
**Development of a Geothermal Resource in a
Fractured Volcanic Formation:
Case Study of the Sumikawa Geothermal Field, Japan**

MASTER

DISTRIBUTION OF THIS DOCUMENT IS UNLIMITED

S. K. Garg
J. Combs
J. W. Pritchett
A. H. Truesdell
J. L. Stevens

Final Report

**Submitted to: The U.S. Department of Energy (DOE-ID)
Idaho Operations Office
850 Energy Drive
Idaho Falls, ID 83404-1563**

**Work completed under the U.S. Department of Energy
Idaho Operations contract DE-AC07-94ID13407**

July 1997

DISCLAIMER

This report was prepared as an account of work sponsored by an agency of the United States Government. Neither the United States Government nor any agency thereof, nor any of their employees, makes any warranty, express or implied, or assumes any legal liability or responsibility for the accuracy, completeness, or usefulness of any information, apparatus, product, or process disclosed, or represents that its use would not infringe privately owned rights. Reference herein to any specific commercial product, process, or service by trade name, trademark, manufacturer, or otherwise does not necessarily constitute or imply its endorsement, recommendation, or favoring by the United States Government or any agency thereof. The views and opinions of authors expressed herein do not necessarily state or reflect those of the United States Government or any agency thereof.

DISCLAIMER

Portions of this document may be illegible electronic image products. Images are produced from the best available original document.

Abstract

The principal purpose of this case study of the Sumikawa Geothermal Field is to document and to evaluate the use of drilling logs, surface and downhole geophysical measurements, chemical analyses and pressure transient data for the assessment of a high temperature volcanic geothermal field. This comprehensive report describes the work accomplished during FY 1993-1996. A brief review of the geological and geophysical surveys at the Sumikawa Geothermal Field is presented (Section 2). Chemical data, consisting of analyses of steam and water from Sumikawa wells, are described and interpreted to indicate compositions and temperatures of reservoir fluids (Section 3). The drilling information and downhole pressure, temperature and spinner surveys are used to determine feedzone locations, pressures and temperatures (Section 4). Available injection and production data from both slim holes and large-diameter wells are analyzed to evaluate injectivity/productivity indices and to investigate the variation of discharge rate with borehole diameter (Section 5). New interpretations of pressure transient data from several wells are discussed (Section 6). The available data have been synthesized to formulate a conceptual model for the Sumikawa Geothermal Field (Section 7).

Acknowledgment

We wish to express our sincere appreciation to the Mitsubishi Materials Corporation, Tokyo, Japan (MMC) for their kind cooperation in making their proprietary data for the Sumikawa Geothermal Field available for the present study.

Table of Contents

Section	Page
Abstract	iii
Acknowledgment	iv
1 Introduction	1-1
2 Geology and Geophysics	2-1
2.1 Regional Geology	2-1
2.2 Geology of the Sumikawa Field	2-5
2.3 Geophysical Surveys	2-5
2.3.1 Heat Flow Studies	2-10
2.3.2 Seismic Surveys	2-10
2.3.3 Gravity Survey	2-10
2.3.4 Electrical and Magnetotelluric Surveys	2-14
2.3.5 Summary	2-16
3 Fluid Chemistry of the Sumikawa Geothermal System	3-1
3.1 Introduction	3-1
3.2 Geothermal Water Types	3-1
3.3 Well Discharge Chemistry	3-4
3.3.1 Well S-1	3-5
3.3.2 Well S-2	3-5
3.3.3 Well S-3	3-8
3.3.4 Well S-4	3-11
3.3.5 Well SA-1	3-14
3.3.6 Well SA-2	3-14
3.3.7 Well SA-4	3-18
3.3.8 Well SB-1	3-18
3.3.9 Well SC-1	3-18
3.3.10 Well SD-1	3-25
3.3.11 Well 52E-SM-2	3-28
3.3.12 Typical Reservoir Water	3-28
3.4 1989 Tests of Cold Water Unloading	3-28

Section	Page
3.5 Interrelation of Sumikawa Water Compositions	3-34
3.5.1 The Combined Na-K and K-Mg Geothermometer Diagram.....	3-37
3.5.2 The Cl-SO ₄ -HCO ₃ Anion Triangular Diagrams.....	3-39
3.5.3 The Cl-B-HCO ₃ Diagram, a Test for Fluid Homogeneity	3-41
3.5.4 The Na-K-Ca Triangular Diagram	3-43
3.6 Chemical Changes Shown by Contour Maps	3-43
3.6.1 Contour Maps of Reservoir Chemistry and Physical State	3-46
3.7 Comparison of Stabilized Sumikawa Fluids and Ohnuma Production Fluids	3-51
3.8 A Model for the Sumikawa-Ohnuma System	3-51
3.8.1 Enthalpy-Chloride Relations	3-54
3.8.2 Isotope Relations	3-55
3.8.3 Isotopic Effects of Cold Water Injection	3-59
3.9 Gas Geothermometer Calculations	3-60
3.10 Equilibria with Rock Minerals	3-75
3.11 Magmatic Constituents	3-78
3.12 Conclusions	3-79
4 Analysis of Downhole Data	4-1
4.1 Slim Hole 50-HM-3	4-1
4.2 Slim Hole N60-KY-1	4-5
4.3 Slim Hole O-5T	4-5
4.4 Slim Hole S-1	4-5
4.5 Slim Hole S-2	4-13
4.6 Slim Hole S-3	4-19
4.7 Well S-4	4-26
4.8 Well SA-1	4-33
4.9 Well SA-2	4-33
4.10 Well SA-4	4-43
4.11 Well SB-1	4-43
4.12 Well SB-2	4-43

4.13	Well SB-3	4-54
4.14	Well SC-1 (original well name: N61-SN-7D)	4-54
4.15	Well SD-1 (original well name: N61-KY-2)	4-63
4.16	Slim Hole 52E-SM-1	4-76
4.17	Slim Hole 52E-SM-2	4-76
4.18	Slim Hole N59-SN-5	4-83
5	Injection and Discharge Tests	5-1
5.1	Determination of Injectivity and Productivity Indices	5-3
	Slim Hole 50-HM-3	5-3
	Slim Hole N60-KY-1	5-3
	Slim Hole O-5T	5-3
	Slim Hole S-1	5-3
	Slim Hole S-2	5-10
	Slim Hole S-3	5-10
	Production Well S-4	5-21
	Production Well SA-1	5-21
	Production Well SA-2	5-28
	Production Well SA-4	5-28
	Production Well SB-1	5-28
	Injection Well SB-2	5-42
	Injection Well SB-3	5-42
	Production Well SC-1	5-42
	Injection Well SD-1	5-42
	Slim Hole 52E-SM-1	5-52
	Slim Hole 52E-SM-2	5-52
	Slim Hole N59-SN-5	5-52
5.2	Comparison of Productivity and Injectivity Indices	5-55
5.3	Characteristic Tests	5-57
5.4	Effect of Borehole Diameter on Discharge Rate	5-71
5.5	Summary	5-74
6	Analysis of Pressure Transient Data	6-1
6.1	Wells S-4 and KY-1	6-2
	6.1.1 Discharge Rate History (1986) for Well S-4	6-3
	6.1.2 Determination of Initial Effective Discharge Rate \dot{M}_o for Well S-4 (1986 test)	6-5

6.1.3	Analysis of 1989 Interference Test	6-9
6.1.4	1986 Pressure Interference Test: Early Response	6-9
6.1.5	1986 Pressure Interference Test: Late Time Response	6-14
6.1.6	Structural Interpretation	6-20
6.2	1989 Injection Test	6-27
6.2.1	Wells KY-1 and SB-1	6-27
6.2.2	Wells KY-1 and SB-2	6-32
6.2.3	Wells SD-1 and SB-3	6-37
6.3	Pressure Transient Tests for Well SC-1	6-37
	The November 1987 Injection Test	6-41
	The June 1988 Injection Test	6-41
	The First 1988 Discharge Test	6-46
	The Second 1988 Discharge Test	6-46
	The 1989 Discharge Test	6-50
	Evaluation of Model Results	6-54
7	A Conceptual Model of the Sumikawa Geothermal Field	7-1
7.1	Fluid State	7-3
7.1.1	Reservoir Pressures	7-3
7.1.2	Reservoir Temperature	7-7
7.1.3	Fluid Chemistry	7-9
7.2	Heat Source	7-9
7.3	Formation Permeability and Hydraulic Boundaries	7-10
7.4	Evolution of Sumikawa Geothermal System	7-11
7.5	Concluding Remarks	7-11
8	References	8-1

1 Introduction

The next major geothermal area in the United States (U.S.) to be developed is likely to be the Cascade volcanic zone in the Pacific Northwest region. At present, detailed practical information pertinent to the development of geothermal resources in fractured volcanic rocks is scarce in the U.S. Geothermal resources in Japan, however, are located in fractured volcanic zones and the development of the Cascade region would likely be expedited by the availability of information concerning the Japanese experience in geothermal exploration and reservoir assessment.

In FY 1993, Maxwell*—under a contract with the U.S. Department of Energy (DOE)/Sandia National Laboratories (Sandia)—approached Mitsubishi Materials Corporation (MMC)** for release of their proprietary data from the Sumikawa Geothermal Field for use in a case study of a high-temperature, fractured, volcanic field. As a result of these negotiations, MMC gave permission to Maxwell to use pertinent Sumikawa data obtained prior to 1990. The Sumikawa Geothermal Field is an especially good candidate for a case study of a high temperature volcanic field. The Sumikawa Geothermal Field is located in the Hachimantai volcanic area in northern Honshu, Japan, about 1.5 kilometers to the west of the Ohnuma geothermal power station operated by MMC. The Hachimantai area also includes the Matsukawa and Kakkonda Geothermal Fields. An extensive well drilling and testing program was ini-

tiated in the Sumikawa area in 1981 with the spudding of boreholes S-1 and S-2 by MMC and the Mitsubishi Gas Chemical Corporation (MGC). The New Energy and Industrial Technology Development Organization (NEDO) became involved in the field characterization effort with the drilling of borehole N59-SN-5 in 1984–1985. During the years 1986–1990, under NEDO sponsorship, Maxwell carried out reservoir engineering studies of the Sumikawa Geothermal Field. The field characterization program at Sumikawa was successfully concluded in 1990 with a decision to build a 50 MWe power plant. The Sumikawa geothermal power plant was commissioned in March 1995.

Because of DOE's budget constraints, the Sumikawa case study has been conducted over several years (FY 1993 - FY 1996). A report (Garg *et al.*, 1994) describing work performed during FY 1993 was approved by MMC for publication in December 1994. DOE decided to fund the second year (FY 1994) of this project through the Idaho National Engineering Laboratory (INEL). A report (Garg *et al.*, 1995) documenting the work carried out during FY 1994 was submitted to INEL in early 1995. In October 1995, the contract for the Sumikawa case study was transferred to DOE's Idaho Operations Office. The work performed during FY 1995 is described by Garg *et al.*, (1996). The present comprehensive report documents the studies carried out by Maxwell during the entire contract period (FY 1993 - FY 1996).

The principal objectives of this study of the Sumikawa Geothermal Field are as follows:

*Formerly S-Cubed Division of Maxwell Technologies.

**Prior to 1990, MMC was known as Mitsubishi Metal Corporation.

- Document and evaluate the use of drilling logs, surface and downhole geophysical measurements, chemical analyses and pressure transient data for reservoir assessment purposes.
- Evaluate the feasibility of predicting the discharge characteristics of large-diameter production wells on the basis of test data from slim holes.
- Demonstrate the usefulness of a map-oriented geothermal database for interpretation of exploration data and analysis of exploration strategies and reservoir information.
- Core data.
- Well histories.
- Downhole logs (pressure, temperature, spinner) in shutin and flowing wells.
- Geochemical data from analyses of well fluids and hot springs.
- Pressure transient data.

With very few exceptions, the above data sets (for the period prior to mid-1990) are now available as part of GEOSYS.

To provide convenient access to the Sumikawa data base, the pertinent Sumikawa data have been incorporated into Maxwell's Geothermal Reservoir Data Management System (GEOSYS).

GEOSYS (Stevens *et al.*, 1992) is an interactive, graphical, map-oriented computer system used to store, display and analyze large volumes of geothermal reservoir engineering data. The design requirements for GEOSYS were defined by Maxwell scientists experienced in the integration/synthesis of geothermal data. GEOSYS consists of a set of independent, integrated modules that analyze and display geographical data, subsurface cross sections, well structure, well logs, and chemical and production data. GEOSYS runs on Unix workstations using the X Window System. More information about GEOSYS is available on the World Wide Web at <http://www.scubed.com/products/geop/GEOSYS/GEOSYS.html>.

The following data have been entered into GEOSYS:

- Surface tectonic and topographic maps.
- Surface geophysics/geological data.
- Well drilling (circulation loss, deviation, stratigraphy) and completion data.

Under its drilling research program, DOE through Sandia, has initiated a research effort to demonstrate that slim holes can be used (1) to provide reliable geothermal reservoir parameter estimates comparable to those obtained from large-diameter wells, and (2) to predict the behavior of large-diameter wells. During FY 1993, S-Cubed was tasked to examine the existing production and injection data for both small-diameter boreholes and large-diameter wells at the Sumikawa Geothermal Field. The major thrust of this work was to evaluate the feasibility of predicting the discharge characteristics of large-diameter production wells on the basis of test data from slim holes. A paper discussing the production/injection characteristics of slim holes and large-diameter wells at the Sumikawa Geothermal Field was presented by Garg and Combs (1995) at the 20th Stanford Geothermal Reservoir Engineering Workshop.

MMC has carried out a series of pressure transient (both single well drawdown/buildup and multiple well pressure interference tests) tests at the Sumikawa Geothermal Field. These test data are invaluable for determining the permeability structure at Sumikawa. During FY 1994, work was initiated on analyzing some of the pressure interfer-

ence tests. Analyses of pressure transient data were continued during FY 1995 and FY 1996. Two papers describing certain aspects of this work were presented at the Twenty-First Stanford Geothermal Reservoir Engineering Workshop (Garg and Owusu, 1996) and at the DOE's Geothermal Program Review XIV (Garg, 1996).

The present report describes the work accomplished during the entire contract period (FY 1993 to FY 1996). A brief review of the surface geological and geophysical surveys is given in Section 2. The Sumikawa geochemical data are dis-

cussed in Section 3. The drilling information and downhole pressure, temperature and spinner surveys for eighteen Sumikawa boreholes are analyzed in Section 4 to determine feedzone locations, pressures and temperatures. Available injection and production data from both slim holes and large-diameter production wells are analyzed in Section 5 to determine injectivity/productivity indices. The variation of discharge rate with borehole diameter is also discussed in Section 5. Results of pressure transient analyses are described in Section 6. Finally in Section 7, a conceptual model for the Sumikawa Geothermal Field is presented.

2 Geology and Geophysics

The Sumikawa Geothermal Field is located in the Hachimantai volcanic area in northern Honshu, Japan, about 2 kilometers to the west of Ohnuma geothermal power station operated by Mitsubishi Materials Corporation (MMC). The Hachimantai area also includes the Matsukawa and Kakkonda Geothermal Fields (Figure 2.1). After the completion of the Ohnuma power station (~ 10 MWe) in 1973, MMC began to conduct exploratory investigations of the Sumikawa geothermal prospect. An extensive well drilling and testing program was initiated in October 1981 with the spudding of boreholes S-1 and S-2 by MMC and the Mitsubishi Gas Chemical Corporation (MGC). The New Energy and Industrial Technology Development Organization (NEDO) became involved in the field characterization effort with the drilling of borehole N59-SN-5 (~ 2 km west of S-1 and S-2) in 1984–1985. During the years 1986–1990, under NEDO sponsorship, Maxwell (formerly S-Cubed) carried out geothermal reservoir engineering studies of the Sumikawa Geothermal Field. All aspects of the five-year study of the Sumikawa Geothermal Field performed by Maxwell have been summarized by Pritchett, *et al.* (1990). The field exploration and characterization program at Sumikawa was successfully concluded in 1990 with a decision to build a 50 MWe power plant. The Sumikawa geothermal power plant was commissioned in March 1995.

In this section, the regional and local geological structures in and around the Sumikawa field (Sections 2.1 and 2.2) are discussed. The geology is synthesized with the results of geophysical studies to produce a model of the structure of the field (Sections 2.3 and 2.4).

2.1 Regional Geology

The Sumikawa/Ohnuma geothermal area is shown in Figure 2.2. The area depicted is about 42 km²; the Sumikawa Geothermal Field lies in the western part of the area. The terrain is extremely irregular. Mt. Yake lies to the southwest of the Sumikawa area, and Mt. Hachimantai is just to the southeast (outside the area illustrated in Figure 2.2, see Figure 2.3). To the north of these volcanic peaks, the terrain drops away rapidly. Between the Sumikawa prospect (which may be regarded as centered in the neighborhood of the S-series boreholes, S-1, S-2, S-3, and S-4) and the Ohnuma borefield is a north-south region of relatively low ground surface elevation where natural hot springs and fumaroles are found (Figures 2.2 and 2.3).

The Sumikawa/Ohnuma area lies within a north-south oriented regional graben structure which extends many kilometers both north and south of the Sumikawa area (see Figure 2.1). It has been postulated that the graben structure extends into the Sumikawa area but the gravity data there do not clearly support this interpretation (KRTA, 1985). The active volcanoes (Mt. Yake to the west and Mt. Hachimantai to the southeast) and the Senosawa uplift have perhaps combined to obscure the local graben structure.

The regional tectonic map (Figure 2.1) shows that the major tectonic features (faults, uplifts and depressions) strike north-south. The faults are evident at the surface in rocks of Miocene age and older but not in surficial Quaternary rocks. Also seen on the map are east-west lineaments which align Quaternary volcanoes in the region, includ-

Continued on page 2-5

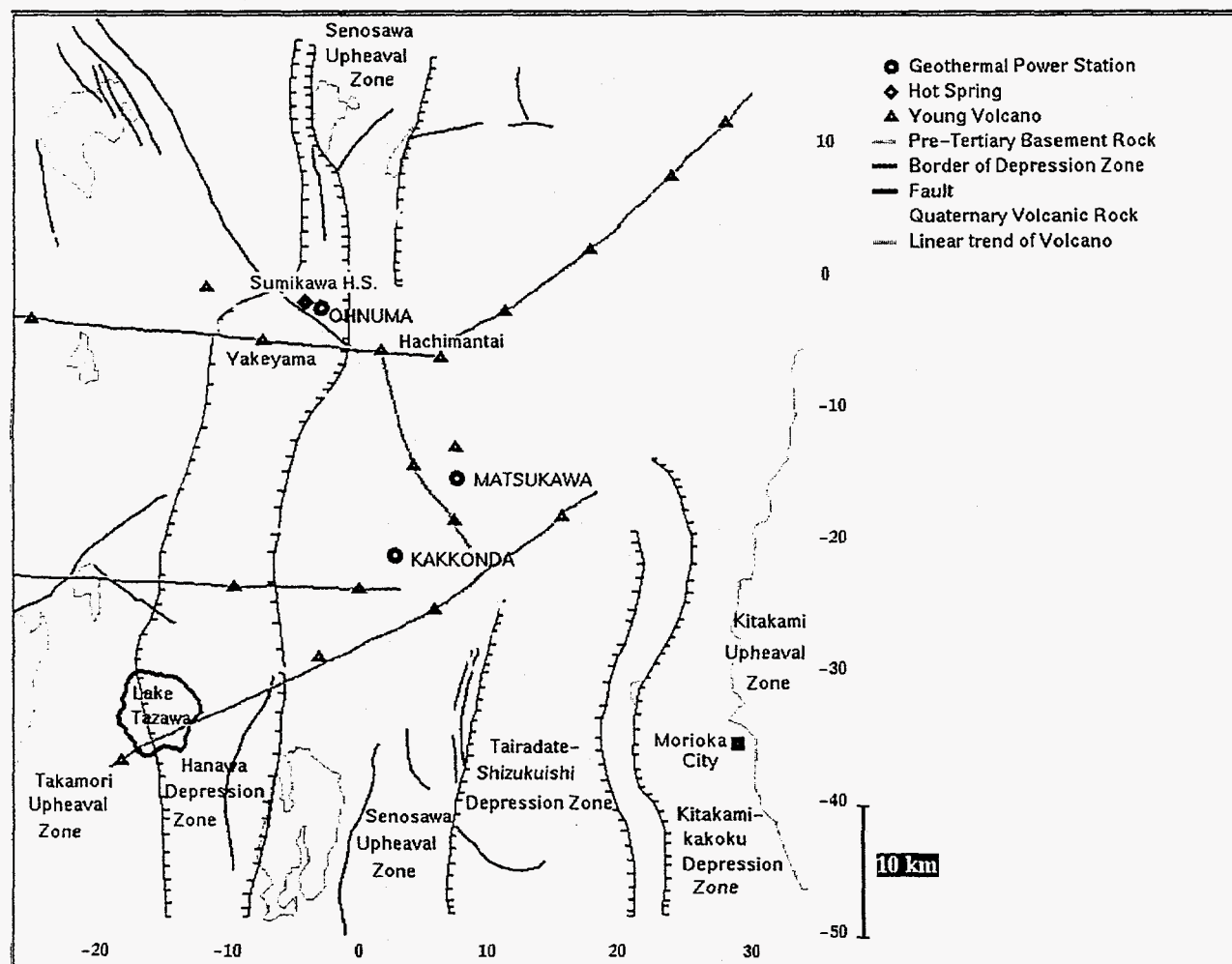


Figure 2.1. Tectonic map of the Hachimantai volcanic area. The origin of the local co-ordinate system is 40°N latitude and 140°50' E longitude. Adapted from MMC (1986).

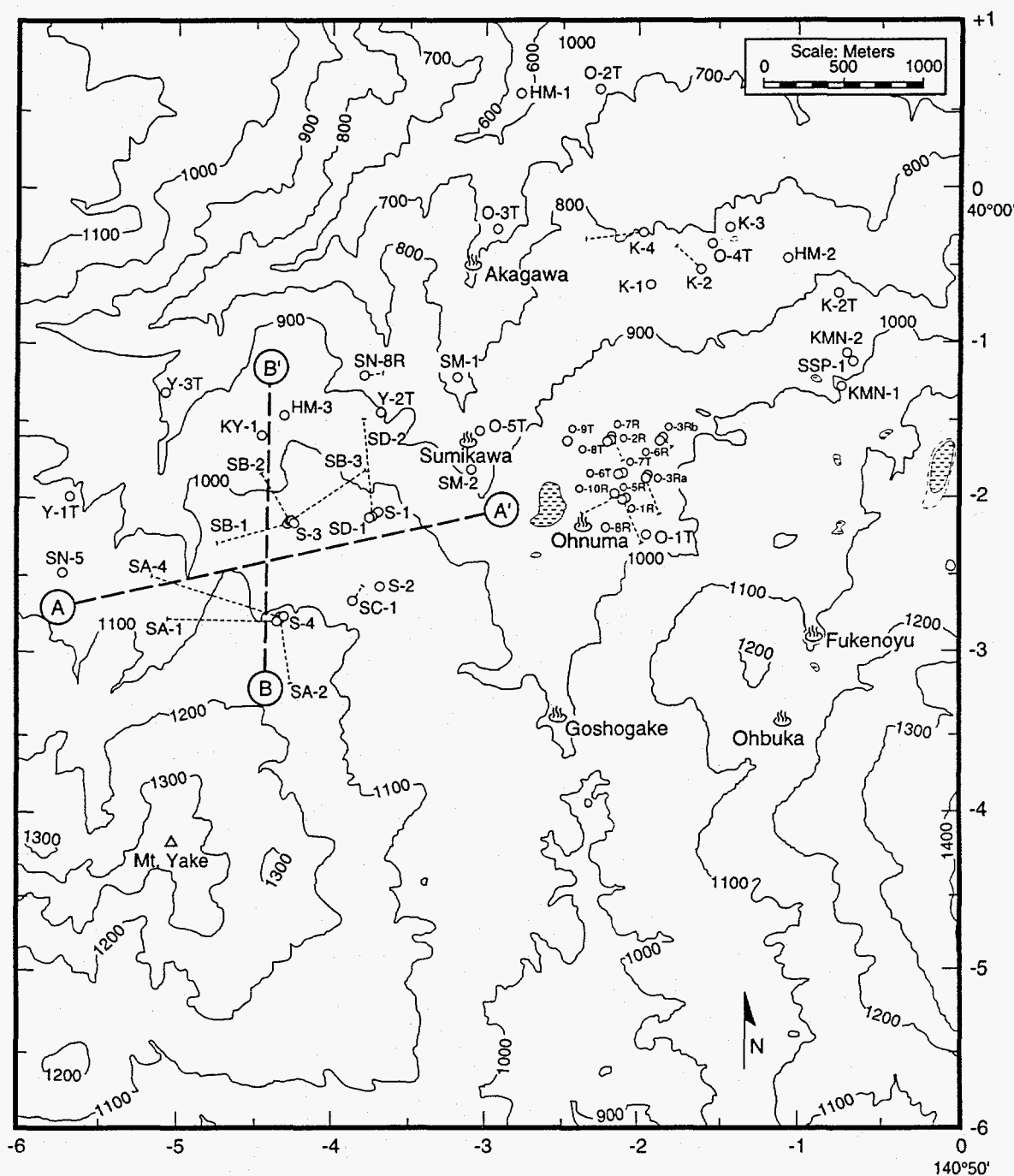


Figure 2.2. The Sumikawa/Ohnuma area, showing locations of wells and cross-sections A-A' and B-B'. The origin of the local co-ordinate system is 40°N latitude and 140°50'E longitude.

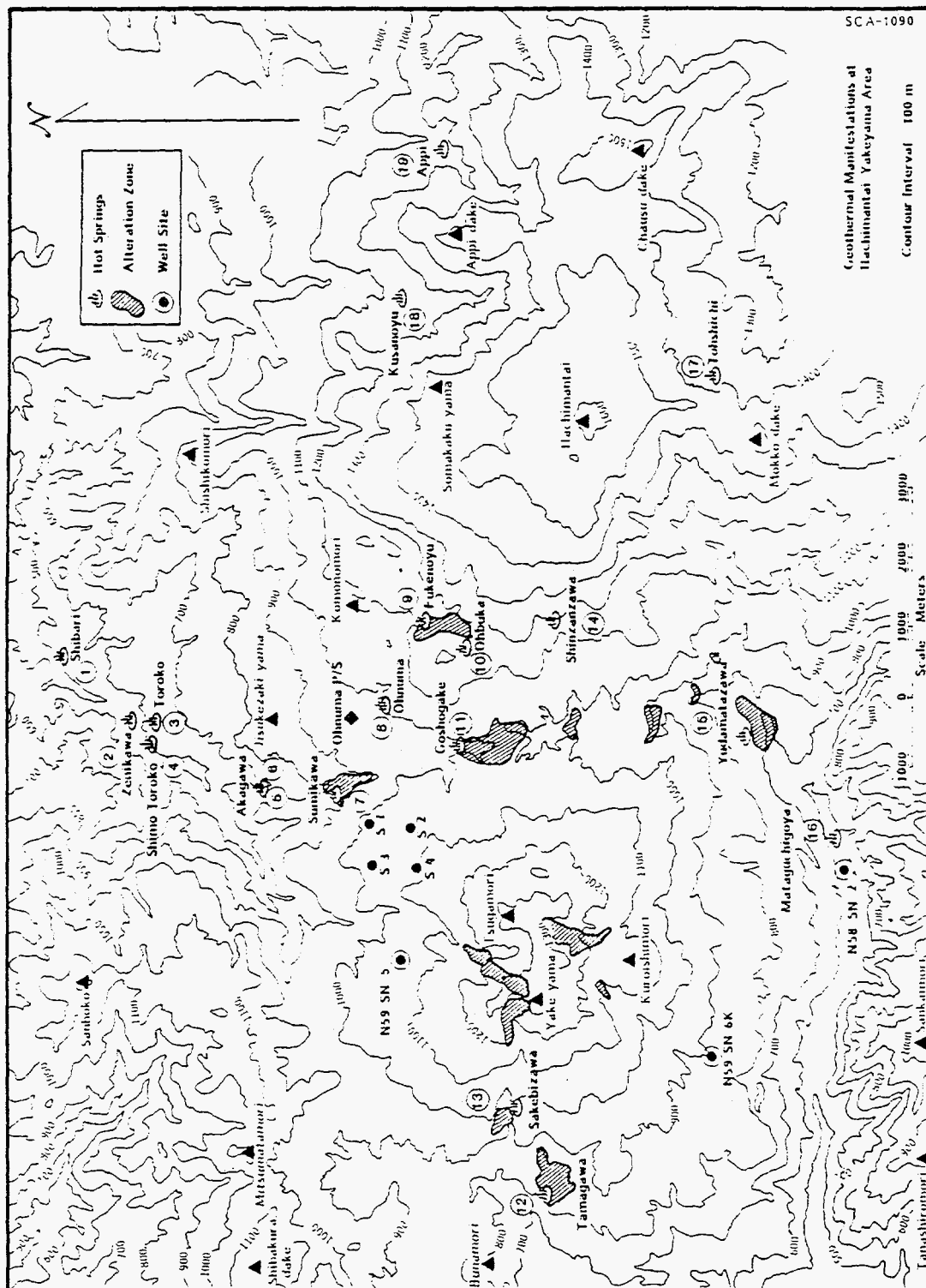


Figure 2.3. Geothermal manifestations in the northern Hachimantai - Yakeyama area.

ing Mt. Yake and Hachimantai, and which are believed to be regional fracture zones.

2.2 Geology of the Sumikawa Field

Surface rocks in the Sumikawa area are andesitic lavas primarily from Mt. Yake and Mt. Hachimantai (Figure 2.4). To the northwest, along the Kumazawa river, are Miocene and older rocks which in addition to andesitic and dacitic lavas include outcrops of tuffaceous mudstones and shale. These rocks are seen in subsurface sections derived from well logs. The geology can be characterized as densely faulted andesitic and dacitic lavas with a bed of black shale under a portion of the field. The average fault spacing is on the order of 200 m, striking predominantly north-south. A summary map, Figure 2.5 (originally from a map made by Compagnie Generale de Geophysique, CGG, and expanded upon for this report), shows the locations of faults inferred from electrical surveys (discussed further in Section 2.3).

Extensive faulting has rendered the detailed geological structure at Sumikawa somewhat obscure, but the abundance of drilling logs from the various boreholes in the area has revealed an underlying geological sequence which applies to most of the area illustrated in Figure 2.2. Schematic cross-sections of the stratigraphy beneath the east-west line AA' and north-south line BB' (Figure 2.2) are shown in Figures 2.6 and 2.7. These structural interpretations are based almost exclusively upon drilling experience.

In order of increasing depth, the formations at Sumikawa are:

ST formation. Surficial andesitic tuffs, lavas, and pyroclastics of recent origin (from Mt. Yake).

LS formation. Lake sediments; Pleistocene tuffs, sandstones, siltstones, and mudstones.

DA formation. Pliocene dacites, dacitic tuffs, and breccias.

MV formation. "Marine/volcanic complex"; interbedded Miocene dacitic volcanic rocks and "black-shale" oxygen-poor marine shales and sediments.

AA formation. Altered andesitic rocks that apparently are extensively fractured.

BA formation. Crystalline intrusive (?) rocks (mainly granodiorite and diorite).

The BA formation is the deepest so far encountered by drilling (well SC-1 bottomed in this formation at 2486 m depth), but the pre-Tertiary basement, which presumably underlies the above sequence, has not yet been reached. Because of a lack of density contrast among the various deep formations in the area, the gravity survey cannot be used to determine the depth to the pre-Tertiary basement. Little evidence exists for significant permeability deep within the BA formation, however, so that it may be permissible to regard this layer as the "basement" from a hydrological standpoint.

2.3 Geophysical Surveys

There have been two sets of geophysical studies performed in the Hachimantai area. The earlier set included gravity, seismic reflection, heat flow and DC resistivity surveys. The second set of studies used similar geophysical techniques except that a long seismic refraction line was run instead of reflection lines, and magnetotelluric surveys were performed. In the following, we discuss the results of the individual surveys and at-

Continued on page 2-10

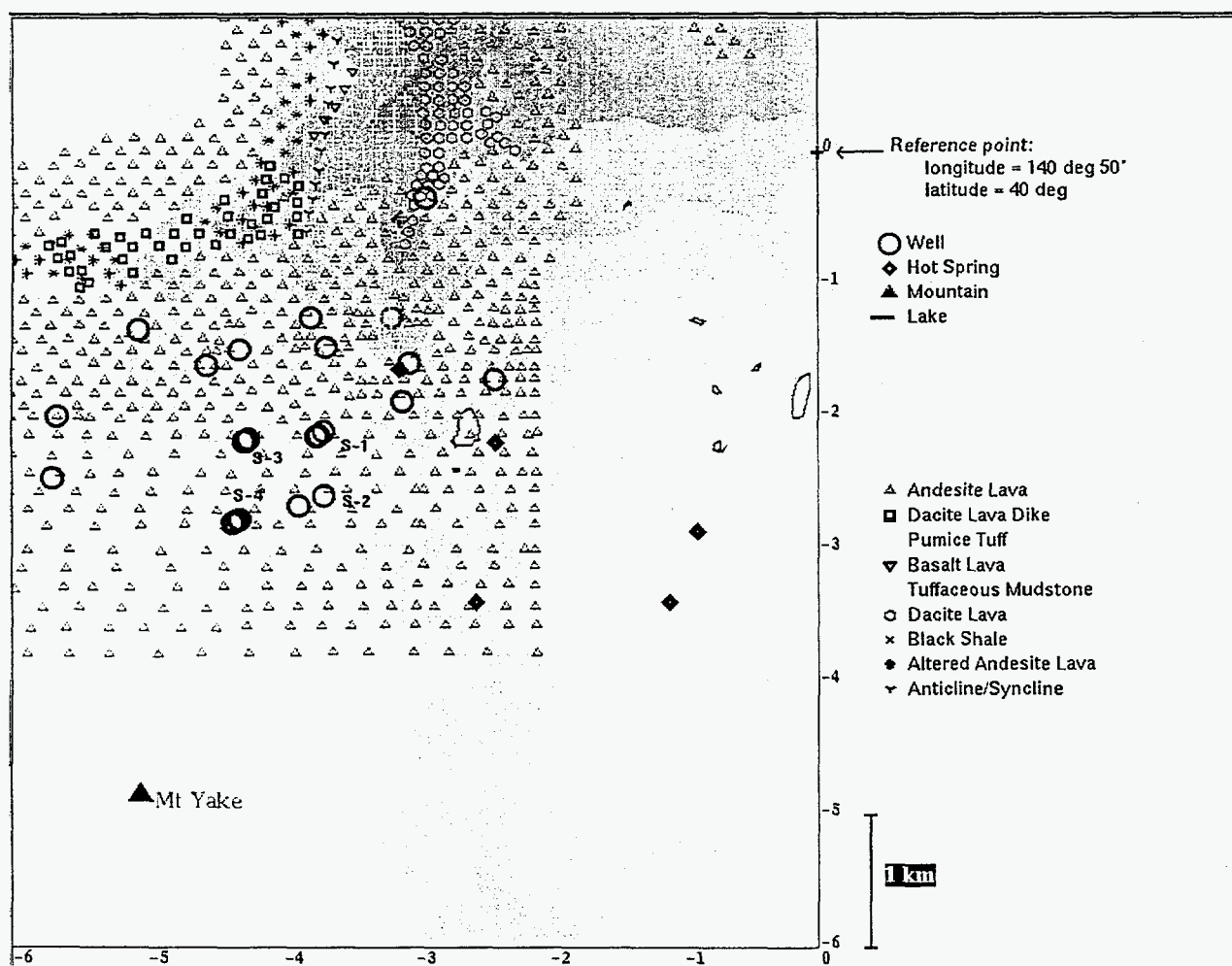


Figure 2.4. Surface geologic map of the Sumikawa area. Adapted from MMC (1986).

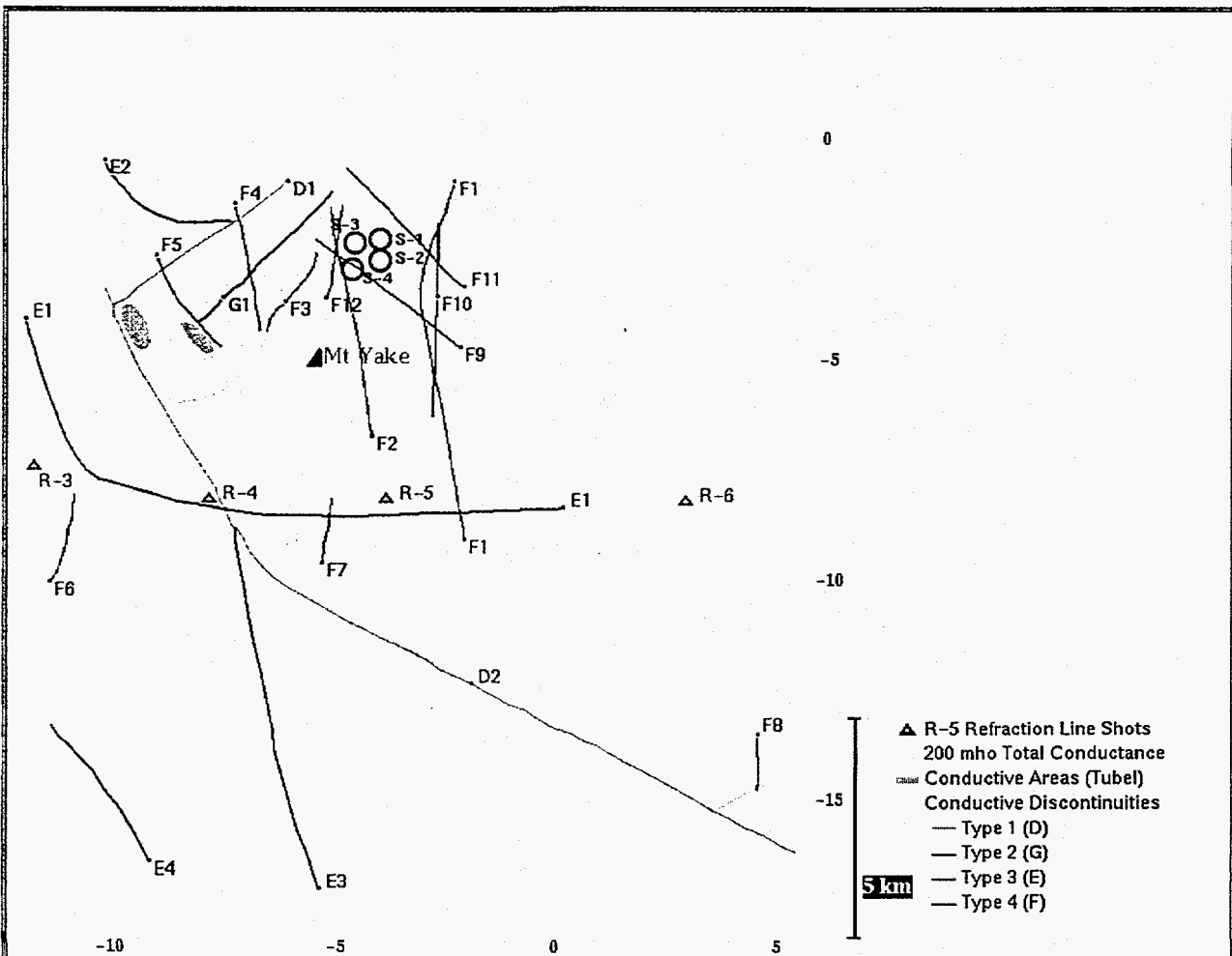


Figure 2.5. Summary map of Sumikawa area showing faults inferred from electrical studies.

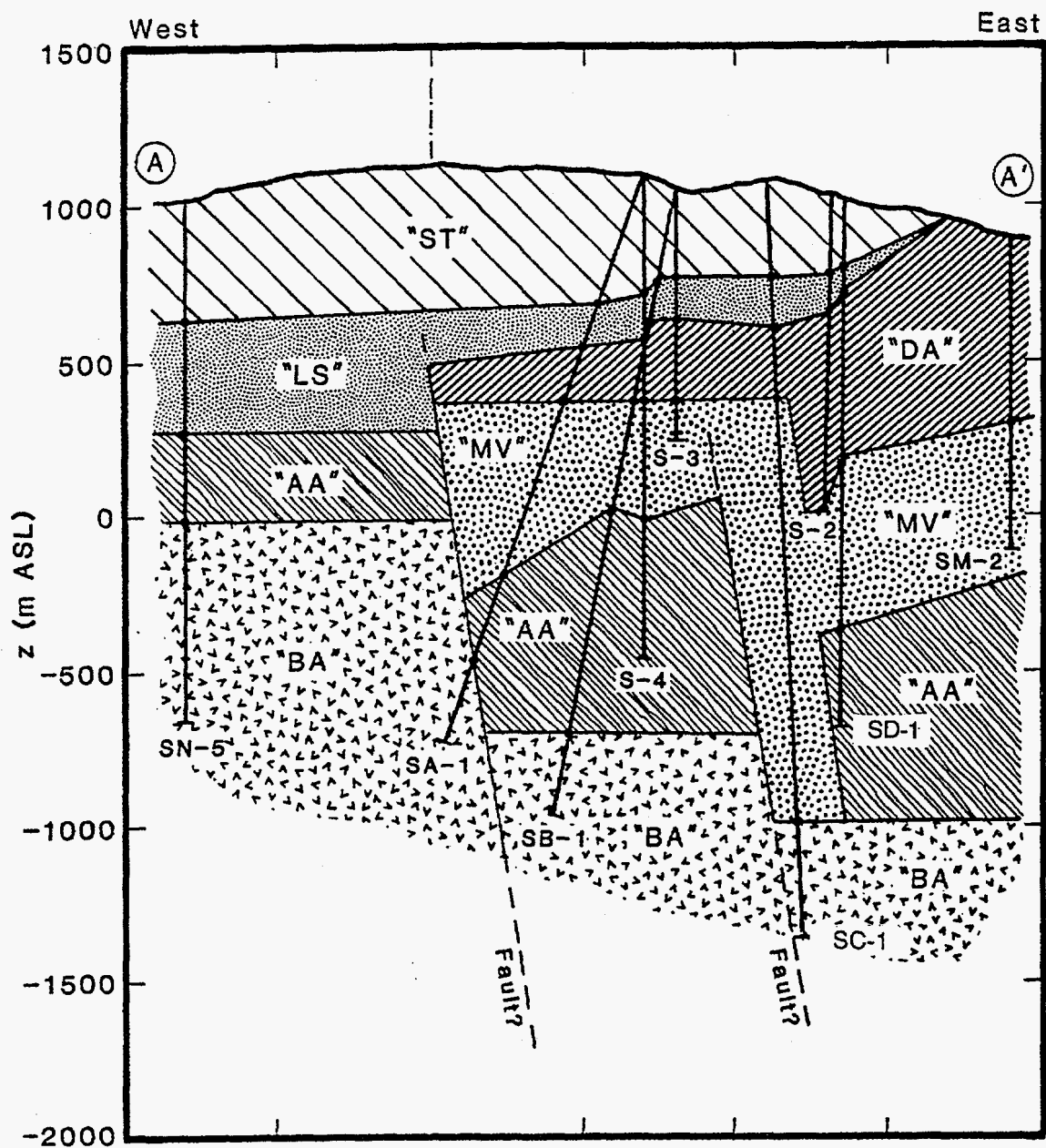


Figure 2.6. East-west A-A' (total length = 3 km) geological cross-section through the Sumikawa area.

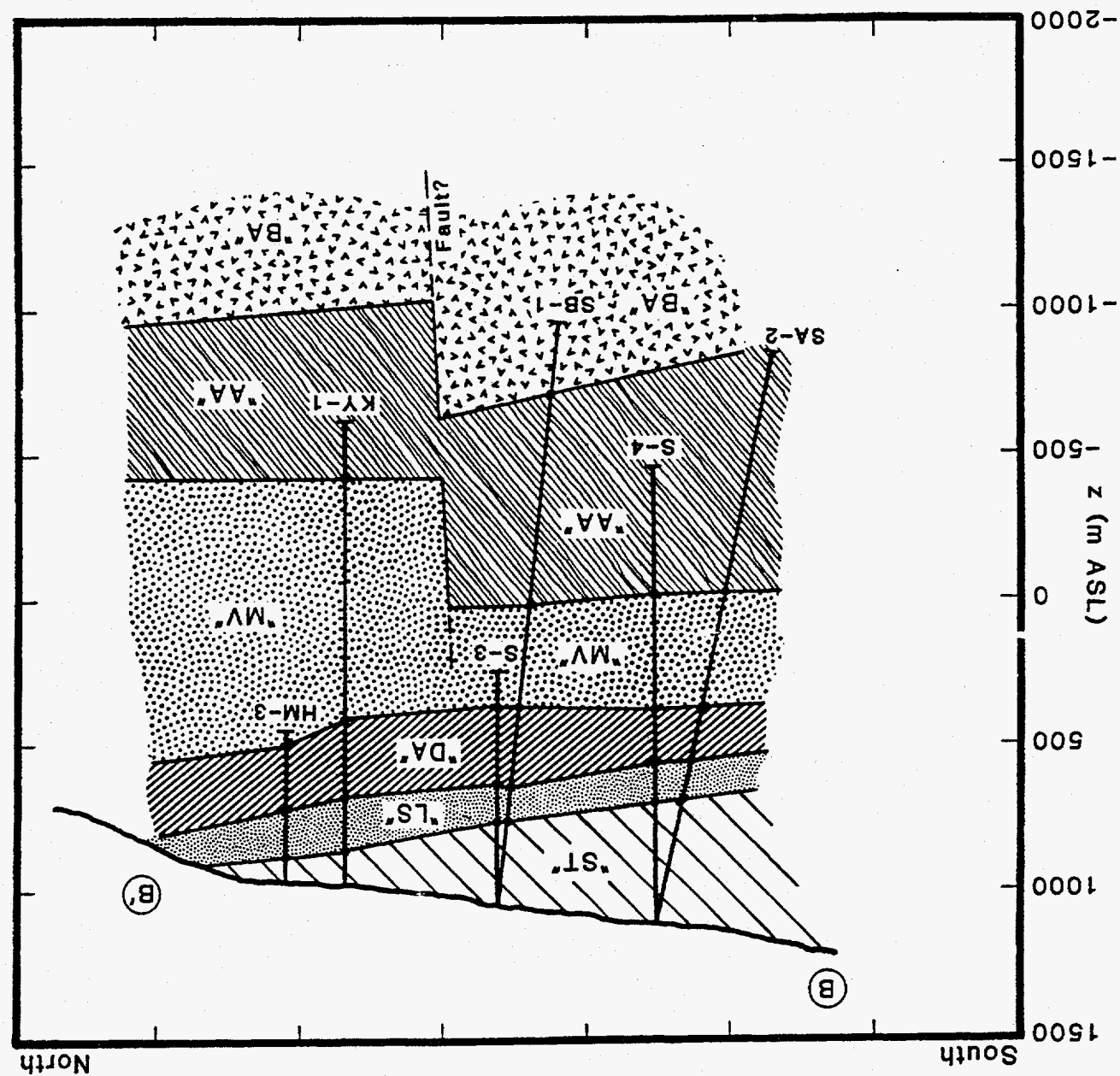


Figure 2.7. North-south B-B' (total length = 3.5 km) geological cross-section through the Sumikawa area.

tempt to synthesize the geological and geophysical findings.

2.3.1 Heat Flow Studies

As part of a heat-flow survey of the Sumikawa/Ohnuma area, temperatures were measured in 36 shallow (80 meter) heat flow holes. The natural heat flow was calculated by assuming purely conductive heat transfer in the near surface zone. The computed heat flow contours along with the locations of heat flow holes are illustrated in Figure 2.8. Although the entire area has elevated heat flow, the detailed interpretation is complicated by topographically induced ground water flow, and convective heat transport in the hot spring areas (KRTA, 1985). Not surprisingly, the highest heat flow appears to occur in the hot spring areas.

The estimated thermal output from the Sumikawa hot spring area (near Wells O-5T, 52E-SM-1 and 52E-SM-2) is about 8 MW, including local conductive flux and convective fluxes from both hot springs and fumaroles. Farther north, at the Akagawa hot spring area (near Well O-3T), the total heat output has been estimated at about 3.3 MW. In addition, about two kilometers north of the Akagawa hot springs, downstream along the Kumazawa river, three more major hot spring areas are located; at Toroko, Zenikawa and Shibari (Figure 2.3). The total thermal output of these three northern hot spring areas is about 24 MW. All estimates of hot spring output quoted above were provided by MMC and GSJ (Geological Survey of Japan). Thus, the thermal output of hot springs is ~35 MW. Taking into account thermal seepages into rivers and conductive heat flow, the total heat flow in the immediate vicinity of the Sumikawa area probably exceeds 70 MW (see also KRTA, 1985).

2.3.2 Seismic Surveys

The seismic reflection survey in the initial set of studies showed a reflector at -600 m ASL which was interpreted by KRTA (1985) as the siliceous shale and sandstone layer seen at -500 m ASL in some Ohnuma wells. The seismic section (Figure 2.9) deduced from the refraction line several kilometers south of the Sumikawa field (see summary Figure 2.5 for location) indicates compressional wave velocities appropriate to crystalline rocks (5.9 to 6.0 km/sec) at elevations of around -500 m ASL on the western half of the line, dropping abruptly to -1500 m ASL near the center, and gradually rising again to -500 m ASL at the eastern end. This seismic section supports the hypothesis that the Sumikawa field is in a graben structure. Because the seismic refraction survey was taken several kilometers to the south of the Sumikawa geothermal field, the results of this survey are less useful for the interpretation of local structure in the vicinity of Sumikawa boreholes. An additional refractor, which is the interface between low velocity rocks (3.0 to 3.4 km/sec) and more competent rocks (4.7 to 5.0 km/sec), also slopes up to the east from about sea level at the center (near the abrupt change in basement) to about 1000 m ASL. We shall refer again to this interface in the discussion of the electrical structure below.

2.3.3 Gravity Survey

The Sumikawa field lies on a steep gravity slope extending from a high centered about 3 km northwest of the field to a low near Goshagake about 500 m southeast of the field (Figure 2.10). The steep change in gravity to the northwest of the Sumikawa geothermal field is probably associated with the presence of low porosity crystalline rocks (mainly grandiorites at shallow depths in this area

Continued on page 2-14

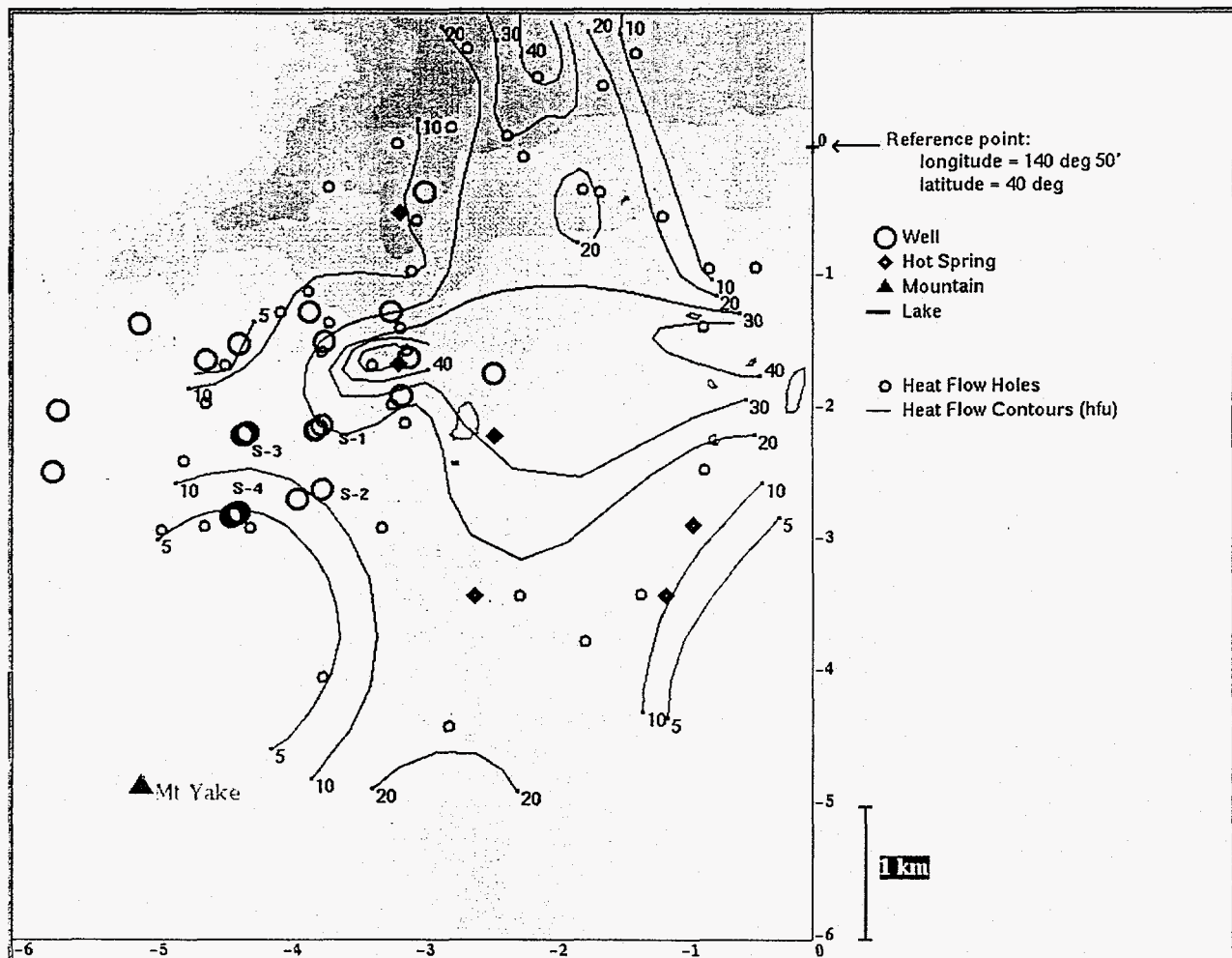


Figure 2.8. Shallow (80 meter) heat flow holes and computed heat flow contours.

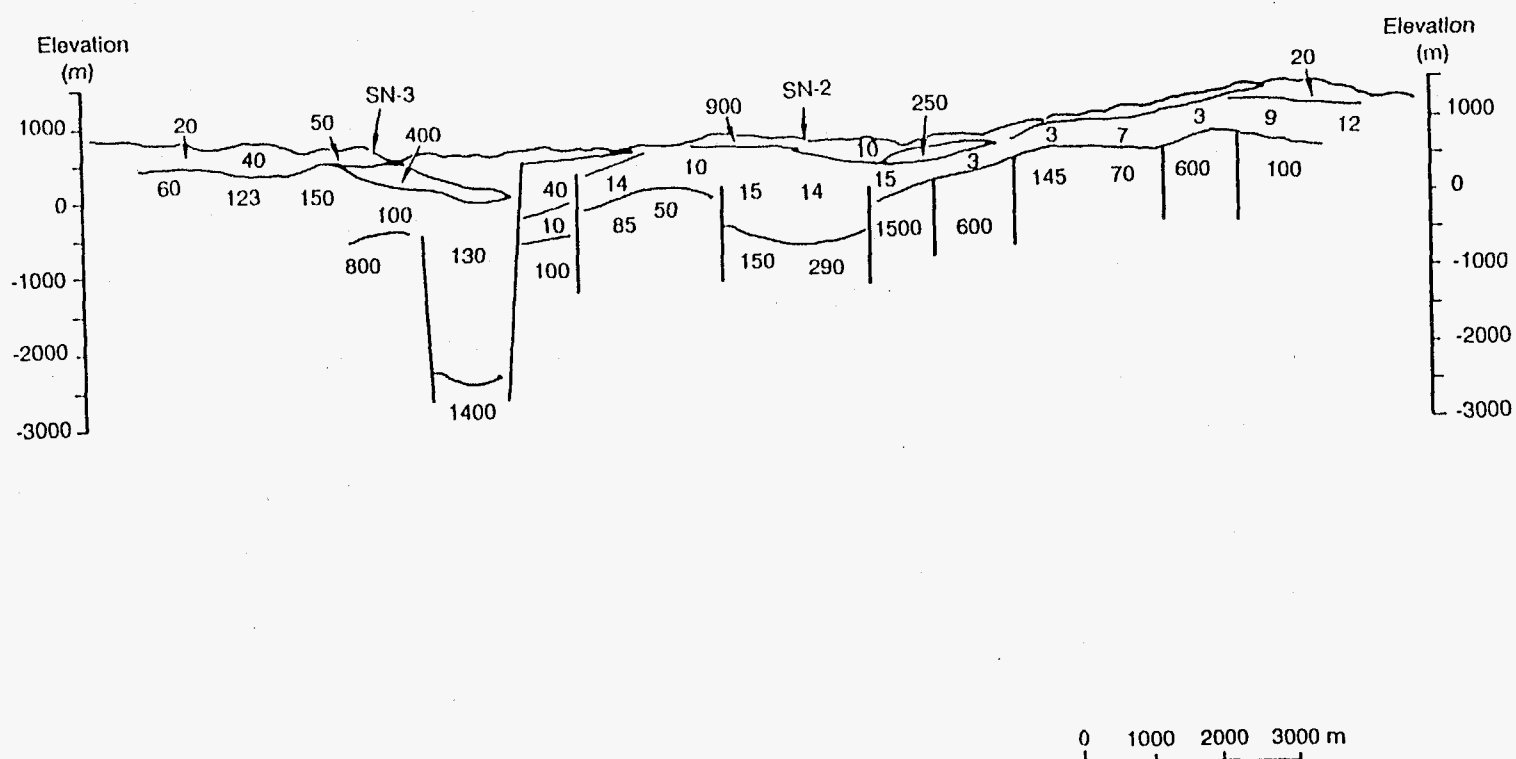


Figure 2.9. Velocity structure section, Hachimantai area. See Figure 2.5 for location of section.

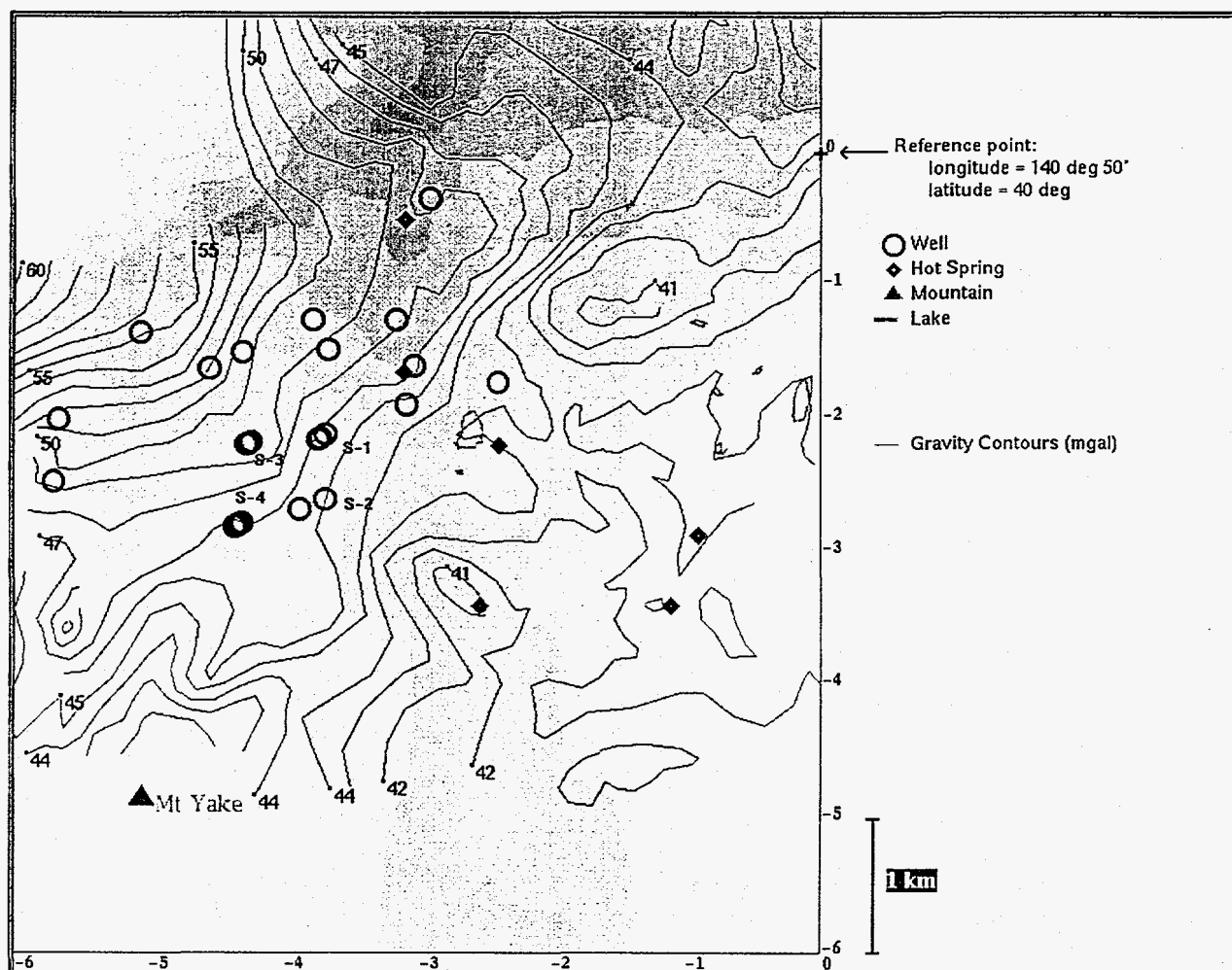


Figure 2.10. Bouguer anomaly in the north Hachimantai area. The gravity low (41 mgal contour) is located near the Goshagake hot spring area.

(see Figure 2.6). A difficulty arises in using gravity to infer changes in deep structure beneath the Sumikawa geothermal field because density logs show that the altered andesites which overlie the basement within the field have densities near 2700 kg/m^3 , which are very near those expected for the granite. These thick deposits would effectively mask the basement gravity signature. In fact, the gravity anomaly is due in part to the presence of lighter lake deposits, shales and pyroclastics in the Hanawa basin. Density logs (MMC, 1986) show densities between 1100 and 2400 kg/m^3 in the upper 300 m of the wells. A 400 m thick layer of deposits with density 2000 kg/m^3 in a basin bounded by material with density 2700 kg/m^3 would produce a gravity anomaly of over 10 mgal . In addition, much of the southern part of the field contains a two-phase mixture of water and steam within the pore spaces at depth, which would further reduce the density and enhance the southern gravity low.

2.3.4 Electrical and Magnetotelluric Surveys

A DC electrical survey (Schlumberger method) was performed along essentially the same line as the seismic refraction line. The section, shown in Figure 2.11 shows that the resistive basement rises to the east at about the same depth as the seismic interface between layers with velocities of 3.0 to 3.4 km/sec and 4.7 to 5.0 km/sec . The resistive basement is deepest in a down-dropped block located about 3 km west of the center of the section, to the west of the seismic discontinuity in crystalline basement.

Magnetotelluric (MT) surveys were conducted in two sets of surveys. The stations of the first set were incorporated into the analysis of the second set. The result are shown in the summary

map (Figure 2.5). Numerous electrical discontinuities mapped by CGG are shown in the figure. They have classified the discontinuities into various types and the details of the classification are not important for the purposes of this report. However, the relationship of the electrical discontinuities to features found in other surveys are important as indications of possible locations of major faults and local system boundaries. The discontinuities labeled F1 and F2 in Figure 2.5 coincide with faults shown on geologic maps. These faults do not penetrate the surface andesite layer in the Sumikawa field.

The electrical discontinuities labelled D1 and D2 in Figure 2.5 are drawn along narrow zones of strong horizontal gradients in conductance. They separate an area of high conductance (the oval-shaped shaded zone) from areas of low conductance (high apparent resistivity) to the northwest and southwest. Mt. Yake is in the high conductance zone. These discontinuities are thought to coincide with the western boundary of the geothermal field. The conductance in the shaded zone is about 300 mhos , while that in the Sumikawa field (near the well field) is near 150 mhos . Electrical feature D2 extends to the southeast past refraction station R4, (where the discontinuity in crystalline basement is inferred) and probably represents a regional fracture in the basement.

Results of electrical studies (Uchida, 1995, Ogawa, et al., 1986 and Uchida, et al., 1986) although different in detail, illustrate the basic structure beneath Sumikawa. The most recent study (Uchida, 1995) uses MT and CSAMT to infer a shallow, thin resistive ($100 \Omega\text{m}$) layer, overlying a conductive ($1 \Omega\text{m}$) layer, which in turn overlies a resistive ($>100 \Omega\text{m}$) layer. The upper layer is associated with the young tuffs and breccias, the intermediate layer with the lake deposits and the deep

Continued on page 2-16

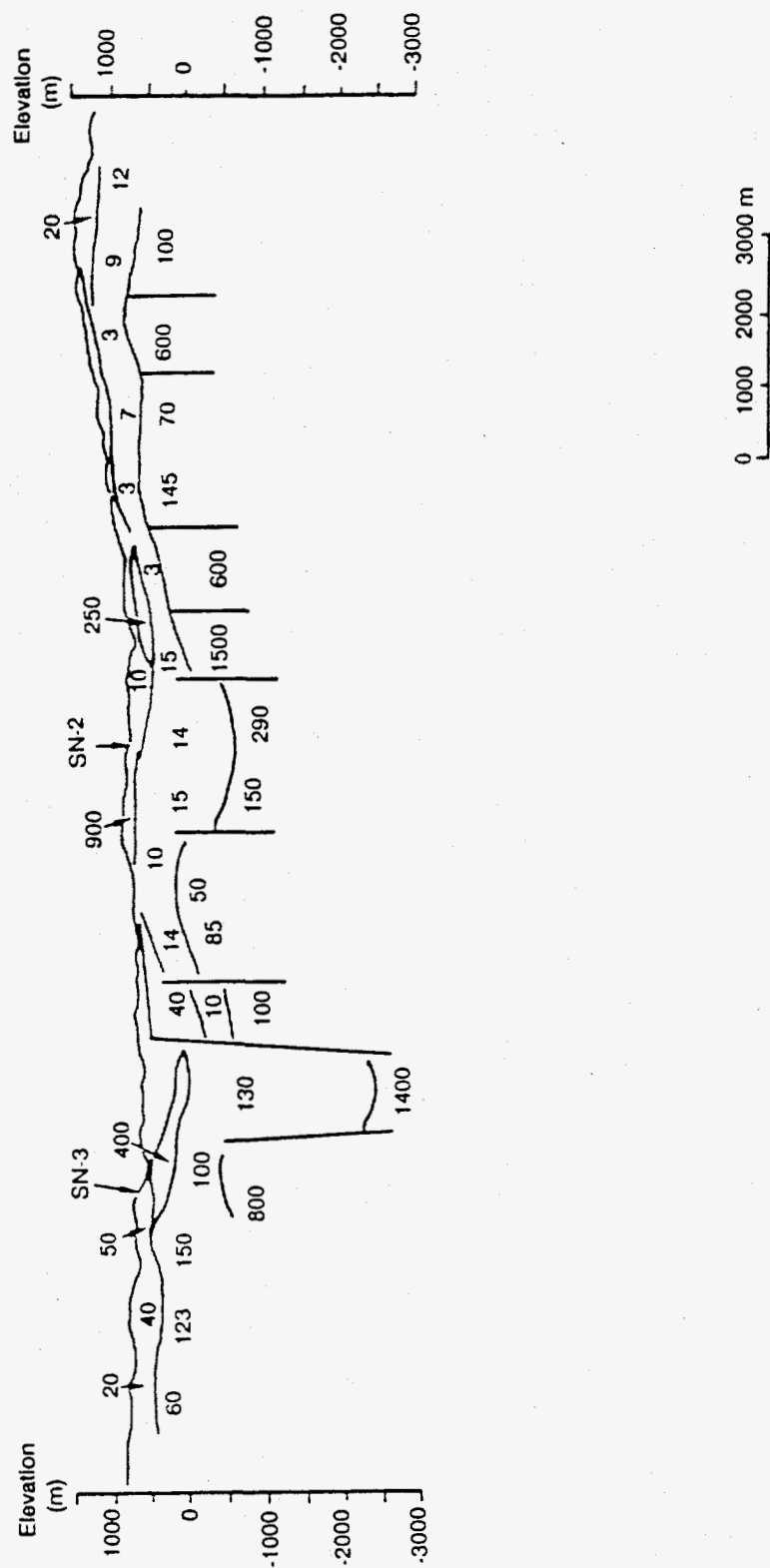


Figure 2.11. Resistivity analysis section, north Hachimnantai area (from NEDO, 1985).

layer with the AA and MV formations (to which Uchida, 1995, refers as intrusive rocks and Green Tuffs, respectively). Although there are substantial amounts of geothermal fluids in the AA and MV formations, the resistivity is high there because the host rock is resistive and the conductive fluids are confined to fractures, according to Uchida (1995).

2.3.5 Summary

The geophysical studies (particularly seismic refraction and DC resistivity) have helped confirm that Sumikawa Geothermal Field is located in a graben structure. The lake sediments, present in

the vicinity of S-series wells, have low resistivities ($\sim 1 \Omega\text{-meter}$). By way of contrast, the reservoir rocks have rather high resistivities ($\sim 100 \text{ ohm-meters}$). Both the gravity and electrical surveys imply that the geothermal field is bounded to the west and the northwest. It is significant that a geological discontinuity (i.e., an abrupt change in the depth to the crystalline granodiorite rocks) is present in this area. Heat flow studies indicate that the entire Sumikawa/Ohnuma area has anomalously high heat flow. Not surprisingly, the highest heat flow is observed in the hot spring areas—located in a north-south region of relatively low surface elevation between the Sumikawa and Ohnuma geothermal fields.

3 Fluid Chemistry of the Sumikawa Geothermal System

3.1 Introduction

The Sumikawa geothermal field is on the north slope of Mt. Yake, an active volcano. Typical volcanic acid sulfate hot springs occur close (~ 1 km) to the field and other types of volcanic hot springs occur at greater distances. Sumikawa well waters are the neutral Na-Cl type with high B and SiO₂ and low Ca and Mg. Figure 3.1 shows general locations of Sumikawa wells, the Ohnuma power plant and area hot springs. Figure 3.2 shows more detailed wellhead and wellbottom locations of Sumikawa and Ohnuma production wells as well as exploratory wells.

Chemical data concerning the Sumikawa field consists of analyses of steam and water discharged from Sumikawa wells S-1, S-2, S-3, S-4, SA-1, SA-2, SA-4, SB-1, SC-1, SD-1 and SM-2 (locations in Figures 3.1 and 3.2). The Sumikawa wells occupy an area of about 4 km², 2 km west of the Ohnuma field. The Sumikawa and Goshogake hot spring areas are nearby (1 km NE and 1 km SE, respectively). Analyses are also available for Ohnuma well discharges and hot spring waters from the general area. In this chapter the chemical data for Sumikawa wells is described and interpreted to indicate compositions and temperatures of reservoir fluids.

3.2 Geothermal Water Types

Based on experience in other volcanic geothermal systems we expect to find a limited number of basic water types in the Sumikawa area resulting from chemical and physical processes re-

lated to deep volcanic heat. Intermediate waters may be formed from the basic types by the action of various physical and/or chemical processes such as boiling, mixing and rock-water reaction.

The deepest waters are of the neutral, sodium-chloride type, which result from deep circulation of meteoric waters with addition of some constituents from deep magmatic fluids. These waters contain "soluble" constituents (such as Cl, B, As and others) contained in rocks and volcanic fluids, and equilibrate with quartz, feldspar and mica to gain SiO₂, Na and K in amounts that depend on temperature. These neutral geothermal waters are the prime target for exploitation because they usually have the highest temperatures at reasonable depths and present few engineering problems.

As the deep neutral chloride waters rise, they boil and release steam containing CO₂, H₂S and other gases. Steam reacting with rock and meteoric water below the surface produces "steam-heated" waters which are low in chloride and high in HCO₃. They may contain moderate amounts of SO₄ resulting from limited oxidation of H₂S by oxygen dissolved in the meteoric water. Most of the H₂S in steam-heated waters is removed by reaction with Fe in rocks to produce pyrite. These waters are found between the zone of boiling and the surface and are cooler than the deep reservoir.

Steam that reaches the surface partially condenses and mixes with surface waters, and H₂S contained in the steam is oxidized by atmospheric oxygen to produce acid-sulfate waters. The sulfuric acid formed is partially neutralized by reaction with rock minerals and leaches Na, K, Ca, Al, SiO₂ and

Continued on page 3-4

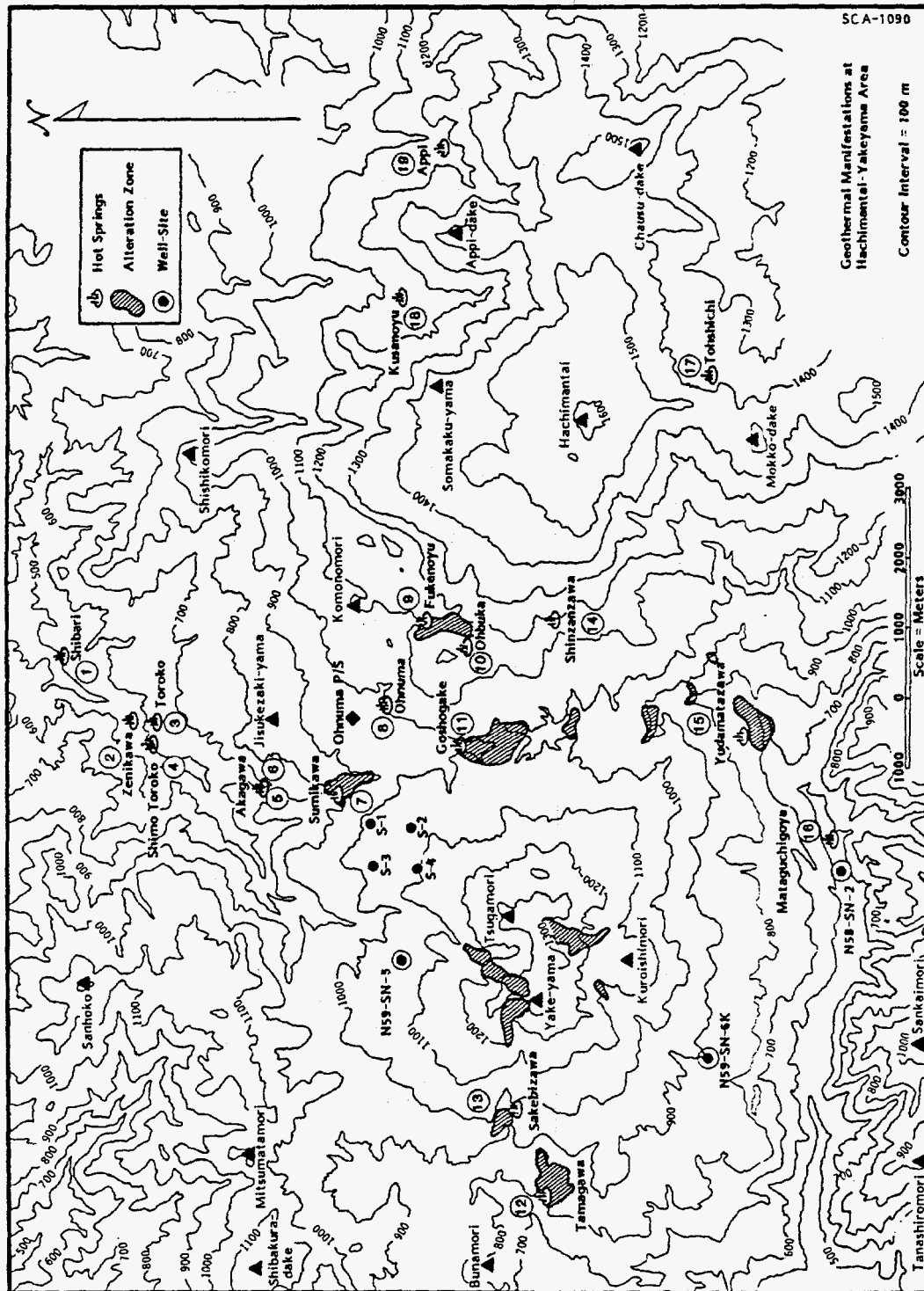


Figure 3.1. Locations of hot springs and older geothermal wells of the Sumikawa-Ohnuma area (from MMC).



Figure 3.2. Locations of geothermal wells and nearby hot springs of the Sumikawa-Ohnuma area. Wellhead locations shown by circles.

other substances from the rock. The chemistry of both acid-sulfate and steam-heated waters is dependent on the reaction of steam with rocks at shallow depth and has little relation to the chemistry of the deep water.

Unusual acid-chloride and acid-chloride-sulfate waters may result from the entry of volcanic gases containing HCl (and possibly SO₂) into a geothermal reservoir that has limited neutralizing capacity (Truesdell, *et al.*, 1989). Acid-sulfate-chloride water may also be produced when surface acid-sulfate waters percolate underground to mix with neutral chloride waters. These acid waters characteristically have much more sulfate than chloride.

At Sumikawa and Ohnuma the primary geothermal reservoir water is of the neutral, high-chloride type. This type of water was found in most wells. The deepened S-2 well at Sumikawa and wells 0-1R and 0-2R at Ohnuma produced acid-sulfate-chloride waters with pH < 3.

Hot springs around Sumikawa (Figure 3.1) are mostly acid-sulfate (Sumikawa, Goshogake, Akagawa and others) with some neutral chloride (Zenikawa, Toroko and Shimo Toroko), steam-heated bicarbonate (Ohnuma and the Akagawa well) and bicarbonate-sulfate waters (Shibari and Mataguchigoya) which are probably mixtures of neutral chloride and steam heated waters. The Tamagawa spring on the west slope of Mt. Yake produces mainly partially altered and diluted volcanic fluid.

3.3 Well Discharge Chemistry

From 1978 to 1989, Sumikawa wells have been discharged and sampled for periods ranging from a few days to six months. Table A.1 (in Ap-

pendix A) shows the period and type of sampling along with physical data for each sampled well. All water samples were collected after flashing to atmospheric pressure and analyses of steam collected at higher pressures were corrected by MMC to atmospheric pressure. During each test, the enthalpy and chemical composition of the discharge changed but showed a tendency to stabilize. Presumably, in each case the stabilized properties approximate those of longer term production.

Chemical analyses of separated water are presented in Table A.2, gas analyses of separated steam along with gas geothermometer temperatures, in Table A.3 and isotope analyses of separated steam and water, in Table A.4. Geothermometer temperatures calculated from the water analyses are given in Table A.5. All of these data (except the geothermometer temperatures) were provided by MMC (MMC, 1985, 1986, 1987, 1988, 1989) and form part of a continuing study by MMC.

All analyses are for (or have been calculated to) collection at atmospheric pressure. This has been assumed to be 0.9 kg/cm² absolute (0.88 bars) based on the elevation of the wells. Water and isotope analyses are presented as they were given by MMC; gas analyses have been recalculated to show percentages of gases on a dry gas basis rather than percent of CO₂, H₂S and residual gas along with residual gas composition. For calculation to aquifer or total discharge basis, discharge enthalpy values are necessary. In most cases these were taken from values provided with the chemical data; in some cases enthalpy was calculated from flows of steam and water at wellhead or atmospheric pressure given with the chemistry data and in a few cases discharge wellhead pressure-enthalpy relationships obtained from "characteristics tests" were used.

The chemical compositions of all Sumikawa well waters are shown as a Schoeller plot in Figure 3.3. In this type of plot, the logarithm of the concentration (in mg/kg) of constituents of an analysis are connected so that each analysis is represented by a line. Where data are missing, the line is broken. With this many data, only general patterns can be seen but the patterns for individual wells can be compared in separate Schoeller plots shown later. In comparing these figures, note that the effect of steam loss or dilution is to move the line up or down parallel to itself.

3.3.1 Well S-1

Well S-1, the shallowest well of the field, was drilled to 448 m in November 1981 (Table A.1). S-1 produced dry steam at 7.9 kg/cm² wellhead pressure and 2760 kJ/kg enthalpy when tested in November 1981 and April 1982. The condensed steam was low in solutes and in particular had low chloride (MMC, 1985) indicating that the reservoir liquid was probably not acid (Truesdell, *et al.*, 1989). The gas was high in CO₂ and H₂S (92 to 95 percent of total dry gas) and was low in N₂ suggesting that air contamination was minor (Table A.3). The reservoir temperature (calculated from downhole pressure) was 213°C. Gas geothermometers based on ratios of single gases to CO₂ indicated temperatures between 100° and 170°C (KRTA, 1985) but the D'Amore-Panichi (1980) geothermometer indicated 240-260°C (Table A.3).

Isotope compositions of steam from Well S-1 are near -72 and -10.2 permil in deuterium and oxygen-18 (Table A.4). The isotope samples were all collected within a day of April 27, 1982 and show no variation with time.

3.3.2 Well S-2

Well S-2 was drilled to 905 m (with open hole below 703 m) and tested in July 1982. This well produced fluids with average enthalpy values near 2260 kJ/kg (11 percent steam by mass in the reservoir fluid) and liquid enthalpy (calculated from geothermometer temperatures) of 1080 kJ/kg from TQA and 995 kJ/kg from T13 (Figure 3.4 and Table A.5). Liquid enthalpy values are used so that they may be compared directly with measured total fluid enthalpy values. Aquifer chloride concentrations calculated assuming these reservoir temperatures increased from less than 250 mg/kg to 540 and 585 mg/kg (Figure 3.5). Aquifer chloride is calculated assuming that all cooling between the aquifer and the surface is by steam loss.

In October 1982 the well was deepened to 1065 m (still with open hole below 703 m). Downhole temperatures measured in the deepened well exceeded 230°C at 700 m and 240°C at 900 m. In November 1982 and May 1983 the well was re-tested. Relative to the July 1982 tests, the enthalpy had decreased to about 1045-1130 kJ/kg and calculated reservoir temperatures increased slightly to 230-260°C. During the tests temperatures seemed to stabilize at 245°C (equivalent to liquid at 1060 kJ/kg enthalpy) in agreement with measured enthalpy values and downhole temperatures. The well was now withdrawing only liquid (no steam) from the reservoir. Aquifer chloride increased through the second and third tests from about 200 mg/kg to about 550-600 mg/kg, nearly the same as during the July 1982 test of the original (shallow) hole. The water feeding the well after deepening was similar to the earlier water in chloride concentration and slightly hotter but with no reservoir steam inflow. Gas temperatures after deepening were very high possibly indicating lack of equilibrium (Table A.3).

Continued on page 3-8

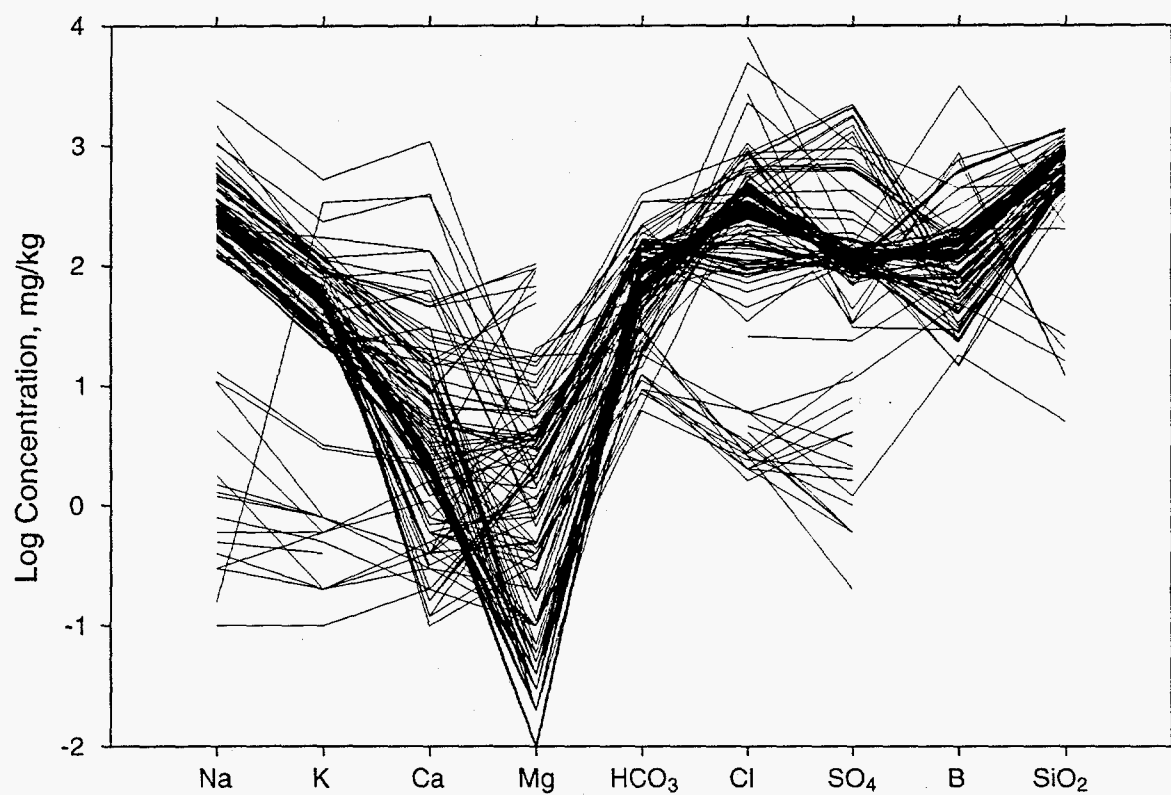


Figure 3.3. Schoeller diameter of all analyses of Sumikawa well waters. See text for explanation.

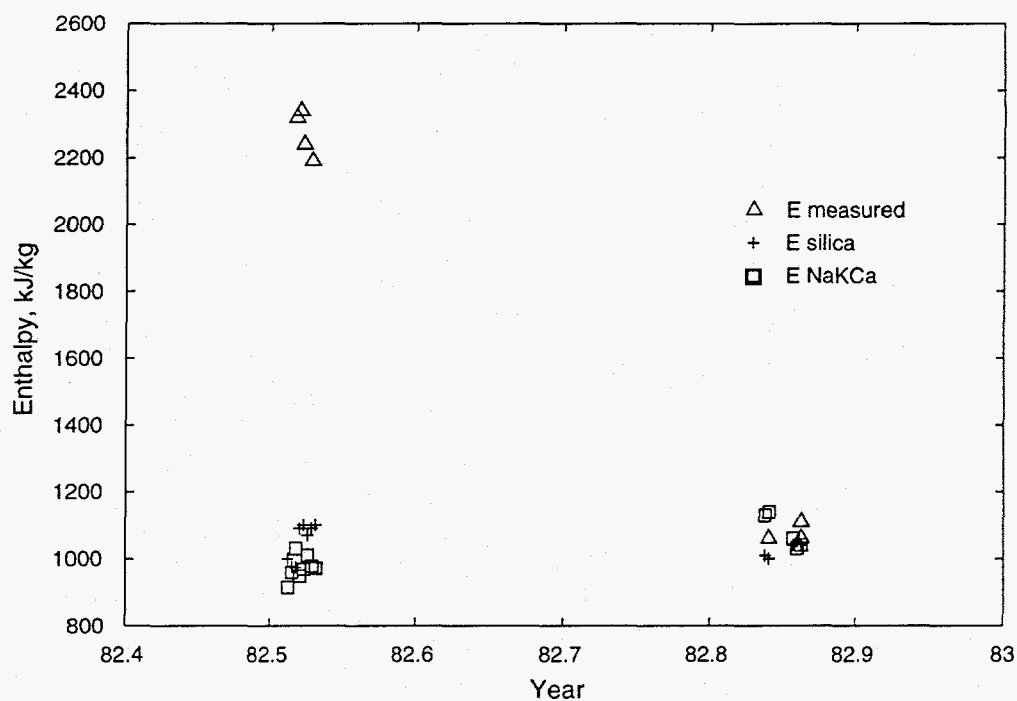


Figure 3.4. Enthalpy of total discharge fluid and aquifer water of Sumikawa well S-2.

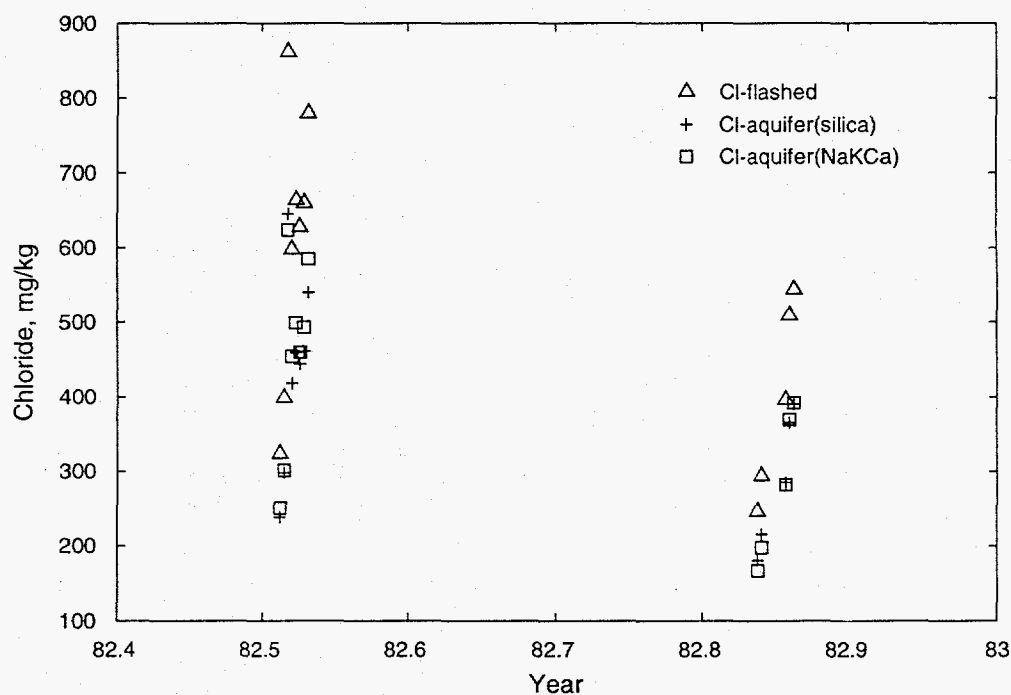


Figure 3.5. Chloride concentrations of flashed and (analyzed) water and aquifer liquid calculated from geothermometer temperatures TQA and T13 for Sumikawa well S-2.

Unfortunately, the deepened well produced acid-sulfate-chloride water (pH 2.6–2.8) whereas the original well had produced neutral water. It seems probable that with continued testing the original well would also have evolved to acid production, because during the first test pH values dropped from 7.2–7.9 to 5.5–5.9 and SO_4 concentrations increased from 655 to 760 mg/kg. The acid waters contained more Mg and Fe, and lower B and (in the last test) Ca. The Fe may have come from corrosion of the casing or possibly from solution of iron-magnesium minerals. Possibly anhydrite and boric acid were precipitated or the newly tapped deeper (?) water contained less B and Ca and more Mg. After deepening, the pH was near 2.6 and the sulfate was about 2000 mg/kg. The chemistry tended to stabilize with time in both cases (before and after deepening), although Cl was probably still increasing during the last test (Figure 3.4). The general trend of increases in solute concentrations with little or no corresponding increases in geothermometer temperatures may have resulted from replacement of shallow neutral water (some possibly from drilling) with deeper acid water while temperatures were controlled by equilibration with rock.

Isotope analyses of steam are limited (Table A.4) but isotope compositions of separated water collected before and after deepening do not vary with time. The total discharge compositions (calculated by MMC) are -73 and -11 permil for δD and $\delta^{18}\text{O}$ before deepening and -69 and -10.9 after deepening.

The chemical pattern of well S-2 waters shown in a Schoeller diagram (Figure 3.6) is quite different from other waters, having higher Mg, Ca and SO_4 and lower B. The change to acid water after deepening accentuated these differences (except in Ca).

3.3.3 Well S-3

Well S-3 was drilled to 805 m between July 1982 and June 1983. The well was cased to 603 m with open hole below. The maximum measured downhole temperature was near 236°C at about 620 m. During the first flow test (July and August 1983) a casing break was discovered and a 3-inch pipe was set near bottomhole. This apparently did not affect fluid compositions. The well was tested again from October 1983 to January 1984.

Chemical analyses of S-3 discharge waters exhibited the effects of flushing of shallow (drilling?) fluids, as was the case with well S-2 (Table A.2). Calculated aquifer chloride increased in the first test from 35 to 110 mg/kg and in the second test from 25 to 140 mg/kg (Figure 3.7). Chloride concentrations did not appear to have stabilized during either test. In contrast, temperatures indicated by geothermometers were apparently stabilized by heat exchange with rock as discussed earlier. Stabilized silica temperatures were similar (225°C) for both tests with 10°C higher temperatures indicated for the last few samples (Figure 3.8). Na-K-Ca temperatures were similar to silica temperatures except for the three last samples which were 20° to 30°C higher. Changes in Na-K-Ca temperatures resulted from a change in reported Ca concentrations from 1–5 mg/kg to 0.4 mg/kg. This could be an analytical or reporting problem and not represent a change in fluid temperature.

The low chloride concentrations were interpreted by KRTA (1985) as resulting from the short time interval between the end of drilling and the start of discharge tests, with large quantities of drilling water remaining in the reservoir near the well. This is possible for the first test starting a month after completion but is less likely for the second test in which initial fluid was even more dilute af-

Continued on page 3-11

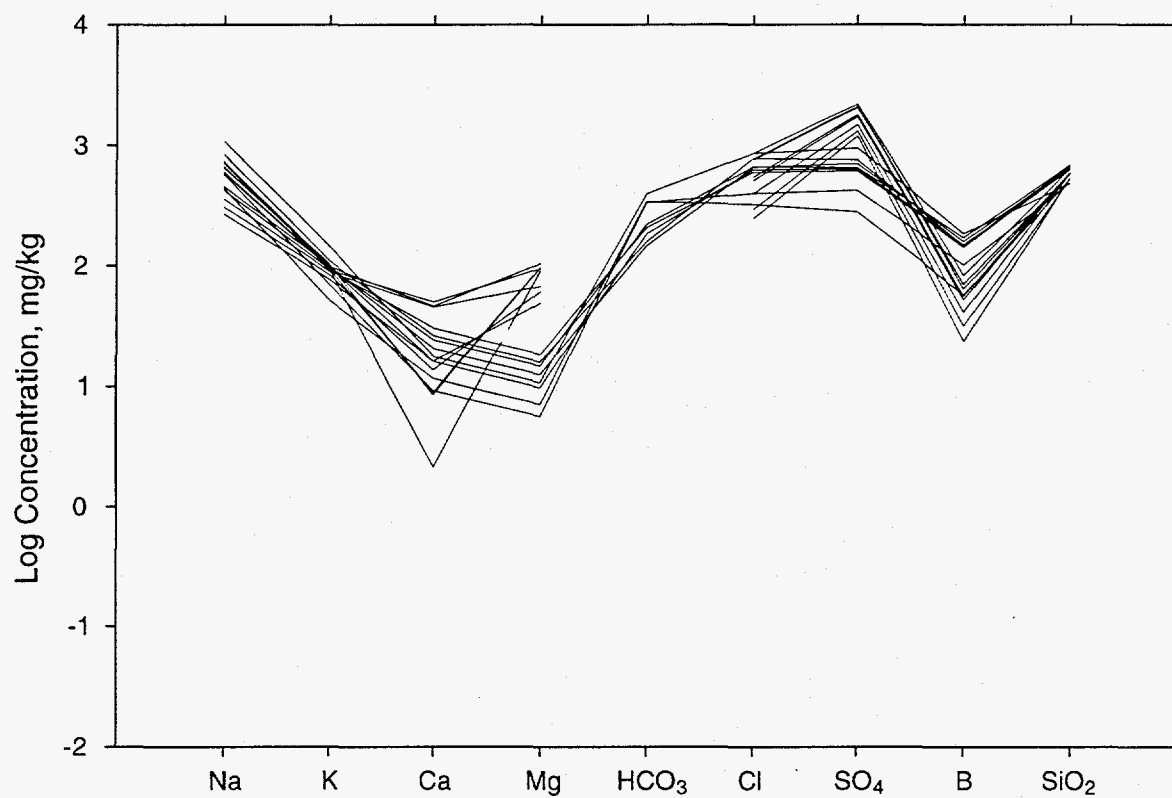


Figure 3.6. Schoeller diagram of well S-2 water analyses. Acid waters from the deepened well lack HCO₃ and are distinctly higher in Mg and SO₄ and lower in B.

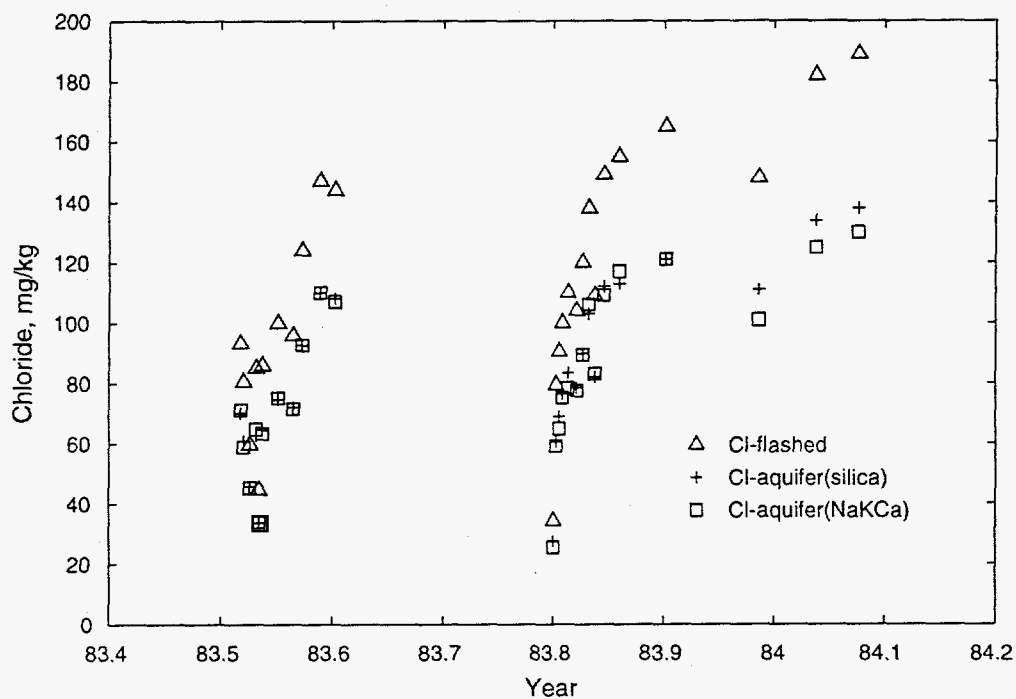


Figure 3.7. Chloride concentrations for flashed and aquifer waters of Sumikawa well S-3.

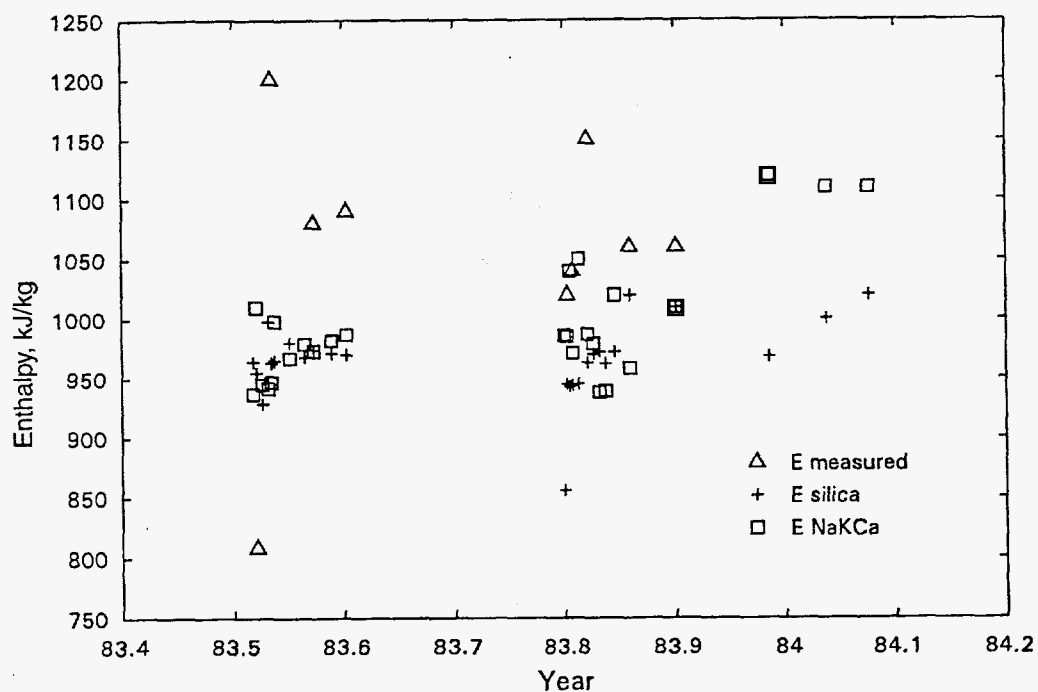


Figure 3.8. Enthalpy of total discharge fluid and aquifer water of Sumikawa well S-3.

ter a two month rest. KRTA (1985) modeled the change in chloride and concluded that the stabilized aquifer concentration was near 150 mg/kg. This is much lower than that found in well S-2. The initial dilute waters in S-3 tests may come from a shallow steam-heated aquifer that has restricted production and is overwhelmed by deeper production as the test continues. This water was replenished during shut in periods.

The total discharge isotope compositions of S-3 fluids vary with time showing initial effects of the near surface fluid. The last analyses are $\delta D = -71.7$ and $\delta^{18}O = -10.1$, nearly identical to the composition of S-1 steam (Table A.4).

Well S-3 water (Figure 3.9) is chemically similar to S-2 water with relatively high Mg and low B even though it is neutral. This water has lower salinity than most others and relatively high HCO_3 and SO_4 compared to Cl. These characteristics suggest that S-2 and S-3 waters contain a component low in B and high in Ca, Mg, SO_4 and, in S-3, HCO_3 . The main difference between S-3 water and neutral S-2 water is that S-3 water is about one-third as concentrated.

3.3.4 Well S-4

Well S-4 was completed in November 1983 to a total depth of 1552 m with open hole below 1071 m. The maximum measured downhole temperature was 300°C near the bottom. The main feed point is also near bottomhole. Prior to 1988, the well was tested three times: in July-November 1984, August-November 1985, and July-November 1986 (Table A.1).

The chemical results from each of these tests were similar in pattern (Figures 3.10 and 3.11). The

enthalpy and geothermometer temperatures were high initially but then rapidly decreased, seeming to stabilize by the latter third of the test. The measured total enthalpy values (reduced by 250 kJ/kg to correct for the difference between 1984–1986 enthalpy values obtained from two-phase flow data and direct measurements made in 1988) are higher than liquid enthalpy values calculated from geothermometer temperatures, indicating that the well is being fed by both steam and water. During each year's test, the decrease in geothermometer temperatures and enthalpies show an apparent rapid transition from a higher-temperature to a lower-temperature fluid supply with time. Chloride concentrations also declined during each test, from high levels (near 300 mg/kg in 1984 and 280 mg/kg in 1985 and 1986) to apparent stabilization at 180–190 mg/kg in 1984 and 1985 and at 170–185 mg/kg in 1986. Oscillatory behavior occurred, particularly in 1984 with 2½ oscillations before the last test (Figure 3.11). The cause of this is not understood but might be due to "geysering" that changed the proportion of the two fluids feeding the well.

In 1988, the same general decrease in chloride occurred with maximum and minimum values lower than in previous years. The behavior of total and liquid enthalpy (Figure 3.10) was different with initially no excess enthalpy (total and liquid enthalpy values nearly the same). In later tests liquid enthalpy values dropped but total enthalpy was nearly constant. The division into high and low enthalpy fluid was less distinct and the average enthalpy was similar to that of the earlier low enthalpy fluid. Although the average was similar, the minimum dropped to unrealistically low values.

These temperature and chloride trends are the opposite of those observed in the S-2 and S-3 tests,

Continued on page 3-14

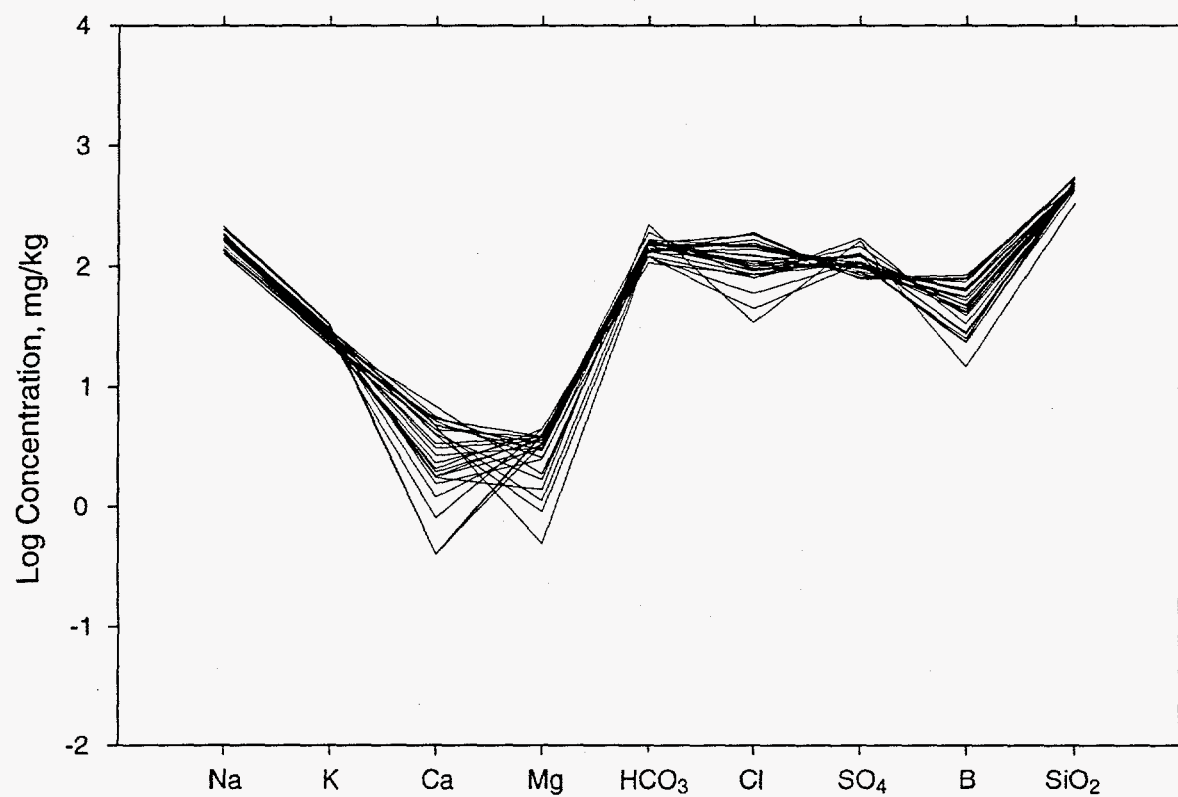


Figure 3.9. Schoeller diagram analyses of waters from well S-3.

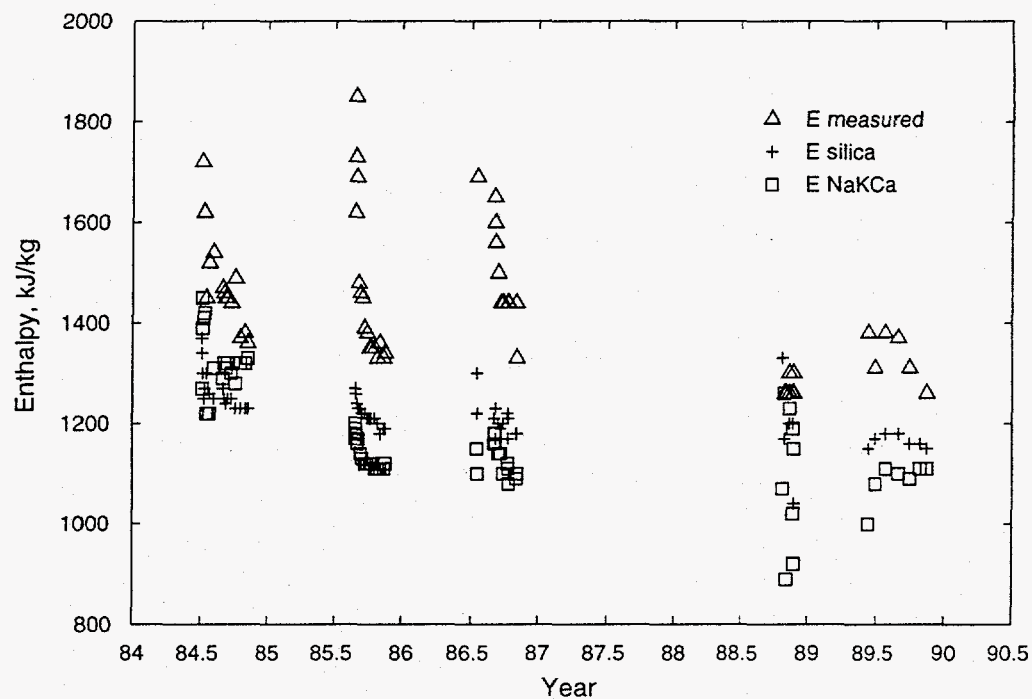


Figure 3.10. Enthalpy of total discharge fluid and aquifer water of Sumikawa well S-4.

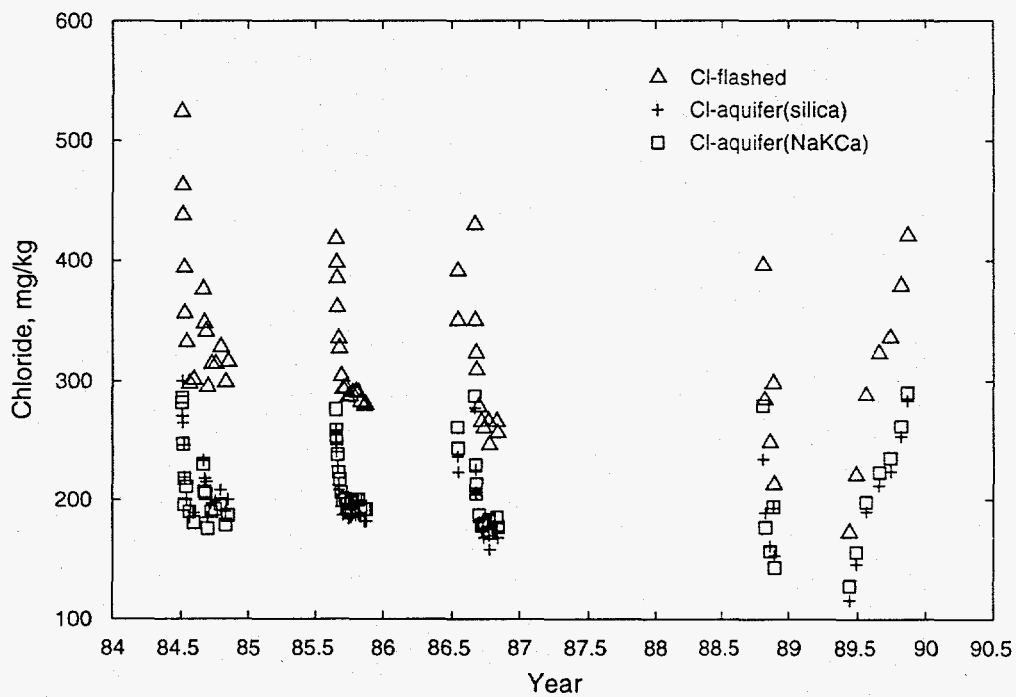


Figure 3.11. Chloride concentrations of flashed and aquifer waters of Sumikawa well S-4.

in which drilling water in the formation made early samples more dilute (and sometimes cooler) than later samples (Figures 3.5 and 3.8). The behavior of S-4 suggests that two zones feed the well: a higher temperature, higher chloride, steam-rich zone and a liquid zone at slightly lower temperature and with much lower chloride. The relative contribution of the high-temperature zone decreases with time during each test and the latter part of each test is dominated by the cooler, more dilute zone. Although the temperature decrease is real it is not large (about 25°C) whereas the change in chloride is much larger—about 100 mg/kg or one third of the total. KRTA (1985) suggested that unloading of drilling mud delayed production from the lower temperature zone. This is not tenable in light of the nearly identical behavior of the 1984, 1985 and 1986 tests.

Isotope compositions of high and low enthalpy fluids were distinct in 1984 and less so in other years (Table A.4). The initial discharge was near $\delta D = -72$, $\delta^{18}O = -9.8$ in 1984, 1985 and 1988, but lower in 1986. The final discharge was much lighter isotopically in 1984 than in other years.

Compositions of S-4 waters (Figure 3.12) vary markedly in Ca and Mg but less so in other constituents. Samples high in Mg tend to be low in Ca and vice versa (also true for some S-3 waters). High Mg, low Ca analyses occur mainly in 1984 with later samples low in Mg and higher in Ca. This may reflect a change in analytical methods. The high-enthalpy, high-Cl water produced at the start of testing in 1984-1986 was relatively low in HCO_3 and SO_4 and high in B suggesting a deeper origin than the cooler, low-Cl water that dominated at the end of each test. This low-Cl water is similar in concentration and constituent pattern

to most waters produced from SA-1, SB-1 and SD-1 and some from SC-1.

3.3.5 Well SA-1

Well SA-1 was directionally drilled in 1987 from near well S-4 to a total depth of 2002 m. The well was tested and sampled in October and November 1988 and from June to November 1989 (1989 tests are described separately). This well discharges almost entirely steam (2090 kJ/kg total enthalpy) with a few water analyses giving scattered indications of liquid enthalpy ranging from 1005 to 1505 kJ/kg with a cluster of values near 1215–1255 kJ/kg (Figure 3.13). Reservoir chloride concentrations are also scattered initially, but stabilized at 500–600 mg/kg (Figure 3.14). MMC has calculated a total discharge isotope composition of $\delta D = -76.8$ and $\delta^{18}O = -9.6$ (Table A.4).

Chemical analyses of waters from SA-1 are few but show a consistent pattern (Figure 3.15) similar to (but more concentrated than) low-Cl S-4 water. The lower Cl analyses in Figure 3.15 are steam condensate or condensate mixed with separated water.

3.3.6 Well SA-2

Well SA-2 was directionally drilled in November 1986 to a total vertical depth (TVD) of 1943 m. In 1987 a temperature of 317°C was measured near the hole bottom. The well apparently was not sampled before the April–May 1989 injection of nearly 30 thousand tons of cold water (Table A.6). Despite the cold water injection 1989 production was almost entirely steam along with

Continued on page 3-18

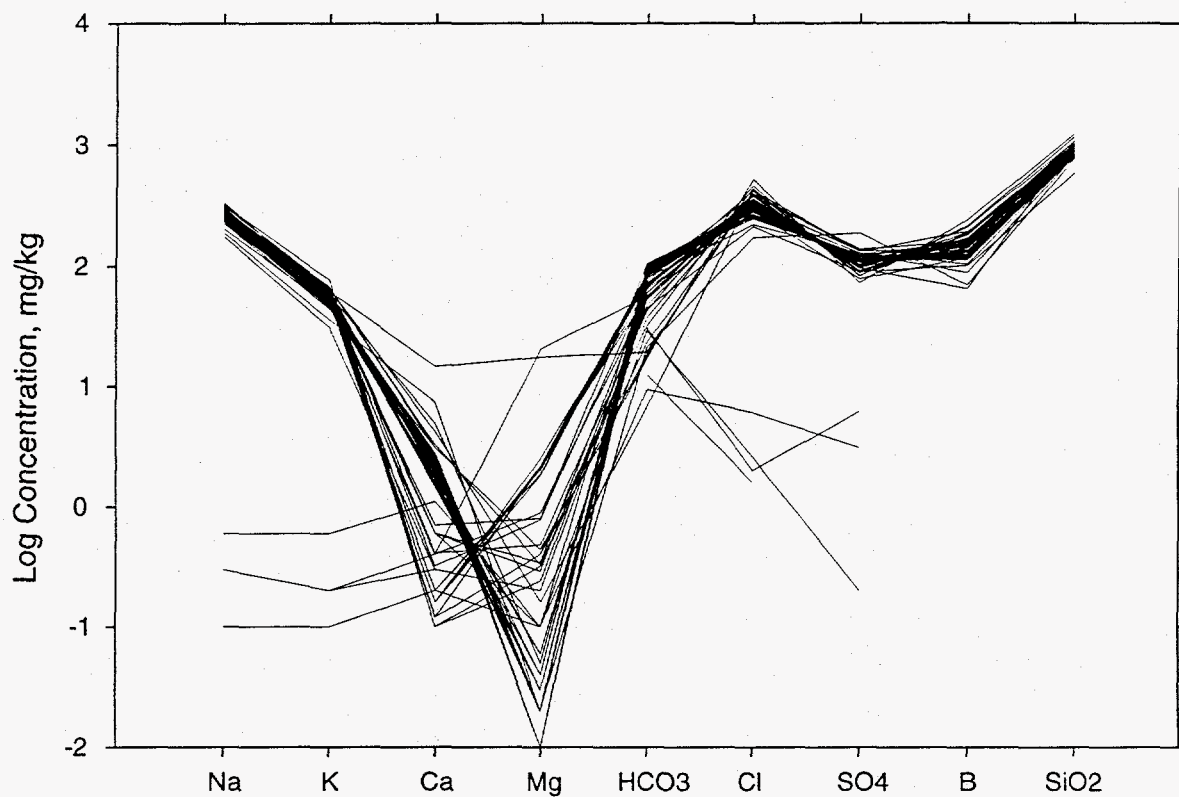


Figure 3.12. Schoeller diagram of well S-4 water analyses. The few very dilute waters in this and following diagrams are steam condensates.

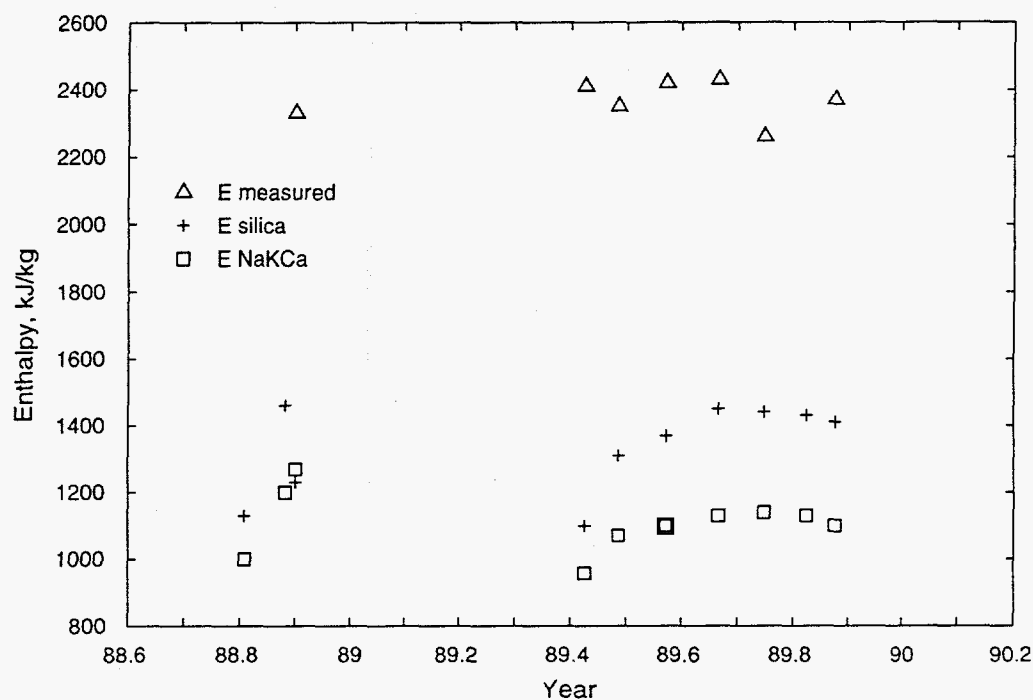


Figure 3.13. Enthalpy of total discharge fluid and aquifer water of Sumikawa well SA-1.

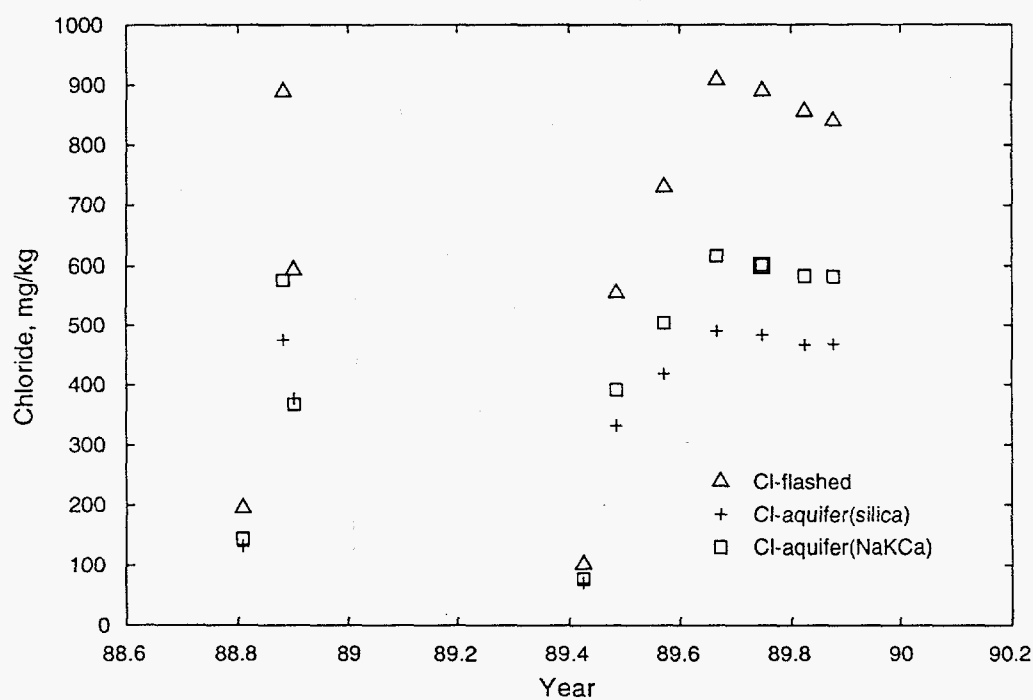


Figure 3.14. Chloride concentrations of flashed and aquifer waters of Sumikawa well SA-1.

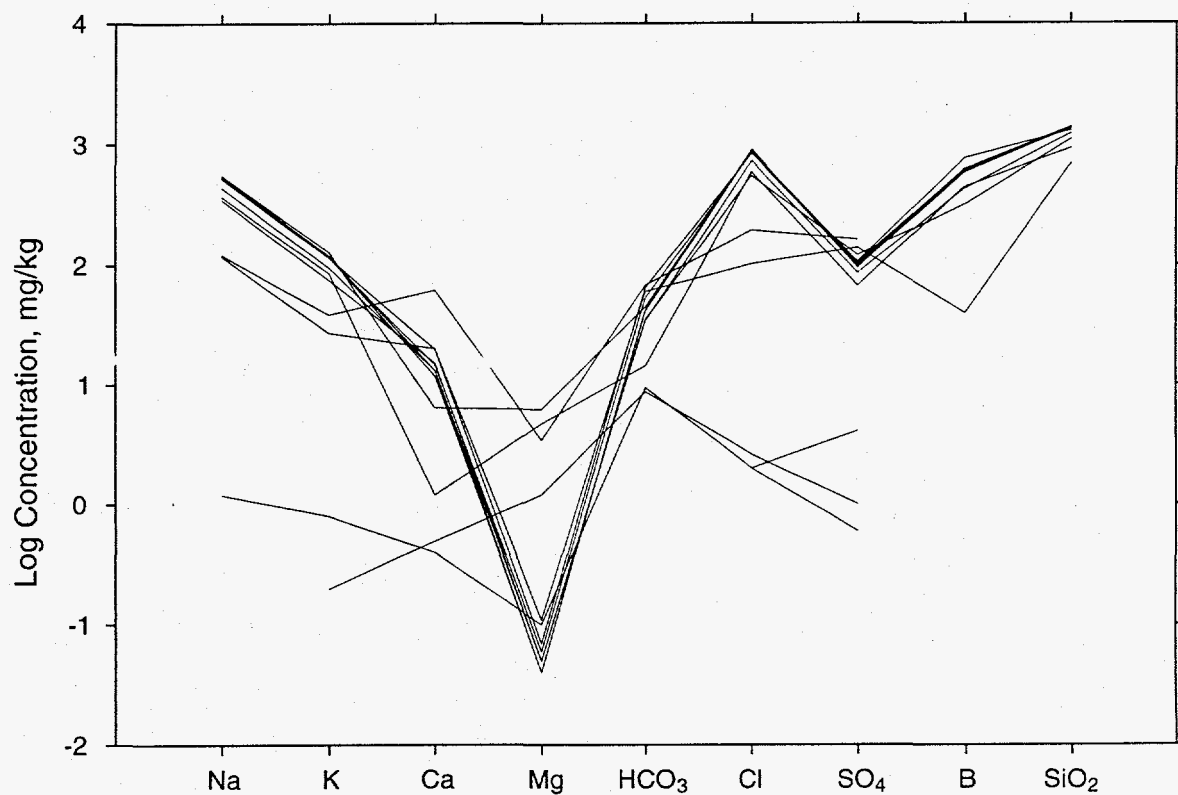


Figure 3.15. Schoeller diagram of analyses of waters from well SA-1.

highly variable, partially evaporated mixtures of condensate and water (Table A.2 and Figure 3.16).

3.3.7 Well SA-4

Well SA-4 produces nearly pure steam. This well was also directionally drilled from a location near well S-4 to a total vertical depth of 1739 m. Tests in 1988 produced only traces of liquid, mainly condensate, from which reservoir liquid enthalpy and chloride could not be reliably calculated (Table A.2). Isotope compositions of steam probably reflect a reservoir liquid with $\delta D = -72.8$ and $\delta^{18}O = -10.4$ in 1988 (Table A.4).

Water analyses from high-enthalpy wells SA-2 and SA-4 show little pattern and extremely varied concentrations (Figures 3.16 and 3.17). These compositions probably are mixtures of steam condensate and some reservoir water that have been affected by evaporation, oxidation and other reactions occurring during production and are not representative of reservoir fluid.

3.3.8 Well SB-1

Well SB-1 was drilled to a total vertical depth of 2006 m in late 1987. The well was tested from June to November 1989 after about 16 thousand tons of cold water were injected in April and May. The fluids produced showed strong effects of the cold water. During the 5 months of the test concentrations of chloride and other solutes increased by a factor of four without leveling out (Figure 3.18). However, total fluid $\delta^{18}O$, geothermometer temperatures and measured enthalpy increased rapidly and became constant after about a month (Figures 3.19 and 3.20).

The Schoeller diagram of SB-1 waters (Figure 3.21) shows changes from a mixed Ca, HCO_3 , SO_4 water, relatively low in Na, K, Cl and B, to a more typical geothermal water high in Na, K, Cl, and B, and low in Ca. Silica, HCO_3 and SO_4 show less change than other components because they are controlled by rock minerals (quartz, calcite and anhydrite) and gases (CO_2 , H_2S).

3.3.9 Well SC-1

Well SC-1 was drilled in 1987 to a total depth of 2486 m. The well was tested in August, October and November 1988 and in 1989. This well produced a mixture of steam and water with total enthalpy similar to the liquid enthalpy computed from geothermometers (Figure 3.22). There is some scatter in enthalpy calculated from the Na-K-Ca geothermometer, but most values of temperature calculated from total enthalpy and from silica concentrations are close to $280^\circ C$ with Na-K-Ca temperatures about $20^\circ C$ lower. During the 1988 test there is no indication of change of total or liquid enthalpy either from flushing of drilling water or multiple feed zones. The aquifer chloride concentration was 300 ± 10 mg/kg (Figure 3.23, Table A.5). During the 1988 tests the total discharge isotope composition showed decreases of 10 permil and 0.5 permil in δD and $\delta^{18}O$ with final values of $\delta D = -74.4$ and $\delta^{18}O = -9.1$ (Table A.4).

Well SC-1 was not subjected to cold water injection in 1989 and chemical and isotopic data from 1989 are similar to those from 1988. Liquid enthalpy values calculated from silica remained unchanged at 1170 kJ/kg and liquid enthalpy from Na-K-Ca showed less scatter than in 1988 and a similar average of 1045 kJ/kg (Figure 3.22). The measured total enthalpy increased to 1260 kJ/kg

Continued on page 3-25

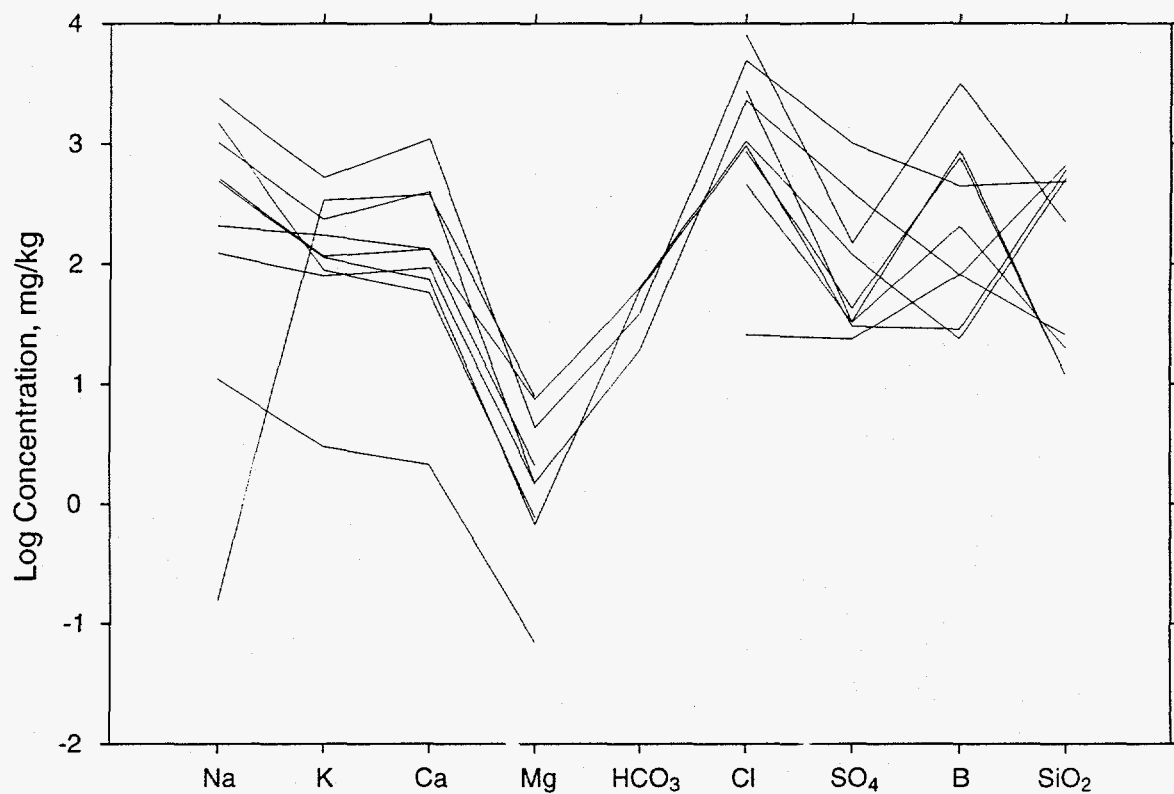


Figure 3.16. Schoeller diagram of water compositions from well SA-2 discharge. The wellhead fluid was almost entirely steam, and liquid water compositions vary widely.

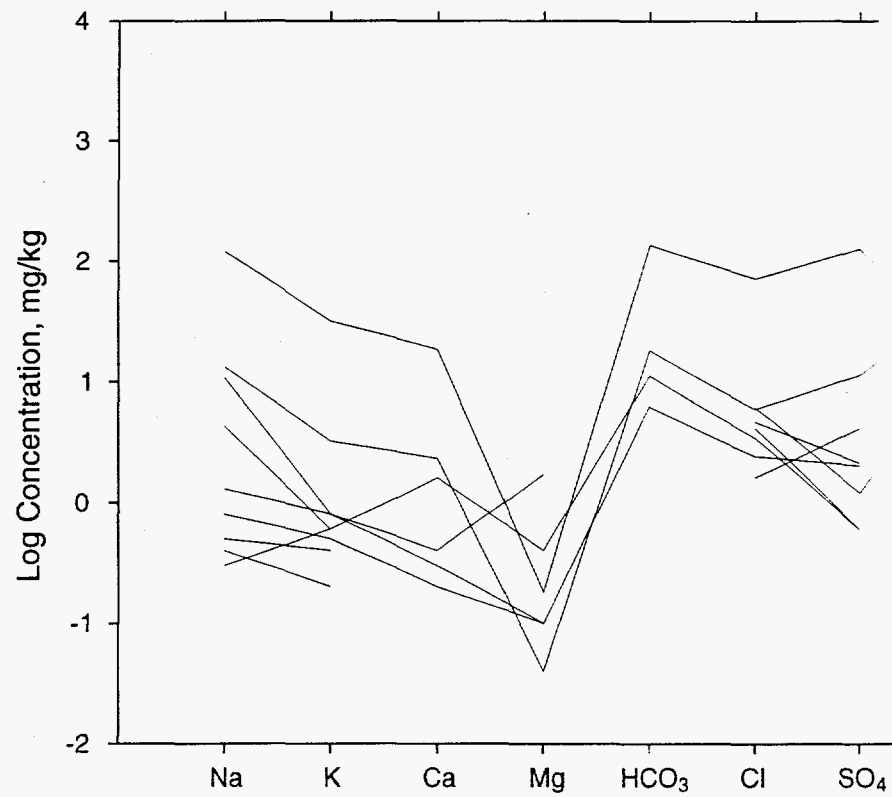


Figure 3.17. Schoeller diagram of water compositions from well SA-4 d. the discharge was almost entirely steam.

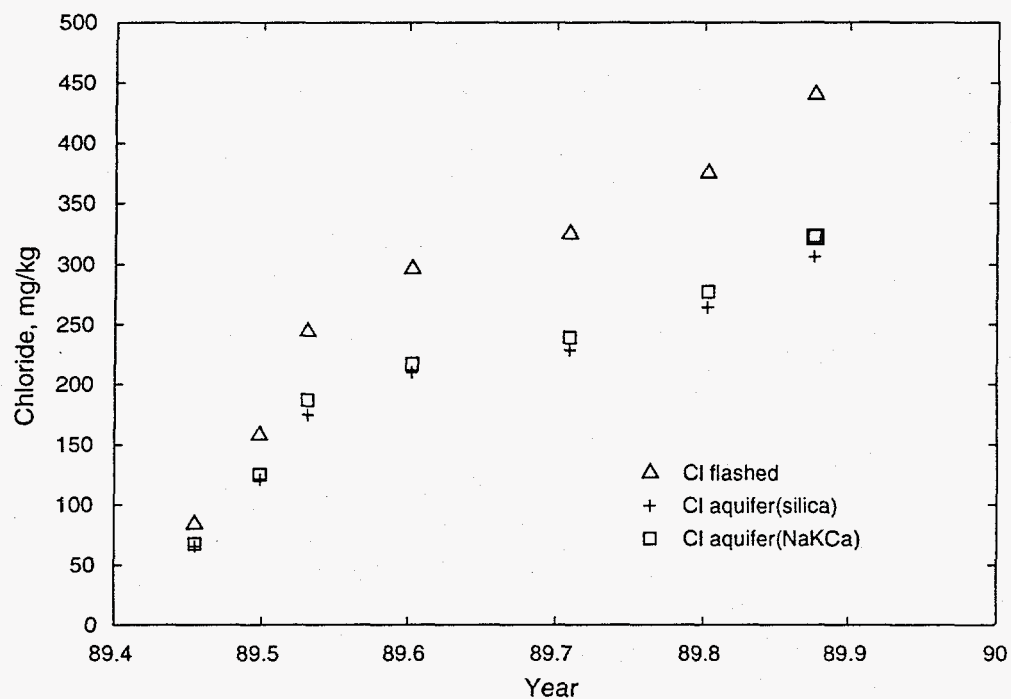


Figure 3.18. Changes in analyzed chloride in separated water from well SB-1 in 1989.

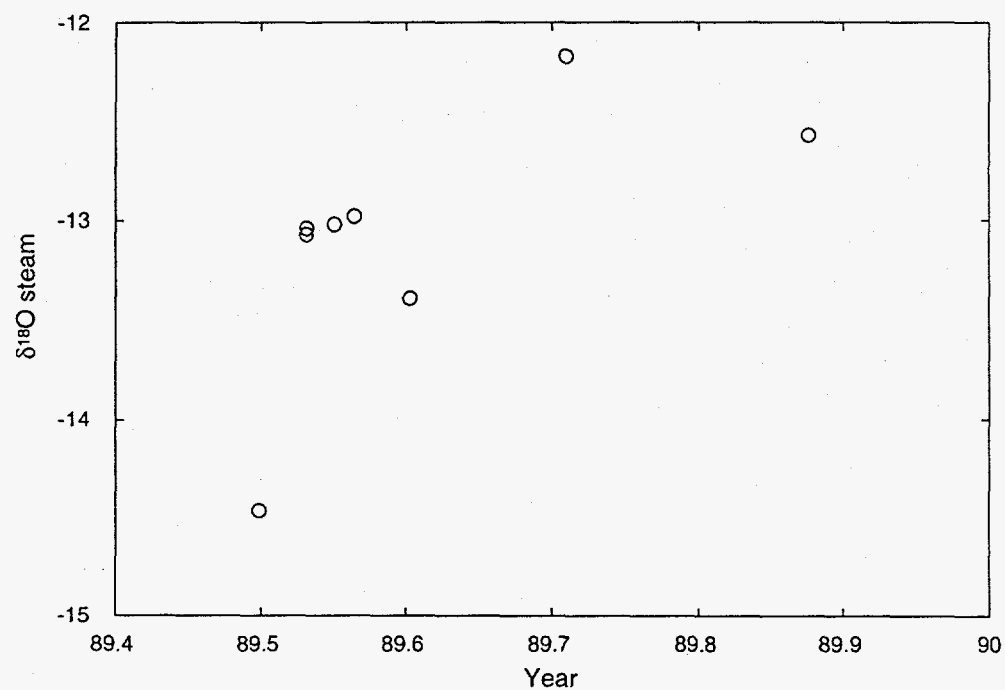


Figure 3.19. Changes in oxygen isotope composition of steam from well SB-1 in 1989. Steam $\delta^{18}\text{O}$ is plotted because other isotopic data are less complete.

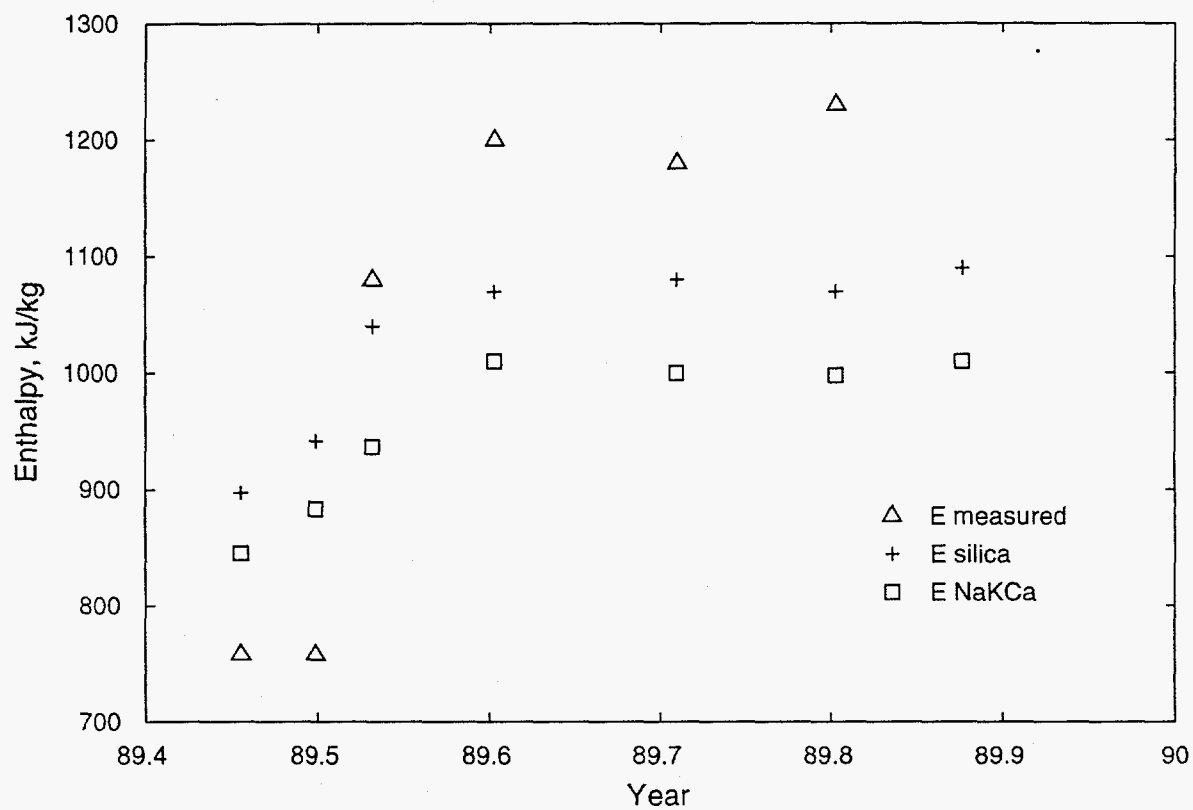


Figure 3.20. Enthalpy of total discharge fluid and aquifer water of Sumikawa well SB-1.

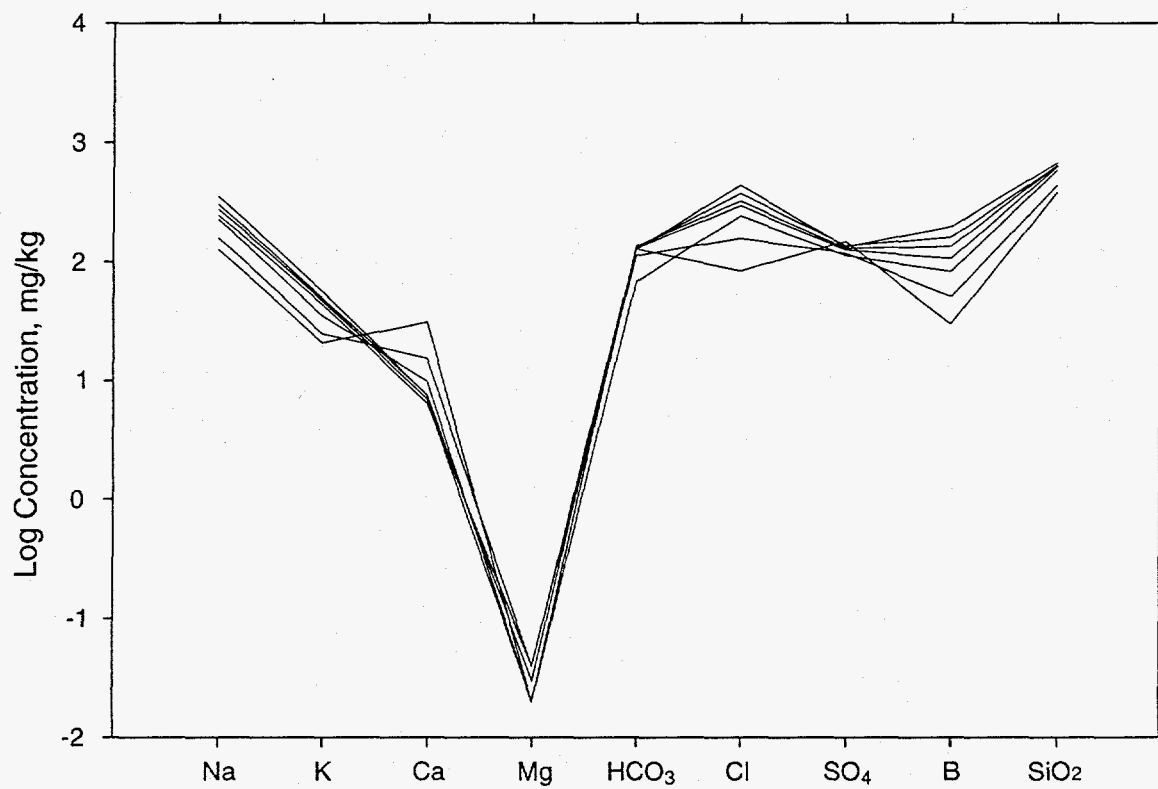


Figure 3.21. Schoeller diagram of well SB-1 water analyses.

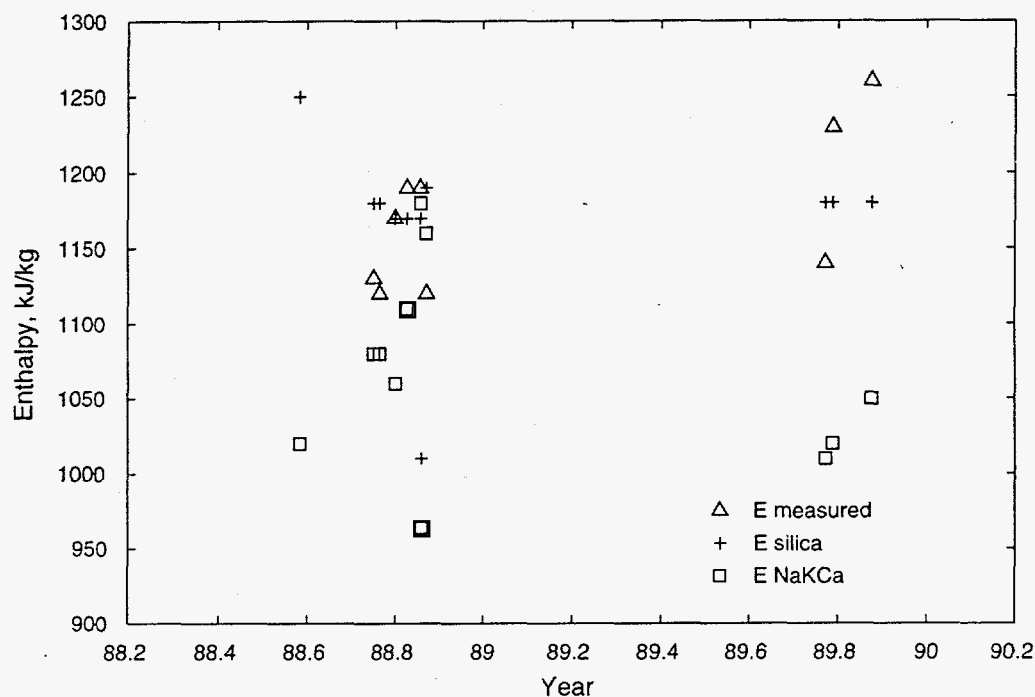


Figure 3.22. Enthalpy of total discharge fluid and aquifer water of Sumikawa well SC-1.

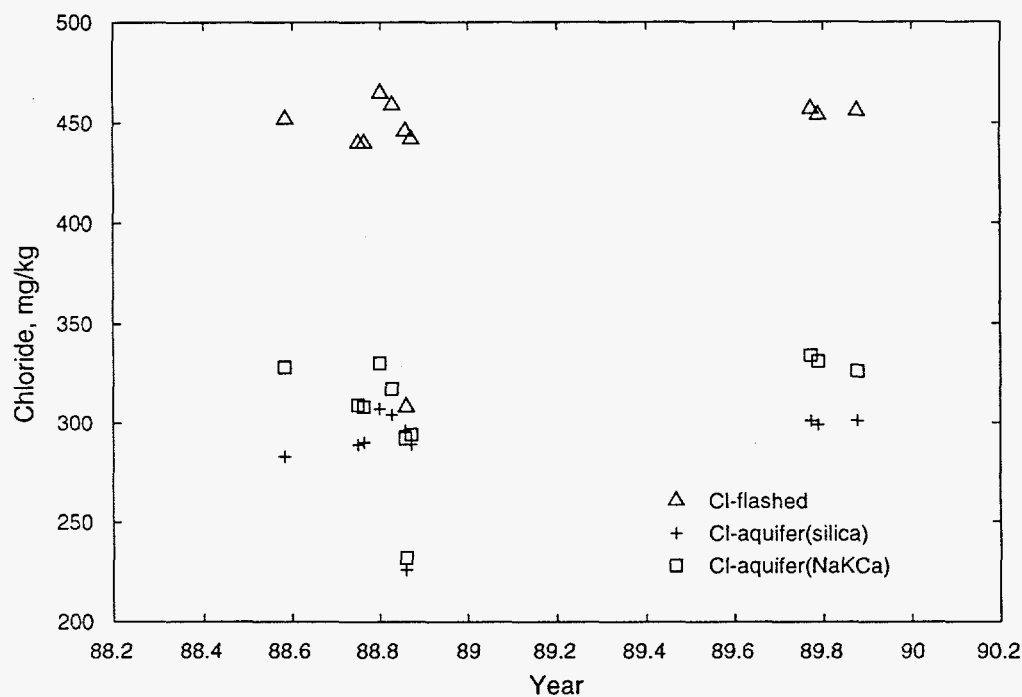


Figure 3.23. Chloride concentrations for flashed and aquifer waters of Sumikawa well SC-1.

(from 1170 kJ/kg) indicating that boiling and excess steam production occurred in the reservoir. Reservoir chloride concentrations remained unchanged at 300 mg/kg (Table A.5). The single 1989 total discharge isotope analysis of $\delta D = -65.8$ and $\delta^{18}O = -8.7$ is significantly heavier than the final 1988 analyses and resembles early 1988 analyses (Table A.4). The reason for this change is not understood. Except for the coincidence of early 1988 and 1989 compositions it might be inferred from the isotope data that cold water injected into other wells in 1989 affected the isotope composition of SC-1 fluid.

The Mg and Ca concentrations of SC-1 waters are quite variable (Figure 3.24 and Table A.2); 1988 analyses are high in Mg and low in Ca relative to 1989 samples. This is probably not due to cold water because Na, K and B do not change significantly between years.

3.3.10 Well SD-1

Well SD-1 was drilled in late 1986 to a depth of 1691 meters. Well SD-1 fluids were first sampled from August to December 1989. Although during 1989 cold surface water was not injected into well SD-1, cold water from a one-month discharge test of well SC-1 was injected into well SD-1 in late 1988. The injection from October to November 1988 involved approximately 150,000 tons of separated water. It is noteworthy that the quantity of water injected into well SD-1 in 1988 is five times greater than that injected into any well in April and May 1989, and is over 60 percent of the total quantity of fluid subsequently discharged from well SD-1 in 1989.

It is therefore not surprising that, unlike other wells, the fluids discharged from well SD-1 did

not attain constant measured enthalpy during the 1989 discharge test (Figure 3.25). At early times, the measured wellhead enthalpy is similar to values computed from silica concentrations suggesting production from an all-liquid reservoir zone. In the later samples, the measured wellhead enthalpies are much higher but the computed liquid enthalpies increase only moderately; this suggests boiling in the formation. Aquifer chloride concentrations increase throughout the test with no stable maximum indicated (Figure 3.26). Since the chloride content of the fluid samples obtained from well SC-1 is significantly greater than the maximum aquifer chloride concentrations indicated by SD-1 discharge, it would appear that the proportion of the previously injected water recovered during the 1989 discharge test of well SD-1 increased with time.

Well SD-1 has several fluid entries in the interval between 800 meters to 1570 meters vertical depth. In geothermal wells with multiple feedzones, the proportion of fluid entering a particular feedzone during injection is often quite different from that produced in a discharge test. Available spinner records for well SD-1 (see Section 4.15) indicate that most (~ 80 percent) of the injected fluid enters feedzones located at or below ~ 1500 meters; these feedzones, however, supply a rather small fraction (~ 20 percent) of the fluid discharged from well SD-1 in 1989. Because of boiling-induced throttling of shallow feedzones, it is likely that the proportion of the fluid contributed by the deeper feedzones increased somewhat with time. It is therefore possible that the fraction of previously injected fluids in the discharge of well SD-1 increased slightly during the 1989 test. Thus the observed geothermometer temperatures and chloride contents are consistent with the production of some previously-injected waters mixed with native reservoir fluids

Continued on page 3-28

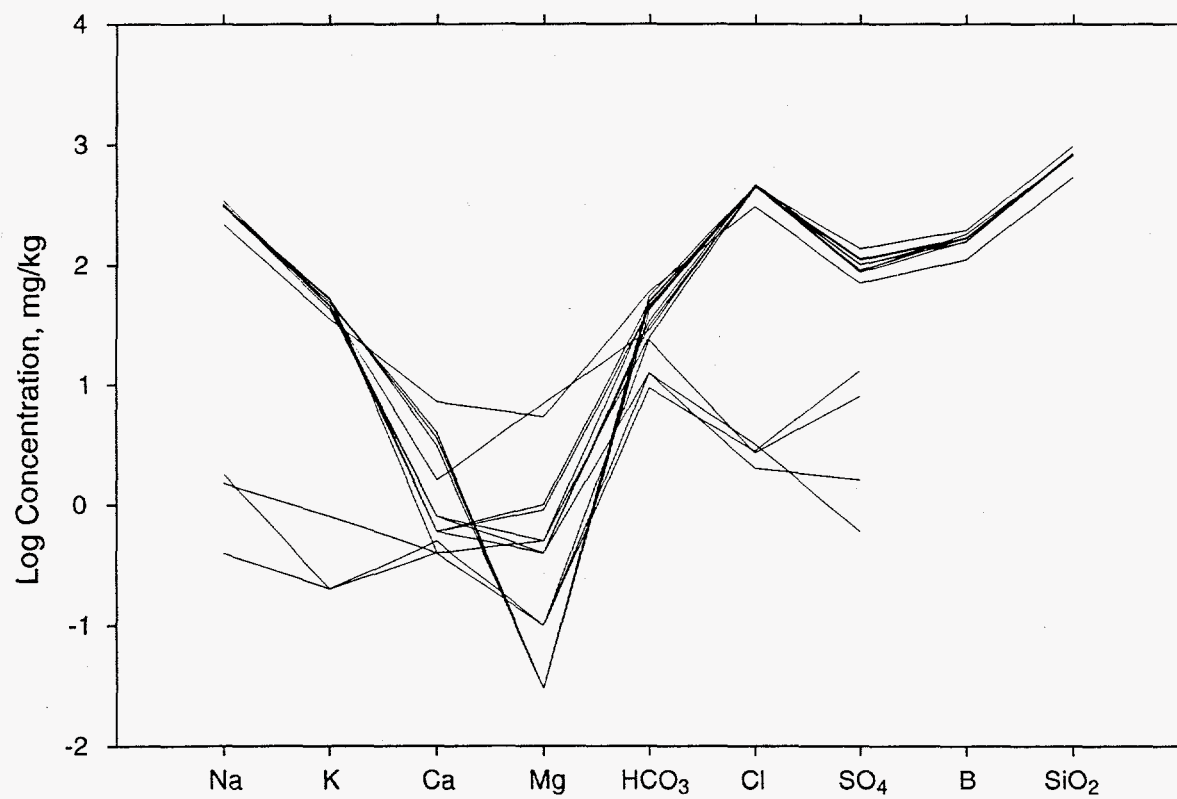


Figure 3.24. Schoeller diagram of water compositions of well SC-1 discharges. Very dilute waters are steam condensates.

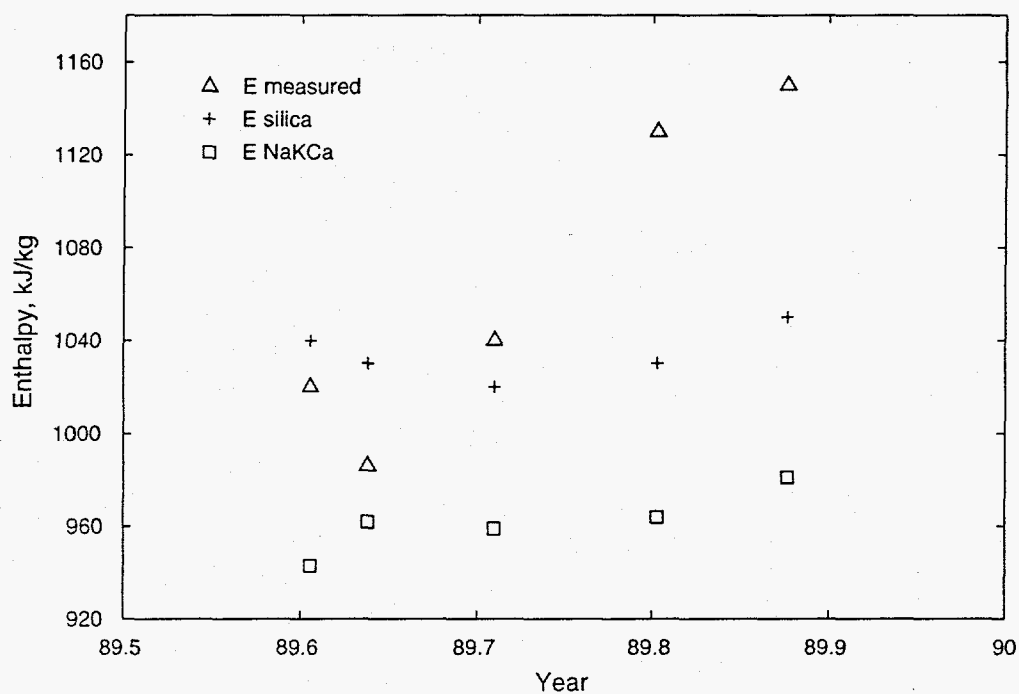


Figure 3.25. Enthalpy of total discharge fluid and aquifer water of Sumikawa well SD-1.

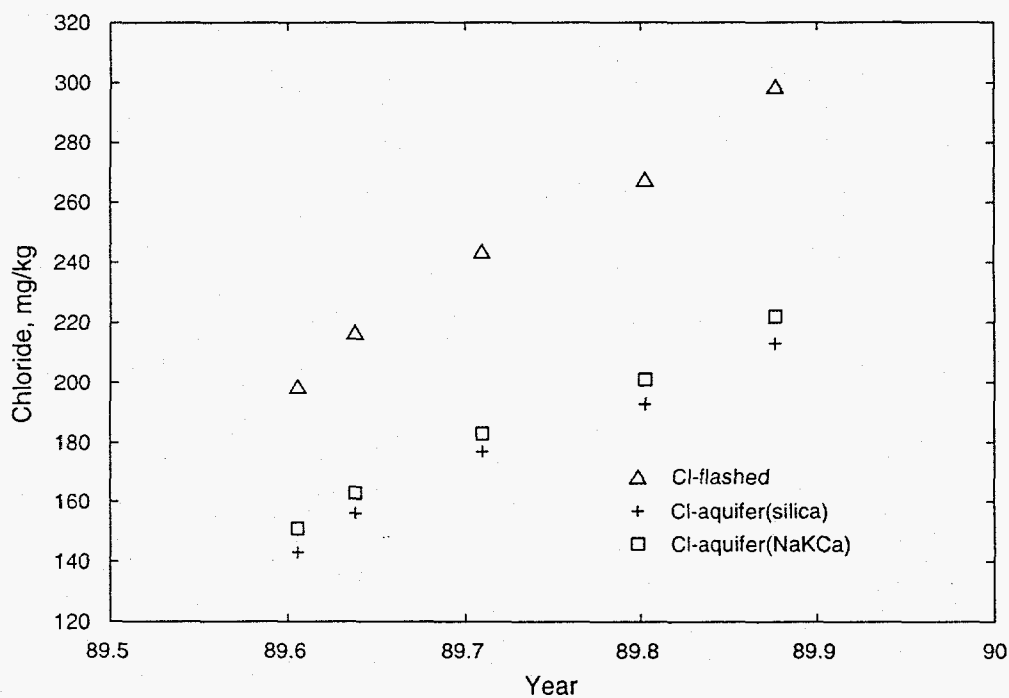


Figure 3.26. Chloride concentrations for flashed and aquifer waters of Sumikawa well SD-1.

3.3.11 Well 52E-SM-2

Well SM-2 was drilled to 803 m in September 1978. After a production test, the well was deepened to 1001 m and casing was installed to 803 m. Well testing and fluid sampling was done from October 1978 through November 1979. Measured enthalpy was more variable than enthalpy from silica which, after the first measurements was constant at 1100 kJ/kg. The NaKCa geothermometer could be applied only to the first analysis as the rest were not analyzed for calcium (Figure 3.28). Similarly aquifer chloride calculated from silica was nearly constant at 325 mg/kg except for the start and end of the period (Figure 3.29). SM-2 water compositions are similar to those for other waters, but possibly have less HCO_3 and B (Figure 3.30). These analyses are, however, much earlier than any others and different analytical methods may have been used.

3.3.12 Typical Reservoir Water

Most waters produced from SA-1, SB-1 and SD-1 and some from SC-1 (Figures 3.15, 3.21, 3.24 and 3.27) are similar in concentration and constituent pattern to the cooler, low-Cl water produced from S-4 (Figure 3.12). The main differences are higher HCO_3 in SC-1, and higher Ca in SB-1 and SD-1. It is likely that the composition common to these wells is representative of most of the Sumikawa reservoir fluids with less volcanic influence than in the high-Cl S-4 and S-2 waters and less surface influence than in S-3 waters. Well SM-2 probably belongs to this group but Mg is much higher and Ca analyses are lacking (Figure 3.30).

3.4 1989 Tests of Cold Water Unloading

In 1989 an experiment was undertaken by MMC to improve the productivity and injectivity of wells. In April and May 1989 large quantities of cold water were injected into each well (Table A.6). For most wells, the cold water changed the composition of produced fluids compared to 1988 samples. These injection-induced changes decreased with time during the 1989 tests but may have been present throughout in some cases. The total and liquid enthalpy values recovered rapidly because the injected water was rapidly heated to rock temperatures. Fluid compositions recovered more slowly with initial produced liquids low in Cl and high in HCO_3 and SO_4 .

A triangular diagram from MMC (Figure 3.31) shows these changes with evolution toward chloride compositions from Cl- HCO_3 - SO_4 and Cl- SO_4 compositions. The initial ratios of SO_4 to HCO_3 were not the same for all wells, with SA-4 and SB-1 having the highest HCO_3 , and S-4 and SD-1 lower in HCO_3 but all about the same SO_4 . Some wells are represented by few points (SA-4, SD-1) and some show little change (SA-2).

A similar diagram (Figure 3.32, also from MMC) shows gas ratios with a clear change from predominance of residual gas (mostly N_2) or H_2S toward dominance of CO_2 . The N_2 was probably introduced along with cold injectate either as a gas (probable for SB-1) or dissolved. The explanation for the evolution towards higher $\text{CO}_2/\text{H}_2\text{S}$ ratios is less clear. HCO_3 introduced in cold water may have been slowly converted to CO_2 or introduced O_2 may have slowly converted H_2S to SO_4 .

Continued on page 3-34

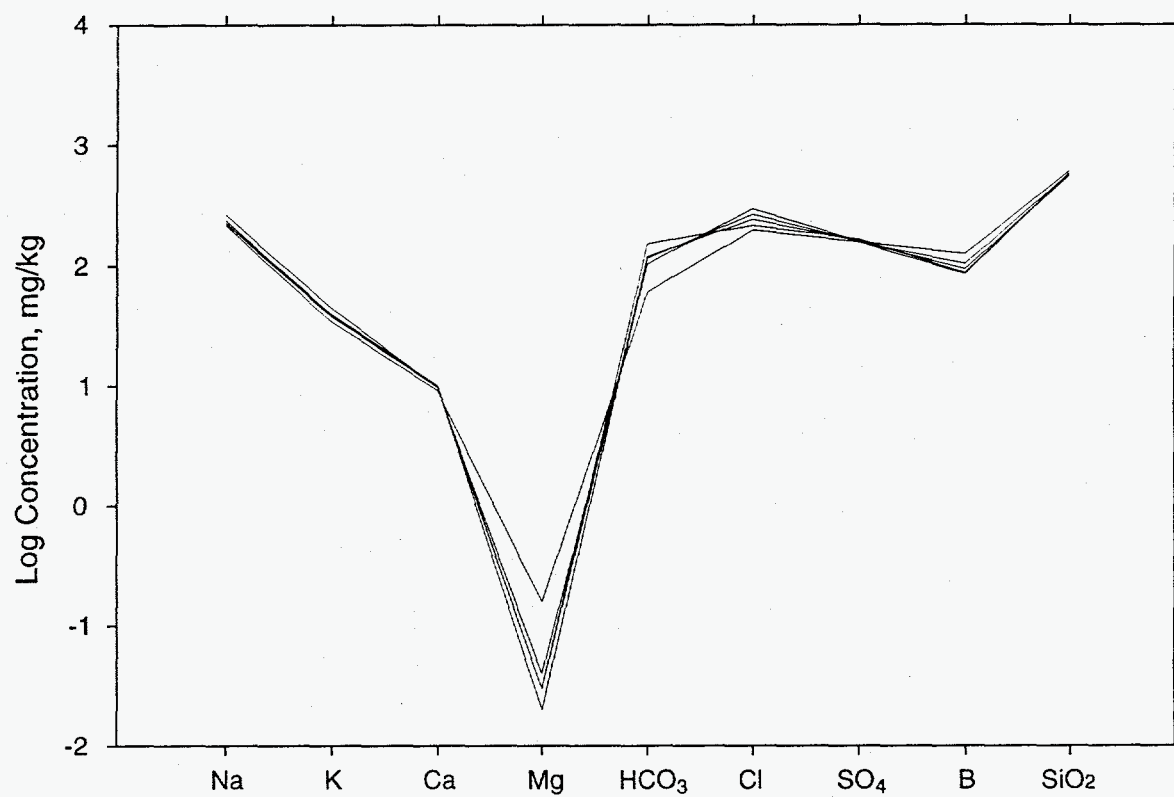


Figure 3.27. Schoeller diagram of well SD-1 water analyses.

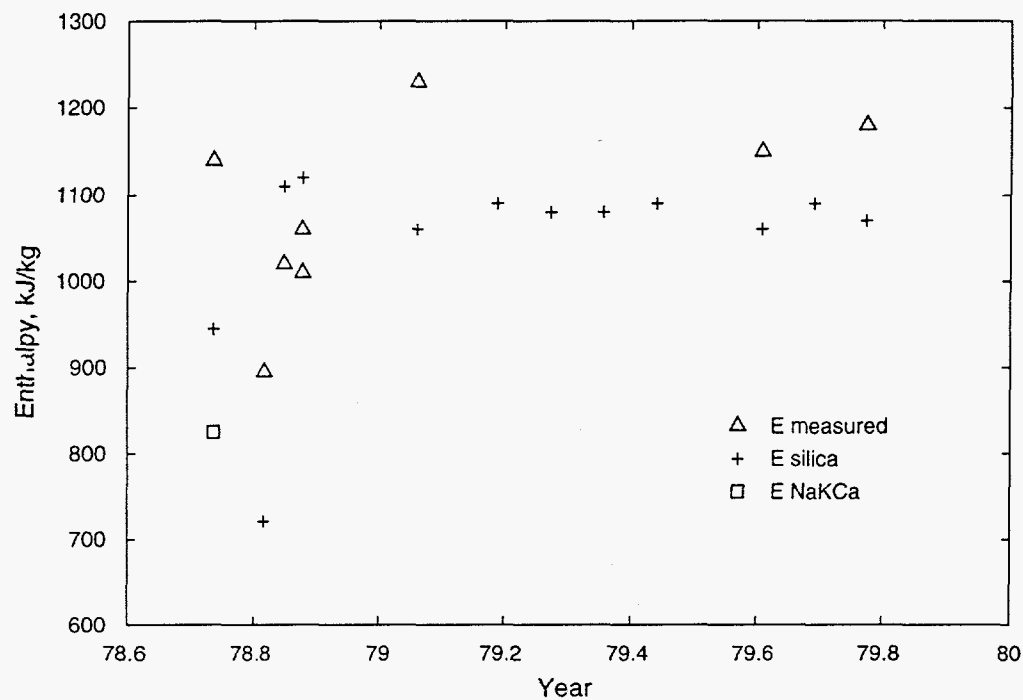


Figure 3.28. Enthalpy of total discharge fluid and aquifer water of Sumikawa well SM-2.

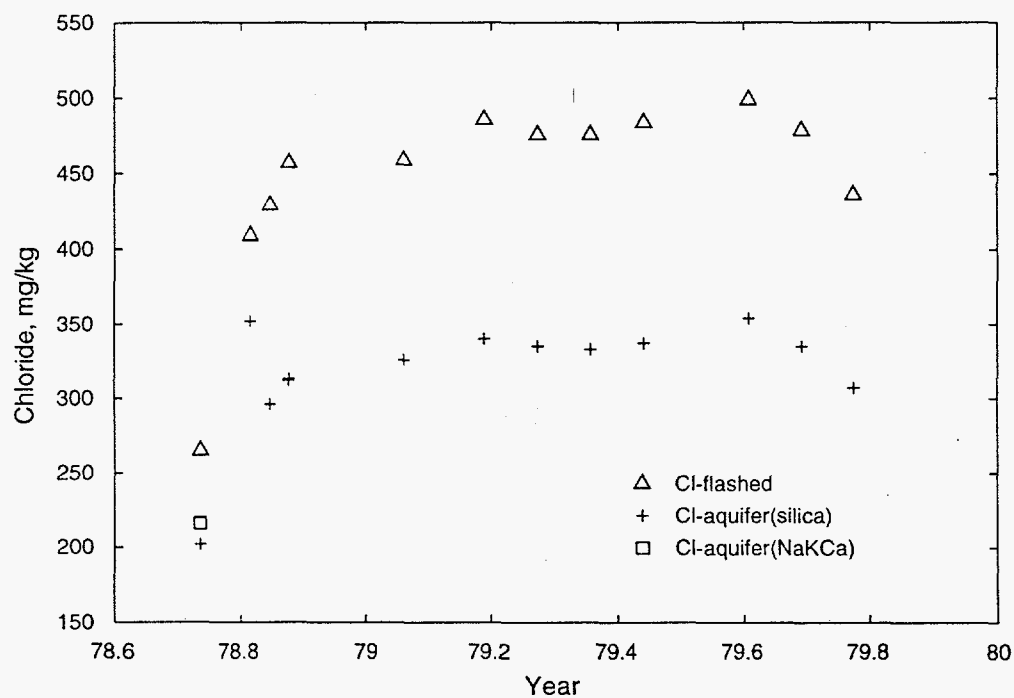


Figure 3.29. Chloride concentrations for flashed and aquifer waters of Sumikawa well SM-2.

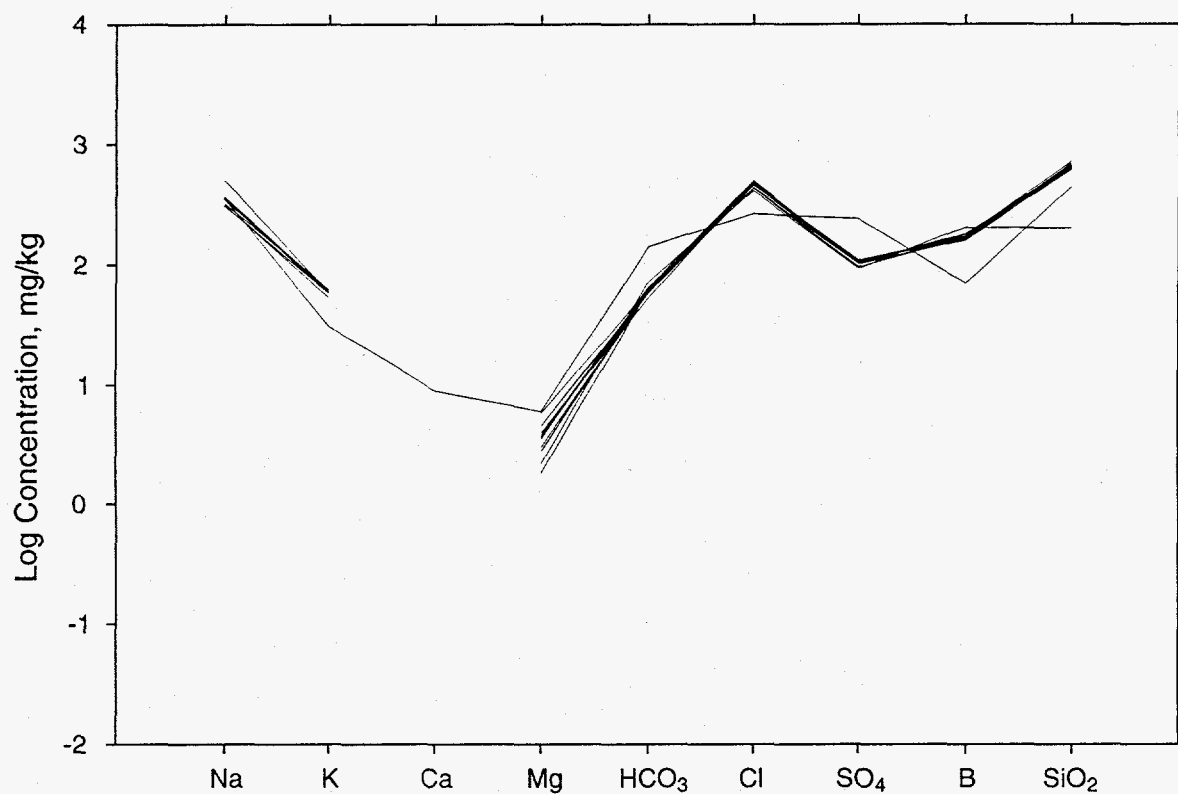


Figure 3.30. Schoeller diagram of well SM-2 water analyses. Calcium was not analyzed in most of this set.

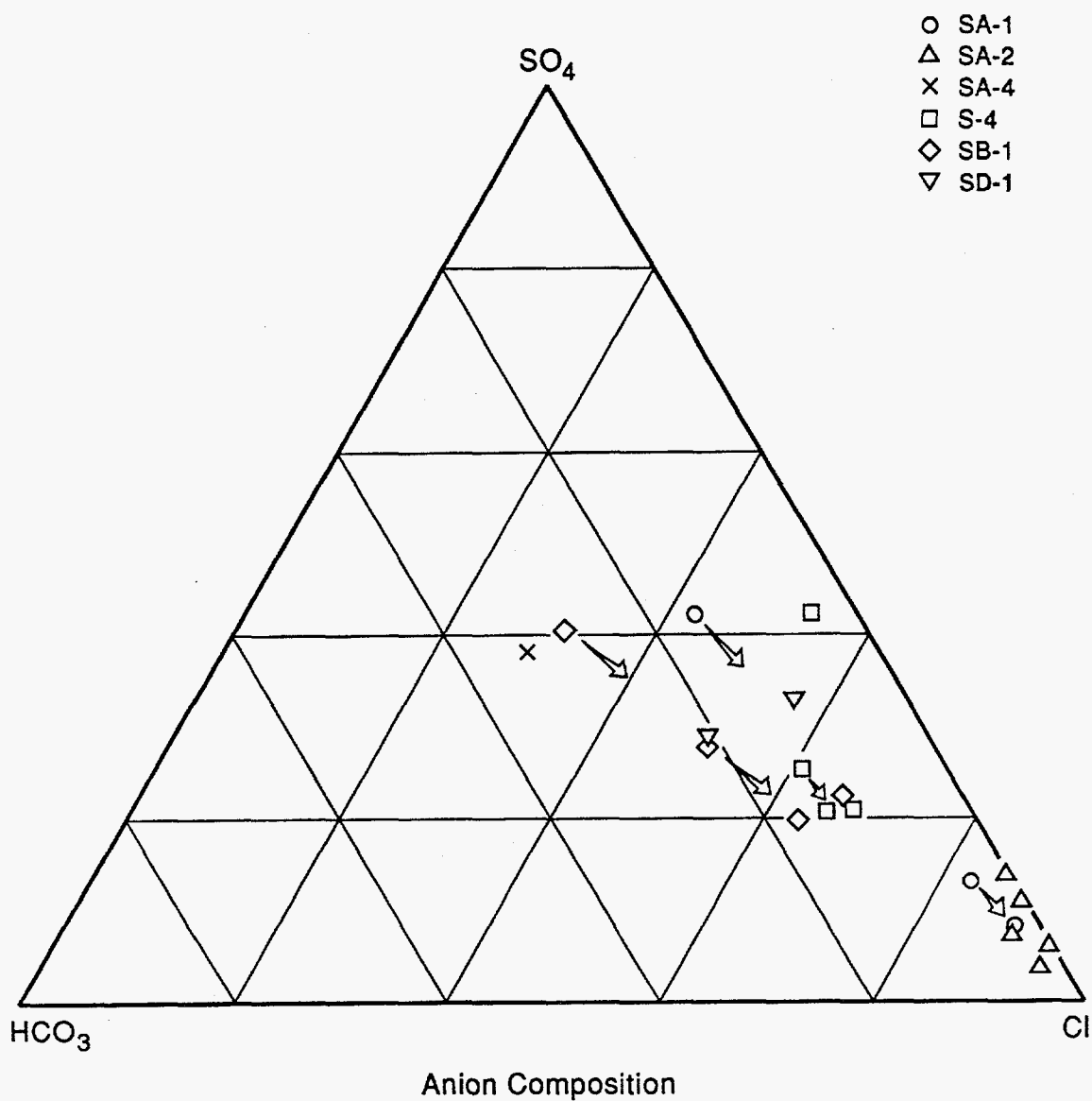


Figure 3.31. Changes in relative anion compositions of separated water during 1989 (from MMC).

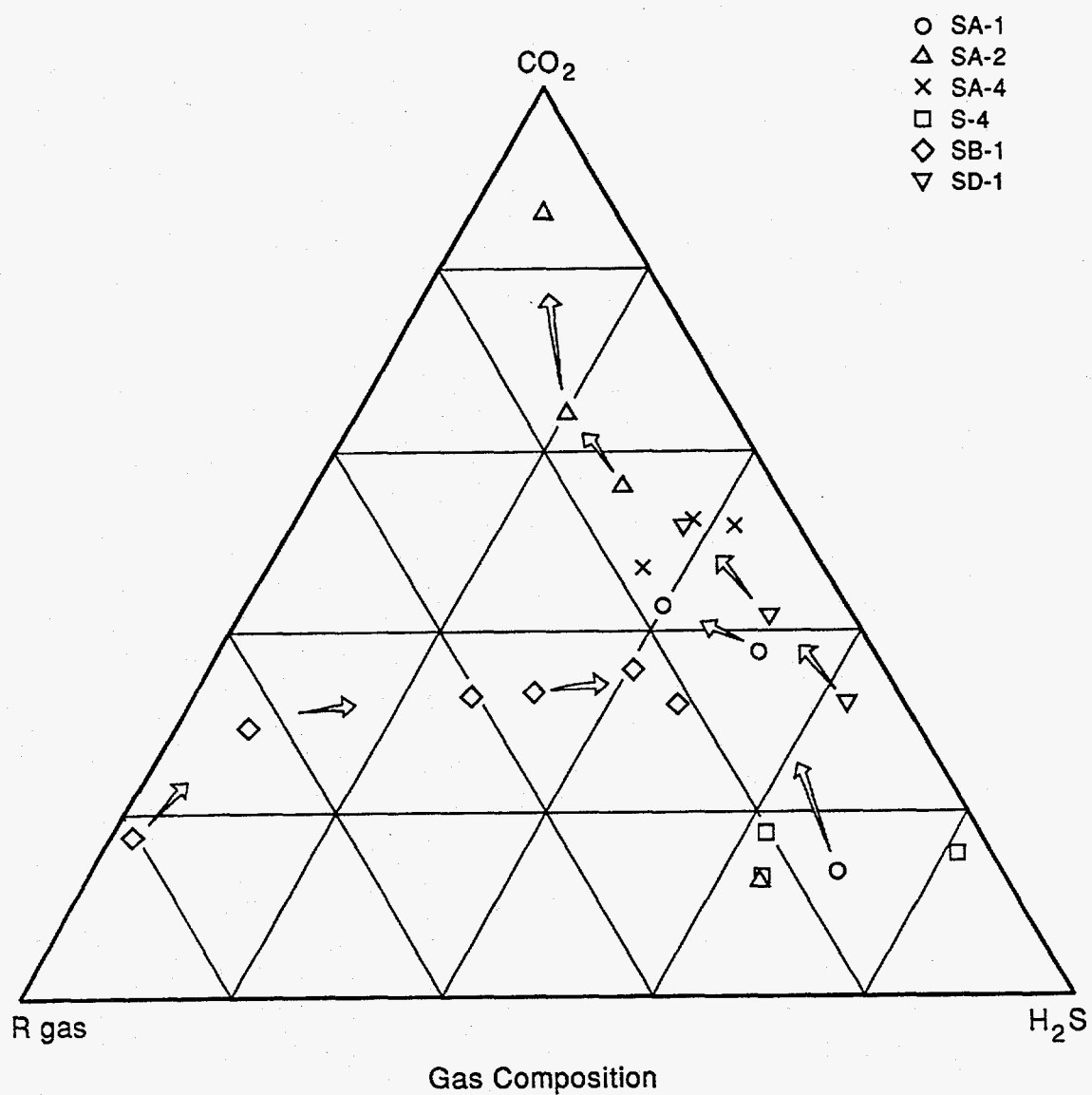


Figure 3.32. Changes in relative gas compositions of separated steam during 1989 (from MMC).

MMC made numerous partial analyses of discharge from wells SB-1, SC-1, and SD-1 to show changes in chloride, silica and enthalpy related to cumulative mass flow after injection (Figures 3.33, 3.34). Some of these analyses are given in Table A.7. It is noteworthy that, except for silica and chloride in discharge from SC-1 (which was not injected with cold water), the data do not reach constant values. The analyses in Table A.7 (unlike Figure 3.34) do not include silica values so reservoir temperatures cannot be exactly compared with data in Tables A.2 and A.5, but the trends in Figures 3.33 and 3.34 are similar to those in Figures 3.18, 3.20, 3.22, 3.23, 3.25 and 3.26.

For wells S-4 and SA-1, stabilized 1989 values of total and liquid enthalpy were similar to those of 1988 (Figures 3.10, 3.13). For these wells, 1989 enthalpy data is less scattered than 1988 data. S-4 and SA-1 show a pattern of enthalpy increase to a broad maximum, sometimes followed by a small decrease. Chloride in S-4 increased without reaching a maximum; this behavior is contrary to that seen in previous years (Figure 3.11).

SB-1 showed depressed enthalpy values at first, but enthalpy increased and became constant in the second half of the test (Figure 3.20). Oxygen isotope compositions similarly increased and became constant (Figure 3.19) while aquifer chloride increased but showed no tendency to constant values (Figure 3.18). This contrasting behavior results from the buffering effect on the fluid enthalpy and oxygen isotope composition of the reservoir heat and oxygen contained in the rock with no similar buffering for chloride. SB-1 gas compositions also changed with increase of CO₂ and H₂S and decrease of N₂ and Ar (Table A.3). This effect was more pronounced than in other wells. More detailed data on the effects of cold water in-

jection on the discharge chemistry of well SB-1 has been published by Ueda, *et al.* (1991).

The 1989 tests of cold water unloading were interesting geochemically to show fluid changes from mixing and reactions with rock minerals but largely obscured determinations of the natural fluid composition and enthalpy. This was a greater problem for chloride, deuterium and other conservative constituents that are not buffered in concentration by interaction with rock. Alkali ratios, silica concentrations, oxygen isotopes and total enthalpy were buffered by heat and rock-water reactions to maintain levels close to pre-injection values.

3.5 Interrelation of Sumikawa Water Compositions

In the previous sections, emphasis was placed on the total composition of fluids from individual wells and on the changes in total enthalpy and in reservoir chloride and liquid enthalpy with time based on data from individual wells. In the following sections emphasis will be on the interrelation of fluid compositions and on the processes which have caused their differentiation.

Showing these interrelations requires graphical methods which allow simultaneous display of fluid compositions from different wells and from different times of collection. Thus use is made of the "grid" method for gas geothermometry (D'Amore and Truesdell, 1985), enthalpy-chloride and isotope-isotope diagrams, and contour maps of reservoir chemistry. To supplement these methods, a plotting program was developed to draw triangular diagrams with numerous symbols and the ability to individually scale each component. Gigenbach (1991) demonstrated that transforma-

Continued on page 3-37

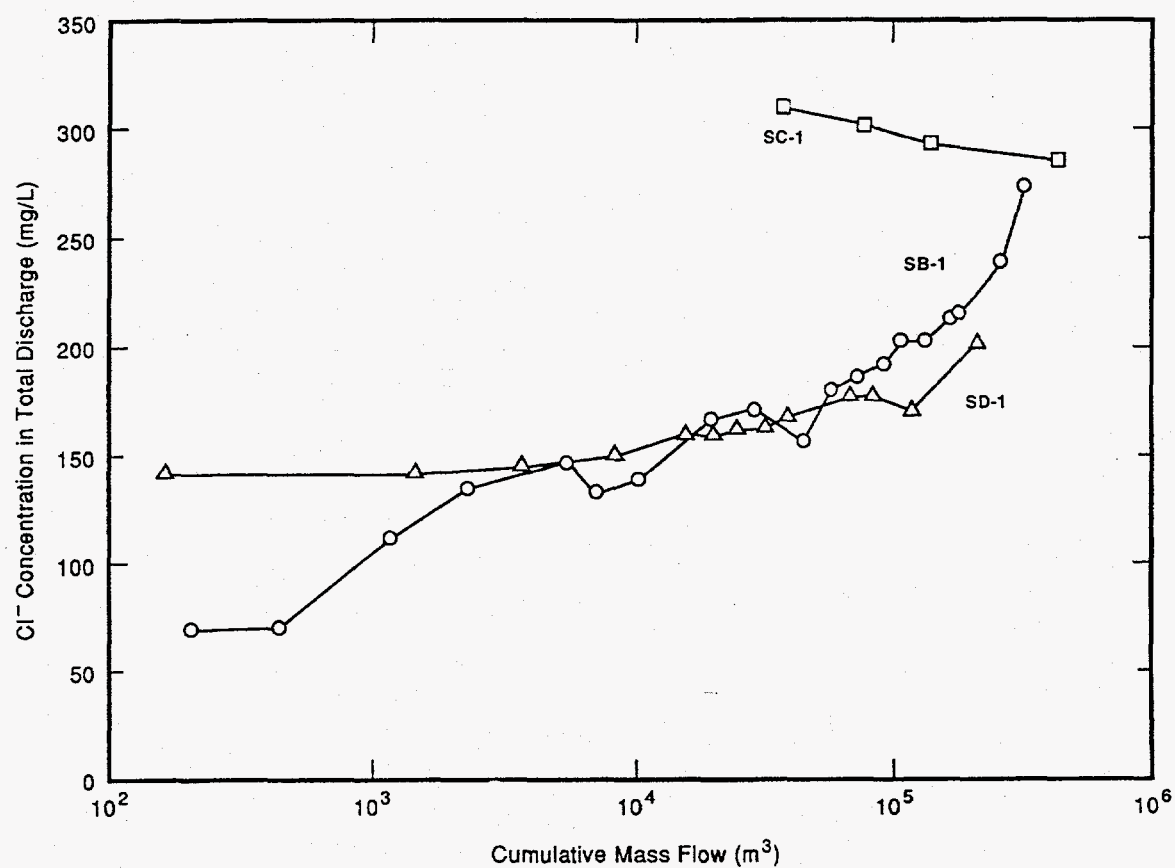


Figure 3.33. Detailed changes in total discharge chloride composition of fluid from three wells with cumulative mass discharge after cold water injection in 1989 (from MMC).

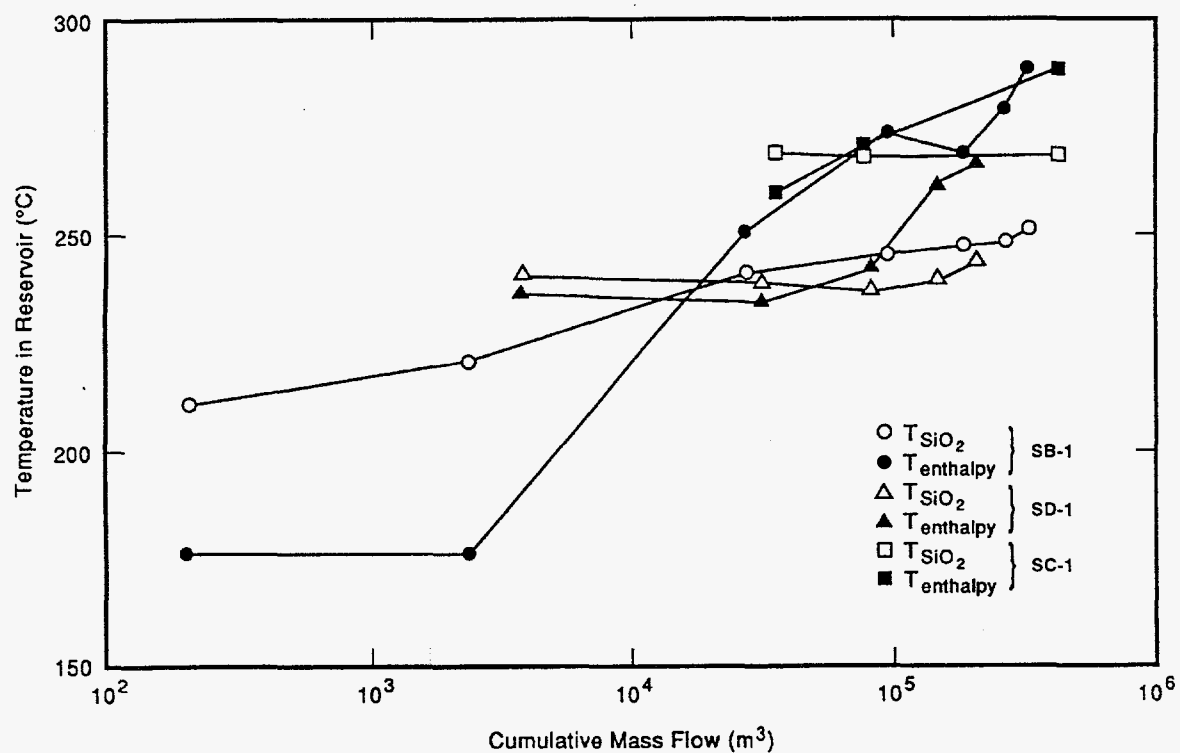


Figure 3.34. Detailed changes in fluid temperatures of three wells indicated by silica concentrations and measured total enthalpy with cumulative discharge after cold water injection in 1989 (from MMC).

tion of these diagrams by separate scaling of each of the components allows the separation of points bunched at one vertex or along one axis without changing the relative geometry of the points. Thus, for example, an alignment of points suggesting mixing remain linear.

3.5.1 The Combined Na-K and K-Mg Geothermometer Diagram

Giggenbach (1988) presented a triangular diagram (Figure 3.35) with the component quantities Na/1000, K/100, and $Mg^{1/2}$ (all concentrations in mg/kg). On this diagram a curve is plotted representing compositions at equilibrium with both Na-K exchange on feldspars and K-Mg^{1/2} equilibrium of feldspar, K-mica, quartz and chlorite. His intention was to increase the reliability of the Na/K geothermometer by including a component characteristic of near surface waters. Thus the compositions near the Mg corner are labeled "immature waters"; compositions near the geothermometer curve, "full equilibration"; and intermediate compositions, "partial equilibration". In practice the rate of reequilibration of Na and K is far slower than that of Mg, so cooling and mixing with near-surface waters generally increases Mg concentrations without changing the ratio of Na to K and the diagram shows lines radial to the Mg corner. Thus the diagram, rather than indicating the state of equilibration, shows essentially Na/K geothermometer temperatures and Na+K vs. Mg mixing. The Na/K geothermometer used by Giggenbach in this diagram yields temperatures that are significantly higher than those indicated by the Na-K-Ca and other Na/K geothermometers (Table A.8).

At Sumikawa the water composition data shows three lineations with constant Na/K ratios,

(and therefore constant Na/K temperatures) and some waters with intermediate compositions (Figure 3.35). The upper of these lines (nearest the Na corner) has all points for Ohnuma wells and Sumikawa wells S-2, some for SC-1, and a few for SM-2. This line intersects the geothermometer curve at 258°C. The second line radial to Mg intersects the geothermometer curve near 274°C. This line consists mostly of waters produced from wells S-3, SB-1, SM-2 and a few from SC-1. The lower line (nearest the K corner) has mostly points for well S-4 and SA-1 along with a few waters from SA-2 and SA-4. The SA-2 points are widely scattered because they represent variable mixtures of water and steam condensate. This line intersects the geothermometer curve just above 300°C. Some of the S-4 waters fall between the two alignments possibly indicating a 290°C source or re-equilibration at this temperature. Note that all of the data lies away from the geothermometer curve at higher Mg than required for equilibrium with respect to K-Mg geothermometry at the indicated Na/K temperatures.

Data for Ohnuma, S-2, S-3 and SM-2 are near the Mg corner suggesting relatively large near-surface influence. SC-1 waters are intermediate and most SB-1 and SD-1 waters approach the geothermometer line suggesting decreasing amounts of near-surface influence. Some S-4 and SA-1 waters have relatively large concentrations of Mg indicating near-surface influence.

It is not clear whether the near-surface influence at Sumikawa consists of mixture with near-surface water or solution of Mg minerals at lower temperatures. In either case equilibration of water with the chlorite bearing assemblage postulated by Giggenbach (1988) does not seem likely. Sumikawa reservoir temperatures from the K-Mg geothermometer are usually 100 to 200°C, with

Continued on page 3-39

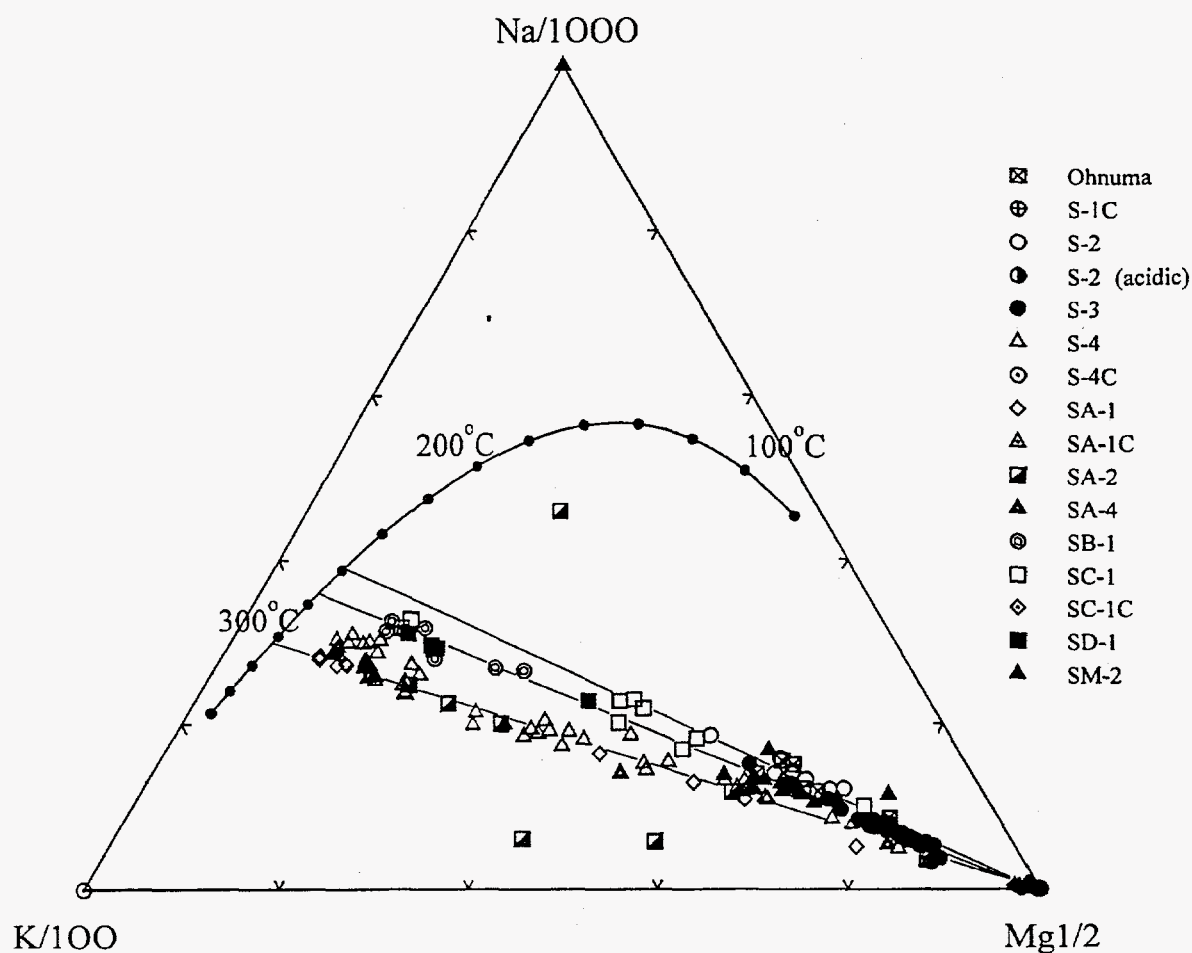


Figure 3.35. The Na-K-Mg geothermometer diagram of Giggenbach (1988) with water compositions from Sumikawa well discharges. The geothermometer curve represents the K-Mg and Na/K geothermometers proposed by Giggenbach. The K-Mg geothermometer equilibrates rapidly at intermediate temperatures and the Na/K geothermometer equilibrates slowly. The Sumikawa pattern suggests relatively low temperature mixing of high Mg water with equilibrated high-temperature waters. See discussion in the text. Temperature is in degrees Celsius and concentrations are by weight.

the maximum about 250°C for S-4 and SA-1 (Table 1). These temperatures are generally too low to represent equilibration in the reservoir. Because high-temperature geothermal waters are generally high in Na and K and very low in Mg, mixture with near surface water could substantially increase Mg without changing the Na/K ratio. This is the most likely case at Sumikawa.

The reservoir temperature of 300+°C indicated by this diagram for well discharge compositions that fall along the lower line is close to maximum measured downhole temperatures (300 to 317°C), but is generally much higher than other geothermometer temperatures (Tsilica, 225 to 277°C; TNaKCa, 255 to 270°C except SA-1, 310°C and early fluids from S-4, ~290°C). Geothermometer temperatures for SA-2 and SA-4 are few and unreliable because these wells discharge mostly steam. The reservoir temperatures of 274°C and 258°C indicated for well discharges falling along the upper two lines are also generally higher than other geothermometer temperatures (Tsilica, 225 to 250°C; TNaKCa, 236 to 255°C except SC-1, 267°C), but generally lower than maximum measured downhole temperatures (300 to 317°C except S-2, 245°C and S-3, 236°C).

In Table A.8 calculated Sumikawa reservoir temperatures from Na/K geothermometers (Truesdell, 1975; Fournier, 1979; Arnorsson et al., 1983; Nieva and Nieva, 1987; and Giggenbach, 1988) are compared with those from the Na-K-Ca and quartz geothermometers. This comparison and the discussion above suggest that, for Sumikawa at least, The Na-K-Mg^{1/2} triangular diagram should be revised to use a more realistic Na/K geothermometer. Figure 3.36 uses the Na/K geothermometer of Nieva and Nieva (1987), which appears closest to the Na-K-Ca geothermometer for Sumikawa wa-

ters. Using this diagram, the high temperature line indicates 280°C, the intermediate temperature line, 250°C and the low temperature line, 240°C. Even though the lowest Mg points are closer to the geothermometer line, there is still no indication that K-Mg equilibrium is achieved.

3.5.2 The Cl-SO₄-HCO₃ Anion Triangular Diagrams.

Another widely used diagram is the anion concentration triangular diagram with Cl, SO₄ and HCO₃ as components. These are the major anions in almost all surface and subsurface waters including geothermal reservoir and discharge waters. In cold waters Cl usually originates from sea spray or solution of evaporites, SO₄ from oxidation of sulfides or from evaporites, and HCO₃ from reaction of (atmospheric or soil) CO₂ with rock minerals and water. In high temperature geothermal reservoir waters Cl dominates because most SO₄ is removed by precipitation of anhydrite and most HCO₃ by precipitation of calcite (due to the very low solubility of both minerals at high temperatures). As geothermal waters migrate towards the surface CO₂ may react with rock to form HCO₃ and at the surface H₂S may be oxidized to SO₄. In acid near-magmatic reservoir waters SO₄ may exist from breakdown of SO₂ contained in magmatic gases or from infiltration of waters with surface-formed SO₄.

At Sumikawa the Cl-SO₄-HCO₃ diagram clearly distinguishes waters of different origins and shows relationships between well waters (Figure 3.37). The HCO₃ corner is occupied by waters dominated by steam condensate with high HCO₃ concentrations formed by reaction of CO₂ in steam with steam condensate. One sample of SC-1 con-

Continued on page 3-41

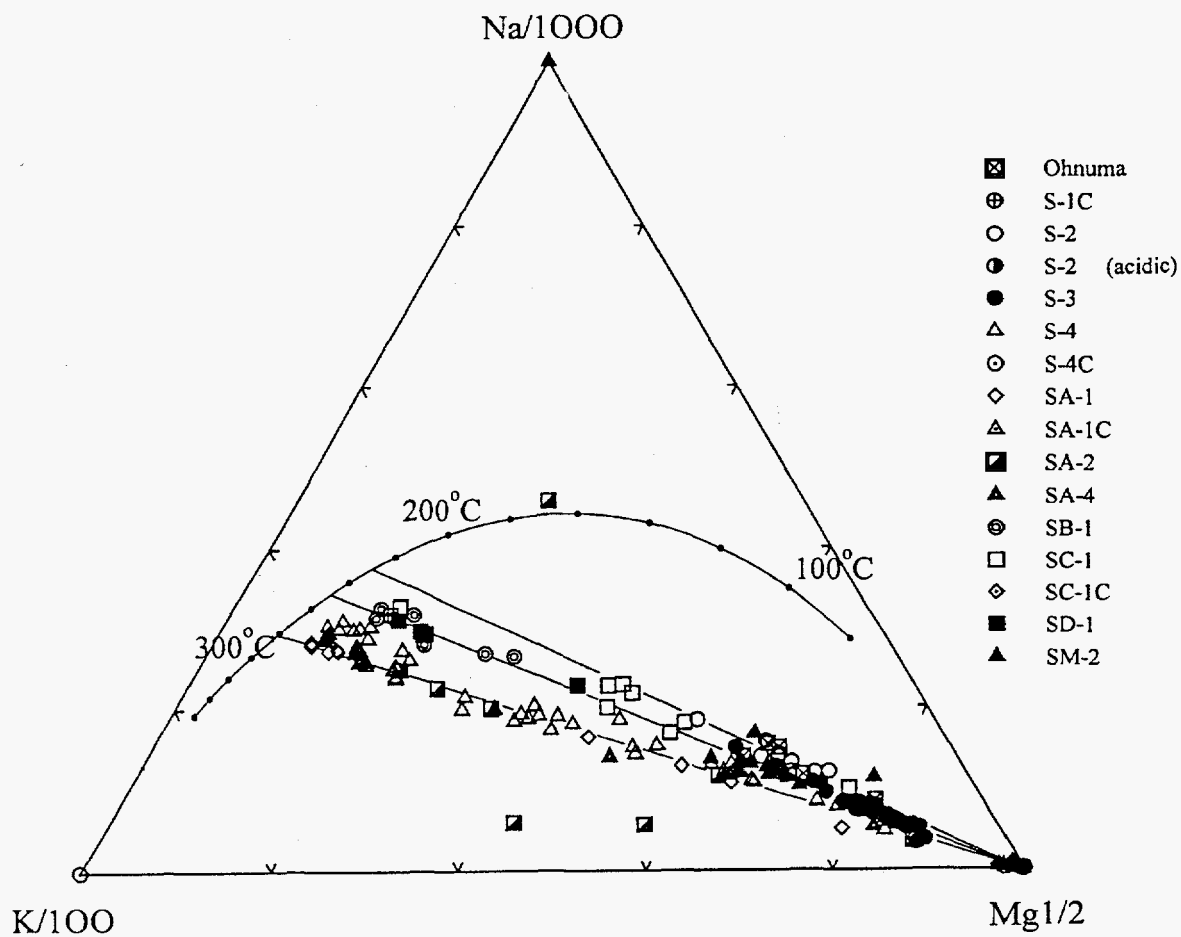


Figure 3.36. The Na-K-Mg geothermometer diagram as in Figure 3.35, but using the Na/K geothermometer of Nieva and Nieva (1987). The indicated Na/K temperatures are more realistic than in Figure 3.35. See text and Table A.8 for discussion of these geothermometers.

densate also has SO_4 indicating oxidation of H_2S , possibly during sampling and one S-4 condensate with higher Cl is similar in anions to reservoir waters indicating that it contained reservoir water as well as steam.

The highest SO_4 waters are acid samples from S-2 with the earlier, near-neutral S-2 waters and some S-3 waters next highest. Well S-2 waters are particularly interesting at Sumikawa. This well was originally completed at 903 m and tested in July 1982. However, the discharge was considered insufficient and the hole was deepened to 1065 m and re-tested in October 1982. Although fluid from the first completion was initially neutral, the pH decreased from 7.9 to 5.5 over the two weeks of the tests. When the deepened hole was re-tested its enthalpy had dropped and the waters were acid (pH 2.6 to 2.8). The near neutral S-2 waters do not have a constant SO_4/Cl ratios but increase in SO_4 with time, possibly indicating increasing magmatic influence. An increase in acidity from mixture with infiltrating acid SO_4 waters produced by surface oxidation of H_2S cannot be ruled out as the major source of acidity in these waters because the concentration of Cl decreased when SO_4 increased and the waters became acid. However the situation is complicated because after a strong decrease, Cl increased along with SO_4 to reach concentrations higher than any of the near neutral waters.

For most waters (other than condensates, S-2 waters and about half the S-3 waters) there is a clear alignment between a high Cl end member with about 10 percent SO_4 and no HCO_3 , and a low Cl end member with about 20 percent Cl and equal amounts of SO_4 and HCO_3 . The high Cl end member is represented by SA-2 waters (with some scatter), and some S-4, and SA-1 waters. Waters from SC-1, SM-2, Ohnuma, SB-1, SD-1 and S-3 fall along the line in order of decreasing Cl.

Samples from S-4 have a wide range of composition and extend from the high Cl end member half way to the high SO_4 , HCO_3 end member. In general, S-3 waters have more SO_4+HCO_3 than Cl indicating partly shallow origin. It is likely that these shallow waters entered the well through a casing break at 268 m depth (MMC, written commun., 1996). About half of the S-3 waters fall off the general alignment in the direction of lower SO_4 . The source of these waters is not clear but they may originate on the margins of the system away from infiltrating SO_4 formed in upflow zones by H_2S oxidation.

In the interpretation of this diagram by Giggenbach (1991), all Cl- SO_4 waters are "volcanic" and Cl- HCO_3 waters in the upper part of the diagram are "mature", while those with high HCO_3 and low SO_4 are "peripheral" and other HCO_3 - SO_4 waters are "steam-heated" (note these labels in Figure 3.37). Applying these classifications to Sumikawa, the high-Cl end member water and most S-2, S-4, SA-2, SB-1 SC-1 and SM-2 waters would be "volcanic", and condensates and S-3 waters would be "peripheral". No waters at Sumikawa would be called "mature".

3.5.3 The Cl-B- HCO_3 Diagram, a Test for Fluid Homogeneity

A different anion diagram was used by Ellis (1970) to differentiate the geothermal fields of New Zealand by their Cl/B ratios. In this plot B, Cl and HCO_3 are used as components. Boron and chloride are considered conservative components that are not affected by water-rock reactions that occur in and above the reservoir and bicarbonate (as noted above) is a reactive component formed at moderate temperatures by reaction of CO_2 with rock minerals. Because Cl and B are conservative, their ra-

Continued on page 3-43

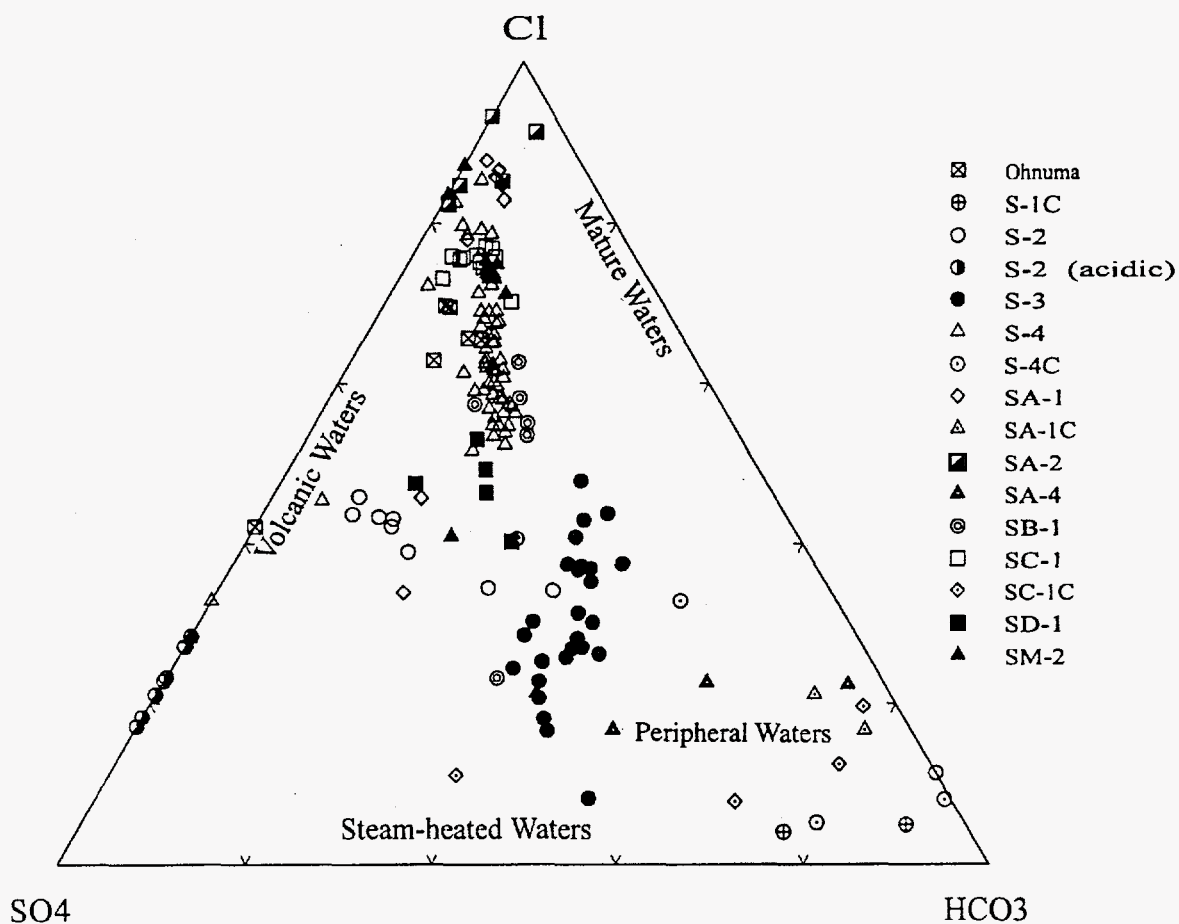


Figure 3.37. The Cl-SO₄-HCO₃ anion diagram which shows the proportions (by weight) of the major anions in Sumikawa and other geothermal waters. Chloride is usually of deep origin and HCO₃, shallow, but SO₄ can originate either shallow, from oxidation of sulfide, or deep from volcanic fluid. The labels are from Giggenbach (1991).

tio is a test for fluid homogeneity. Ellis found that the Cl/B ratios of New Zealand geothermal waters varied from 7 to 30 and, except for Broadlands, were constant within each field, while the fraction of HCO_3 varied widely. Variation in Cl/B may indicate several reservoirs or several rock types. At Broadlands part of the field is hosted in graywacke and part in andesite.

Sumikawa waters show as much variation in Cl/B as all of the geothermal fields in Ellis' diagram (Figure 3.38). The acid S-2 waters and SA-2 waters contain almost entirely Cl with Cl/B ratios between 10 and 20. Neutral S-2 waters and Ohnuma waters have Cl/B near 5 and SB-1, SC-1 and SM-2 Cl/B ratios are near 2.6. Most other waters (S-3, S-4 and SD-1) have Cl/B ratios of 2 to 2.3, except SA-1 waters some of which are as low as 1.5. The reason for this wide range is not clear but may result from the nearness of Sumikawa to Mt. Yake volcano, with the most volcanic waters high in chloride and evolved waters having increasingly more boron. The New Zealand areas are related to rhyolite calderas and all are about equally far from crystallizing magma. The wide range in Cl/B ratios suggests that the Sumikawa waters are relatively inhomogeneous and have not mixed extensively. This may be due to permeability barriers or be characteristic of a young, volcanic-related fluid.

3.5.4 The Na-K-Ca Triangular Diagram

Some features of both Cl-SO₄-HCO₃ and Na-K-Mg geothermometer diagrams are combined in the Na-K-Ca diagram (Figure 3.39). By showing Na/K ratios, this diagram distinguishes waters with different high temperature end members, and Ca indicates mixture with cooler, near-surface water.

Because calcite is less soluble at higher temperatures, Ca concentrations are low at high temperatures (>275°C), but increase at lower temperatures from water-rock reactions. This also provides indication of the tendency to calcite scaling. High temperature waters seldom produce calcite scale but waters at intermediate temperatures (~200°C) often scale rapidly.

The Sumikawa waters with the highest Ca are steam condensates, waters from high enthalpy wells that are mixed with steam condensate, and acid waters from well S-2. The steam condensates lack Na and K, and all of these waters are mildly or strongly acidic when collected. Calcium in these waters could originate in part from rock leaching or from solution of Ca from concrete silencers or weir boxes. The acid reservoir waters from well S-2 have no HCO₃ and can readily dissolve Ca feldspars and calcite. The low Ca waters, presumably from higher temperature zones, show three alignments; a lower K/Na, lower-temperature line with Ohnuma, neutral S-2 and some SC-1 waters; an intermediate line with mostly well S-3 waters and some acid S-2, SB-1 and SC-1 waters; and a high K/Na, high-temperature line with entirely S-4 waters at the low Ca end and SA-1 waters, along with some acid S-2 waters with higher Ca. The high K/Na line is broader than the others with most variation in the S-4 waters. The high Ca end member also has a significant but small K fraction and no Na. This is typical of low temperature (<100°C) waters and results in very-high, misleading Na/K geothermometer temperatures.

3.6 Chemical Changes Shown by Contour Maps

In order to show the chemistry of the entire field, the parameters indicated to differentiate the

Continued on page 3-46

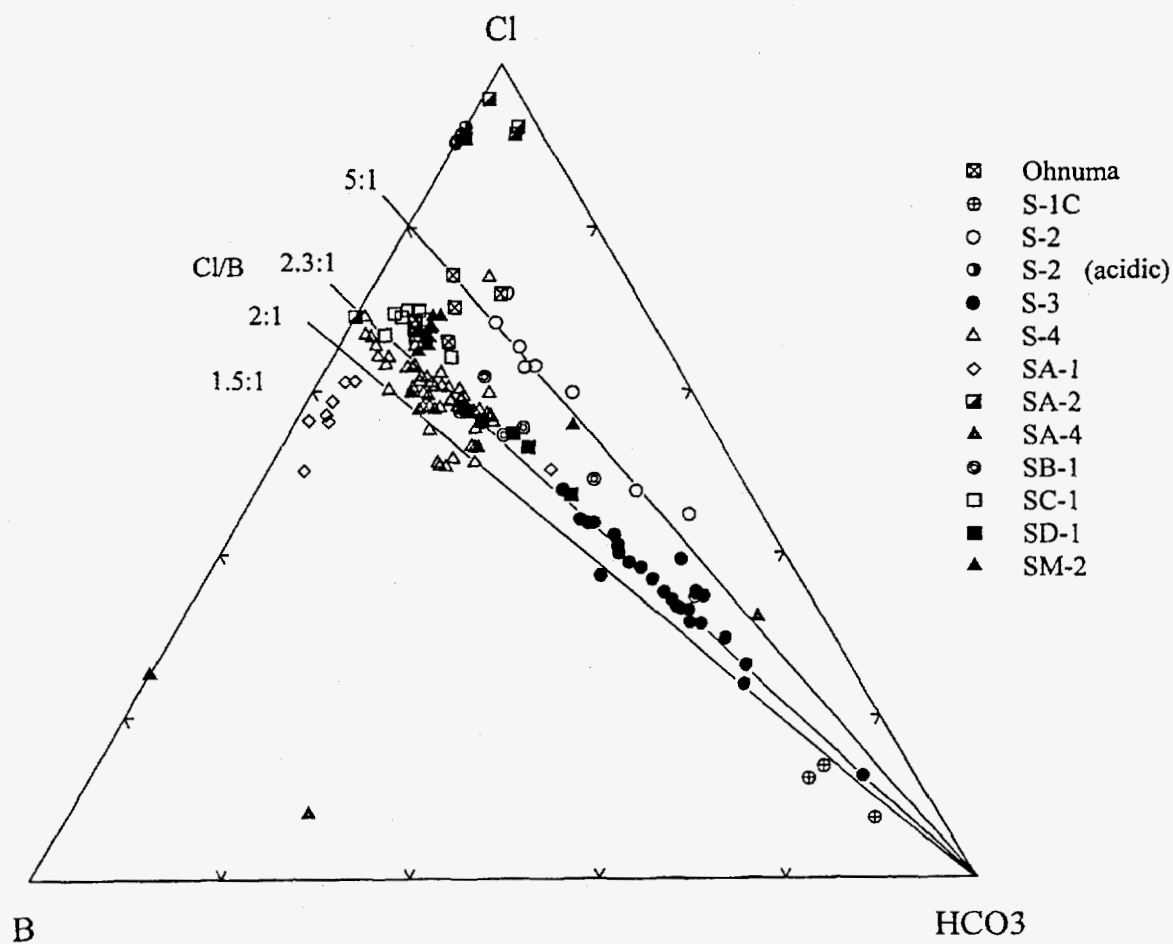


Figure 3.38. The Cl-B-HCO₃ diagram showing Sumikawa waters. In this diagram Cl and B are deep conservative (or "soluble") constituents not generally available from reservoir rocks, while HCO₃ is formed at shallower depths where CO₂ reacts with rock at moderate temperatures. The wide range of Cl/B ratios suggests a near volcanic source for these constituents.

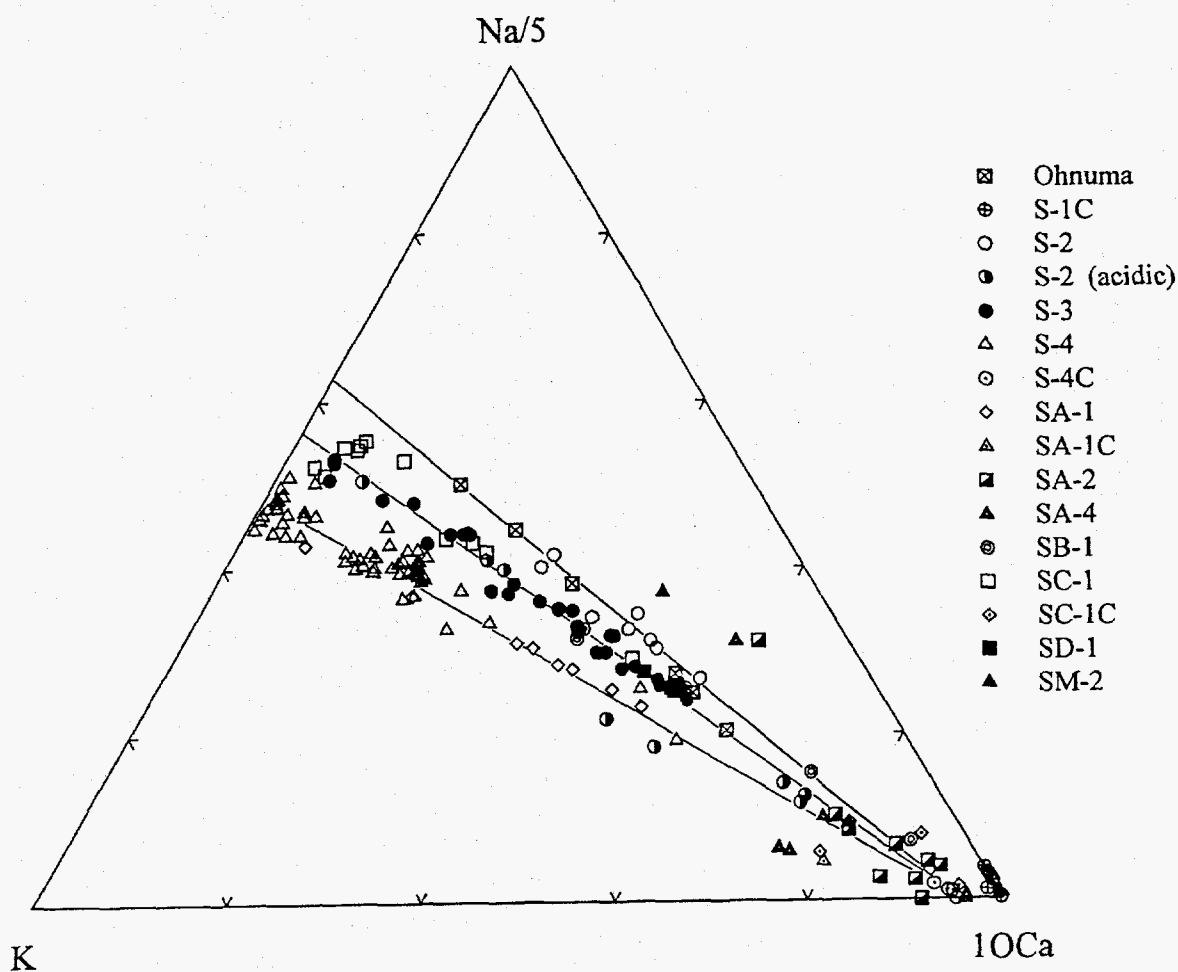


Figure 3.39. The Na-K-Ca diagram is similar to the Na-K-Mg diagram in showing Na/K temperatures and mixture with near surface (Ca-bearing) water. The Sumikawa waters show a range of Ca concentrations that may indicate possible calcite scaling if lower temperature waters are produced.

Sumikawa fluids (e.g. Na/K, Cl/B) can be mapped using estimated locations of mean inflow zones based on well downhole characteristics (see Section 4). This method has been used effectively to show reservoir processes at Cerro Prieto (Truesdell et al., 1992). However the short production tests and cold water injection along with the small number of wells have made the application to Sumikawa less informative. Despite this a few maps have been constructed of Sumikawa data.

3.6.1 Contour Maps of Reservoir Chemistry and Physical State

The contour maps found most useful for indicating reservoir processes at Cerro Prieto are reservoir temperature, chloride concentrations and well inlet vapor fraction (IVF). (IVF is a measure of excess enthalpy or excess steam. For a well fed entirely by liquid, IVF (the calculation of these quantities is described by Truesdell, *et al.*, 1989) is zero and for an all steam well, IVF is one.) The quantity of data for Sumikawa is so limited and the variations within each year's tests were so large, that contouring of 1983 data from wells S-1, S-2, and S-3 was not informative. The major changes were between data from the 1984-1988 period and data from 1989. Therefore two sets of maps, one for 1982 to 1988 and one for 1989, were constructed using data averaged for each well. This showed general reservoir processes without short term variations. The effects on reservoir fluids of the 1989 cold water injection are indicated by some decreases in reservoir chloride and temperature and an increase in both deuterium and oxygen-18. The isotopic changes will be discussed further in connection with isotope-isotope diagrams (section 3.8); other changes were discussed in section 3.3.

The pre-1989 patterns are dominated by a east-west gradient in temperature, chloride and IVF

(Figure 3.40). All quantities generally increase from north to south (or north central to southeast and southwest); temperature from 200 to 270°C, chloride from 100 to 400 mg/kg, and IVF from <0.1 to 0.7. The exclusion of SA-2, SB-1 and SD-1 (with no pre-1989 water analyses), has contributed to this gradient but the 1989 data for these wells may not reflect natural reservoir conditions. 1989 data for SA-2 in particular shows high temperatures and chloride in these calculations, but these may have resulted from variable amounts of evaporation and precipitation before collection (see section 3.3.6). The 1982-1988 $\delta^{18}\text{O}$ data show a similar northeast-southwest pattern with SA-2 isotopically heavy and a general decrease in δO and δD to the northeast and northwest (Figure 3.41). Deuterium, however, is highest in the east and decreases to the west and well S-4.

The 1989 maps (Figures 3.42) show more uniform calculated temperatures (range 220-250°C), chloride decreases for wells S-4 and SA-4 with no changes for other wells, and a reversal in gradient for IVF. Isotopes show a general change toward heavier δO and δD values (Figure 3.43). Wells S-4, SC-1, and SA-4 increased in δD by 5 permil and in δO by 0.5 to 1.4 permil. In both periods δO generally decreased to the south and southwest. In 1989 the δD pattern was similar to that of δO , but it was quite different in 1982-1988. The interpretation of deuterium in high temperature geothermal fluids is difficult because above 220°C there is a deuterium fractionation reversal with vapor heavier than liquid. Thus at higher temperatures, the separation of steam leaves water enriched in δO and depleted in δD . Thus the 1982-1988 patterns of δO and δD differ because boiling was dominant, but the 1989 patterns of both isotopes are similar because mixture with cold water was the dominant process. The 1982-1988 data shows increase of δO to the south. This prob-

Continued on page 3-51

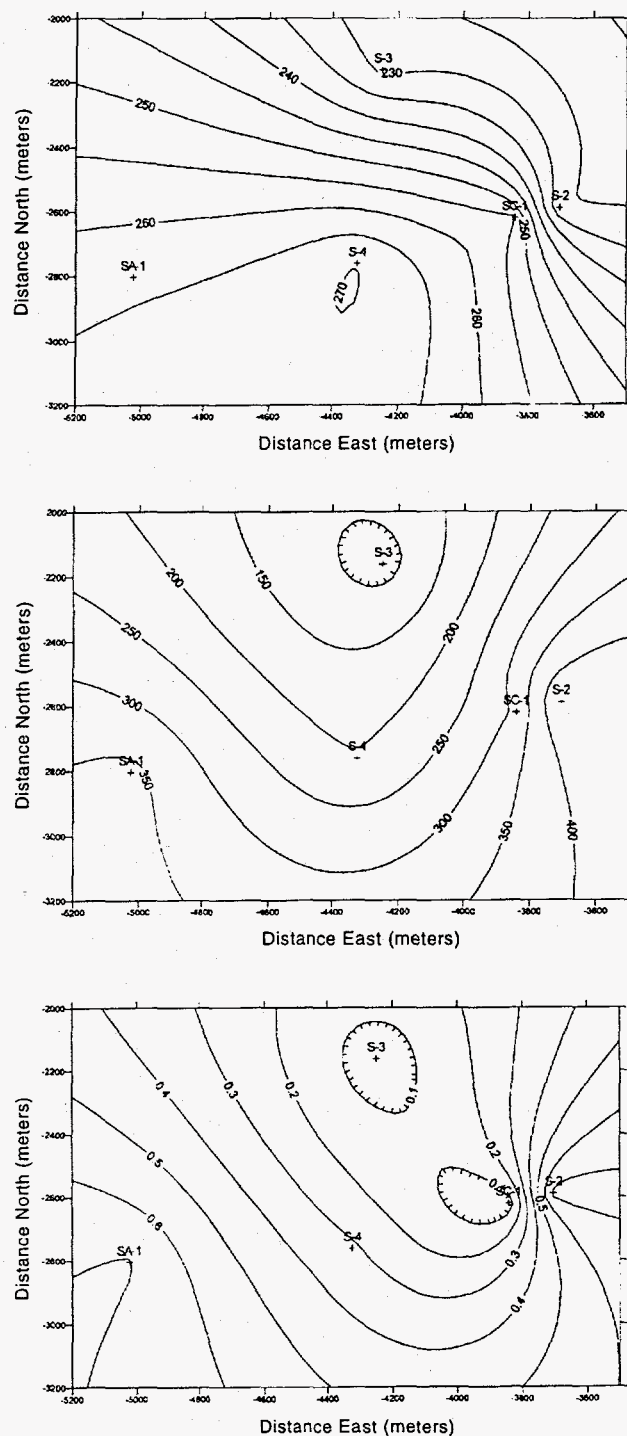


Figure 3.40. Contour map of average Sumikawa reservoir (a) temperatures (degrees Celsius), (b) chloride concentrations (mg/Kg), and (c) inlet vapor fractions (IVF) for 1982 through 1988 calculated using Na-K-Ca geothermometer temperatures. Data from Table A.5.

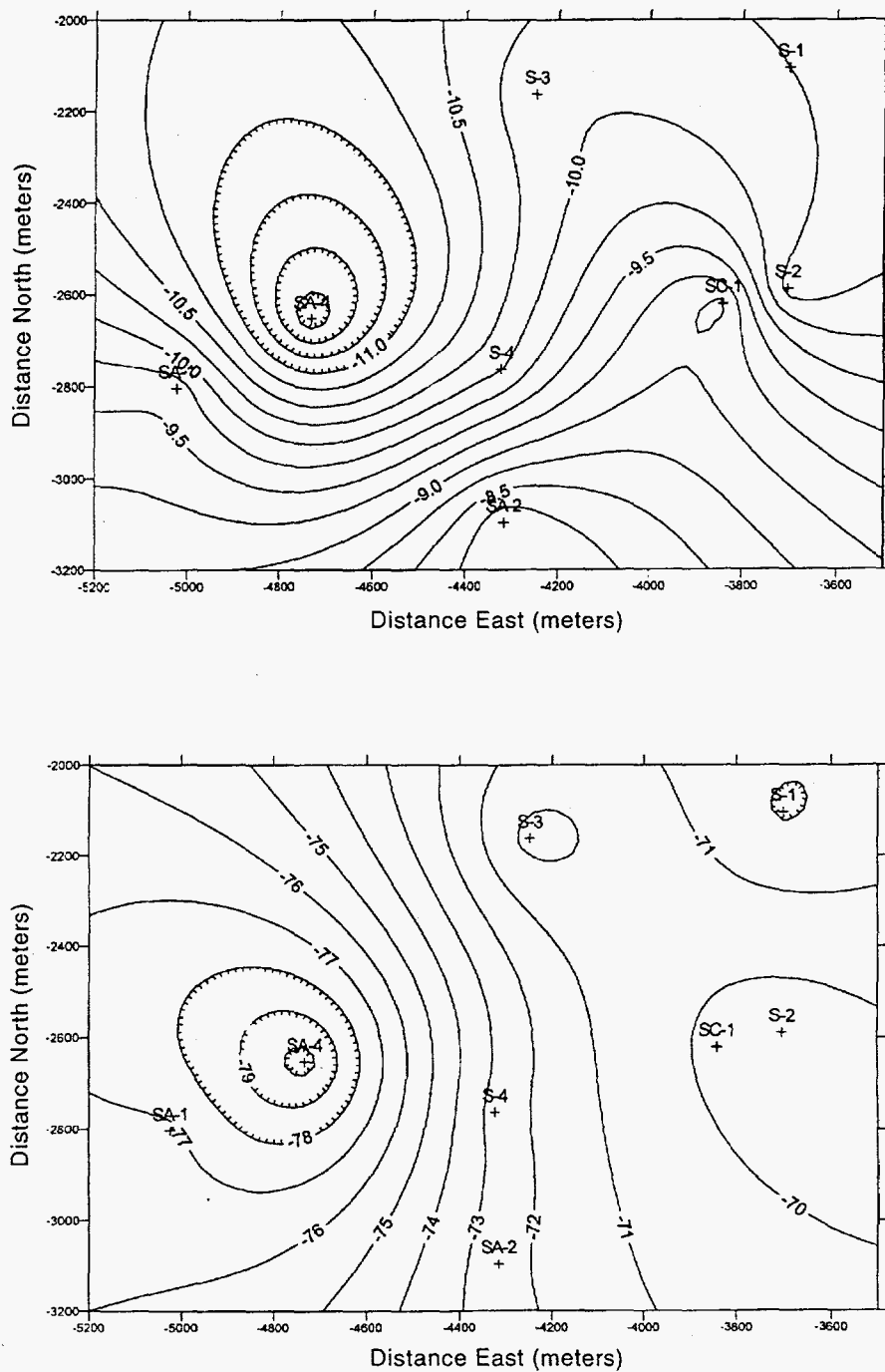


Figure 3.41. Contour map of average Sumikawa total discharge (a) δO (permil SMOW) and (b) δD (permil SMOW) for 1982 through 1988. Data from Table A.4.

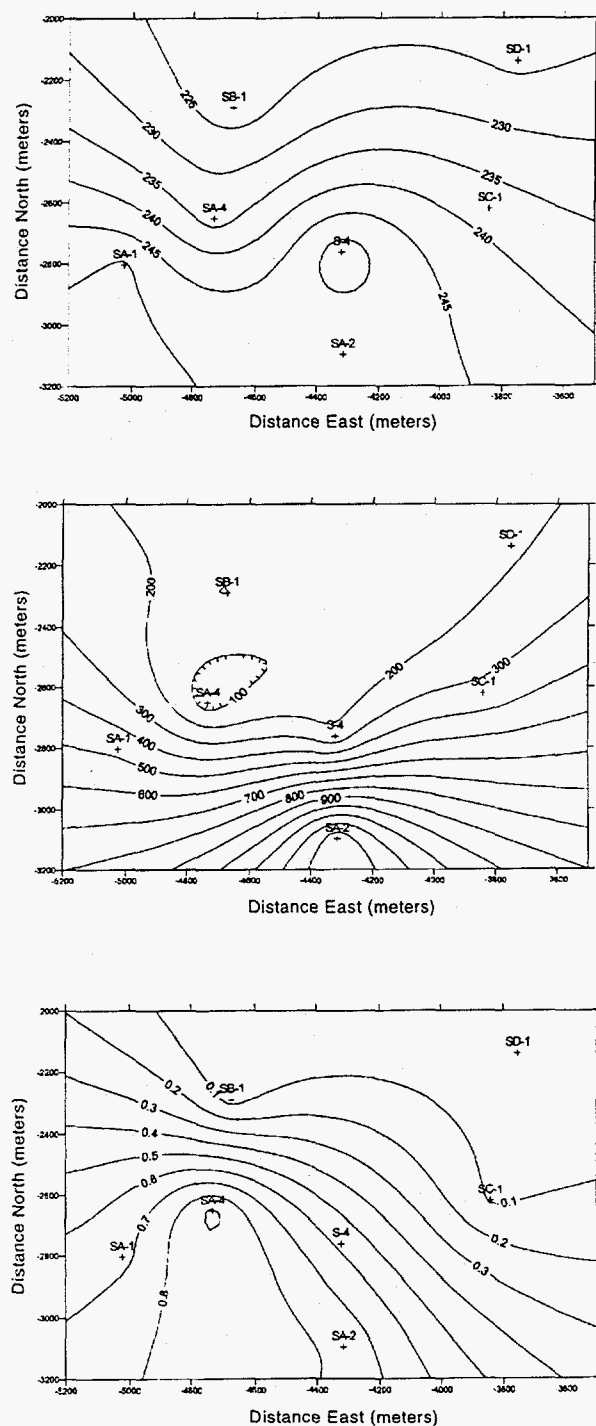


Figure 3.42. Contour map of average Sumikawa reservoir (a) temperatures, (b) chloride concentrations, and (c) IVF for 1989. Calculated as described for Figure 3.40.

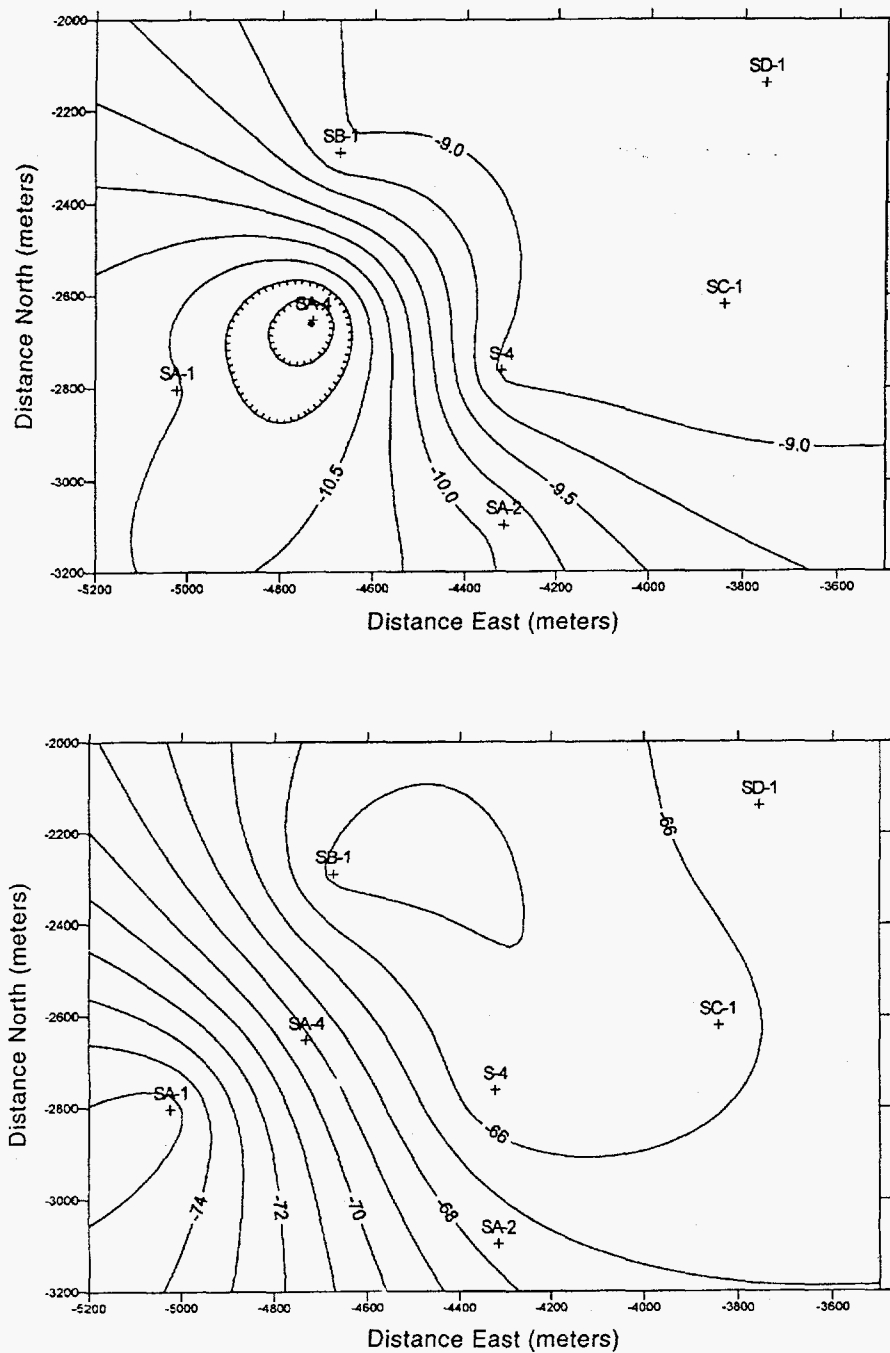


Figure 3.43. Contour map of average Sumikawa total discharge (a) δO (permil SMOW) and (b) δD (permil SMOW) for 1989. Data from Table A.4.

ably results from mixture with high-salinity, isotopically-heavy water of magmatic origin from the upflow zone near Mt. Yake.

3.7 Comparison of Stabilized Sumikawa Fluids and Ohnuma Production Fluids

In Section 3.3, we showed that in most discharge tests of Sumikawa wells, stabilized fluid compositions and temperatures were obtained. These compositions and temperatures along with characteristic ratios are shown in Table 3.1 (detailed data in Table A.6) together with similar data for Ohnuma well fluids and neutral hot spring waters.

Geothermometer temperatures for most Sumikawa wells are similar, with Na-K-Ca temperatures (T13) tending to 250°C. Wells SA-1 and SC-1 are significantly (270°C) hotter, and Ohnuma fluids are cooler at 220-230°C. Sumikawa aquifer chloride concentrations tend toward 140-200 mg/kg for wells S-3, S-4 and SD-1, 300 mg/kg for S-4 (high Cl), SB-1 and SC-1, and 500-600 mg/kg for wells S-2 and SA-1. Chloride concentrations of Ohnuma fluids (290-480 mg/kg) are significantly more concentrated than those of S-3, S-4 (low Cl) and SD-1 fluids but similar to that of fluids from other wells. Cl/B ratios are similar for all neutral samples (1.5-5), but acid S-2 waters have high Cl/B (~10). Cl/SO₄ ratios are also similar for Sumikawa and Ohnuma neutral, medium-enthalpy waters (1-5), but highly variable for high-enthalpy, SA-1 and SA-2 fluids. Acid S-2 waters are much lower in Cl/SO₄ (0.3) and acid Ohnuma waters are intermediate (0.7-1.9). Cl/As ratios range from 20-65 in most Sumikawa and Ohnuma neutral waters but are higher in S-2 and SA-2.

In general the comparisons show that a genetic relationship is possible between Sumikawa

and Ohnuma fluids with differences in temperature and salinity that could result from boiling and mixing processes. In particular, the lower temperatures and higher Cl concentrations are most probably caused by repeated production, boiling with separation of steam, and injection of residual water (see the next section). Ratios of conservative constituents (Cl/B, Cl/As) and some less conservative components (Cl/SO₄) tend to be very similar in Sumikawa and Ohnuma neutral waters.

3.8 A Model for the Sumikawa-Ohnuma System

The interrelations of thermal fluids in a geothermal system may be best understood using enthalpy-chloride and isotope diagrams. These diagrams reflect dominant boiling and mixing mechanisms as well as gain or loss of steam and conductive heating and cooling. In an enthalpy chloride diagram, processes which change the temperature and salinity of a fluid can be shown. (Enthalpy is used rather than temperature because it is a conservative quantity.) The direction of change of liquid enthalpy and chloride due to some of these processes is shown schematically in the upper right corner of Figure 3.44. These processes can be generally divided into those which occur slowly, usually in the natural state, and those which occur in response to a rapid change, usually due to exploitation. Slow processes might include boiling and steam loss taking place over a long enough time for rock temperatures to have adjusted to fluid temperatures so that no heat is transferred to or from the rock. Similarly, mixing with cooler water is usually also such a process because rock and fluid temperatures equalize rapidly. Rapid processes occurring in response to changes imposed during exploitation include isothermal evaporation during exploitation of a vapor-dominated system in which the heat in the rock maintains near-constant temperature while liquid boils in place to produce

Continued on page 3-54

Table 3.1. Comparison of Aquifer Temperature, Chloride Concentrations and Characteristic Ratios for Sumikawa and Ohnuma Well Fluids and Neutral Spring Waters Expressed in °C, mg/kg and Ratios by Weight.

	TQA	T13	Cl (aquif.)	Cl/B	Cl/SO ₄	Cl/As
S-2	230→255	215→245	238→540	3.9–5.7	0.9–1.1	45–75
S-2A*	233–248	238–260	181610	9.4–12.0	0.2→0.4	100–520
S-3	220–235	220–255	70→140	1.8–2.5	0.9→2.4	30–60
S-4	305→270	320→250	300→170	1.6–2.5	7.2→2.2	20–35
SA-1	259–279	232→286	132→470	1.1–1.5	7–9	18–23
SA-2	226–251	233–241	—	1.1–44	5–80	160–6000
SB-1	210–252	198–234	65→306	3→2.2	0.6→3.3	40–62
SN-7D	234–283	237–270	226–307	2.3–2.8	3.3→5.2	31–34
KY-2	236–243	220–228	143→213	2.3–2.6	1.3→1.9	38–62
Ohnuma neutral fluid	215–230	220–230	290–480	2.8–5.1	2.2–3.0	33–65
Ohnuma acid fluid	220–235	227–229	370–440	—	0.7–1.9	—
Neutral spring waters	110–177	123–186	82–295**	—	1.2–2.9	—

* Acid fluids after deepening

** Surface chloride

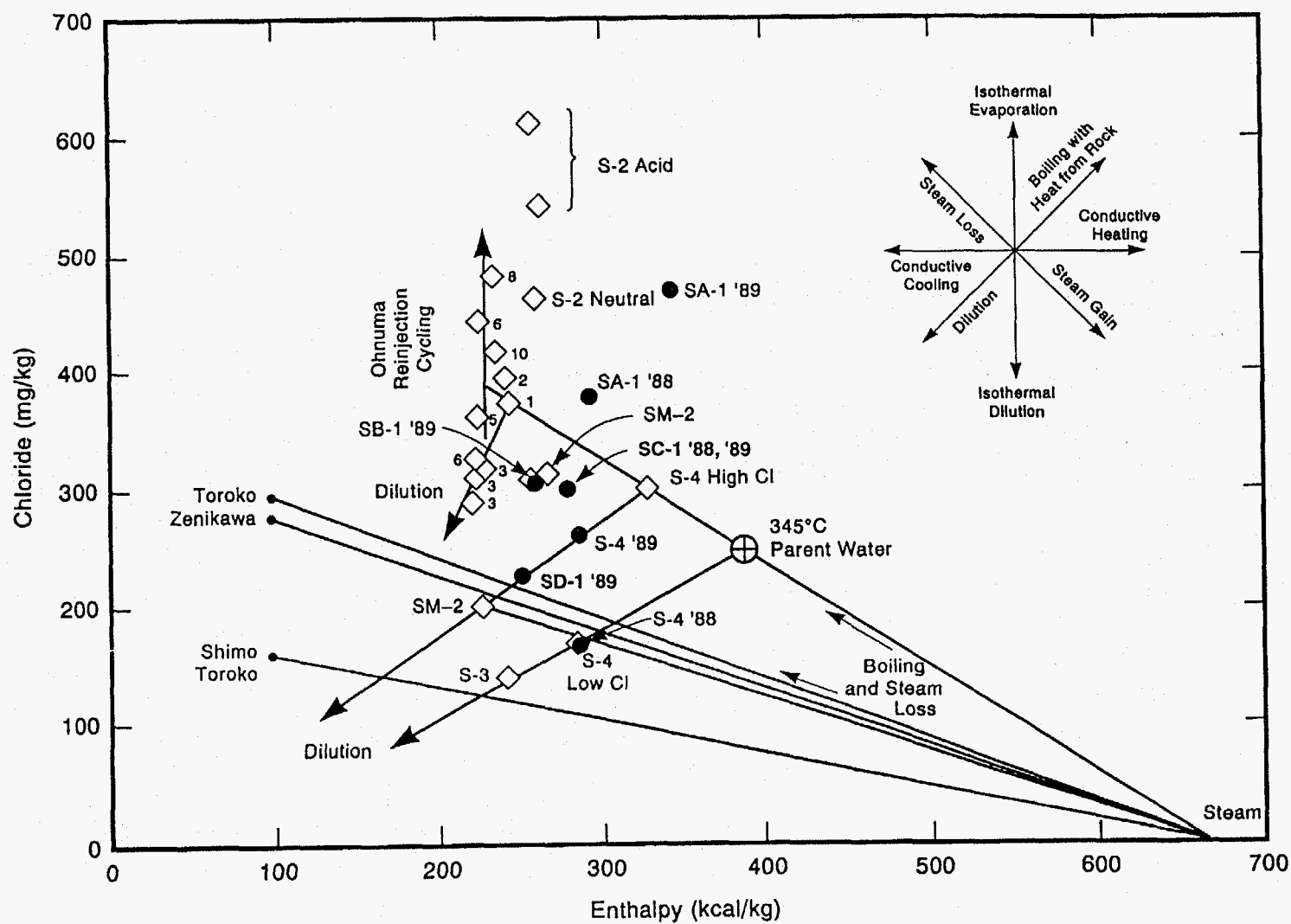


Figure 3.44. Enthalpy-chloride relations for aquifer fluids of Sumikawa and Ohnuma wells and for some related hot spring waters. Diamonds indicate 1984–1986 samples; circles indicate 1988 and 1989 samples.

steam. A somewhat less extreme example is boiling in response to pressure lowering when a well is opened. Boiling fluids cool and pick up heat from rock so that solute concentrations increase. Cooling takes place (so the process is not isothermal) but there is less cooling than would have occurred if the rock had not been present. In order to emphasize natural (slow) processes, the enthalpy values plotted in these diagrams are for reservoir liquid as calculated from geothermometer temperatures, rather than measured total discharge enthalpy values.

3.8.1 Enthalpy-Chloride Relations

Figure 3.44 shows enthalpy-chloride relations for reservoir fluids at Sumikawa and Ohnuma, and some neutral spring waters. The characteristics of Ohnuma waters are based on the few available analyses (usually only one per well) and Sumikawa waters were chosen to represent (as nearly as possible) the end member composition produced from the well. For wells S-2 and S-3 this is the stabilized composition after unloading of drilling water. For well S-4, the high chloride, high temperature water produced at the beginning of each test and the stabilized low-chloride water from the end of the tests are both represented. Samples collected between 1983 and 1986 are somewhat more consistent than 1988 samples and much more consistent than 1989 samples. The earlier samples are indicated by a diamond; later samples, by circles. For wells affected by 1989 cold water injection both 1989 and earlier compositions are shown. Fluids from wells that produced only steam (S-1, SA-2, SA-4) cannot be shown. Aquifer liquid enthalpy values were calculated assuming that the quartz-adiabatic geothermometer indicated true aquifer temperatures and liquid enthalpy values. Aquifer liquid chloride concentrations were calculated using these enthalpy values.

This diagram suggests that a parent water at 345°C with about 250 mg/kg chloride could produce the low-chloride S-4 water and the S-3 water by mixing with a low-chloride, slightly heated ground water (possibly at about 70°C and near zero chloride). The parent water could also produce the high-chloride S-4 water and the Ohnuma waters by boiling and steam loss. The Ohnuma waters have a small range of fluid enthalpy but a large range in chloride, which was suggested by Ito, *et al.* (1977) and KRTA (1985) to result from reinjection and cycling of residual water after steam separation. Some additional variation in chloride could also result from dilution with a low chloride, slightly heated groundwater (as for S-4 low-chloride and S-3). SB-1, SM-2 and SC-1 waters could be produced from the parent water by boiling followed by dilution. SD-1 (1989), S-4 (1989) and some SM-2 waters could be formed from dilution of S-4 high chloride water.

The temperature of 345°C indicated for the parent water is similar to that observed in high-temperature geothermal systems (e.g. Cerro Prieto, Baca) and is related to the solubility maximum of quartz at about 340°C, with quartz precipitation reducing permeability at higher temperatures. It may be possible to verify the presence of a reservoir at 345°C by using slow-reacting isotope geothermometers such as $\delta\text{O}(\text{SO}_4\text{-H}_2\text{O})$ or $\delta\text{C}(\text{CO}_2\text{-CH}_4)$ on some of the Sumikawa well fluids.

The only Sumikawa waters that do not fit into this genetic model are those from wells S-2 and SA-1. These waters are much higher in chloride than all other Sumikawa waters and almost all Ohnuma waters. Concentration by residual water recycling (as at Ohnuma) is not reasonable and solution of chloride-containing evaporites is very unlikely. These waters may contain a magmatic

component that has not been diluted or, in the case of S-2, fully neutralized.

3.8.2 Isotope Relations

Additional indications of relations among Sumikawa and Ohnuma thermal waters may be obtained from oxygen and hydrogen isotope analyses. Meteoric waters that have not evaporated or reacted with rocks fall along a "meteoric water line" characteristic of the geographical area. The line for Japan suggested by Sakai and Matsubaya (1977) is $\delta D = 8 \delta^{18}O + 18$. Geothermal waters usually have nearly the same δD values as local meteoric waters but have higher δO because of the "oxygen isotope shift" in which aqueous oxygen-18 is enriched by exchange with rock oxygen. Rock hydrogen is so scarce that it has negligible effect. Some "volcanic" geothermal waters may show increases in $\delta^{18}O$ and δD related to "andesitic" water (Giggenbach, 1991).

Boiling and mixing also affect isotope compositions. Boiling enriches residual liquid in oxygen-18 and (below 220°C) in deuterium. Between 220°C and the critical point, the deuterium fractionation is small and inverse, so boiling above 220°C does not greatly affect δD values. Mixing with meteoric waters generally decreases δO values and may either increase or decrease δD values according to whether the deuterium content of the meteoric water is higher (lower altitude) or lower (higher altitude) than the thermal water. Evaporation increases both δO and δD and these values are usually high for acid sulfate waters.

Isotope compositions of waters of the Sumikawa-Ohnuma area are shown in Figures 3.45, 3.46 and 3.47. Well waters are plotted in Figure 3.45 at their total discharge compositions calculated from separate analyses of steam and water (MMC, 1985;

with additional data from Ueda, *et al.*, 1991). The analyses of all waters are given in Table A.5 and selected analyses (used in the figures) are given in Table A.4. The river and creek analyses fall close to the meteoric water line; all thermal waters fall to the right of the line showing the effects of oxygen isotope shift or boiling. As pointed out by KRTA (1985) there is a general correspondence between the chloride contents and the δO values, with the Ohnuma waters the most concentrated and highest in δO and Sumikawa waters the most dilute and lowest in δO . In Figure 3.45 the analyses are numbered in order of collection. There is unfortunately a wide range of analyses for all Sumikawa well samples; wider than would be expected from analytical variation (usually ± 0.1 in δO and ± 1 in δD). Some of this variation is due to transients, such as the unloading of drilling water in S-3 (the later analyses are probably more characteristic) and the initial high chloride, high temperature flow of S-4 before 1988. The S-4 analyses in particular vary widely; one analysis is similar to Ohnuma waters and others are as much as 2 permil (parts per thousand) lower in δO and almost 12 permil lower in δD than the average. Generally the S-3 water seems to have resulted from mixing low-Cl S-4 water with river water, and the Ohnuma waters, from boiling and low-temperature evaporation of high-Cl S-4 water. The Ohnuma waters have been repeatedly flashed and reinjected, producing increases in δD and δO relative to their calculated composition. The increase in δD indicates evaporation at temperatures below 200°C.

Locating the parent water on this graph is difficult. From the enthalpy-chloride plot, S-4 high-chloride water is produced from the parent water by boiling and S-4 low-chloride water is formed by dilution. Therefore, the parent water should have higher δO than S-4 low chloride water (and be on a line with it and meteoric waters)

Continued on page 3-59

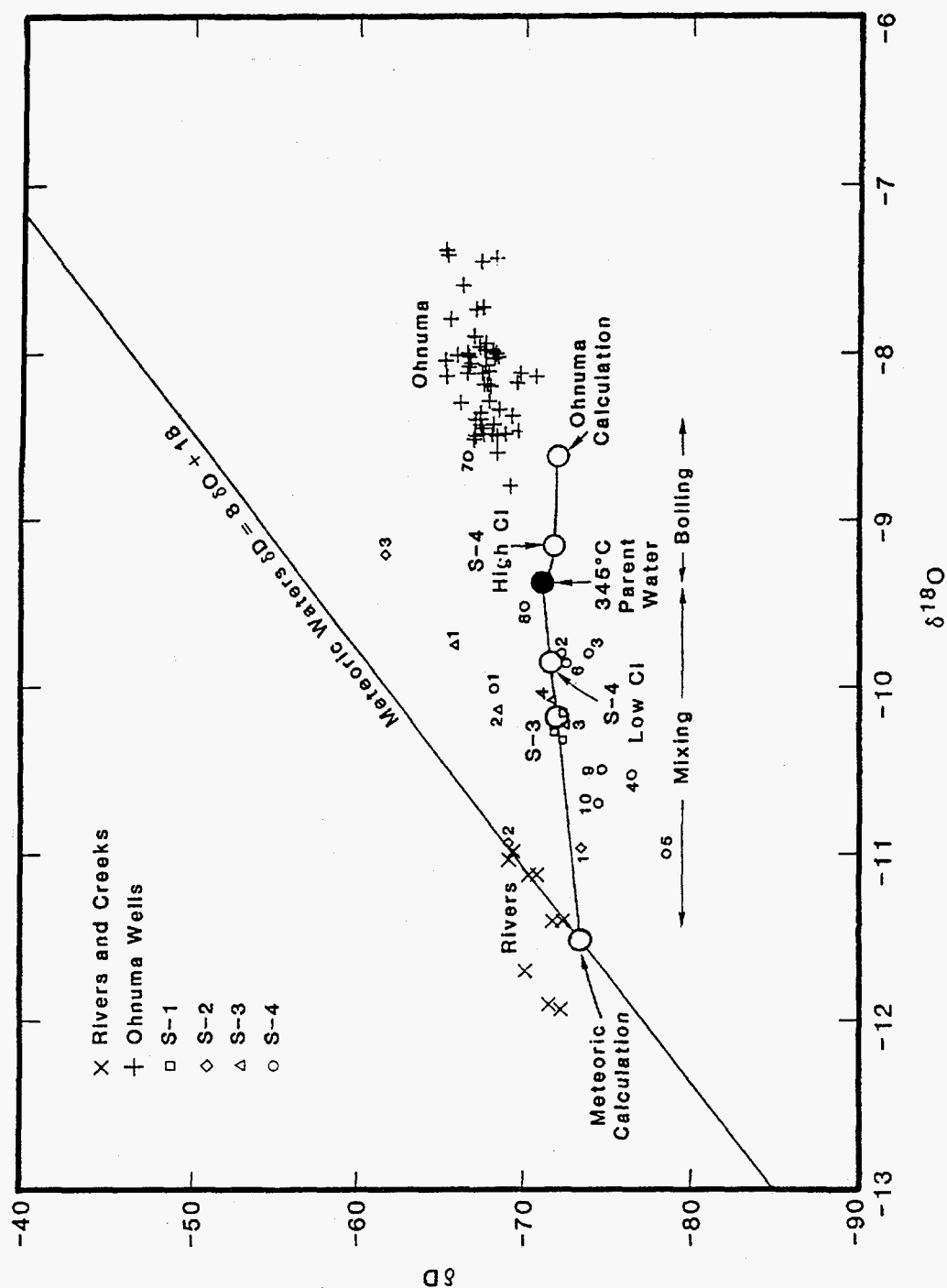


Figure 3.45. Isotope relations for 1983 to 1986 Sumikawa and Ohnuma total discharge fluid compositions and local meteoric waters with processes from Figure 3.44 indicated. Numbers next to points indicate time sequence of samples for each well. Large circles are calculated.

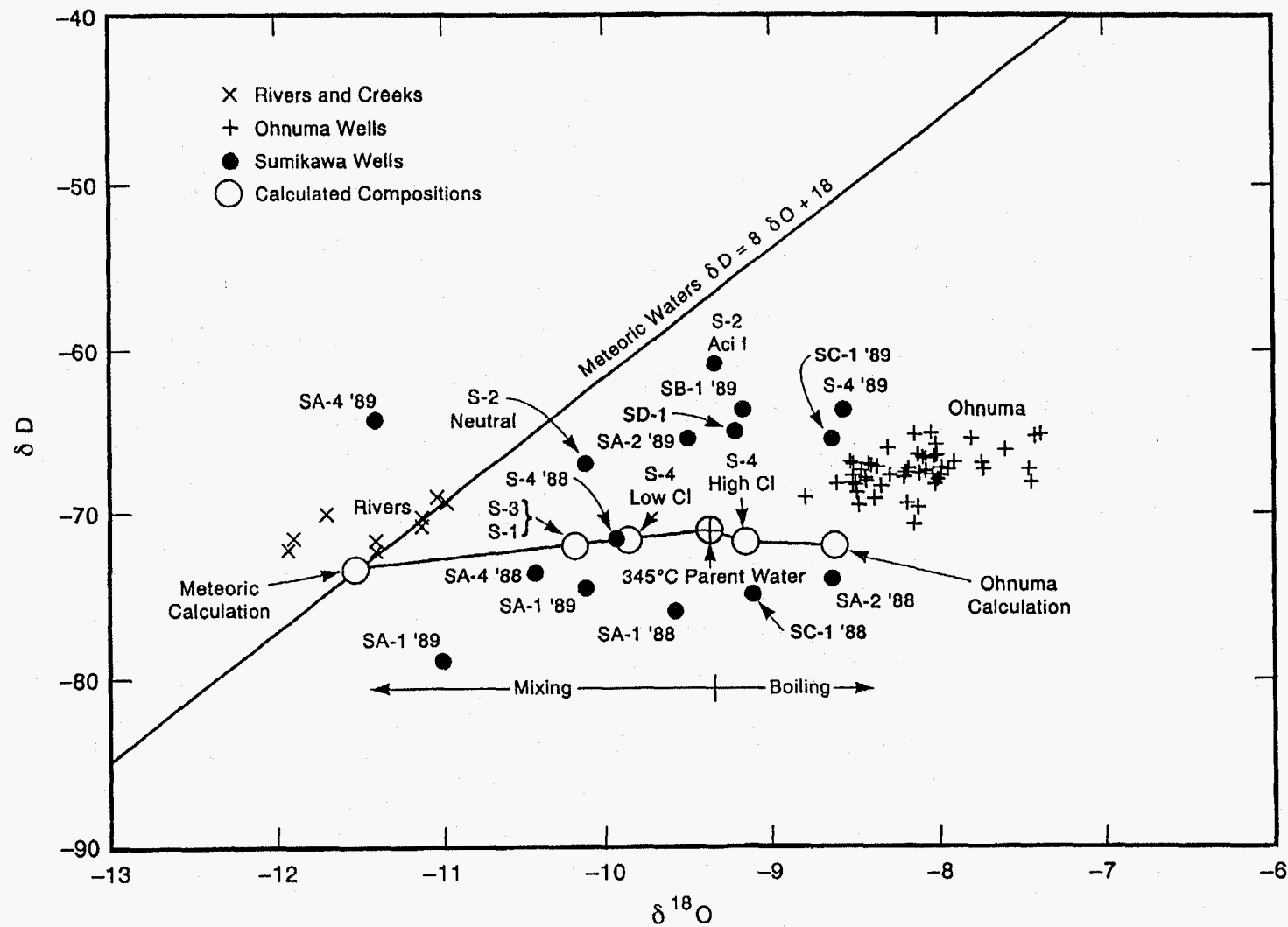


Figure 3.46. Isotope relations for 1988 to 1989 Sumikawa (and Ohnuma) total discharge fluid compositions with calculated compositions from Figure 3.45.

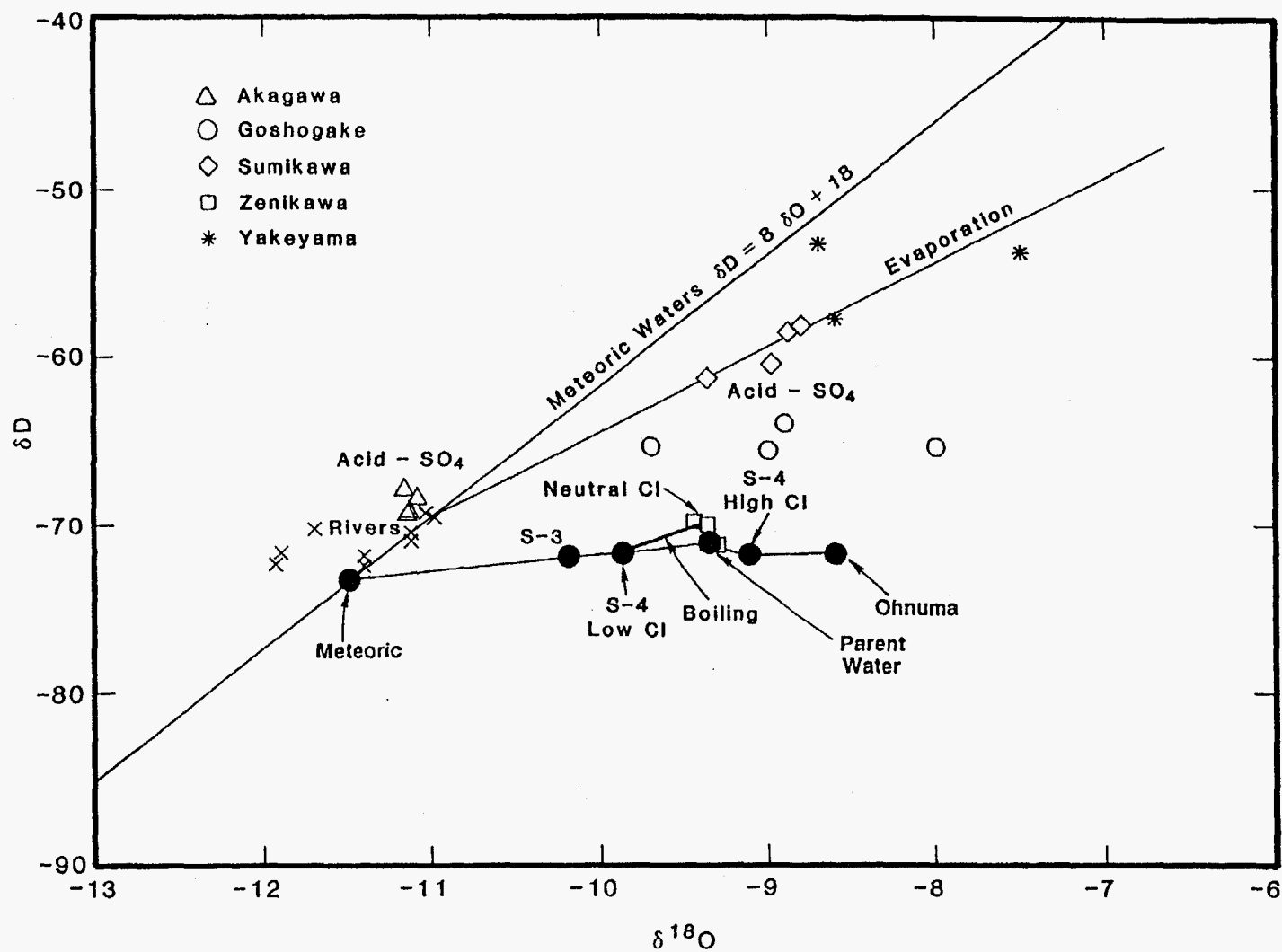


Figure 3.47. Isotope relations for hot springs of the Sumikawa area and meteoric waters with processes from Figures 3.44 and 3.45 indicated. Solid circles are calculated.

and it should have lower δO than S-4 high-chloride water. The isotope analyses and the mixing proportions (from the Cl-enthalpy diagram) of meteoric water, S-3 and low-Cl S-4 waters indicate the δO and (less certainly) δD composition of the parent water.

The variability of the S-4 isotope analyses provides considerable freedom of interpretation. The intermediate isotope compositions correspond reasonably well with that of the calculated low-Cl, low-enthalpy fluid, and a few analyses appear to be mixtures of the high-chloride and low chloride waters, but the high-chloride water was only produced at the start of each year's test and isotope analyses of this water are lacking. The magnitudes of isotope changes due to boiling are relatively small (Henley, et al., 1984). For boiling from 345°C to 300°C (parent to S-4 high-chloride), δO would change by 0.19 and δD by -0.7 permil. For boiling from 300°C to 220°C (S-4 high-chloride to Ohnuma) δO would change by 0.45 and δD by 0.02 permil. Locations are shown on Figure 3.45 that would satisfy these values and the mixing proportions of parent waters, S-4 low-chloride waters and S-3 waters required by the enthalpy-chloride diagram. Although steam-only samples cannot be plotted on a Cl-enthalpy diagram, they can appear on isotope diagrams. The isotope composition of S-1 steam appears to be very similar to that of S-3 water.

Isotopic compositions of samples collected in 1988 and 1989 are shown in Figure 3.46 along with the calculated isotope compositions (from Figure 3.45) related to processes indicated by the enthalpy-chloride diagram (Figure 3.44).

Hot spring analyses are shown on a separate diagram (Figure 3.47). In this figure the acid-sulfate springs are seen to be either the same as mete-

oric water (Akagawa) or related along an evaporation line (Sumikawa and Yakeyama). Only Zenikawa water relates to the well waters. These spring waters appear to be boiled from S-4 low-chloride water with continuous steam separation suggesting a change in δO of +1.0 permil (versus +0.5 observed) and in δD of +4.1 permil (versus +3.0 observed).

3.8.3 Isotopic Effects of Cold Water Injection

As discussed earlier, the 1989 tests for recovery from cold water injection produced only short term changes in liquid and total enthalpy because these quantities were buffered by heat contained in the rock. Chloride recovery was slower and in some cases not complete in 1989 because chloride is contained only in fluids and is not buffered by interaction with rock. Isotope compositions are also not buffered because oxygen isotope exchange is slow and would probably not equilibrate during the test and because rocks contain so little hydrogen that they cannot buffer fluid δD values.

In Figure 3.46 and Table 3.1 the isotopic compositions of the best stabilized 1988 and 1989 samples are shown. Usually these samples were collected last. Both 1988 and 1989 data are identified where they differed. The 1988 data appear similar to earlier data but most 1989 data are markedly higher in both deuterium and oxygen-18.

The 1988 S-4 total discharge composition is nearly the same as the earlier low-chloride S-4 composition as was the case in the enthalpy-chloride diagram. The total discharge isotope composition from SA-4 in 1988 is similar to earlier S-3 compositions and could also have formed by dilution of the S-4 low-chloride water. SC-1 and SA-2 total discharge compositions are similar to earlier S-4 high-chloride and Ohnuma

compositions, respectively, which were indicated to have formed from the 345°C parent water by boiling and steam loss. SA-1 compositions in 1988 and 1989 do not fit the model nor do any 1989 compositions.

The cold water injected into the wells in early 1989 must have higher deuterium than the reservoir waters by 5 permil or more because even the least diluted samples are displaced to higher deuterium compositions by up to 5 permil. The 1989 compositions are probably also displaced to higher oxygen-18 by up to 1.5 permil (S-4) but the difference is less striking.

The results of comparisons of 1988 and 1989 samples on enthalpy-chloride and isotope diagrams has shown that generally the newer well samples are genetically similar to earlier samples from wells S-3 and S-4. Without the distortions caused by cold water injection in 1989 this conclusion would probably be more definite.

3.9 Gas Geothermometer Calculations

Equilibria between gases contained in reservoir fluids are the only indicators of reservoir temperature for dry steam discharges and provide independent temperature indications for reservoirs with two phase production. Perhaps more importantly they indicate the fractions of vapor and liquid in the reservoir that contribute to the production fluid. These indications can be used to estimate reserves of vapor-dominated systems and show the extent and location of boiling in hot water systems. Calculations of reservoir temperatures and reservoir steam fractions were first described by Giggenbach (1980) and D'Amore and Celati (1983). They are presented in detail in Appendix A based on D'Amore and Truesdell (1985).

These calculations are based on the assumption that certain gas reactions are in equilibrium in both liquid and vapor phases in the reservoir and that the fluid produced is a mixture of reservoir liquid and reservoir vapor. If two equilibria are considered, each in equilibrium in the reservoir in both liquid and vapor, then both the reservoir temperature and the fraction of vapor ("y") contributing to production can be calculated graphically with constant values of each quantity shown as lines that form a grid (Figures 3.48–3.59). The isothermal lines are more or less S-shaped, and in a complete grid (approximated in Figure 3.48) increase from 125°C on the left to 350°C on the right in 25 degree increments. Lines of constant y value (steam fraction) are less curved (y=0 is almost straight) and increase from -0.1 on the lower right to 1.0 on the upper left. The increase is approximately logarithmic. While positive y values indicate the relative amounts of steam and water contributing to production, negative values indicate the degree of depletion of gas in a recently-boiled water that has not yet equilibrated with coexisting steam.

At Sumikawa, gas analyses of steam samples have been made from collections during each flow test. Application of the gas geothermometer to all samples (Figure 3.48) shows that many analyses do not give reasonable results. Many points fall outside the grid of possible equilibrium compositions and there is a wider spread of calculated temperature and steam fraction than would be reasonable for a single geothermal reservoir.

Study of the data suggests that there are possibly two problems with the application of this method to these Sumikawa gases. Samples collected from 1983 to 1986 (and some from 1988) show generally reasonable temperatures (reservoir steam fractions cannot be independently calculated), but with a spread of points that may be due

Continued on page 3-73

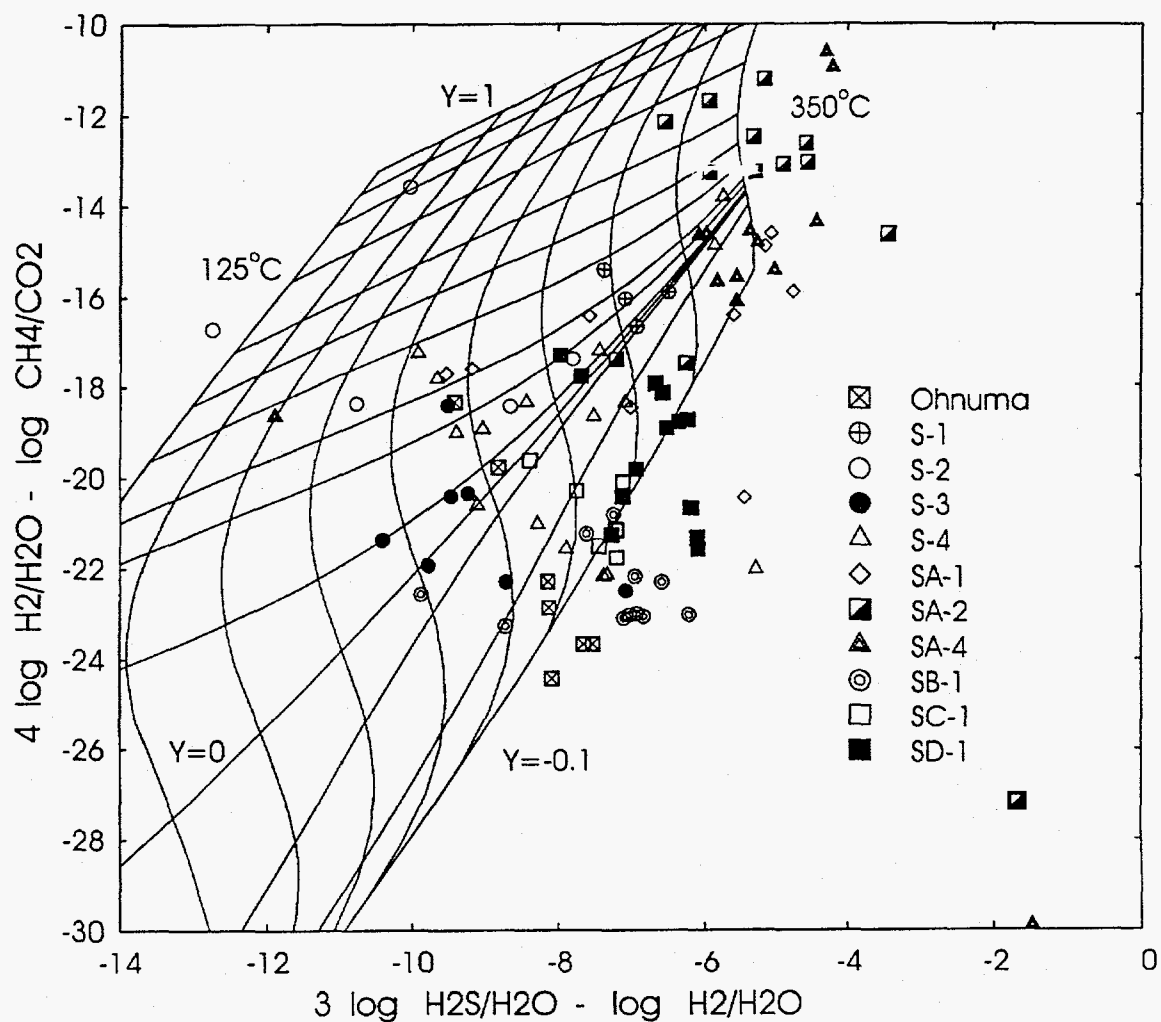


Figure 3.48. Gas geothermometer grid diagram for Ohnuma and Sumikawa wells using all available data. For this diagram (and those that follow), grid lines for temperature are (left to right) 125, 150, 175, 200, 225, 250, 275, 300, 325 and 350 degrees celsius and gridlines for reservoir steam fraction, Y, are (top to bottom) 1.0, 0.75, 0.5, 0.25, 0.1, 0.05, 0.025, 0.01, 0.005, 0.001, 0.0, -0.001, -0.01 and -0.1.

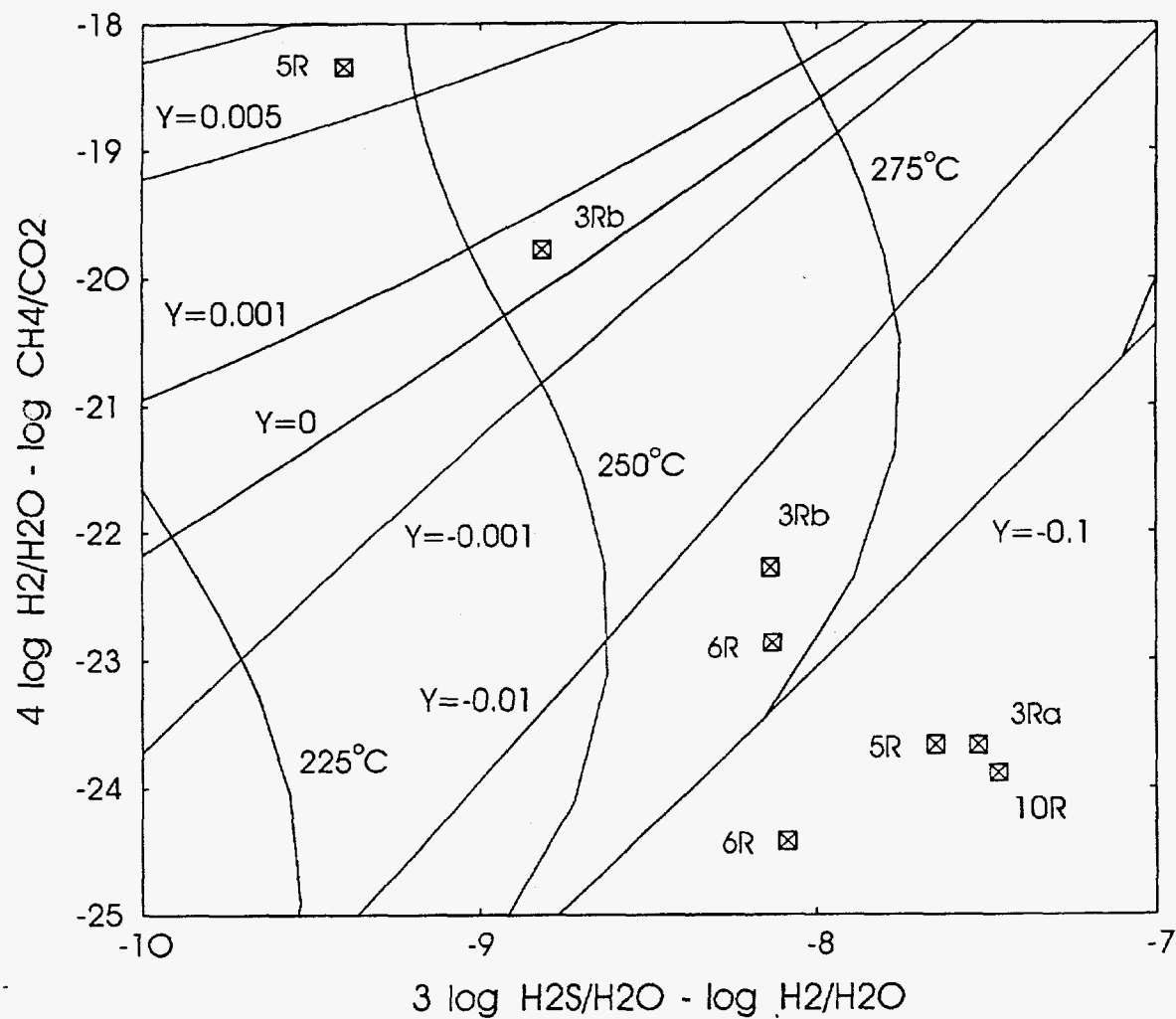


Figure 3.49. Gas geothermometer grid diagram for Ohnuma wells. Grid shown in this and following figures is part of the grid shown in Figure 3.48. See text for discussion.

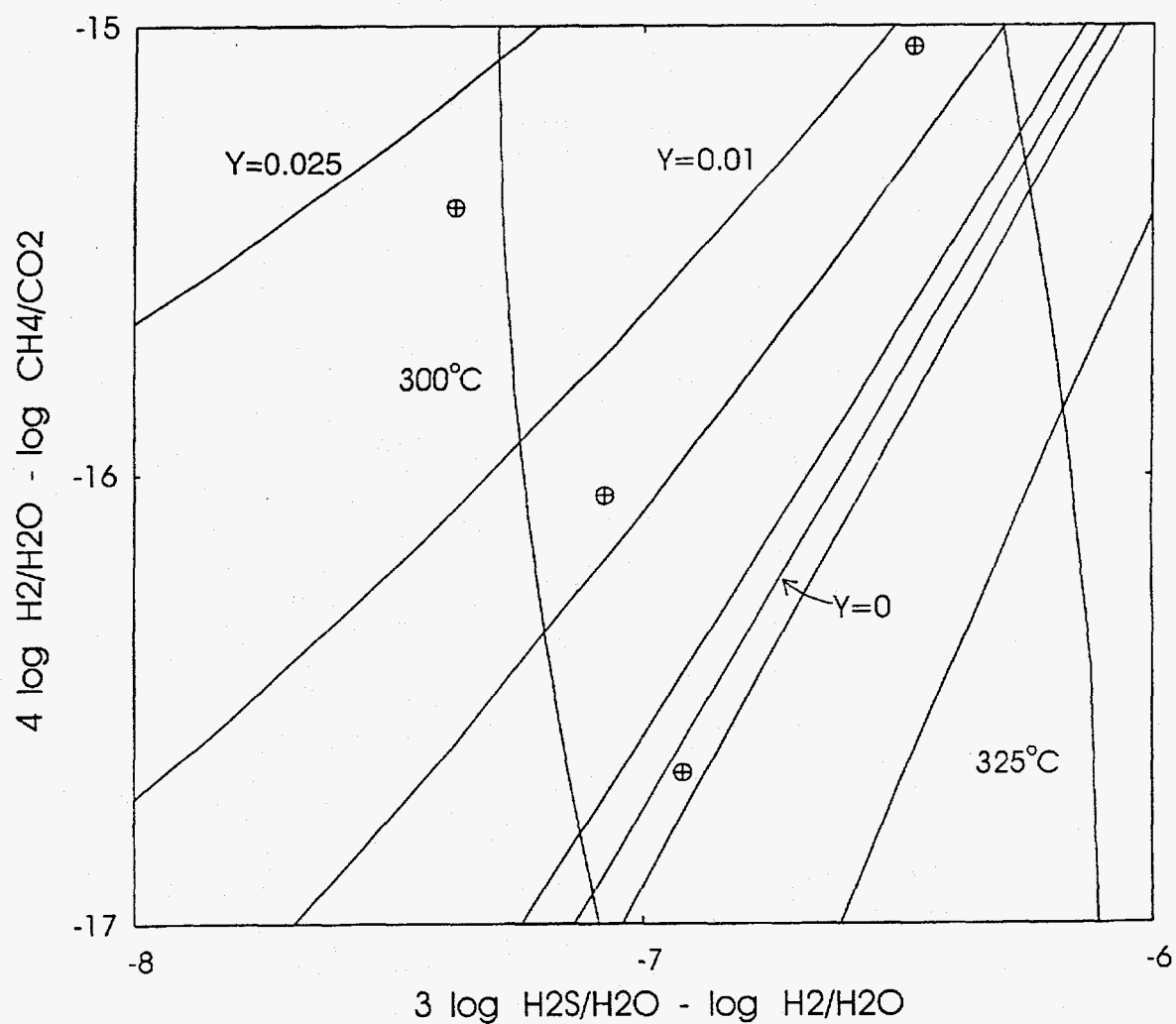


Figure 3.50. Gas geothermometer grid diagram for Sumikawa well S-1. Grid shown is part of the grid shown in Figure 3.48. Note the limited ranges of Y and T . This well produced pure steam but the diagram indicates that the reservoir contained less than two percent vapor.

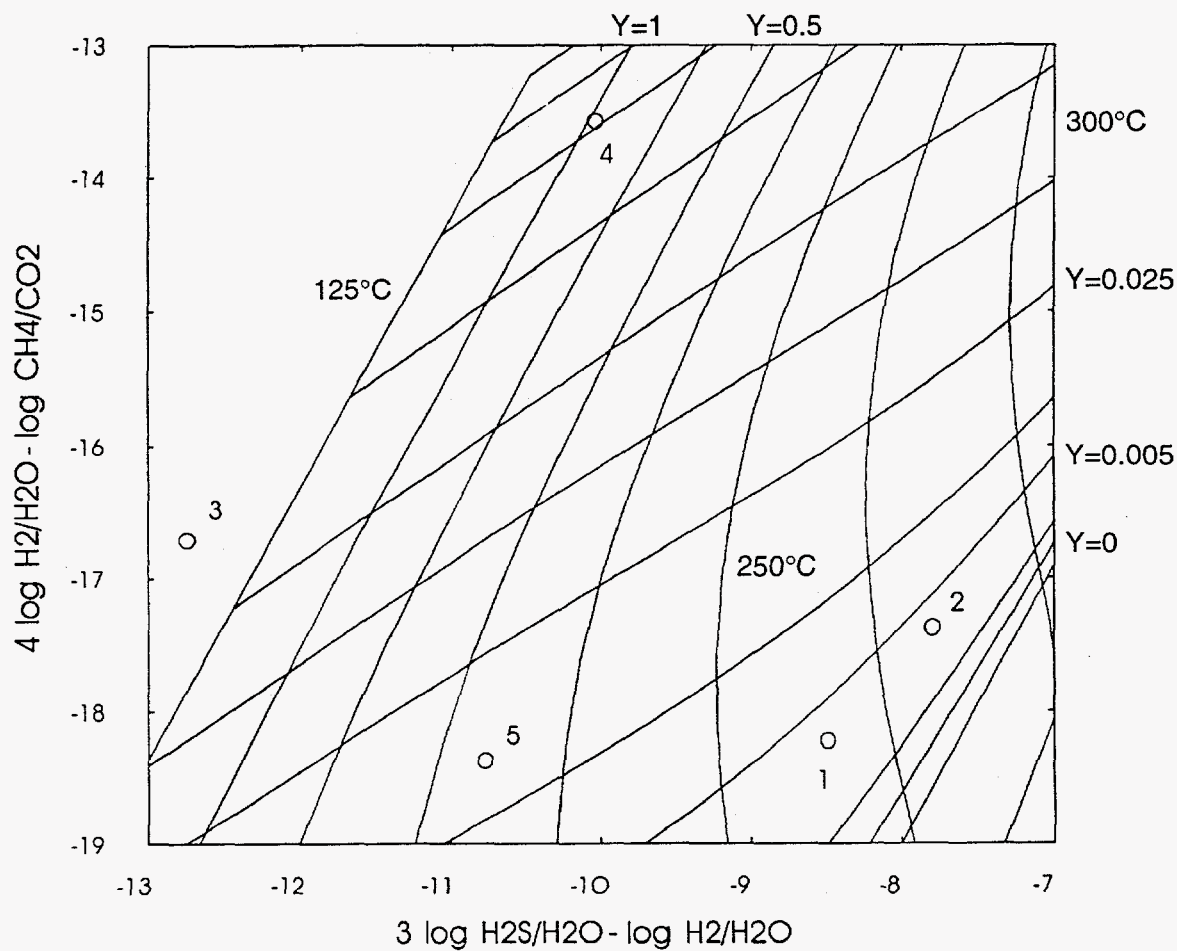


Figure 3.51. Gas geothermometer grid diagram for Sumikawa well S-2. Points 3-5 are samples collected after the well was deepened and fluids became acid.

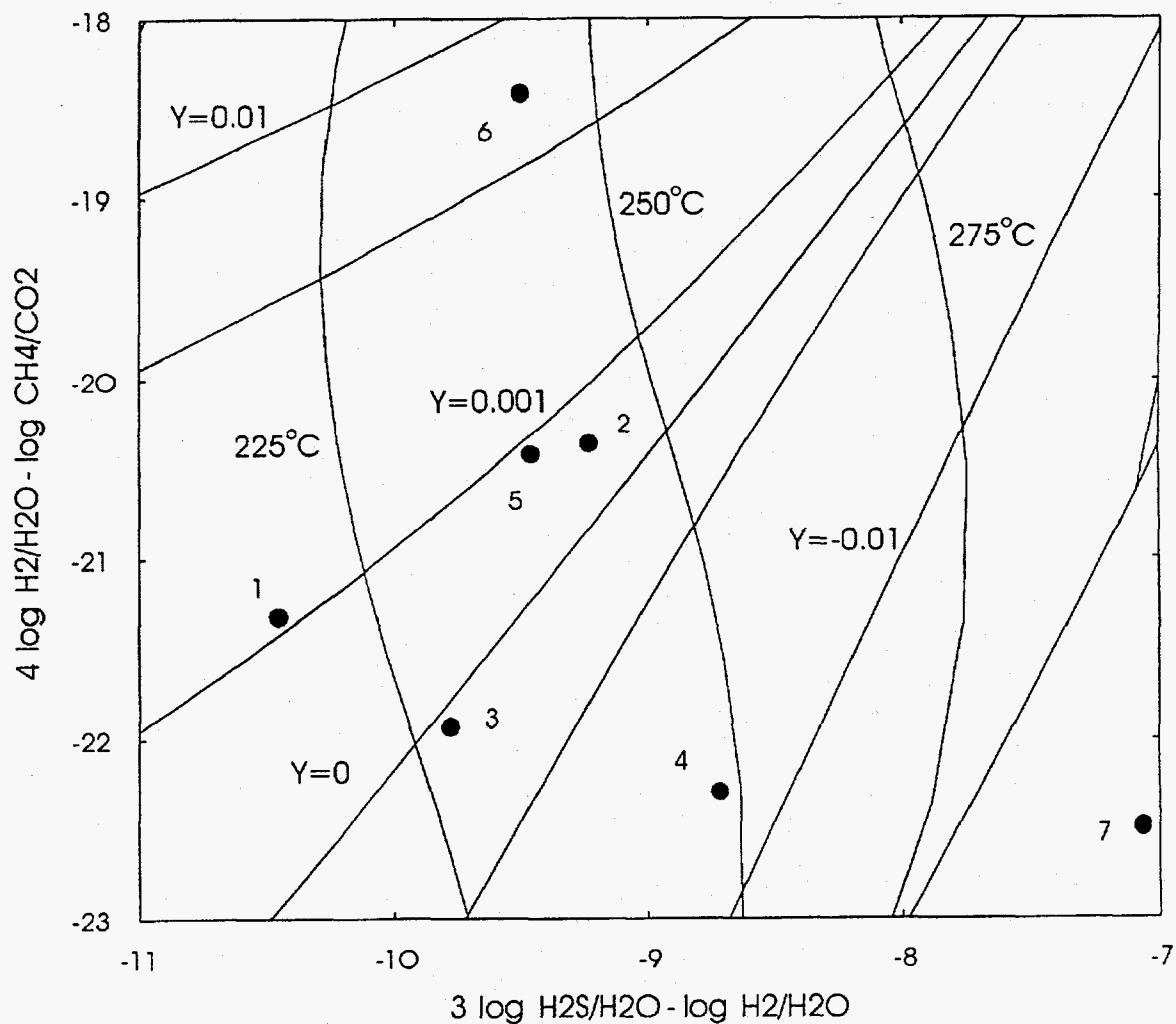


Figure 3.52. Gas geothermometer grid diagram for Sumikawa well S-3. All but the last point indicate equilibrated liquid at 220 to 250°C.

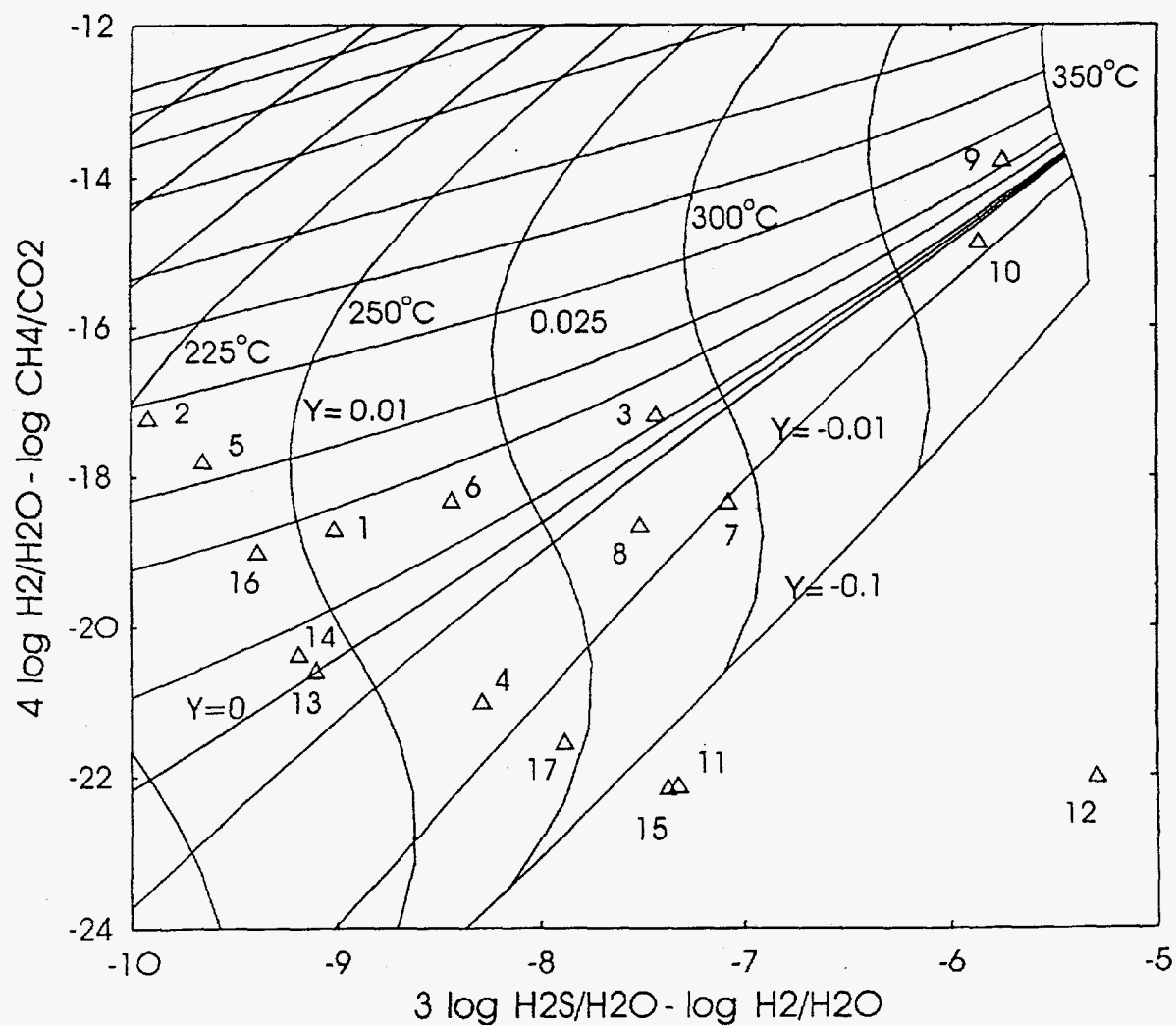


Figure 3.53. Gas geothermometer grid diagram for Sumikawa well S-4. The first eight points from 1984 to 1986 indicate equilibrated liquid. The other points possibly indicate disequilibrium in part caused by cold injection.

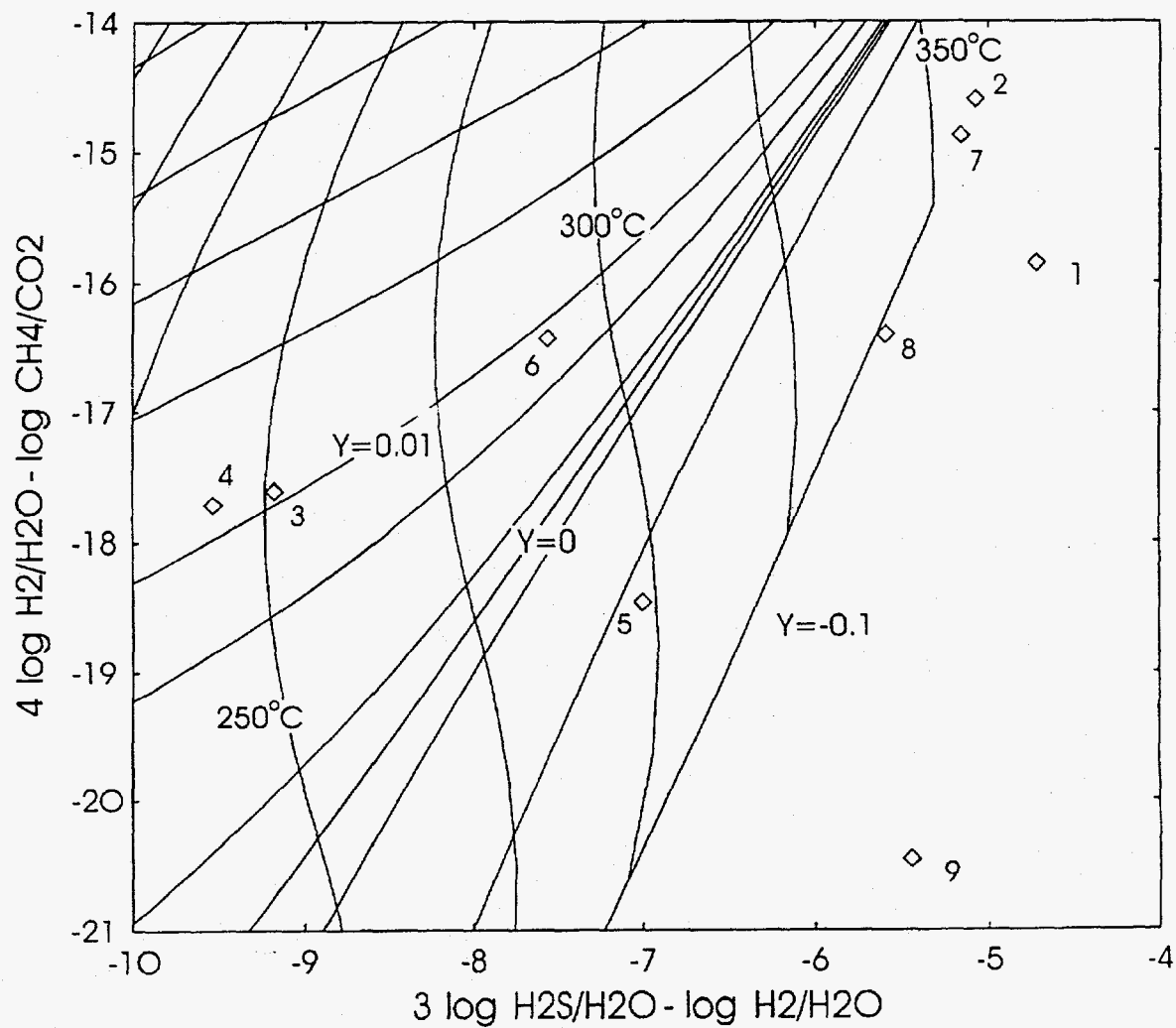


Figure 3.54. Gas geothermometer grid diagram for Sumikawa well SA-1. The last points indicate gas depletion caused by cold water injection.

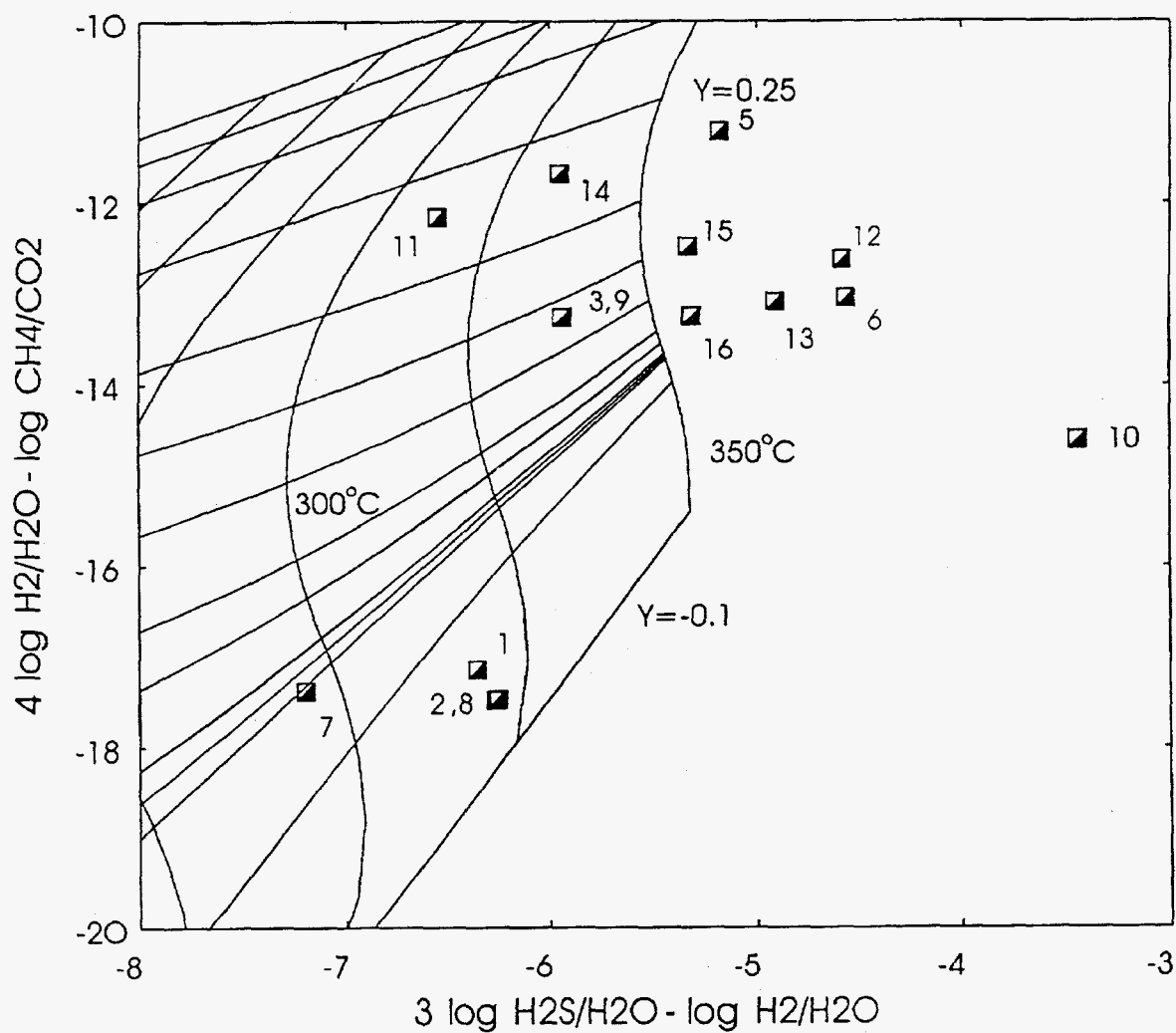


Figure 3.55. Gas geothermometer grid diagram for Sumikawa well SA-2. This well and SA-4 produce nearly pure steam and indicate unreasonably high temperatures on this diagram.

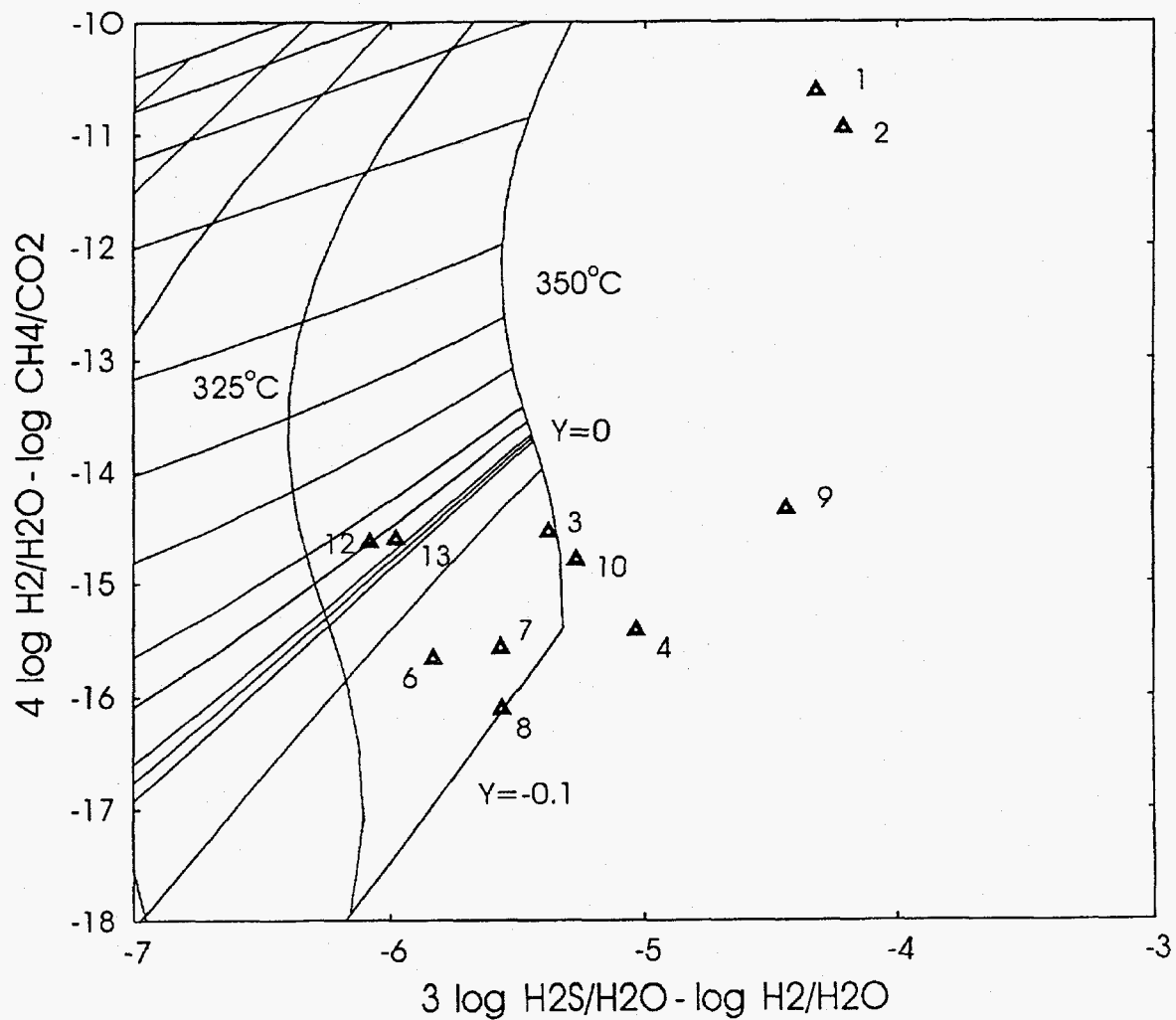


Figure 3.56. Gas geothermometer grid diagram for Sumikawa well SA-4.

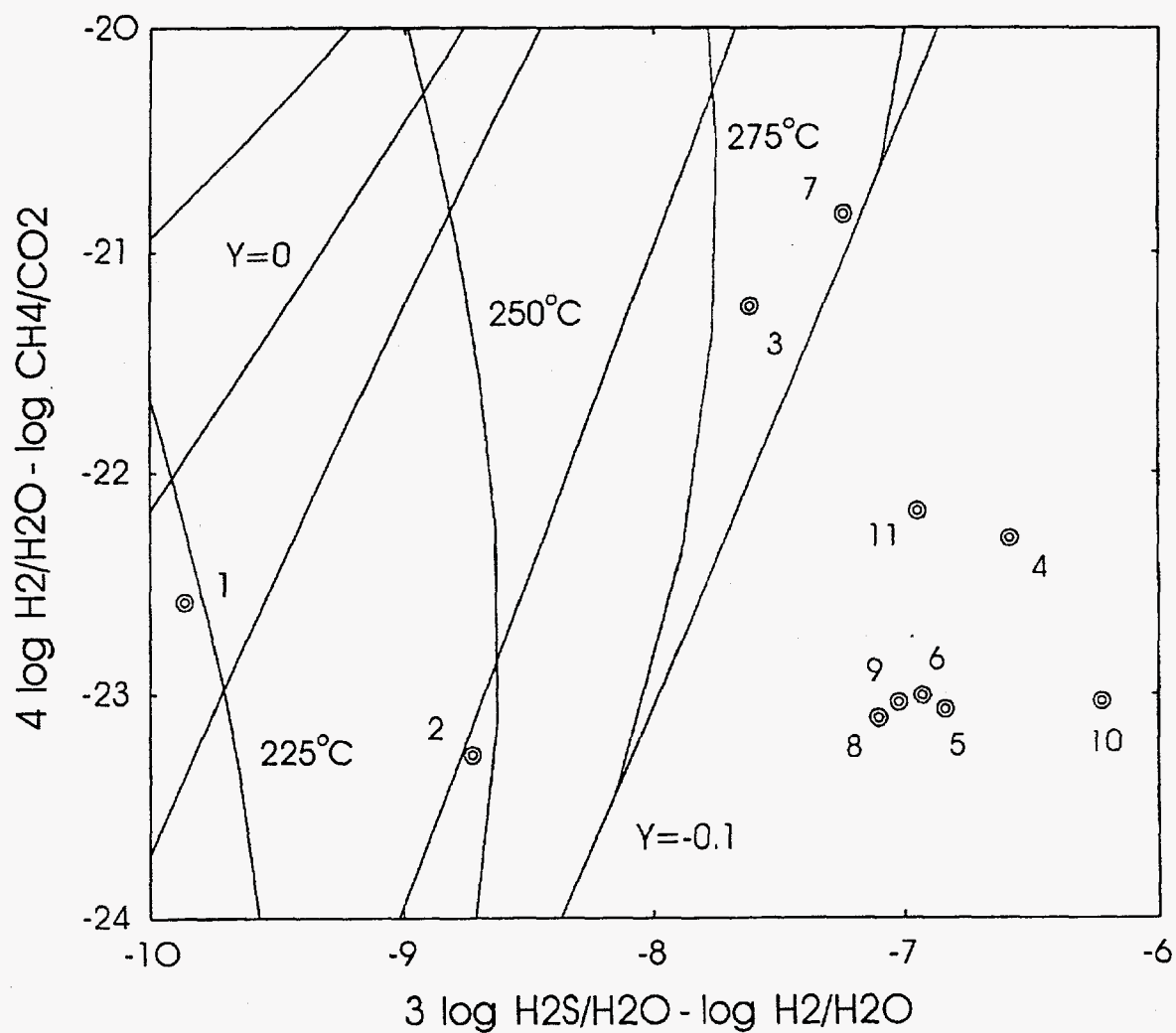


Figure 3.57. Gas geothermometer grid diagram for Sumikawa well SB-1. All collections from this well (as well as SC-1 and SD-1) were in 1989 after the field-wide injection of cold water probably causing the strong gas depletion indicated for most samples.

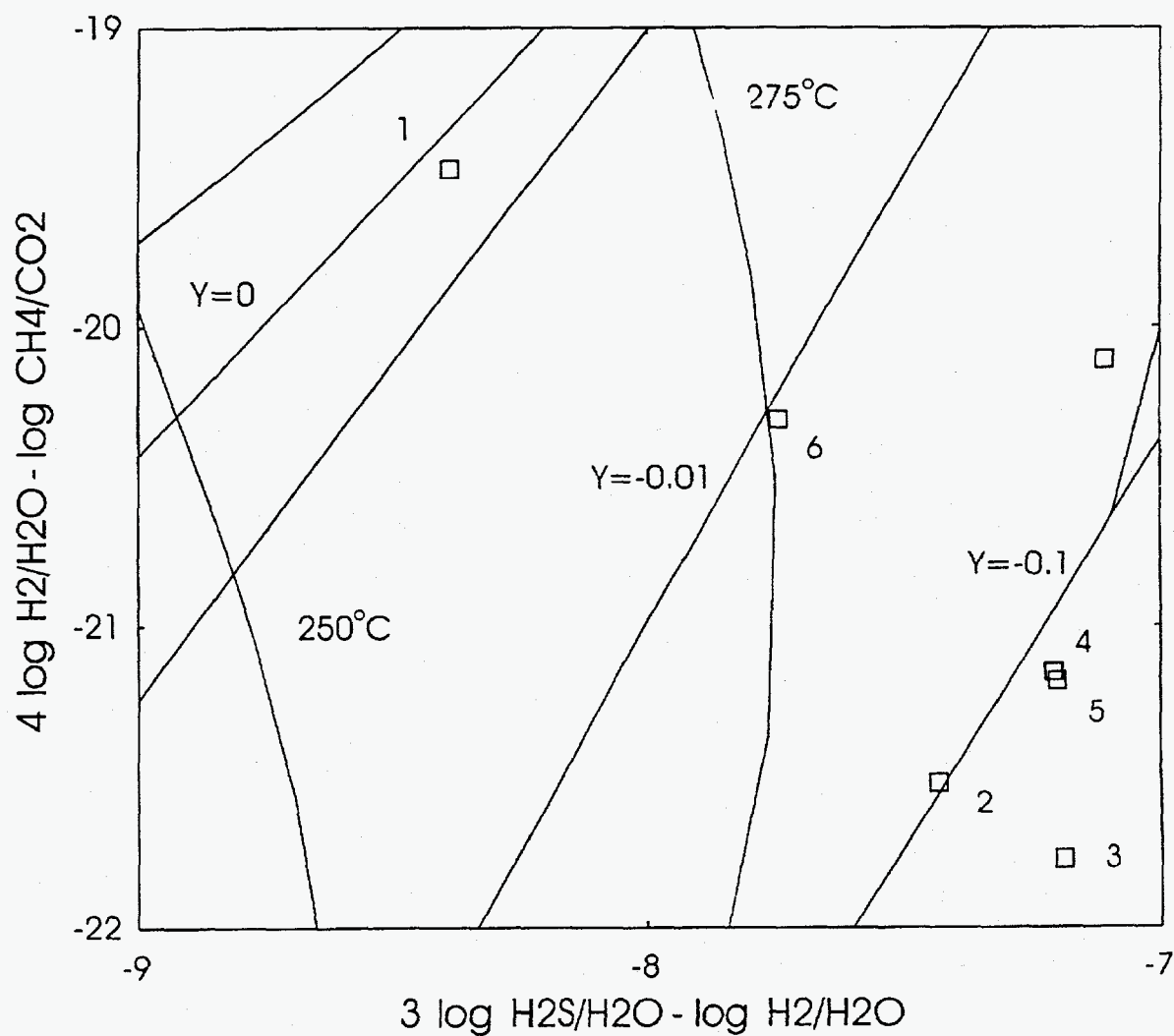


Figure 3.58. Gas geothermometer grid diagram for Sumikawa well SC-1. Although cold water was not injected in this well most points show more than 10 percent gas depletion, possibly influenced by cold water injected elsewhere.

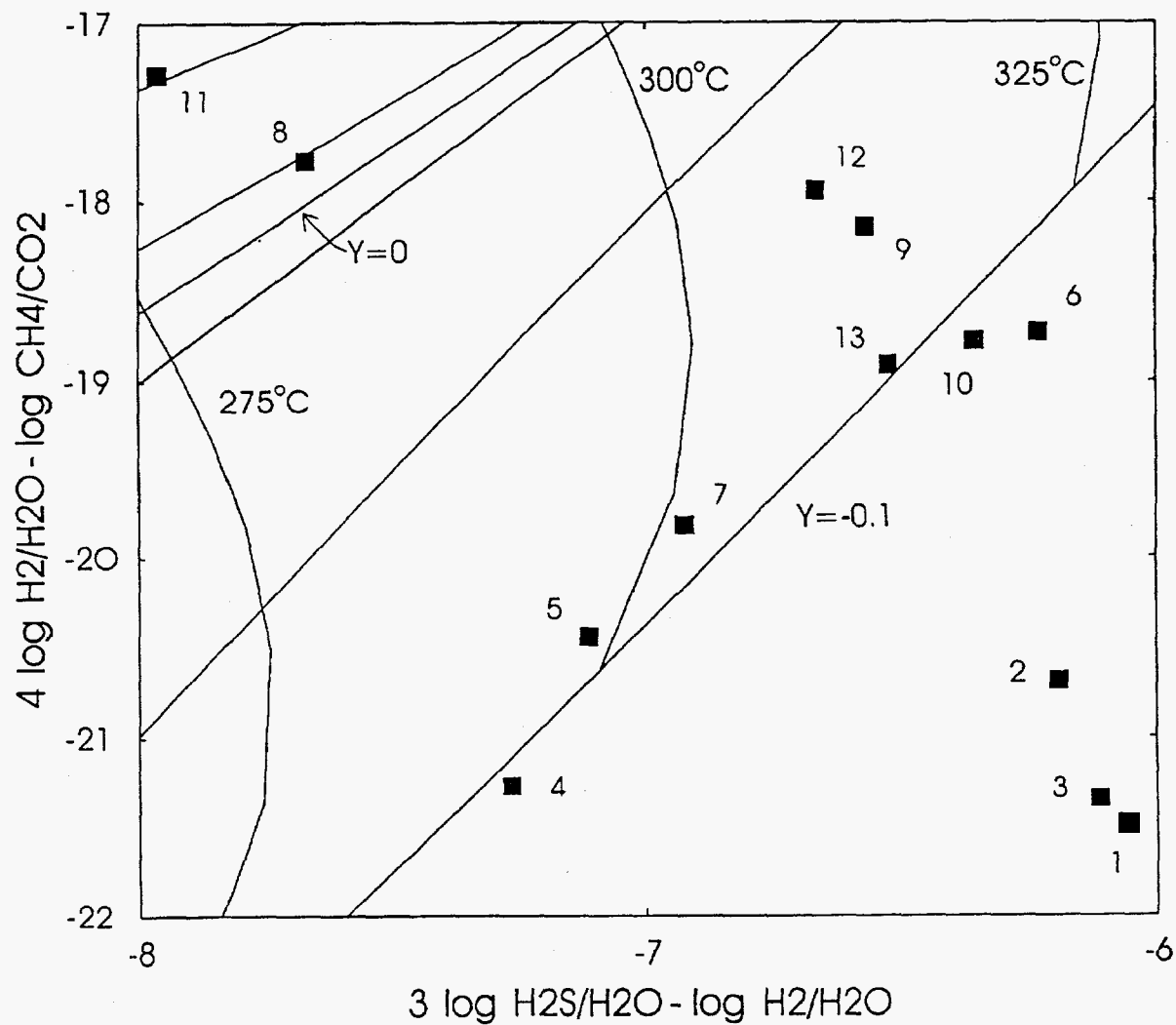


Figure 3.59. Gas geothermometer grid diagram for Sumikawa well SD-1. This well also shows gas depletion but with some recovery in the later samples.

to the discontinuous production history. Gas compositions of samples collected in 1989 generally plotted outside the grid. It appears that in 1989 disequilibrium caused by cold water injection had affected gas compositions.

In order to show the changes with time of calculated points for individual wells, plots were made for each well with points numbered to show the sequence of sampling. Almost all complete analyses in Table A.3 were plotted, although estimated steam fractions were necessary for some. Each plot shows only the part of the grid with points for the well considered.

The published Ohnuma gas analyses with complete data are shown in Figure 3.49 (well names rather than sampling numbers are shown). The indicated temperatures (240 to 270°C) are higher than those from solute geothermometers (220 to 230°C), and half the points show a range of y of +0.01 to -0.01 (liquid only) with the rest more negative indicating gas depleted waters. This indicated depletion probably results from injection of degassed, residual water from separators.

Well S-1 produced only steam and all reported samples were collected in April 1982. Figure 3.50 shows a small range of temperature from 295 to 320°C and of y from 0 to 0.02. The y values indicate nearly all liquid and the temperatures are nearly 70°C higher than those measured at the feed to the well (Table A.1). This suggests that the liquid boiled and cooled during flow to the well, with excess enthalpy resulting from heat transfer from the rock.

Gases from well S-2 before it became acid (points 1 and 2 in Figure 3.51) show essentially all liquid at 265 to 280°C suggesting that the high total enthalpy and moderate feed temperature

(245°C) of the well fluid resulted from boiling similar to that inferred for S-1 fluids. After the well was deepened and the fluid became distinctly acid, the calculated temperatures dropped and the y values increased suggesting intense boiling, (which is unlikely because the total enthalpy decreased) or that the gases were no longer in equilibrium as a result of mixing with a chemically different fluid.

Well S-3 fluids (all from 1983) show near-equilibrium reservoir liquid at 220 to 245°C with less than 1 percent reservoir steam (Figure 3.52). This agrees with solute geothermometer temperatures of 220 to 250°C and total well head fluid enthalpy of 1075 to 1150 kJ/kg indicating 0.3 to 6 percent steam at 240°C. The last analysis, indicating extreme gas depletion, may be bad.

Temperatures and steam fractions calculated from well S-4 gas analyses have varied considerably with time (Figure 3.53). The eight samples from 1984 to 1987 give temperatures of 240 to 280°C and y values within 2 percent of zero indicating reservoir liquid at temperatures somewhat lower than those measured downhole (300°C) or indicated by solute geothermometers (255 to 295°C). The two 1988 analyses (points 9 and 10) indicated a high temperature liquid at 335°C, and in 1989 all but two of the calculations indicated more or less strongly gas depleted liquid at temperatures similar to those for steam sampled before 1988. The behavior of the 1988 samples is not understood, but the 1989 results are probably due to the injection of cold water which was heated by conduction from rocks to near original reservoir temperatures, but did not attain the gas contents of original fluids.

The rest of the gas analyses considered are from wells sampled only in 1988 and 1989. Some of the 1988 samples, which were collected before

the injection of cold water, appear to yield information on natural state conditions, but other 1988 samples (like those from well S-4) are strange and appear to indicate out of equilibrium fluids or possibly bad analyses. Samples from well SA-1 (Figure 3.54) behave this way with the two 1988 samples falling outside the grid at temperatures above 350°C. The first 4 samples from 1989 are reasonably consistent with a reservoir liquid at 250 to 300°C (silica indicated 310°C) with about 1 percent vapor. However the last three analyses again fall outside the grid, close to the 1988 analyses.

Analyses of SA-2 steam (Figure 3.55) seem to fall randomly on the diagram, almost half outside the grid above 350°C and the rest from 300 to 350°C and from 20 percent steam to 10 percent gas depleted. Well SA-4 is similar (Figure 3.56) with even higher temperatures. Both of these wells have high-enthalpy discharge, essentially all steam. This may affect the behavior of the gas grid method, but it has been very successfully applied to all-steam discharges of The Geysers and Larderello.

All samples of well SB-1 steam were collected after the 1989 cold water injection. The gas geothermometer diagram (Figure 3.57) shows that all samples were gas depleted with the smallest depletions among the first samples and the largest depletions among the last samples. The initial temperatures are indicated to have been 225 to 250°C, not far from the first solute geothermometer temperatures of 200 to 230°C. The rapid increase in enthalpy after the early samples (from 750 to 1200 kJ/kg) suggests that the injected gas-poor water was heated and boiled becoming increasingly gas depleted as suggested by the gas diagram.

Although there was no injection of cold water into well SC-1, the gas geothermometer diagram (Figure 3.58) looks similar to that for SB-1 with the earliest sample showing all equilibrated liquid (265°C and $y = 0$) and later samples 10 percent or more gas depleted. Some of the gas-depleted samples are from 1988, so the apparent depletion cannot be due to cold water injected into other wells affecting SC-1 (as was suggested by isotope data). However both 1988 and 1989 SC-1 water samples showed large variations in calculated temperatures and reservoir chloride, and reservoir processes may be complex.

In late 1988 well SD-1 was injected with massive quantities of cooled, degassed discharge from well SC-1. This probably explains why the first 1989 samples from SD-1 show strongly gas-depleted water (Figure 3.59). This gas depletion decreased with time and some of the last samples show a slight steam excess. There is considerable scatter and gas temperatures (280 to 310°C) are considerably above either measured or solute geothermometer temperatures (240 to 250°C). This well (and several others) appears to have not been in gas equilibrium during 1989.

The use of the gas geothermometer grid diagram has been somewhat disappointing when applied to Sumikawa fluids, particularly those from 1988 and 1989. The reasons are several. Clearly injection of cold water not only upset reservoir thermal equilibrium, but also disturbed chemical equilibrium in and between water and steam phases, and between fluid phases and rock minerals. Reactions in which participating species are contained in excess (e.g., silica, water) reequilibrated rapidly while those in which the species are scarce (gases, isotopes) reequilibrated slowly and still showed the effects of cold injection in the most recent available analyses.

Using pre-1988 gas data, reasonable reservoir temperatures and vapor fractions were calculated for Ohnuma and Sumikawa wells S-1 through S-4 (Figures 3.49–3.53). Almost all indicated y values are within ± 0.01 of $y = 0$ suggesting all-liquid reservoir fluid with $< 1\%$ vapor or $< 1\%$ gas depletion. Indicated temperatures are 300–325°C for S-1, 260°C for S-2 before deepening, 220–240°C for S-3, and 230°C (with 2.5 percent vapor) to 290°C (with a small gas deficiency) for S-4. S-2 after deepening shows probable disequilibrium with 100–150°C and 10–25 percent vapor indicated. In most cases the range in temperatures indicated by the gas method is within 15 to 30°C of that indicated by solute geothermo-meters with well S-2 fluid after deepening, a notable exception. The reservoir steam fraction (y value) is particularly interesting for S-1 which produced only steam. The y value near 0 indicates that at equilibrium only liquid existed in the reservoir so all the steam must have been produced by production-induced boiling. The temperature at the feed point to the well was 230–240°C indicating that cooling of about 70°C occurred due to boiling and evaporation from pure liquid to pure vapor.

Although gas-water equilibrium was not achieved in Sumikawa fluids after the cold injection, the direction of change toward equilibrium indicated the nature of the disequilibrium. From samples collected over the next 3 to 5 years after the injection, the return to equilibrium would probably have been observable and yielded information on the rates of the processes involved.

3.10 Equilibria with Rock Minerals

Chemists and geochemists have developed methods for modeling the species present in solutions (ions, complex ions, molecular species) that

allow the calculation of ion “activities” or thermodynamically effective concentrations. If a mineral solution reaction is written so that the products are species in solution and the activities of these species are calculated water composition, then their product (the “activity product” or “ion activity product”) can be compared with the equilibrium solubility product and the state of saturation of the mineral calculated. For example, if the ion activity product (IAP) of Na^+ and Cl^- ($a_{\text{Na}^+}a_{\text{Cl}^-}$) were equal to the equilibrium solubility product for the solution of halite $K_{\text{eq}} = a_{\text{Na}^+}a_{\text{Cl}^-}$ [equilibrium halite-water] then halite (NaCl) would be exactly saturated. If the IAP were less than K_{eq} halite would be undersaturated and if the IAP were greater than K_{eq} halite would be supersaturated. The calculation of activity products and equilibrium solubility products must be made for the in situ temperature of the water.

Calculations for geothermal waters are complicated by the necessity of combining water and steam analyses to reconstitute the aquifer water composition and by the necessity of calculating the pH (because it cannot be measured) in order to form the model. Calculation of saturation with aluminosilicate minerals requires analytical values of aluminum as well as complete water and gas analyses and measured enthalpy. In order to apply these methods to Sumikawa fluids, the computer program WATCH by Arnorsson et al., (1982) was used to calculate solution models and mineral saturation with reservoir minerals.

All available Sumikawa and Ohnuma analyses that were sufficiently complete were modeled with the results presented in Table A.10. An example of a calculation using data from well S-4 is discussed here in detail (Table 3.2). This sample did not have analyzed aluminum but a range of 0.1 to 0.5 mg/kg Al was found in other samples

Continued on page 3-78

Table 3.2. Output from WATCH1 calculation of mineral saturation at 267°C reservoir water from Well S-4, September 26, 1986 water and steam samples. Aluminum ppm of 0.136 used for microcline saturation.

Water sample (mg/kg)		Steam sample			
pH/deg.C	7.90/ 20.0	Gas (volume %)		Reference	deg.C : 267.0
CO2	66.00	CO2	74.80		
H2S	.00	H2S	21.50	Sampling pressure	bar abs. : 1.0
NH3	.00	NH3	.00	Discharge enthalpy	kJ/kg : 1690.
B	160.00	H2	1.38	Discharge	kg/s : .0
SiO2	879.00	O2	.00	Steam fraction at collection	: .5631
Na	238.00	CH4	.08		
K	46.80	N2	2.20	Measured temperature	deg.C : .0
Mg	.010				
Ca	2.30	Liters gas per kg			
F	.000	condensate/deg.C	.75/20.0	Condensate (mg/kg)	
Cl	260.00			pH/deg.C	.00/ .0
SO4	123.00	Total steam (mg/kg)		CO2	.00
Al	.136	CO2	.00	H2S	.00
Fe	.090	H2S	.00	NH3	.00
TDS	2130.00	NH3	.00	Na	.00

Ionic strength = .01318

Ionic balance : Cations (moleq.) = .01162631 Anions (moleq.) = .01208418 Diff(%) = -3.86

Deep water components (mg/kg)		Deep steam (mg/kg)		Gas pressures (bara)	
B	100.77	CO2	30.70	CO2	1910.61
SiO2	553.62	H2S	23.78	H2S	366.25
Na	149.90	NH3	.00	NH3	.00
K	29.48	H2	.00	H2	1.59
Mg	.006	O2	.00	O2	.00
Ca	1.45	CH4	.00	CH4	.73
F	.000	N2	.08	N2	35.13
Cl	163.76			N2O	.586E+02
SO4	77.47			Total	.586E+02
Al	.0854				
Fe	.0567				
TDS	1341.54	Aquifer steam fraction =	.3064		

Ionic strength = .00783

1000/T (Kelvin) = 1.83

Ionic balance : Cations (moleq.) = .00705534 Anions (moleq.) = .00734552 Diff(%) = -4.03

Oxidation potential (volts) : Eh H2S= -.709 Eh CH4= -.740 Eh H2= -.649 Eh NH3= 99.999

Chemical geothermometers (degrees C)

Quartz 267.0 (Fournier & Potter, GRC Bulletin, pp. 3-12, Nov. 1982)

Chalcedony 254.1 (Fournier, Geothermics, vol. 5, pp. 41-50, 1977)

Na/K 265.8 (Amorsson et al, Geochim. Cosmochim. Acta, vol. 47, pp. 567-577, 1983)

Activity coefficients in deep water

H+	.845	KSO4-	.830	Fe++	.481	FeCl+	.824
OH-	.821	F-	.821	Fe+++	.219	Al+++	.219
H3SiO4-	.824	Cl-	.819	FeOH+	.828	AlOH++	.475
H2SiO4--	.475	Na+	.824	Fe(OH)3-	.828	Al(OH)2+	.830
H2BO3-	.816	K+	.819	Fe(OH)4--	.471	Al(OH)4-	.826
HCO3-	.824	Ca++	.481	Fe(OH)++	.471	AlSO4+	.826
CO3--	.465	Mg++	.500	Fe(OH)2+	.830	Al(SO4)2-	.826
HS-	.821	CaHCO3+	.833	Fe(OH)4-	.830	AlF++	.475
S-	.471	MgHCO3+	.824	FeSO4+	.828	AlF2+	.830
HSO4-	.826	CaOH+	.833	FeCl++	.471	AlF4-	.826
SO4--	.460	MgOH+	.835	FeCl2+	.828	AlF5--	.465
NaSO4-	.830	NH4+	.816	FeCl4-	.824	AlF6---	.179

Table 3.2. Output from WATCH1 calculation of mineral saturation at 267°C reservoir water from Well S-4, September 26, 1986 water and steam samples. Aluminum ppm of 0.136 used for microcline saturation (continued).

Chemical species in deep water - ppm and log mole					Deep water pH is 7.523			
H+	.00	-7.450	Mg++	.00	-7.490	Fe(OH)3	.00	-7.745
OH-	6.66	-3.407	NaCl	3.73	-4.195	Fe(OH)4-	.12	-6.001
H4SiO4	864.55	-2.046	KCl	.29	-5.413	FeCl+	.00	-16.683
H3SiO4-	19.14	-3.696	NaSO4-	9.74	-4.087	FeCl2	.00	-19.946
H2SiO4--	.00	-7.575	KSO4-	10.80	-4.097	FeCl++	.00	-28.348
NaH3SiO4	2.07	-4.757	CaSO4	2.62	-4.716	FeCl2+	.00	-30.090
H3BO3	560.51	-2.043	MgSO4	.01	-7.066	FeCl3	.00	-32.569
H2BO3-	15.63	-3.590	CaCO3	.06	-6.196	FeCl4-	.00	-35.382
H2CO3	29.30	-3.326	MgCO3	.00	-10.173	FeSO4	.00	-16.761
HCO3-	13.49	-3.656	CaHCO3+	.36	-5.450	FeSO4+	.00	-27.081
CO3--	.00	-7.352	MgHCO3+	.00	-9.259	Al+++	.00	-28.085
H2S	13.08	-3.416	CaOH+	.06	-5.947	AlOH++	.00	-18.630
HS-	10.38	-3.503	MgOH+	.01	-6.853	Al(OH)2+	.00	-10.090
S--	.00	-10.558	NH4OH	.00	.000	Al(OH)3	.25	-5.502
H2SO4	.00	-13.495	NH4+	.00	.000	Al(OH)4-	.00	-7.787
HSO4-	.46	-5.327	Fe++	.00	-16.262	AlSO4+	.00	-26.689
SO4--	59.63	-3.207	Fe+++	.00	-32.392	Al(SO4)2-	.00	-27.186
HF	.00	.000	FeOH+	.00	-13.950	AlF++	.00	.000
F-	.00	.000	Fe(OH)2	.00	-12.552	AlF2+	.00	.000
Cl-	161.36	-2.342	Fe(OH)3-	.00	-11.720	AlF3	.00	.000
Na+	146.15	-2.197	Fe(OH)4--	.00	-16.230	AlF4-	.00	.000
K+	26.20	-3.174	Fe(OH)++	.00	-22.177	AlF5--	.00	.000
Ca++	.47	-4.935	Fe(OH)2+	.00	-13.212	AlF6---	.00	.000

Log solubility products of minerals in deep water (Al based on microcline)

	Theor.	Calc.		Theor.	Calc.		Theor.	Calc.
Adularia	-14.372	-14.982	Albite, low	-13.943	-14.002	Analcime	-11.587	-11.956
Anhydrite	-8.554	-8.798	Calcite	-13.401	-12.938	Chalcedony	-1.902	-2.046
Mg-Chlorite	-86.903	-84.198	Fluorite	-11.091	99.999	Goethite	3.631	-2.590
Laumontite	-24.782	-24.603	Microcline	-14.982	-14.982	Magnetite	-14.576	-28.744
Ca-Montmor.	-72.579	-86.515	K-Montmor.	-33.830	-43.892	Mg-Montmor.	-74.085	-89.053
Na-Montmor.	-34.114	-42.912	Muscovite	-17.840	-19.162	Prehnite	-38.193	-34.796
Pyrrhotite	-7.333	-54.900	Pyrite	-24.059	-68.513	Quartz	-2.022	-2.022
Wairakite	-25.049	-24.603	Wollastonite	7.094	7.746	Zoisite	-39.106	-36.886
Epidote	-38.870	-37.385	Marcasite	-8.041	-68.513	Talc	7.849	13.581
Chrysotile	13.947	17.673	Sil. amorph.	-1.595	-2.046			

(Table A.1). An Al concentration of 0.136 was chosen to produce exact saturation with K-feldspar (microcline). The solution model shows limited ion pairing with weak acid complexes (H_2BO_3^- , H_3SiO_4^-) the most prominent. The calculated pH of 7.5 is similar to the analytical value of 7.9 because gas concentrations were relatively low. The assumed temperature of equilibration was 267°C based on the quartz geothermometer. If saturation is taken as ± 1.0 log units in IAP/K (in the table, IAP = calc. and K = theoretical) then saturated minerals include adularia, anhydrite, laumontite, wairakite, epidote, low albite, calcite, (microcline), analcime, chalcedony and (quartz). Many of these minerals (laumontite, wairakite, quartz, calcite, anhydrite and K-feldspar) have been observed at Sumikawa (MMC unpublished data, 1989).

Calcite is supersaturated in the model by about 0.5 log units and might be expected to form scale during production. However, large amounts of calcite probably would not form in S-4 because calcium concentrations are low (< 3 mg/kg) and bicarbonate concentrations are high. When Ca and HCO_3^- concentrations are more nearly equal then more scale can be formed. The small change in pH upon flashing also suggests that major calcite scaling may not occur. High Ca in other Sumikawa wells such as SD-1 (10 mg/kg Ca) and SB-1 (7 mg/kg Ca) may show the influence of cold water injection and original values may be lower.

The results of other calculations are similar (Table A.10). Almost all fluids studied are near saturation with both calcite and quartz. Silica scaling is only a problem for high-temperature ($> 300^\circ\text{C}$) waters because silica in waters saturated with quartz at these temperatures becomes supersaturated with amorphous silica as it cools and loses steam. Calcite scaling is usually a problem only for waters cooler than about 220 to 250°C. This is

because at high temperatures the solubility of calcite is lower and less calcite is carried in solution. If CO_2 concentrations are high, then during flashing the pH increases and CO_3^{2-} ion is formed causing calcite precipitation. Some Sumikawa reservoir fluids are cool enough that calcite scaling could be a problem. Scaling inhibitors can be very successful in preventing calcite scaling, but usually they must be injected in wells below the flash point, a process that can be expensive. A more complete study of the potential for calcite scaling could be made modeling wellbore flashing using WATCH to track calcite saturation.

3.11 Magmatic Constituents

As mentioned in sections 3.1-3.2, The Sumikawa field is located on the N slopes of Mt. Yake not far from the Tamagawa hot spring discharging partially altered volcanic acid chloride-sulfate water. The high temperatures measured at Sumikawa are also of undoubted volcanic origin. It is reasonable therefore, that the Sumikawa fluids would show evidence of volcanic origin, unless during the alteration of acid, oxidized volcanic fluid to neutral, reduced geothermal waters, all of the chemical evidence was lost.

In some geothermal waters associated with andesitic volcanoes, isotopes show that the waters are mixtures of local meteoric water and an "andesitic" water characterized by high $\delta^{18}\text{O}$ and δD values along with high Cl concentrations (Giggenbach, 1991). However, this is not observed at Sumikawa probably because of high dilution with meteoric water and possibly also because most heat entered the reservoir by conduction rather than in volcanic fluid. Another more-definite indication would be a high $^3\text{He}/^4\text{He}$ ratio in the gases, because ^3He is an indicator of direct mantle origin

while most ^4He originates in the crust. Unfortunately no He isotope analyses have been made on Sumikawa fluids.

However, Giggenbach (1991) has shown that the He-Ar- N_2 compositions of andesitic volcanic gases are distinct from those of air, air-saturated water and gases in crustal rocks. Figure 3.60 shows the He-Ar- N_2 compositions of Sumikawa fluids along with the compositions of air and air-saturated water (ASW), and the general compositions of Japanese magmatic gases (from Matsuo, *et al.*, 1982). On this figure most Sumikawa gas compositions fall near the air composition and only gases from SA-2 and SD-1 (along with one from SA-4) contain significant He. The SA-2 gases show a strong lineation in the direction of magmatic gas with gases of some samples mostly from magma. In 1988 and 1989 the fraction of magmatic indicator gases increased with time suggesting that diluting air gases were being progressively purged.

In order to compare fluids from wells S-1, S-2 and S-3 (without He data) with fluids from newer wells, all N_2/Ar mole ratios are plotted against date of collection in Figure 3.61. This figure shows that from 1982 to 1988 almost all N_2/Ar ratios are within the range between air-saturated water (~40:1) and air (~80:1). In 1988, with more analyses, the range is the same, but in 1989 most points fall near the air value. This probably results from the injection of cold water in late 1989, during which slugs of air were injected along with water. In 1988 and 1989 SA-2 samples and possibly others with N_2/Ar higher than air are evident.

These indications of magmatic influence at Sumikawa do not necessarily indicate that there are significant unaltered acid magmatic fluids in the system. The magmatic constituents detected are inert (Ar, He) or relatively so (N_2) and would

be preserved through the dilution and rock reactions involved in the alteration of magmatic gas to geothermal fluid. Well SA-2 with the strongest magmatic signal is closest to Mt Yake and, along with well S-2, has the most saline waters and the highest $\delta^{18}\text{O}$ values (outside the enthalpy-chloride-isotope pattern of other wells). These wells also have the highest Mg and the highest C1/B which are used in Philippine fields to detect acid magmatic inflow (PNOC, pers. commun, 1996). Therefore, It may be important to monitor frequently the chemistry of fluids from SA-2 and other wells drilled near Mt Yake.

3.12 Conclusions

The Sumikawa geothermal field being exploited by the Mitsubishi Metals Corporation (MMC) appears highly promising from a geochemical perspective. Most drilled wells produce fluids that can be exploited easily for electricity production using conventional technology. The field appears to be larger than the present (1990) drilled area and probably extends from Mt. Yake to Ohnuma and some distance to the north. The Sumikawa and Ohnuma fluids are genetically connected, originating from boiling and dilution of a 345°C parent fluid.

The Sumikawa reservoir fluid samples collected and analyzed by MMC are generally neutral to alkaline sodium chloride-sulfate-bicarbonate waters (except the later discharge from well S-2), originate at temperatures of 230 to 310°C, and exist in the reservoir as liquid or mixtures of liquid and vapor. The salinity is variable but low with most waters having 200 to 250 mg/kg chloride before flashing. In general these waters should present no unusual chemical problems during exploitation.

Continued on page 3-82

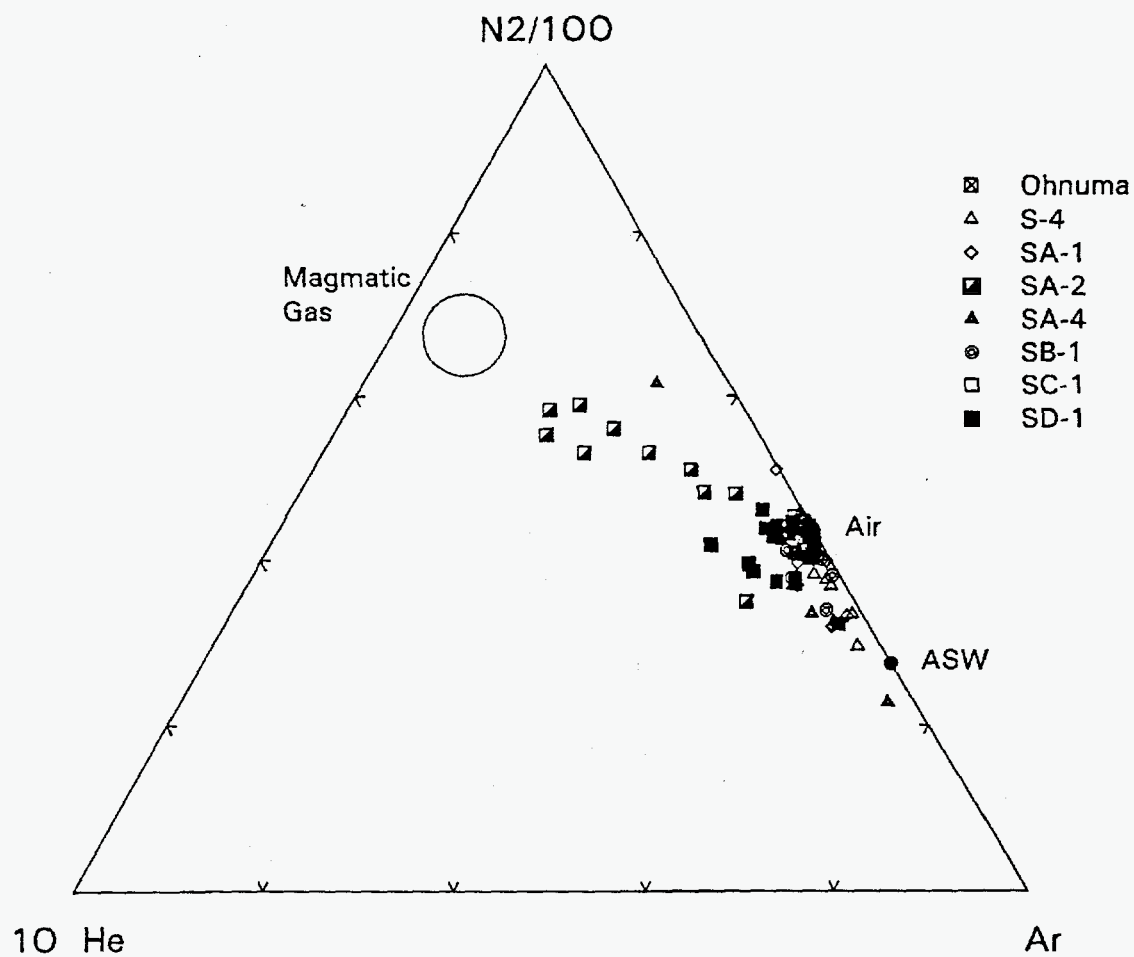


Figure 3.60. He-Ar-N₂ compositions of Sumikawa fluids along with the compositions of air and air-saturated water (ASW).

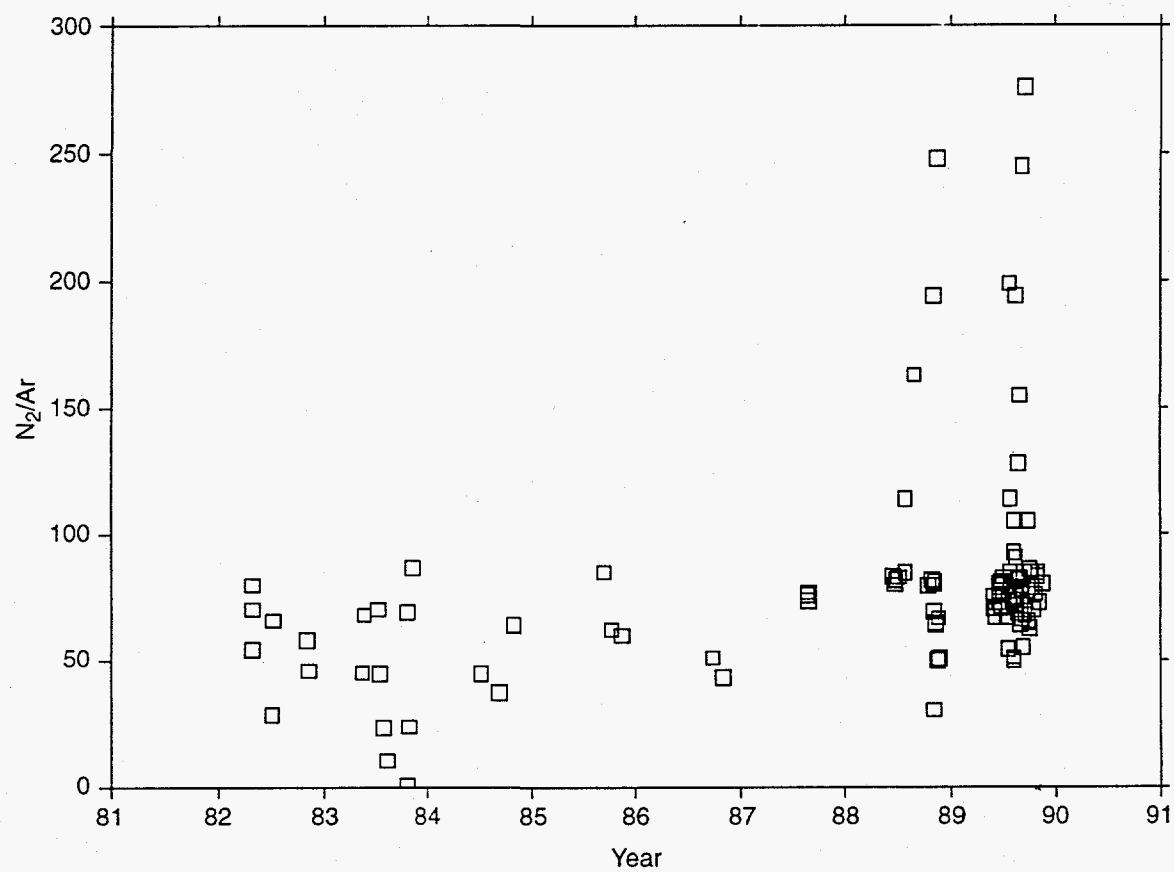


Figure 3.61. N_2/Ar ratios for Sumikawa wells.

The cold water injection test has made the calculation of undisturbed reservoir fluid composition for some wells difficult. The recovery curves from this injection are interesting and may yield estimates of reservoir volumes. However, some wells were only sampled after the cold injection and other wells have had only a few samples collected earlier. Methods of estimating reservoir temperatures and *in situ* vapor fractions worked well on earlier, uncontaminated samples as did calculation of mineral saturation using a chemical solution model. These methods should be applied to analyses of future, uncontaminated samples.

The presence of gases derived from a magmatic source has been demonstrated from wells

near Mt. Yake. Development in this sector should consider the possibility of residual acid magmatic fluids.

More sampling of fluids from existing wells during long term flow tests would add to our knowledge of the field. Future testing should include chemical, gas and isotope analysis of samples collected at the same time as the measurement of flow and enthalpy. Slow reacting $\text{SO}_4\text{-H}_2\text{O}$ and $\text{CO}_2\text{-CH}_4$ isotope geothermometers should be applied to try to verify the presence of the hypothesized 345°C parent fluid.

4 Analysis of Downhole Data

As of early-1990, MMC and NEDO had drilled and tested thirteen slim holes (diameter ≤ 6 inches) and eleven large-diameter (diameter > 6 inches) wells. With the exception of four slim holes (0-3T, Y-1T, Y-2T, and Y-3T) and two large-diameter wells (SD-2, SN-8R), some injection and/or production data are available for all of the Sumikawa boreholes. In this section, we will analyze available drilling (circulation losses, well completion and geologic data) and downhole PTS (*i.e.*, pressure, temperature, and spinner) surveys to obtain feedzone depths, pressures and temperatures for the eighteen wells listed in Table 4.1. The essential drilling and well completion data, required in the interpretations, are given in Appendix B.

At the Sumikawa Geothermal Field, downhole pressures are usually measured with Kuster gauges. Since these Kuster gauges are not recalibrated in the field, it is highly desirable to have repeat measurements with different tools. It is also possible to utilize the water level and temperature gradient data to deduce the downhole pressure distribution in the borehole; this pressure distribution can in turn be used to verify the accuracy of downhole pressure measurements. The importance of ensuring the accuracy and reliability of measuring tools cannot be overemphasized. It appears that the downhole pressure measurements made with a Kuster pressure tool (KPG-29846) during 1987 at Sumikawa are incorrect. We were also advised by MMC that many of the pressure/temperature measurements taken by an experimental PTS tool (PTS 350) during 1988 are suspect.

Some of the Sumikawa boreholes were directionally drilled; because of borehole deviation the measured depths along the borehole (MD) do not necessarily indicate true vertical depths (TVD) from the surface. To derive true vertical depths from the measured depths, it is thus necessary to correct for borehole deviation. Depths will also be sometimes given in terms of elevation (meters) above sea level; thus -800 ASL denotes an elevation of 800 meters below sea level. Casing, liner and borehole dimensions are generally given in mm for slim holes (borehole diameter ≤ 6 inches) and in inches for large-diameter (borehole diameter > 6 inches) wells.

4.1 Slim Hole 50-HM-3

The borehole appears to heat up conductively (Figure 4.1) and temperature surveys provide no clear indications of permeability. A temperature profile at a nominal shutin time of three hours recorded on November 27, 1975 shows a change in temperature gradient at ~ 460 m; if real, this may indicate the permeable horizon for 50-HM-3. The latter depth (~ 460 m) corresponds to a sandstone stringer embedded in the black shales.

Selected water level data and computed downhole pressures are shown in Figure 4.2. The water level stood at 14 m on November 22, 1975 (ST ~ 3 hours); it then fell to 139 m on December 2, 1975 (ST ~ 120 hours). Since it is not known if the water level at 120 hours represents the stable water level for 50-HM-3, we can only place an upper

Continued on page 4-5

Table 4.1. Sumikawa boreholes with production or injection data.

Borehole Name	Measured Depth (meters)	Vertical Depth (m TVD)	Feedzone Depth (m TVD)	Final Diameter (mm)	Feedzone Temperature (°C)	Production/ Injection Data
50-HM-3	501	501	460?	79	—	I
N60-KY-1	1604	1604	1560	101	205	I
O-5T	749	749	747?	64	>210	I
S-1	448	448	436	143	—	P,I
S-2*	905	905	900	101	>225	P,I
S-2	1065	1065	940	101	240	P,I
S-3	805	805	700	101	240	P,I
S-4	1552	1552	1520	159	295	P,I
SA-1	2001	1832	1800	216	305	P,I
SA-2	2005	1943	1450	216	≥300	P,I
SA-4	2009	1739	1240	216	≥290	P,I
SB-1	2086	2006	1600	216	>260	P,I
SB-2	1384	1308	1270	216	~250	I
SB-3	1542	1366	880	216	~210	I
SC-1	2486	2472	2310	216	246	P,I
SD-1	1704	1691	1550	216	250	P,I
52E-SM-1	1003	1003	730?	79	—	I
52E-SM-2*	803	803	550	101	>170	P,I
52E-SM-2	1001	1001	980	79	>230	P
N59-SN-5	1701	1701	1600	101	>260	I

*Intermediate depth

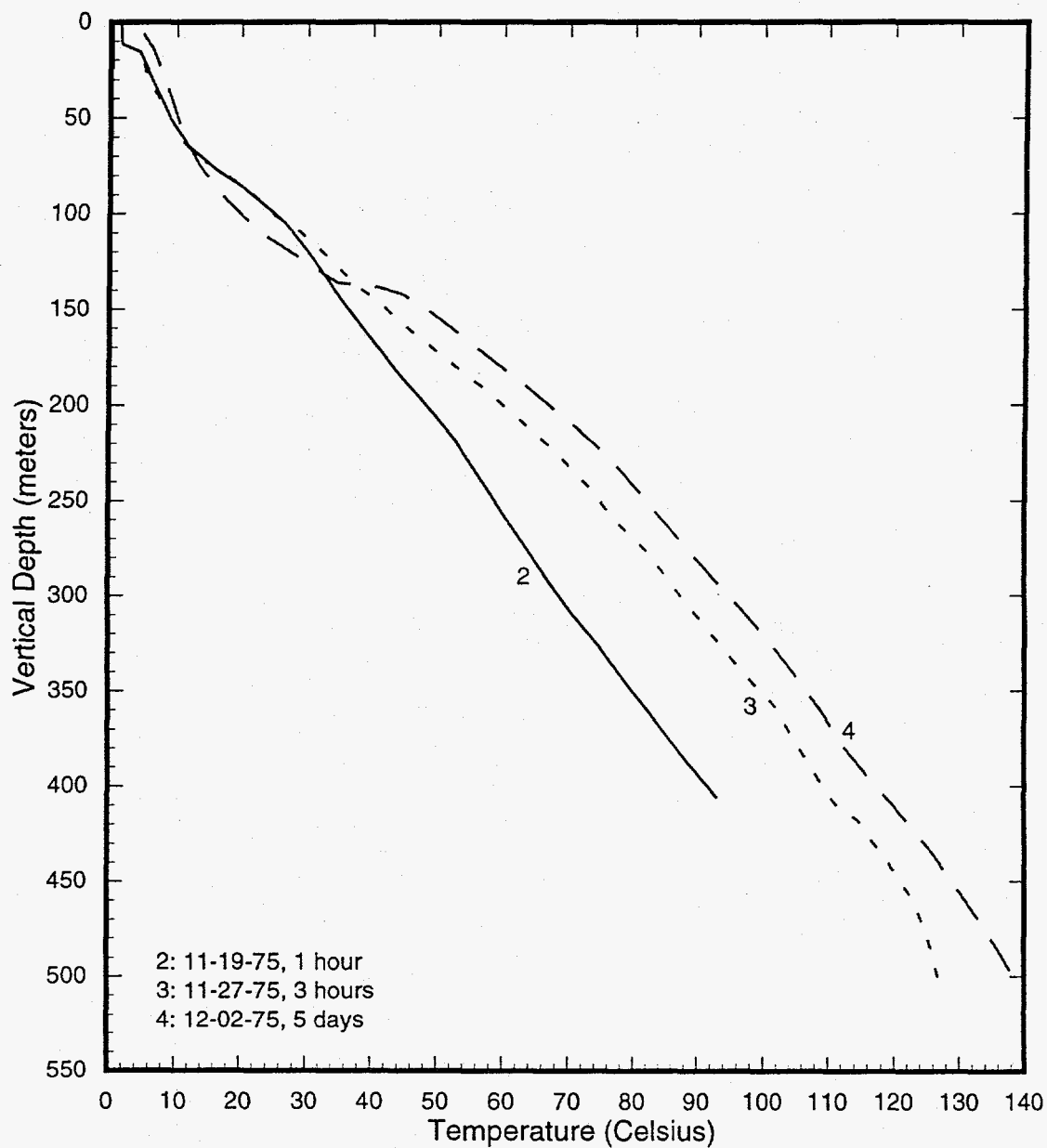


Figure 4.1. Temperature profiles for 50-HM-3.

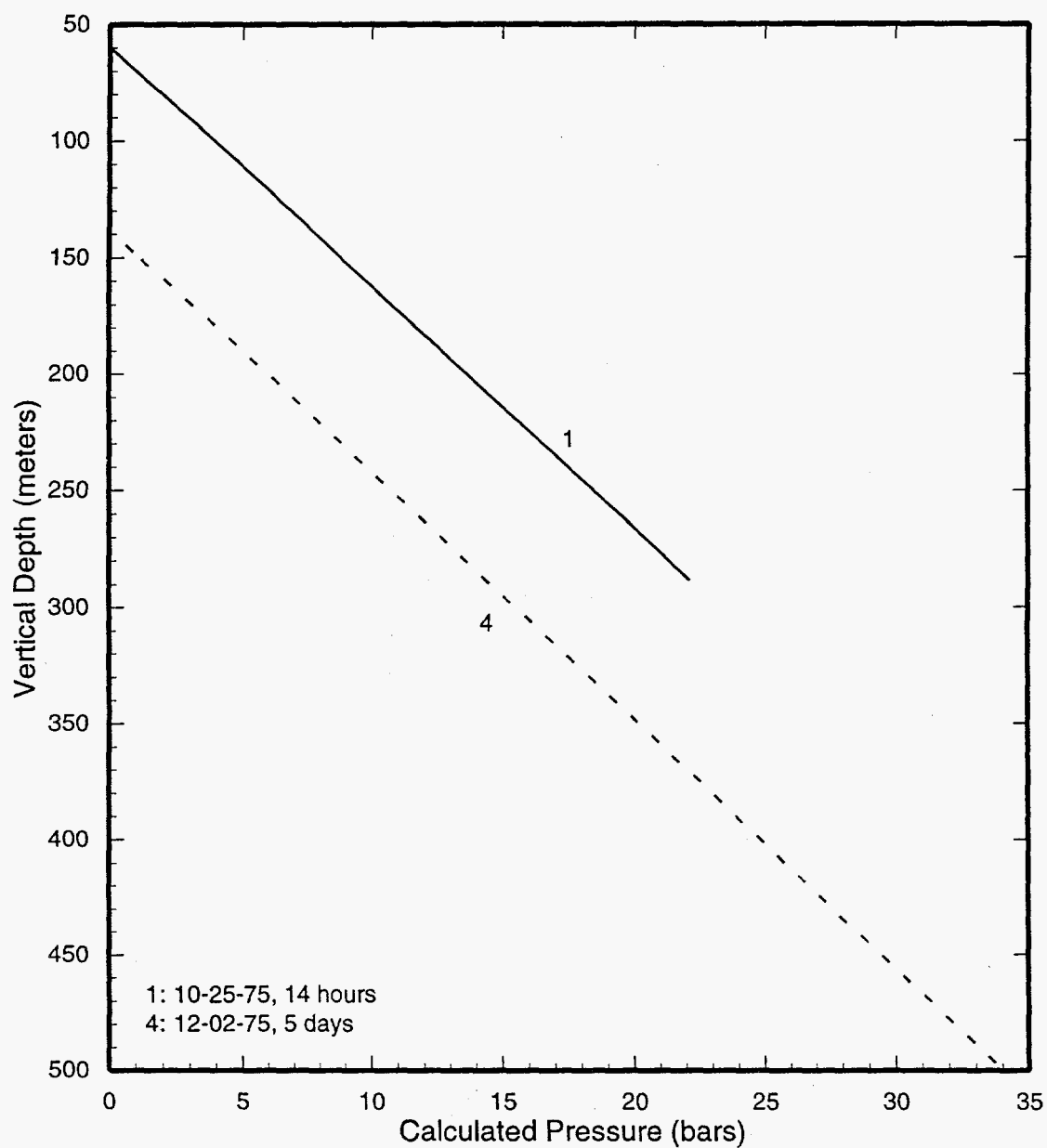


Figure 4.2. Pressure profiles computed from water level and temperature data for 50-HM-3.

bound on the formation pressure. The pressure at a depth of 460 m is:

$$p(460 \text{ m}) = p(514 \text{ ASL}) < 31 \text{ bars}$$

4.2 Slim Hole N60-KY-1

Heat up surveys in the partially drilled hole (drilled depth ~ 880 meters) show a thermal feature in the depth interval from 500 to 540 meters (Figure 4.3); this probably corresponds to the lost circulation zone at 530 meters. After over four months of shutin, the water level in the partially drilled borehole was recorded on April 26, 1986; the computed pressure profile is shown in Figure 4.4. The pressure at 530 meters is ~ 38.5 bars. It is significant that the heatup surveys in the completed borehole (Figure 4.5) do not show any thermal feature at 500 to 540 meters; in addition, the pressures in the completed borehole are much lower than those implied by the water level measurements in the partially drilled borehole.

The completed borehole heats up very slowly below the casing shoe at ~ 1001 meters; available temperature profiles provide no clear indications of formation permeability. Only two mud loss zones (at 1160 m and at 1562 m) were encountered in the uncased interval for this borehole. We will tentatively assume that the major feedzone for KY-1 is located at ~ 1560 meters. Like the temperatures, water levels did not show much variation during the heat up period; representative computed pressure profiles are shown in Figure 4.6. The pressure at 1560 meters is ~ 104 bars. The latter pressure value is in substantial agreement with that (~ 103 bars) recorded on May 10, 1988 (Figure 4.7). The stable pressure at 1560 meters is, therefore, 103.5 (± 0.5) bars. The stable temperature at 1560 meters is about 205°C.

4.3 Slim Hole O-5T

The heatup profiles (Figure 4.8) show marked features at ~ 260 m and ~ 380 m; also a small break in temperature gradient is seen at ~ 450 m. The break in temperature gradient at ~ 260 m is probably associated with the water level in the well; the feature at ~ 450 m corresponds to the change from cased to open hole. Temperature data, however, fail to show any thermal anomaly at the lost circulation horizon at ~ 747 m. Maximum temperature occurs towards bottomhole and exceeds 210°C (shutin time ~ 76 hours).

Well logs indicate that the water level in the borehole stood at 261.5 m at a shutin time of ~ 3 hours (8/13/77); it then fell to 262.5 m at ~ 4 hours and stayed at this level until the end of the observation period (shutin time ~ 76 hours). The above water level for 76 hours cannot be correct since the corresponding temperature profile would imply the presence of superheated steam below the water level. Table 6-3-1 (MMC, 1985) gives a water level of 150 m at the same time. Assuming that the latter water level is correct, the pressure at 750 m (see Figure 4.9) is about 54.5 bars.

4.4 Slim Hole S-1

During the drilling of S-1, partial circulation losses were recorded at 436 m and 438 m. While drilling at 448 m, a blowout occurred and no further drilling was undertaken. The blowout was probably caused by total circulation loss at 448 m. These mud loss and drilling data suggest that the fluid entry for this borehole is located at 436 to 448 m.

Prior to setting the 6-inch casing at 305 m, heat up surveys (shutin time 3 to 12 hours) were

Continued on page 4-13

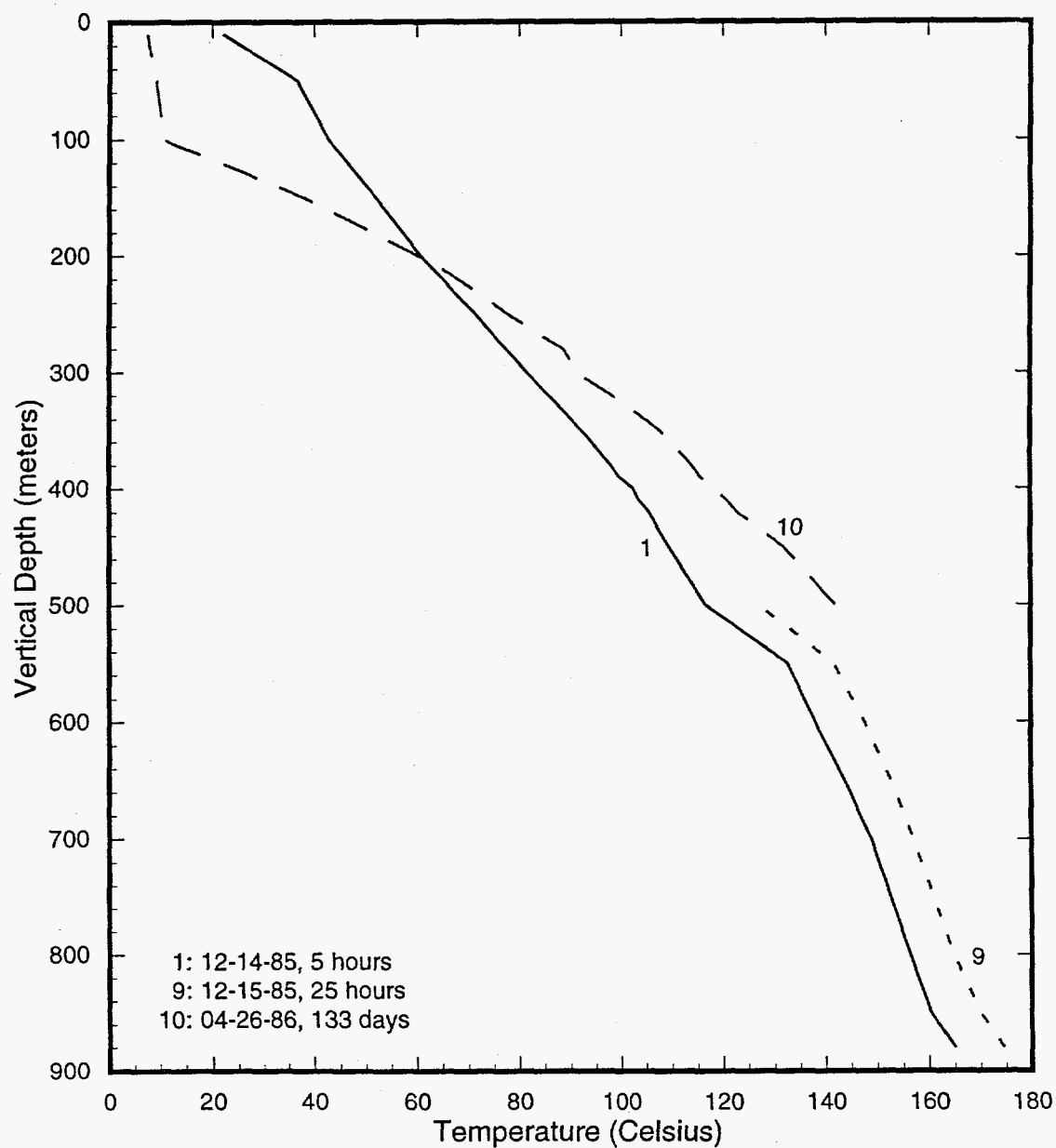


Figure 4.3. Temperatures in partially drilled borehole N60-KY-1 (drilled depth ~ 880 meters).

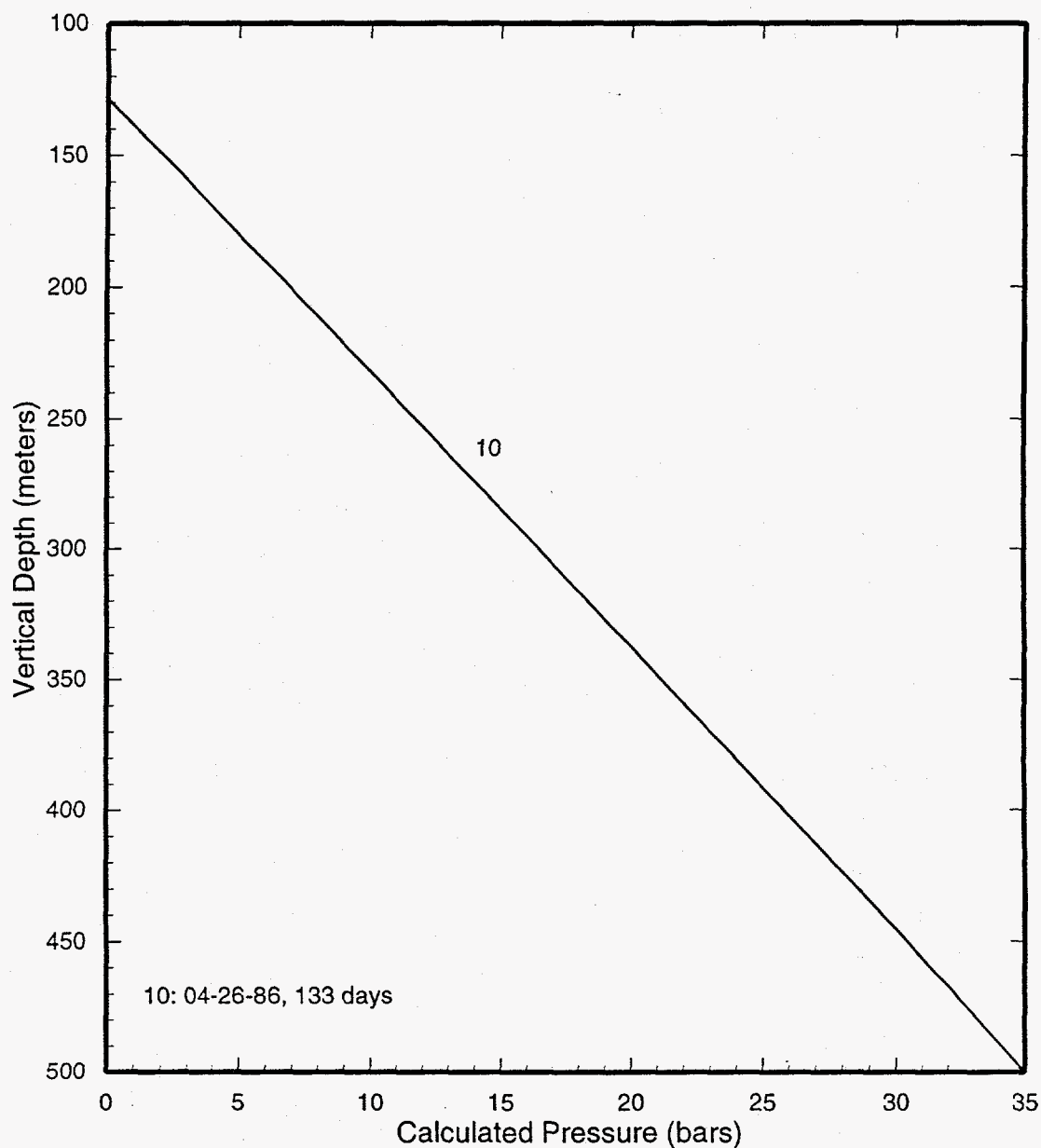


Figure 4.4. Pressures computed from water level and temperature data in partially drilled borehole N60-KY-1.

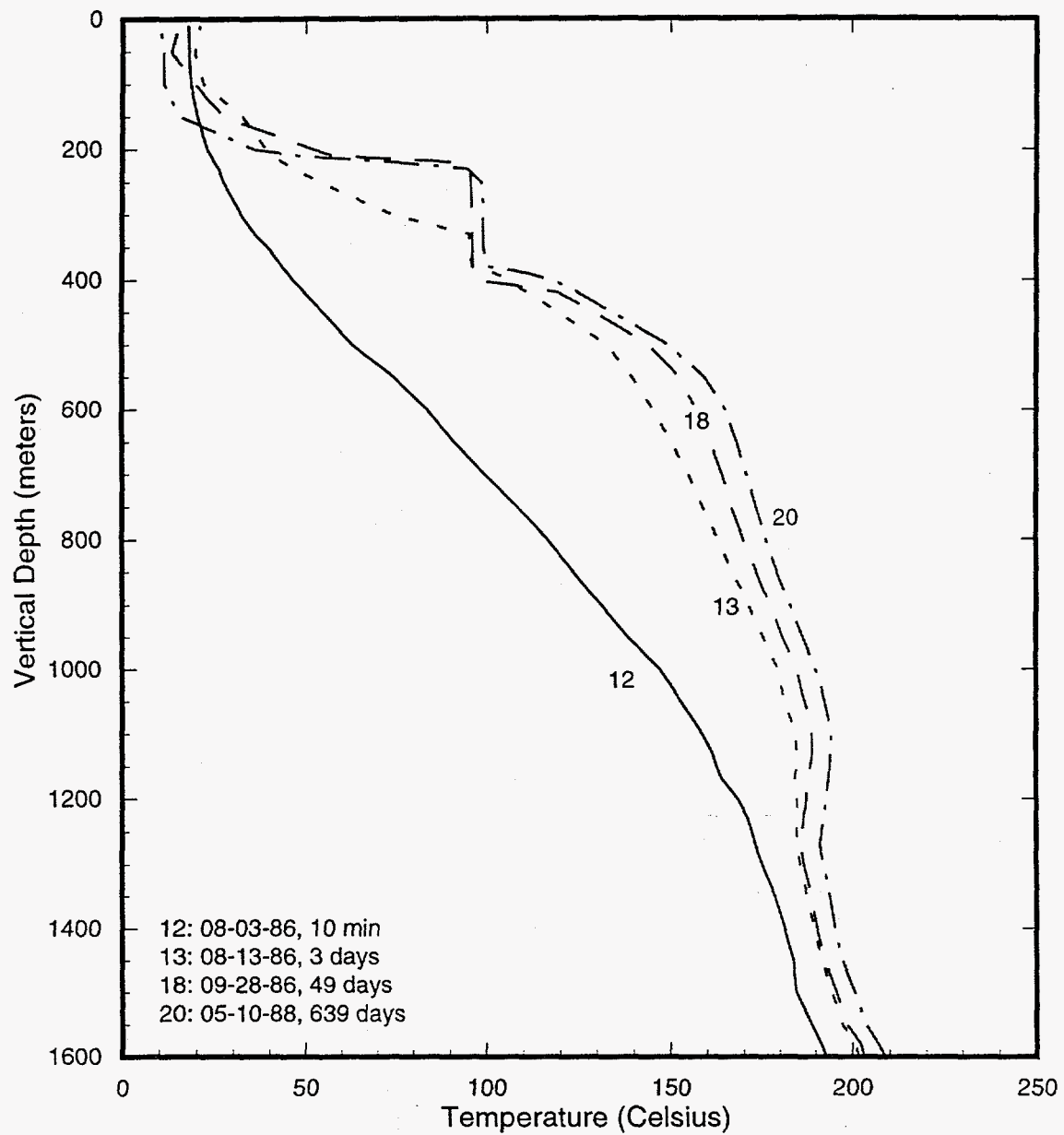


Figure 4.5. Temperatures in borehole N60-KY-1.

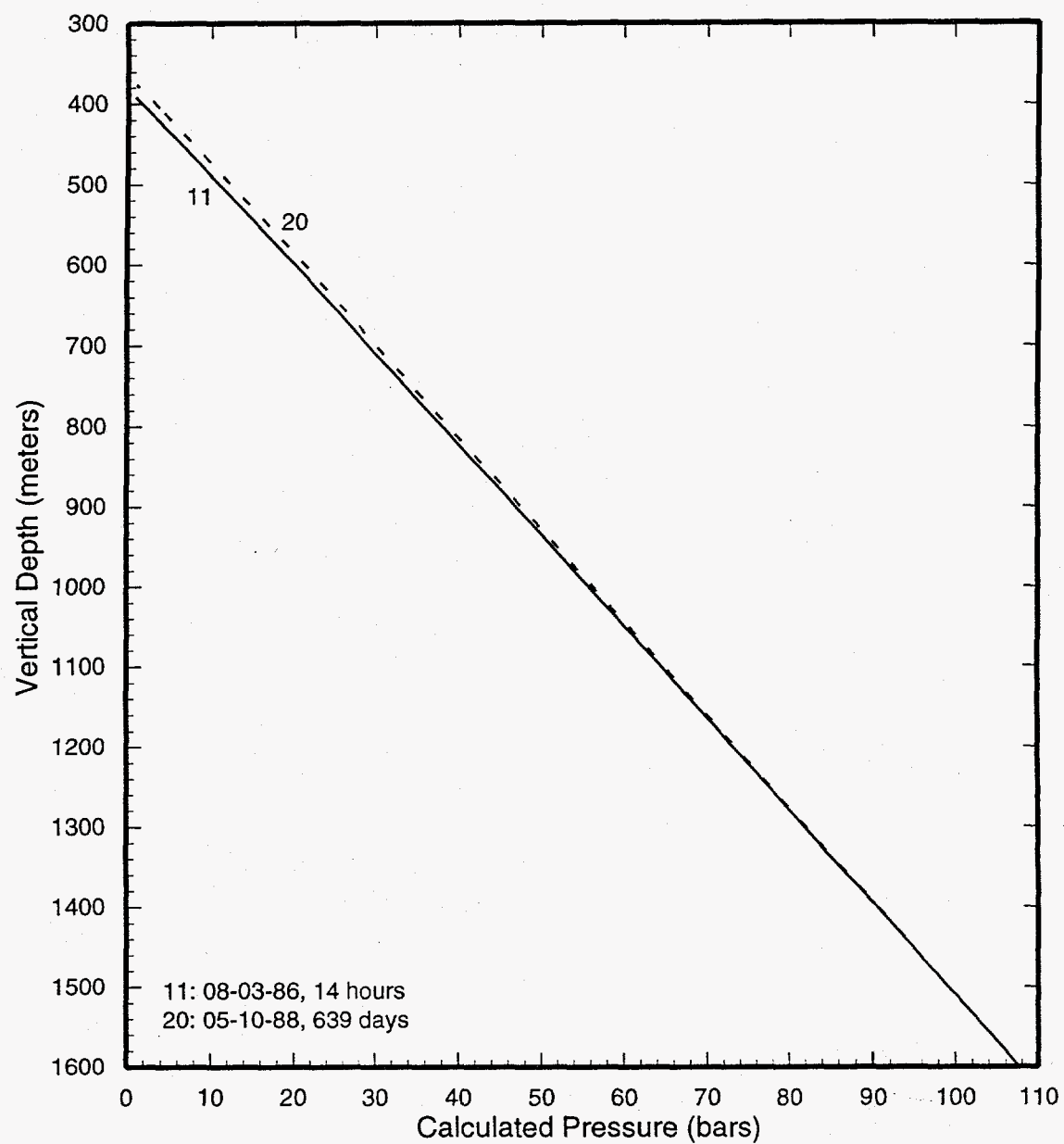


Figure 4.6. Pressures computed from water level and temperature data for borehole N60-KY-1.

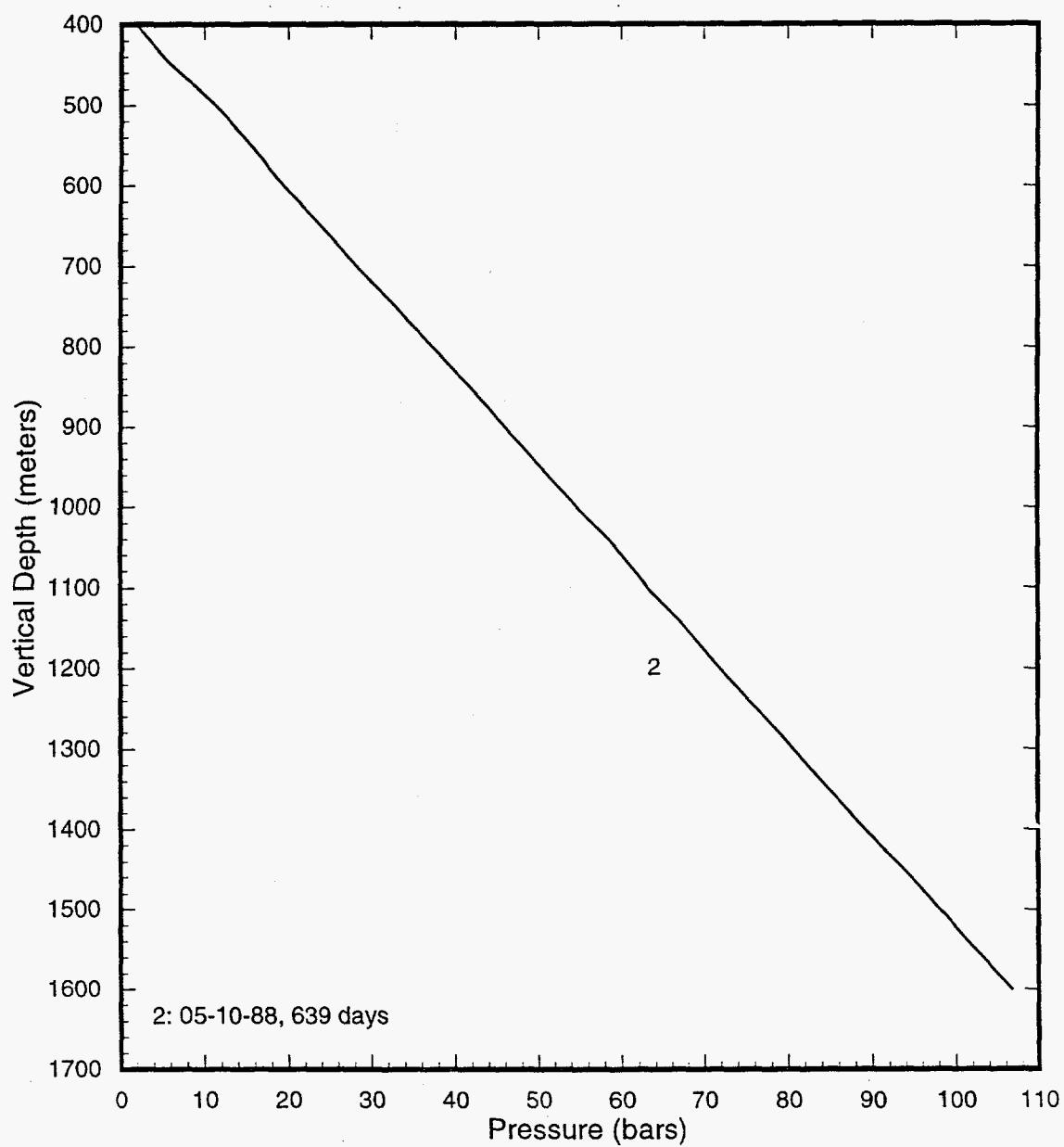


Figure 4.7. Measured pressure profile in borehole N60-KY-1 on May 10, 1988.

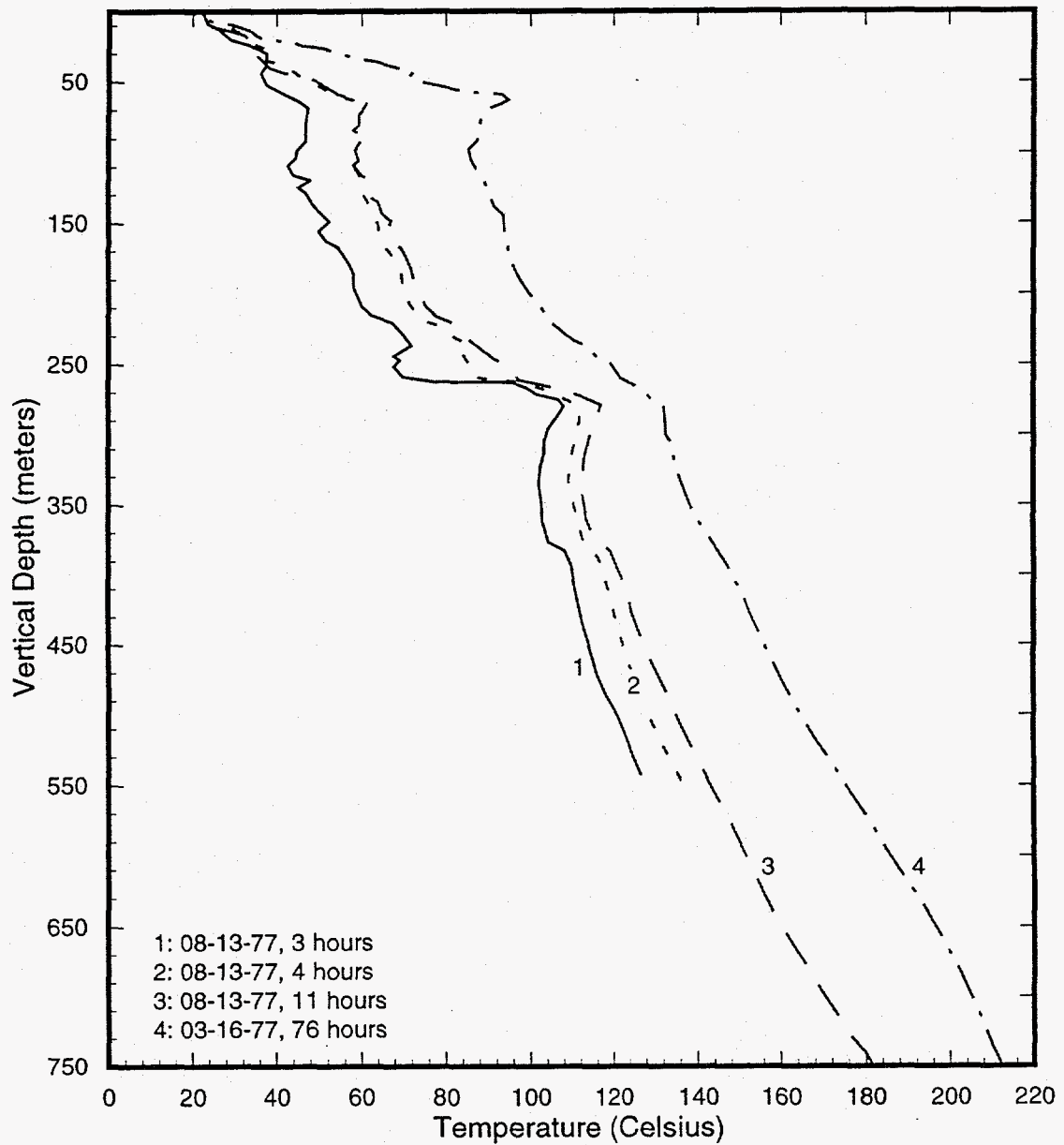


Figure 4.8. Heatup profiles for O-5T.

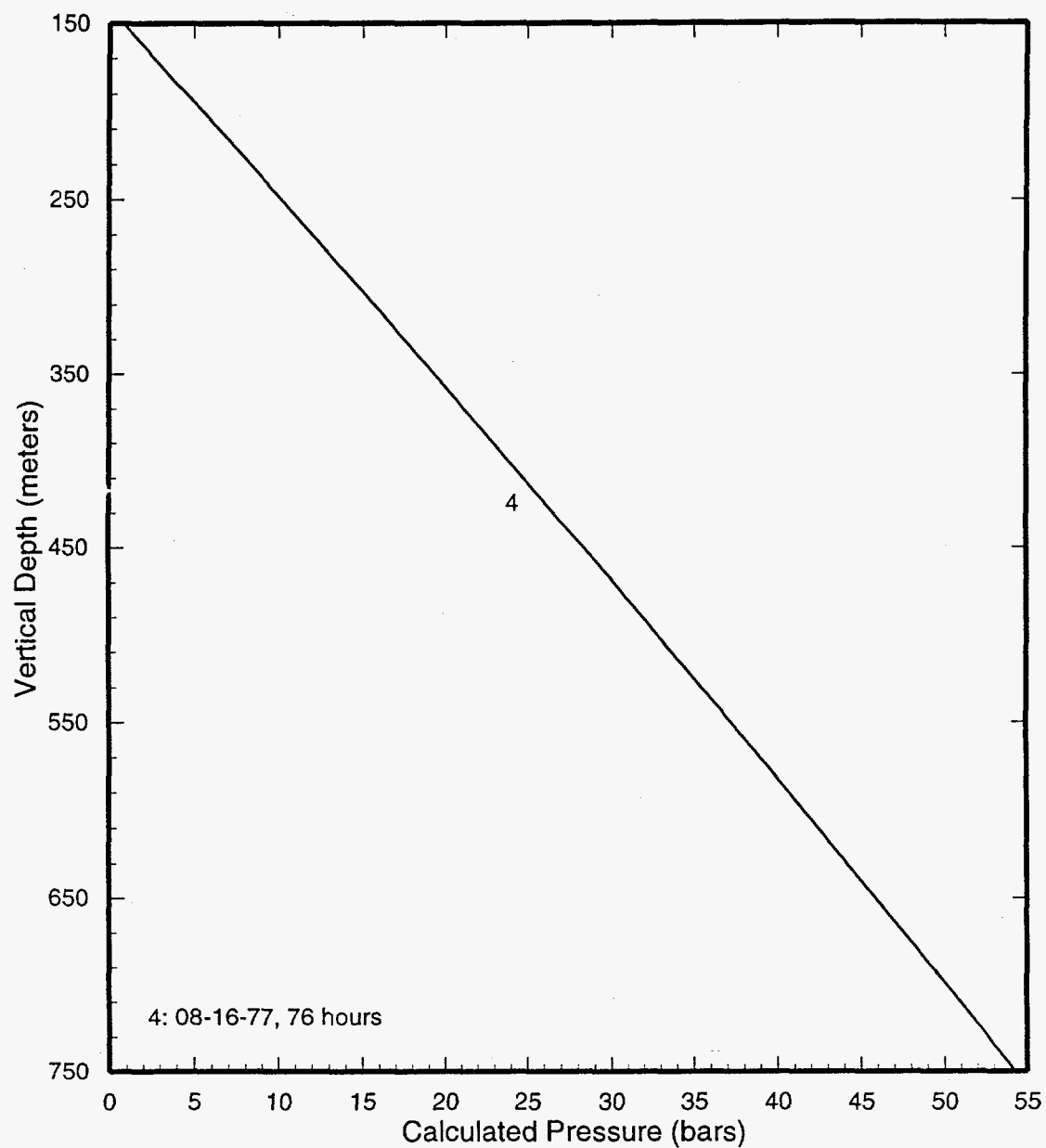


Figure 4.9. Pressure profile computed from water level and temperature data in O-5T at a shut-in time of ~76 hours.

recorded on November 4 and 5, 1981 (see Figure 4.10). The 12-hour temperature survey suggests the possibility of an entry at ~ 270 m; this is, however, not confirmed by the temperature survey at 3 hours. No heat up profiles deeper than 305 m are available.

The pressure survey of April 30, 1982 (see Figure 4.11) was run to a maximum depth of 300 m. The interval from 100 m to 300 m depth is certainly two-phase; extrapolating the pressure gradient over the interval 150 m to 300 m, a bottomhole (448 m) pressure of ~ 20.3 bars is obtained. This pressure is only approximate since (1) the pressure gradient below 300 m may not be the same as that above 300 m and (2) the borehole is discharging internally.

The borehole was flow tested for several days in April 1982. The well output consisted entirely of dry steam with no water phase present. It appears that the reported wellhead enthalpies were determined by assuming that the steam is saturated at the measured wellhead pressure. The steam flow rate declines linearly with pressure and can be extrapolated to give a pressure of ~ 20.1 bars at zero flow rate. Allowing for the weight of the steam column, this suggests a bottomhole (~ 448 m) pressure of ~ 20.5 bars. The latter pressure value agrees closely with that obtained from an extrapolation of the pressure survey of April 30, 1982. Assuming that the reservoir in the neighborhood of S-1 contains saturated steam, the reservoir temperature is estimated to be ~ 213°C (corresponding to a reservoir pressure of ~ 20.4 bars).

The above inferred value for reservoir pressure is, however, at considerable variance with the pressure value given in Table II-3-1 of MMC (1986). According to the latter, a pressure survey run on December 17, 1981 (shutin time ~ 1 hour,

9 minutes) indicated a pressure of 25.3 bars at 436 m. The corresponding water level (pressure ~ 0.9 bars) depth in the borehole was ~ 187 meters (*i.e.*, 249 meters above the pressure measurement depth). These water level and pressure data imply the presence of a very dense fluid (density ~ 1000 kg/m³) in the borehole at the time of pressure survey on December 17, 1981. The drilling operations were completed on or about November 20, 1981. We are unable to explain the presence of a dense fluid (density ~ 1000 kg/m³) in the borehole on December 17, 1981. It is therefore, suggested that the pressure measurement of December 17, 1981 is unreliable.

4.5 Slim Hole S-2

The borehole was originally (October 1981) drilled to a total depth of ~ 905 meters. The bottom of the 4-inch casing was set at 703 meters, and an open hole completion was used below this depth. In October 1982, the hole was sidetracked at 747 meters, and drilled to a depth of ~ 1065 meters. The redrilled hole (like the original hole) was left open below 703 meters.

The single shutin survey (Figure 4.12) in the original hole was recorded during swabbing operations on July 2, 1982; the temperature at 900 meters depth exceeds 225°C. A spinner survey recorded during an injection test on July 16, 1982 (Figure 4.13) indicates that the major feedzone for the original S-2 is located at 900 meters. Temperature (Figure 4.12) and pressure surveys (Figure 4.14) taken during a production test on July 11, 1982 show two-phase conditions in the borehole at the feedzone depth; apparently, production is accompanied by *in situ* boiling. MMC (1986; Table II-3-1) lists a pressure (computed from water level and temperature data) of 49.5 bars (June 24,

Continued on page 4-19

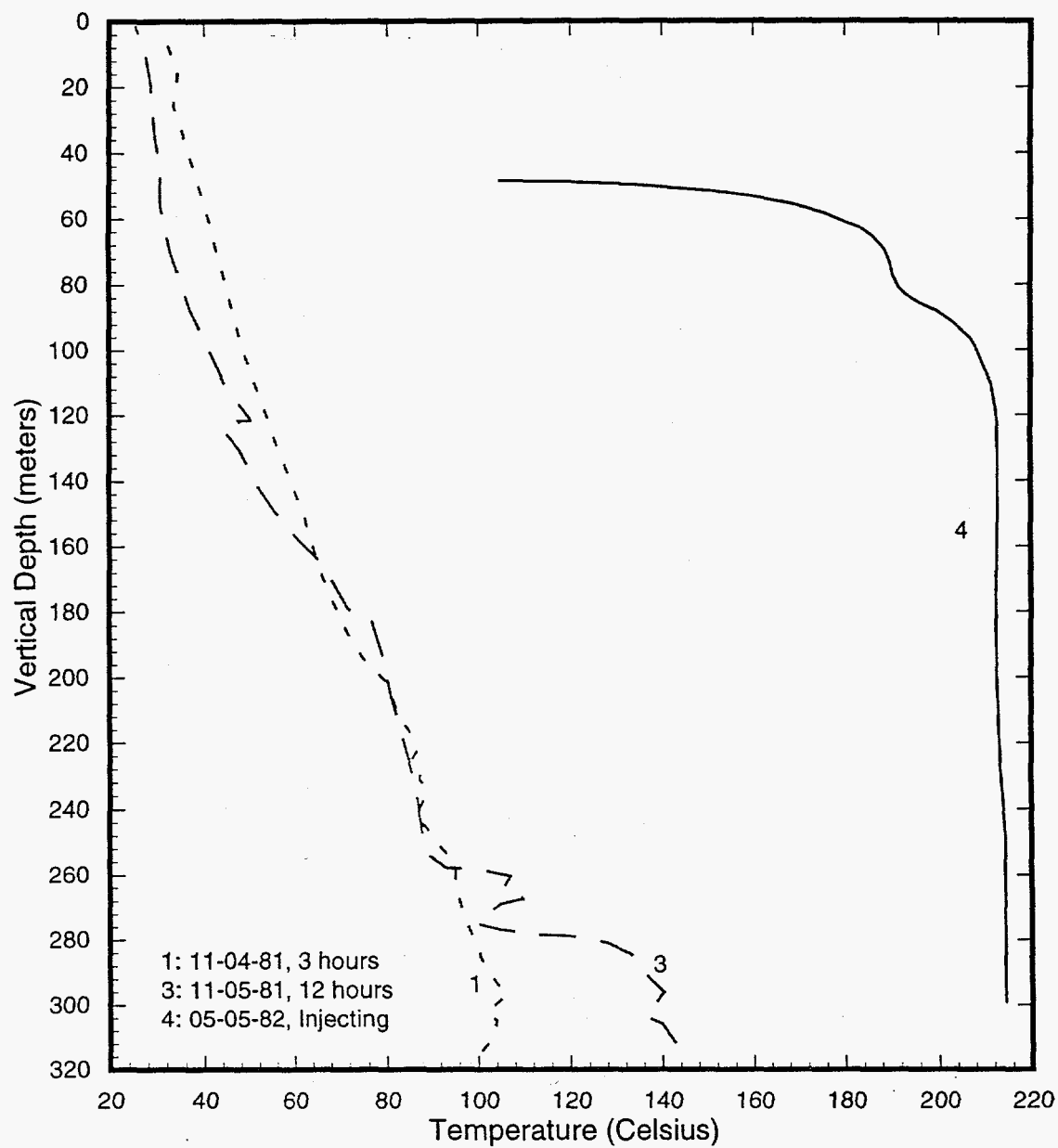


Figure 4.10. Temperature surveys in slim hole S-1.

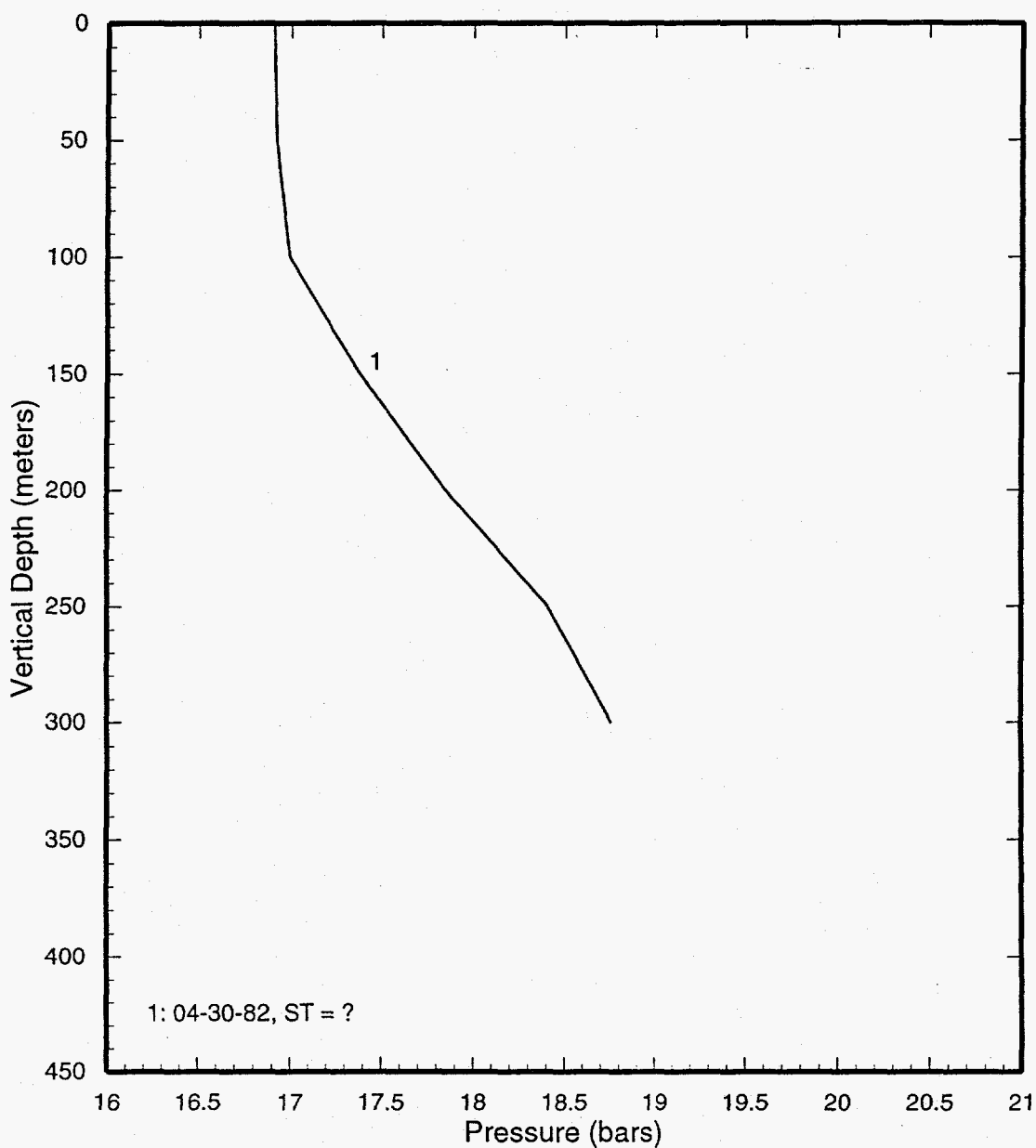


Figure 4.11. Pressure survey recorded in slim hole S-1 on April 30, 1982 shortly after a production test.

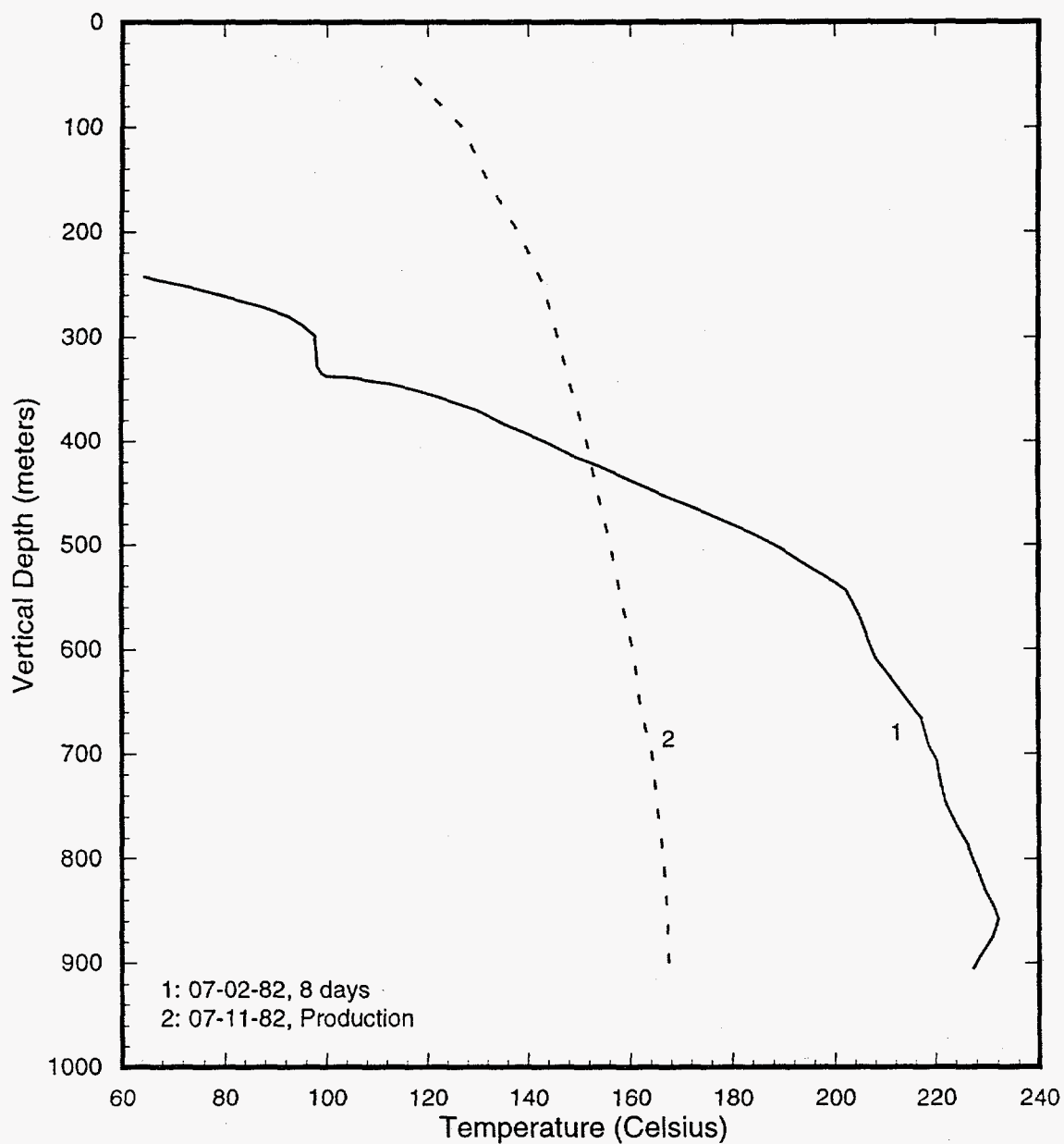


Figure 4.12. Temperature surveys in the original slim hole S-2 (drilled depth = 904.6 m).

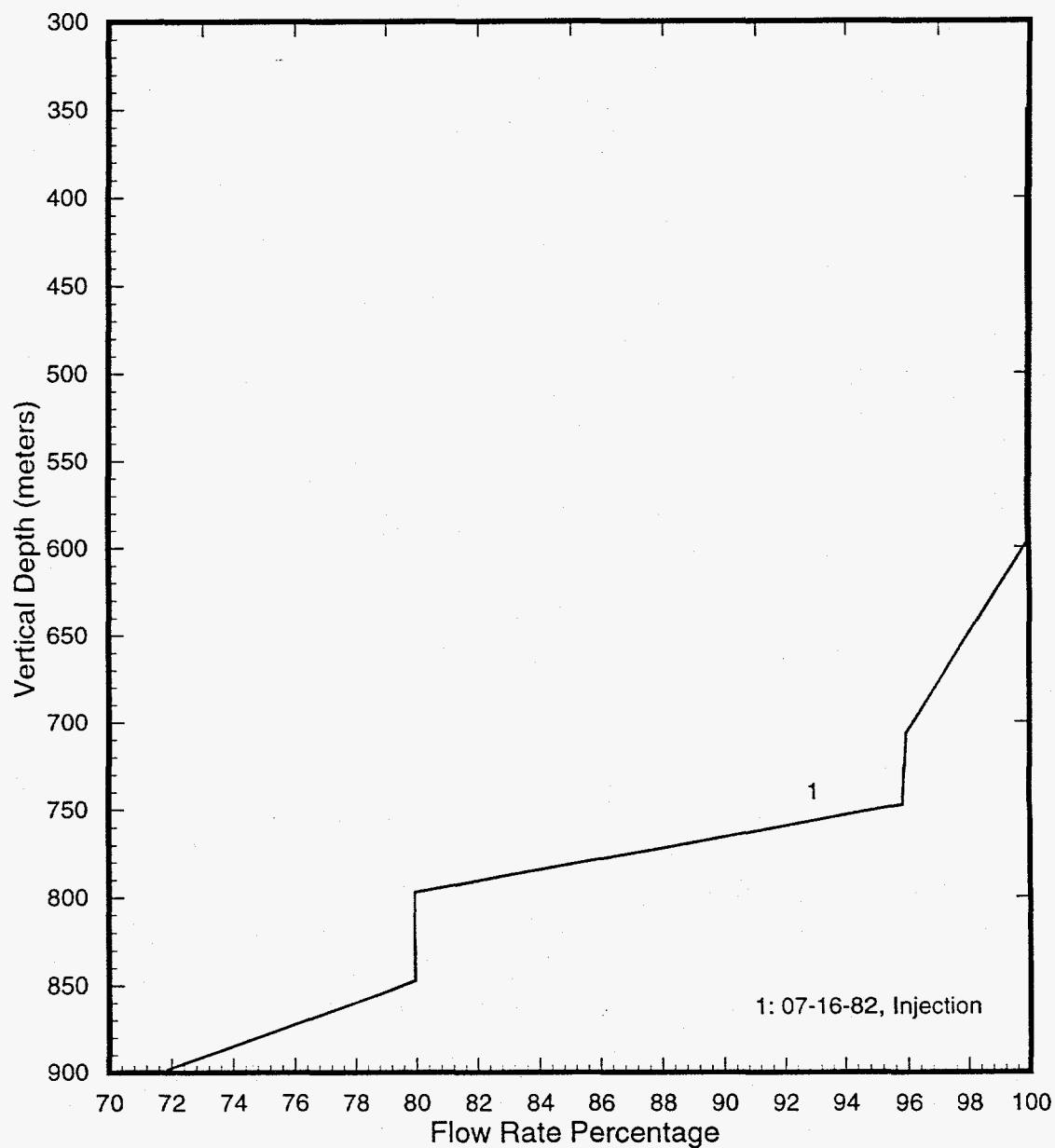


Figure 4.13. Spinner survey (interpreted by MMC) run in the original slim hole S-2 (drilled depth = 904.6 m) during an injection test on July 16, 1982.

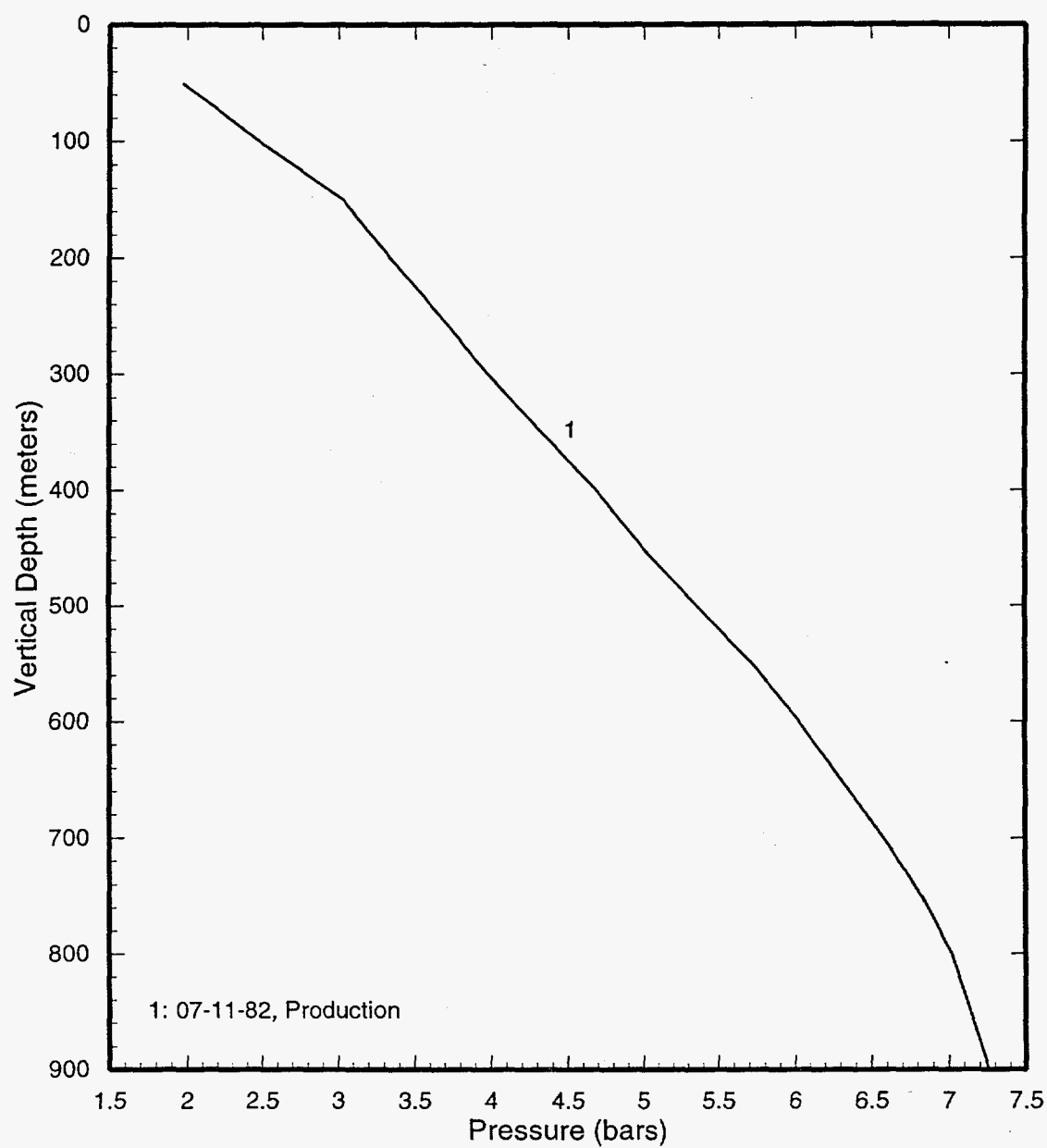


Figure 4.14. Pressure survey recorded in the original slim hole S-2 (drilled depth = 904.6 m) during a production test on July 11, 1982.

1982; shutin time ~ 13.3 hours) at 903.4 meters. The temperature and water level data recorded on June 24, 1982 are unavailable for the present study.

Selected heat up surveys in the redrilled hole are plotted in Figure 4.15. The persistence of low temperatures at ~ 600 m, ~ 735 m and ~ 880 m indicates the presence of permeable horizons. Also, an abrupt change in temperature gradient at ~ 940 m implies a fluid entry at this depth. The temperature at ~ 940 m (see temperature surveys taken on May 10, 1983 and November 10, 1982) is ~ 240°C. The fluid entry at ~ 600 m is also confirmed by several flow meter surveys (see Figure 4.16). It is therefore likely that there is a break in casing at this depth. All of the flow meter surveys in the redrilled hole indicate that most of the injected water is lost over the depth interval 900 to 940 m; this is clearly the most permeable horizon for S-2.

Several water level readings are available for the redrilled S-2. The water level reading corresponding to a shutin time of 179 days appears to be incorrect; this is probably due to boiling in the upper part of S-2 at this time. The pressure profiles (Figure 4.17) other than that for a shutin time of 179 days appear to coincide at ~ 900 to 1000 m. The pressure at a depth of 940 m is 52.5 bars. The latter value is close to the pressure of ~ 51 bars (depth ~ 935 m) recorded on November 6, 1982 (Table II-3-1, MMC, 1986). The slight discrepancy (~ 1 bar) between the two values may be due to borehole deviation. The saturation temperature corresponding to a pressure of 51 bars is ~ 265°C. Since it is unlikely that the stable temperature at ~ 940 m exceeds 250°C, we conclude that the reservoir fluid at this depth is single-phase liquid. The reservoir at shallower depths may, however, contain a two-phase fluid.

Temperature (Figure 4.15) and pressure (Figure 4.18) surveys taken in the redrilled hole during a production test on November 10, 1982 show the presence of single-phase liquid in the borehole at the feedzone (900–940 meters) depth. During the November 1982 production test, the redrilled S-2 discharged fluid with an enthalpy of about ~ 250 (± 10) kcal/kg; this is consistent with production from a liquid reservoir of about 240 to 250°C at a depth of ~ 940 m.

4.6 Slim Hole S-3

The available temperature surveys for S-3 are shown in Figure 4.19. A pronounced feature in temperature profiles 2 and 3 identifies a permeable zone at ~ 450 m. Temperature surveys 2 to 4 also show permeable zones at 650 to 750 m and at ~ 780 m. The permeable zone at 650 to 750 m may not be a continuous zone; the isothermal interval indicates permeability at both the endpoints and interzonal flow. Two flow-meter surveys conducted on June 13, 1983 (Figure 4.20) show that most of the injected water is lost over the depth interval 650 to 750 m; thus it would seem that the principal feed point for S-3 is located in this depth interval.

Temperature surveys conducted after long standing times (see profiles 7 and 10, Figure 4.19) appear to follow the boiling point versus depth curve down to ~ 650 m; the water levels associated with these profiles (see profiles 7 and 10, Figure 4.21) are useless for determining reservoir pressures due to boiling in the borehole. The maximum temperature in S-3 measured on May 16, 1983 was ~ 236°C at ~ 620 m. The enthalpy of the fluid produced from S-3 is approximately equal to the enthalpy of liquid water at ~ 240°C. Thus, it is likely

Continued on page 4-26

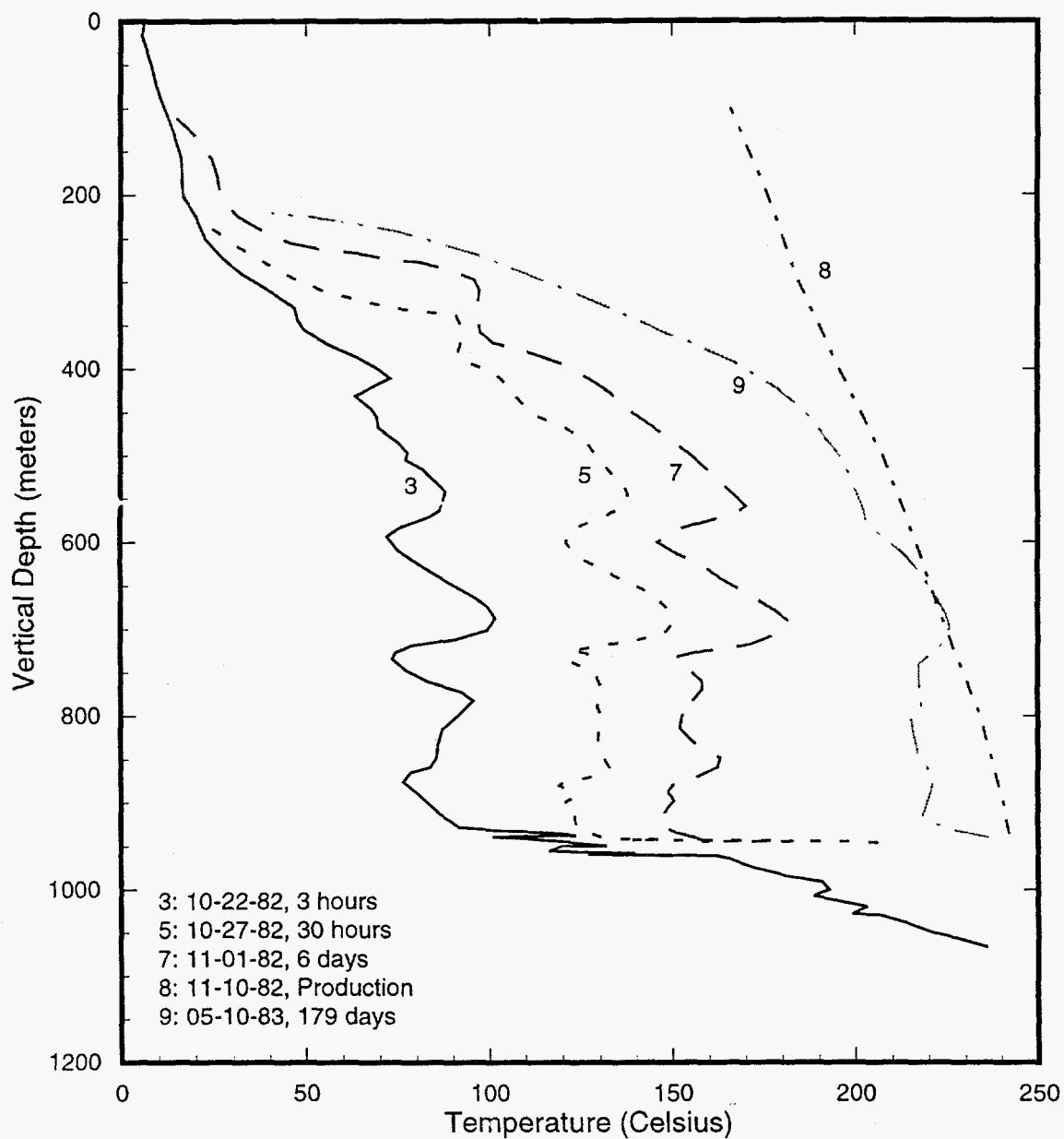


Figure 4.15. Temperature surveys in slim hole S-2 (drilled depth = 1065.1 m).

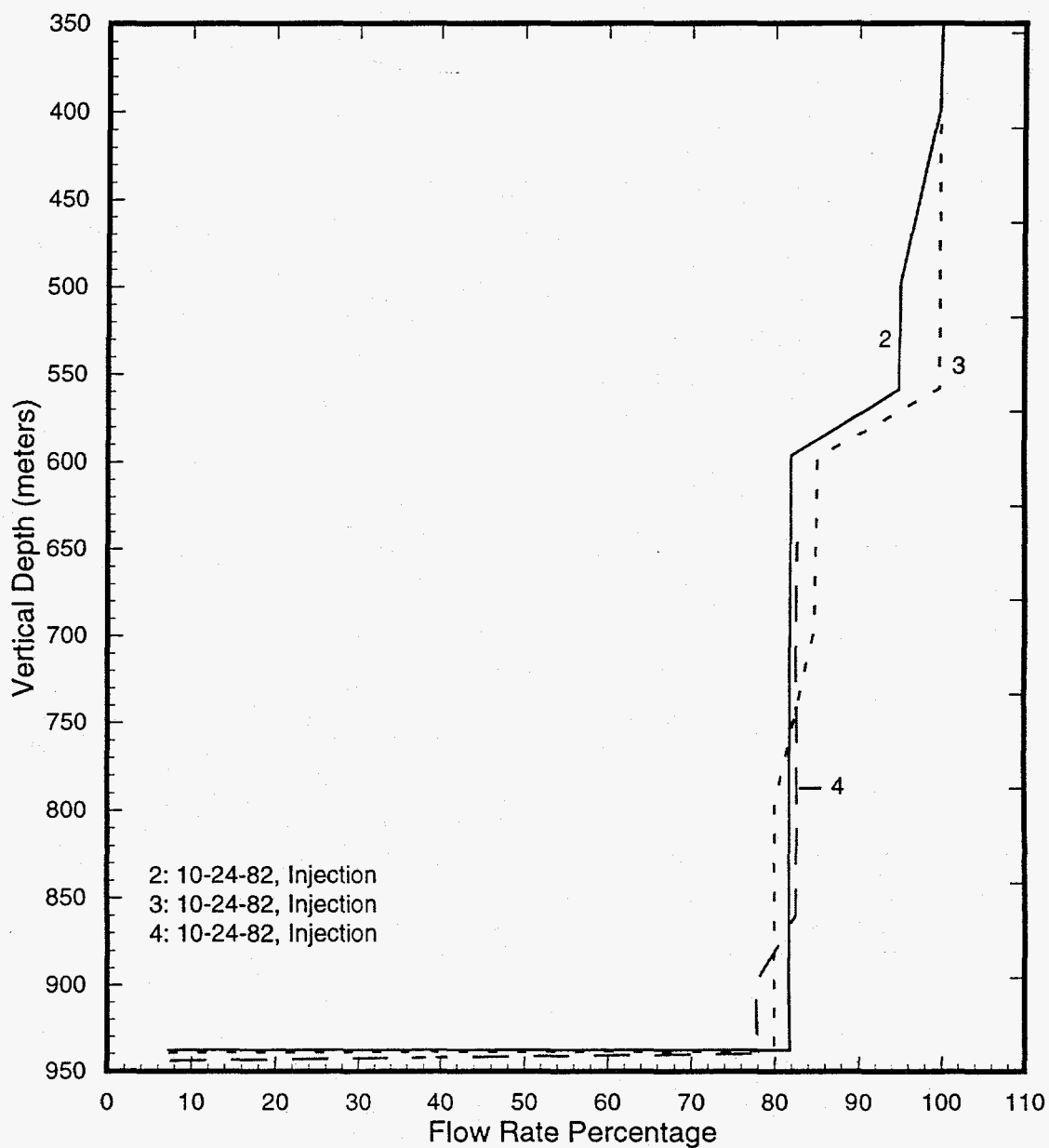


Figure 4.16. Spinner surveys (interpreted by MMC) in slim hole S-2 (drilled depth = 1065.1 m) taken during an injection test on October 24, 1982.

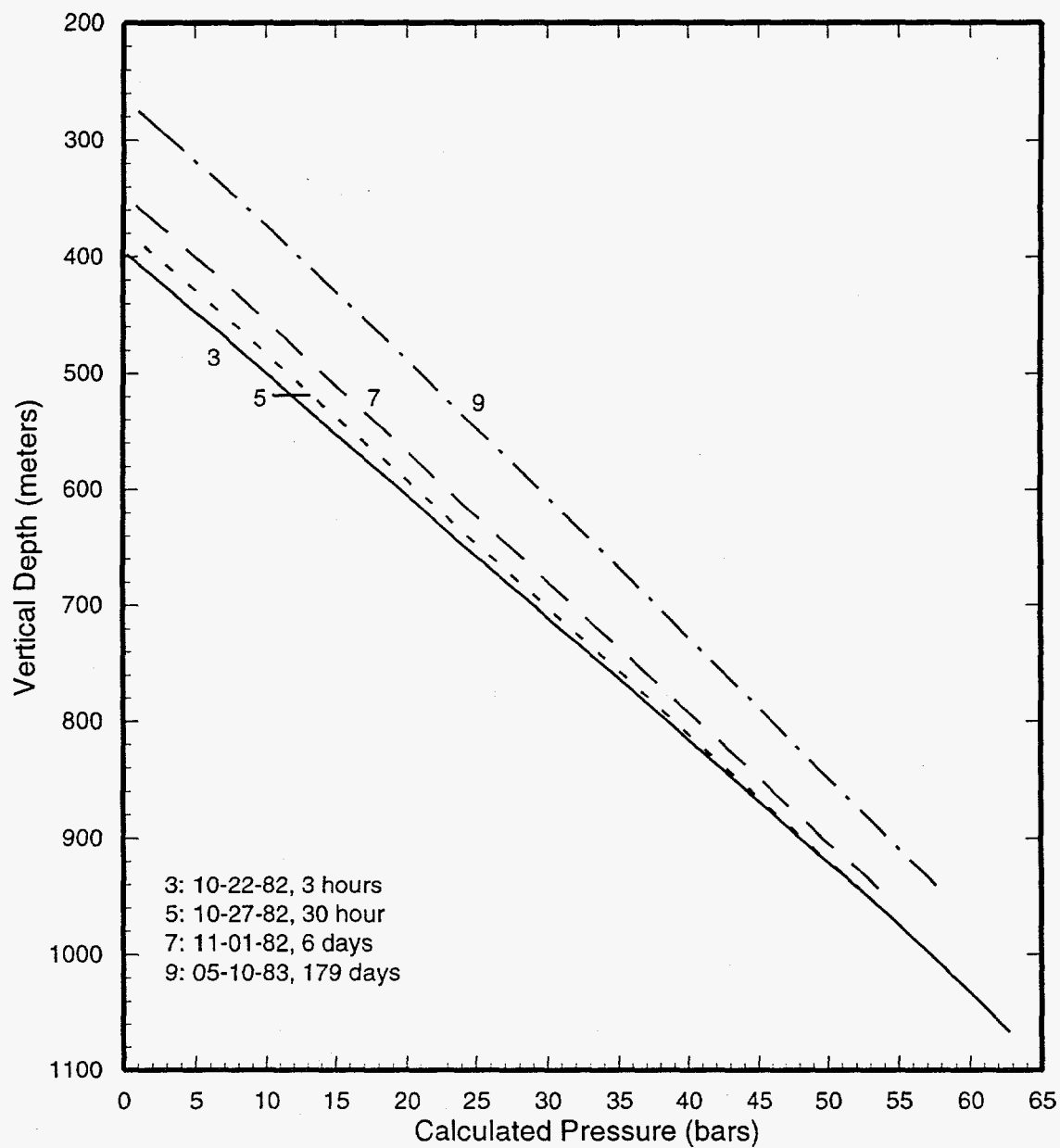


Figure 4.17. Pressure profiles computed from temperature and water level data in slim hole S-2 (drilled depth = 1065.1 m).

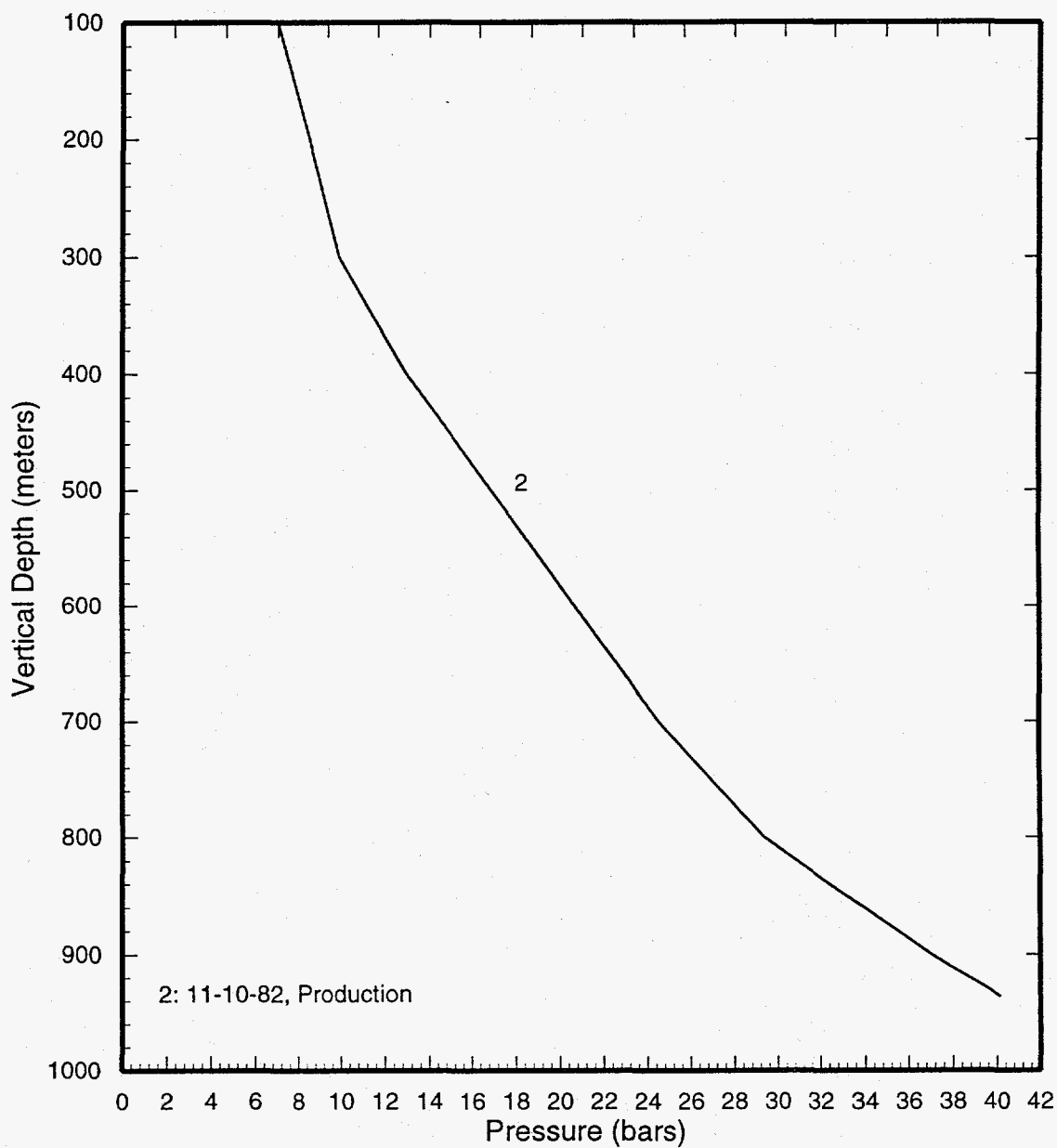


Figure 4.18. Pressure survey in slim hole S-2 (drilled depth = 1065.1 m) run during a production test on November 10, 1982.

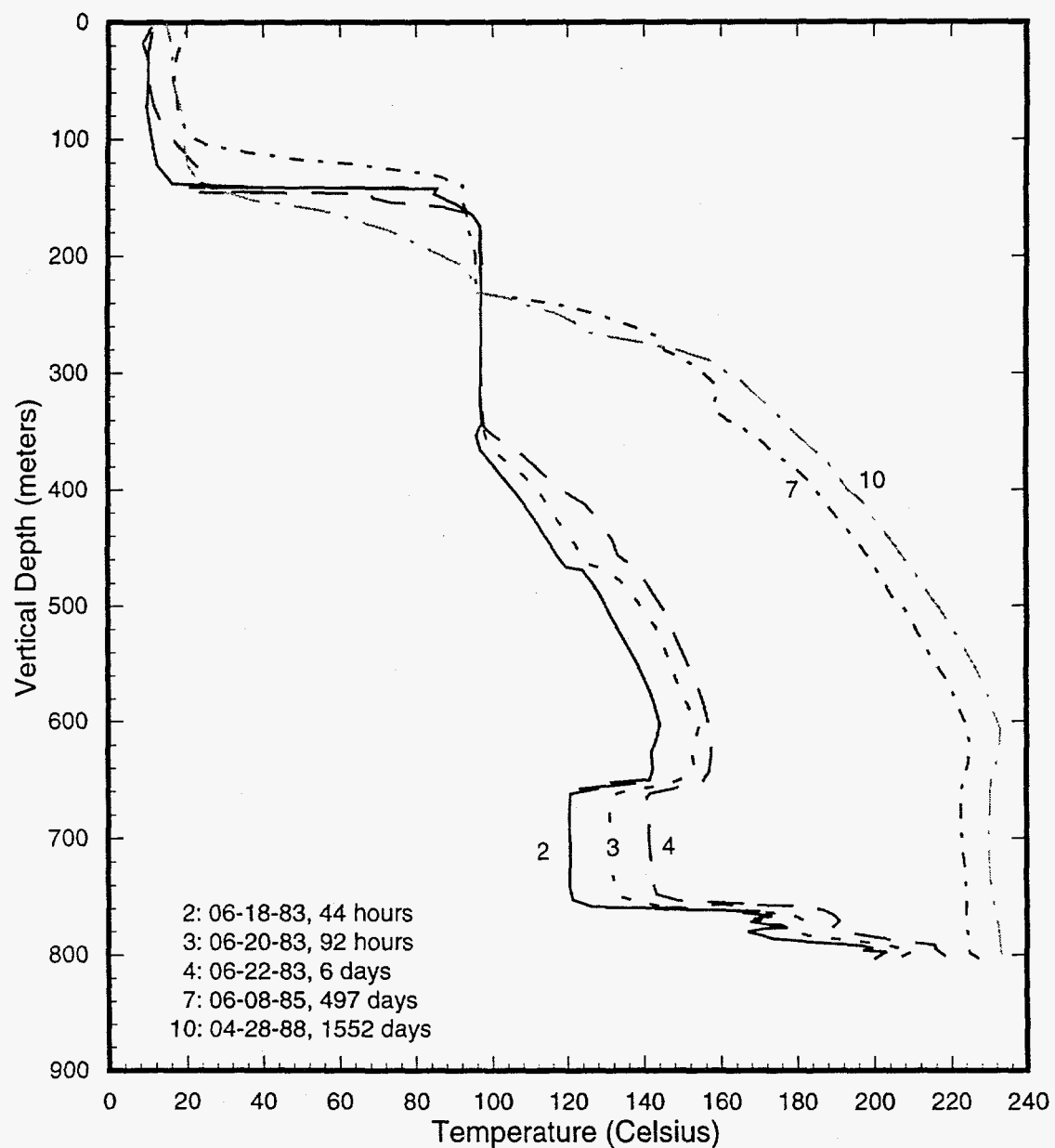


Figure 4.19. Selected temperature profiles for slim hole S-3.

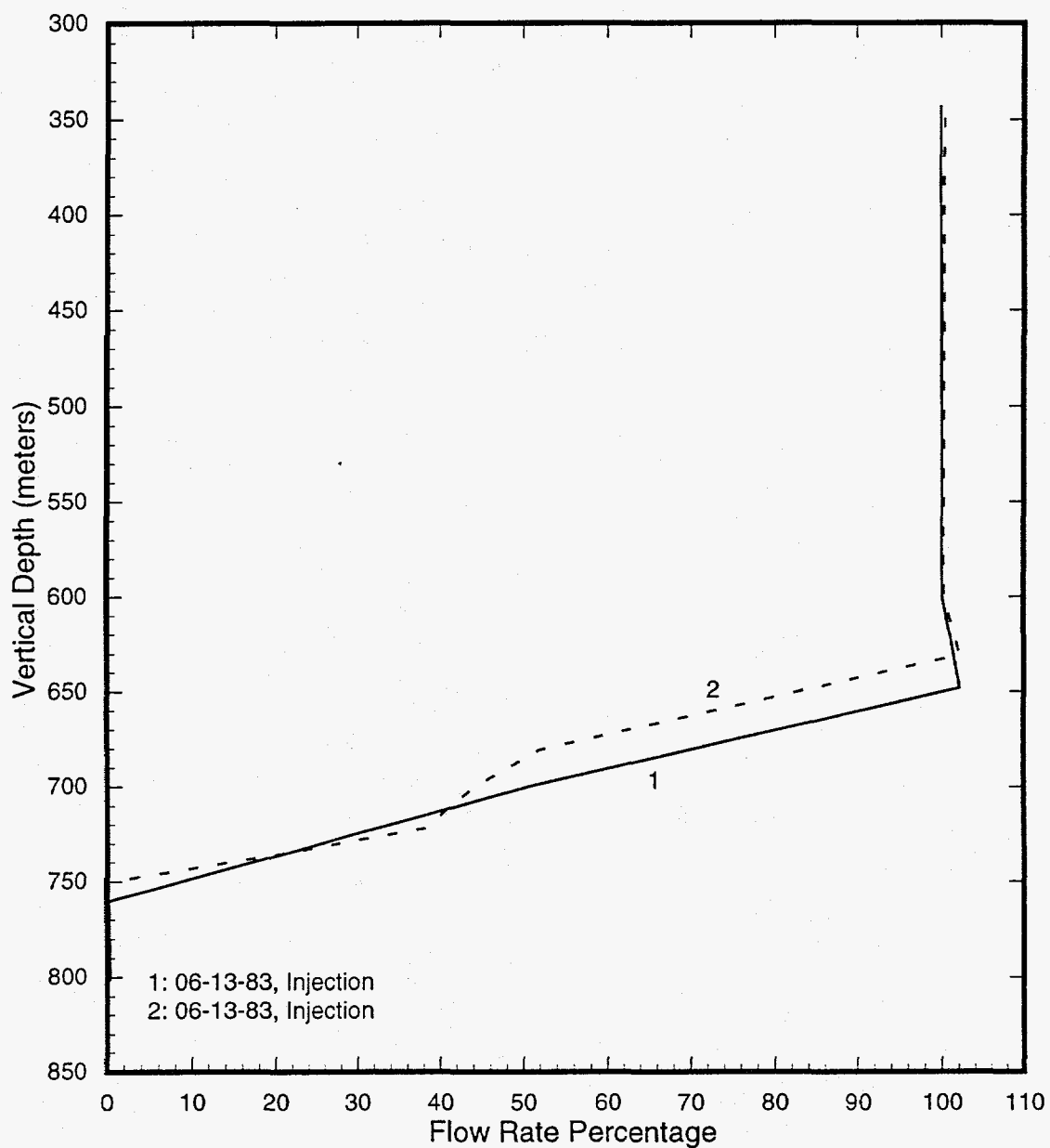


Figure 4.20. Spinner surveys (interpreted by MMC) in S-3 taken during an injection test on June 13, 1983.

that the main feed zone for S-3 (depth ~ 650 to 750 m) contains liquid water at ~ 240°C.

Several bottomhole pressure surveys are available for S-3. Two of these surveys (September 2, 1982, $p = 27.6$ bars at 428 m; May 16, 1983, $p = 32.6$ bars at 648 m) were made in the partially drilled hole (see Table II-3-1 in MMC, 1986). Since the reservoir is most likely two-phase down to a depth of ~ 650 m, these pressure values may be used to estimate the corresponding formation temperatures ($T = 229^\circ\text{C}$ at 428 m, and $T = 238^\circ\text{C}$ at ~ 648 m). We note that for borehole S-1, the estimated temperature at 436 m depth is at least 213°C .

Pressure profiles computed from water level and temperature data are shown in Figure 4.21. Pressure profiles (7 and 10) cannot be used to determine the feedzone pressure due to the presence of two-phase conditions in the wellbore. The pressure at the midpoint (700 m) of the permeable zone at 650 to 750 m can be estimated from profiles 2 and 4, and is ~ 33.5 bars. The latter pressure value is in substantial agreement with that obtained (~ 32.5 bars) from downhole pressure surveys (see e.g., pressure survey 3, Figure 4.22) conducted prior to June 1986. Later downhole pressure surveys (surveys 4 and 5, Figure 4.22) give substantially higher pressures; these higher pressures may be the result of a shallow casing leak in S-3.

4.7 Well S-4

Selected temperature profiles for S-4 are shown in Figure 4.23. Temperature profile 1 was measured in the partially drilled hole, and indicates a temperature of ~ 245°C at a depth of 650 m. The measured temperature implies two-phase (or even steam) conditions at this depth in the reservoir. The shape of the temperature profile (i.e., linear gradi-

ent above ~550 m) suggests that two-phase conditions may extend up to ~550 m.

The short-time heat-up profiles (see profiles 2 through 4) indicate permeable zones at 1120 to 1180 m and at ~1525 m. These permeable zones are also confirmed by a flow-meter test carried out on November 7, 1983. The flow-meter also indicates water loss at 1200 to 1300 m (Figure 4.24). Temperature profile 12 (Figure 4.23) shows an isothermal zone from 1250 to 1350 m; an isothermal zone implies permeability at both its end points. The maximum temperature (Profile 6) occurs towards bottomhole and is ~ 300°C .

Pressure profiles calculated from water level and temperature data are shown in Figure 4.25. Pressure profiles 2 and 4 (corresponding to temperature profiles 2 and 4, Figure 4.23) coincide towards bottomhole; this indicates that the primary permeable zone for S-4 is at ~1520 to 1530 m. The computed pressure at ~1520 m is ~94 bars, and is in good agreement with a bottomhole pressure survey ($p = 94.9$ bars at 1523 m) made on June 29, 1984 (MMC, 1986; Table II-3-1). It is noteworthy that the water level and temperature data recorded on the latter date yield a higher pressure value (see profile 6 in Figure 4.25). The water level data of June 29, 1984, and April 3, 1989 (Figure 4.25), cannot be used to calculate downhole pressures due to the presence of boiling conditions in the wellbore at that time. The measured pressure profiles for well S-4 are shown in Figure 4.26; these pressure profiles indicate a pressure of ~92 bars at ~1520 m. Based on the preceding discussion, the stable pressure at ~1520 m is estimated to be $93 (\pm 1)$ bars.

Continued on page 4-33

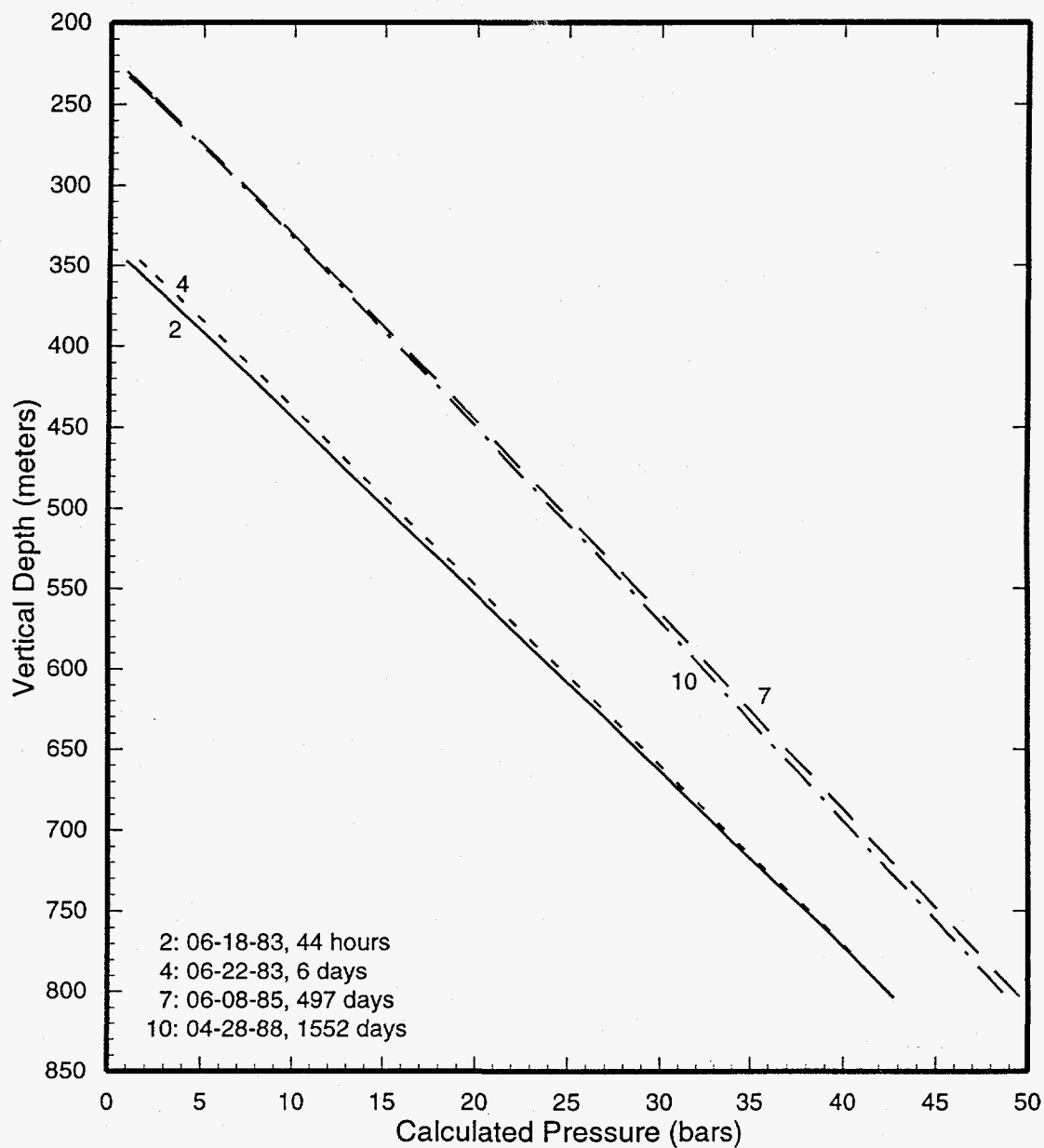


Figure 4.21. Pressure profiles computed from water level and temperature data for slim hole S-3.

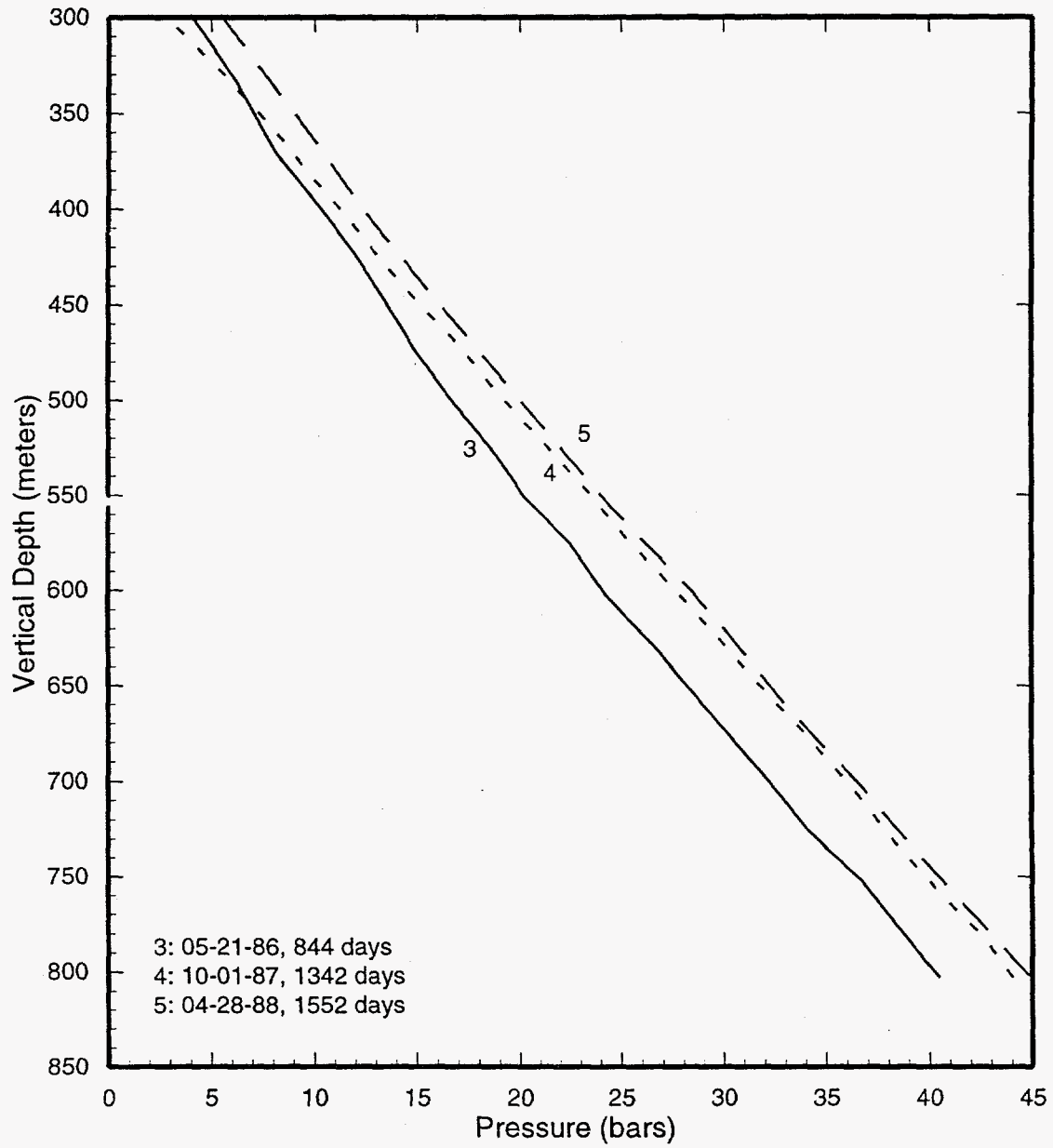


Figure 4.22. Measured pressure profiles for slim hole S-3.

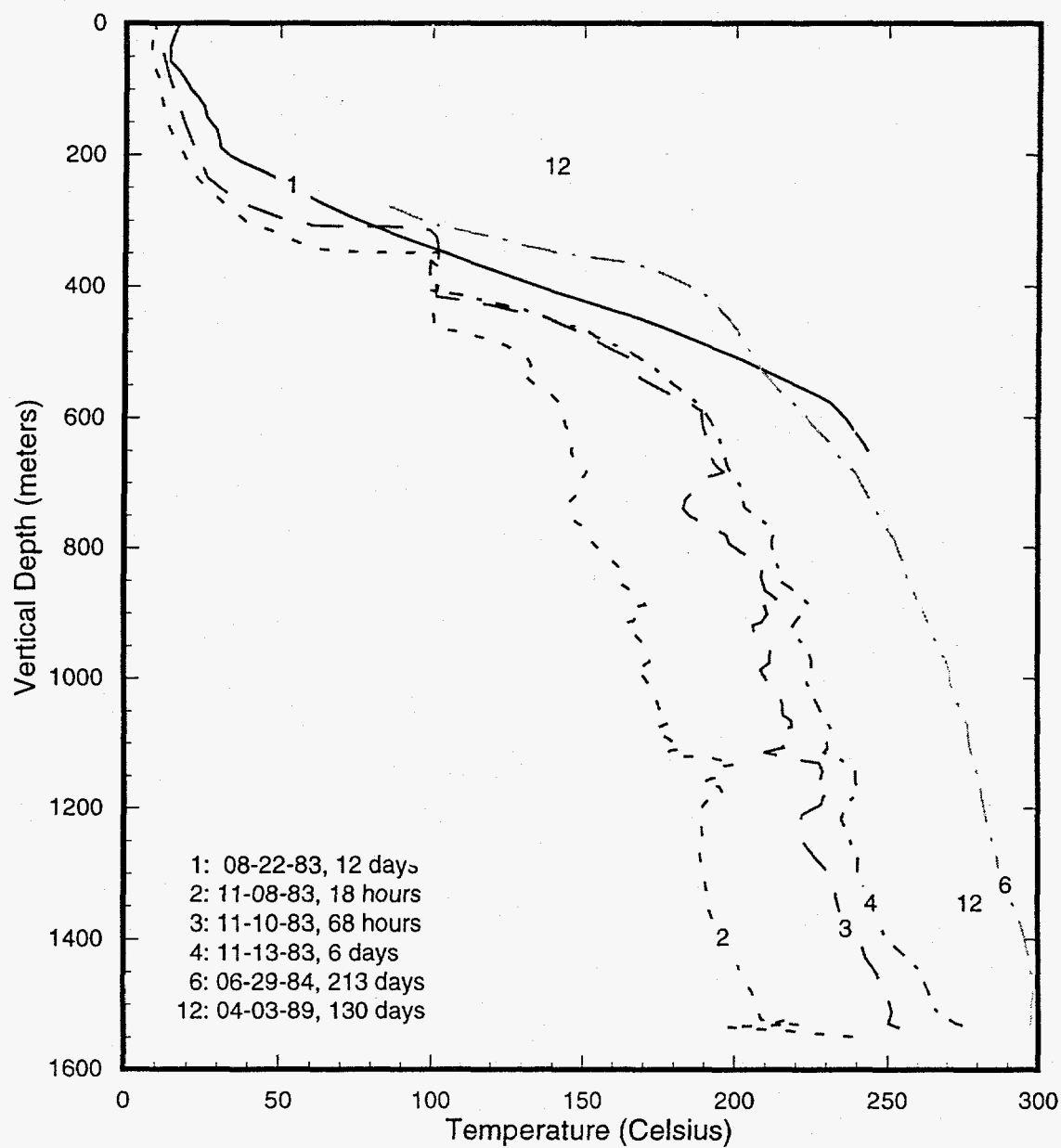


Figure 4.23. Temperature surveys for well S-4.

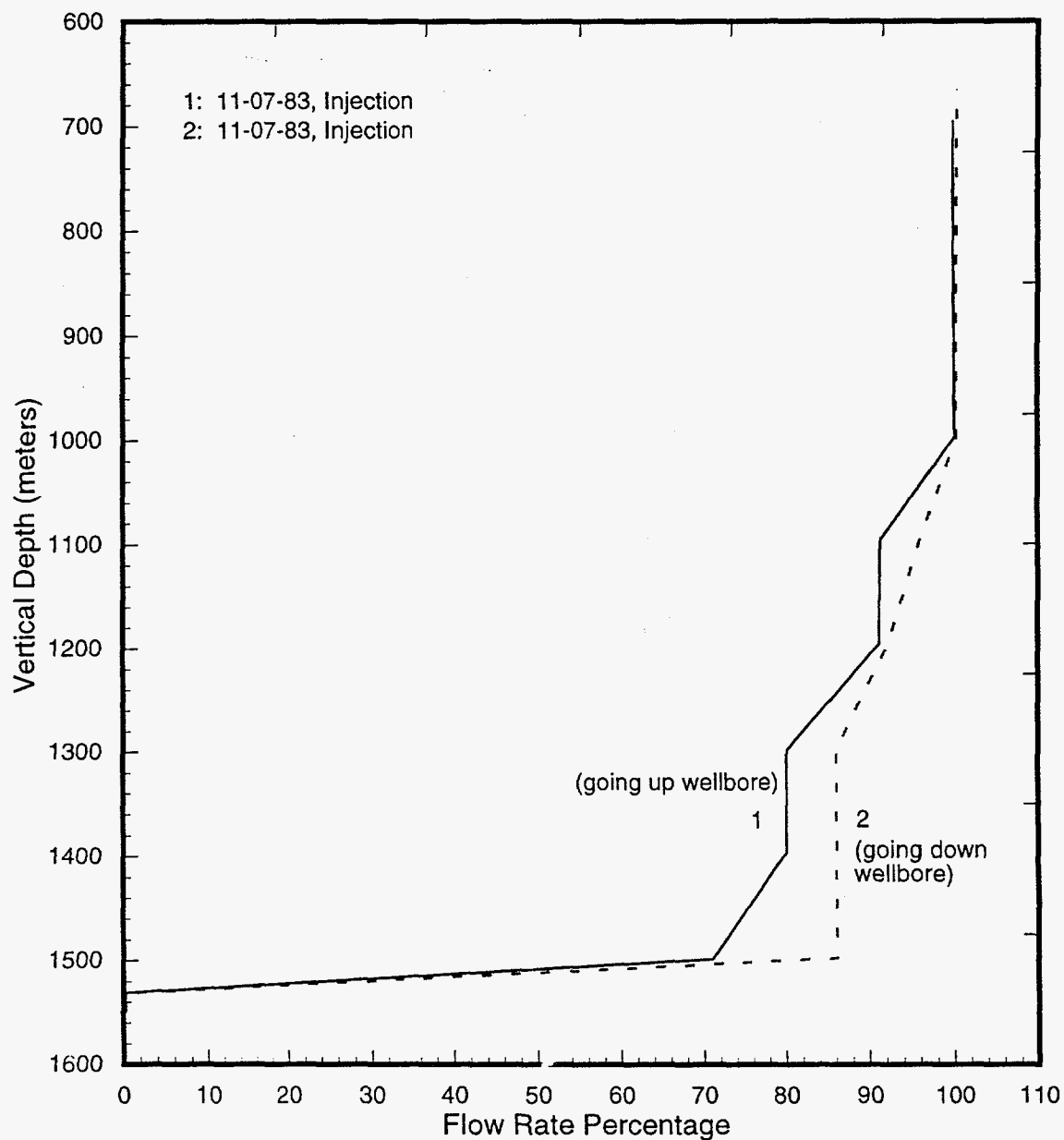


Figure 4.24. Spinner surveys (interpretation by MMC) recorded in well S-4 during an injection test on November 7, 1983.

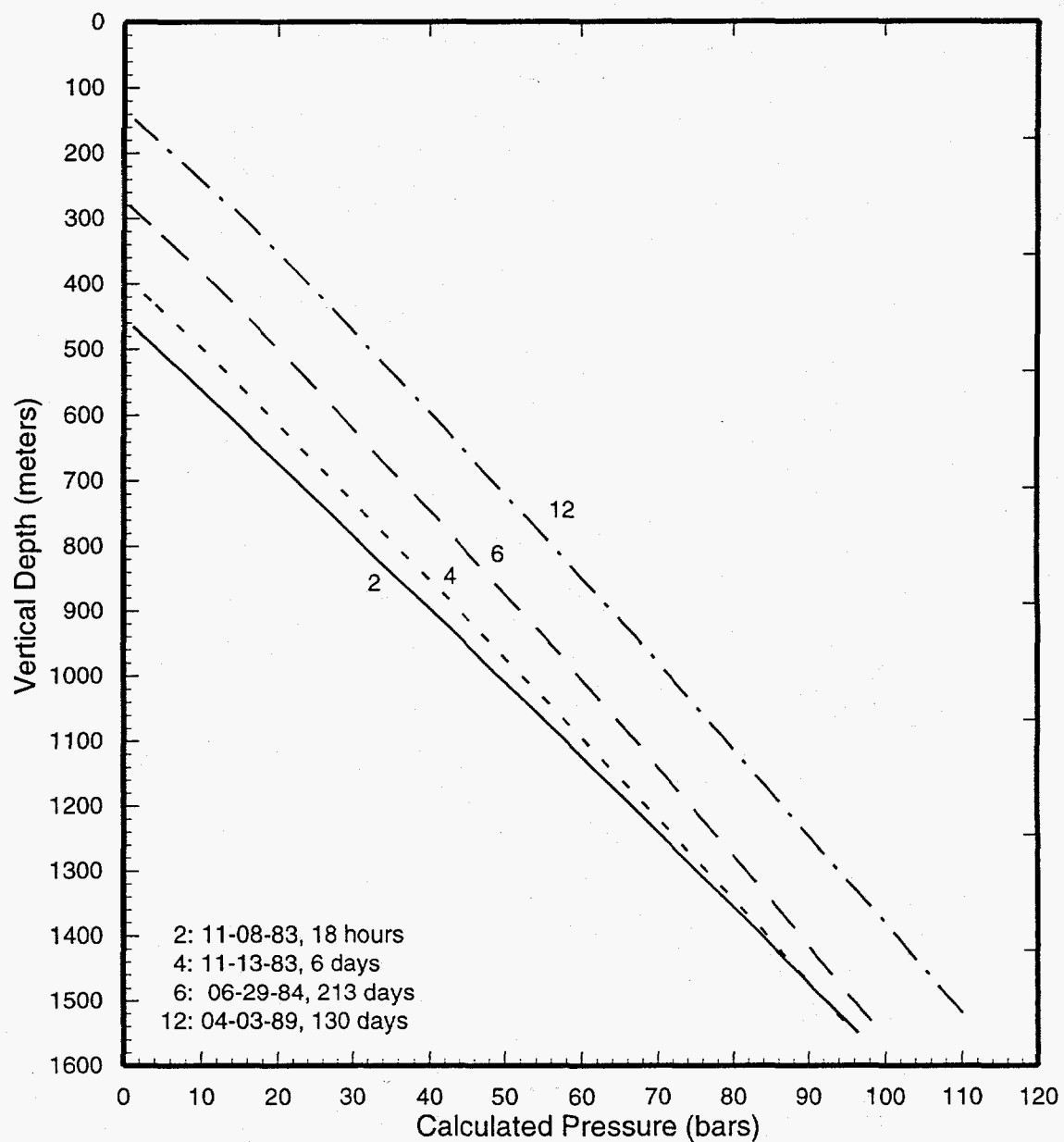


Figure 4.25. Pressure profiles computed from water level and temperature data for well S-4.

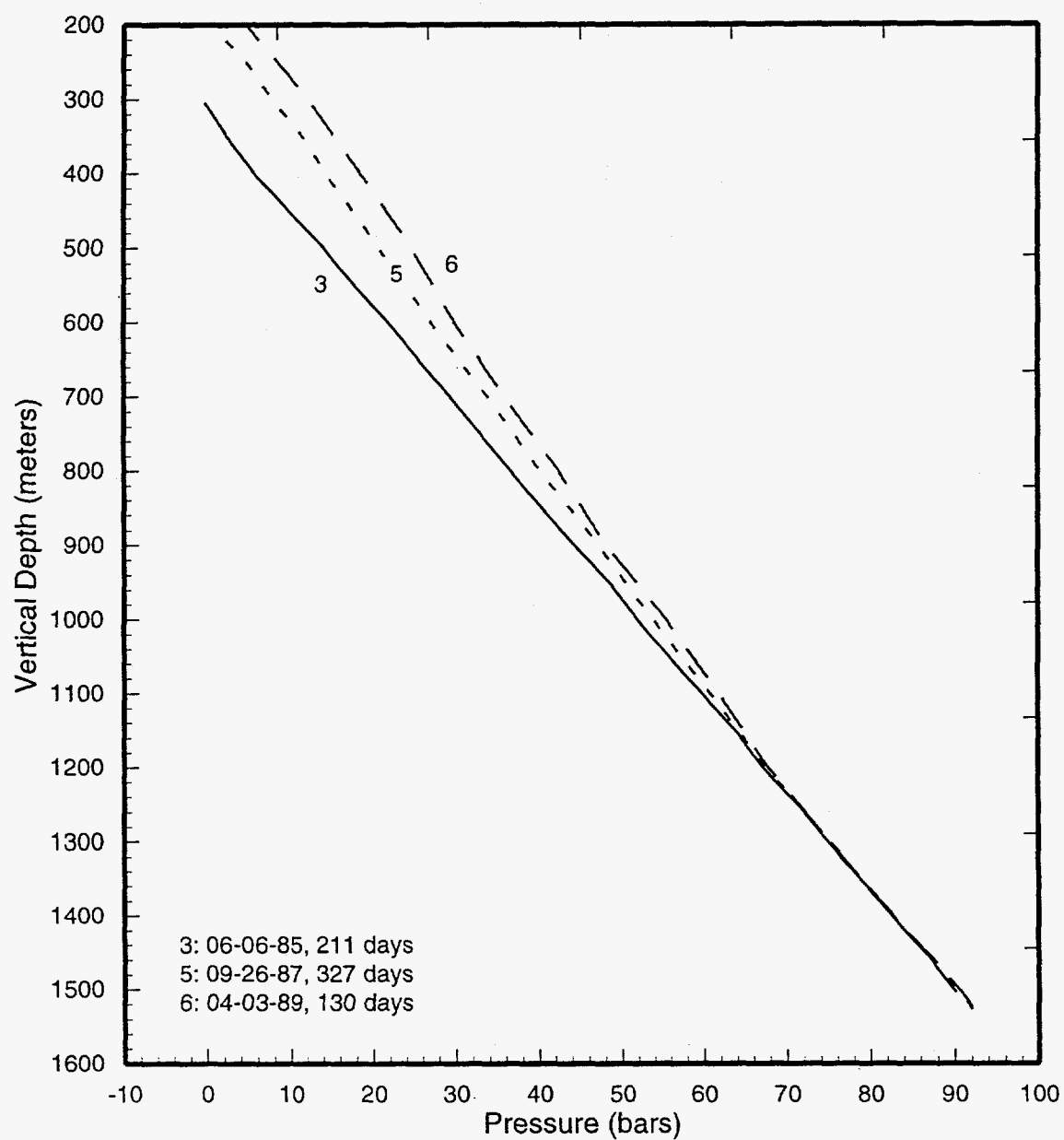


Figure 4.26. Measured pressure profiles for well S-4.

4.8 Well SA-1

Selected temperature surveys for well SA-1 are displayed in Figure 4.27. The temperature survey recorded on October 10, 1986 while injecting cold water shows an anomalously warm interval from ~1250 m TVD to ~1450 m TVD. This anomaly is most likely associated with the particular liner arrangement (slotted/blank/slotted/blank/slotted) employed in the hole over the latter depth interval. A spinner survey taken during an injection test on October 15, 1987 (Figure 4.28) shows a complex flow pattern in the well from ~1250 m TVD to ~1450 m TVD. All the available spinner surveys (Figures 4.28 and 4.29) indicate that the major permeable zone for SA-1 is located at ~1790 m TVD. The maximum temperature occurs towards bottomhole and exceeds 305°C.

Pressures computed from measured temperature profiles and water level data are shown in Figure 4.30. Interestingly, the pressures appear to increase with increasing shutin time, and do not form a pivot. This may be indicative of poor formation permeability; alternatively, it could be due to inaccuracies in water level data. It is often difficult to measure water levels accurately in wells which are boiling. The computed pressure (Figure 4.30) at 1800 m TVD is $\sim 114.5 \pm 2$ bars. This value is in good agreement with that (~ 113 bars) recorded on April 22, 1988 with a downhole pressure gauge (see Figure 4.31).

4.9 Well SA-2

A temperature survey taken during cold water injection on September 28, 1987 (Figure 4.32) shows that part of the injected fluid is lost into a fracture zone at ~1450 m TVD, and that the rest of the injected fluid travels down the hole. Heat up

surveys (Figure 4.32, profiles 1 and 2) indicate additional permeable zones at ~1150 m TVD and at ~1900 m TVD. The permeable zone at ~1900 m TVD is probably associated with the lost circulation zone recorded near this depth. A spinner survey taken during cold water injection on September 28, 1987 (Figure 4.33) indicates that most of the water loss occurs from ~1380 m TVD to ~1500 m TVD. Thus, it would appear that the major feed point for Well SA-2 is located at ~1450 m TVD. The maximum temperature occurs towards bottomhole and is ~320°C. The feedzone temperature exceeds 300°C.

No reliable downhole pressure measurements are available for this well. (Downhole pressure measurements were made with KPG-29846 and PTS-350. As discussed elsewhere in this report, these measurements are not reliable.) Pressure profiles computed from water level and temperature data are shown in Figure 4.34. The water level for profile 1 was obtained from an electric survey, and may be in substantial error. The pressure survey conducted with Kuster tool KPG-29846 (Figure 4.35) was used to determine the water level for profile 8. Although the two pressure profiles in Figure 4.34 appear to pivot at ~1220 m TVD, we do not attach any significance to this observation; a pressure pivot should be an intersection of at least three pressure profiles. Assuming that pressure profile 8 represents stable pressures, the pressure at 1450 m TVD is ~95.5 bars; by comparison, the downhole pressure recorded directly by KPG-29846 (see Figure 4.35) is ~94.5 bars. At present, the feedpoint pressure for Well SA-2 must be regarded as uncertain. The available estimates for feedzone pressure and temperature imply that two-phase conditions may be present at the feedzone.

Continued on page 4-43

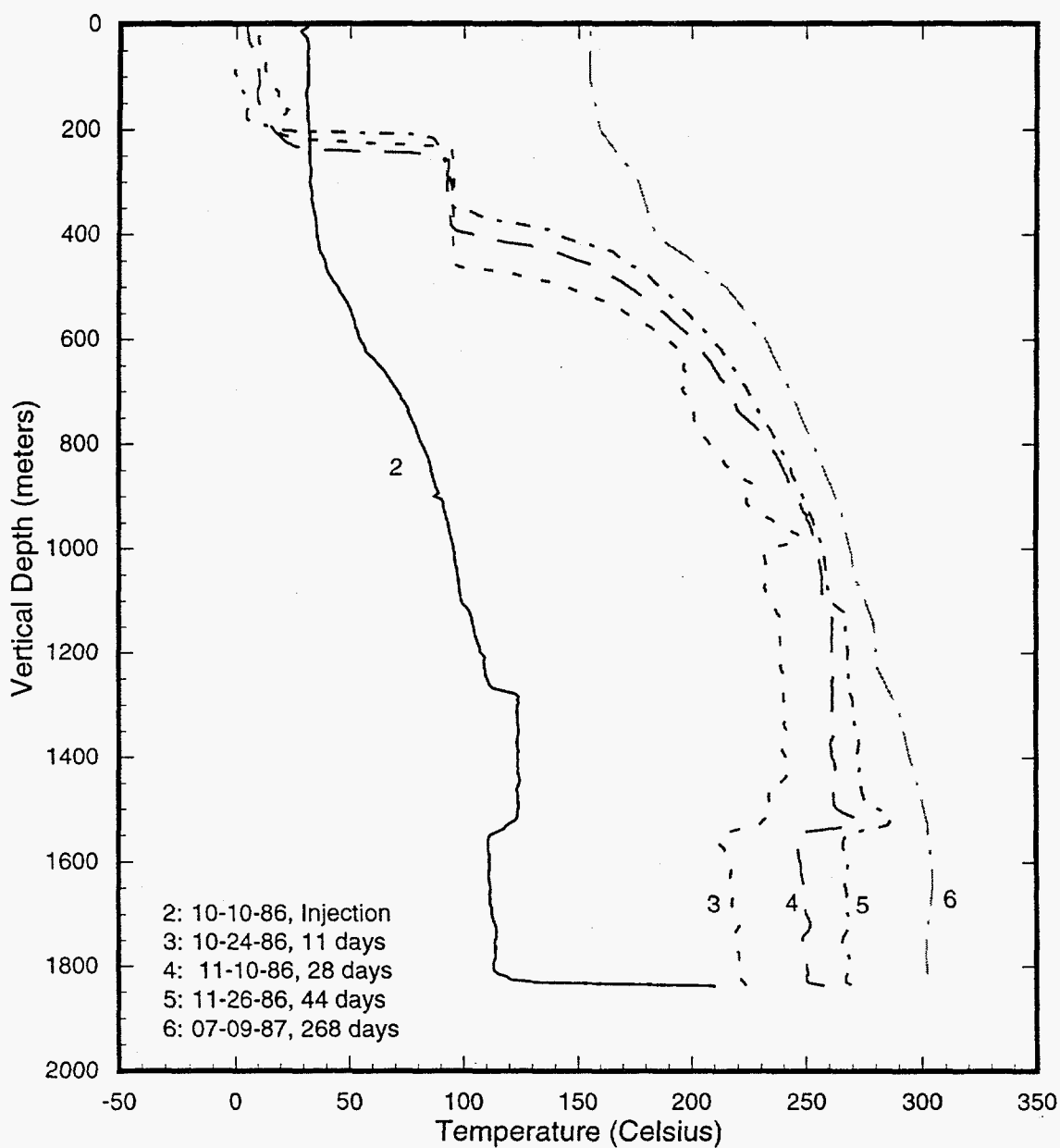


Figure 4.27. Temperature surveys in well SA-1.

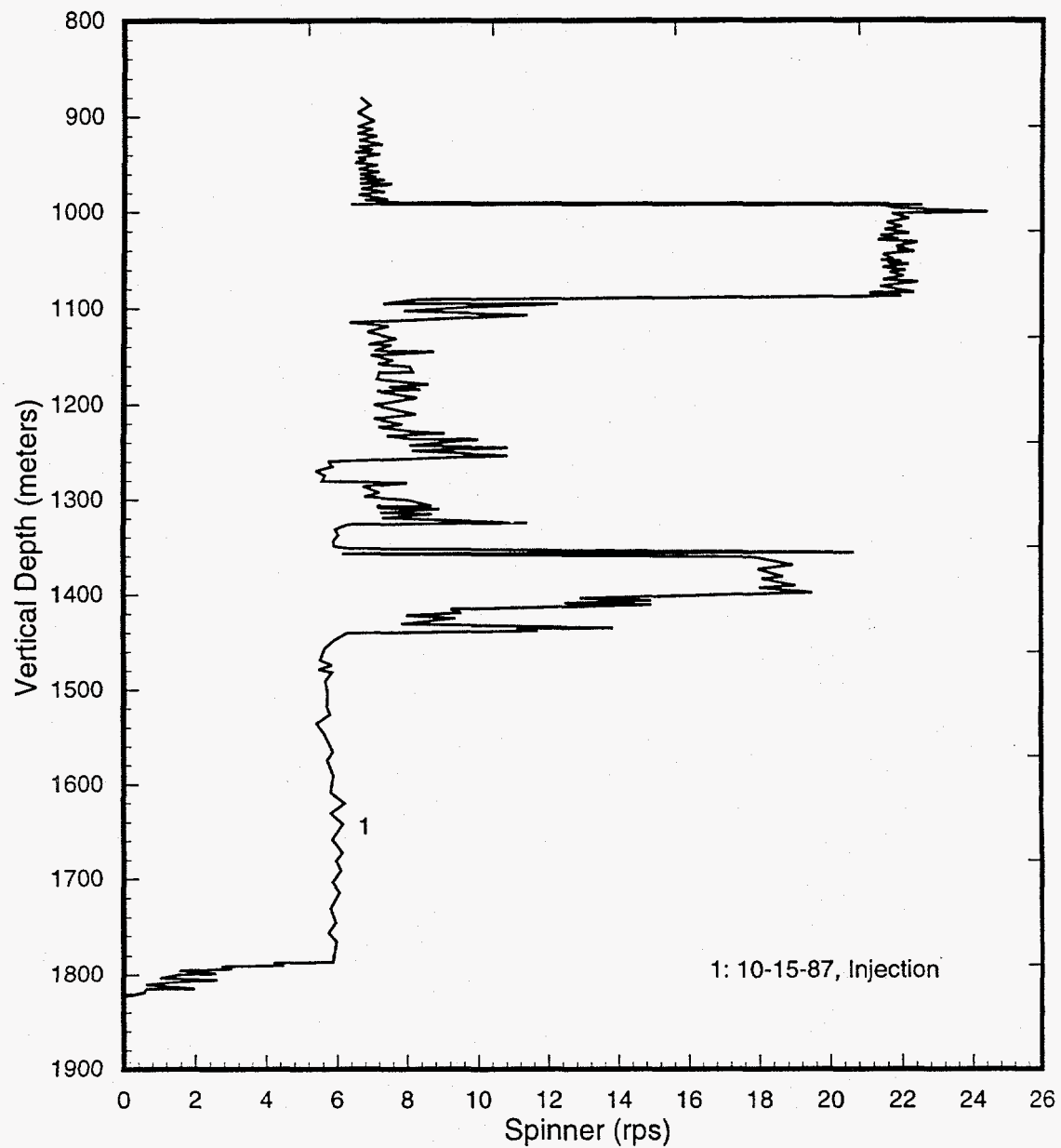


Figure 4.28. A spinner survey recorded (tool moving up wellbore) while injecting cold water in well SA-1 on October 15, 1987.

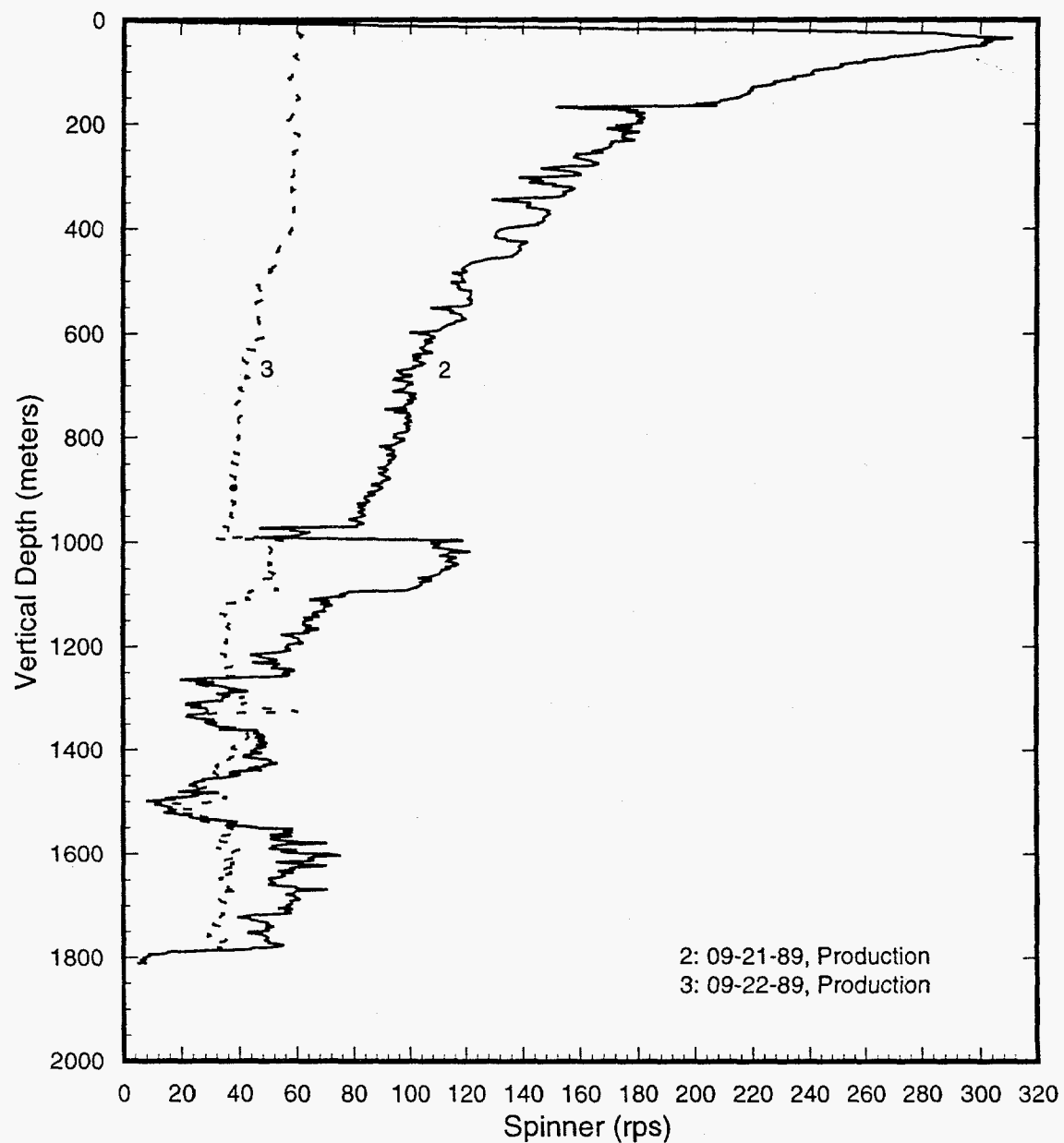


Figure 4.29. Spinner surveys recorded in well SA-1 during a discharge test in September 1989.

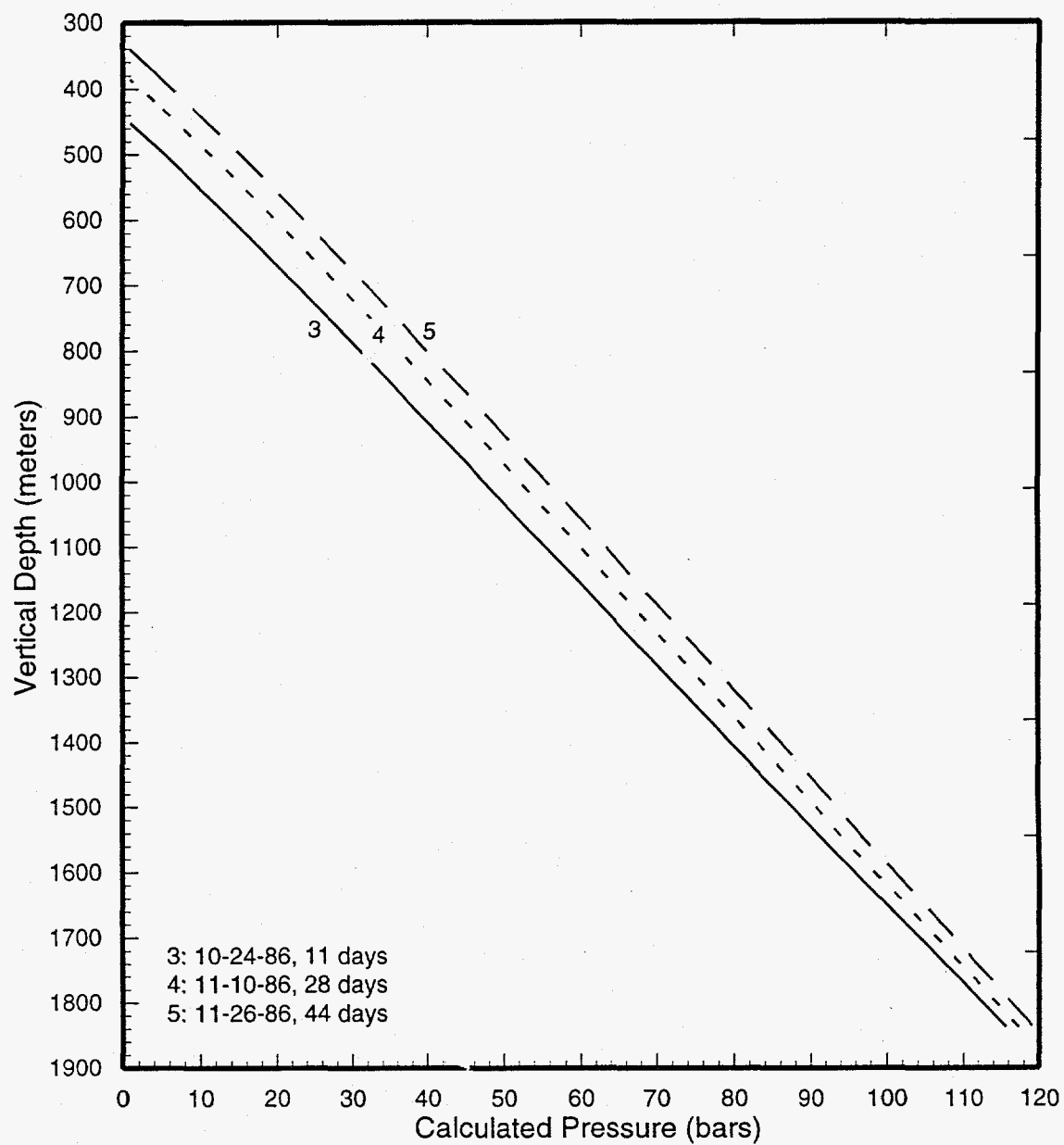


Figure 4.30. Pressures (computed from water level and temperature data) in well SA-1.

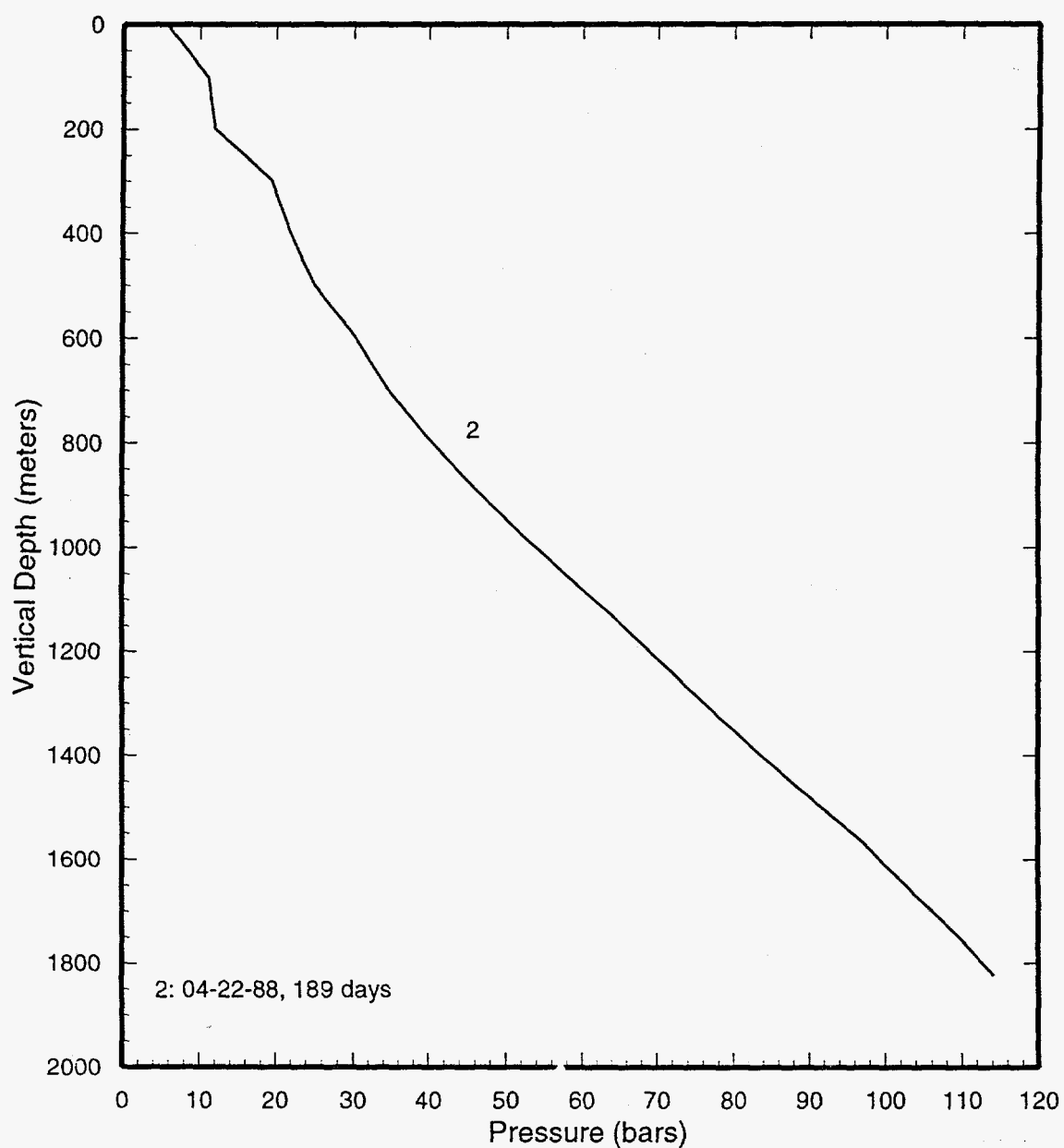


Figure 4.31. A measured pressure profile in well SA-1.

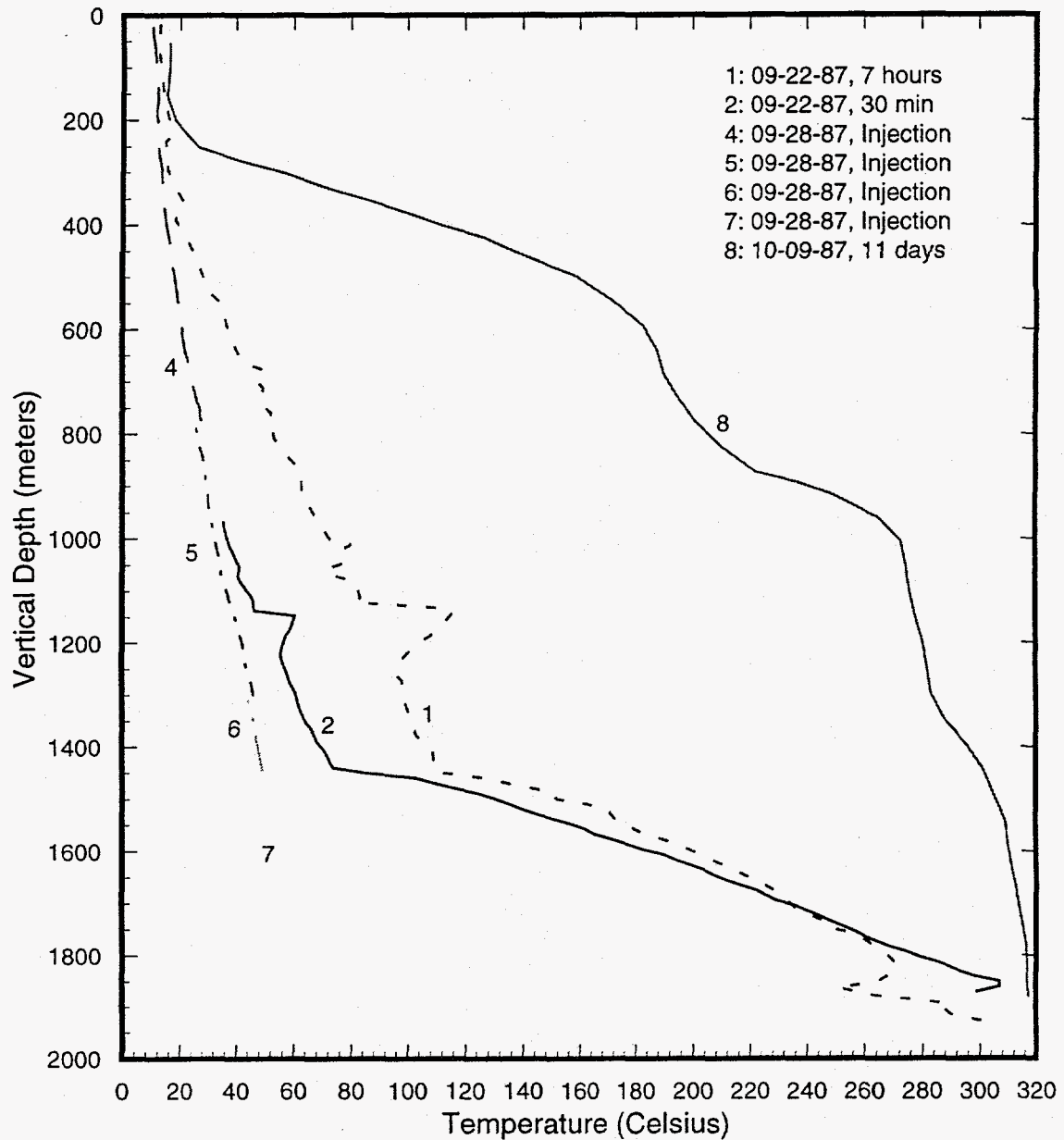


Figure 4.32. Temperature surveys in well SA-2. Breaks in injection temperature profile of September 28, 1987 indicate stops at these locations.

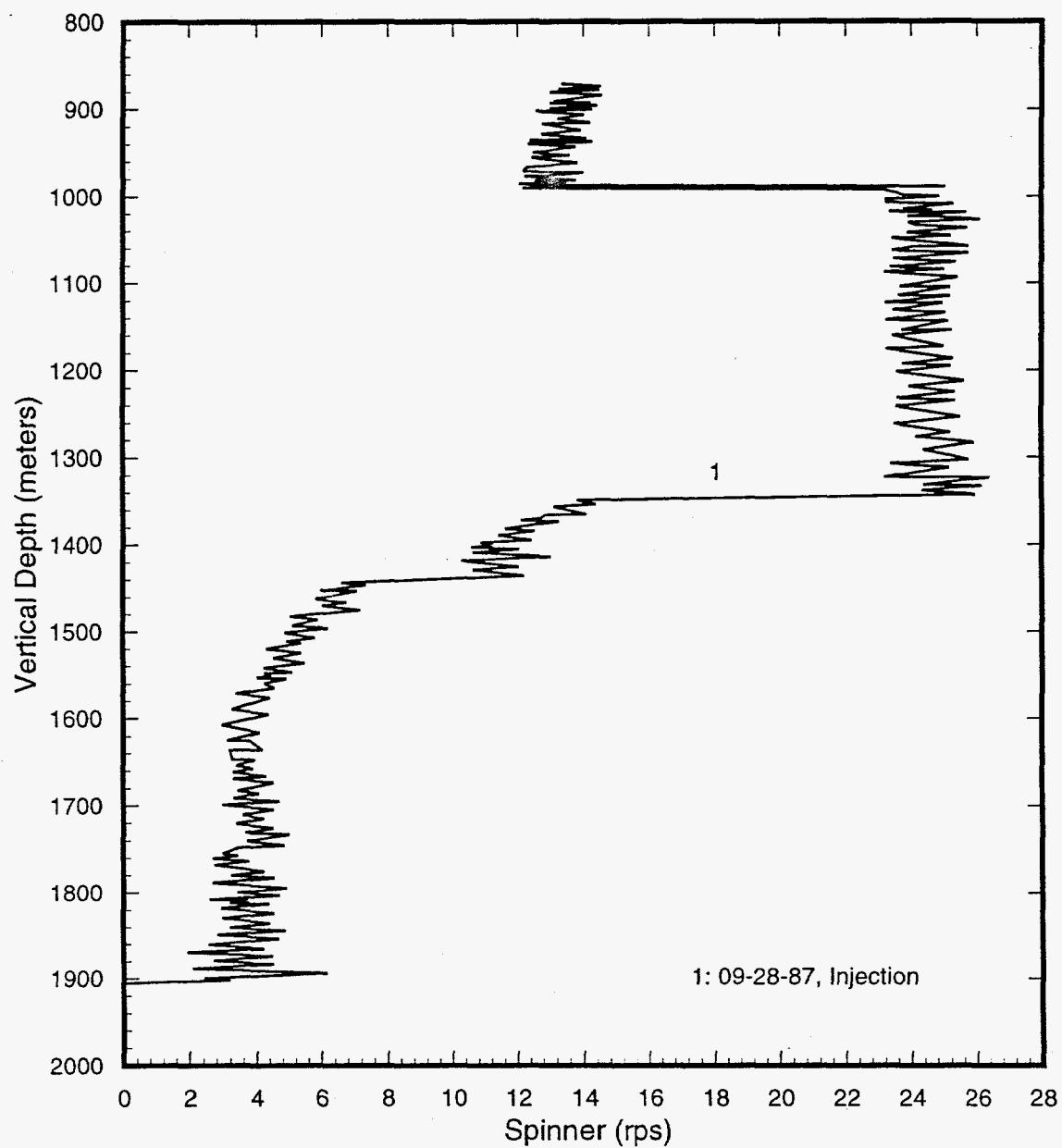


Figure 4.33. A spinner survey (tool moving up the hole) recorded in well SA-2 during an injection test on September 28, 1987.

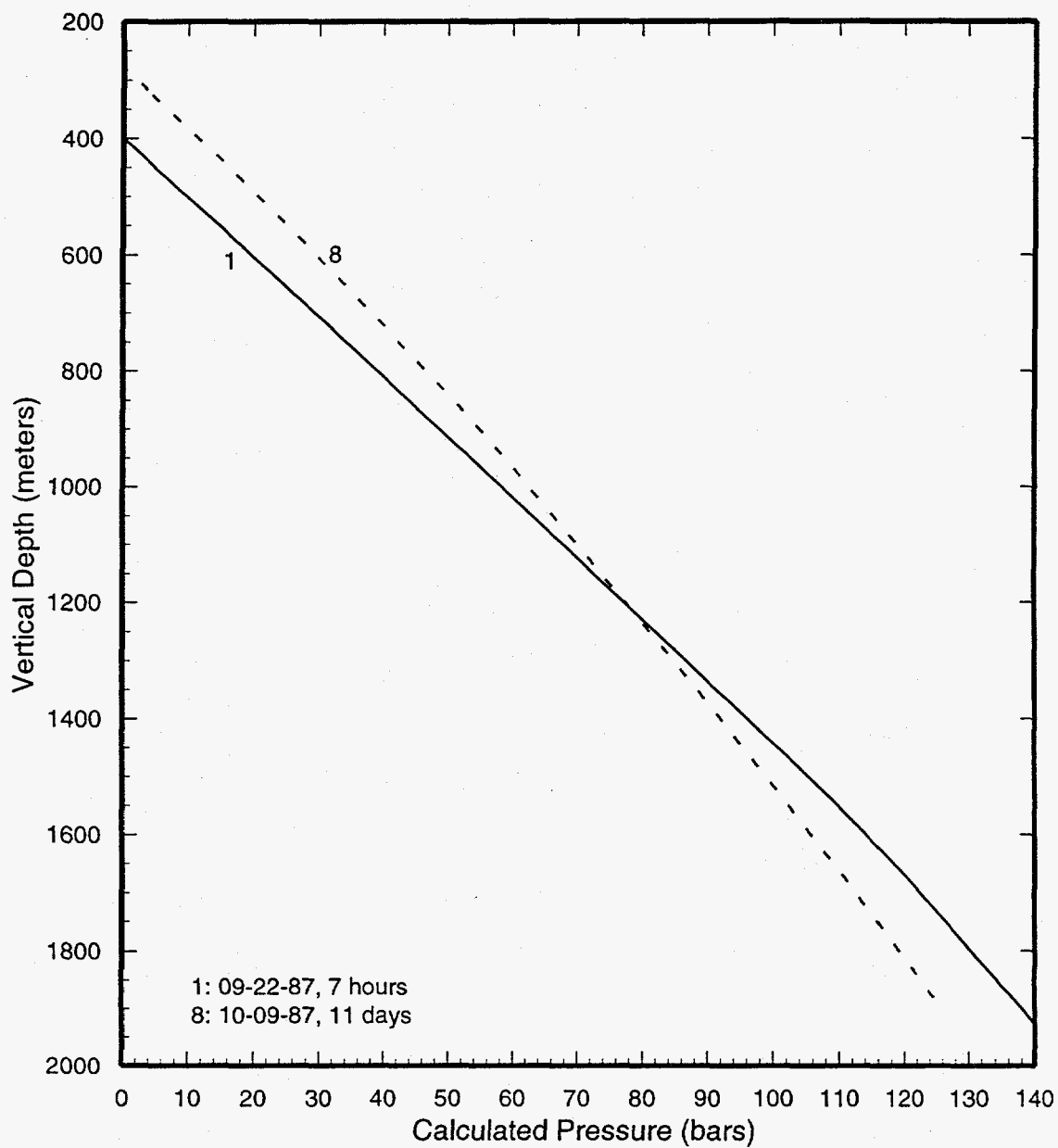


Figure 4.34. Pressures computed from water level and temperature data in well SA-2.

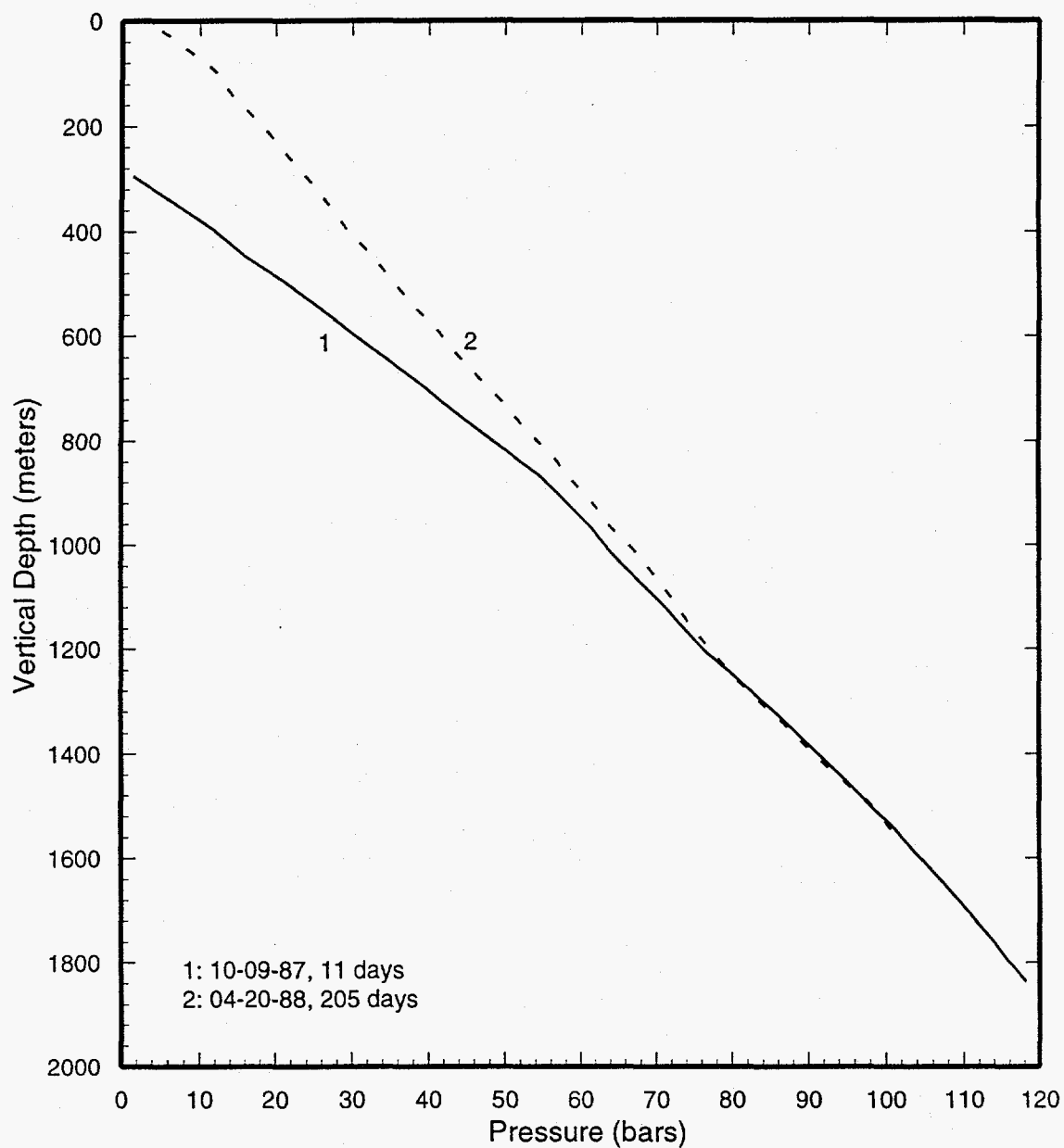


Figure 4.35. Pressure surveys in well SA-2.

4.10 Well SA-4

Temperature surveys taken during and shortly after injection (see profiles 9 and 3, Figure 4.36) imply that most of the water loss occurs from ~1240 m TVD to ~1420 m TVD; this depth interval is characterized by numerous lost circulation zones. Rapid temperature recovery at ~1240 m TVD (profiles 2 and 6, Figure 4.36) indicates that the major feed zone for SA-4 is located at this depth. A spinner survey recorded in the discharging well (Figure 4.37) supports the conclusion that the major permeable horizon is situated at ~1240 TVD. Offsets in the spinner and temperature survey at ~920 TVD (Figures 4.38 and 4.39) indicate the presence of a casing break and a minor inflow zone at this depth. The pressure and temperature surveys in the discharging well indicate that the entry at ~920 TVD supplies steam to the well. The maximum temperature occurs towards bottomhole and exceeds 300°C. The feedzone temperature exceeds 290°C.

Shutin pressure surveys of June 11, 1988 and June 26, 1988 (Figure 4.40) were both made with tool PTS-350. Pressure profiles computed from water level and temperature data are displayed in Figure 4.41. The pressure (Figure 4.41) at 1240 m TVD is ~80 bars, and is not too different from that (~81.5 bars) recorded downhole by PTS-350. The estimated feedzone temperature and pressure values indicate that two-phase conditions are likely at the feedzone depth.

4.11 Well SB-1

Selected temperature surveys in well SB-1 are shown in Figure 4.42. Short-time heat up surveys after cold water injection (see Profiles 2, 3 and 4) indicate permeable horizons at ~1520 m TVD and

at ~1650 m TVD. A minor entry may also be present just below the casing shoe at ~1060 m TVD. The persistence of a low temperature zone at ~1520 m TVD may imply that the major permeable horizon for SB-1 is located at this depth. The maximum temperature occurs towards bottomhole and is ~300°C. By comparison with measured temperatures above and below the feedzone, the temperature at 1600 m TVD is estimated to be at least 260°C.

Pressure profiles computed from water level and temperature data are displayed in Figure 4.43; profiles 5, 8 and 9 (Figure 4.43) intersect at about ~1600 m TVD. The pressure at 1600 m TVD is ~103 bars. Measured pressure profiles for SB-1 are displayed in Figure 4.44. The pressure survey of May 7, 1988 – conducted with PTS-350 – exhibits strange behavior below ~1650 m TVD. Pressure surveys 2 and 3 (Figure 4.44) give a pressure of ~103 bars at 1600 m TVD; the latter value is identical with that computed from temperature and water level data.

4.12 Well SB-2

Brief shutin time heatup surveys (see profiles 1, 2 and 3, Figure 4.45) indicate several permeable horizons (740 m TVD, 1020 m TVD, 1160 m TVD and 1270 m TVD). The permeable horizons at 1020 m TVD, 1160 m TVD and 1270 m TVD correspond closely to lost circulation zones. The persistence of a cold zone at ~1270 m TVD even at late times (profiles 4 and 5, Figure 4.45) implies that the major feed point for SB-2 is located at about this depth. By comparison with the temperatures measured above the feedzone, the temperature at 1270 m TVD is estimated to be about 250°C.

Continued on page 4-54

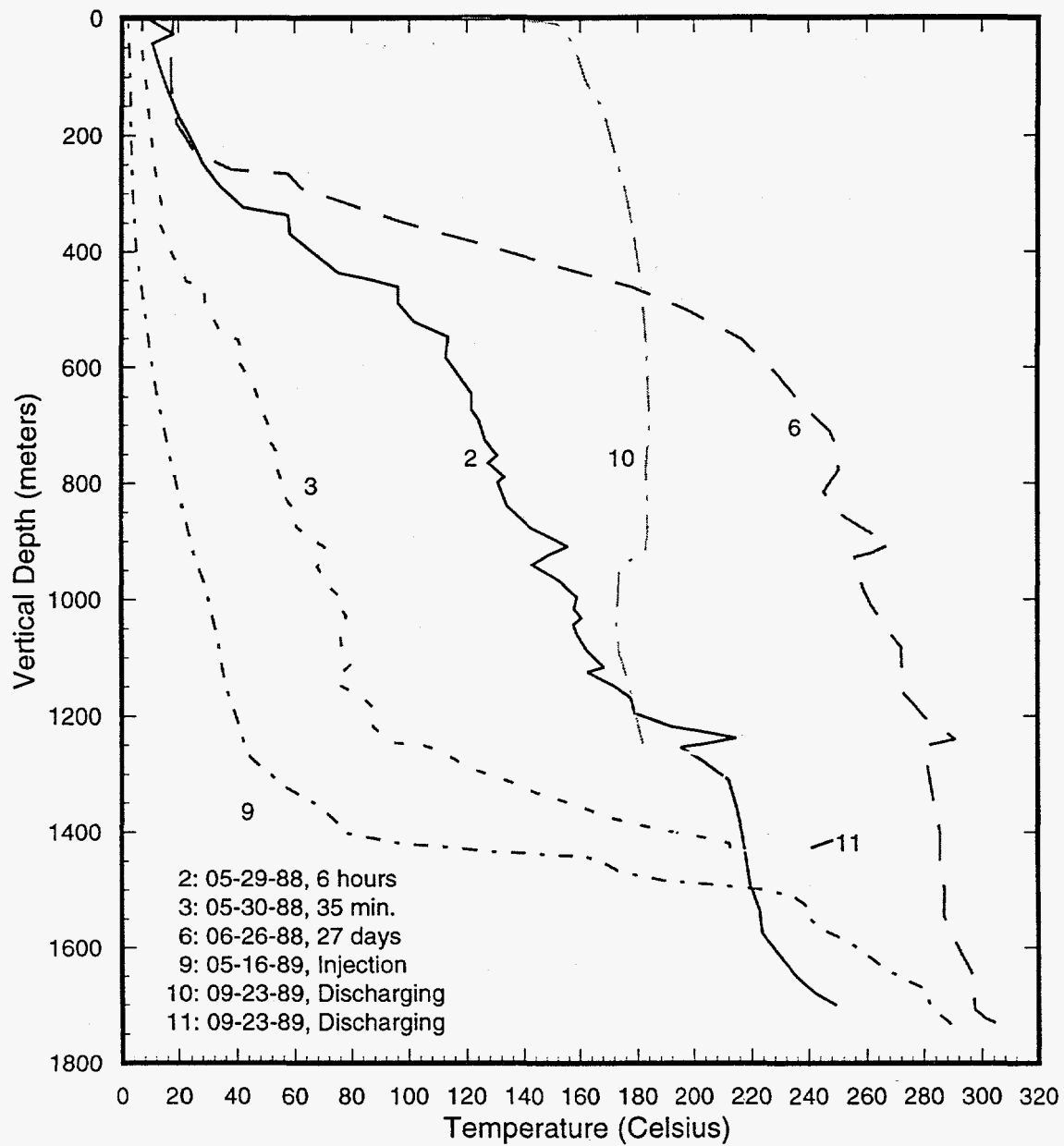


Figure 4.36. Selected temperature surveys in well SA-4.

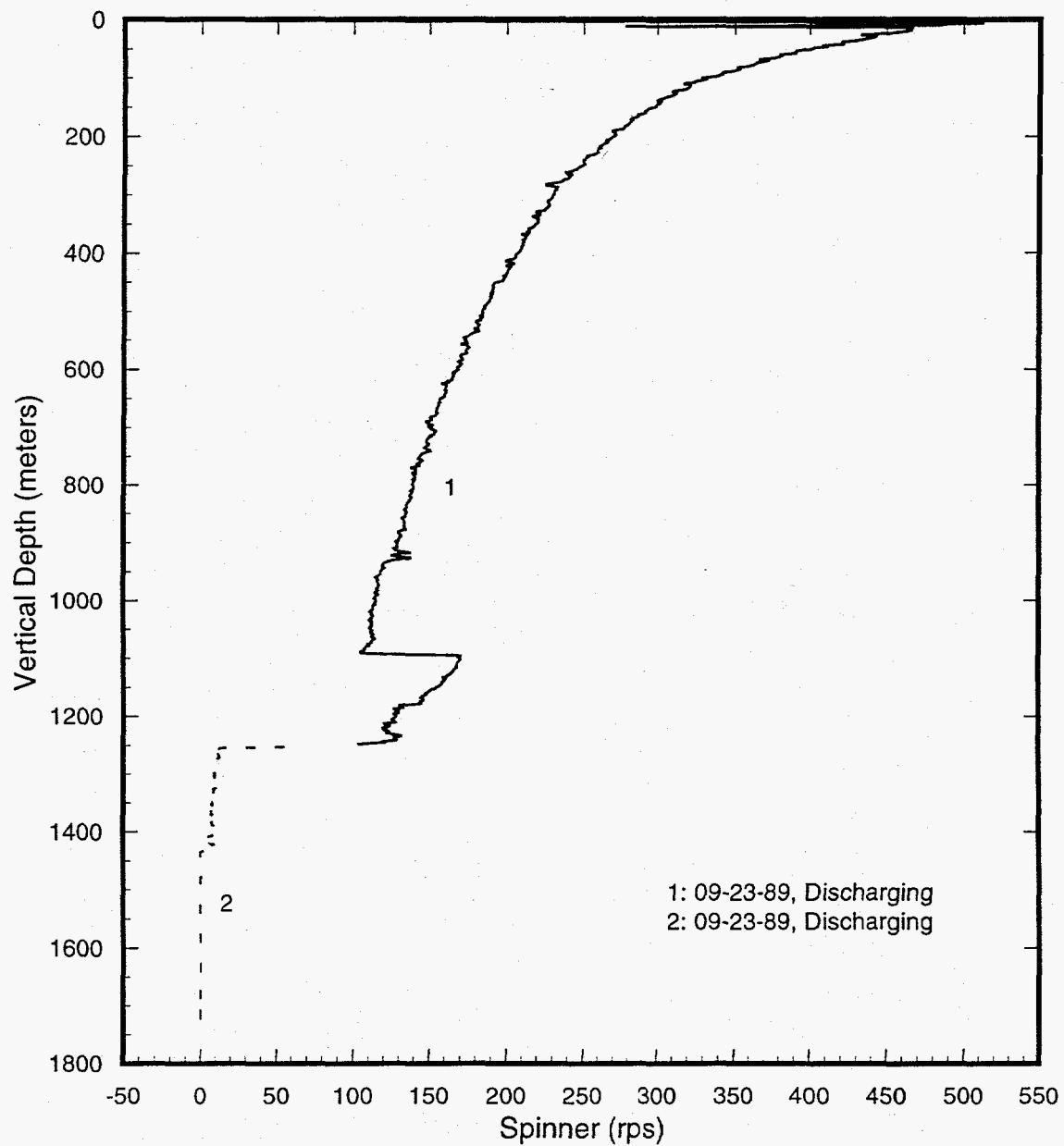


Figure 4.37. A spinner survey recorded during a discharge test in well SA-4 on September 23, 1989.

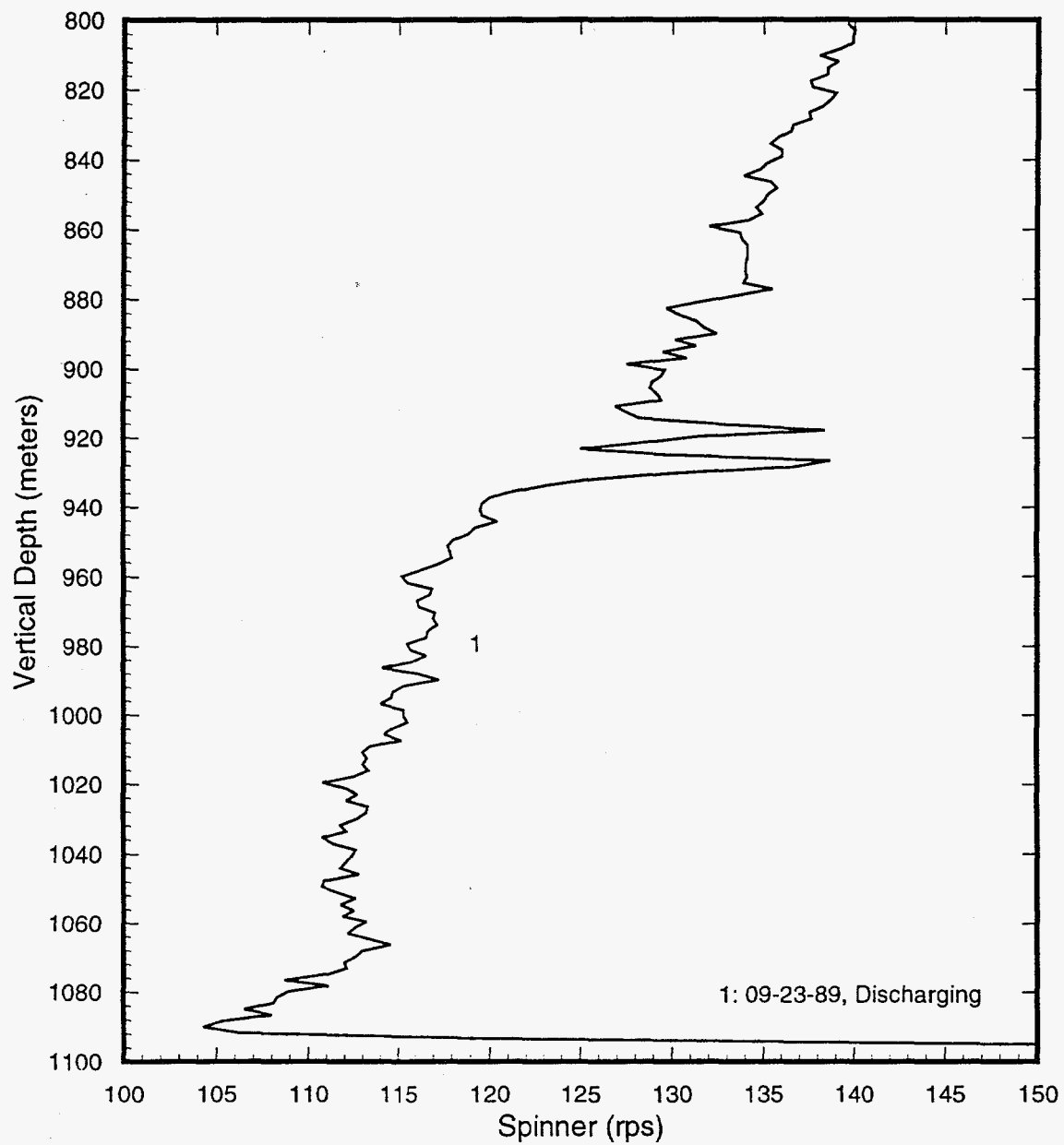


Figure 4.38. An expanded view of the spinner survey taken on September 23, 1989. See Figure 3.37 for complete record.

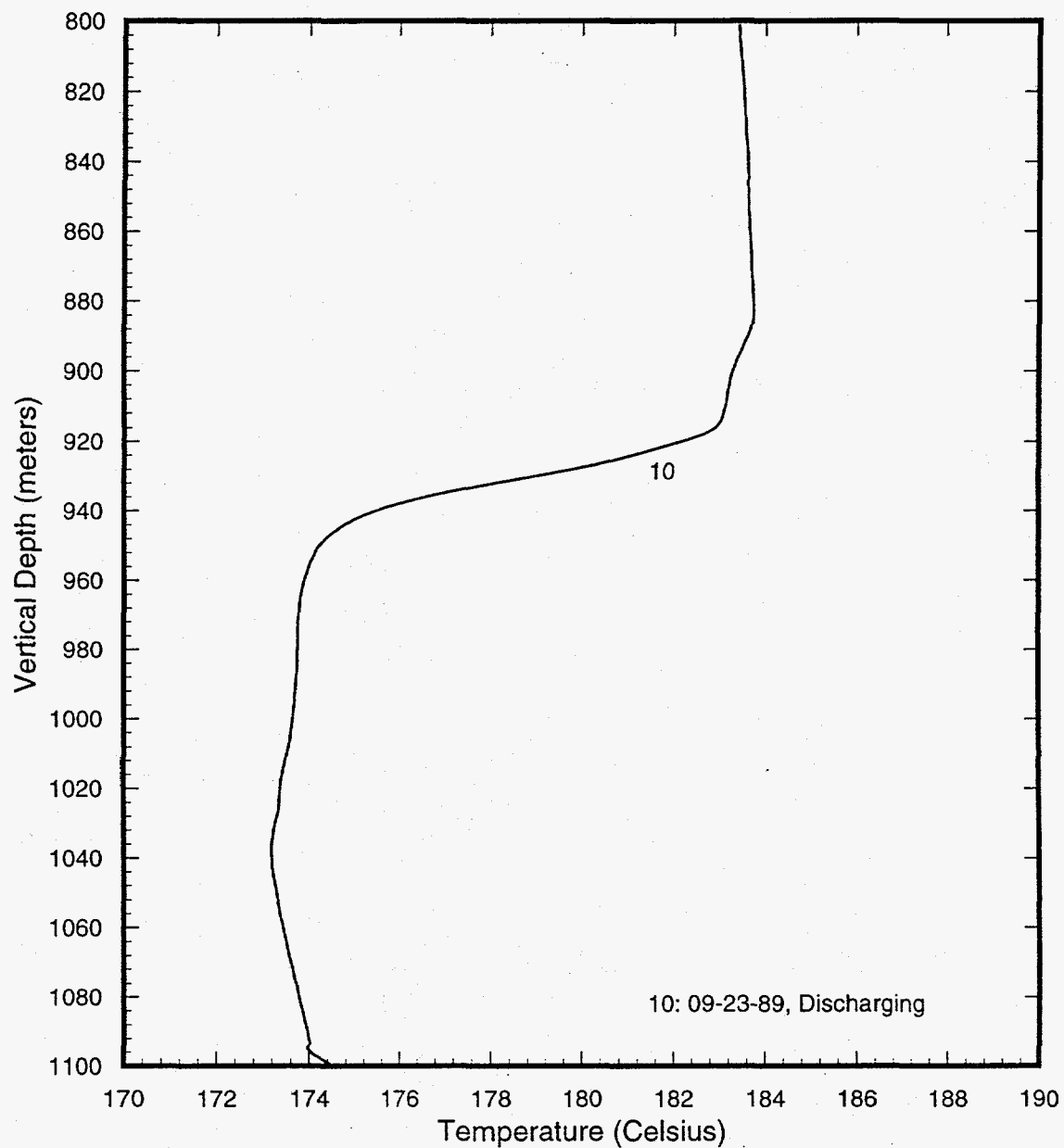


Figure 4.39. An expanded view of the temperature survey taken on September 23, 1989. See Figure 4.36 for the complete profile.

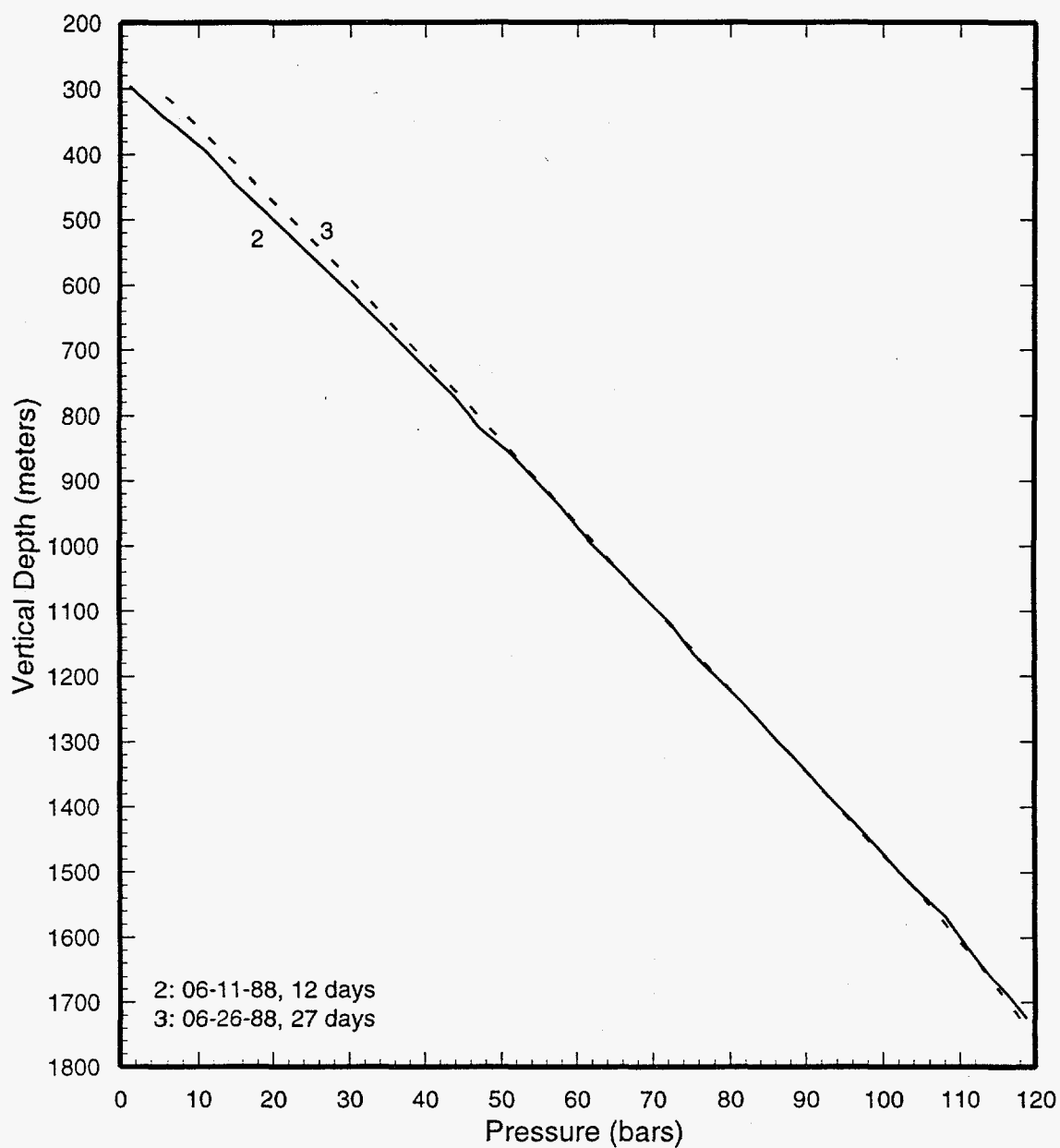


Figure 4.40. Pressure surveys recorded in well SA-4 with an experimental pressure/temperature/spinner tool (PTS-350).

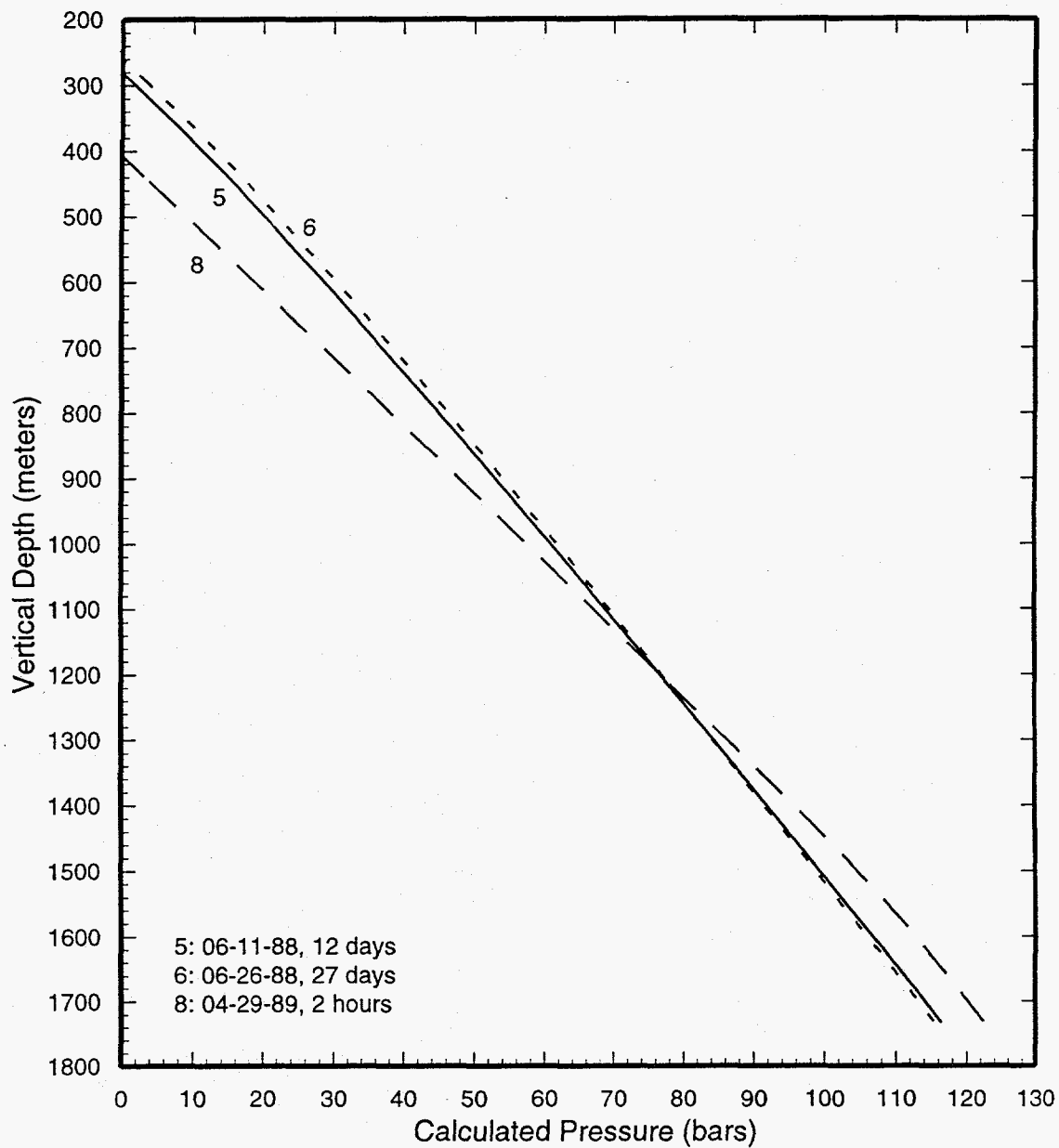


Figure 4.41. Pressure profiles computed from water level and temperature data for well SA-4.

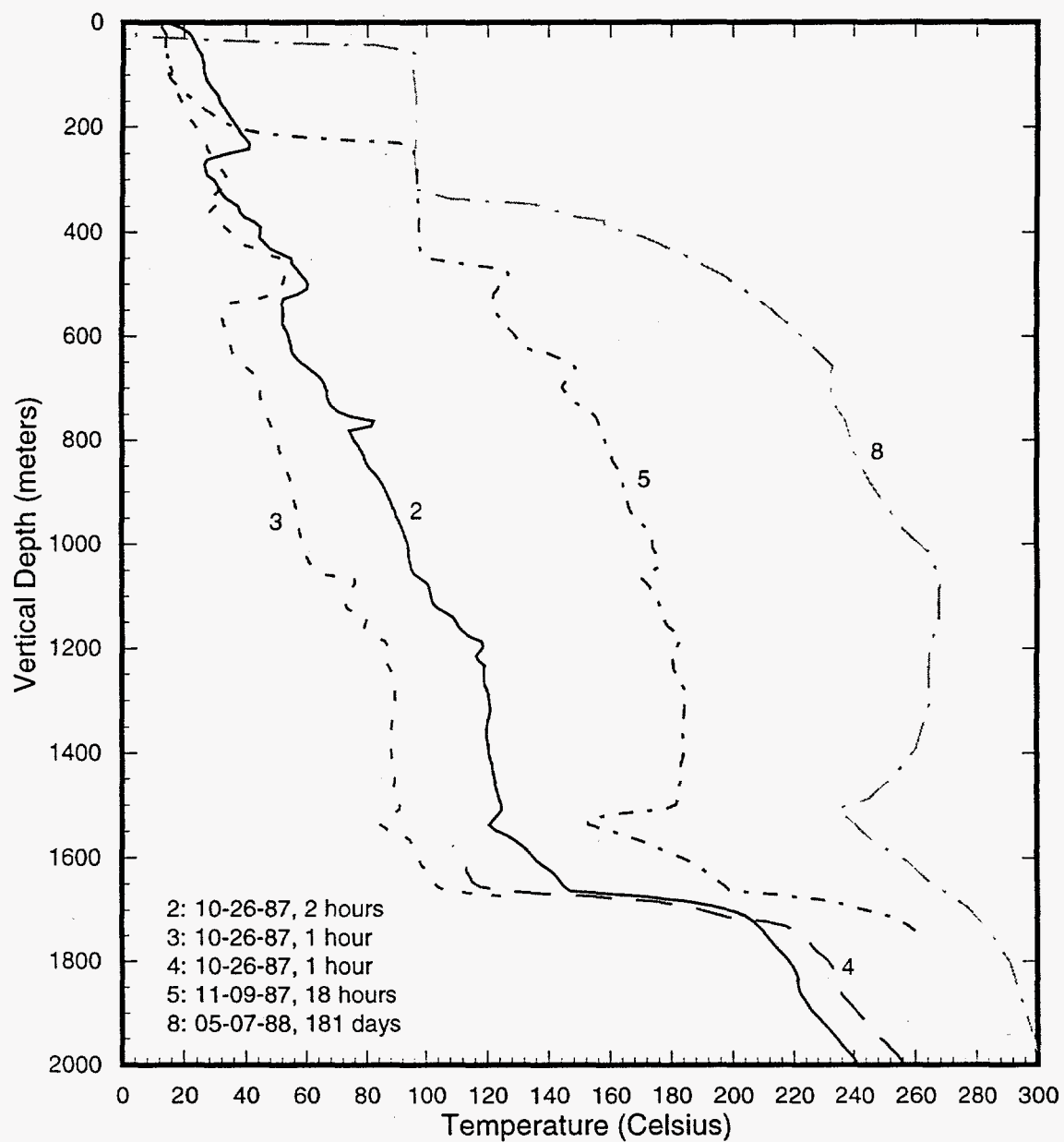


Figure 4.42. Selected temperature surveys in well SB-1.

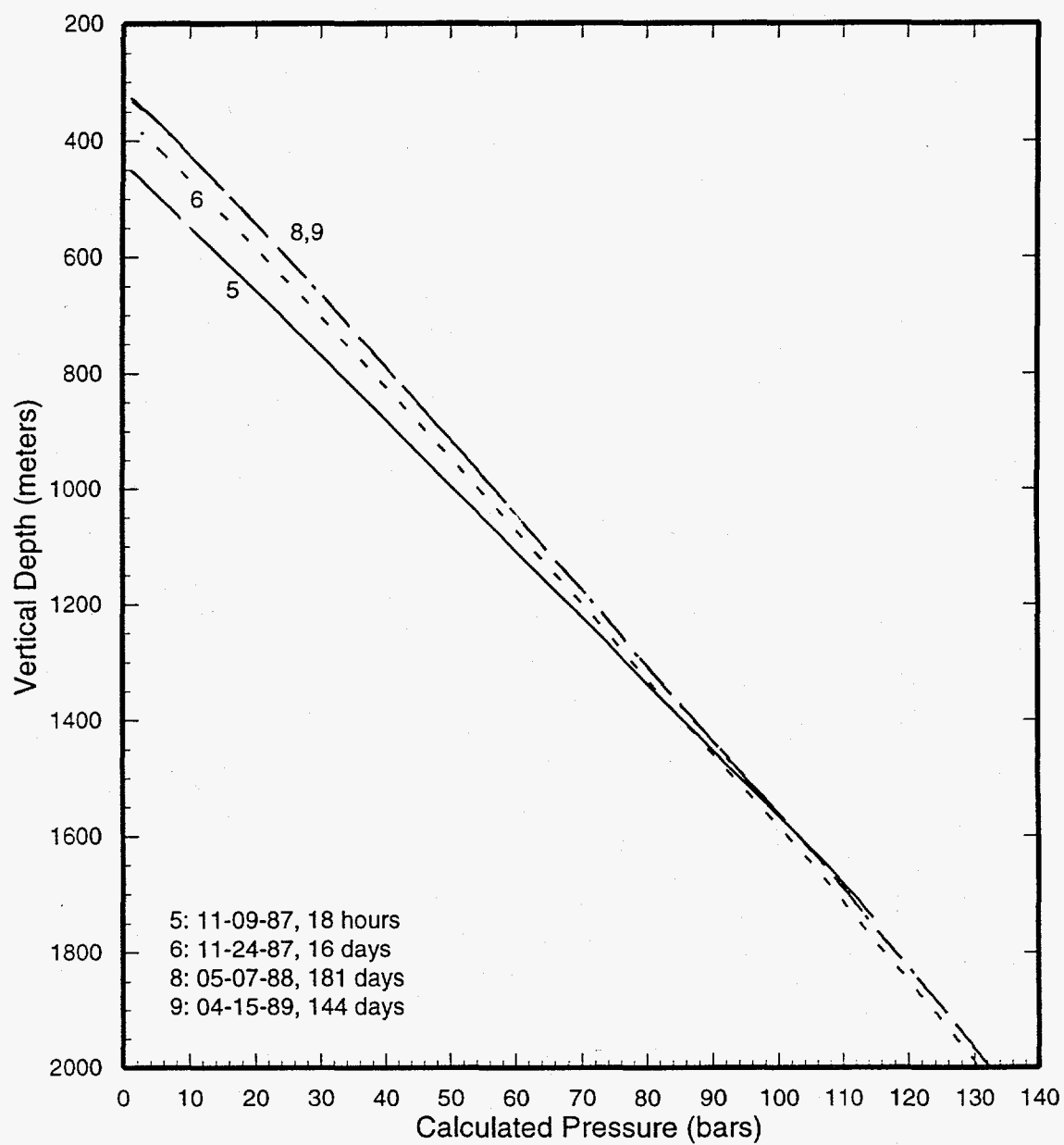


Figure 4.43. Pressure profiles computed from water level and temperature data for well SB-1.

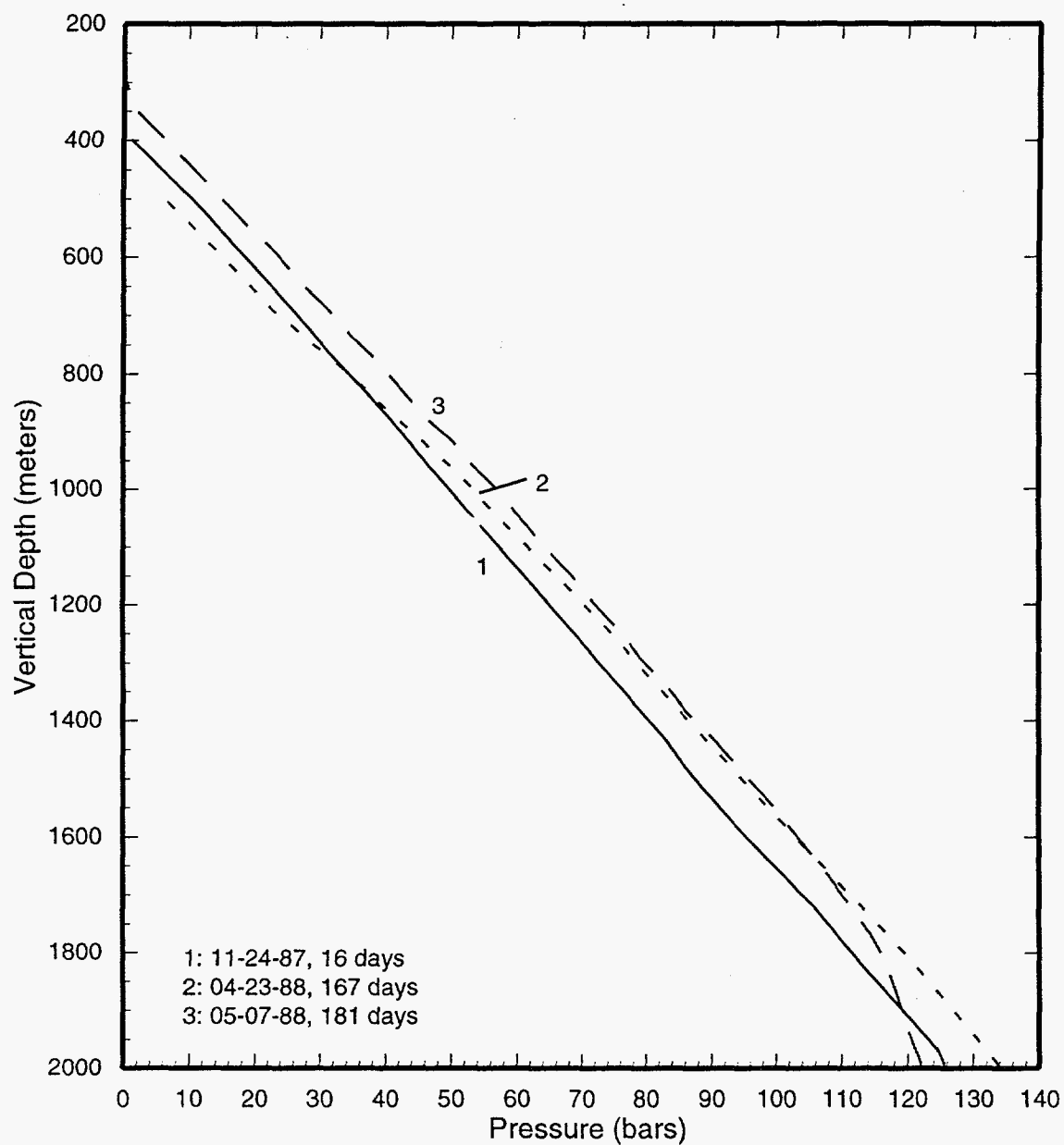


Figure 4.44. Measured pressure profiles in well SB-1.

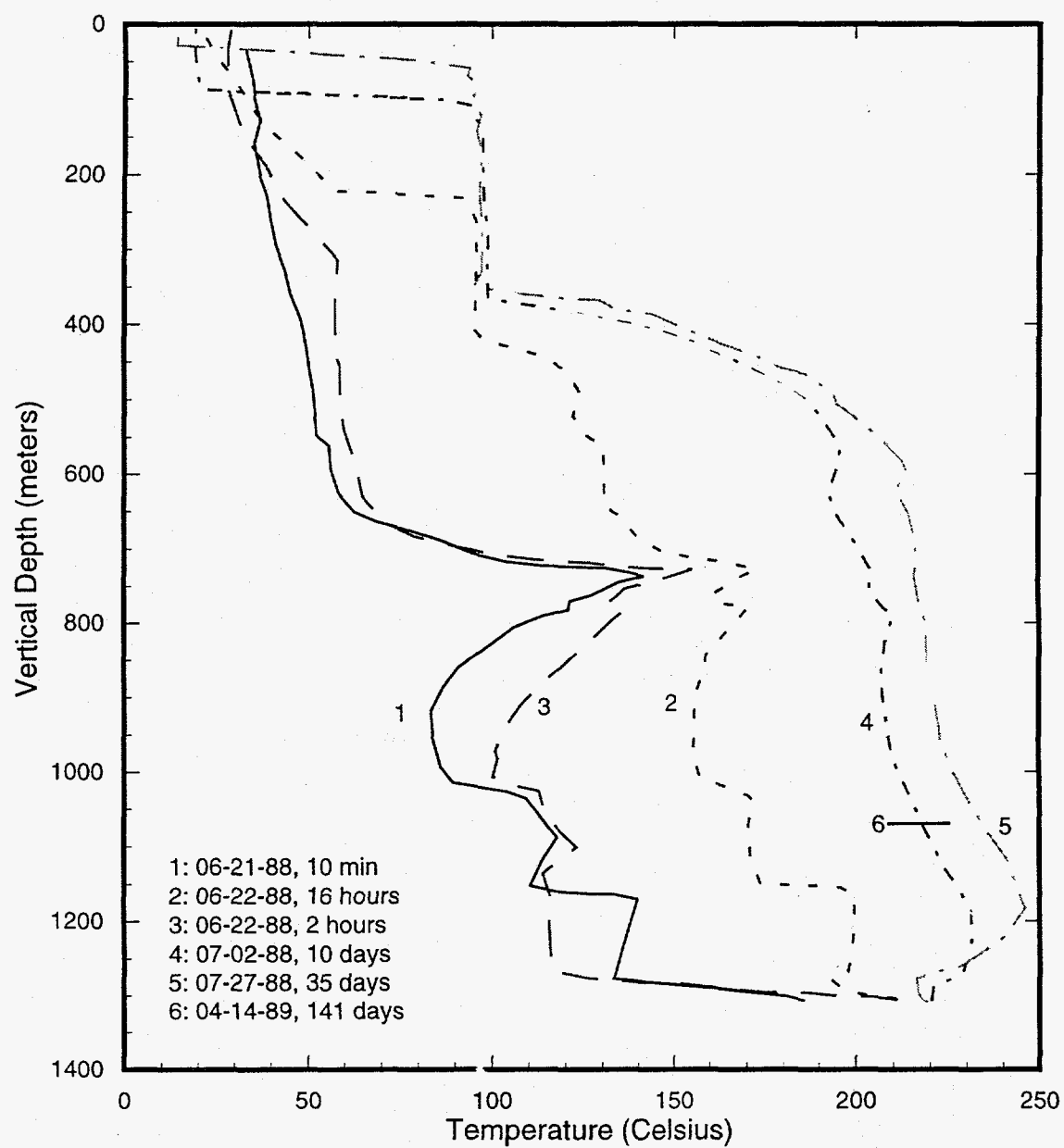


Figure 4.45. Temperature profiles for well SB-2.

Pressure profiles computed from water level and temperature data are shown in Figure 4.46. The computed pressure at 1270 m TVD is ~77.5 bars. The measured pressure (see Figure 4.47) at 1270 m TVD is ~78.5 bars. Thus, the best estimate for feed point (1270 m TVD) pressure is ~78 bars.

4.13 Well SB-3

Selected heatup surveys for well SB-3 are displayed in Figure 4.48. Temperature surveys taken shortly after cold water injection (Profiles 2 and 4, Figure 4.48) suggest that most of the water loss occurs from ~800 m TVD to ~960 m TVD. Relatively rapid heatup at ~1100 m TVD may be evidence of a minor feed zone at this depth. The feedzone temperature is estimated to be about 210°C.

Pressure profiles computed from water level and temperature data are shown in Figure 4.49, the pressure at 880 m TVD is ~46.5 bars. This pressure value is in substantial agreement with that (~45.5 bars) recorded downhole by a pressure gauge (Figure 4.50). Accordingly, the pressure at 880 m TVD is estimated to be ~46 bars.

4.14 Well SC-1

(original well name: N61-SN-7D)

Selected temperature surveys for well SC-1 are shown in Figures 4.51 and 4.52. The temperature profile measured during cold water injection on June 7, 1988 shows a water loss zone at ~2300 m TVD. Heat up surveys 4, 10, and 14 (Figures 4.51 and 4.52) show large temperature gradients at ~1740 m TVD and at ~1900 m TVD; these thermal features do not denote the presence of permeable horizons. It appears that rapid heatup at

~1740 m TVD and ~1900 m TVD is the direct result of well completion. During cold water injection or fluid production (see below), part of the fluid flows in the annulus between the 7-inch liner and the 9⁵/₈-inch casing (or 12¹/₄-inch hole) from 1740 m TVD to 1900 m TVD. Temperature profile 14 (Figures 4.51 and 4.52) also implies a permeable zone at ~2030 m TVD. Temperature profile 11 (Figures 4.51 and 4.52) was recorded after the well had been shut in for approximately 6 months. It is significant that the cold zone at ~2300 meters has not disappeared even after 6 months; the recorded temperature at ~2300 m TVD is ~246°C. The maximum temperature (~310°C) occurs in the depth range 1800 m TVD to 1900 m TVD. The temperature inversion is confirmed by pressure/temperature/spinner (PTS) surveys taken while the well was discharging.

The PTS logs taken during a production test in November 1988 are displayed in Figure 4.53. The spinner logs clearly confirm fluid flow behind the liner between ~1740 m MD and ~1900 m MD. Temperature logs imply permeable horizons at 1950–1970 m MD (1947–1967 m TVD), 2030–2050 m MD (2026–2046 m TVD), 2120–2130 m MD (2114–2124 m TVD), 2230–2250 m MD (2222–2242 m TVD), and 2320 m MD (2310 m TVD). Since the temperature distribution below the shallowest feedpoint does not depend upon the flow rate, it would appear that the fraction of fluid contributed by each feed zone is essentially independent of the pressure drawdown inside the wellbore. To estimate the flow fractions emanating from the various feed zones, we need stable feedpoint temperatures. For present purposes, we shall assume that the feed zone temperatures are given sufficiently accurately by the temperature survey taken on May 11, 1988 (Figure 4.51). Given feedpoint temperatures (T_i , $i = 1, 2, \dots, 5$) and the temperature distribution in the

Continued on page 4-63

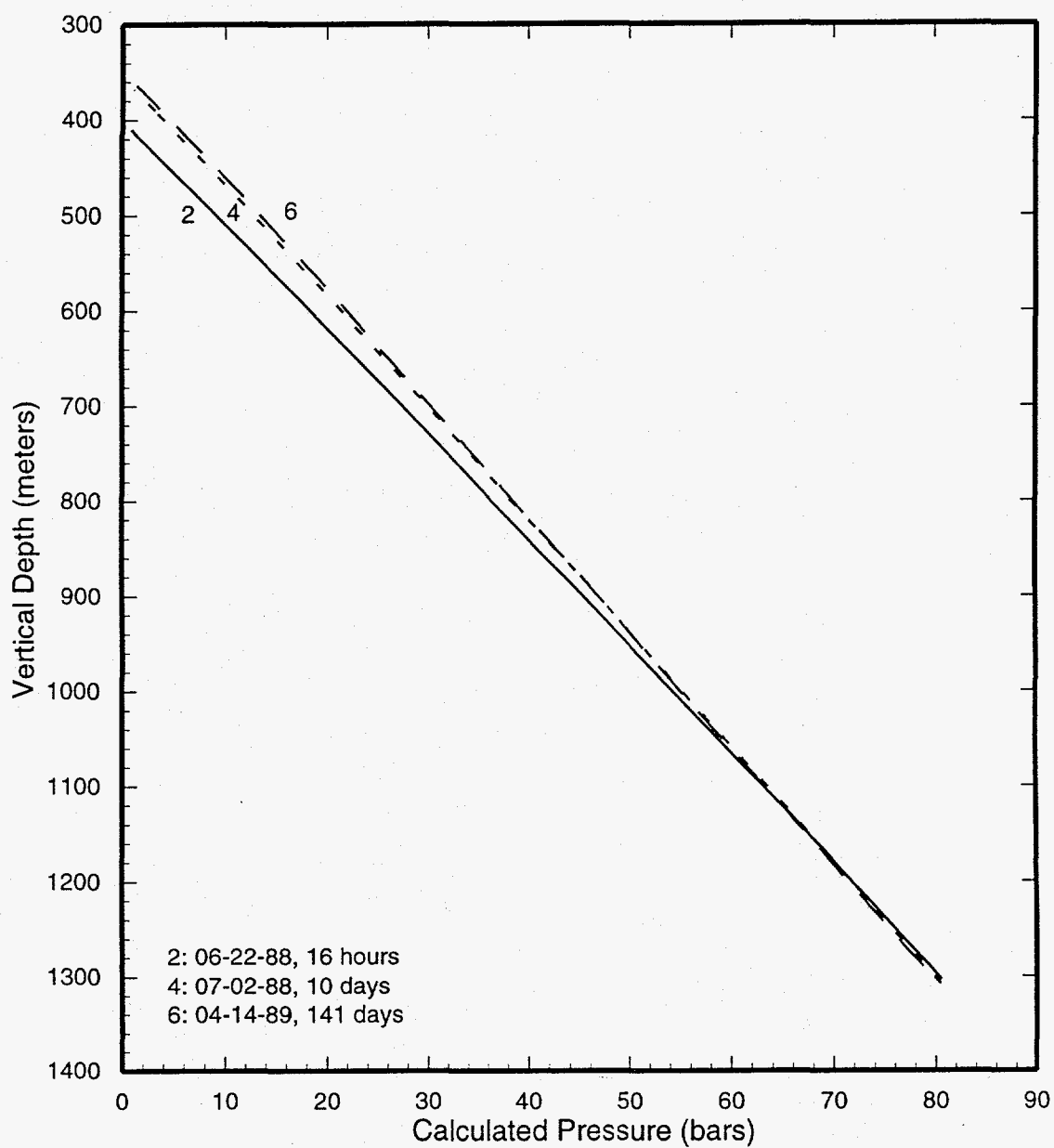


Figure 4.46. Pressure profiles computed from water level and temperature data for well SB-2.

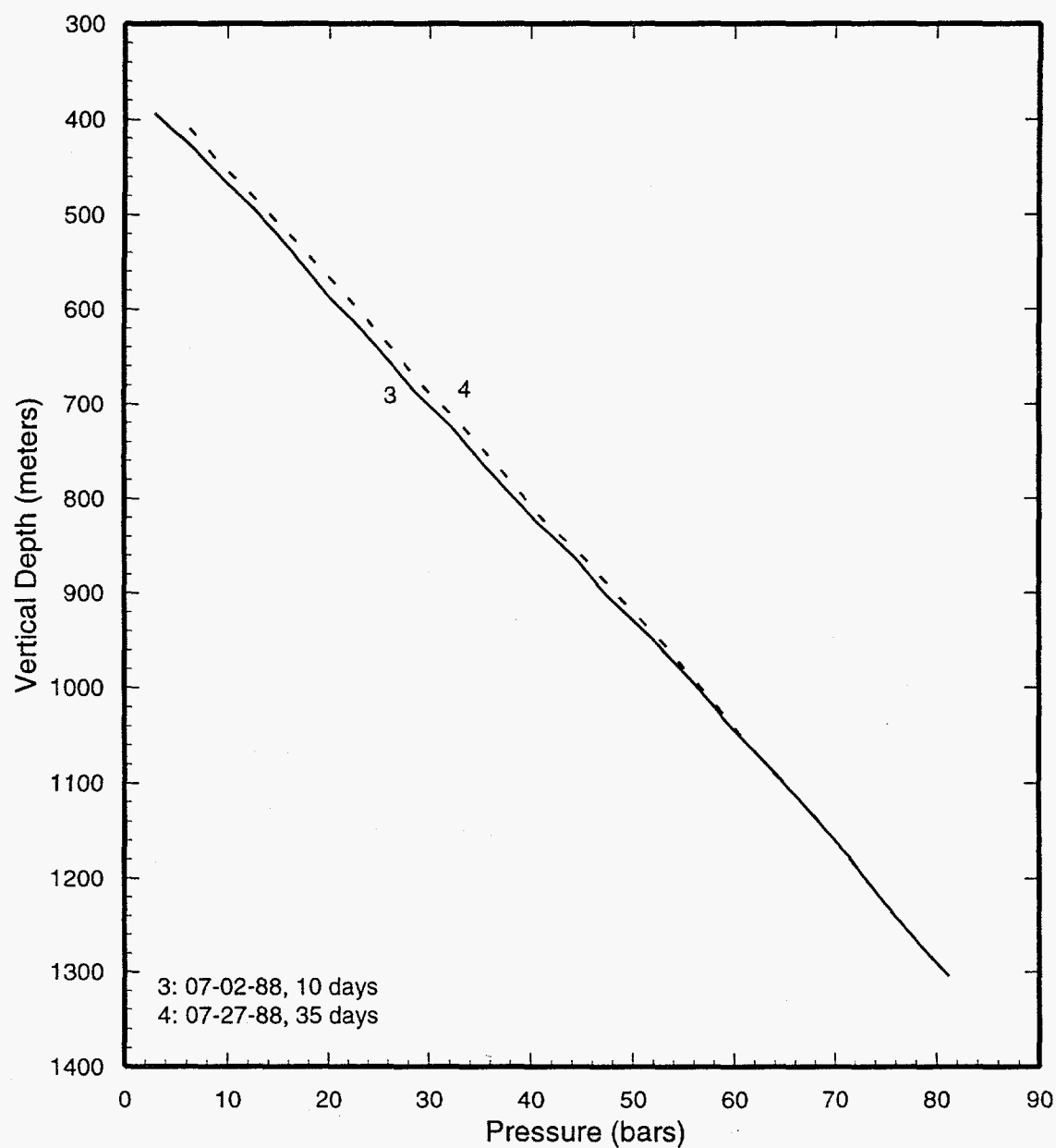


Figure 4.47. Measured pressure profiles for well SB-2.

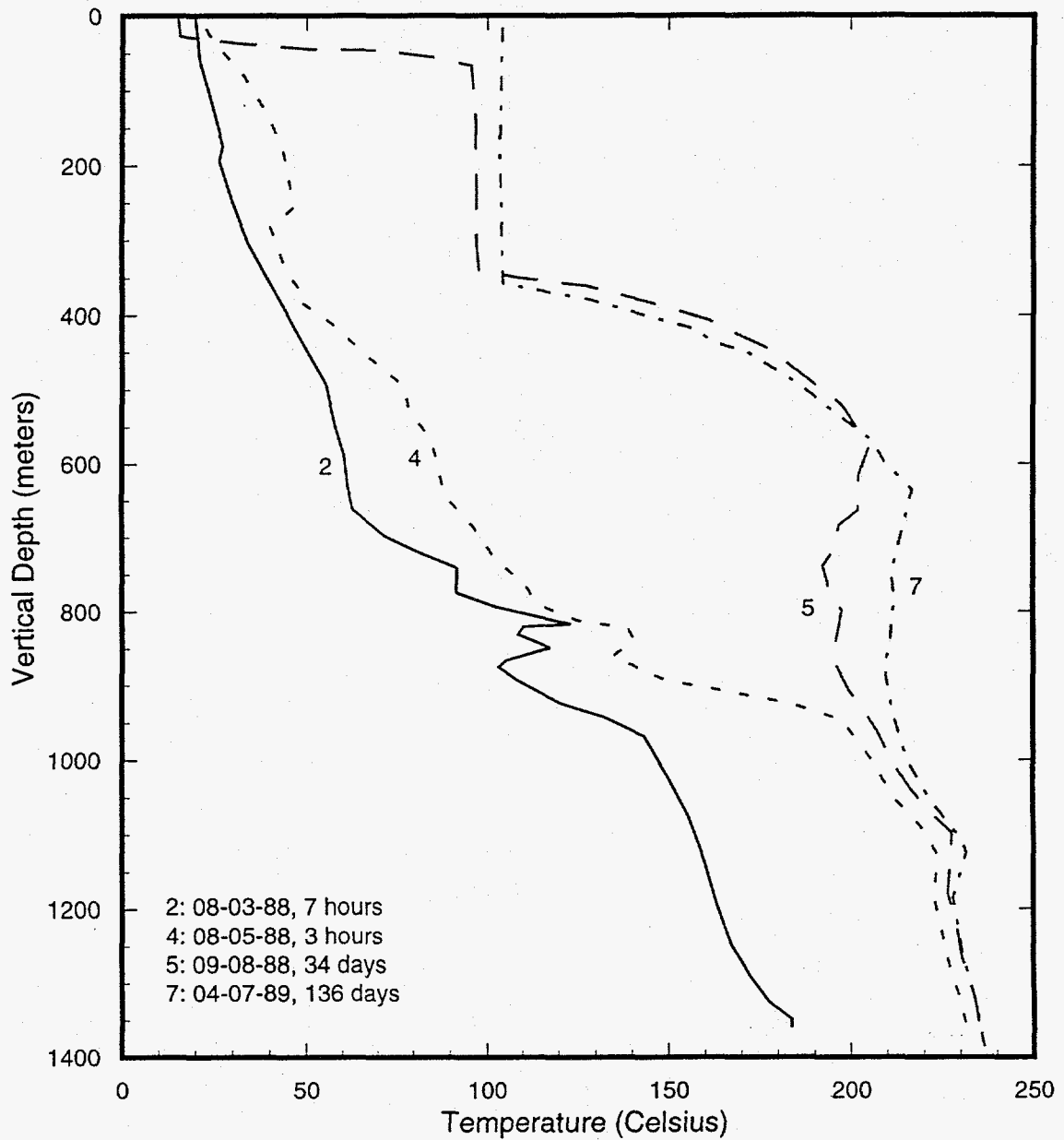


Figure 4.48. Selected heatup surveys for well SB-3.

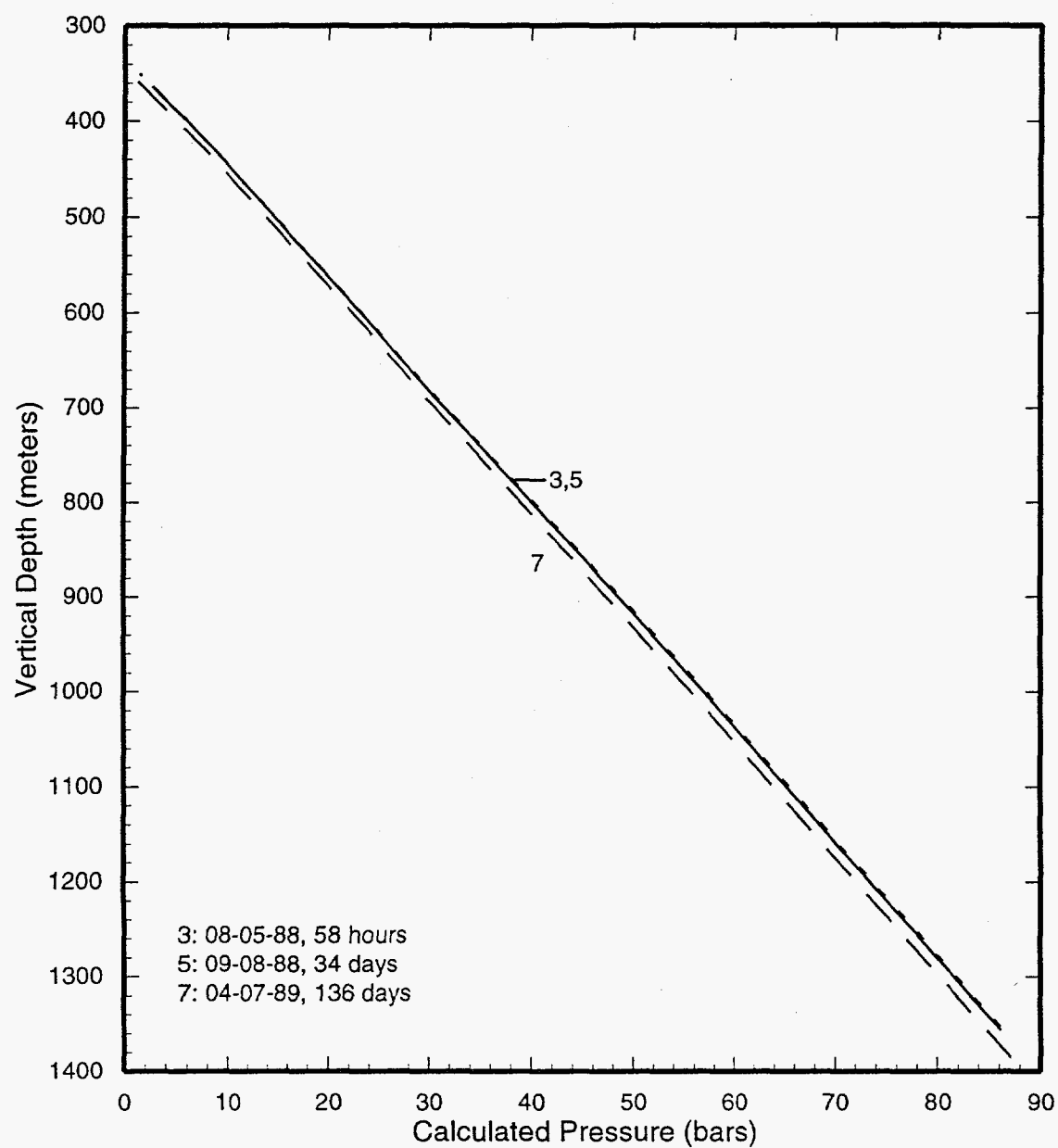


Figure 4.49. Pressure profiles computed from water level and temperature data for well SB-3.

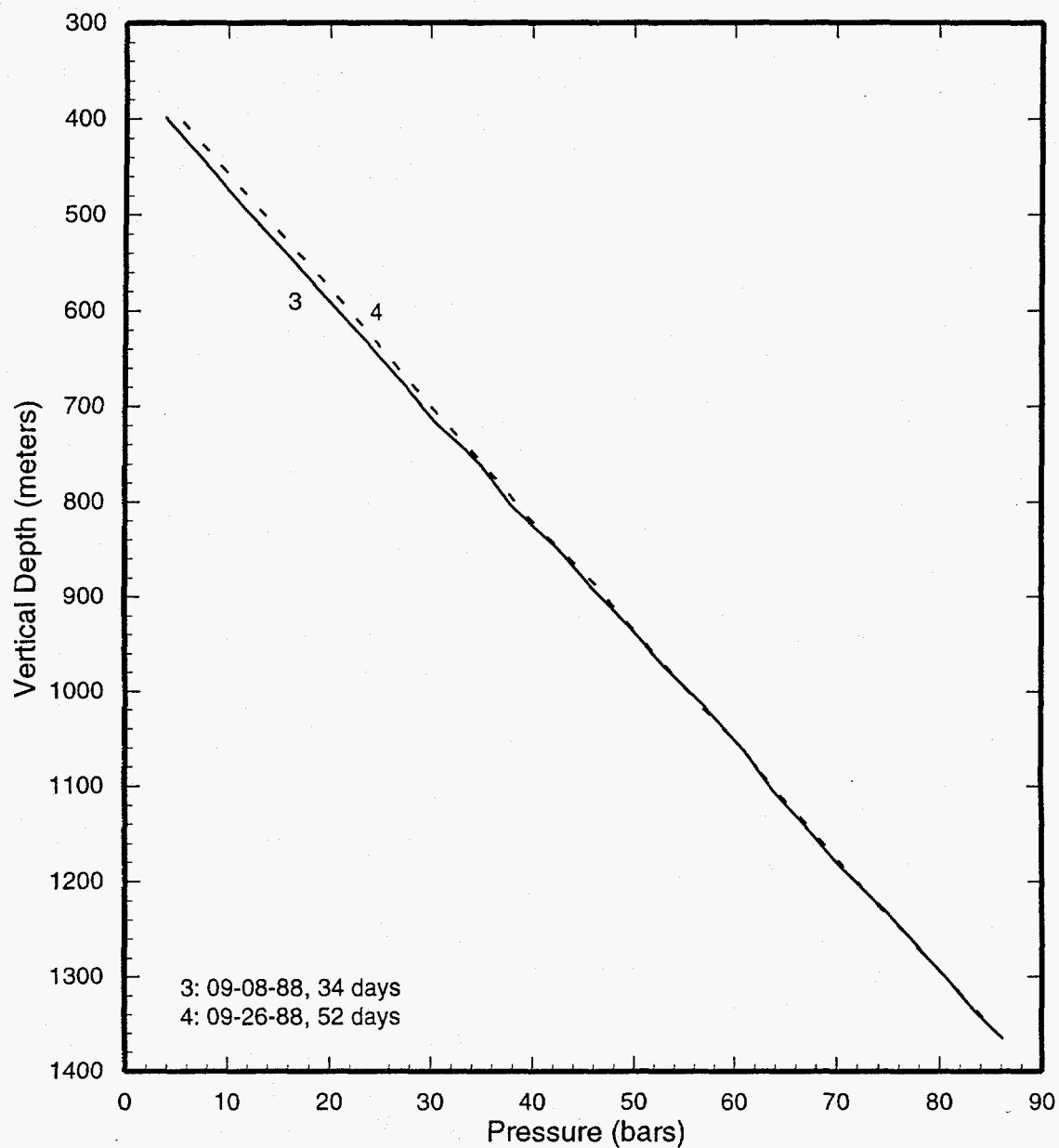


Figure 4.50. Measured pressures in well SB-3.

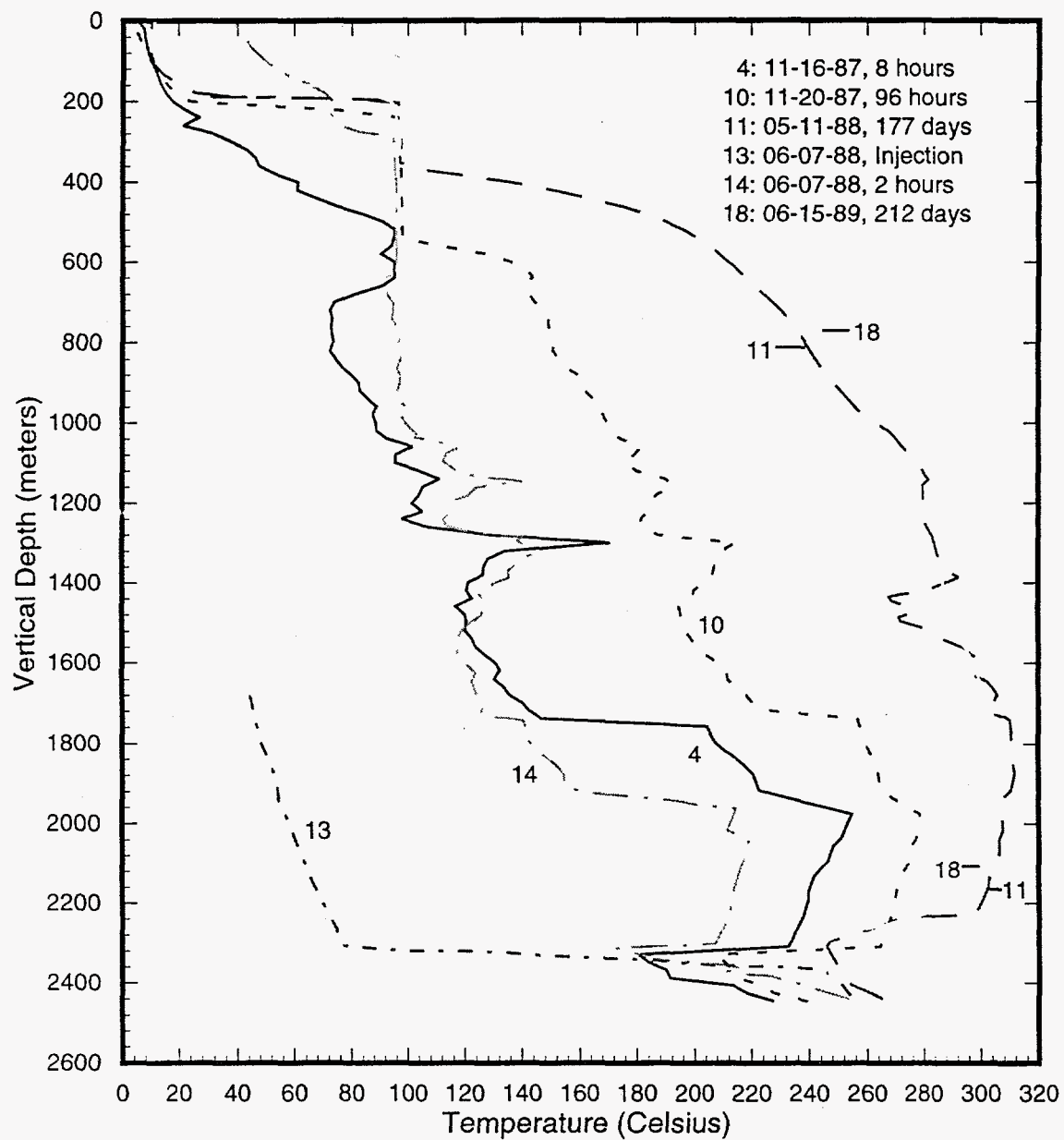


Figure 4.51. Selected temperature surveys for well SC-1.

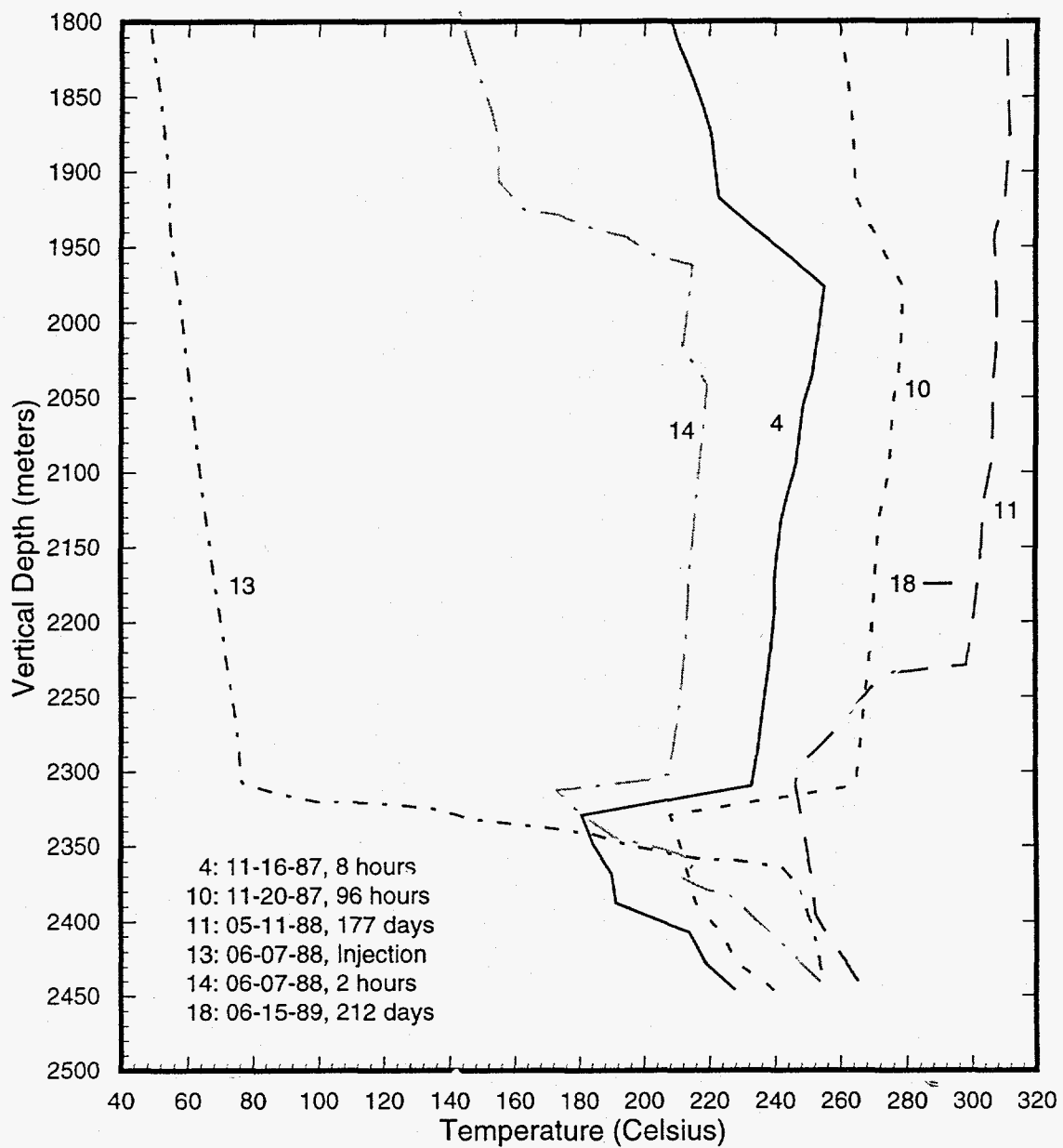


Figure 4.52. Deep portion of selected temperature surveys for well SC-1 (see Figure 4.51 for complete profiles).

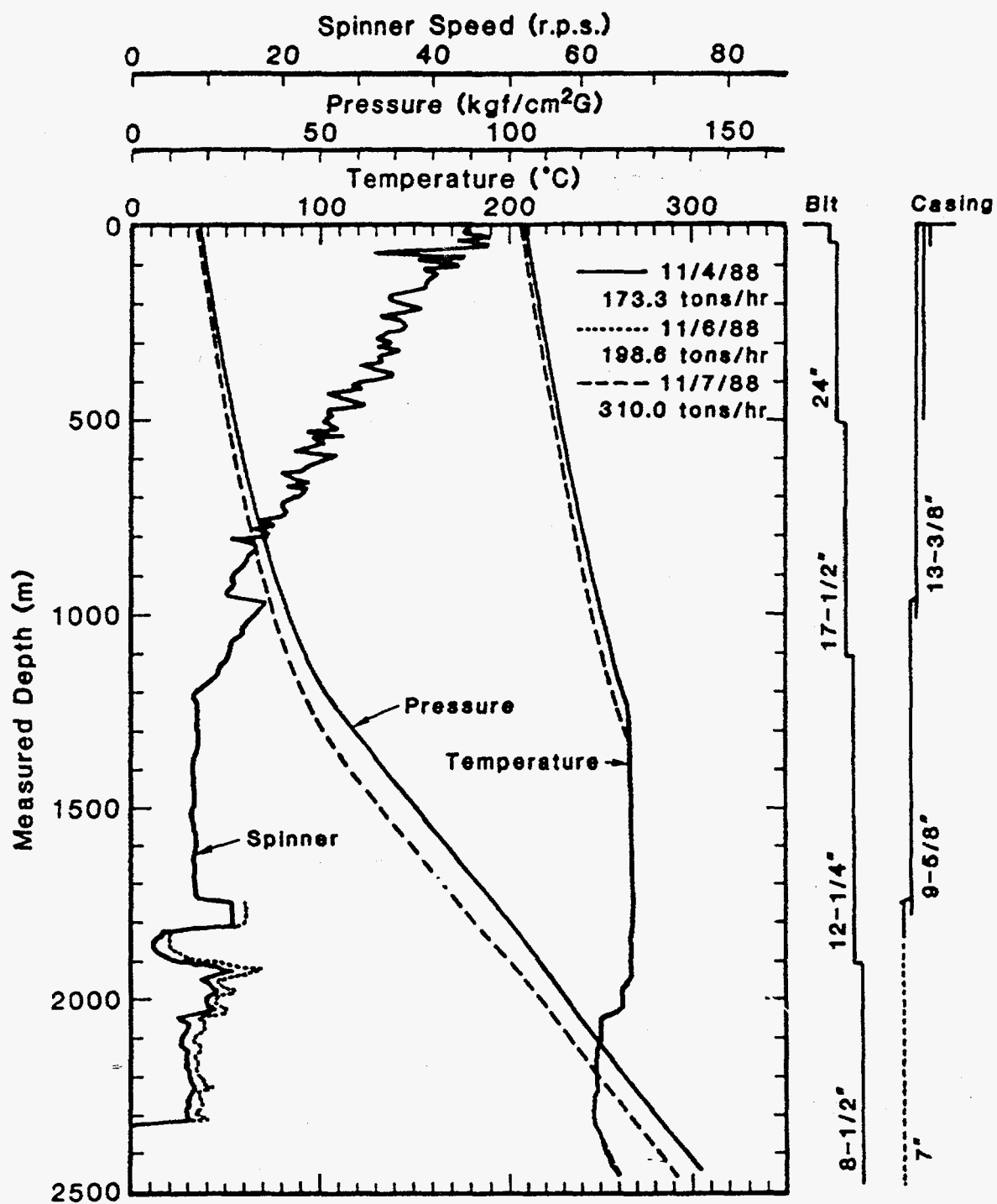


Figure 4.53. Pressure/temperature/spinner logs taken during production testing of well SC-1.

wellbore, the fluid fractions (x_i , $i = 1, 2, \dots, 5$) contributed by the various feed zones can be obtained by solving the following set of linear algebraic equations:

$$\begin{aligned}(x_1 + x_2 + x_3 + x_4)H(T_{-5}) + x_5H(T_5) &= \\ & (x_1 + x_2 + x_3 + x_4 + x_5)H(T_{+5}) \\ (x_1 + x_2 + x_3)H(T_{-4}) + x_4H(T_4) &= \\ & (x_1 + x_2 + x_3 + x_4)H(T_{+4}) \\ (x_1 + x_2)H(T_{-3}) + x_3H(T_3) &= (x_1 + x_2 + x_3)H(T_{+3}) \\ x_1H(T_{-2}) + x_2H(T_2) &= (x_1 + x_2)H(T_{+2}) \\ (x_1 + x_2 + x_3 + x_4 + x_5) &= 1,\end{aligned}$$

where index i increases from the deepest to the shallowest feedpoint and

$H(T)$ = Fluid enthalpy at temperature T ,
 $T_{-i} (= T_{+(i-1)})$ = Fluid temperature just below
 (just above) feedzone $i(i-1)$.

The numerical results for x_i are given in Table 4.2. Almost two-thirds of the total flow is contributed by the deepest feed zone at or below 2320 m MD (2310 m TVD), and most of the remainder comes

from the two feed zones at 1950–1970 m MD and 2030–2050 m MD.

Selected pressure profiles computed from water level and temperature data are displayed in Figure 4.54. The pressure profiles tend to coincide in the depth range from ~2200 m TVD to ~2400 m TVD. The computed pressure at 2310 m TVD is ~148 bars and is in reasonable agreement with that (~150 bars) recorded with downhole gauges (Figure 4.55).

4.15 Well SD-1

(original well name: N61-KY-2)

Temperature surveys taken during a break in drilling of well SD-1 (drilled depth ~700 meters) are shown in Figure 4.56; the change in temperature gradient at about 380 meters is most likely associated with the lost circulation zone at 387 meters. Since the water level did not stabilize prior to the restart of drilling (see profiles 4 and 6 in Figure 4.57), it is only possible to place an upper limit on shallow pressures. Thus, the pressure at a depth of 400 meters does not exceed 37 bars.

Continued on page 4-68

Table 4.2. Fluid fractions x_i contributed by the various feedzones in well SC-1.

Feedpoint Depth (m MD)	Fluid Temp. Below Feedpoint (°C)	Fluid Temp. Above Feedpoint (°C)	Feedzone Temperature (°C)	Fluid Fraction x_i
1950—1970	262	268	307.4	0.13
2030—2050	250.5	262	306.8	0.17
2120—2130	249.5	250.5	303.8	0.01
2230—2250	246	249.5	286.4	0.06
2320	—	246	246	0.64

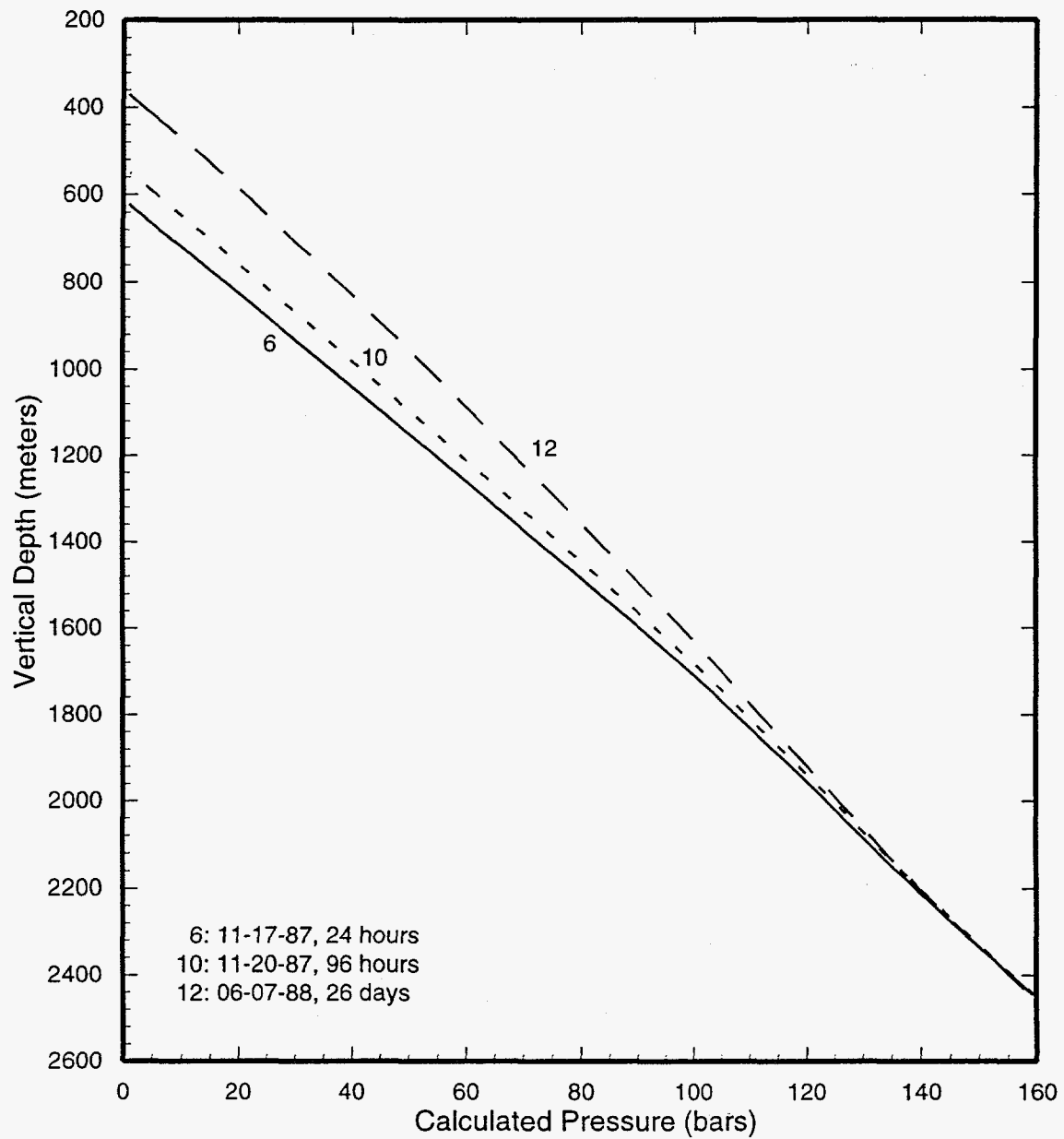


Figure 4.54. Pressure profiles computed from water level and temprature data for well SC-1.

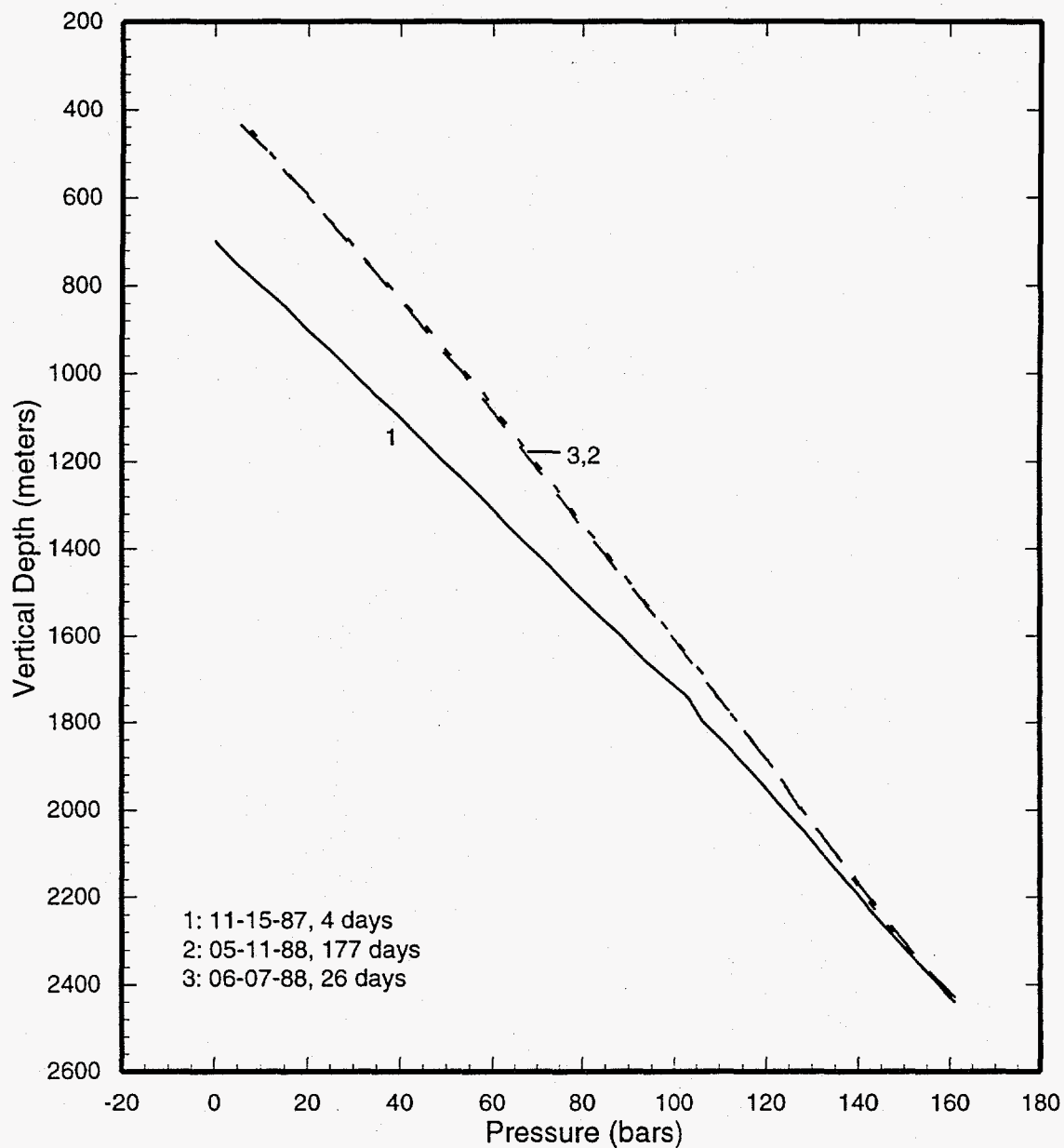


Figure 4.55. Measured pressures in well SC-1.

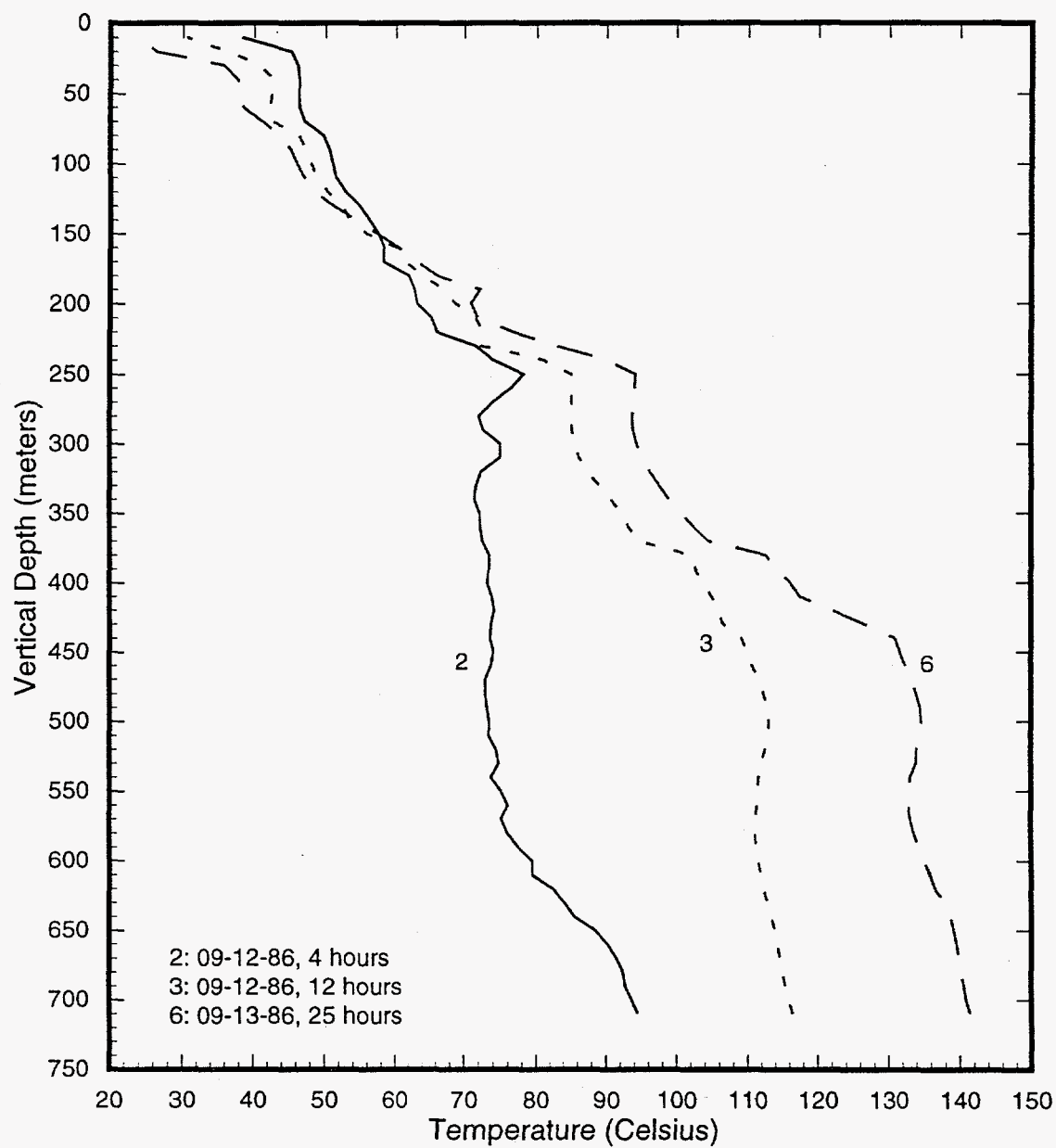


Figure 4.56. Temperature surveys in partially drilled well SD-1.

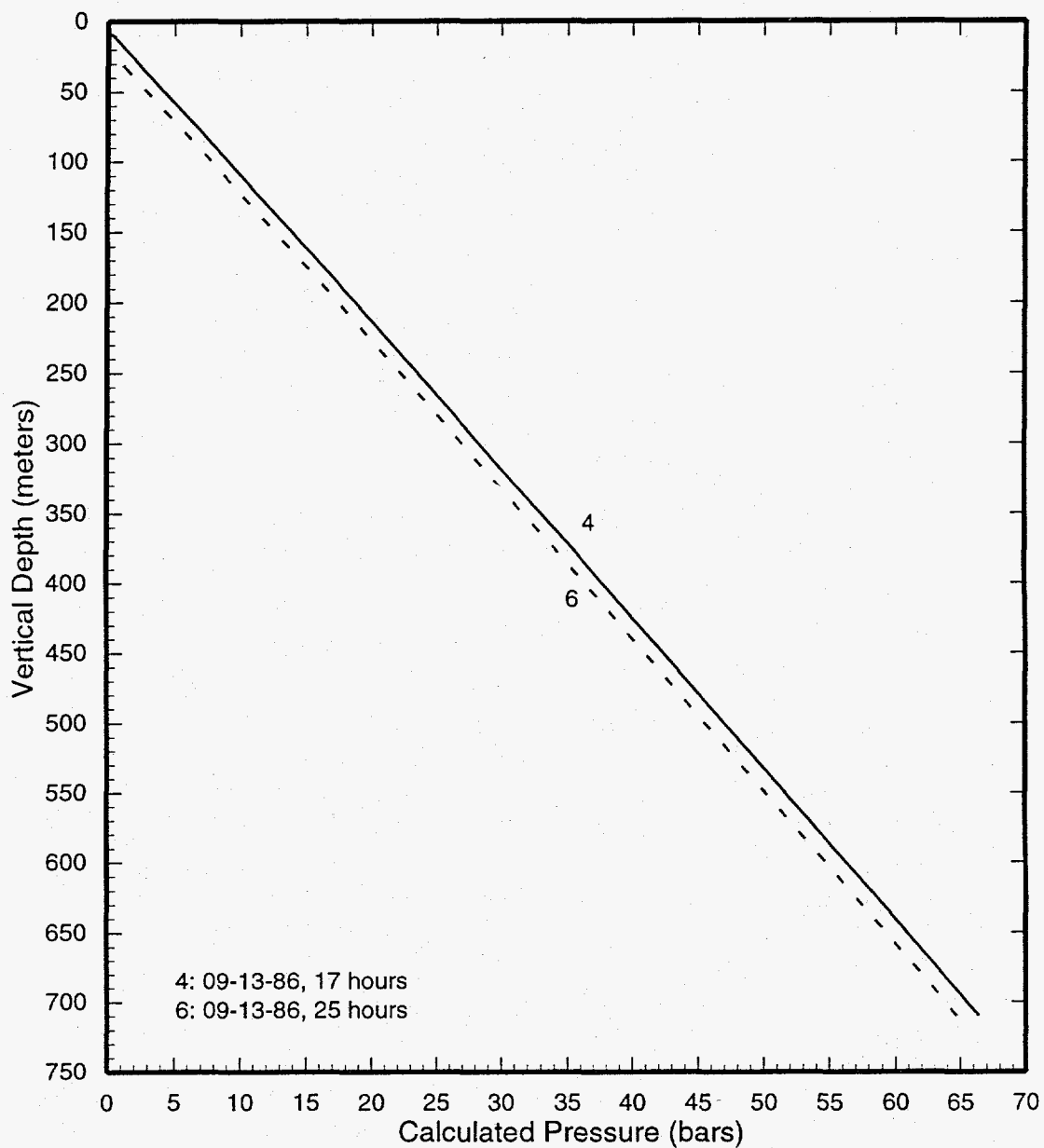


Figure 4.57. Pressures computed from water level and temperature data in partially drilled well SD-1.

Temperature surveys in the completed well are displayed in Figures 4.58 and 4.59. The injection survey of October 17, 1986 (Figure 4.58) shows sharp changes in temperature gradient at ~650 m, ~800 m, ~930 m and ~1100 m. A spinner survey taken while injecting at a low flow rate (~500 liters/min) indicates that not all of these depth intervals correspond to water loss zones; the gradient changes at ~650 m and ~1100 m are very likely associated with variations in pipe conditions (diameter; slotted versus cased interval, *etc.*). The injected water is lost in the depth intervals from 783 to 926 meters and from 1445 to 1526 meters (Table 4.3). Interestingly, the temperature survey taken during high rate injection on October 26, 1988 shows no clear indication of water loss in the zone at 783 to 926 meters; instead, it appears that the water is not lost at or below a depth of 1500 meters. Apparently, the water injection rate during the latter test was high enough to cool the hole down to a depth of 1500 meters, and thus obscure the upper water loss zone. The deep water loss zone at ~1500 meters is also confirmed by a break in temperature gradient at this depth in heat up surveys (see profiles labeled 11 and 12 in Figure 4.59).

Long-term heatup surveys in the completed well show a boiling point temperature profile down to a depth of ~620 meters. The boiling point to depth (BPTD) profile represents the highest temperature that a liquid water column can attain, and thus cannot reflect the effects of a higher formation temperature outside the well. Presumably, the temperature of the formation outside the well in this region exceeds that inside the well. Temperature surveys 11 and 12 (Figure 4.59) show an essentially isothermal region in the depth range from ~800 meters to ~1500 meters. This indicates interzonal flow between these two feed zones in well SD-1.

Because of interzonal flow in well SD-1, shut-in temperature surveys provide no information regarding permeability and temperature distributions in the depth interval from ~800 to ~1500 m. During a discharge test of well SD-1 in September 1989, two pressure/temperature/spinner surveys were run. These PTS surveys (Figures 4.60–4.62) are invaluable for deciphering the permeability and thermal structure in the vicinity of well SD-1. An examination of spinner surveys indicates fluid entries at 1550–1570 m, 1530–1550 m, 1450–1490 m, 1300–1360 m, 1040–1060 m and 800–900 m. In the absence of calibration data for the spinner logs, we shall assume that the fluid velocity v_f is linearly related to the spinner revolutions R as follows:

$$R = m(v_s + v_f) \quad ,$$

where v_s is the line speed and m is a constant. Assuming that there are no fluid entries below 1570 m ($v_f \equiv 0$), the two spinner surveys yield:

$$m \sim 4.07 \text{ RPM/m/min} \quad .$$

The fluid velocity (v_f) and temperature distribution in the wellbore can be combined to yield feedzone temperatures (see Tables 4.4 and 4.5). Temperature and pressure surveys (Figures 4.60 and 4.62) indicate the presence of boiling conditions at shallow depths (~1200 meters on September 18, 1989, and ~900 meters on September 19, 1989). In the two-phase zone, the fluid speed v_f (and hence R) increases due to a decrease in fluid density. Therefore, no attempt was made to analyze the spinner data in the boiling region. The temperature of the liquid in the wellbore above the shallowest single-phase entry is (Tables 4.4 and 4.5) ~220°C (enthalpy ~940 kJ/kg). Since the enthalpy of the produced fluid is greater than 940 kJ/kg, it follows that the fluid entering SD-1 from

Continued on page 4-76

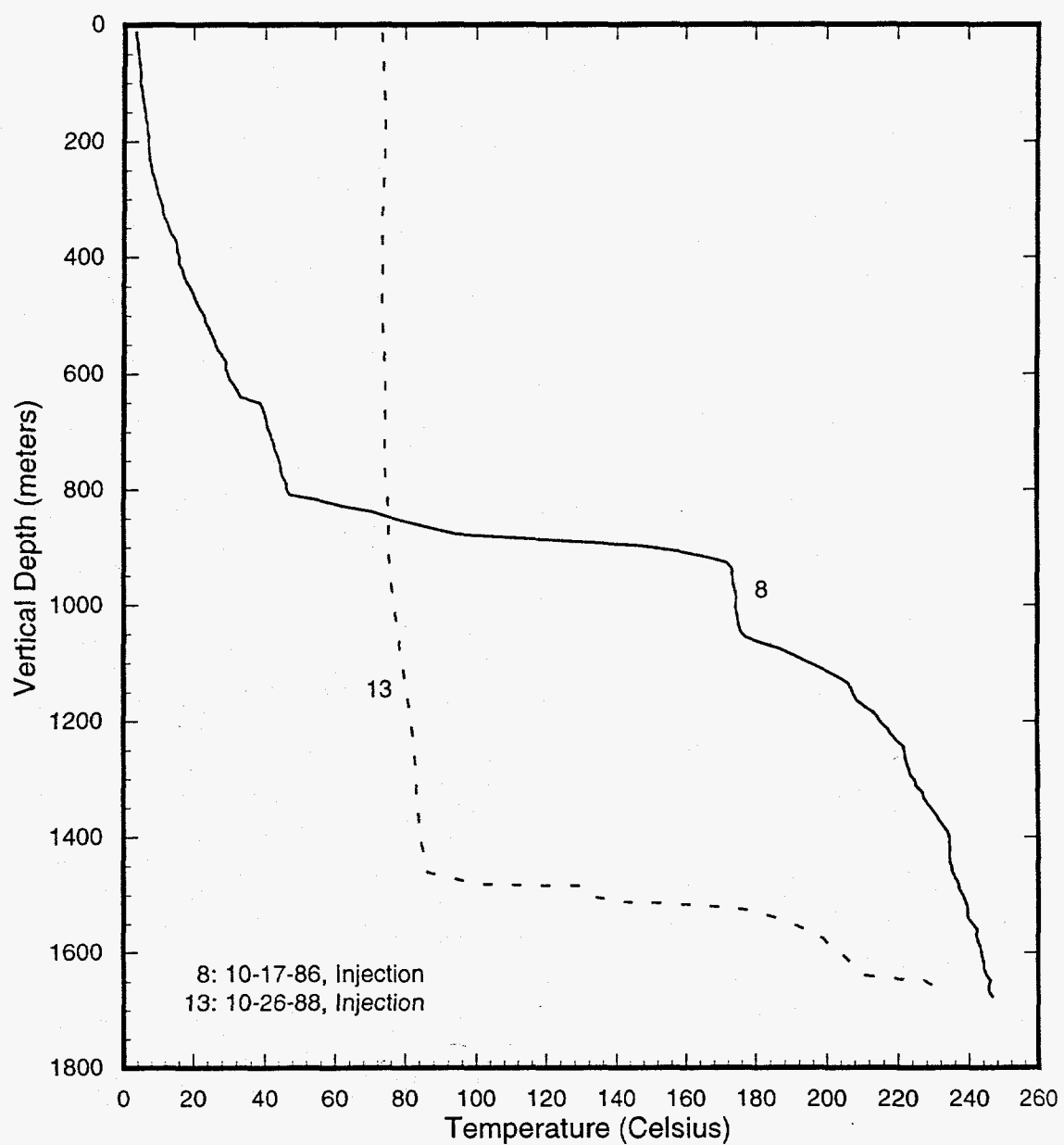


Figure 4.58. Temperature surveys during cold water injection in well SD-1.

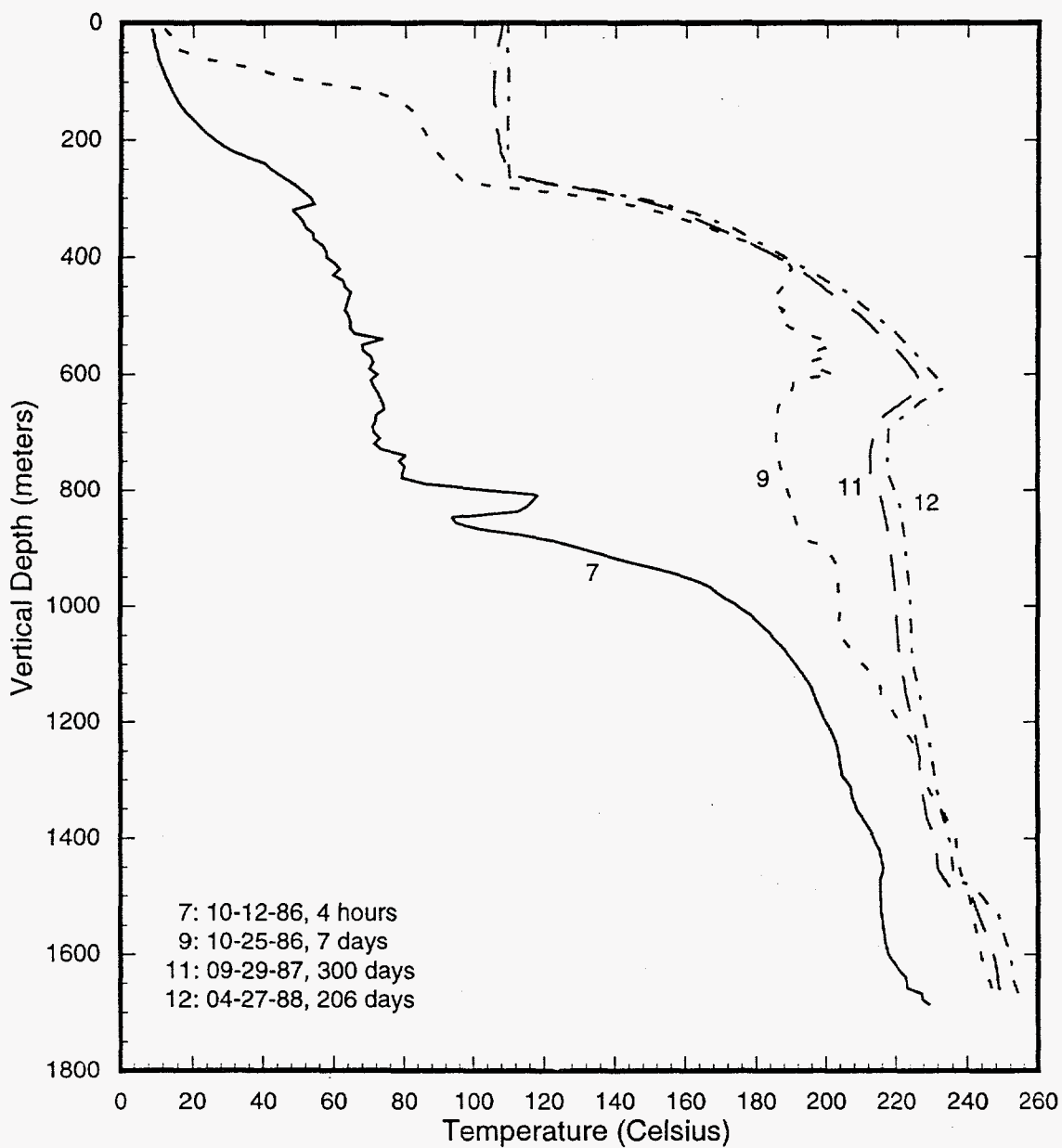


Figure 4.59. Temperature surveys in well SD-1 prior to, and after, an injection test performed on October 17, 1986.

Table 4.3. Results of a spinner test conducted in well SD-1 (MMC, 1988).(Flow Rate , $q \sim 0.5 \text{ m}^3/\text{min.}$; Cable Velocity, $v_s \sim 29 \text{ m/min.}$)

Depth Interval	Inside Pipe/Well Diameter	Spinner (RPM)	Flow Velocity (v_f , m/min)
~641 m	0.224 m	280	12.7
641 ~ 783 m	0.162 m	370	24.3
783-926 m	Loss Zone		
926-1045 m	0.162 m	340 ± 10	
1045-1394 m	Flow in Annulus	(No Net Fluid Loss)	
1394-1445 m	0.162 m	340 ± 10	
1445-1526 m	Loss Zone		
1526 ~ m	0.162 m	0	

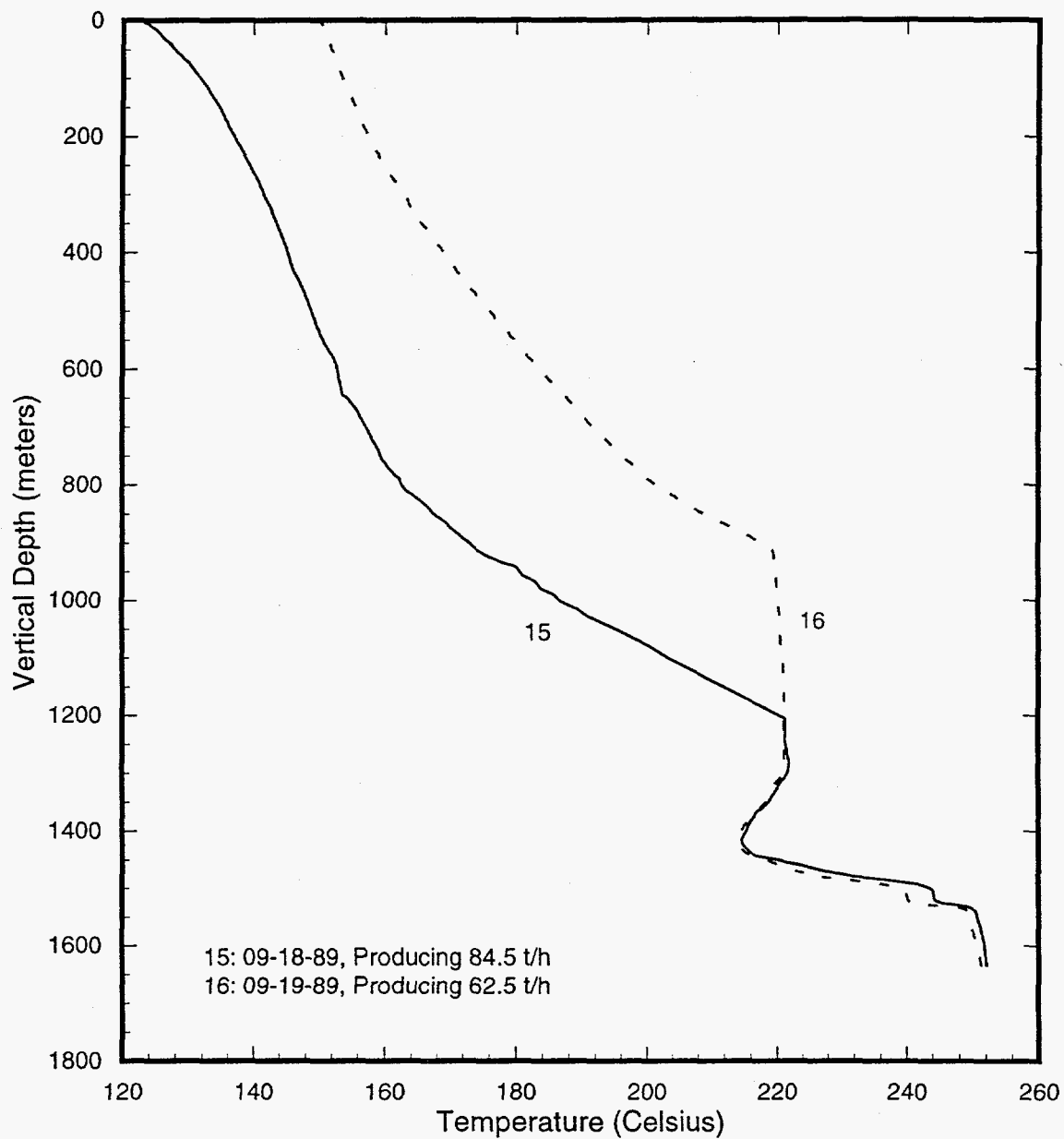


Figure 4.60. Temperature surveys run under discharge conditions in well SD-1 in September 1989. For corresponding spinner and pressure surveys, see Figures 4.61 and 4.62, respectively.

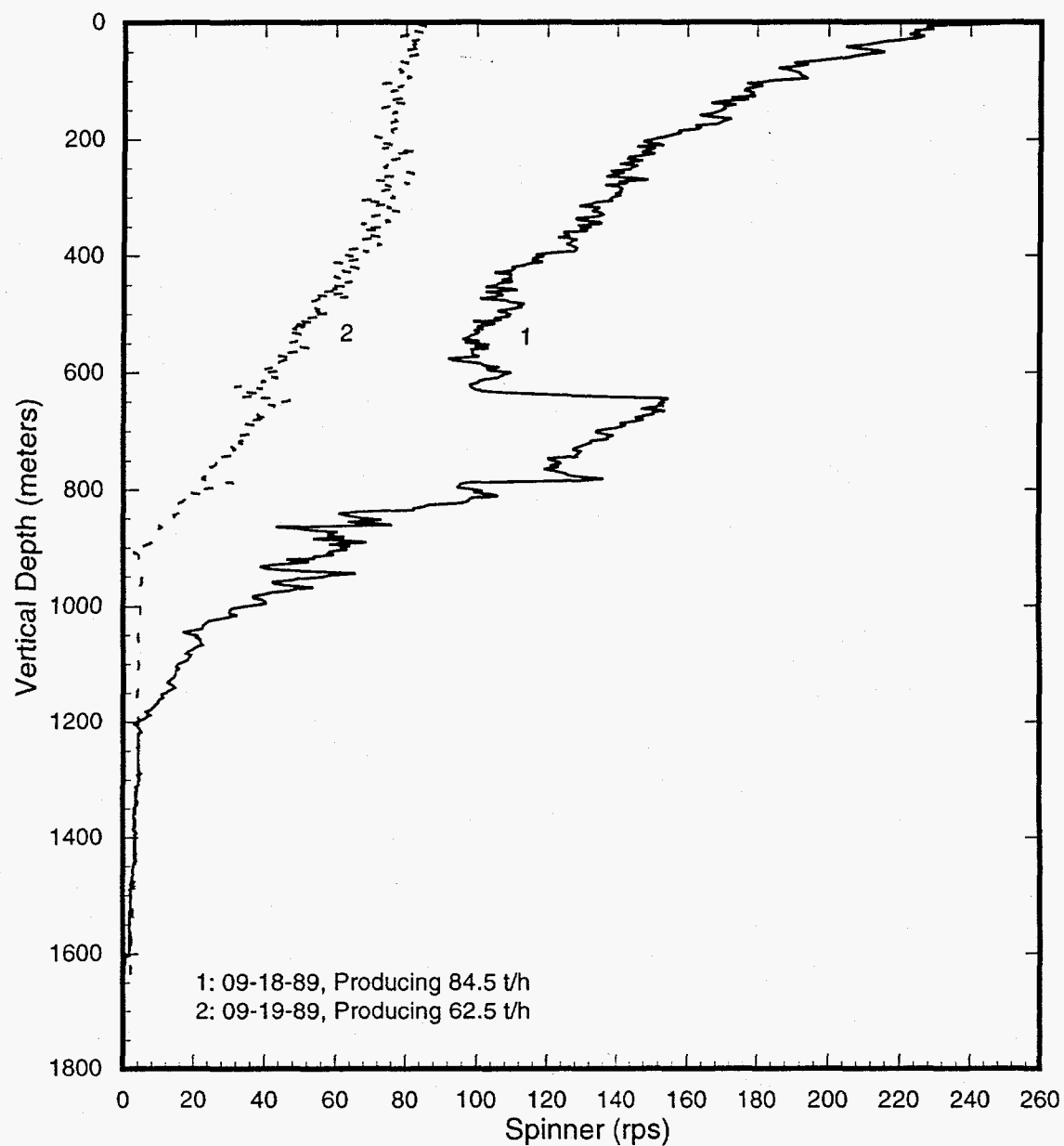


Figure 4.61. Spinner surveys run under discharge conditions in well SD-1 in September 1989. For corresponding temperature and pressure surveys, see Figures 4.60 and 4.62, respectively.

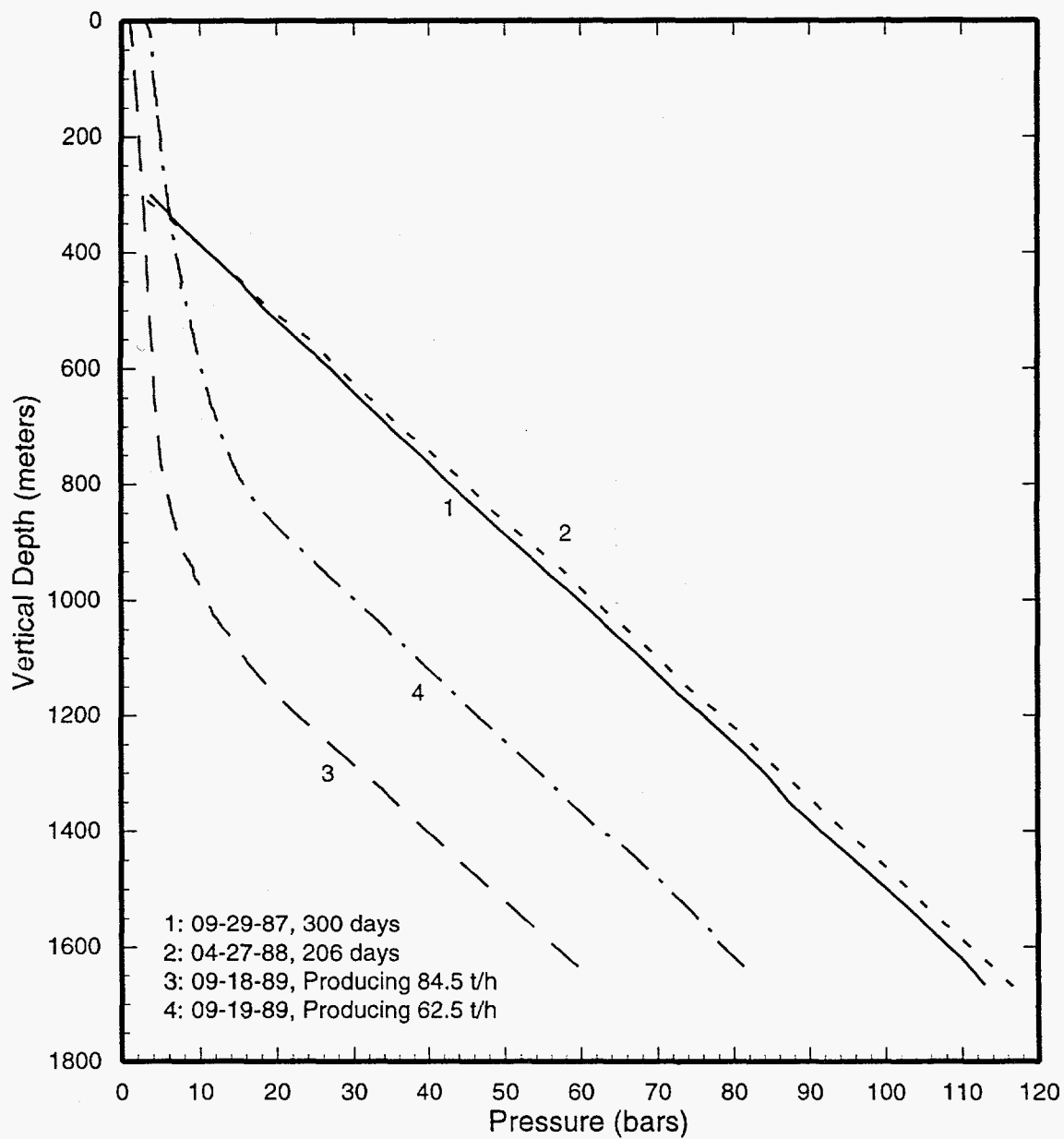


Figure 4.62. Pressure surveys recorded in well SD-1.

Table 4.4. Results of spinner test conducted on September 18, 1989 (discharge rate ~84.5 tons/hour, flowing enthalpy ~1100 kJ/kg).

Feedpoint Depth (m)	Spinner Revolutions Above Feedzone (RPM)	Line Speed v_s (m/min)	Fluid Speed v_f (m/min)	Temp. Below Feedzone T_- (°C)	Temp. Above Feedzone T_+ (°C)	Fluid Mass Flux M_+ (tons/hour)	Formation (Feedzone) Temp. (°C)
1550—1570	111	26.4	0.9	250.9	250.4	1.5	250.4
1530—1550	125	26.7	4.0	250.4	244.3	7.3	242.7
1450—1490	189	27.8	18.6	233.1	216.4	34.4	211.9
1300—1360	239	28.7	30.0	218.5	221.8	55.4	227.2
1040—1060	Two-Phase Flow						
800—900	Two-Phase Flow						

Notes: 1. $v_f = \frac{\text{RPM}}{4.07} - v_s$

2. $M \sim A v_f \rho_{T_+}$; A (well cross-section) $\sim 0.0366 \text{ m}^2$, ρ_{T_+} = water density at T_+

3. Formation Temperature, $T = (T_+ M_+ - T_- M_-) / (M_+ - M_-)$; $M_+(M_-)$ = Mass Flux above (below) feedzone.

Table 4.5. Results of spinner test conducted on September 19, 1989 (discharge rate ~62.5 tons/hour, flowing enthalpy ~1010 kJ/kg).

Feedpoint Depth (m)	Spinner Revolutions Above Feedzone (RPM)	Line Speed v_s (m/min)	Fluid Speed v_f (m/min)	Temp. Below Feedzone T_- (°C)	Temp. Above Feedzone T_+ (°C)	Fluid Mass Flux M_+ (tons/hour)	Formation (Feedzone) Temp. (°C)
1550—1570	162	36.5	3.3	249.6	249.1	5.8	249.1
1530—1550	172	36.2	6.1	249.1	240.2	11.0	230.3
1450—1490	196	35.9	12.3	227.0	215.6	22.6	204.8
1300—1360	242	37.2	22.3	218.2	221.0	41.1	224.4
1040—1060	284	38.3	31.5	220.4	220.4	58.1	220.4
800—900	Two-Phase Flow						

Notes: 1. $v_f = \frac{\text{RPM}}{4.07} - v_s$

2. $M \sim A v_f \rho_{T_+}$; A (well cross-section) $\sim 0.0366 \text{ m}^2$, ρ_{T_+} = water density at T_+

3. Formation Temperature, $T = (T_+ M_+ - T_- M_-) / (M_+ - M_-)$; $M_+(M_-)$ = Mass Flux above (below) feedzone.

the uppermost feedzone(s) is two-phase. The estimated feedzone temperatures (Table 4.6) imply a temperature inversion in the vicinity of well SD-1. The minimum temperature ($\sim 208^{\circ}\text{C}$) occurs in the depth interval 1450–1490 m.

Table 4.6. Feedzone temperatures (see Tables 4.4, 4.5).

Feedzone Depth (meters)	Temperature ($^{\circ}\text{C}$)
1550–1570	250
1530–1550	236 ± 6
1450–1490	208 ± 3
1300–1360	226 ± 1
1040–1060	220
800–900	$219 \pm 2^*$

*Estimated from shutin temperature profiles

Pressure profiles computed from the water level and temperature data are shown in Figure 4.63. Because of boiling in the wellbore (see Figure 4.59), downhole pressures calculated from water level data are not reliable. The pressures recorded by downhole gauges are displayed in Figure 4.62. The pressure at 800 m TVD (top of upper feedzone) is $\sim 44 (\pm 1)$ bars, and the pressure at 1200 m TVD (middle of permeable interval 800–1570 m) is ~ 77 bars.

4.16 Slim Hole 52E-SM-1

The borehole appears to heat up conductively in the upper part (Figure 4.64); no heat up below ~ 730 m is observed. A break in temperature gradient at the latter depth indicates the presence of a permeable horizon at ~ 730 m.

The water level in 52E-SM-1 stood at the wellhead at a shutin time of ~ 3 hours on September 27, 1978. It then fell to 19 m at a shutin time of 12 hours (9/27/78) and to 42 m at a shutin time of 36 hours (9/28/78). It is unlikely that a stable water level was attained during the observation period. Consequently, it is only possible to place an upper limit on the reservoir pressure. The pressure at a depth of 730 m is (Figure 4.65) less than 63.5 bars.

4.17 Slim Hole 52E-SM-2

Temperature surveys 1 and 2 (Figure 4.66) were recorded in the partially-drilled hole (depth = 803 m) on August 21, 1978. The change in temperature gradient at ~ 550 m corresponds to a lost circulation horizon, and represents the principal feedzone for the partially-drilled hole. The feedzone temperature exceeds 170°C . Pressure profiles computed from water level and temperature data are shown in Figure 4.67. The pressure at 550 m (profiles 1, 2; Figure 4.67) is less than 38.5 bars.

Temperature surveys recorded on October 15 and 16, 1978 in the completed borehole (Figure 4.68) show a sharp increase in temperature at ~ 470 m; this feature is absent from the temperature profiles recorded in the partially drilled hole on August 21, 1978 (see Figure 4.66). We speculate that a casing break is present at ~ 470 m. A break in temperature gradient at ~ 980 m identifies the permeable horizon for the completed 52E-SM-2. The feedzone temperature is at least 230°C . During the observation period in October 1978, the water level (Profiles 3–5, Figure 4.67) continued to rise; it is impossible to tell whether a stable water level was reached. The pressure at 980 meters is estimated to be ~ 69 bars (see Profile 5, Figure 4.67).

Continued on page 4-83

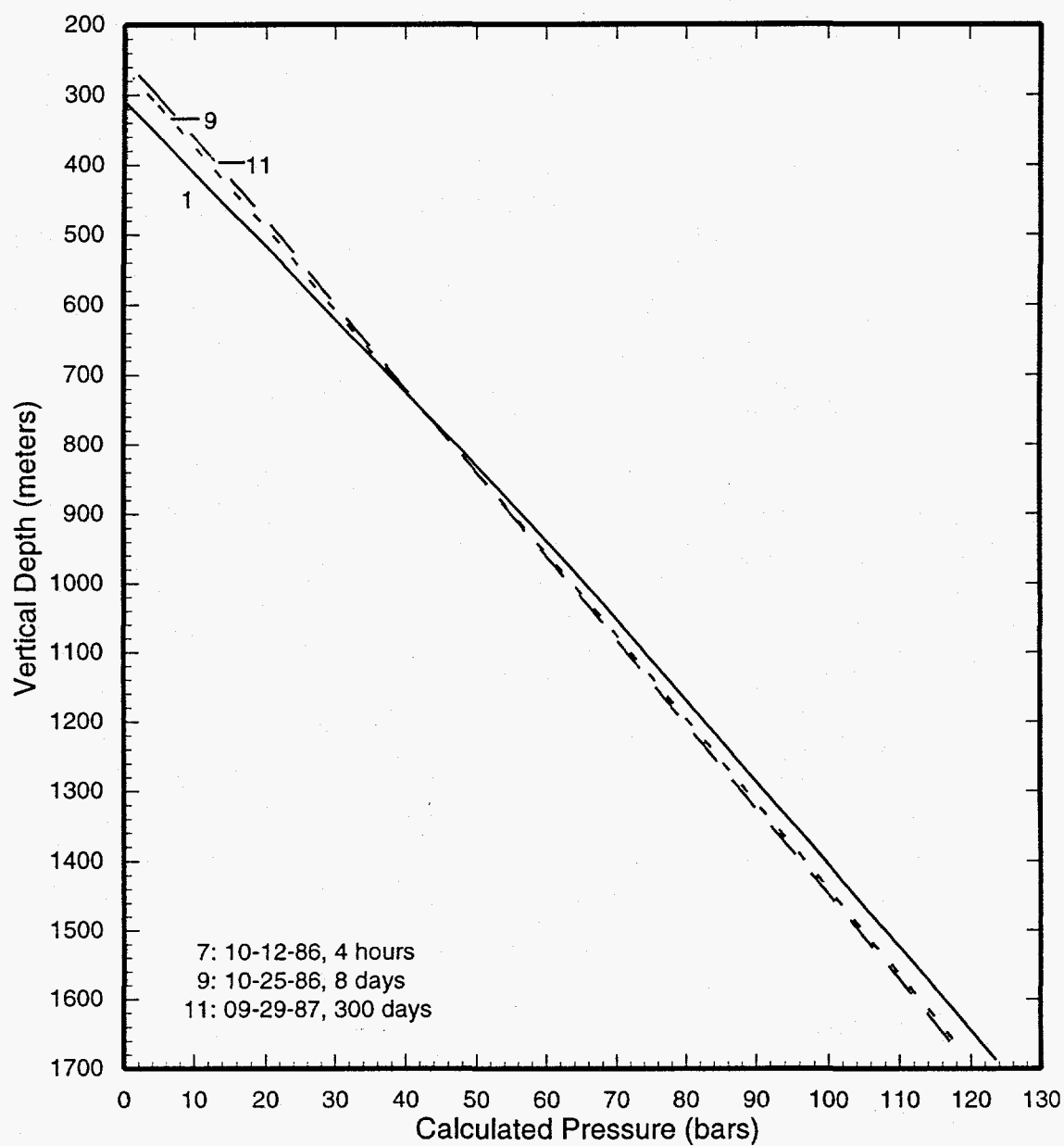


Figure 4.63. Selected pressure profiles computed from water level and temperature data in well SD-1.

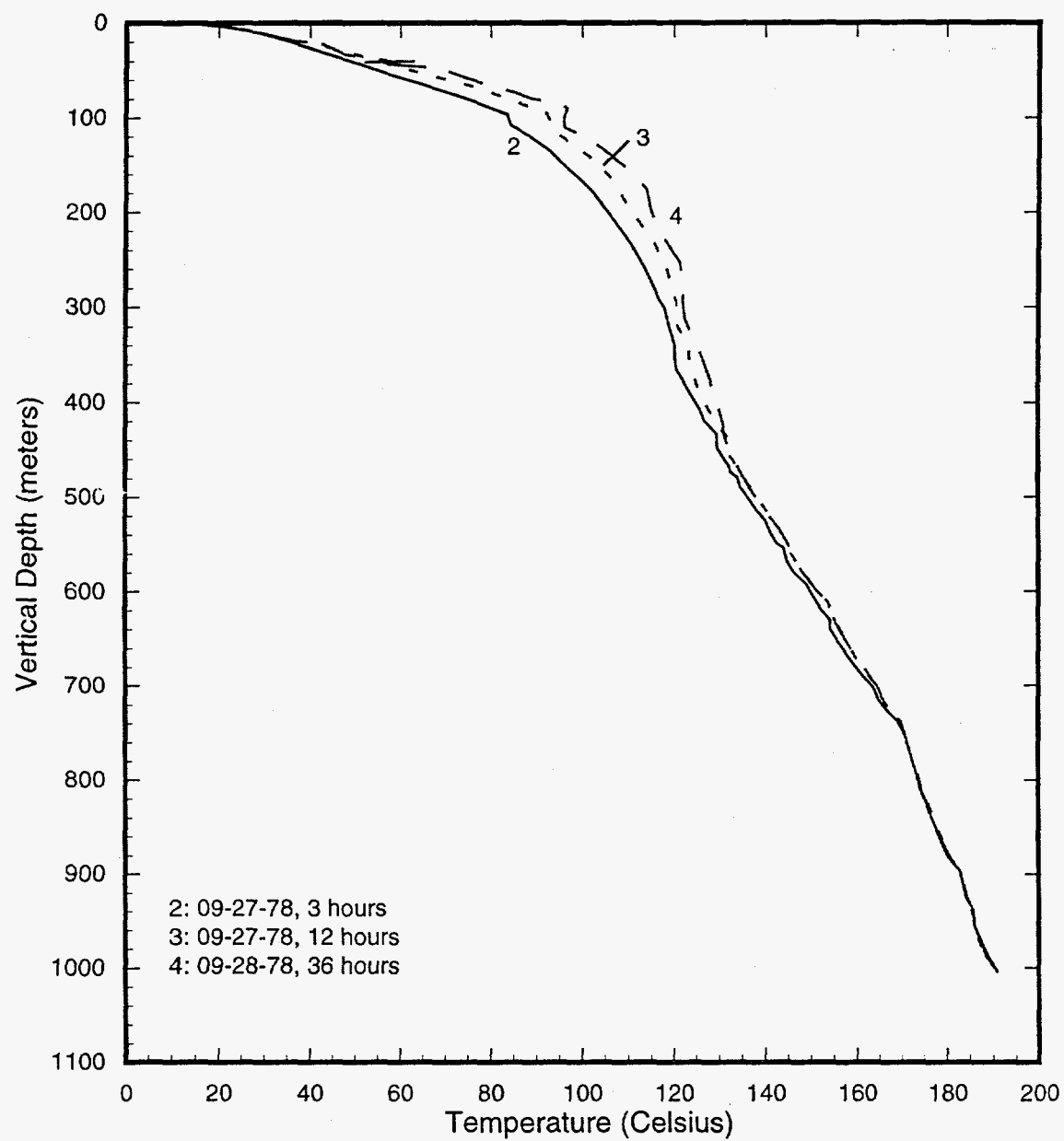


Figure 4.64. Selected temperature profiles for 52E-SM-1.

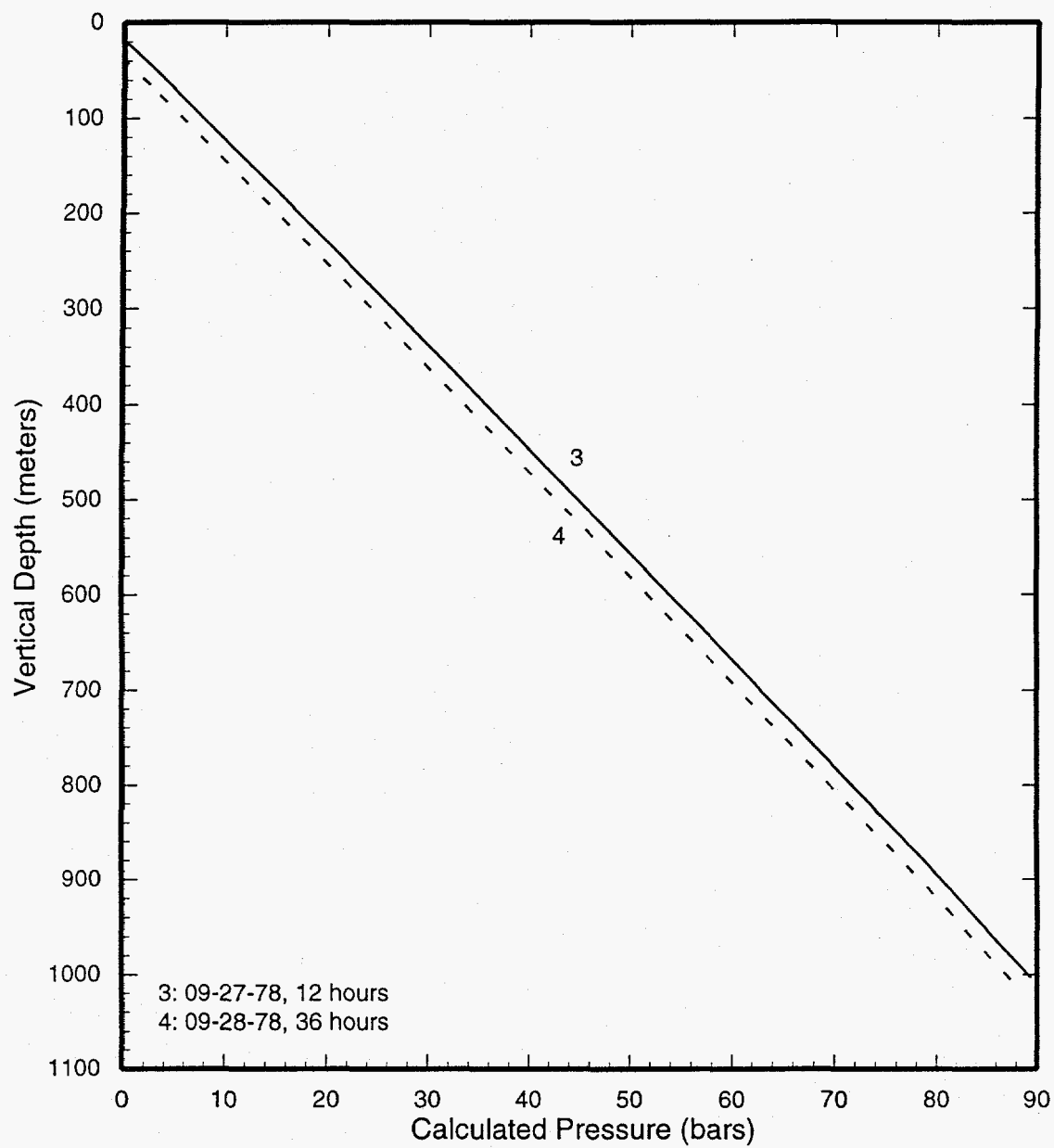


Figure 4.65. Pressure profiles computed from water level and temperature data for 52E-SM-1.

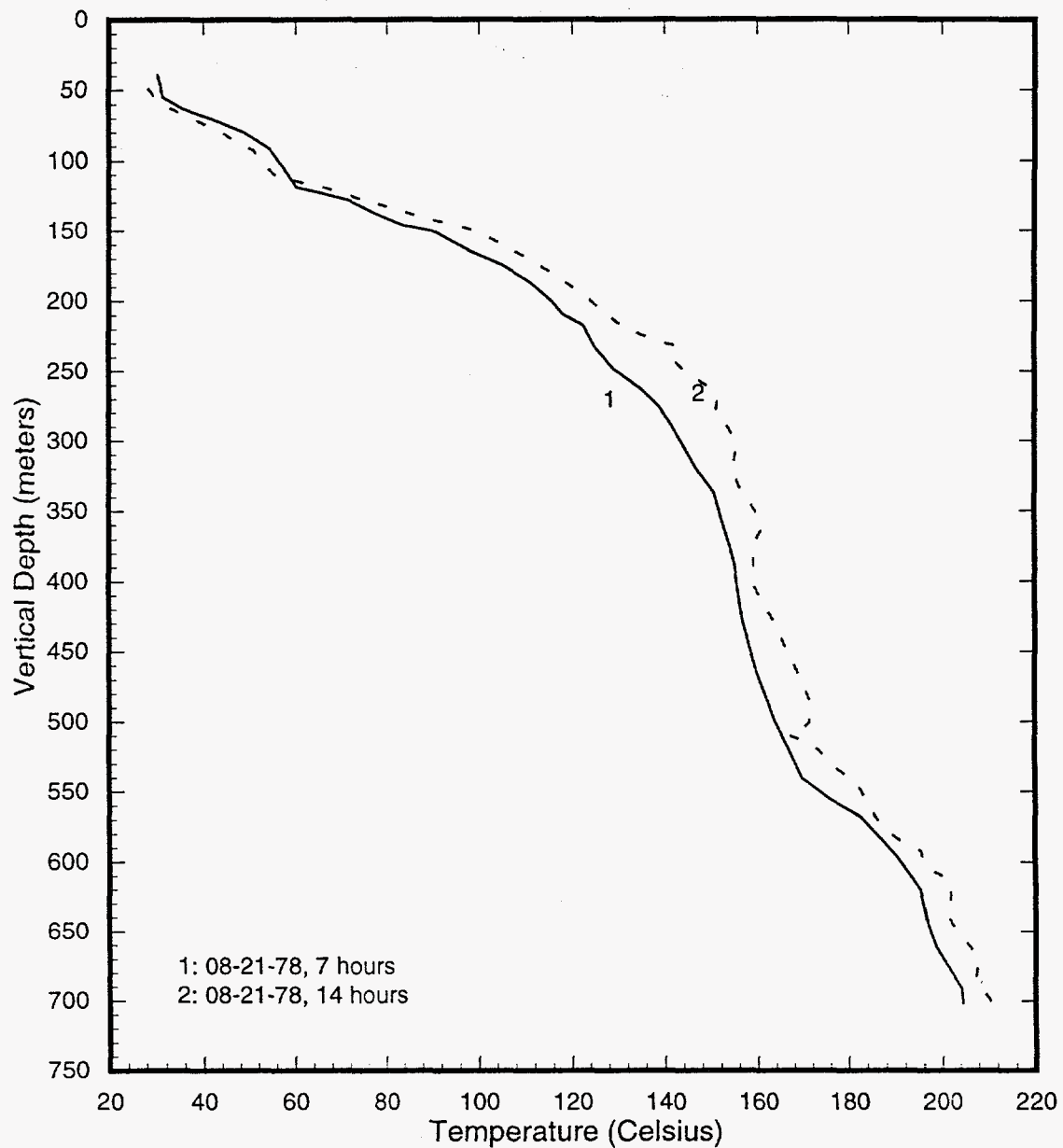


Figure 4.66. Temperature profiles in partially-drilled (depth = 803 m) 52E-SM-2 recorded on August 21, 1978.

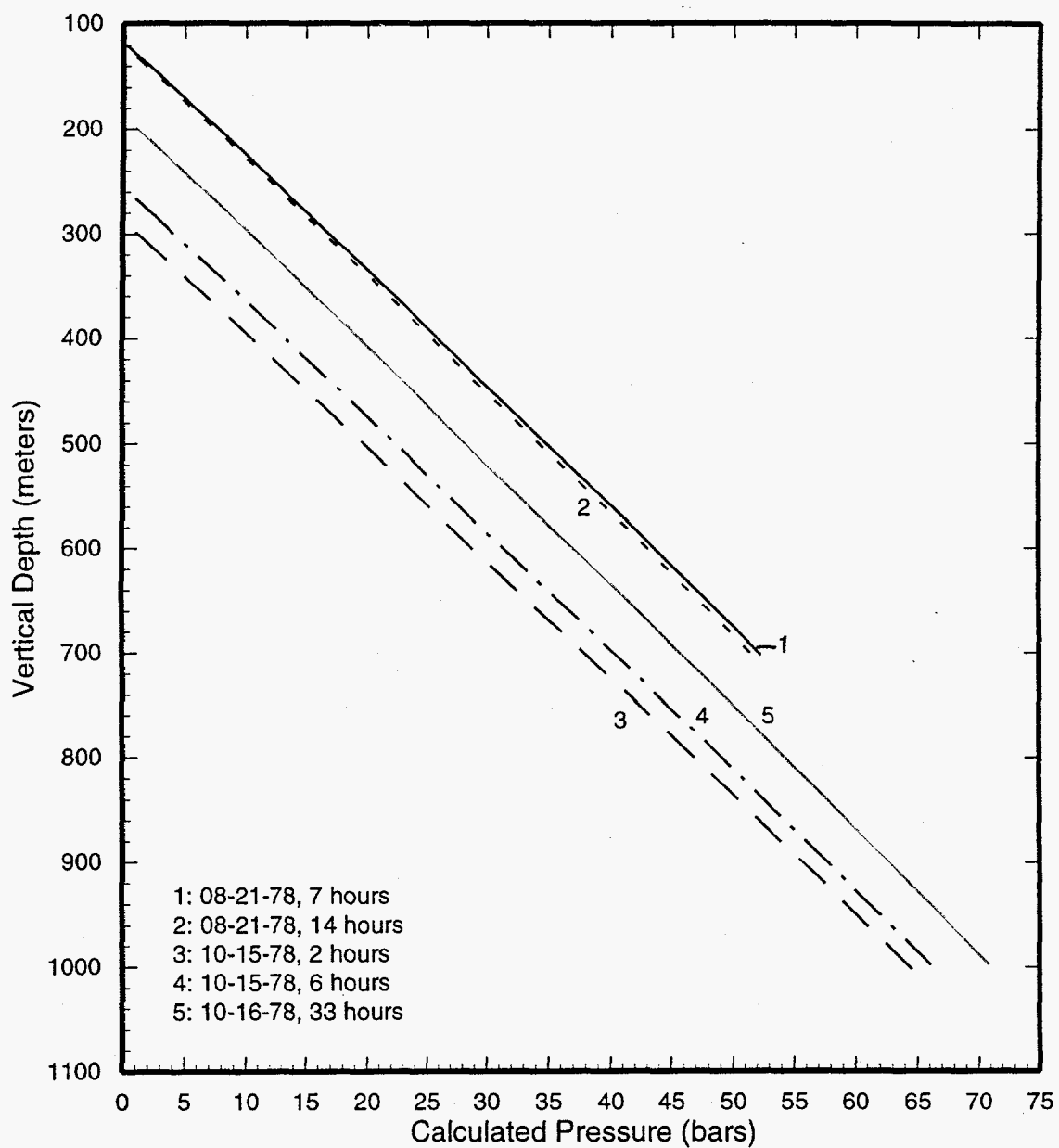


Figure 4.67. Pressure profiles computed from water level and temperature data for 52E-SM-2.

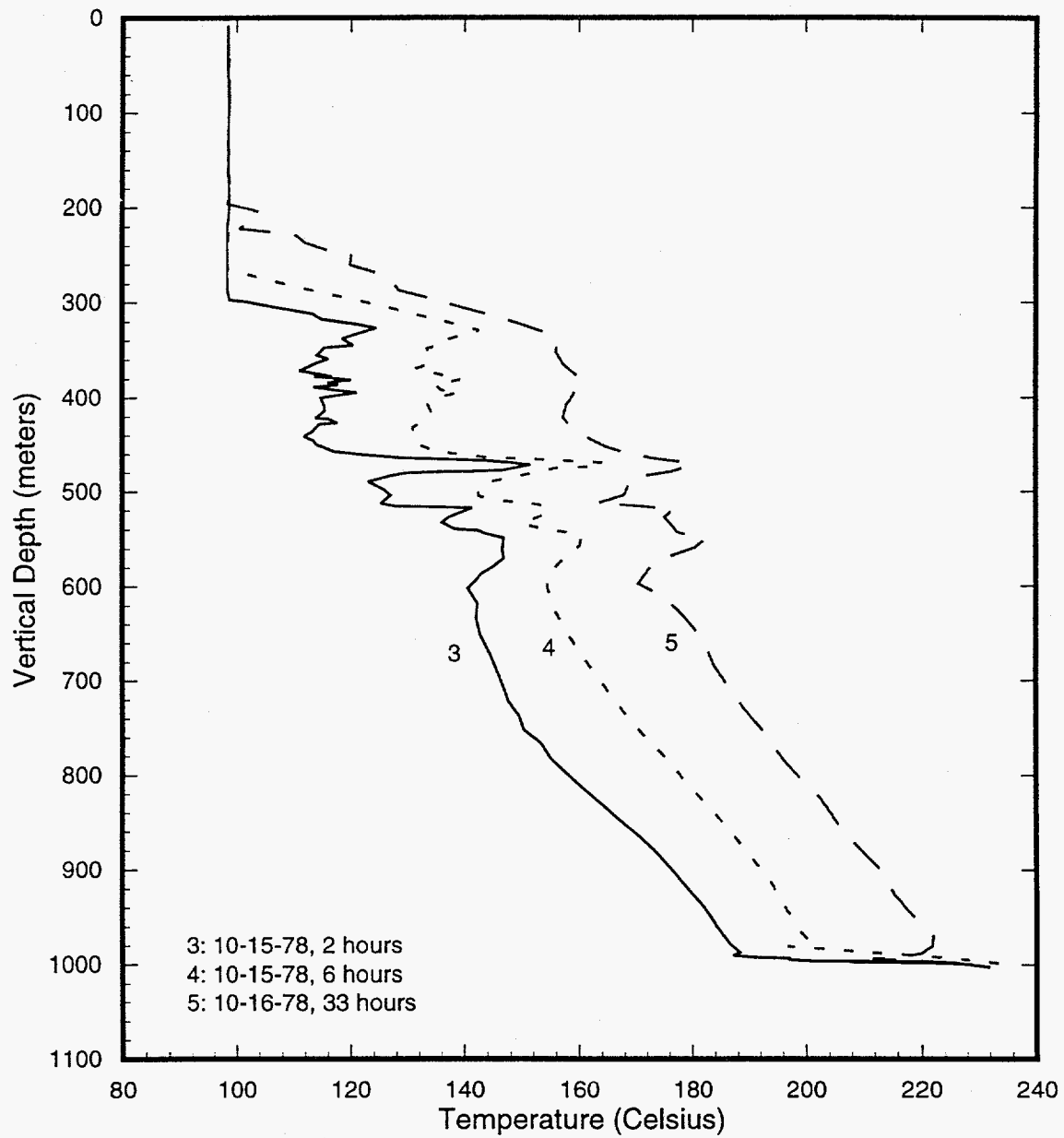


Figure 4.68. Temperature surveys in completed 52E-SM-2 taken on October 15 and 16, 1978.

4.18 Slim Hole N59-SN-5

The temperature survey of November 7, 1985 (Figure 4.69) was taken after the hole had reached 1700 m. An injection test was performed on November 13, 1985. Heat-up surveys subsequent to the injection test show a large change in temperature at ~750 m; this temperature feature is absent from the temperature survey of November 7, 1985. We therefore speculate that injection caused a break in casing at ~750 m. Temperature profiles recorded on November 13, 1985 (Figure 4.69) show depressed temperatures at ~1425 m and ~1600 m. An abrupt break in temperature gradient at ~1600 m identifies the principal feedzone for N59-SN-5.

Only three short shutin time (ST ~5 and 8 hours on November 13, 1985 and ST ~16 hours on November 14, 1985) water level readings are available. The borehole has poor permeability, and it is almost certain that the water level did not attain its

stable value at these early times; these water levels are, therefore, useless for determining reservoir pressures.

On November 20 and 21, 1985, two pressure gradient surveys were taken with a Kuster gauge. Unfortunately, these surveys were confined to the upper 800 m of the hole. There appears to be something wrong with these pressure data since the measured pressure gradients imply the presence of two-phase fluid in the depth interval 200 to 800 m. (The temperatures in this depth interval are simply too low to sustain two-phase conditions). In any case, the measured pressure at 800 m depth was 34 to 38 bars. Assuming that the pressure at 800 m is indeed 34 to 38 bars and taking the average temperature between 800 m and 1600 m to be ~238°C (see Figure 4.69), the pressure at 1600 m is estimated to be 99 to 103 bars.

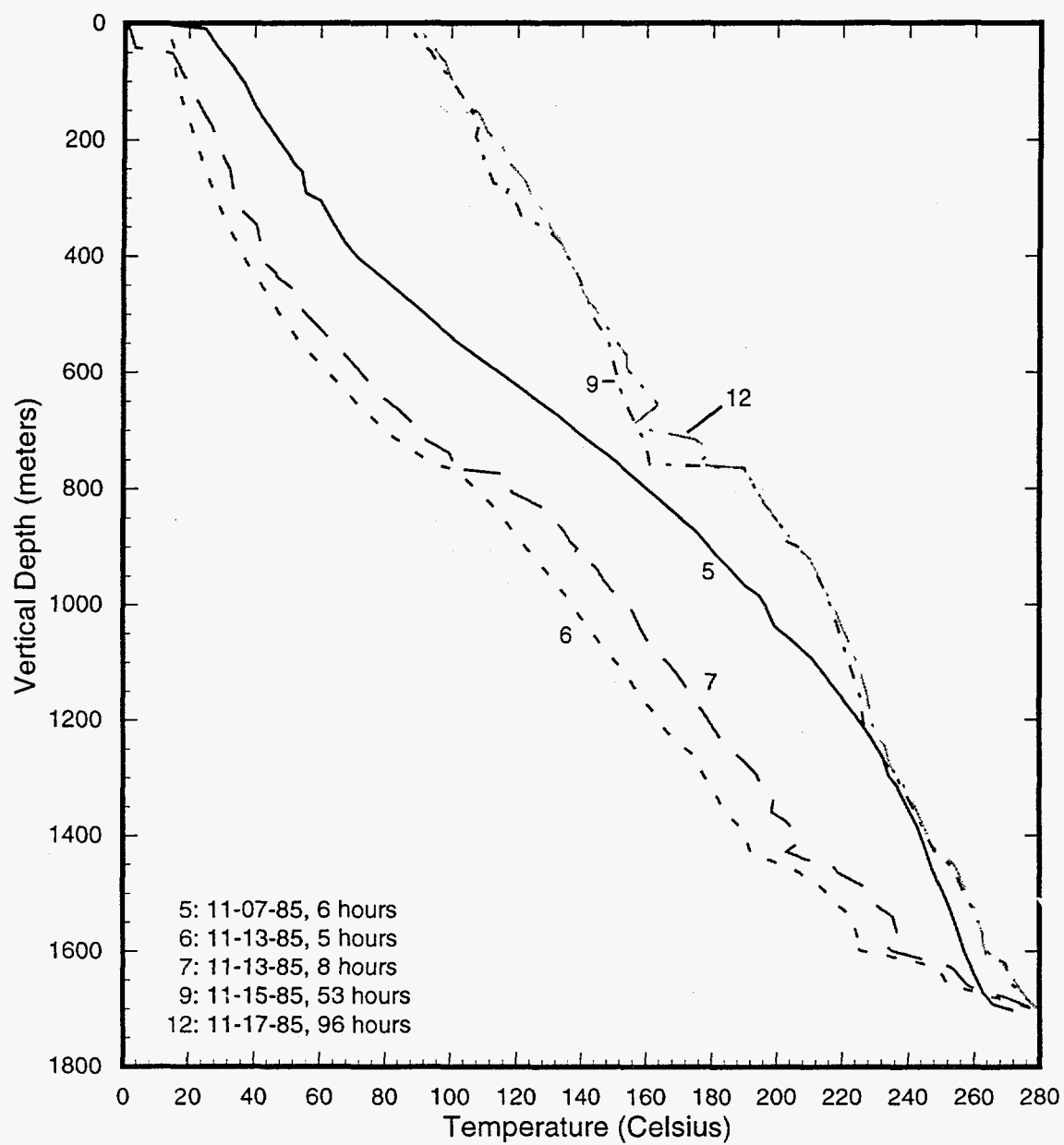


Figure 4.69. Selected temperature surveys in N59-SN-5.

5 Injection and Discharge Tests

Injection tests have been performed on eighteen Sumikawa boreholes. It is a standard practice at Sumikawa to perform a short (a few hours) injection test soon after the (usually within a few days) drilling and completion of a borehole. In an effort to improve the productivity and injectivity of wells SA-1, SA-2, SA-4, S-4, SB-1, SB-2 and SB-3, MMC injected large amounts of cold river water in these wells in April and May 1989; step rate injection tests were performed (with downhole pressure gauges) both prior to (wells SA-1, SA-2, and SA-4 only) and subsequent to (all 7 wells) the river water injection. A typical injection test at Sumikawa consists of injecting cold water into a borehole at several different rates and simultaneously monitoring pressure (and temperature) downhole. While exceptions do exist, in most of the tests, the pressure tool was placed substantially above the feedzone depth. Because of wellbore cooling, the measured change in pressure at the gauge depth (gauge depth \ll feedzone depth) will underestimate the change in pressure at the feedzone depth. The discrepancy in rates of change at the gauge and feedzone depths will decline with continued injection. After the injection of a few wellbore volumes (say 2 or 3), the rates of pressure change at the two depths should be similar. Since in most of the Sumikawa injection tests several wellbore volumes of cold water were injected, the measured pressures can be used to infer the injectivity index (II). The injectivity index (II) is defined as follows:

$$II = \frac{\Delta M}{\Delta P}$$

Here $\Delta M/\Delta P$ is the slope of the straight-line fit to the multi-step injection rate versus injection pressure (at gauge depth) data.

The available injection test data are, however, less useful for inferring formation transmissivity. During the injection phase, the pressures (at a constant rate) are often observed to decline due to borehole cooling and/or borehole washing effects. The fall-off pressure data from most of the tests are corrupted by borehole heating. Borehole heating causes the apparent pressure decline rate at the gauge depth to be smaller than the corresponding decline rate at the feedzone depth.

The determination of injectivity indices for individual Sumikawa boreholes is described in Section 5.1. The injectivity data are summarized in Table 5.1.

A total of four slim holes and seven large-diameter Sumikawa wells have been discharged at one time or another. Five of the Sumikawa boreholes (slim holes S-2, S-3 and 52E-SM-2, large diameter wells SB-1 and SC-1) produce from all liquid feedzones. Discharge from other Sumikawa boreholes (slim hole S-1, intermediate depth slim holes S-2 and 52E-SM-2, large-diameter wells S-4, SA-1, SA-2, SA-4 and SD-1) is accompanied by *in situ* boiling. As part of the discharge tests, the characteristic output curves (*i.e.*, mass and enthalpy versus wellhead pressure) were also obtained. These characteristic data are discussed in Section 5.3.

During the discharge tests of seven boreholes (slim hole S-2, original slim hole S-2, large-diameter wells S-4, SA-1, SA-4, SC-1 and SD-1), pressure and temperature (or pressure, temperature and spinner) surveys were run. These pressure/temperature surveys are used to calculate the productivity indices for the Sumikawa boreholes

Continued on page 5-3

Table 5.1. Injectivity indices for Sumikawa boreholes.

Borehole Name	Final Diameter (mm)	Feedzone Depth (m TVD)	Test Date	Pressure Gauge Depth (m TVD)	Injectivity Index (kg/s-bar)	Remarks
50-HM-3	79	460	12-02-75	0	0.016	After well completion
N60-KY-1	101	1560	08-07-86	1177	0.012	After well completion
O-5T	64	747	09-22-78	280	0.28	
S-1	143	436	05-20-82 05-26-82	250 300	1.3 6.8	Injection into a shallow horizon (70–100 meters) through a casing break
S-2	101	900 900 ? 940 940	06-23-82 07-16-82 10-04-82 10-16-82 10-23-82	400 500 450 500 500	0.76 0.76 0.52 1.62 1.76	Original completion, hole depth = 904.6 m Original completion, hole depth = 904.6 m Redrilled hole, hole depth = 906 m Final completion Final completion
S-3	101	? ? ? 700	09-02-82 10-06-82 05-16-83 06-12-83	400 300 600 600	0.79 0.43 0.25 1.4	Intermediate depth, hole depth = 603 m? Intermediate depth, hole depth = 603 m? Intermediate depth, hole depth = 656 m After well completion
S-4	159	1520	11-06-83 11-07-83 05-19-89	700 700 700	1.4 1.4 4.9	After well completion After well completion After 1989 injection
SA-1	216	1800	10-11-86 04-16-89 05-16-89	1057 1726 1726	1.5 0.90 2.0	After well completion Before 1989 injection After 1989 injection
SA-2	216	1450	09-22-87 09-22-87 04-16-89 05-17-89	968 968 1062 1061	1.0 1.2 1.3 1.7	After well completion After well completion Before 1989 injection After 1989 injection
SA-4	216	1240	05-30-88 04-17-89 05-18-89	1127 1262 1262	0.31 0.88 1.0	After well completion Before 1989 injection After 1989 injection
SB-1	216	1600	10-25-87 10-26-87 11-08-87 05-27-88 08-15-88 05-28-89	0 0 965 965 1665 1626	0.98 1.5 0.37 0.49 0.44 2.0	After well completion After well completion After well completion After well completion After well completion After 1989 injection
SB-2	216	1270	06-22-88 05-29-89	674 684	1.8 1.6	After well completion After 1989 injection
SB-3	216	880	08-05-88 05-30-89	678 678	0.41 1.5	After well completion After 1989 injection
SC-1	216	2310	11-15-87 06-07-88	2290 2329	5.5 4.9	After well completion
SD-1	216	? 1550 1550	09-04-86 10-12-86 10-17-86	387 700 799	2.7 0.65 0.92	Intermediate depth; hole depth = 396 m After well completion After well completion
52E-SM-1	79	730	09-30-78	0	0.002	After well completion
52E-SM-2	101	550	08-26-78	0	0.068	Intermediate depth; hole depth = 803 m
N59-SN-5	101	1600	11-12-85	0	0.068	After well completion

- Notes: 1. After well completion = within 1 month of drilling and well completion.
 2. 1989 injection test: cold river water was injected into SA-1, SA-2, SA-4, S-4, SB-1, SB-2 and SB-3 during April and May 1989

in Section 5.1. Productivity index, PI, is defined as follows:

$$PI = \frac{M}{P_{ns} - P_{fp}}$$

where M is the mass discharge rate, P_{ns} is the stable (static) feedzone (or gauge depth) pressure, and P_{fp} is the flowing feedzone (or gauge depth) pressure. The static feedzone (or gauge depth) pressure was estimated from shutin pressure surveys discussed in Section 4. The pressure surveys in the discharging boreholes were used to obtain the flowing pressures. The productivity indices for individual Sumikawa boreholes are summarized in Table 5.2.

5.1 Determination of Injectivity and Productivity Indices

The injection rates are usually given as volume injection rates (m^3/s or liters/s). For present purposes, it is satisfactory to assume that the density of injected water is 1000 kg/m^3 ; therefore, a volume flow rate of 1 liter/s equals a mass flow rate of 1 kg/s.

Slim Hole 50-HM-3

A multi-rate injection test was performed on December 2, 1975; the pressures were recorded at the wellhead. The straight-line fit to the pressure versus injection rate data (Figure 5.1) yields an injectivity index of 0.016 kg/s-bar . Slim hole 50-HM-3 is located in a low-permeability zone to the north of the Sumikawa field.

Slim Hole N60-KY-1

A single multi-rate injection test was performed shortly after drilling and completion of the

borehole on August 7, 1986; the pressures were recorded at 1177 m TVD. The straight-line fit to the pressure and injection rate data (Figure 5.2) gives an injectivity index of 0.012 kg/s-bar . The poor injectivity exhibited by N60-KY-1 is rather surprising in view of the results of later pressure interference tests. During discharge from wells S-4 and SB-1 and injection into wells S-4, SB-1 and SB-2, strong pressure interference was observed in N60-KY-1. These pressure interference data have been interpreted to imply the existence of a high permeability zone in the "altered andesite" formation (N60-KY-1 has feedzones in the altered andesite and marine-volcanic complex formations), and a modest permeability dacite layer in the "marine-volcanic complex" formation. In view of these pressure interference results, it is possible that the poor injectivity for N60-KY-1 is caused by the plugging of permeable fractures by the drilling mud.

Slim Hole O-5T

An injectivity test for slim hole O-5T was carried out on September 22, 1978 with the pressure gauge set at 280 m TVD. Slim hole O-5T is located to the east of the Sumikawa field (*i.e.*, between the Sumikawa and Ohnuma Geothermal Fields). The pressure and injection data shown in Figure 5.3 give an injectivity index of 0.28 kg/s-bar .

Slim Hole S-1

The pressure and flow rate data obtained during the two injection tests of S-1 in May 1982 (approximately six months after drilling and completion of S-1) are displayed in Figures 5.4a and 5.4b. It is apparent from Figures 5.4a and 5.4b that the pressures fluctuated considerably during these in-

Continued on page 5-10

Table 5.2. Productivity indices for Sumikawa boreholes.

Borehole Name	Final Diameter (mm)	Feedzone Depth (m TVD)	Test Date	Total Flow Rate (kg/s)	Static Pressure (bars)	Flowing Pressure (bars)	Productivity Index (kg/s-bar)	Remarks
S-1	143	436	04-25-82 04-27-82 04-30-82	—	—	—	0.86	Produced dry-steam. PI estimated from mass flow rate and wellhead pressure (see text).
S-2	101	900	07-11-82	1.10	47.3*	7.26	0.027	Original completion, hole depth = 904.6 m Two-phase feed
	101	940	11-10-82	13.4	51.0	40.5	1.3	Liquid feed
S-4	159	1520	10-04-84	37.5	93.0	51.3	0.90	Two-phase feed. Flowing pressure extrapolated from pressure surveys to 1050, 1050 and 1070 meters depth (see text).
			10-31-84	39.1		49.4	0.90	
			10-12-85	35.1		58.2	1.01	
SA-1	216	1800	09-21-89	13.6	114.0	26.5	0.16	Well produces mostly steam Two-Phase feed
			09-22-89	13.7		34.6	0.17	
SA-4	216	1240	09-23-89	8.06	81.0	10.8	0.11	Well produces dry steam from a two-phase feed
SC-1	216	2310	11-04-88	48.1	149.0	139.7	5.2	Liquid feeds (several entries)
			11-06-88	55.2		140.1	6.2	
			11-07-88	86.1		133.6	5.6	
SD-1	216	1200 (middle of permeable interval)	09-18-89	23.5	77.0	23.8	0.44	Several entries. Shallowest (800–900 m) two-phase; deeper entries liquid.
			09-19-89	17.4		47.0	0.58	

*Estimated from a fit to feedzone pressures for Sumikawa wells (Pritchett et al., 1990)

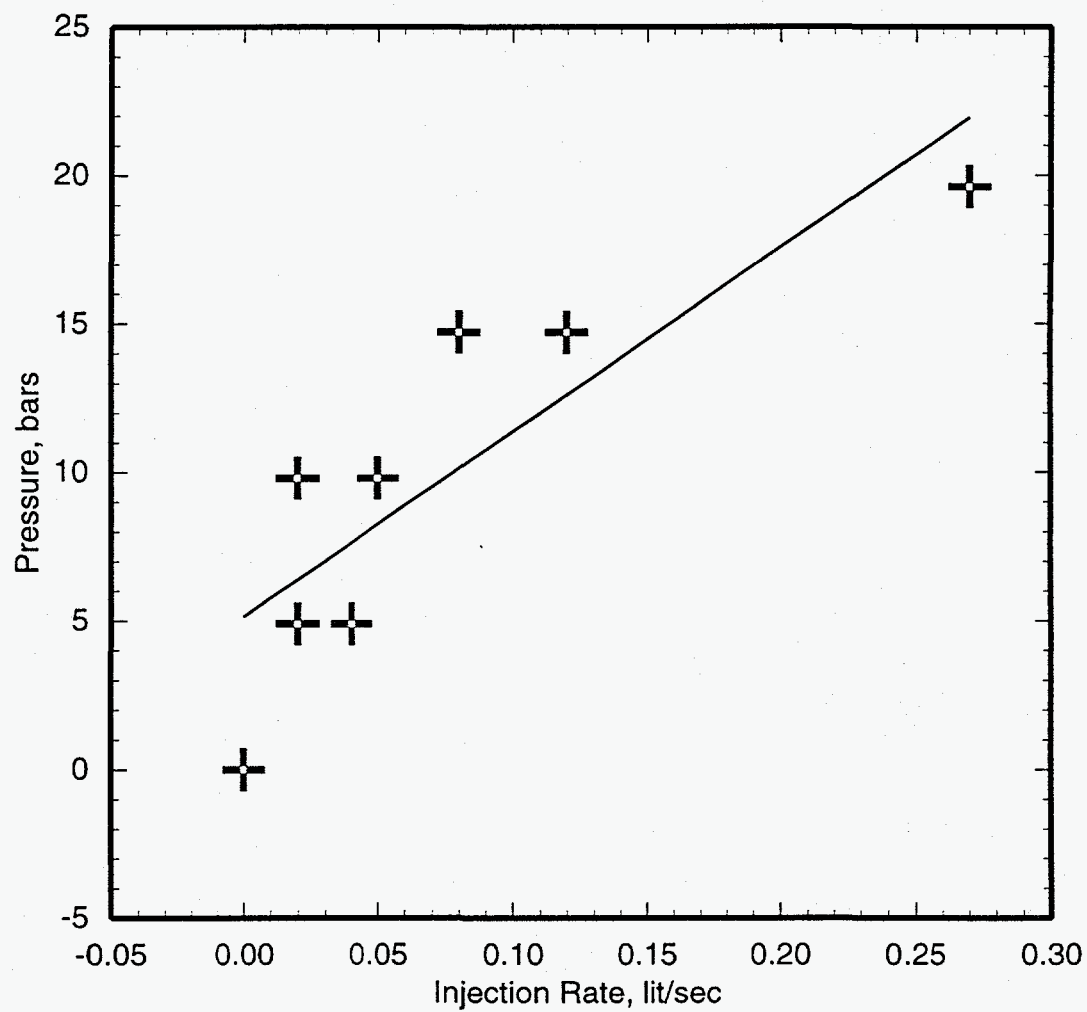


Figure 5.1. Injectivity test for slim hole 50-HM-3 performed on December 2, 1975. The pressure gauge was set at wellhead.

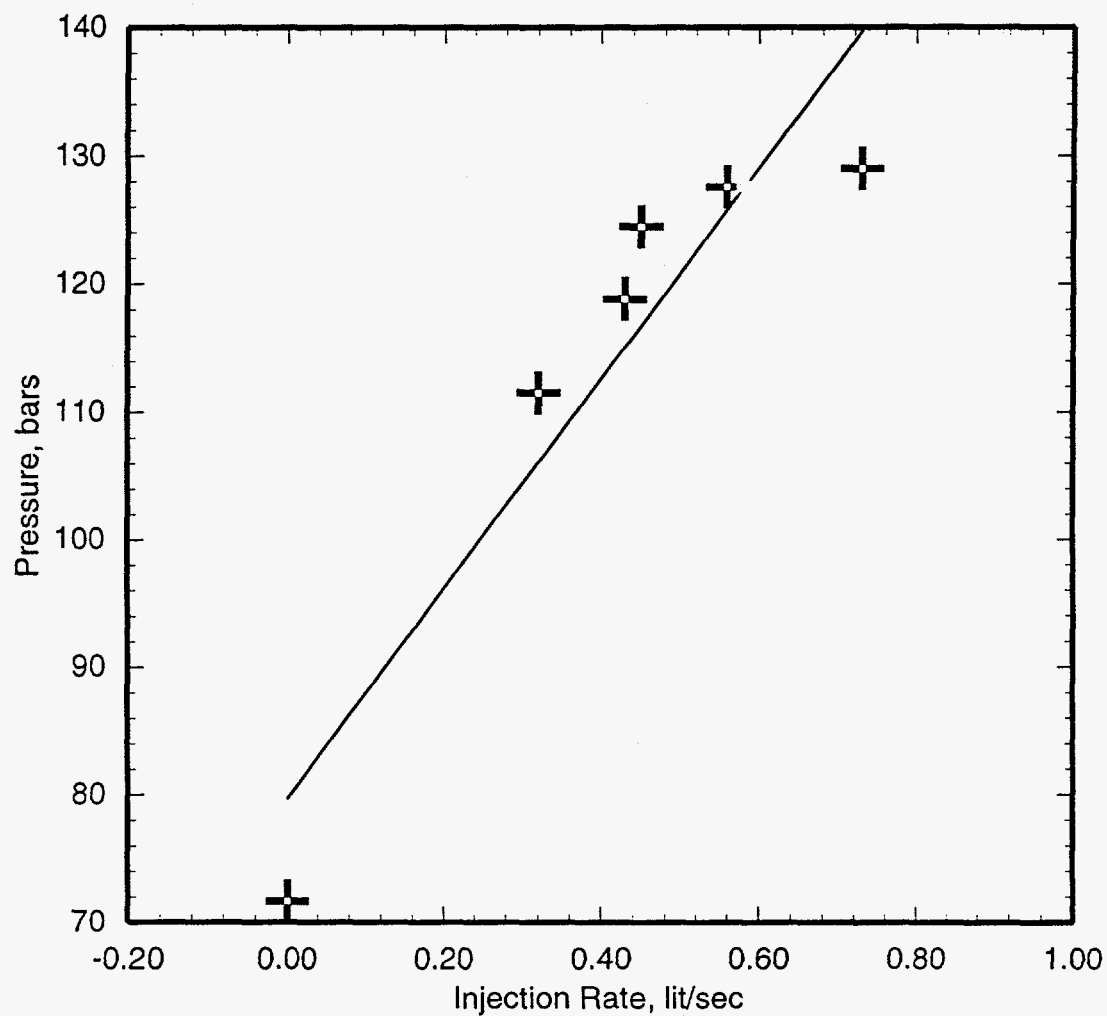


Figure 5.2. Injectivity test for slim hole N60-KY-1 performed on August 7, 1986. The pressure gauge was set at 1177 m MD (1177 m TVD).

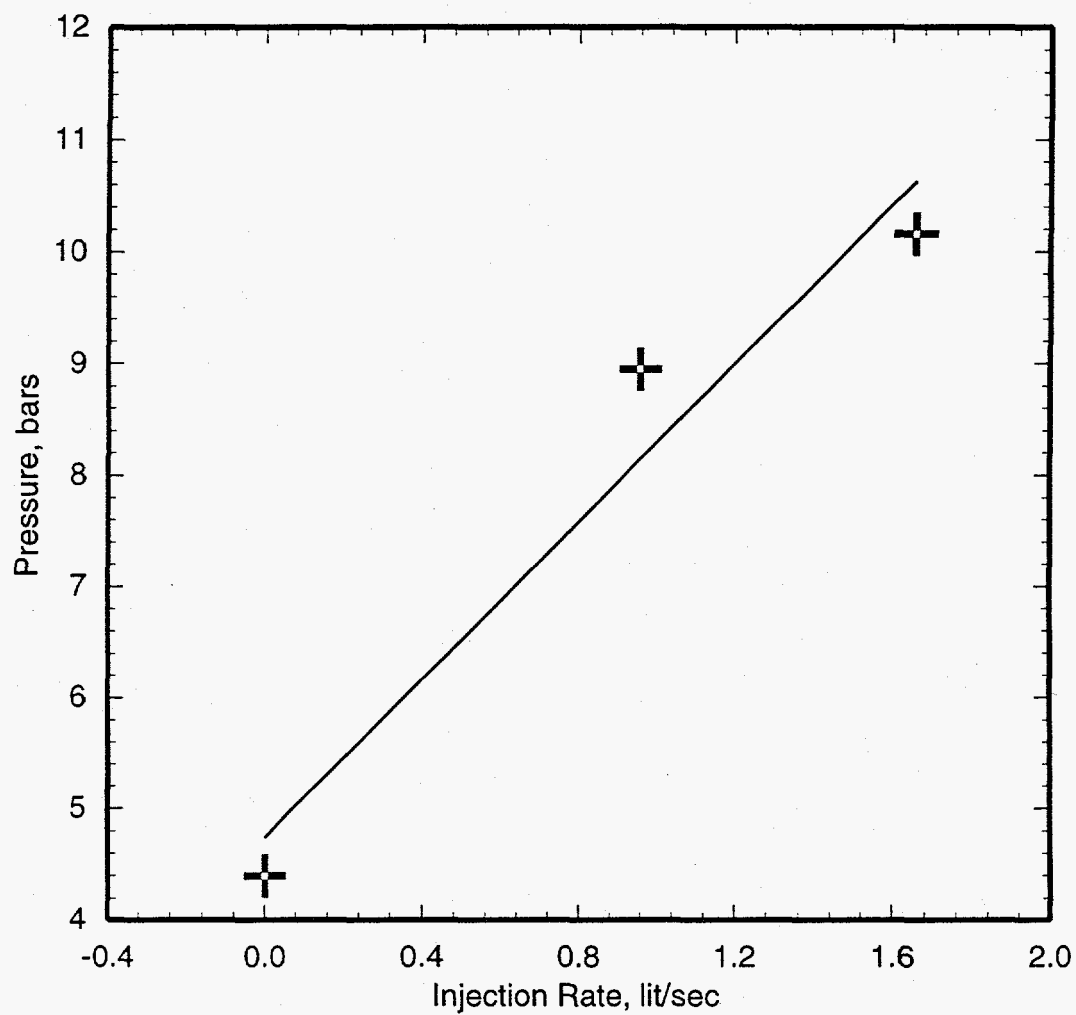


Figure 5.3. Injectivity test for slim hole O-5T performed on September 22, 1978. The pressure gauge was set at 280 m MD (280 m TVD).

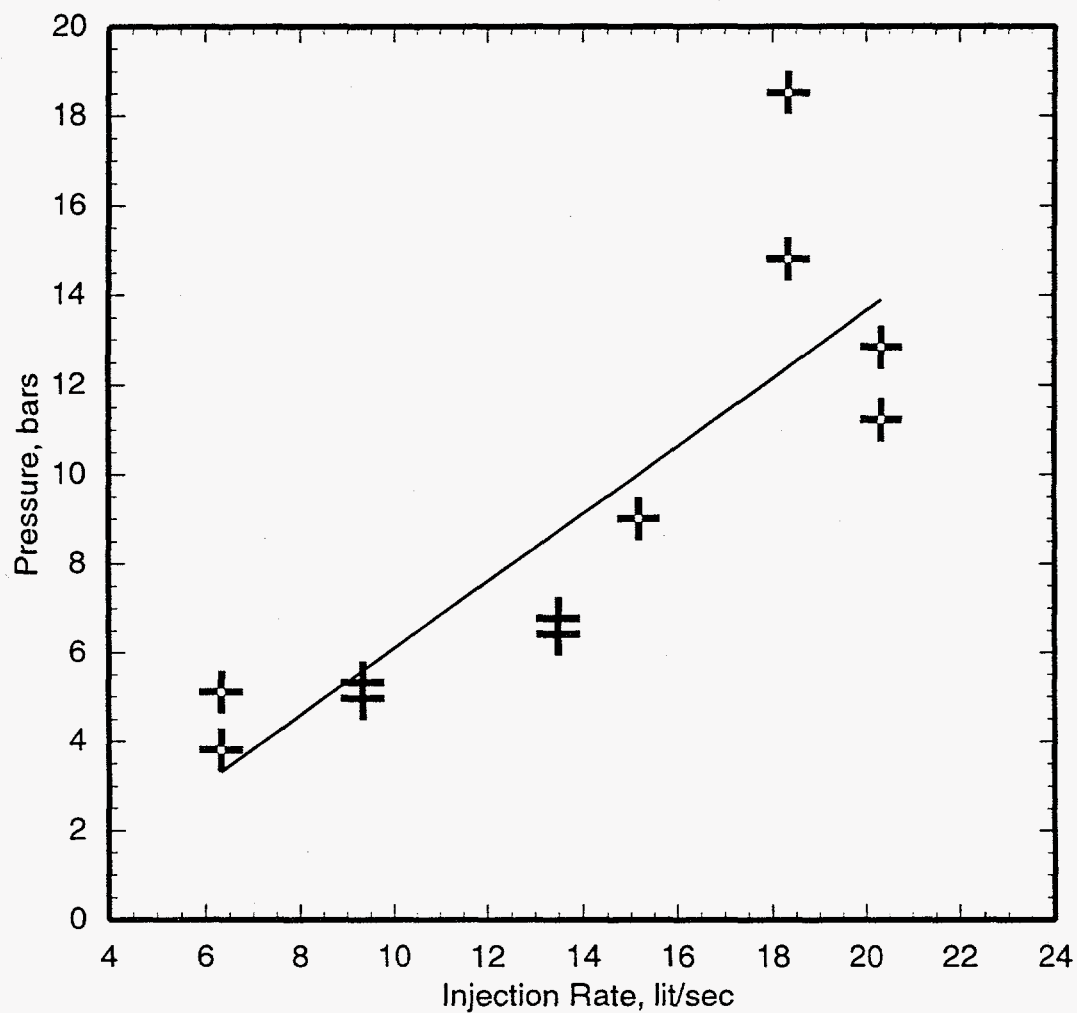


Figure 5.4a. Injectivity test for slim hole S-1 performed on May 20, 1982. The pressure gauge was set at 250 m MD (250 m TVD).

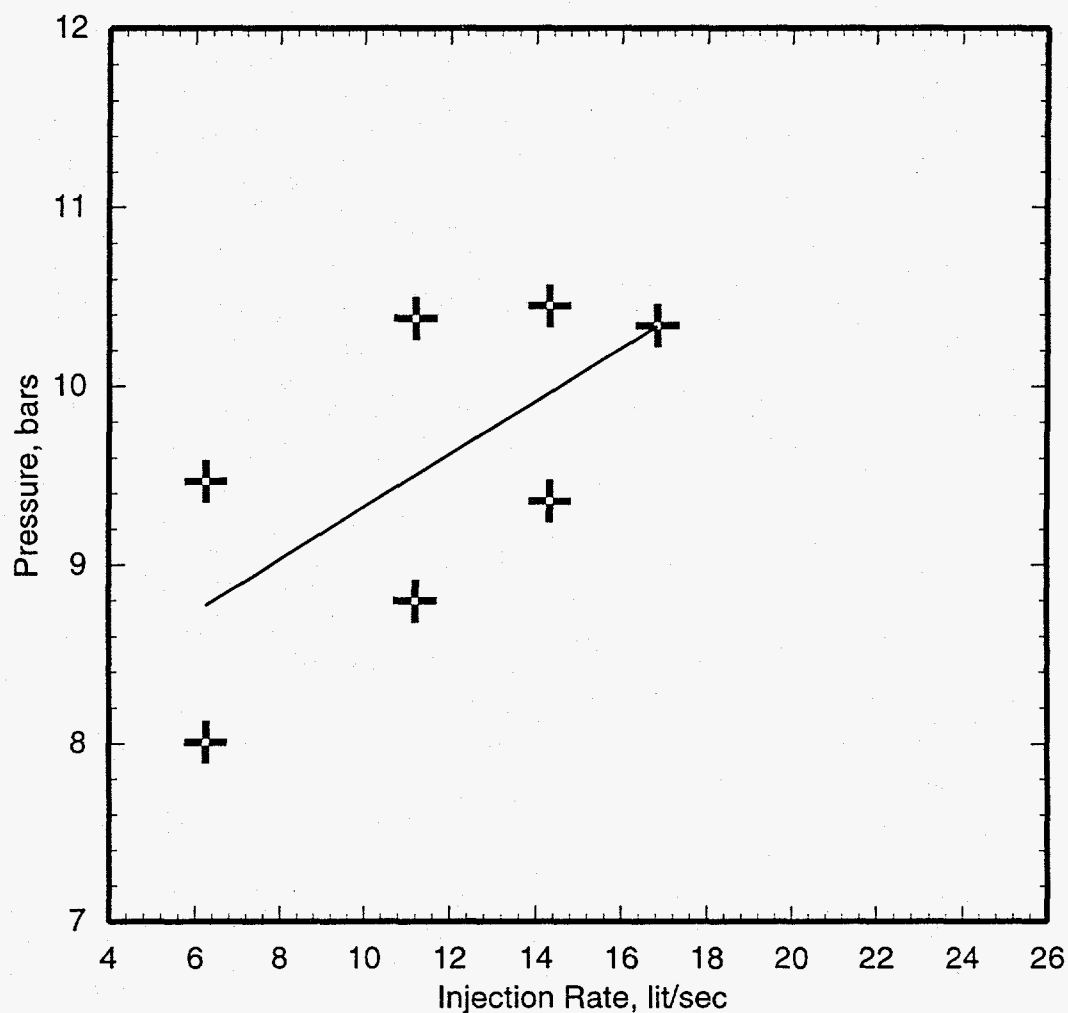


Figure 5.4b. Injectivity test for slim hole S-1 performed on May 26, 1982. The pressure gauge was set at 300 m MD (300 m TVD).

jection tests. The two injection tests (Figures 5.4a,b) yield rather disparate values (1.3 kg/s-bar and 6.8 kg/s-bar) for the injectivity index.

Slim hole S-1 was discharged for several days in April 1982 (*i.e.*, prior to injection tests discussed above). The slim hole produced dry steam. No downhole pressure and temperature surveys were taken in the discharging borehole. The discharge rate versus wellhead pressure data (Figure 5.5) can be fit closely by a straight-line; the discharge rate is inversely proportional to the wellhead pressure. The slope of the straight-line gives a value of 0.86 kg/s-bar for the productivity index.

Slim Hole S-2

After the borehole had been drilled to 904.6 m, both injection and discharge tests were performed. The major feedpoint for the original hole S-2 (drilled depth = 904.6 m) is located a depth of about 900 m. The injectivity tests performed on June 23, 1982 and July 16, 1982 (Figures 5.6a and b) both yield an injectivity index of 0.76 kg/s-bar. During discharge tests from July 8 to July 12, 1982 of the 904.6 m hole, two-phase fluids with an enthalpy well above that of liquid water at reservoir temperature were produced. The amount of excess enthalpy decreased with increasing wellhead pressure. It is, therefore, likely that the excess enthalpy is the result of production induced flashing in the formation. An alternative explanation is that the borehole taps a two-phase reservoir at shallow depths. A pressure survey run in the discharging hole on July 11, 1982 gave a pressure of 7.26 bars at 900 m depth. Assuming a stable feedzone pressure of 47.3 bars (pressure computed from Sumikawa pressure correlation, Section 7) and a discharge rate of 1.10 kg/s, a productivity index of 0.027 kg/s-bar is obtained. The large dif-

ference between the productivity and injectivity indices is due to *in situ* boiling induced by borehole discharge; the formation transmissivity is severely reduced by two-phase flow.

Injectivity tests of October 16 and October 23, 1982 (Figures 5.6d,e) were performed on the redrilled hole (final depth = 1065.1 m). The feedzone for the redrilled hole is at ~940 m. The injectivity index for S-2 (Figures 5.6d,e) is ~1.7 kg/s-bar. During a discharge test in November 1982, slim hole S-2 produced fluid with an enthalpy of about 250 (± 10) kcal/kg; this is consistent with production from a liquid reservoir of about 240 to 250°C. A pressure survey run in discharging S-2 on November 10, 1982, gave a pressure of 40.5 bars at 940 m. With a stable feedzone pressure of 51.0 bars (Section 4.5) and a discharge rate of 13.4 kg/s, a productivity index of 1.3 kg/s-bar is obtained. Unlike the original hole, the productivity and injectivity indices for the completed hole are not all that different. Both the injection and production tests imply that the redrilled hole has higher transmissivity than the original hole.

Slim Hole S-3

Injectivity tests of September 2, 1982, October 6, 1982 and May 16, 1983 (Figures 5.7a-c) were performed in the partially drilled hole. After the hole was drilled to the target depth (805.1 m) and completed, another injectivity test was carried out on June 12, 1982 (Figure 5.7d). The injectivity index for the completed hole is 1.4 kg/s-bar.

During discharge tests carried out in October 1983, slim hole S-3 produced fluids with an enthalpy equal to that of liquid water at ~240°C. This suggests that the main feedzone for S-3 contains liquid water. Slim hole S-3 exhibited some cycling

Continued on page 5-21

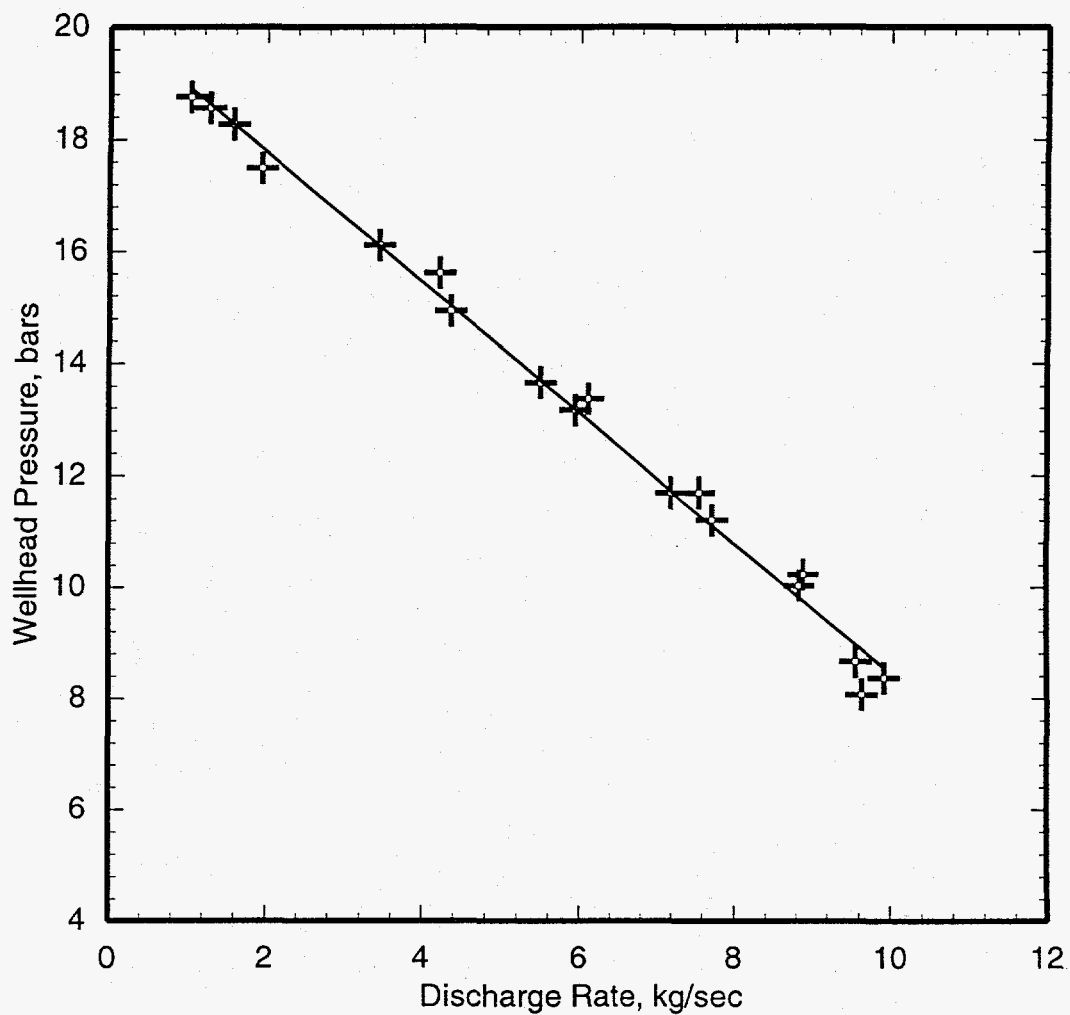


Figure 5.5. Productivity test for slim hole S-1 performed from April 25, 1982 to April 30, 1982. S-1 discharged dry steam.

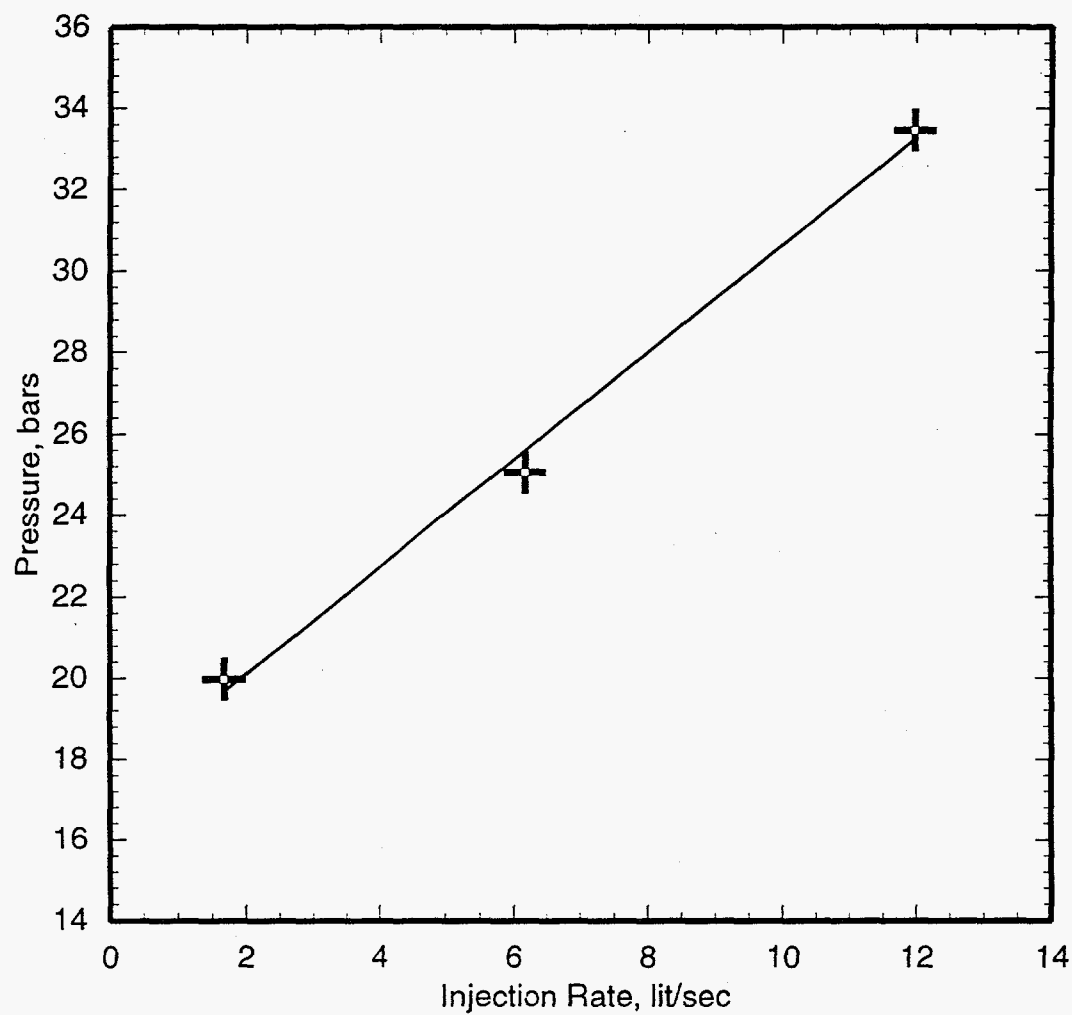


Figure 5.6a. Injectivity test for original slim hole S-2 (drilled depth = 904.6 m) performed on June 23, 1982. The pressure gauge was set at 400 m MD (400 m TVD).

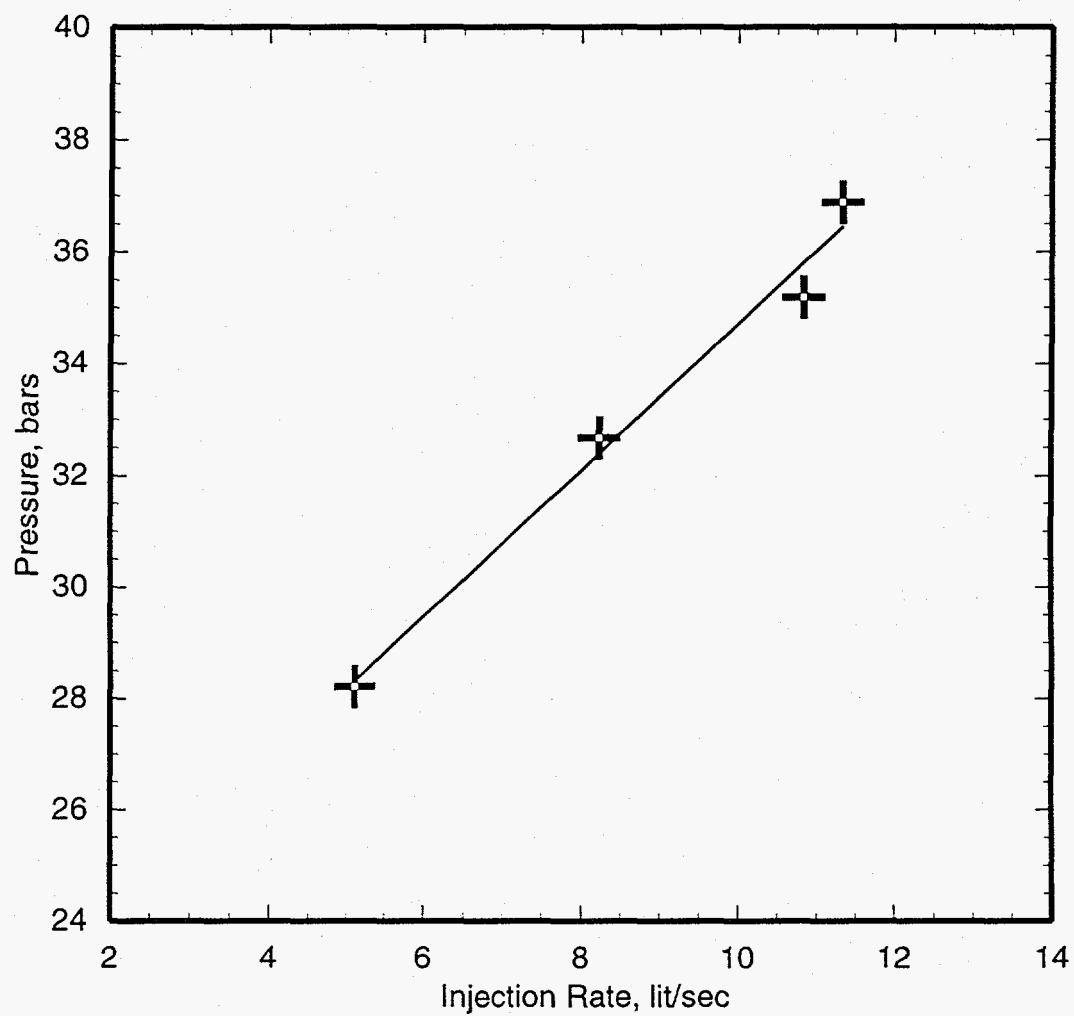


Figure 5.6b. Injectivity test for original slim hole S-2 (drilled depth = 904.6 m) performed on July 16, 1982. The pressure gauge was set at 500 m MD (500 m TVD).

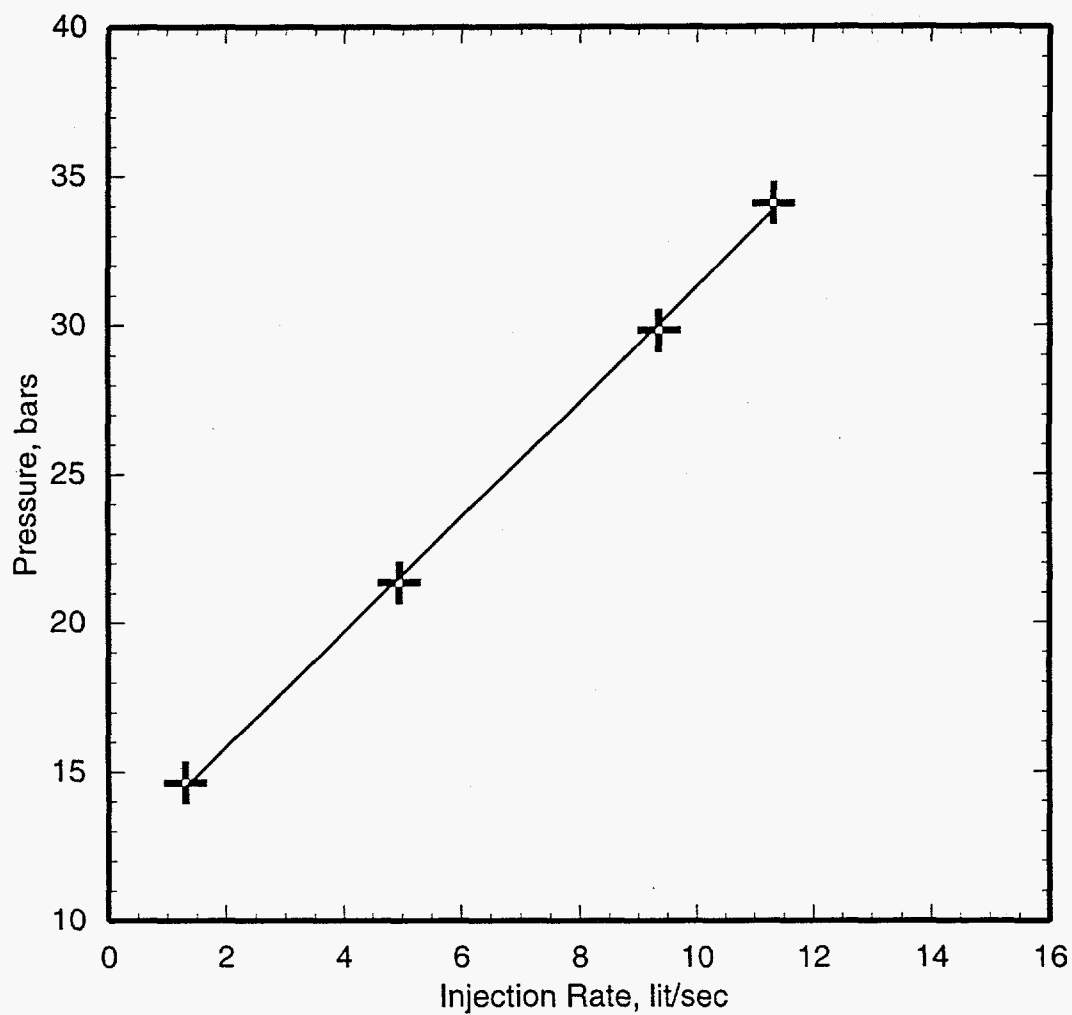


Figure 5.6c. Injectivity test for redrilled slim hole S-2 (drilled depth \approx 906.0 m) performed on October 4, 1982. The pressure gauge was set at 450 m MD (450 m TVD).

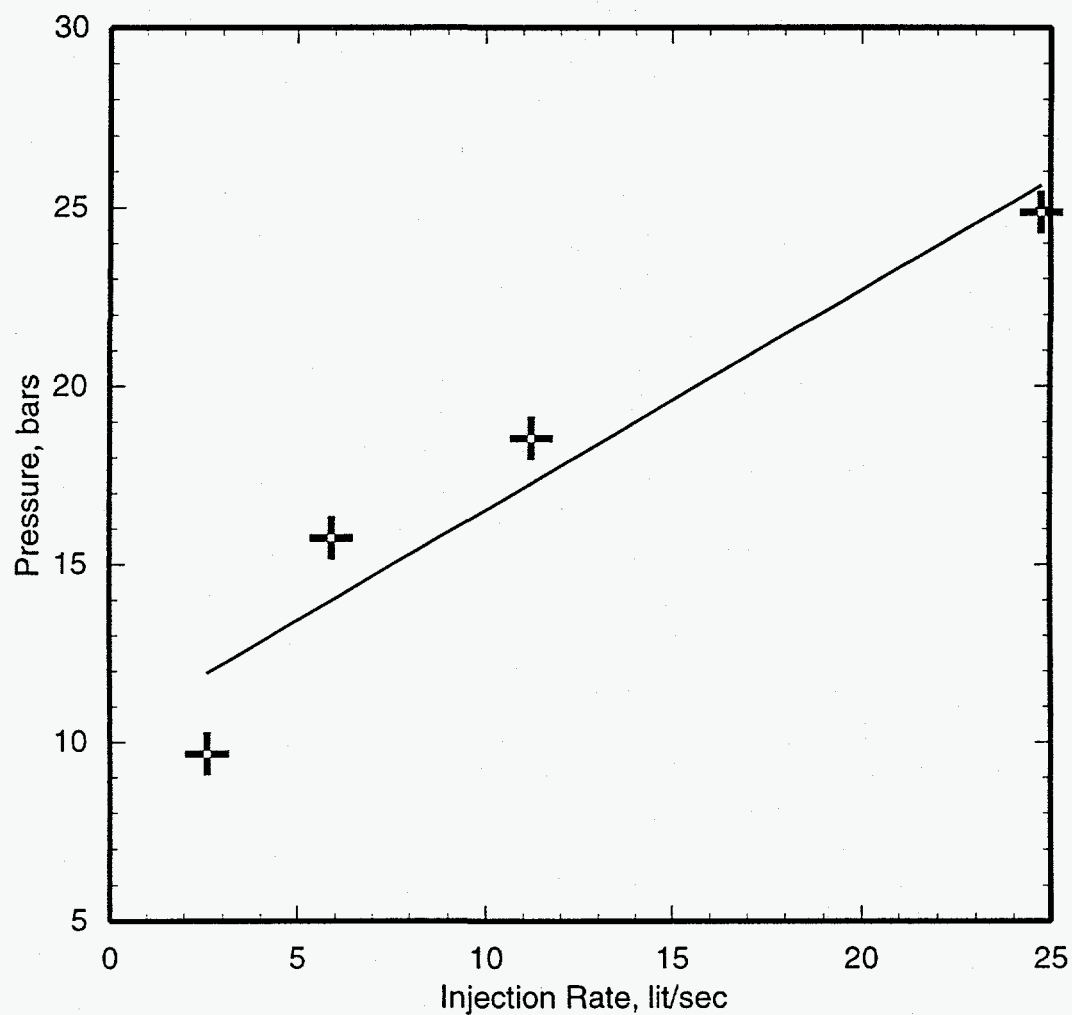


Figure 5.6d. Injectivity test for redrilled slim hole S-2 performed on October 16, 1982. The pressure gauge was set at 500 m MD (500 m TVD).

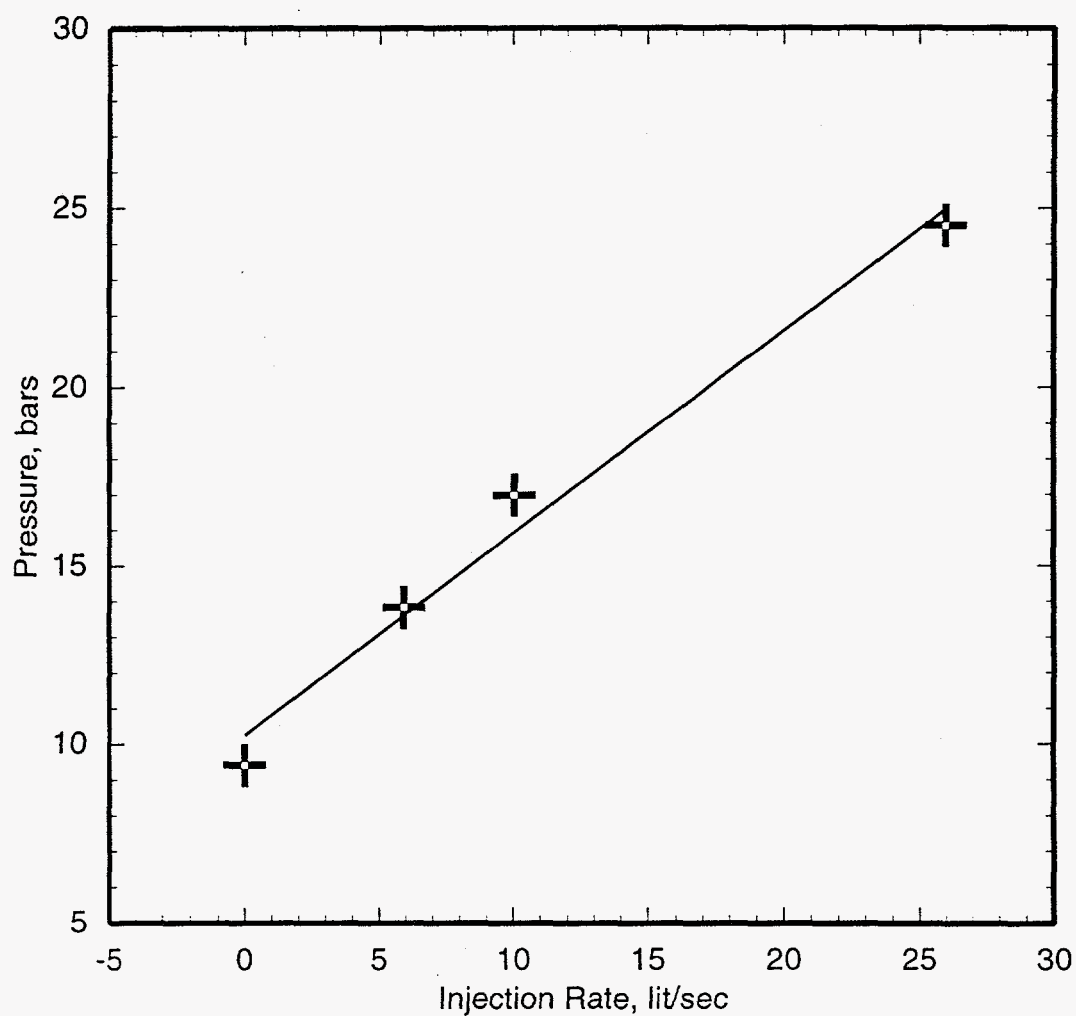


Figure 5.6e. Injectivity test for redrilled slim hole S-2 performed on October 23, 1982. The pressure gauge was set at 500 m MD (500 m TVD).

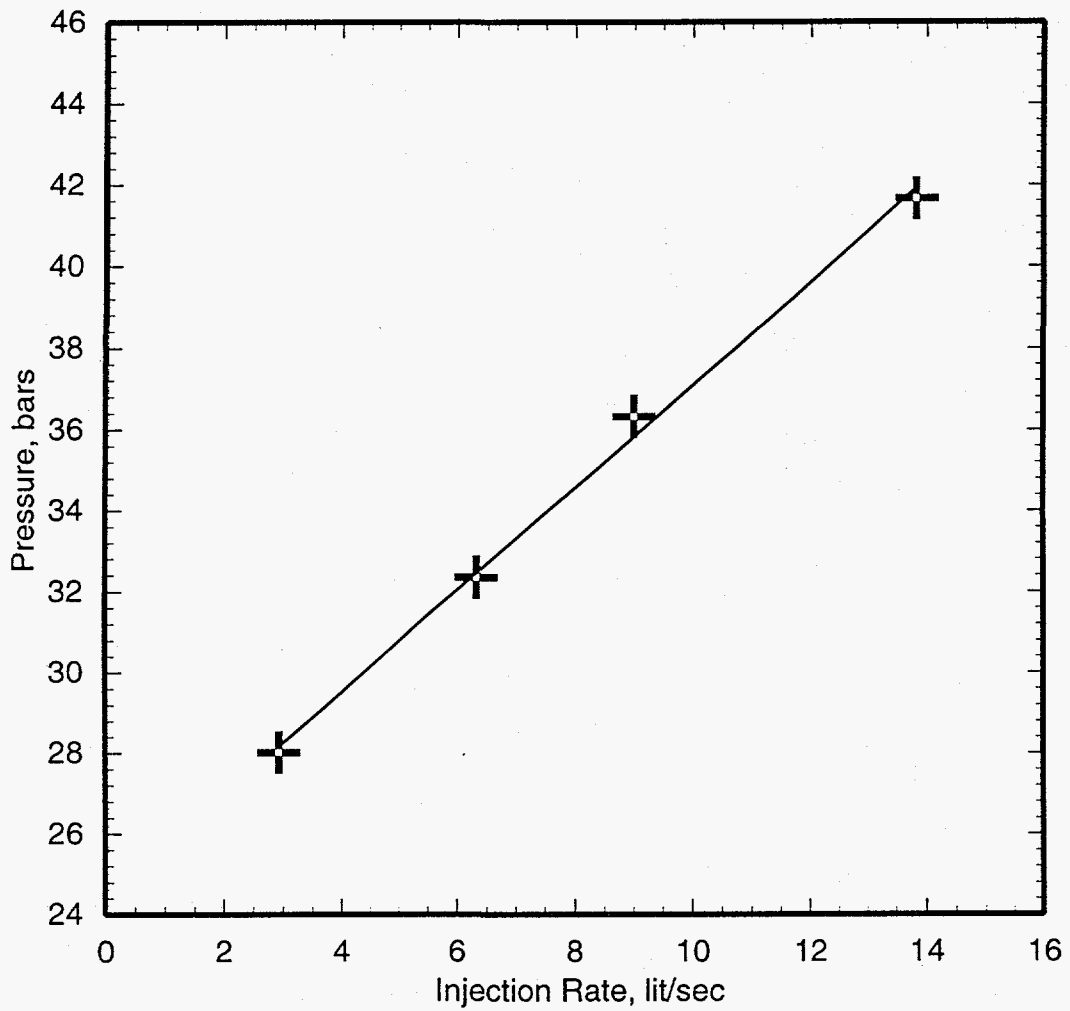


Figure 5.7a. Injectivity test for intermediate depth slim hole S-3 (drilled depth = 603 m?) performed on September 2, 1982. The pressure gauge was set at 400 m MD (400 m TVD).

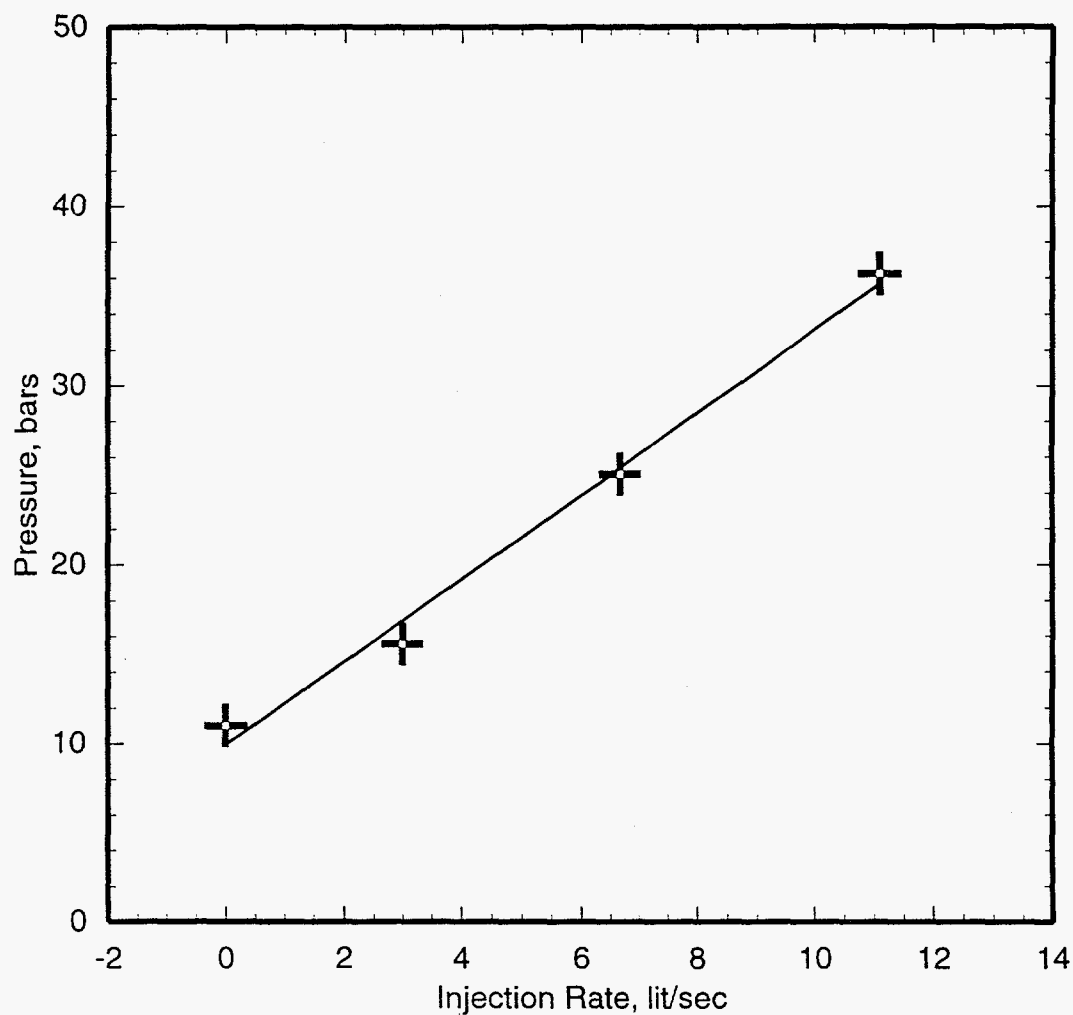


Figure 5.7b. Injectivity test for intermediate depth slim hole S-3 (drilled depth = 603 m?) performed on October 6, 1982. The pressure gauge was set at 300 m MD (300 m TVD).

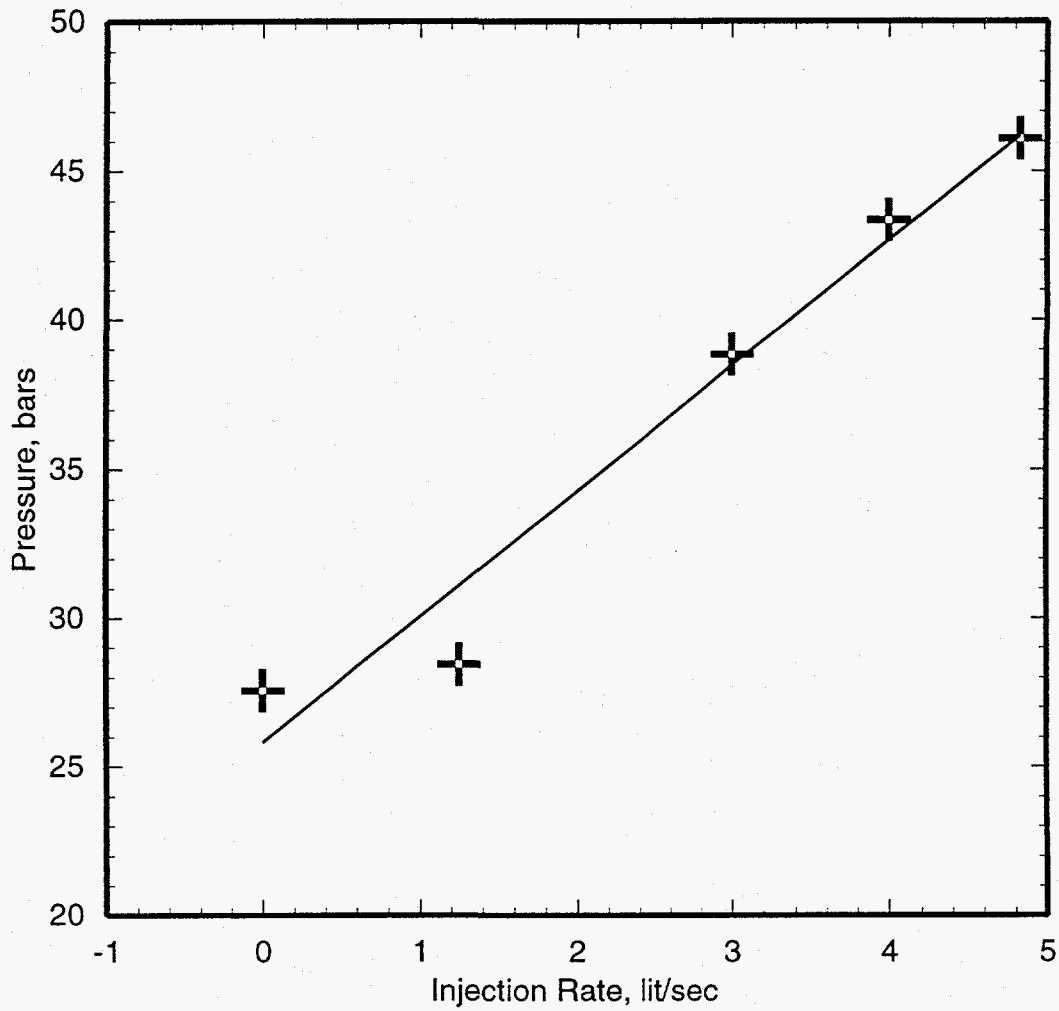


Figure 5.7c. Injectivity test for intermediate depth slim hole S-3 (drilled depth = 656 m?) performed on May 16, 1983. The pressure gauge was set at 600 m MD (600 m TVD).

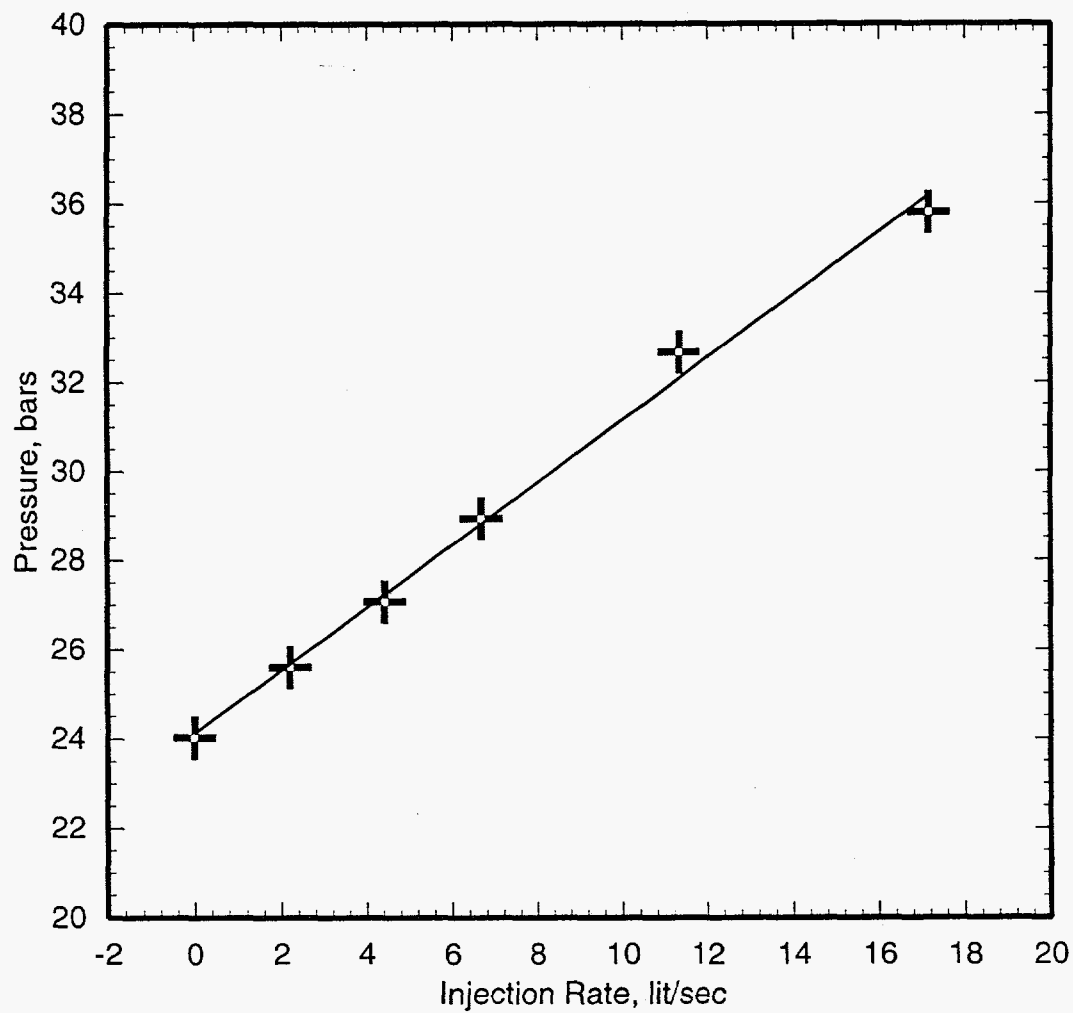


Figure 5.7d. Injectivity test for slim hole S-3 performed on June 12, 1983. The pressure gauge was set at 600 m MD (600 m TVD).

of steam and water flows and wellhead pressure. The period of the cycle is ~10 minutes. Considering the low discharge rate (< 15 tons/hour) and the absence of a two-phase zone in the open part (601 to 805 meters) of the hole, it is likely that the cycling was induced by the wellbore. Apparently, no downhole pressure surveys were carried out in S-3 under discharge conditions; it is, therefore, not possible to compute a productivity index for S-3.

Production Well S-4

Injectivity tests of November 6 and 7, 1983 (Figures 5.8a,b), carried out shortly after well drilling and completion, both gave an injectivity index of 1.4 kg/s-bar. A sharply higher value of injectivity index (4.9 kg/s-bar) is implied by an injectivity test performed on May 19, 1989 (Figure 5.8c) after the injection of cold river water in April and May 1989. Discharge tests carried out prior to and after the May 1989 injection test, however, failed to show any increase in well productivity. As a matter of fact, the maximum discharge rate for S-4 did not exhibit any substantial variation during the years 1984 to 1990.

Well S-4 produces a two-phase mixture from several feedzones in the depth interval from 1071 to 1552 m. The wellhead enthalpies indicate some *in situ* boiling. During discharge tests in October 1984 and December 1985, pressure surveys were run in the cased part of the hole; these pressure surveys imply the upflow of a two-phase mixture above 1070 meters. The principal feedzone for S-4 is at a depth of 1520 meters; the stable feedzone pressure (Section 4.7) is 93.0 bars. The measured pressure gradients in the shallow part of the hole (*i.e.*, above ~1050 meters) were used to estimate the flowing pressures at 1520 meters. The estimates of productivity index for S-4 range from 0.90 to

1.01 kg/s-bar (Table 5.2). *In situ* boiling during discharge is most likely responsible for the productivity index being lower than the injectivity index.

Production Well SA-1

An injectivity test was performed on well SA-1 on October 11–12, 1986 shortly after well drilling and completion; the pressure gauge was set 1057 m TVD (~750 meters above the principal feedzone at 1800 m TVD). The October 1986 injection test (Figure 5.9a) gave an injectivity index of 1.5 kg/s-bar. In April and May 1989 (Figures 5.9b,c), two additional injectivity tests were performed; the pressure gauge in these tests was set at 1726 m TVD (*i.e.*, ~75 meters above the principal feedzone). The injectivity test carried out prior to cold river water injection (Figure 5.9b) gave an injectivity index of 0.90 kg/s-bar. Injection of cold river water resulted in a large increase in the injectivity index; the injectivity index after cold water injection (Figure 5.9c) is seen to be 2.0 kg/s-bar. Apparently, injection of cold river water also resulted in a large increase in well productivity. The maximum discharge rate for SA-1 prior to injection was ~34 tons/hour at a wellhead pressure of ~4.9 bars. After cold water injection, the maximum discharge rate increased to ~62 tons/hour at a wellhead pressure of ~4.2 bars.

Production well SA-1 produces a two-phase mixture (steam is over 80 percent by mass at atmospheric pressure) from a feedzone at ~1800 m TVD. The stable feedzone pressure is 114.0 bars (Section 4.8). During a discharge test in September 1989, two downhole pressure/temperature/spinner surveys were run in SA-1; these surveys show the existence of two-phase conditions in the wellbore above the feedzone. Using the measured

Continued on page 5-28

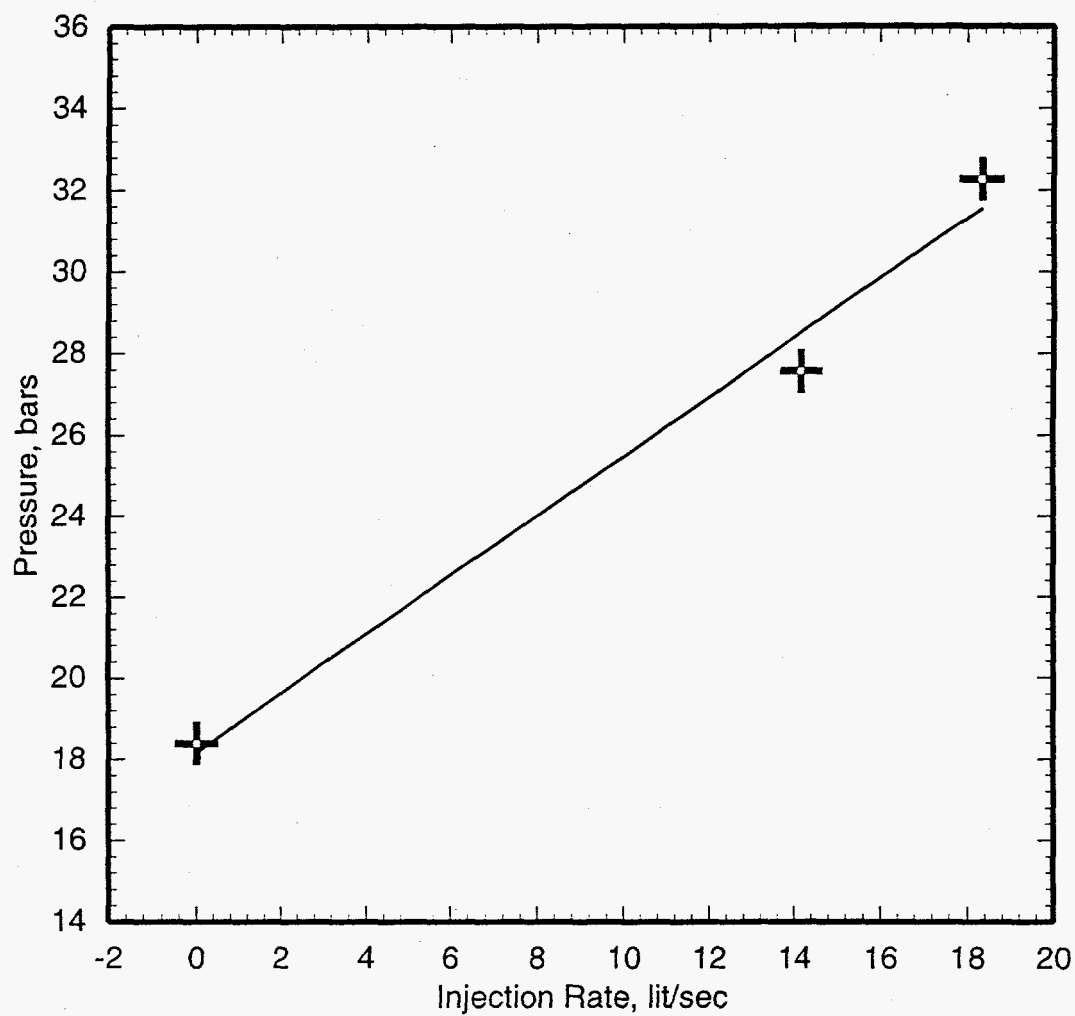


Figure 5.8a. Injectivity test for production well S-4 performed on November 6, 1983. The pressure gauge was set at 700 m MD (700 m TVD).

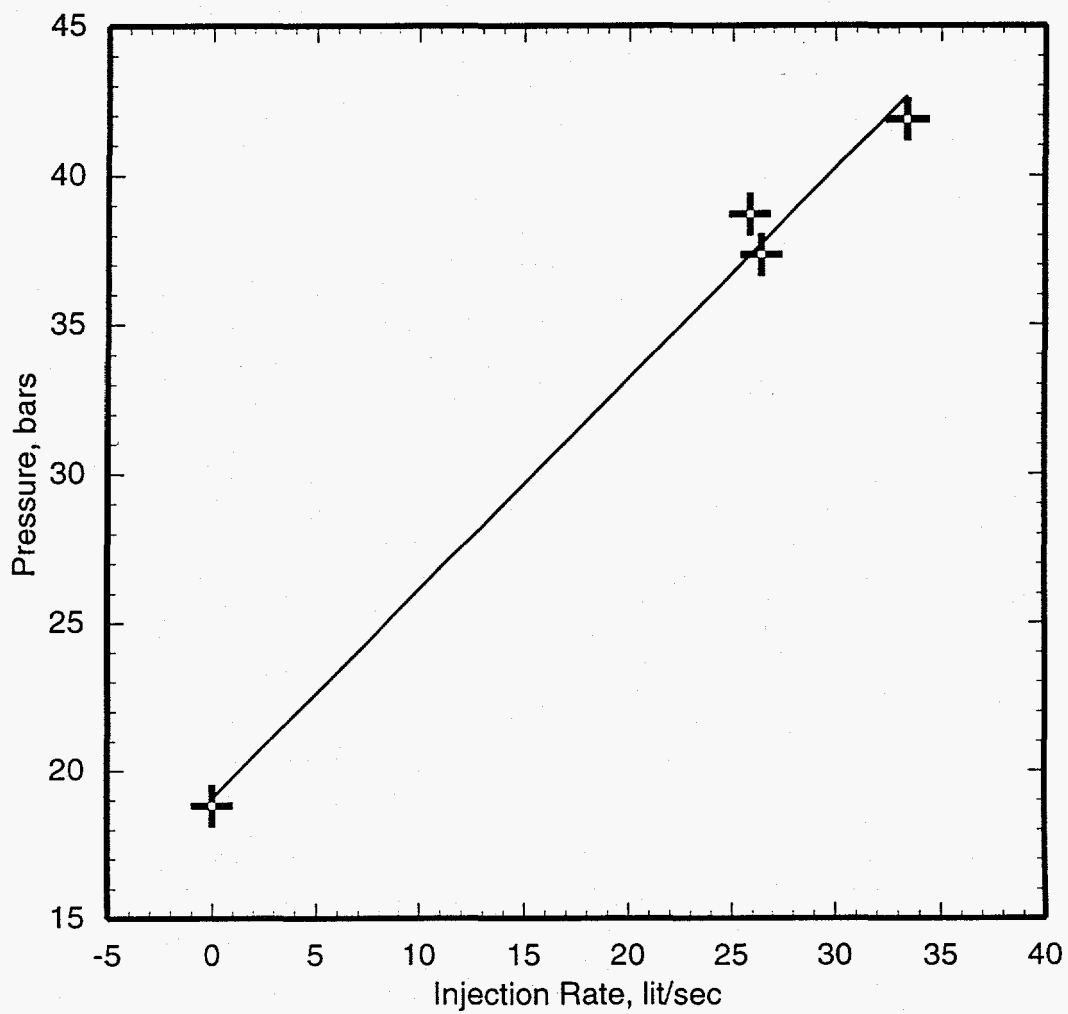


Figure 5.8b. Injectivity test for production well S-4 performed on November 7, 1983. The pressure gauge was set at 700 m MD (700 m TVD).

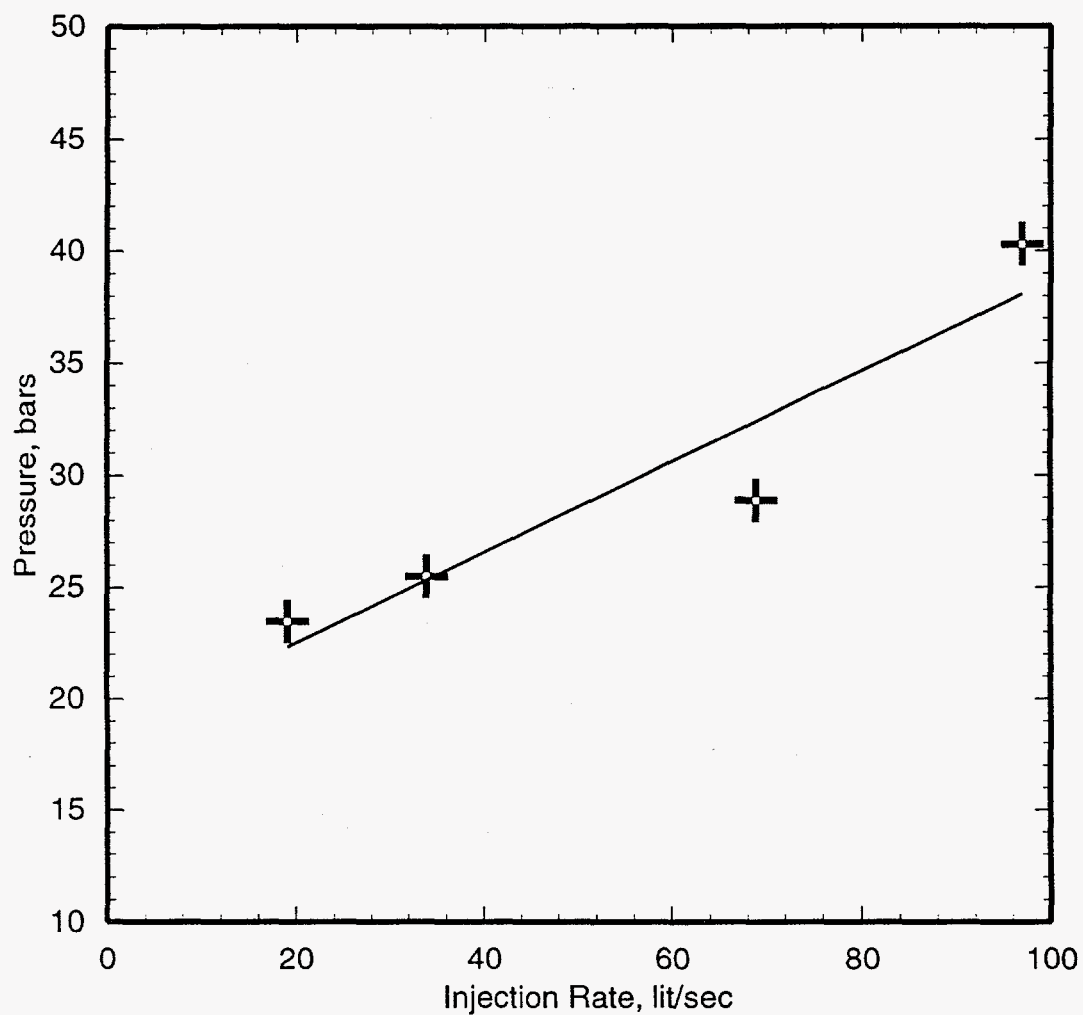


Figure 5.8c. Injectivity test for production well S-4 performed on May 19, 1989 after injection of cold river water. The pressure gauge was set at 700 m MD (700 m TVD).

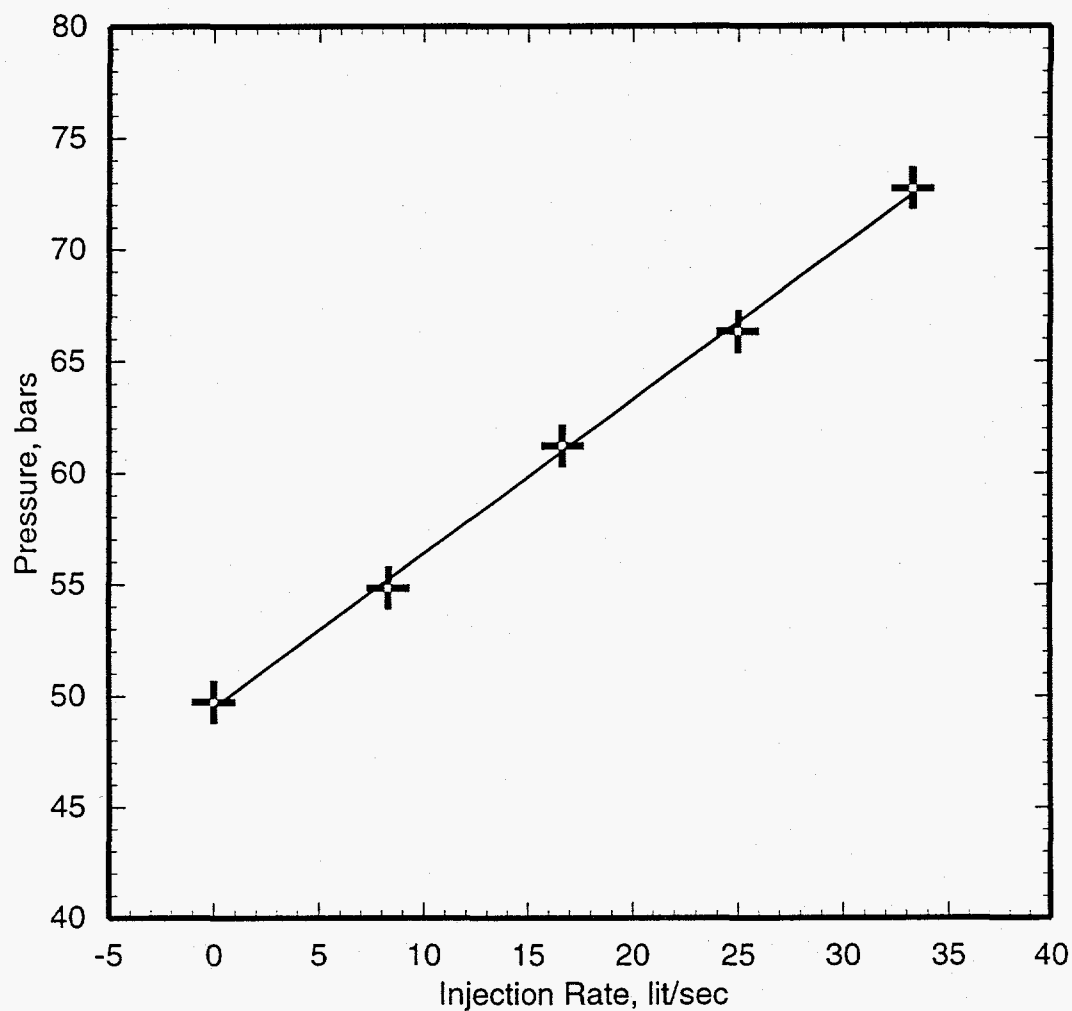


Figure 5.9a. Injectivity test for production well SA-1 performed on October 11–12, 1986. The pressure gauge was set at 1100 m MD (1057 m TVD).

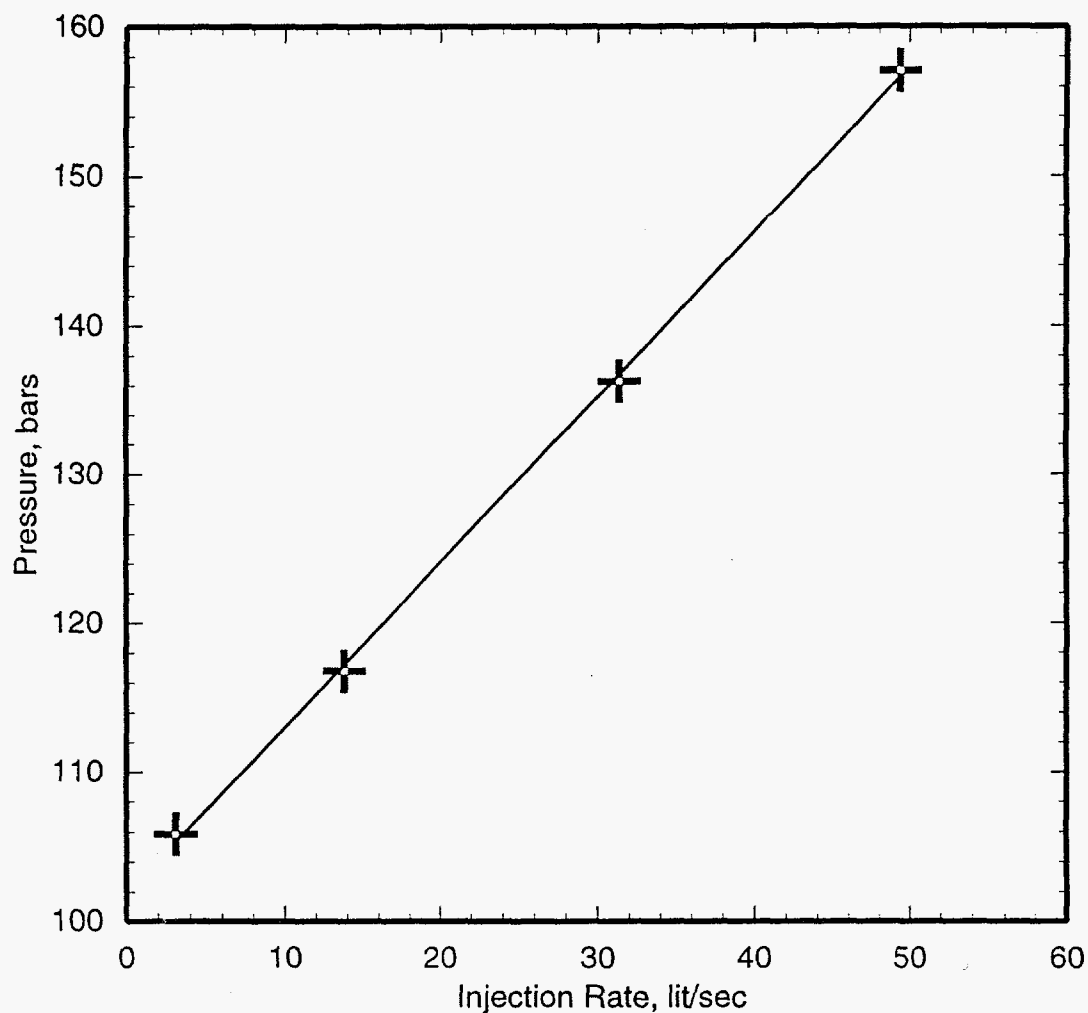


Figure 5.9b. Injectivity test for production well SA-1 performed on April 16, 1989 just prior to injection of cold river water. The pressure gauge was set at 1879 m MD (1726 m TVD).

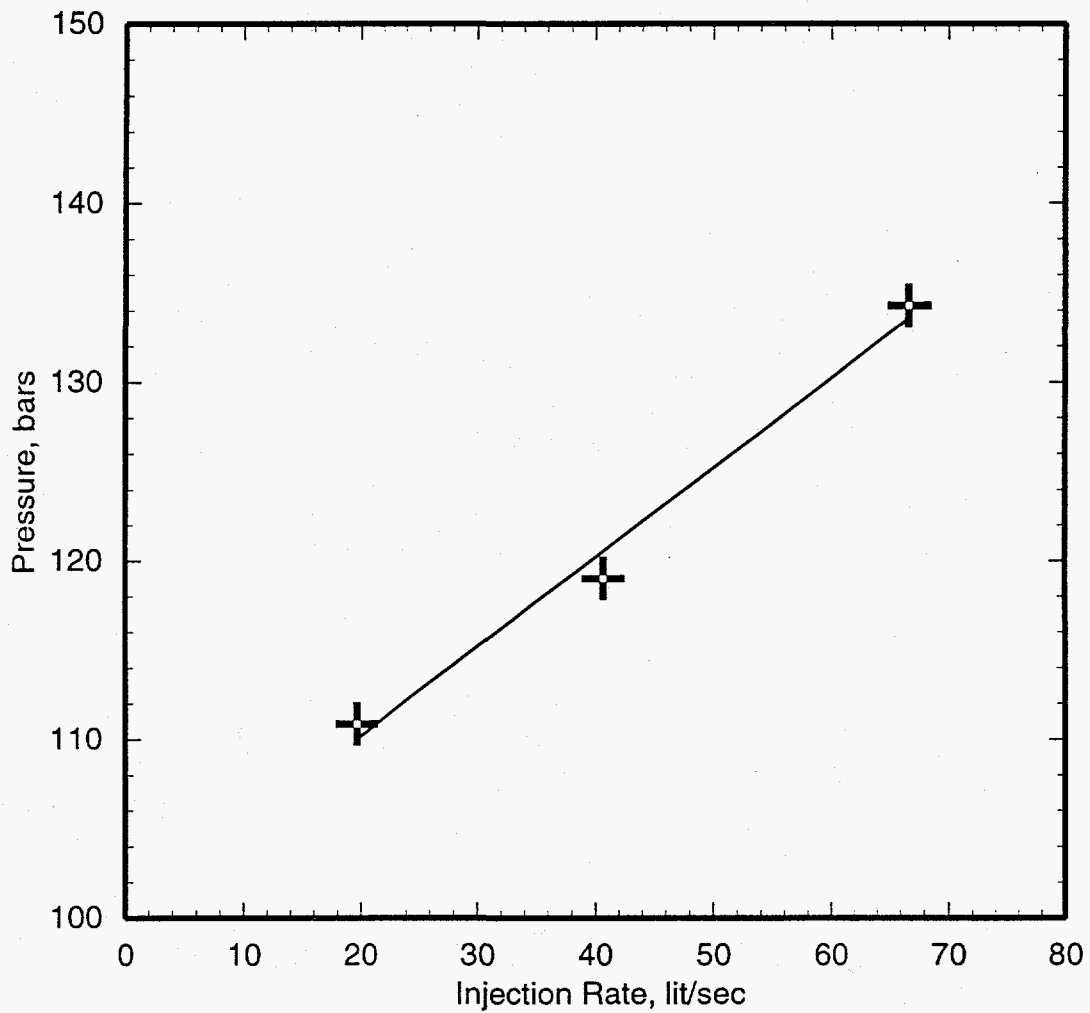


Figure 5.9c. Injectivity test for production well SA-1 performed on May 16, 1989 after injection of cold river water. The pressure gauge was set at 1879 m MD (1726 m TVD).

values for flowing feedzone pressure, the productivity index for SA-1 is estimated to be 0.16–0.17 kg/s-bar (Table 5.2). The large discrepancy between the productivity and injectivity indices is due to *in situ* boiling during discharge tests.

Production Well SA-2

The two injectivity tests performed on September 22 and 23, 1987 just after well completion (Figure 5.10a,b) gave injectivity indices of 1.0 and 1.2 kg/s-bar. These injectivity indices are in substantial agreement with that (1.3 kg/s-bar) obtained from a test carried out on April 16, 1989 prior to the injection of cold river water (Figure 5.10c). The injectivity did not improve much with the injection of cold river water in April and May 1989; the injectivity index after cold water injection was 1.7 kg/s-bar (Figure 5.10d). Like the injectivity index, production from SA-2 showed little or no increase as a result of injection.

Production well SA-2 produces essentially all steam from a feedzone at 1450 m TVD. No down-hole pressure surveys were run in the discharging well; consequently, it is not possible to calculate the productivity index for SA-2.

Production Well SA-4

The injection test performed on May 30, 1988 shortly after well completion (Figure 5.11a) gave a relatively low value (0.31 kg/s-bar) for the injectivity index. The injectivity tests carried out on April 17, 1989 (prior to cold river water injection) and May 18, 1989 (after cold river water injection) imply substantially higher values for the injectivity index (0.88 kg/s-bar and 1.0 kg/s-bar, respectively). Apparently, injection of cold river water in April and May 1989 (Figure 5.11b,c) resulted in a modest improvement in well productivity. The

maximum discharge rate increased from ~24 tons/hour (prior to injection) to ~30 tons/hour (after injection).

Production well SA-4 produces dry steam from a feedzone at about 1240 m TVD. The stable shutin pressure at 1240 m TVD is 81.0 bars (Section 4.10). A pressure/temperature/spinner survey run in the discharging well on September 23, 1989 gave a pressure of 8.06 bars. With a mass discharge rate of 10.8 kg/s, the productivity index is estimated to be 0.11 kg/s. The productivity index is an order of magnitude smaller than the injectivity index.

Production Well SB-1

Five injection tests of production well SB-1 (Figures 5.12a–e) were conducted in the period from October 25, 1987 to August 15, 1988. The best estimate for the injectivity index prior to April/May 1989 cold river water injection is provided by the test run on August 15, 1988. In the latter test, the pressure gauge was set 65 meters below the main feedzone at 1600 m TVD; in all other tests (Figure 5.12a–d) the pressure gauge was set hundreds of meters above the feedzone.

Injection of cold water in April and May 1989 appears to have improved the well injectivity. The injectivity index increased from 0.44 kg/s-bar on August 15, 1988 (prior to river water injection) to 2.0 kg/s-bar on May 28, 1989 (after river water injection, Figure 5.12f). Since no discharge tests of SB-1 were performed prior to cold river water injection in April/May 1989, it is not possible to ascertain the effect of cold water injection on well productivity.

A discharge test of well SB-1 was conducted from June 4, 1989 to November 26, 1989. Well

Continued on page 5-42

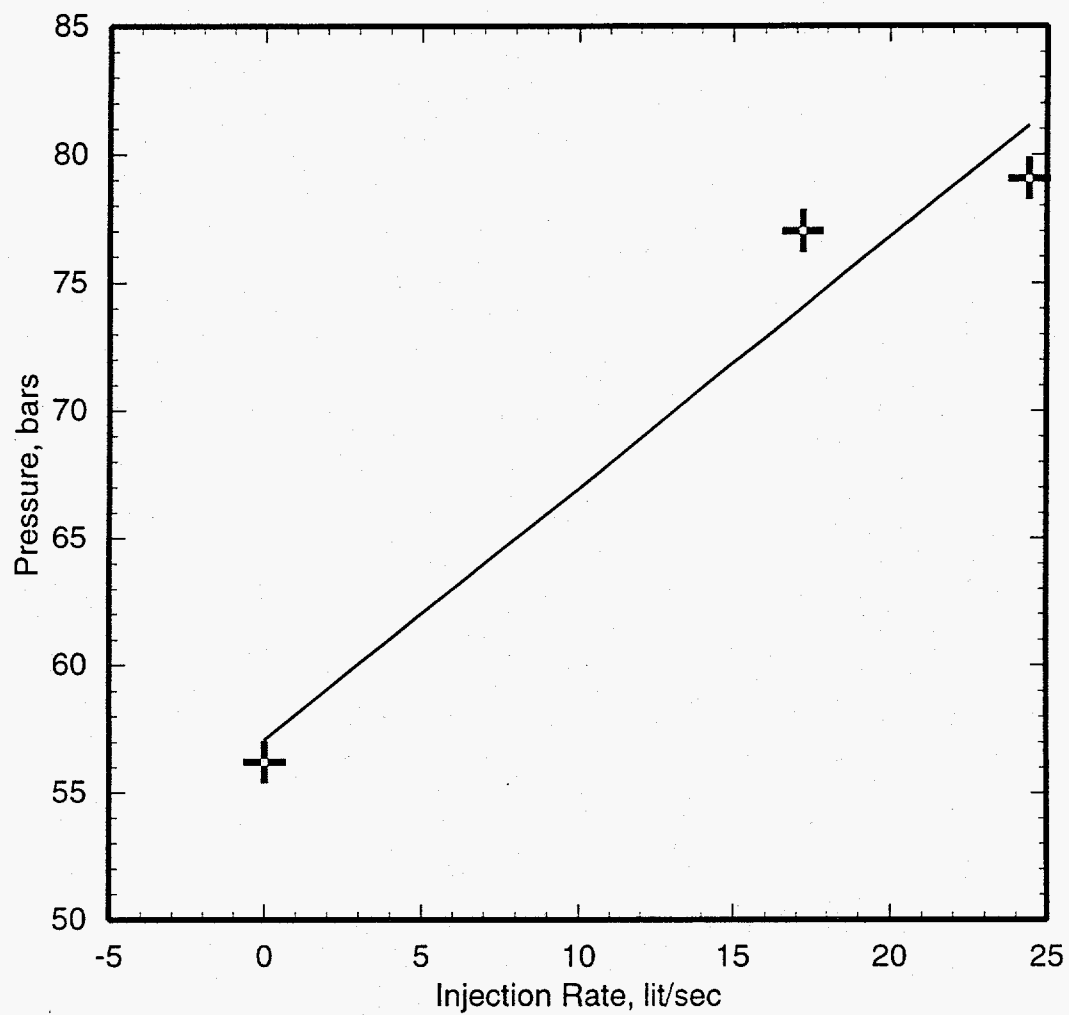


Figure 5.10a. Injectivity test for production well SA-2 performed on September 22, 1987. The pressure gauge was set at 1000 m MD (968 m TVD).

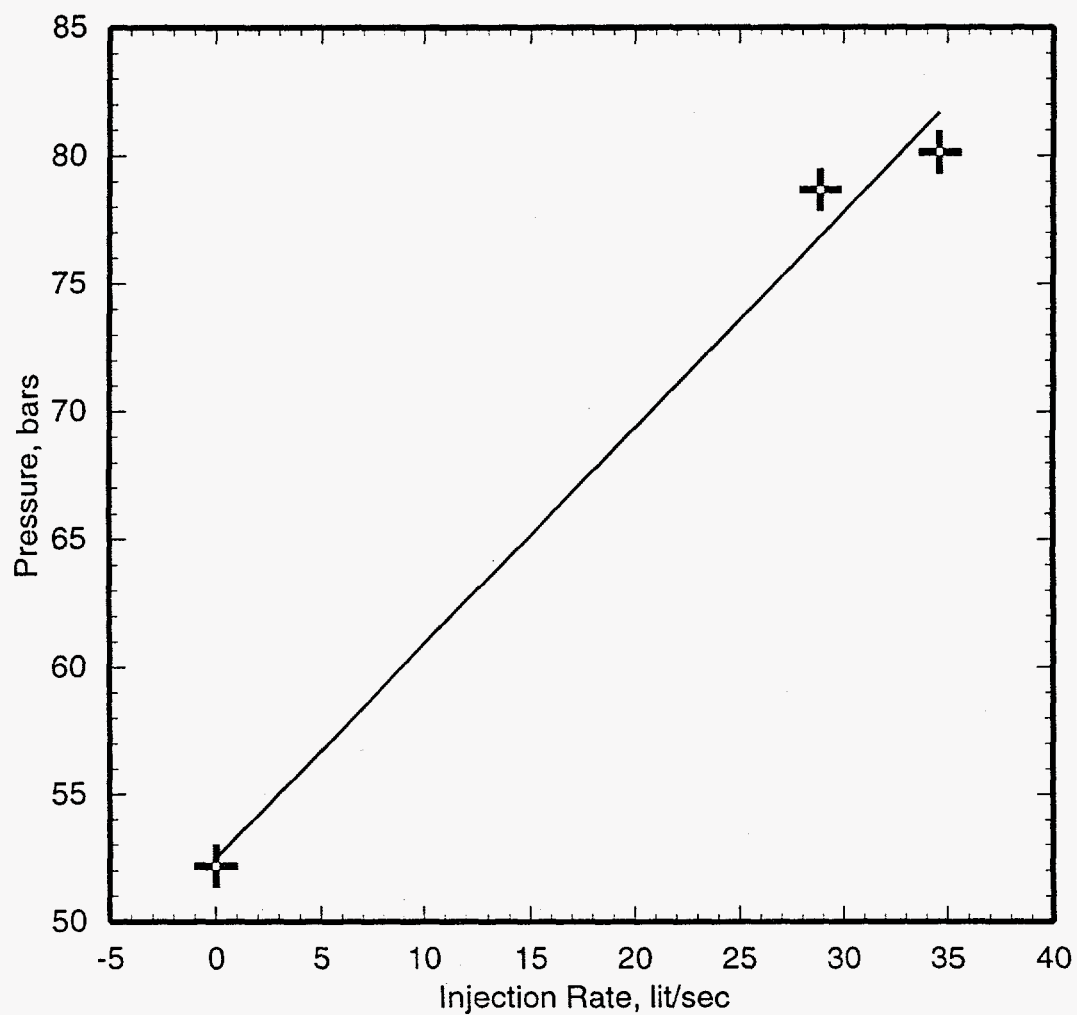


Figure 5.10b. Injectivity test for production well SA-2 performed on September 22–23, 1987. The pressure gauge was set at 1000 m MD (968 m TVD).

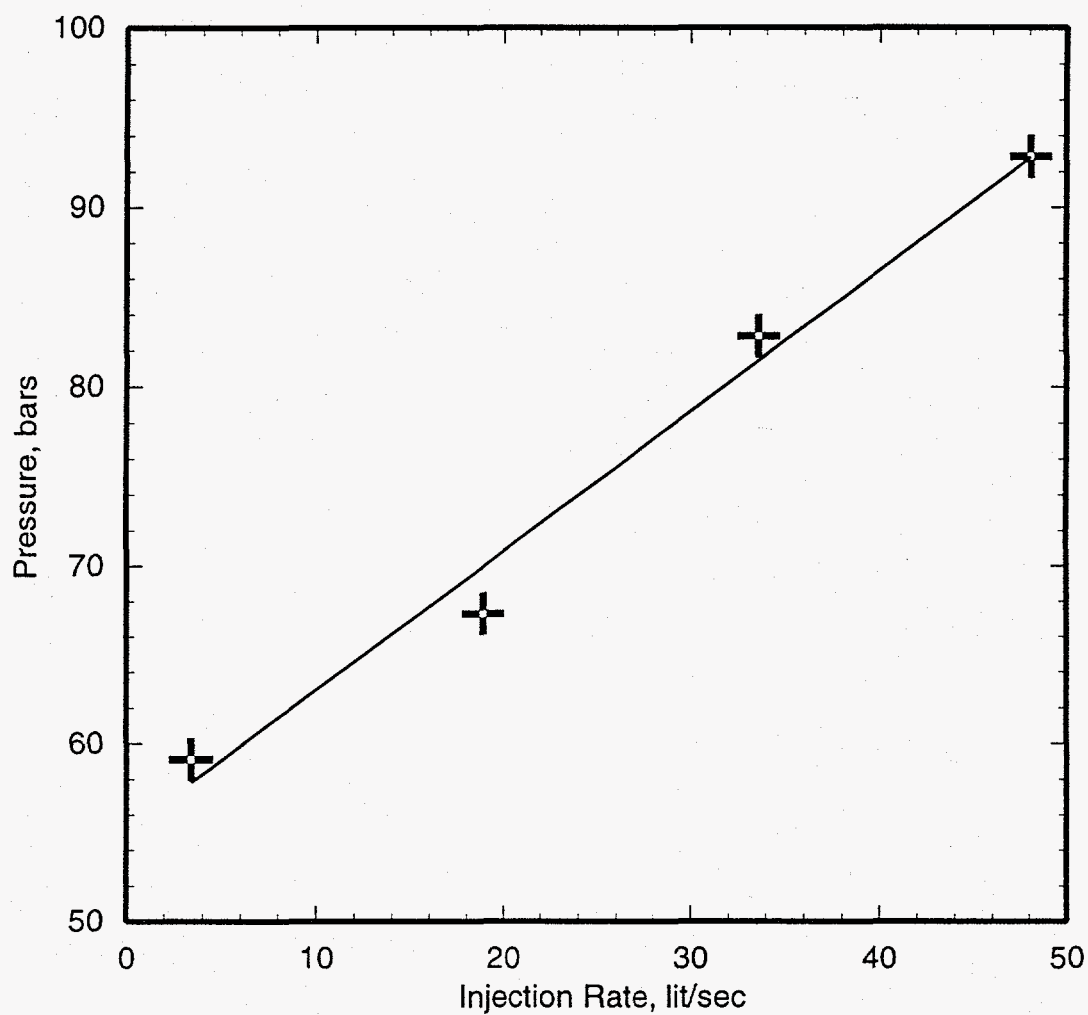


Figure 5.10c. Injectivity test for production well SA-2 performed on April 16–17, 1989 prior to injection of cold river water. The pressure gauge was set at 1100 m MD (1062 m TVD).

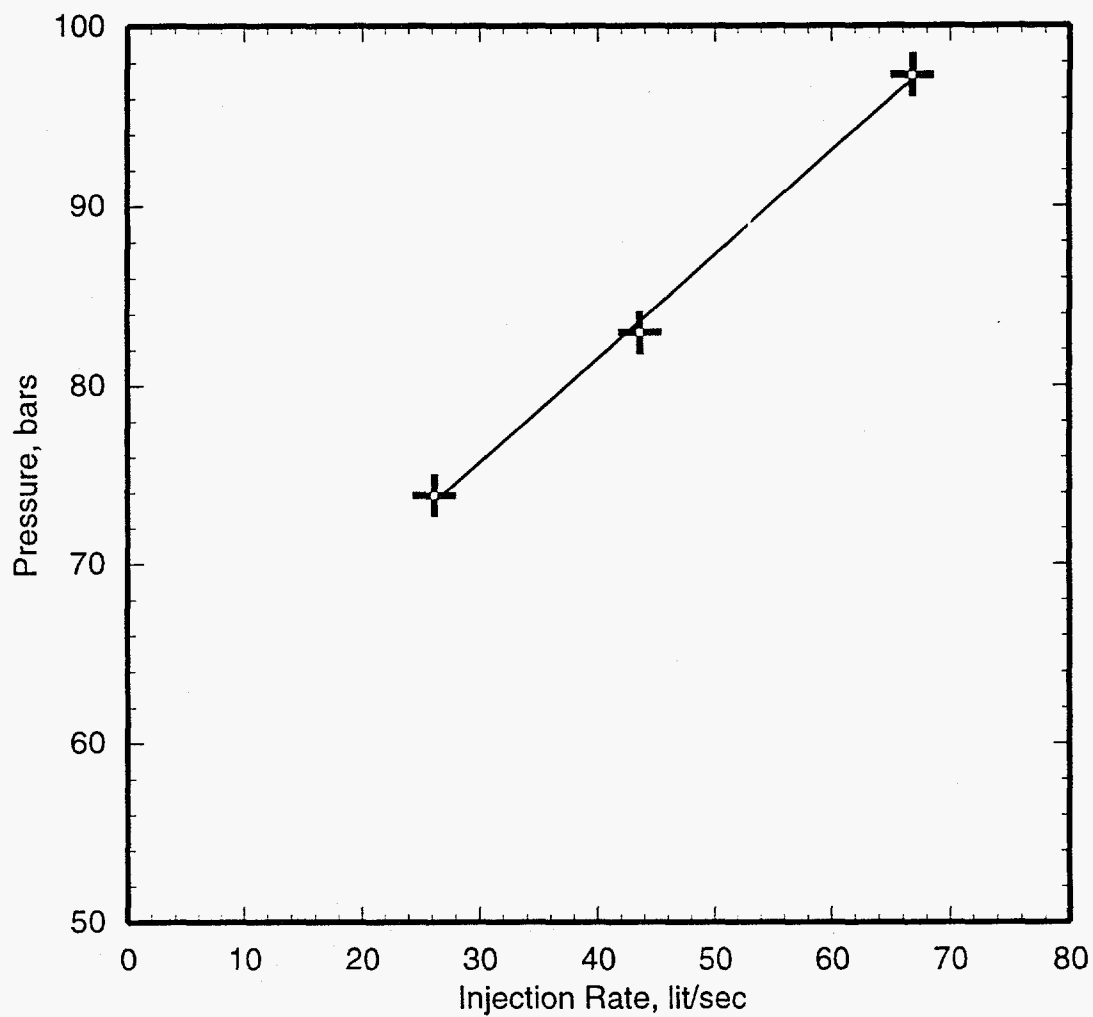


Figure 5.10d. Injectivity test for production well SA-2 performed on May 17, 1989 after the injection of cold river water. The pressure gauge was set at 1099 m MD (1061 m TVD).

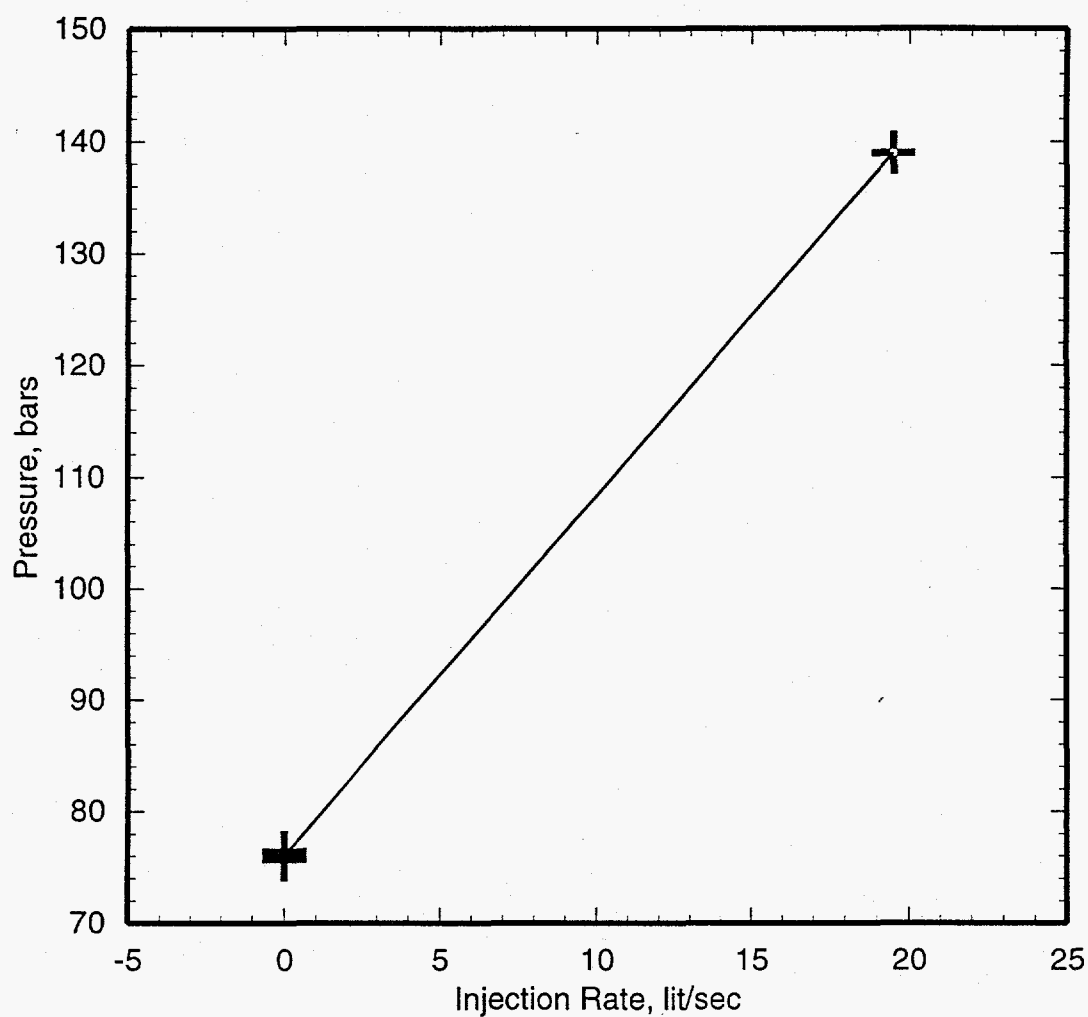


Figure 5.11a. Injectivity test for production well SA-4 performed on May 30, 1988. The pressure gauge was set at 1200 m MD (1127 m TVD).

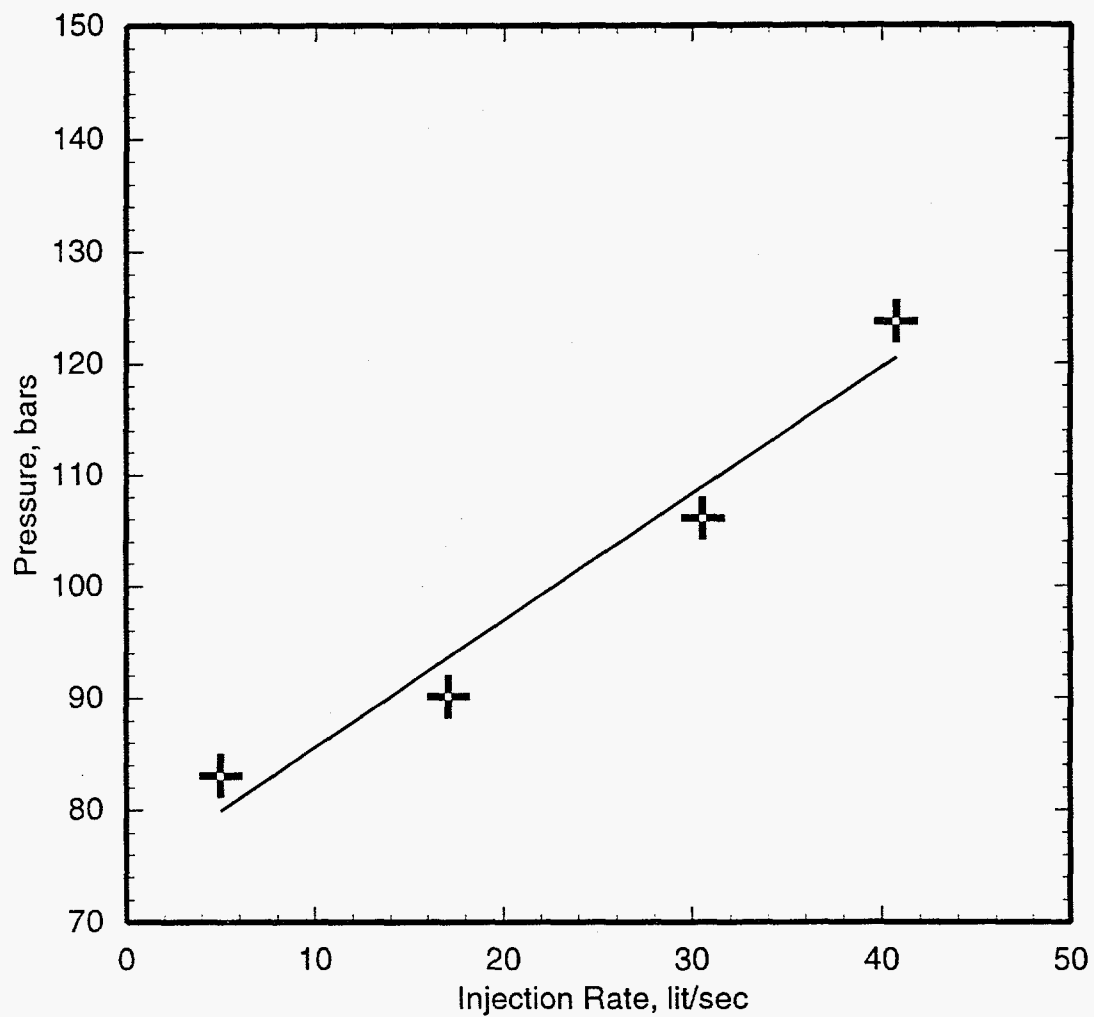


Figure 5.11b. Injectivity test for production well SA-4 performed on April 17–18, 1989 prior to cold river water injection. The pressure gauge was set at 1366 m MD (1262 m TVD).

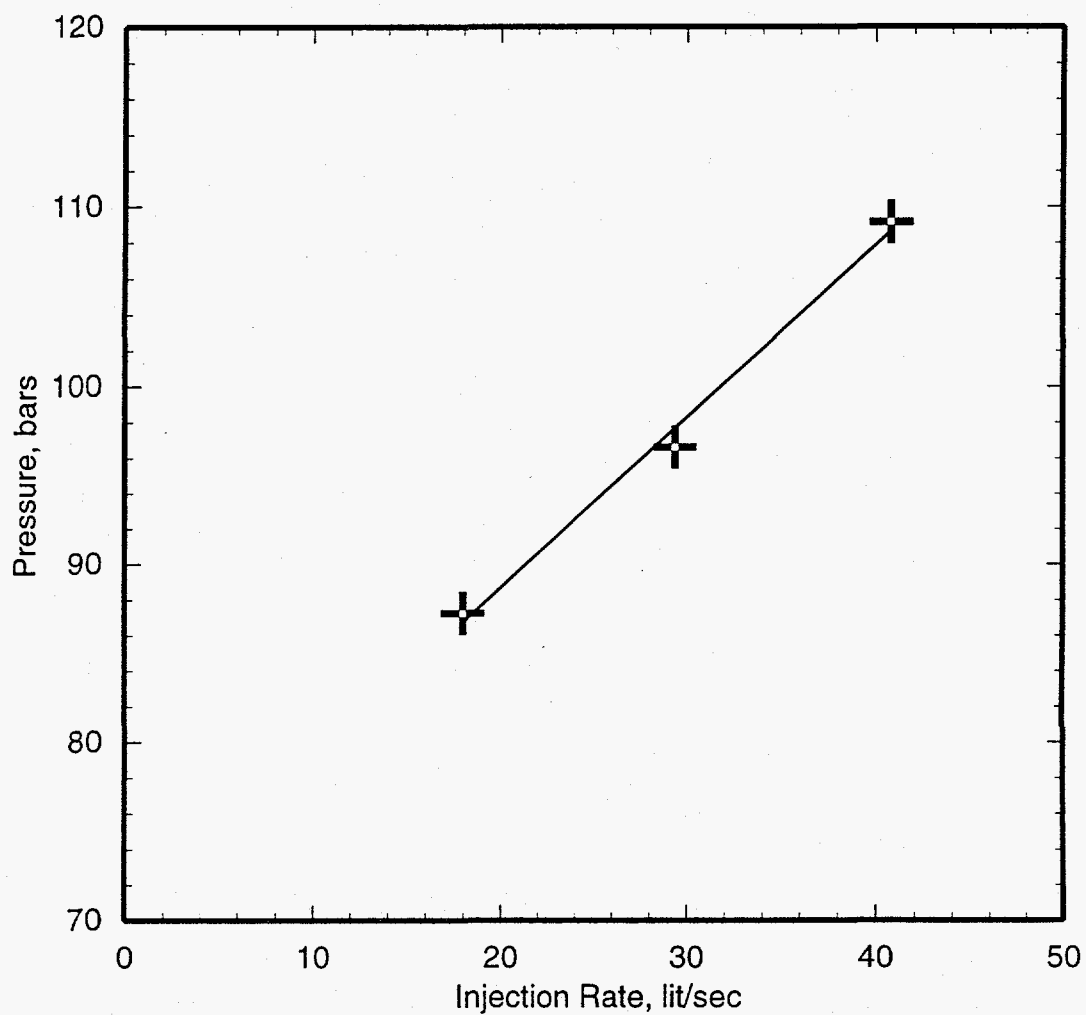


Figure 5.11c. Injectivity test for production well SA-4 performed on May 18, 1989 after cold river water injection. The pressure gauge was set at 1366 m MD (1262 m TVD).

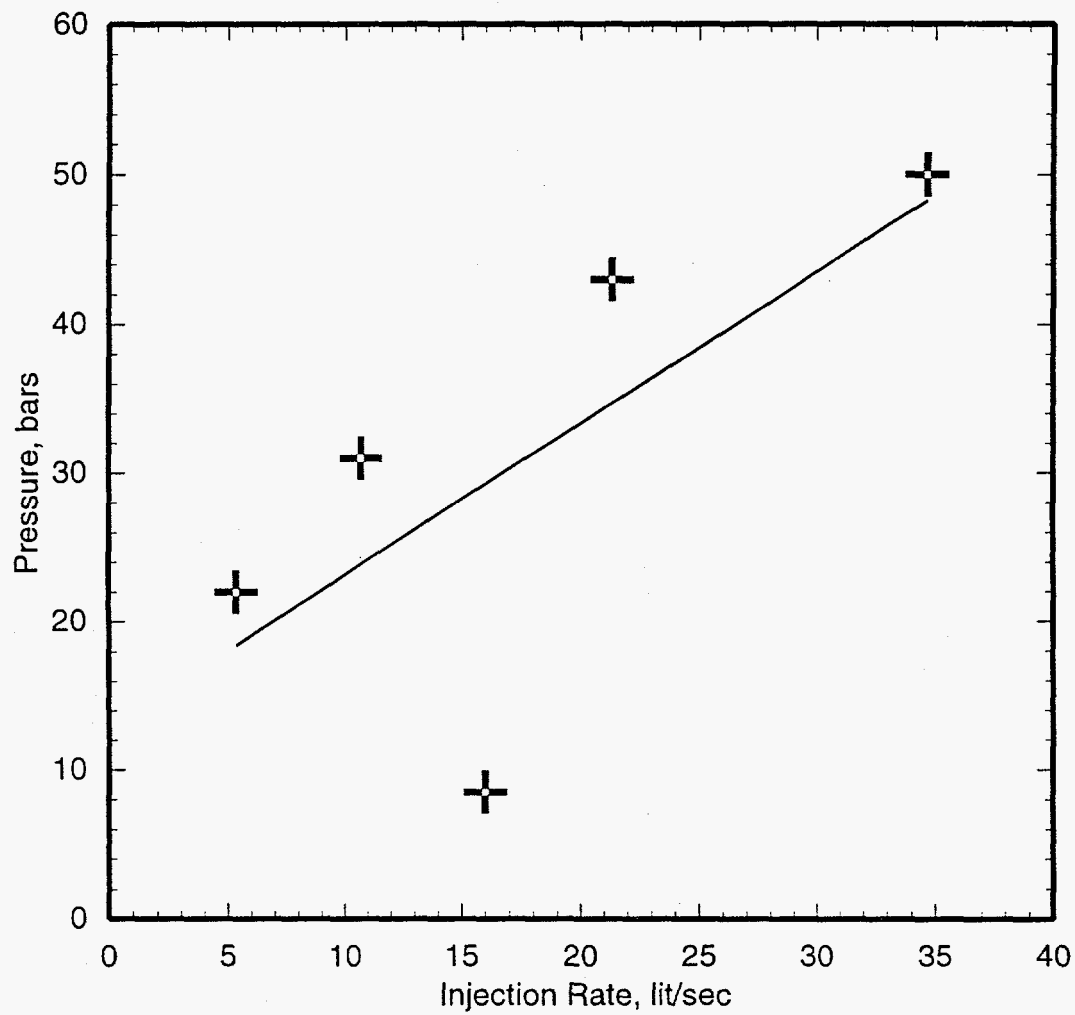


Figure 5.12a. Injectivity test for production well SB-1 performed on October 25, 1987. The pressure gauge was set at wellhead.

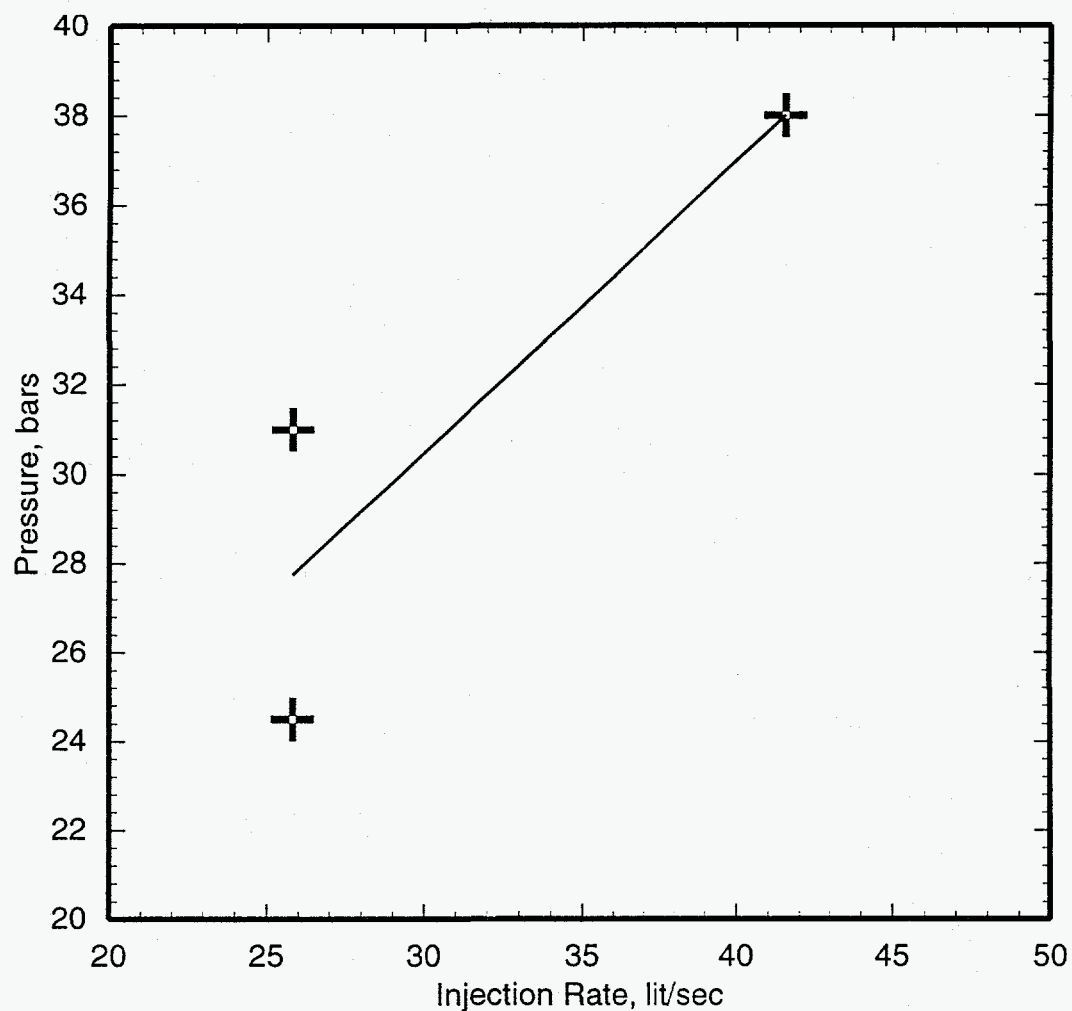


Figure 5.12b. Injectivity test for production well SB-1 performed on October 26, 1987. The pressure gauge was set at wellhead.

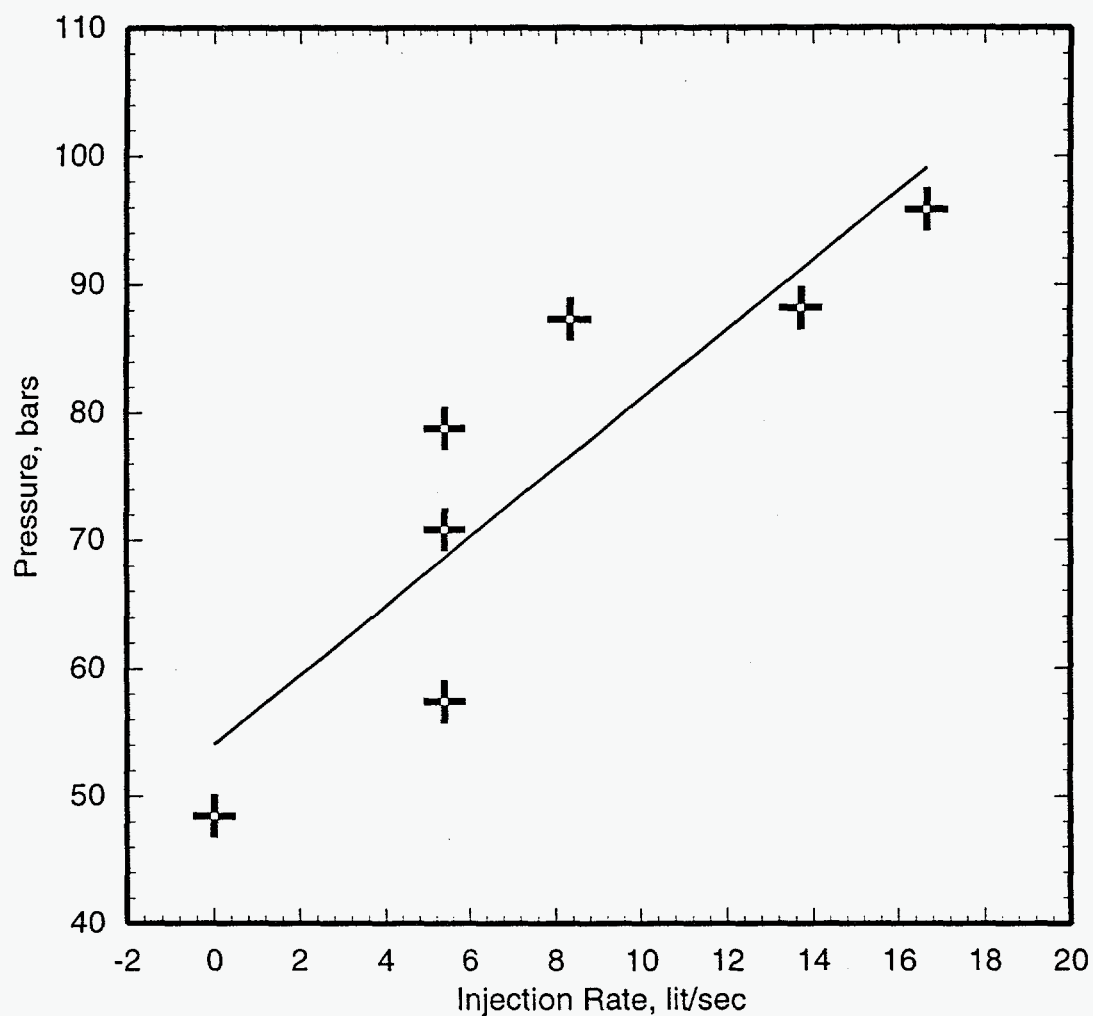


Figure 5.12c. Injectivity test for production well SB-1 performed on November 8, 1987. The pressure gauge was set at 1000 m MD (965 m TVD).

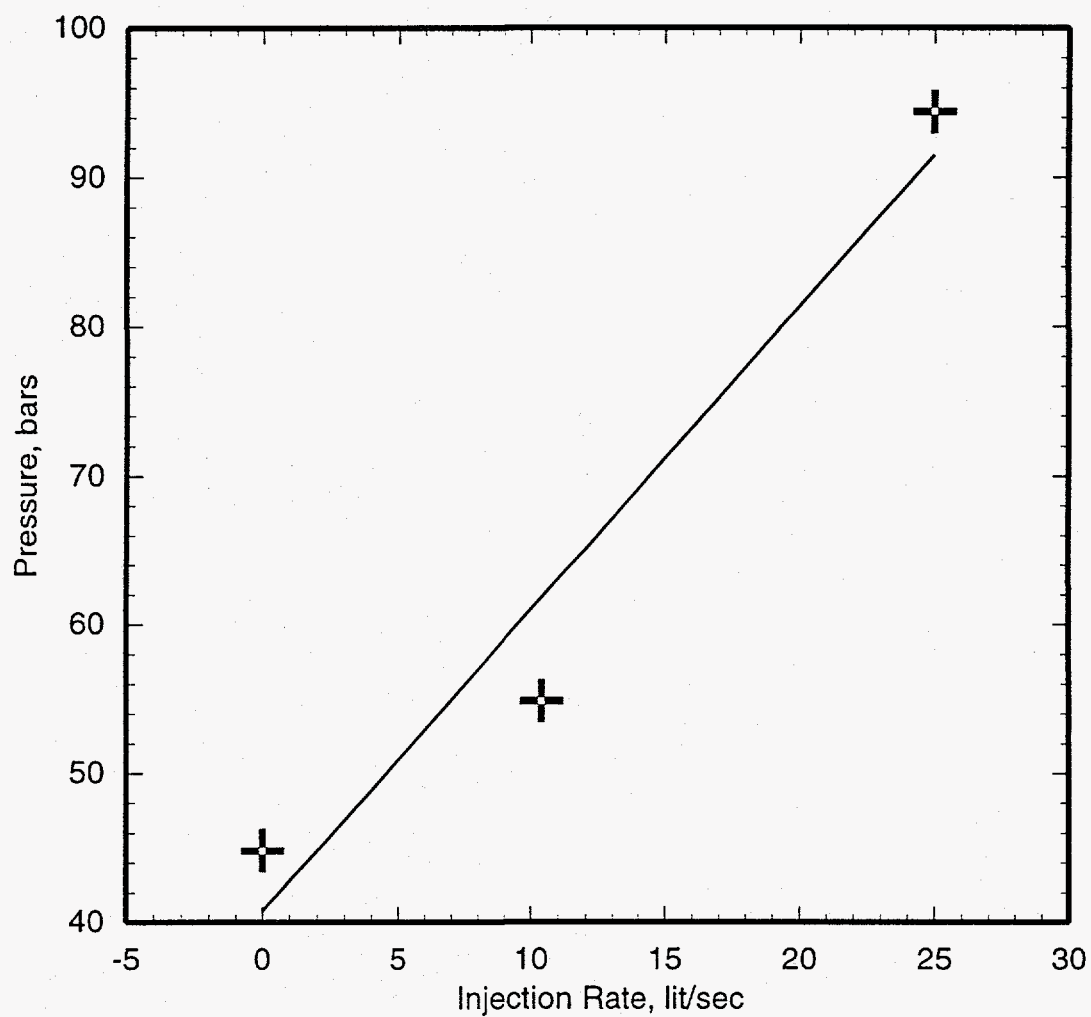


Figure 5.12d. Injectivity test for production well SB-1 performed on May 27, 1988. The pressure gauge was set at 1000 m MD (965 m TVD).

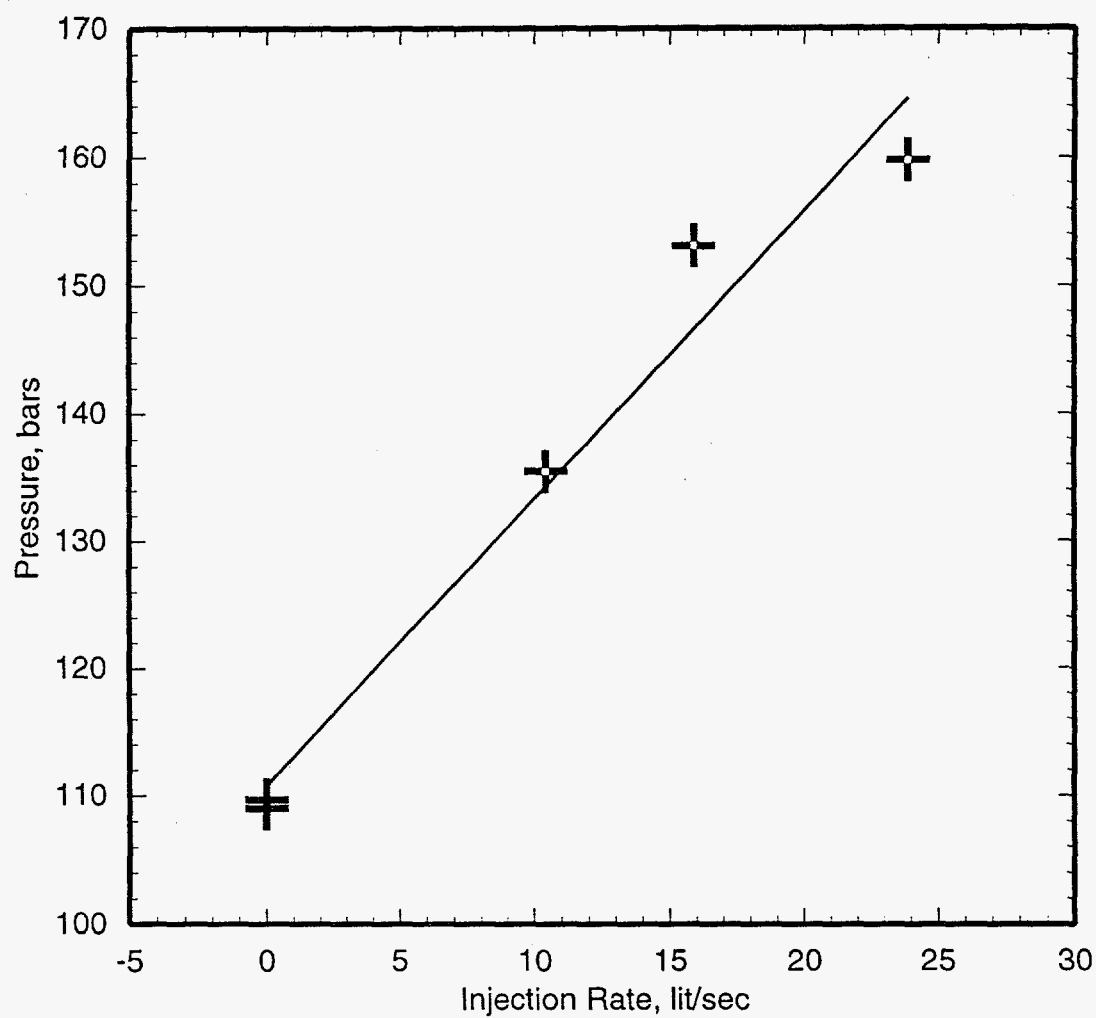


Figure 5.12e. Injectivity test for production well SB-1 performed on August 15, 1988. The pressure gauge was set at 1740 m MD (1665 m TVD).

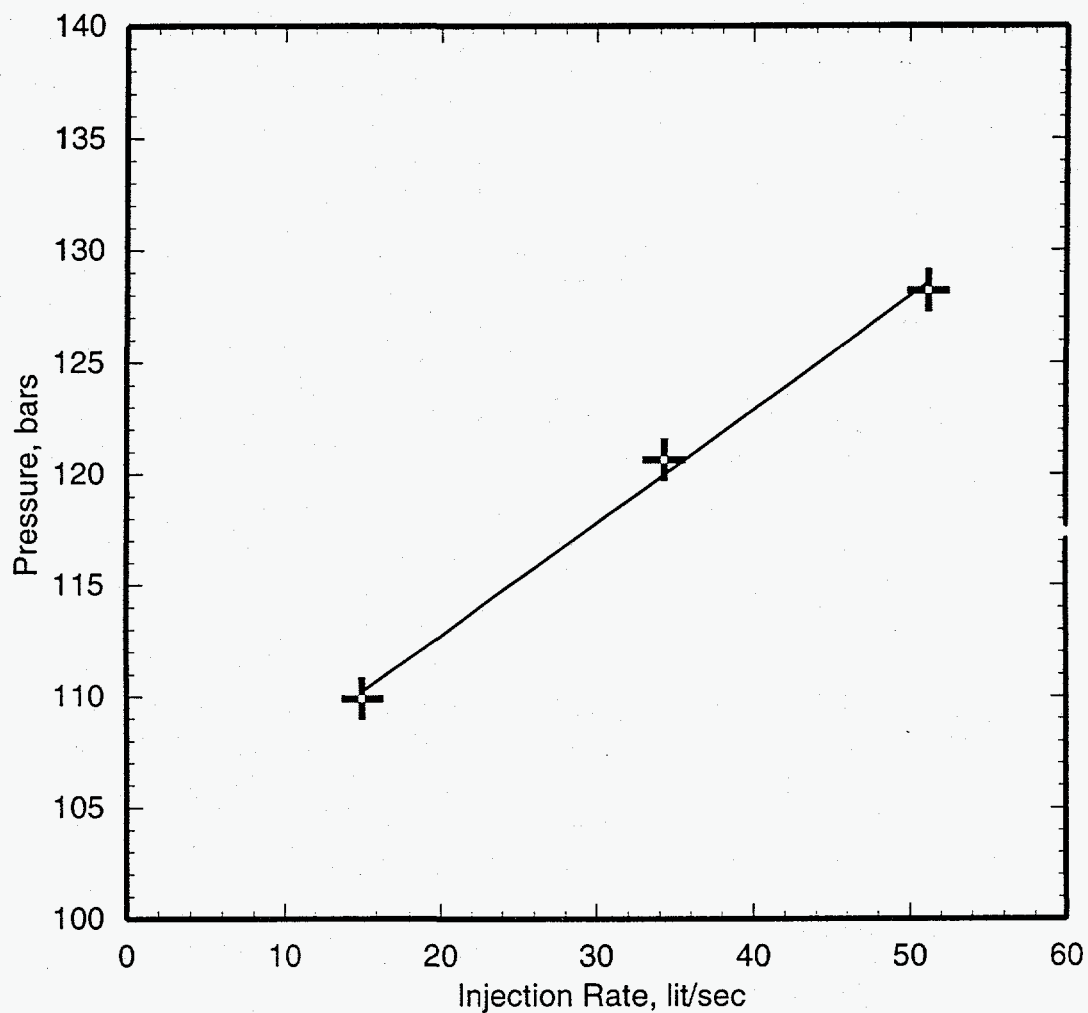


Figure 5.12f. Injectivity test for production well SB-1 performed on May 28–29, 1987. The pressure gauge was set at 1700 m MD (1626 m TVD).

SB-1 produces liquid water from a feedzone at 1600 m TVD; the feedzone temperature is ~280°C. No downhole pressure surveys were made in the discharging well. It is, therefore, not possible to compute a value for the productivity index.

Injection Well SB-2

An injectivity test of well SB-2 was performed on June 22, 1988 shortly after well drilling and completion (Figure 5.13a). After cold river water injection in April/May 1989, a second injectivity test was performed on May 29–30, 1989 (Figure 5.13b). The two injection tests yield essentially the same value (1.8 and 1.6 kg/s-bar) for the injectivity index.

Injection Well SB-3

An injection test of well SB-3 was performed on August 5, 1988 shortly after well drilling and completion; an injectivity index of 0.41 kg/s-bar is inferred for this test (Figure 5.14a). Apparently, the injection of cold river water in April/May 1989 was accompanied by a large increase in well injectivity. A test performed on May 30–31, 1989 (Figure 5.14b) yields an injectivity index of 1.5 kg/s-bar.

Production Well SC-1

An injection test was performed on November 15, 1987 soon after well drilling and completion. A second injectivity test was carried out several months later on June 7, 1988. The pressure gauge in both the tests was set fairly close to the principal feedzone at 2310 m TVD. Both the tests

(Figure 5.15a,b) gave essentially the same value (5.5 and 4.9 kg/s-bar) for the injectivity index.

Production well SC-1 is by far the most productive well at Sumikawa. The well produces liquid water from several feedzones between 1950 m MD (temperature = 307°C) and 2320 m MD (temperature = 246°C). Over 60 percent of the production is derived from the feedzone at 2320 m MD (2310 m TVD). The stable pressure at 2310 m TVD is 149.0 bars (Section 4.14). During a discharge test in November 1988, three downhole pressure/temperature/spinner surveys were run. Using the flowing pressures measured in the latter surveys, the productivity index for SC-1 is estimated to be 5.7 (± 0.5) kg/s-bar.

The productivity and injectivity indices for SC-1 are more or less equal. Furthermore, the productivity (injectivity) index for SC-1 is substantially larger than for other Sumikawa wells. It is interesting to note here that no altered andesite layer was encountered in SC-1; instead, an unusually thick layer of "marine volcanic complex" formation was found to overlie the "granodiorite" formation. No other Sumikawa well has been drilled (as of early 1990) through this unusual geologic structure.

Injection Well SD-1

The injectivity test of September 4, 1986 (Figure 5.16a) was run after the hole had been drilled to 396 meters. Shortly after reaching target depth and completing the well, two other injectivity tests (Figure 5.16b,c) were run. The pressure gauge in the latter two tests was set at the top of the permeable interval. The injectivity test run on October 17, 1986 gave a slightly higher value (0.92 kg/s-bar) for the injectivity index than that (0.65 kg/s-bar) obtained from the test of October 12, 1986.

Continued on page 5-52

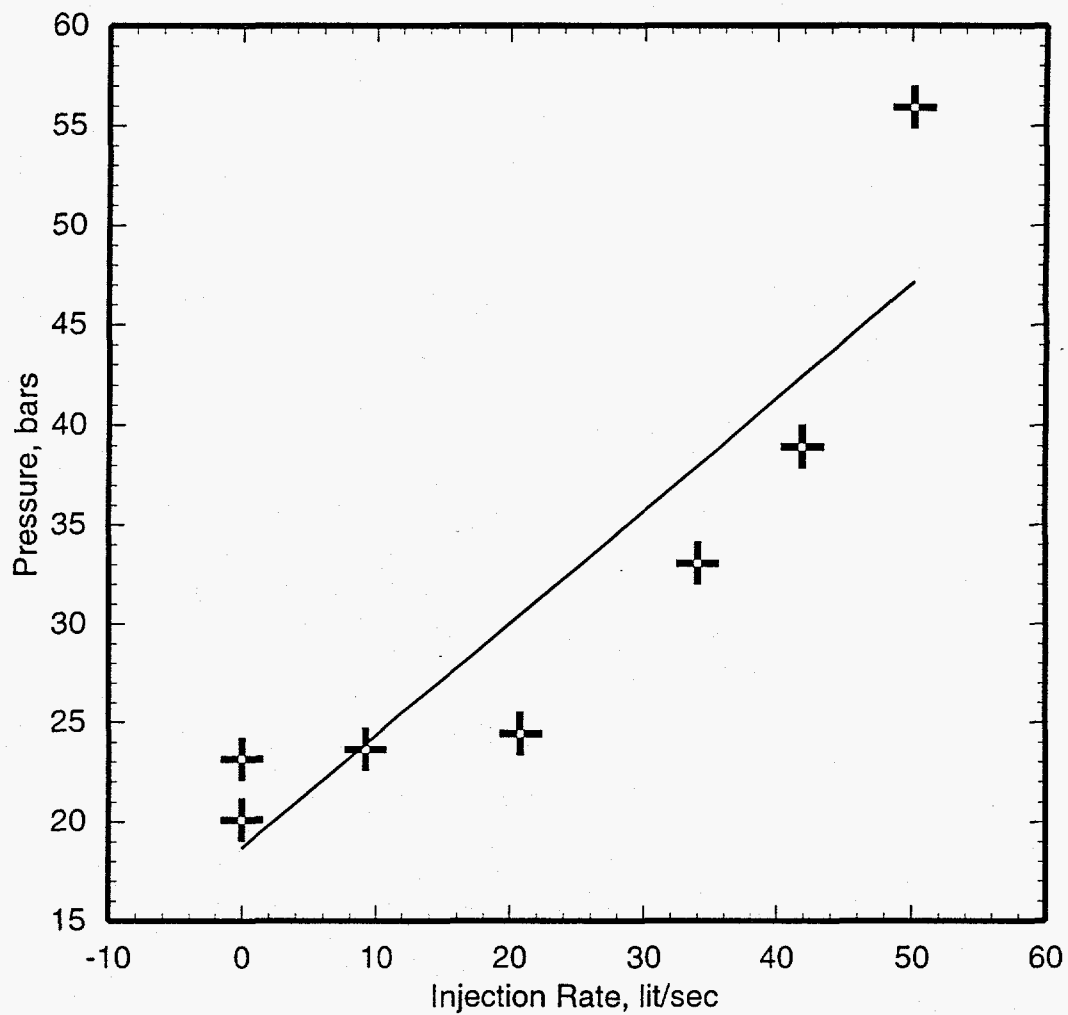


Figure 5.13a. Injectivity test for injection well SB-2 performed on June 22, 1988. The pressure gauge was set at 690 m MD (674 m TVD).

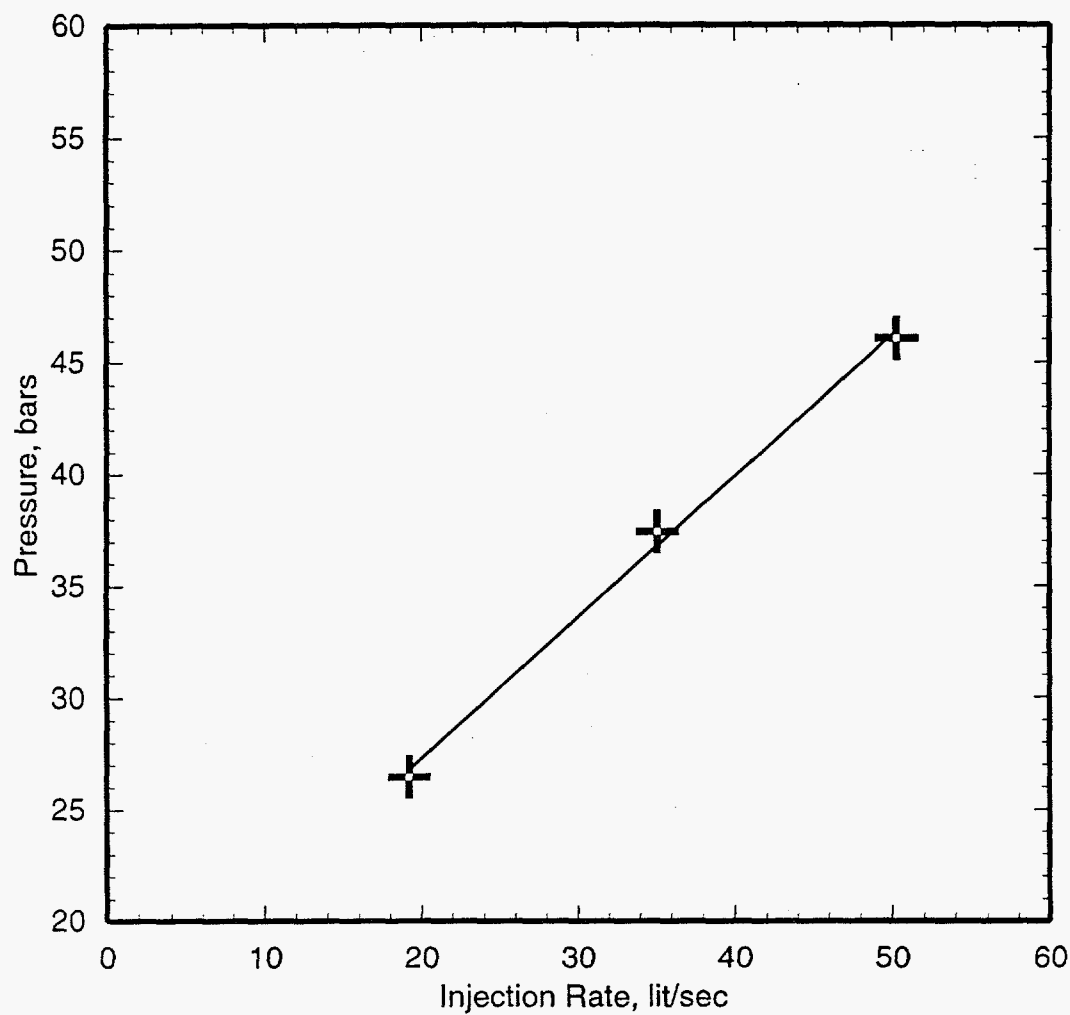


Figure 5.13b. Injectivity test for injection well SB-2 performed on May 29–30, 1989 after the injection of cold river water in April/May 1989. The pressure gauge was set at 700 m MD (684 m TVD).

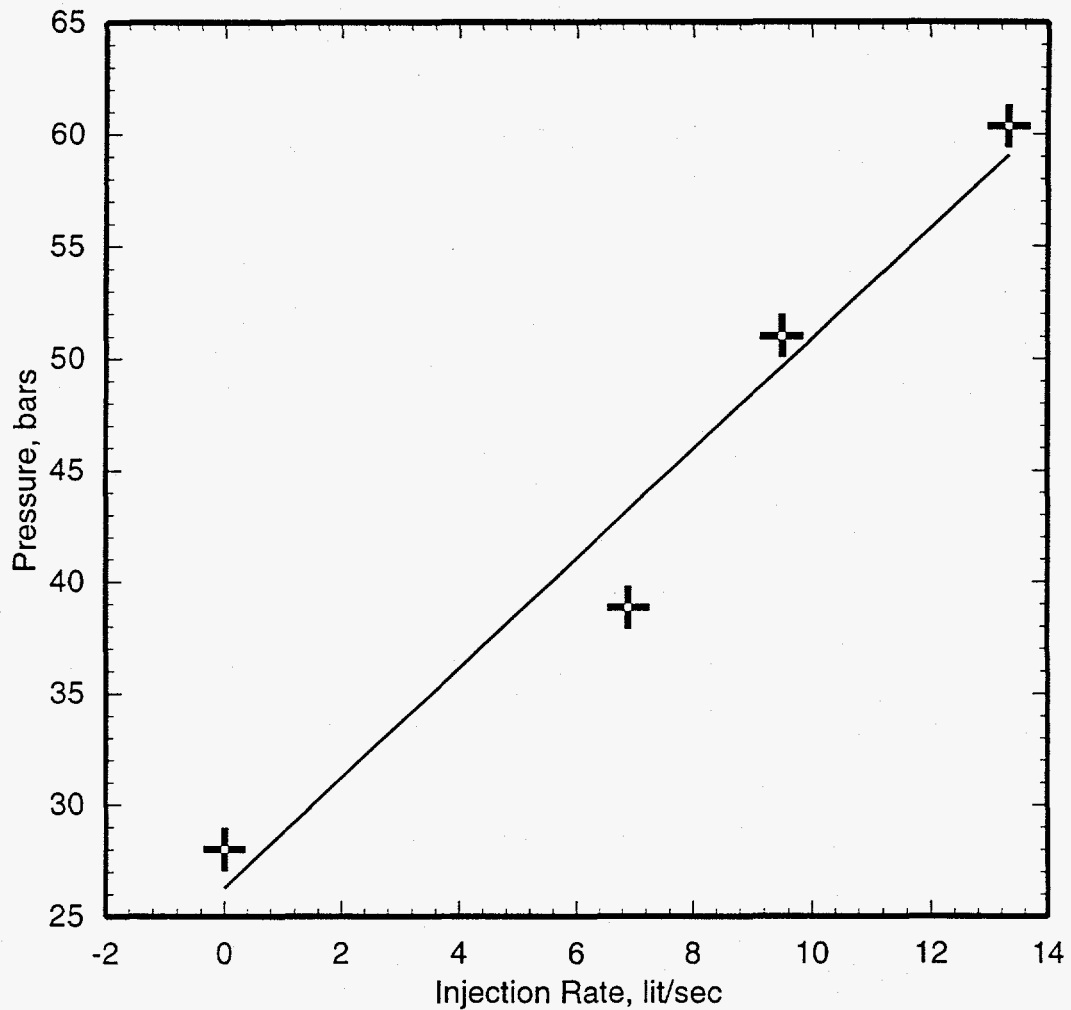


Figure 5.14a. Injectivity test for injection well SB-3 performed on August 5, 1988. The pressure gauge was set at 700 m MD (678 m TVD).

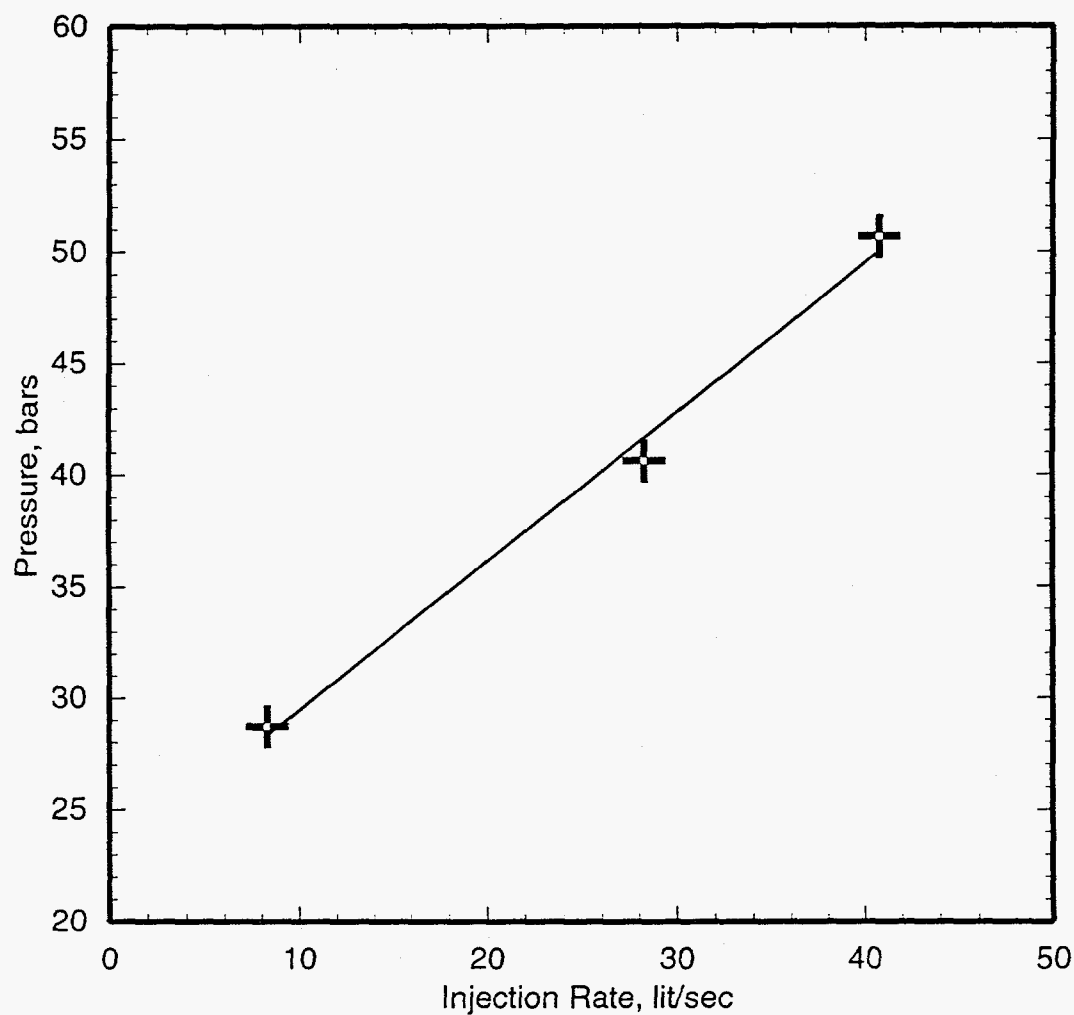


Figure 5.14b. Injectivity test for injection well SB-3 performed on May 30–31, 1989 after cold river water injection. The pressure gauge was set at 700 m MD (678 m TVD).

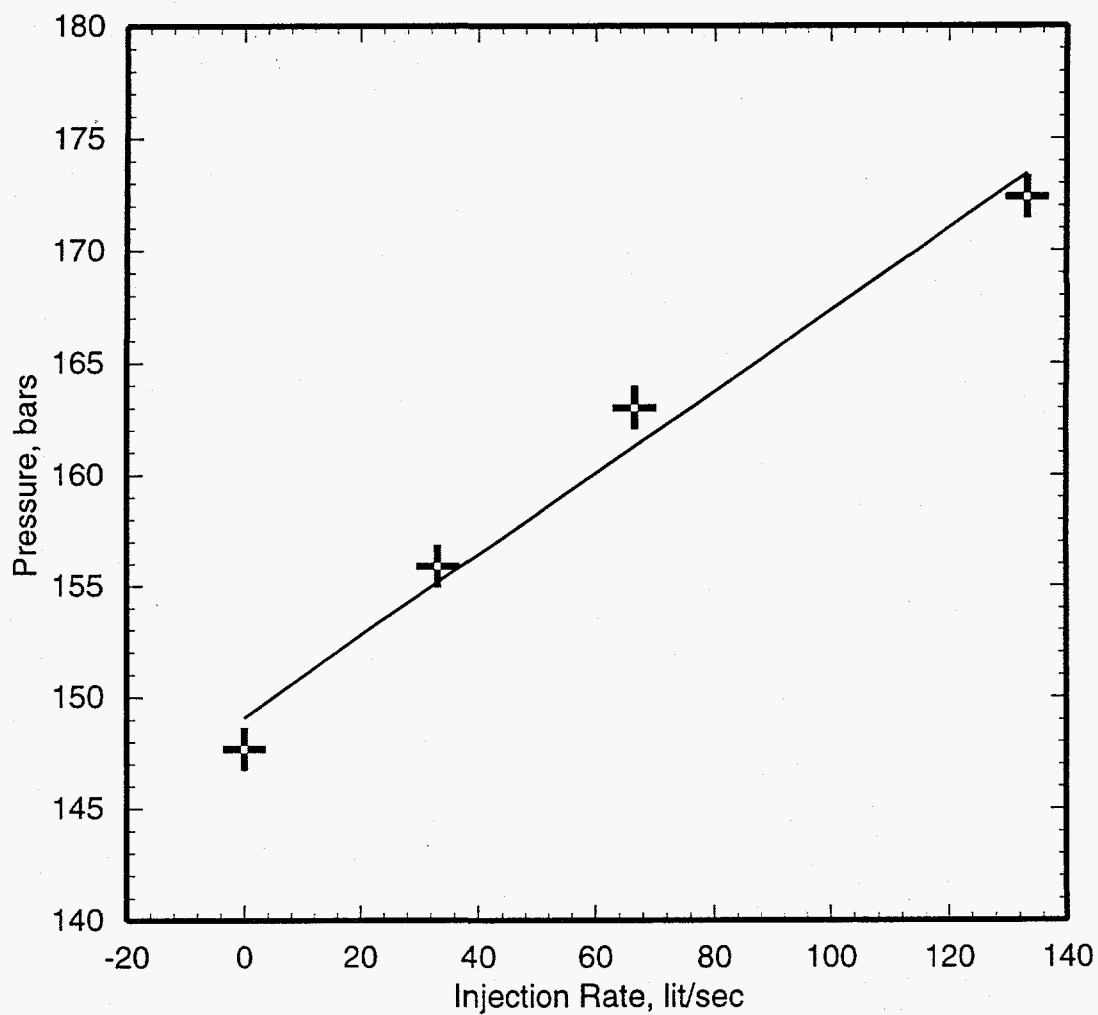


Figure 5.15a. Injectivity test for production well SC-1 performed on November 15, 1987. The pressure gauge was set at 2300 m MD (2290 m TVD).

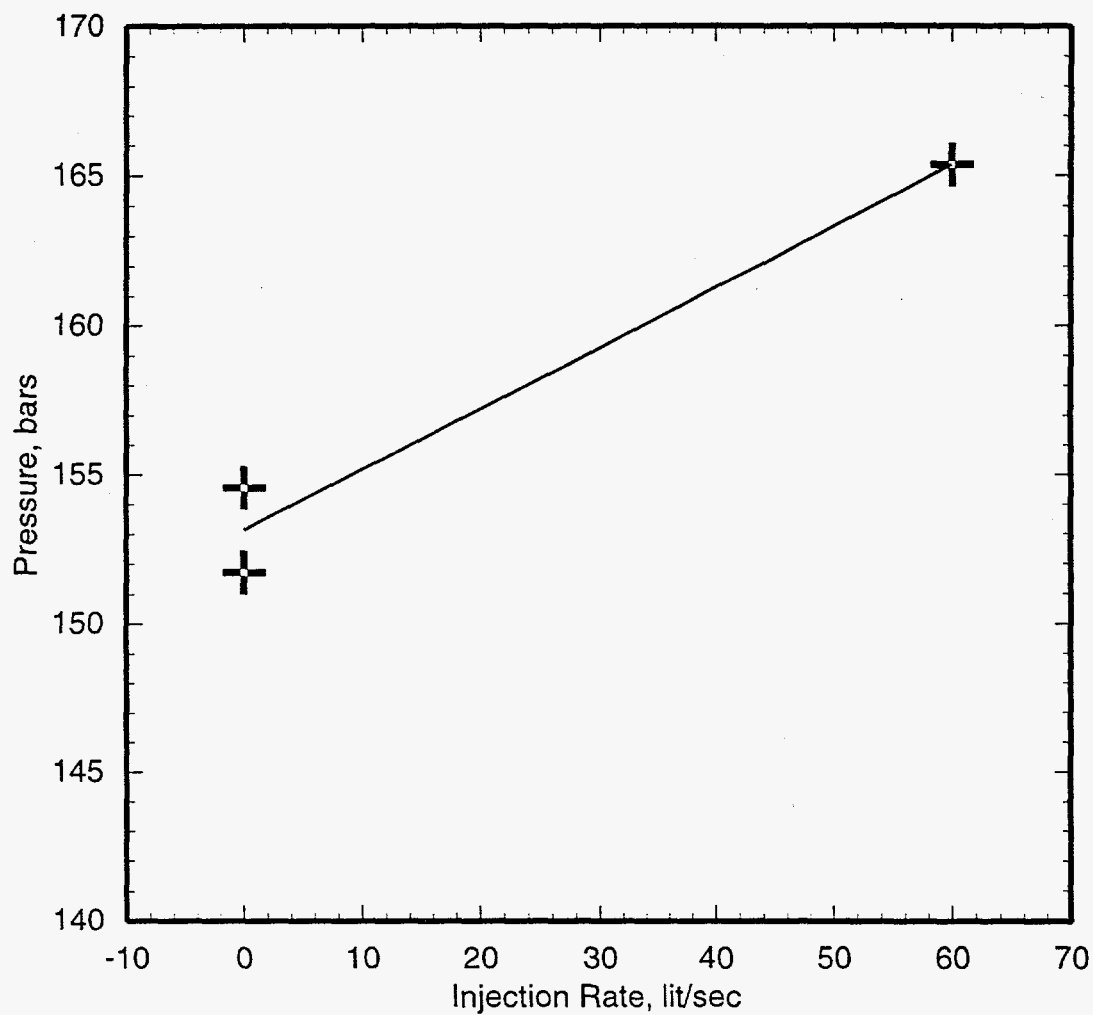


Figure 5.15b. Injectivity test for production well SC-1 performed on June 7, 1988. The pressure gauge was set at 2340 m MD (2329 m TVD).

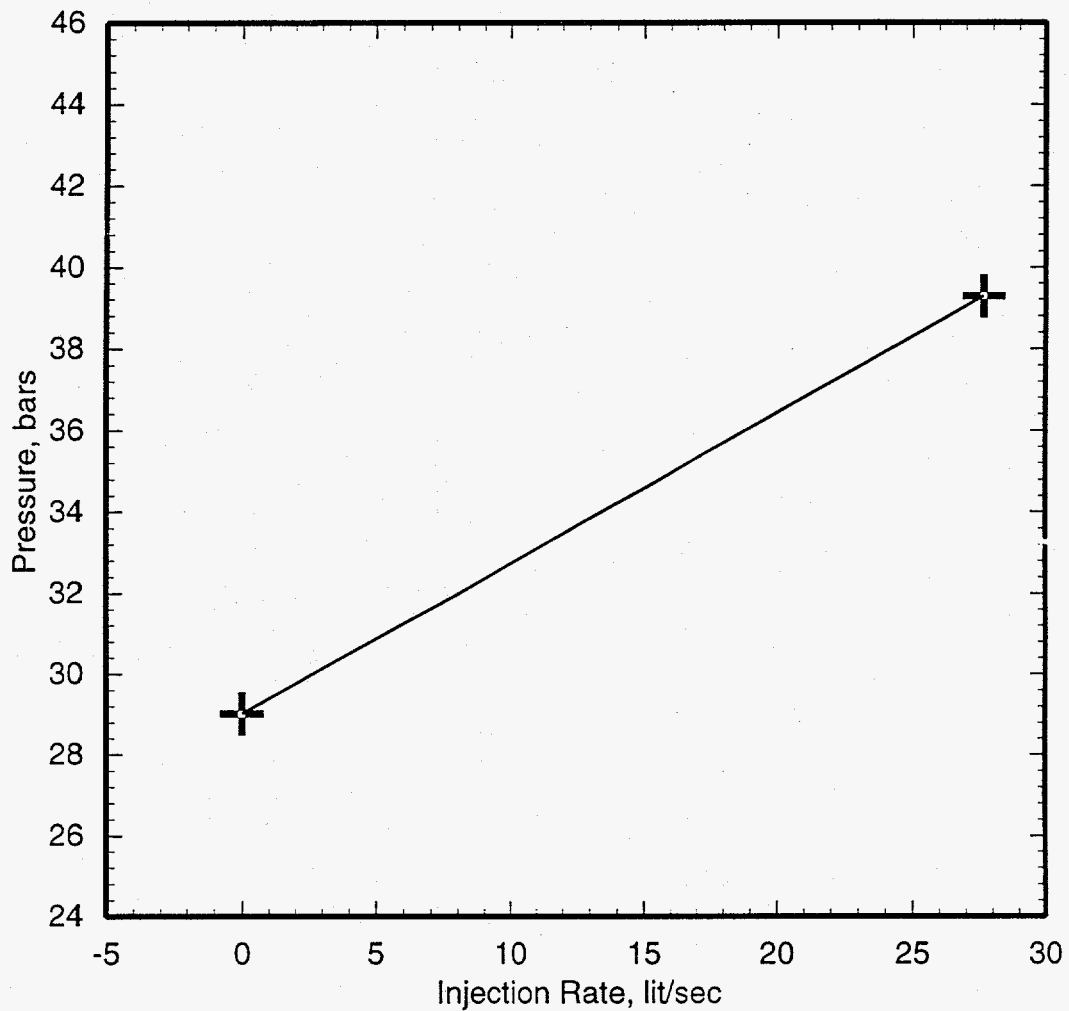


Figure 5.16a. Injectivity test for intermediate depth (drilled depth = 396 m) injection well SD-1 performed on September 4, 1986. The pressure gauge was set at 387 m MD (387 m TVD).

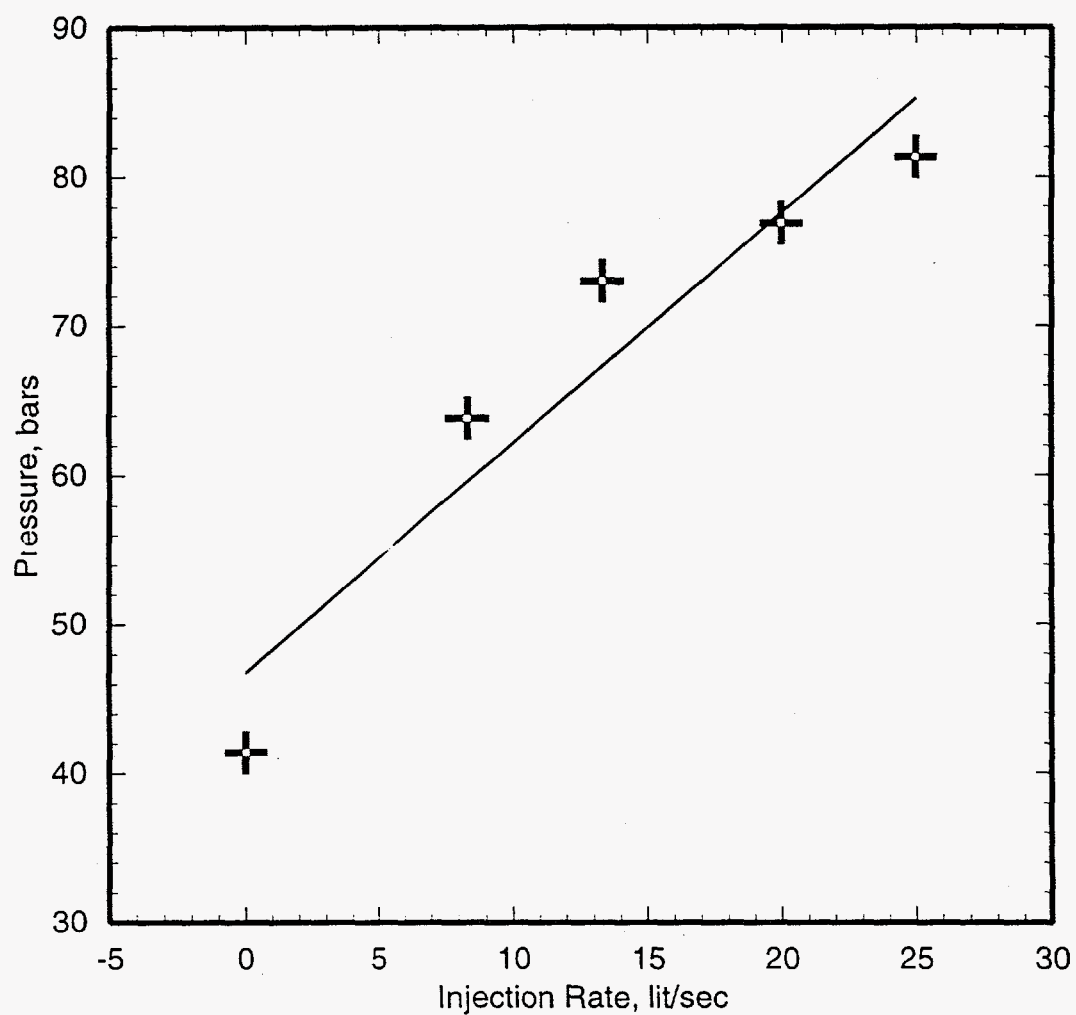


Figure 5.16b. Injectivity test for injection well SD-1 performed on October 12, 1986. The pressure gauge was set at 700 m MD (700 m TVD).

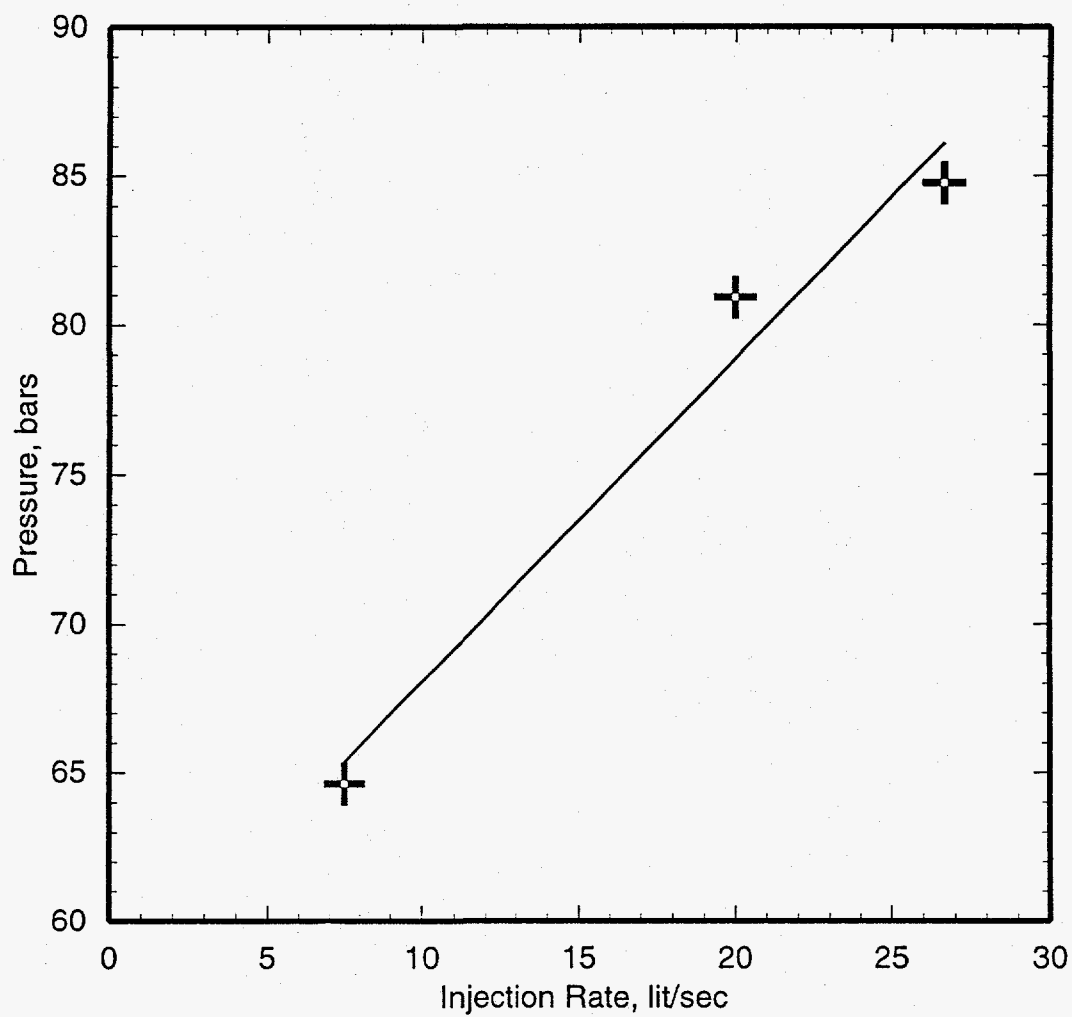


Figure 5.16c. Injectivity test for injection well SD-1 performed on October 17, 1986. The pressure gauge was set at 800 m MD (799 m TVD).

The improvement in well injectivity between the two tests may be due to borehole washing.

During a discharge test run from August 8, 1989 to December 1, 1989, injection well SD-1 produced from several feedzones in the depth interval from 800 m MD to 1570 m MD. At the start of the production test, *in situ* boiling was limited to the shallowest feedzone at 800 m MD; as production continued, boiling conditions extended to the deeper feedzones. The stable feedzone pressure at 1200 m TVD (approximately the middle of the permeable interval) is 77.0 bars (Section 4.15). During the 1989 production test, two downhole pressure/temperature/spinner surveys were run in SD-1 on September 18 and 19, 1989. At the time of these pressure/temperature/spinner surveys, *in situ* boiling was limited to the shallowest feedzone (800–900 meters). Using the flowing pressures measured in these pressure/temperature/spinner surveys, the productivity index for SD-1 is estimated to be ~ 0.51 (± 0.07) kg/s-bar (Table 5.2). It is almost certain that the productivity index for SD-1 goes down with continued production as boiling extends to deeper feedzones.

Slim Hole 52E-SM-1

Slim hole 52E-SM-1, located to the northeast of the Sumikawa Geothermal Field, did not encounter any circulation losses during drilling; this indicates poor formation permeability. An injection test was performed shortly after well completion on September 30, 1978 (Figure 5.17). The very small value (0.002 kg/s-bar) of the injectivity index obtained from this test is consistent with indications of poor permeability provided by the absence of circulation losses while drilling.

Slim Hole 52E-SM-2

After slim hole 52E-SM-2 had been drilled to a depth of 803 m, an injection test was performed on August 26, 1978 (Figure 5.18). The injectivity index inferred from the latter test is rather small (0.068 kg/s-bar). The intermediate depth hole was also discharged on September 23, 1978. The measured wellhead enthalpies suggest *in situ* boiling. The maximum discharge rate was about 5 tons/hour. No downhole pressure surveys were made in the discharging borehole.

No injection data are available for the completed 52E-SM-2. The principal feedzone for the completed slim hole is at a depth of 980 meters. The measured wellhead enthalpies during a discharge test performed in October 1978 suggest that the borehole feeds from a liquid zone at about 230–240°C. (Later discharge tests indicate some *in situ* boiling.) The maximum discharge rate during the October 1978 test was ~ 35 tons/hour.

The absence of downhole pressure measurements makes it impossible to compute the productivity index for either the intermediate depth or the completed slim hole. The measured discharge rates/enthalpies do, however, imply that the completed hole has higher transmissivity and productivity than the intermediate depth borehole. Slim hole 52E-SM-2 is located to the south of O-5T (*i.e.*, between the Ohnuma and Sumikawa fields).

Slim Hole N59-SN-5

Slim hole N59-SN-5 is located to the west of the Sumikawa field. No circulation losses were encountered in the open part of the borehole. An injection test performed shortly after drilling and completion on November 12, 1985 (Figure 5.19) implies that the injectivity index for N59-SN-5 is

Continued on page 5-56

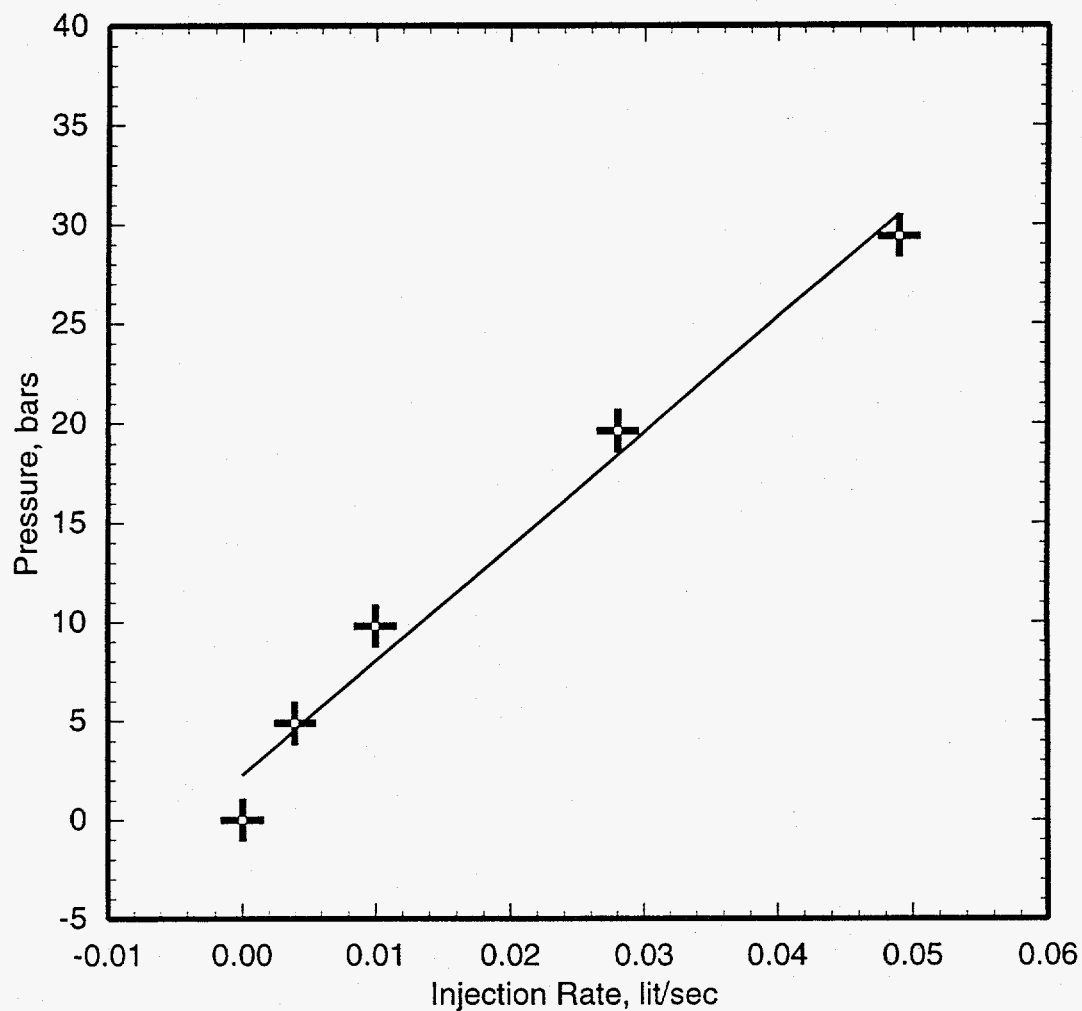


Figure 5.17. Injectivity test for slim hole 52E-SM-1 performed on September 30, 1978. The pressure gauge was set at the wellhead.

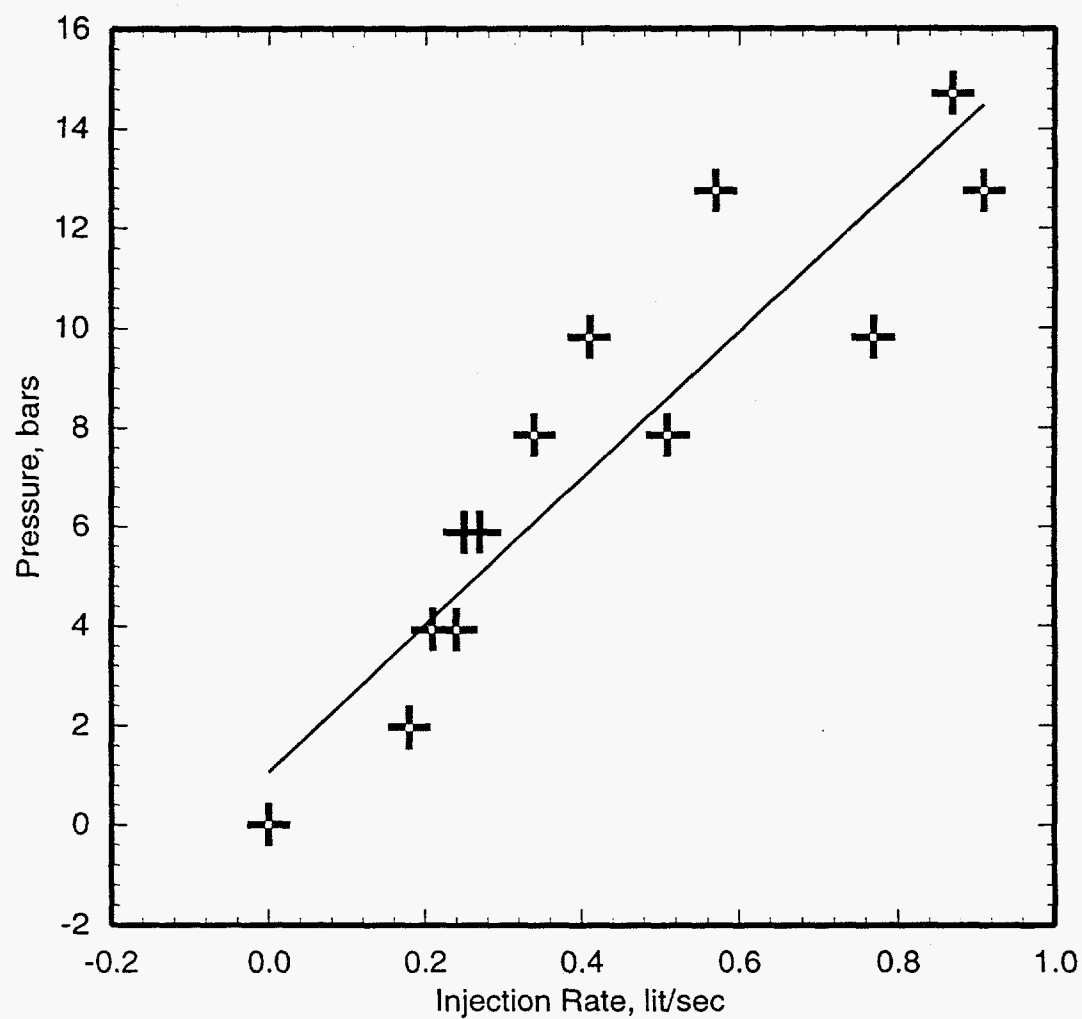


Figure 5.18. Injectivity test for the intermediate depth (drilled depth = 550 m) slim hole 52E-SM-2 on August 26, 1978. The pressure gauge was set at the wellhead.

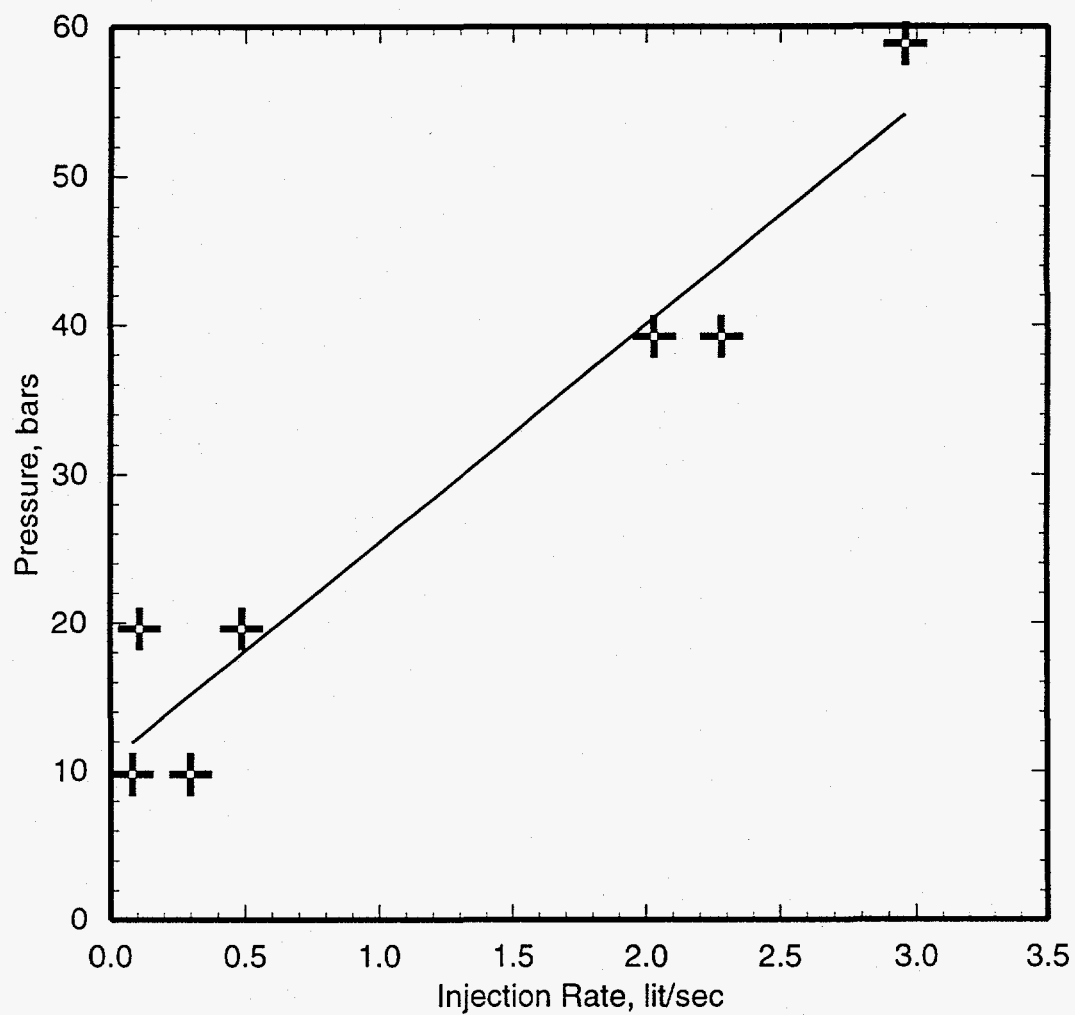


Figure 5.19. Injectivity test for slim hole N59-SN-5 performed on November 12, 1985. The pressure gauge was set at the wellhead.

small (0.068 kg/s-bar). The small injectivity index is consistent with low formation permeability indicated by the absence of circulation losses during drilling.

5.2 Comparison of Productivity and Injectivity Indices

Apart from transient effects associated with the initiation of discharge (or injection) from a borehole, the flow resistance (*i.e.*, pressure losses) of the reservoir rocks can be represented by the productivity (or injectivity) index. Injectivity indices are available for eighteen Sumikawa boreholes (Table 5.1). Five of the boreholes listed in Table 5.1 (50-HM-3, O-5T, 52E-SM-1, 52E-SM-2, and N59-SN-5) are located outside the permeable zone of the Sumikawa field. Slim hole N60-KY-1 within the Sumikawa field displays excellent pressure communication with several Sumikawa wells (S-4, SB-1, and SB-2); this slim hole has, however, very limited injectivity (Table 5.1). As mentioned elsewhere in this report, slim hole N60-KY-1 was injection tested only once (shortly after drilling); it is likely that the permeable fractures at the time of the test were laden with drilling mud and/or rock flour. In the following discussion, we will not further consider injectivity data for the aforementioned six boreholes. Of the remaining twelve boreholes (S-1, S-2, S-3, S-4, SA-1, SA-2, SA-4, SB-1, SB-2, SB-3, SC-1, SD-1), productivity indices (Table 5.2) are available for seven boreholes (S-1, S-2, S-4, SA-1, SA-4, SC-1, SD-1). The productivity and injectivity indices for the latter seven boreholes are compared in Table 5.3.

The injectivity indices for ten of the twelve boreholes (the two exceptions are S-1 and SC-1) are all of the order of unity. The injectivity indices for Sumikawa boreholes do not depend in any sys-

tematic manner on the borehole diameter. This result is in agreement with theoretical results of Pritchett (1993) and of Hadgu, *et al.*, (1994). Both of these authors have suggested that apart from any differences associated with differences in wellbore skin (*i.e.*, near wellbore formation damage or stimulation), the productivity (or injectivity) should exhibit only a weak dependence on borehole diameter. The Sumikawa results are, however, at variance with results for the Oguni Geothermal Field (Garg, *et al.*, 1994b). Both the productivity and injectivity indices for the Oguni wells display a strong dependence on borehole diameter. At Oguni, most of the slim holes were drilled with a complete loss of circulation; the drilling mud and/or rock flour may have plugged some of the permeable fractures. In the case of Sumikawa slim holes, no blind drilling was necessary. Rotary drilling—employed to drill large-diameter holes in both the Sumikawa and Oguni Geothermal Fields—is rarely carried out with complete loss of circulation. Thus, it is possible that formation plugging is responsible for the apparent variation of productivity/injectivity indices with diameter at Oguni; apparently, formation plugging does not vary with diameter at Sumikawa. Data from other geothermal fields should be examined to determine the frequency of the occurrence of excess formation plugging with core drilling.

The injectivity indices for Sumikawa boreholes ($\sim 0(1)$) are significantly smaller than productivity/injectivity indices for Oguni production wells (productivity indices for Oguni wells range from 4 kg/s-bar to 15 kg/s-bar). Liquid conditions prevail at the feedzone depth during production from Sumikawa boreholes S-2 (redrilled hole only) and SC-1; the productivity indices for these boreholes are more or less the same as the corresponding injectivity indices. The latter conclusions are in accord with results from the Oguni boreholes

Table 5.3. Comparison of productivity and injectivity indices for Sumikawa boreholes.

Borehole Name	Final Diameter (mm)	Feedzone Depth (m TVD)	Injectivity Index (kg/s-bar)	Productivity Index (kg/s-bar)	Remarks
S-1	143	436	1.3–6.8	0.86	Borehole produces dry steam.
S-2	101	900	0.76	0.027	original hole, hole depth = 904.6 m. <i>In situ</i> boiling on discharge.
	101	940	1.7	1.3	Redrilled hole, Liquid feed.
S-4	159	1520	1.4	0.94	<i>In situ</i> boiling on discharge; 1983 Injectivity Index
SA-1	216	1800	1.5	0.16	<i>In situ</i> boiling on discharge; 1989 Injectivity Index
SA-4	216	1240	0.94	0.11	1989 Injectivity Index; <i>in situ</i> boiling on discharge.
SC-1	216	2310	5.2	5.7	Liquid feeds.
SD-1	216	1200 (middle of permeable interval)	0.78	0.51	Shallowest feedzone two-phase, deeper feeds liquid.

(Garg, *et al.*, 1994b). Production from Sumikawa boreholes other than S-2 (redrilled hole only) and SC-1 is accompanied by *in situ* boiling. Low formation permeability and high formation temperatures ($250^{\circ}\text{C} < T < 320^{\circ}\text{C}$) are responsible for *in situ* boiling on discharge. The formation transmissivity for two-phase flow is always smaller than that for liquid flow. For Sumikawa boreholes with *in situ* boiling (S-1, S-4, SA-1, SA-4 and SD-1), the productivity index is, as expected, smaller than the corresponding injectivity index.

5.3 Characteristic Tests

A total of eleven Sumikawa boreholes (slim holes S-1, S-2, S-3, and 52E-SM-2; production wells S-4, SA-1, SA-2, SA-4, SB-1, and SC-1; in-

jection well SD-1) have been discharged at one time or another. In addition, two intermediate depth slim holes (S-2 and 52E-SM-2) were discharged for brief periods. The discharge test data are needed to define the characteristic output curves (*i.e.*, mass and enthalpy versus wellhead pressure). Wellhead enthalpy measurements suggest that slim holes S-2 (final completion), S-3 and 52E-SM-2 (final completion), and production wells SB-1 and SC-1 produced from all liquid feedzones with little or no *in situ* boiling. Production from all the other Sumikawa boreholes is accompanied by *in situ* boiling. Slim hole S-1 and production wells SA-2 and SA-4 discharge only steam. The mass output curves for the various Sumikawa boreholes are shown in Figures 5.20 through 5.32 (tables of data are given in Appendix C). Interestingly, production from intermediate depth slim holes S-2 and

Continued on page 5-71

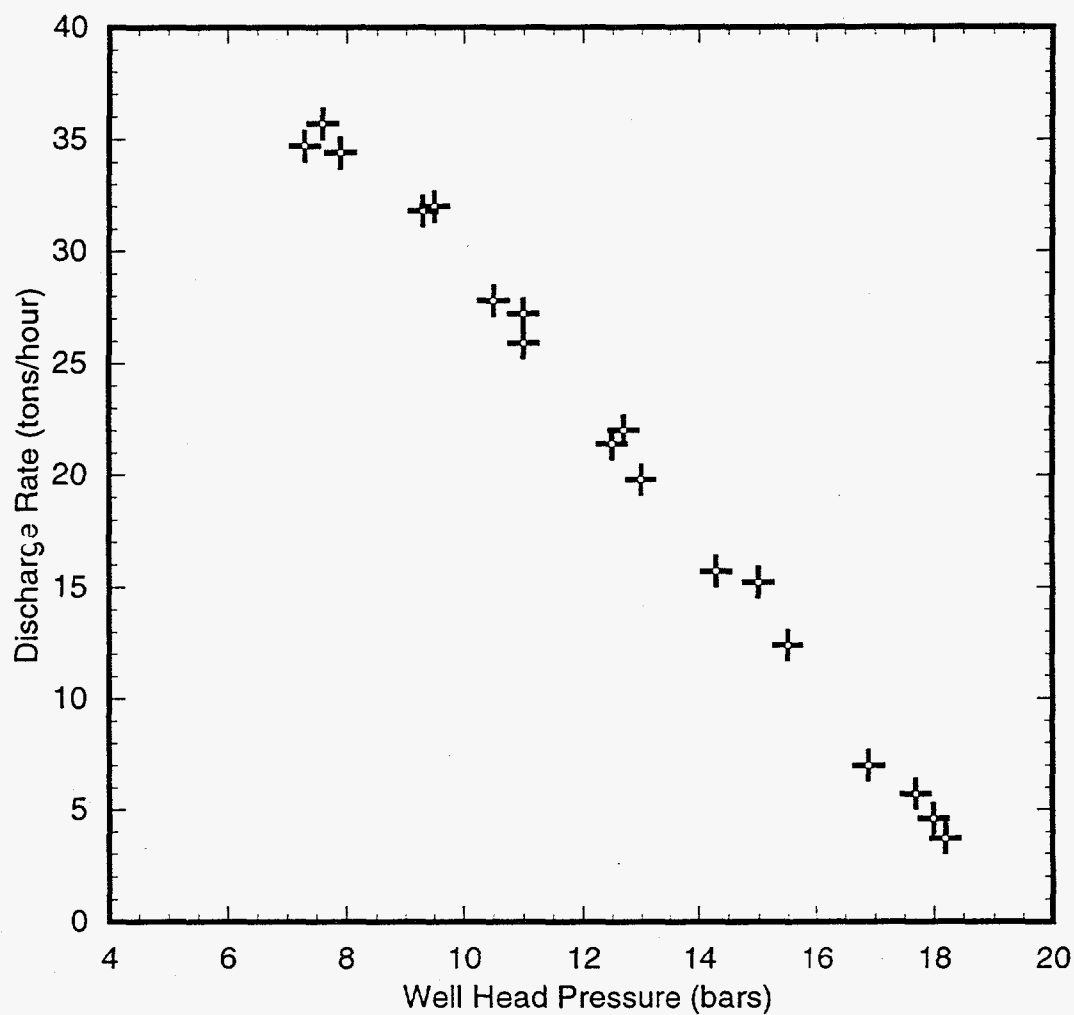


Figure 5.20. Discharge rate versus wellhead pressure for slim hole S-1 (April 1982).

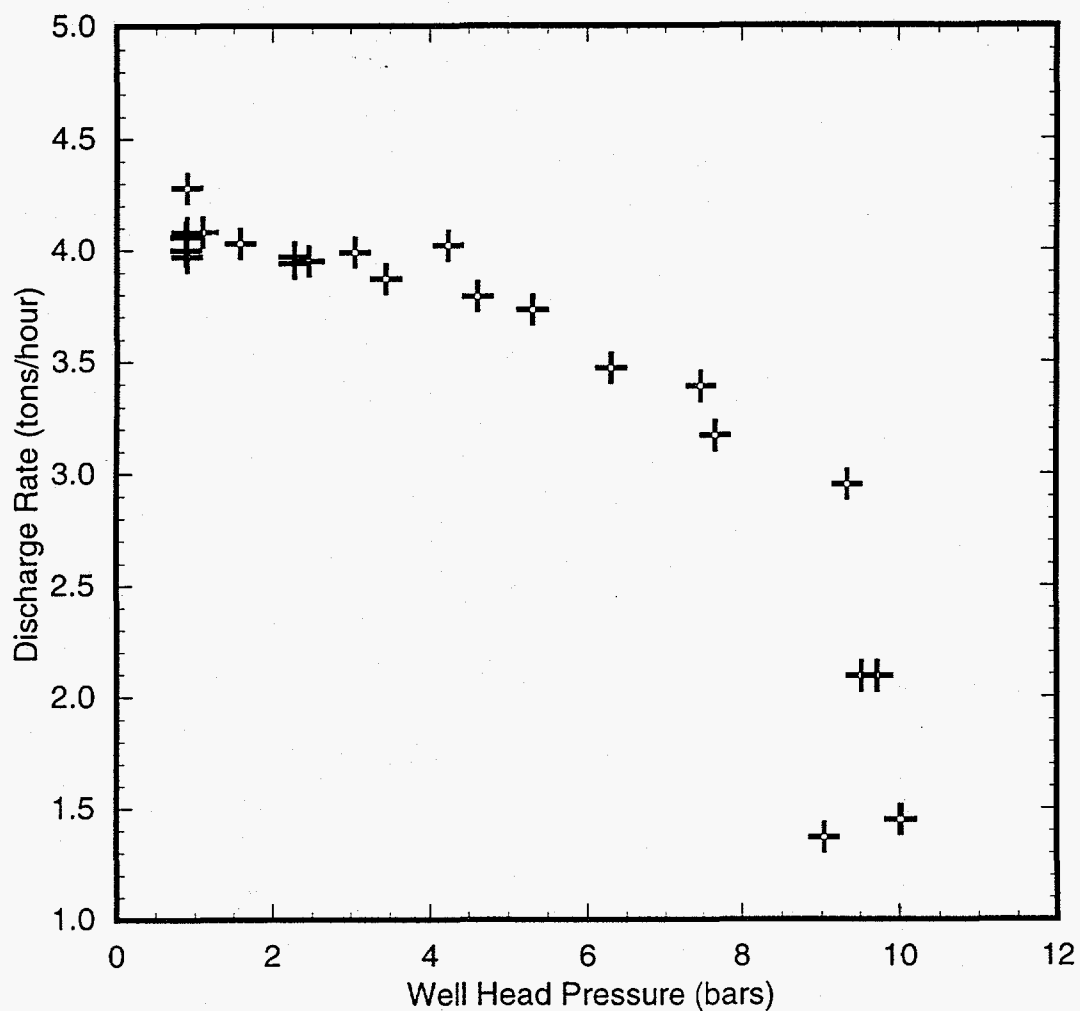


Figure 5.21. Discharge rate versus wellhead pressure for original (drilled depth = 904.6 m) slim hole S-2 (July 1982).

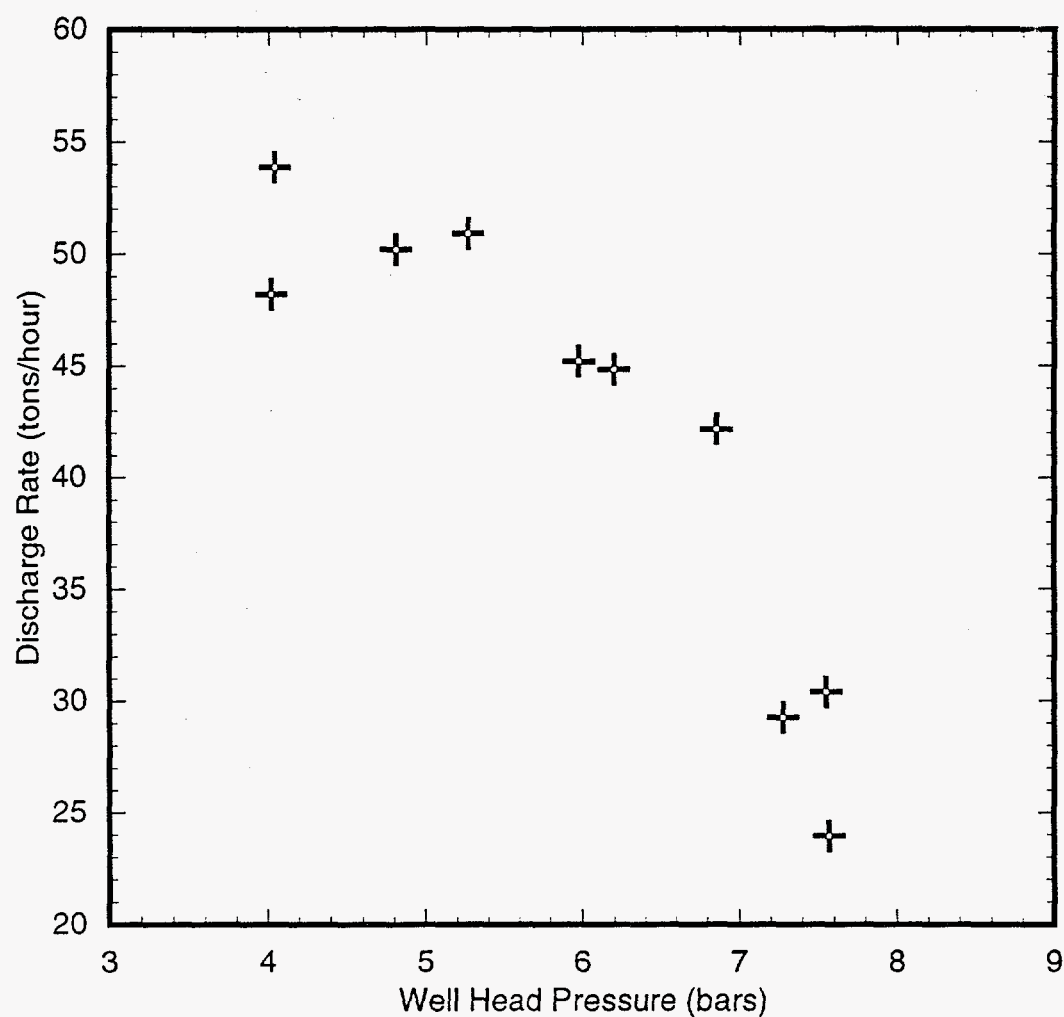


Figure 5.22. Discharge rate versus wellhead pressure for redrilled slim hole S-2 (final completion) (November, 1982).

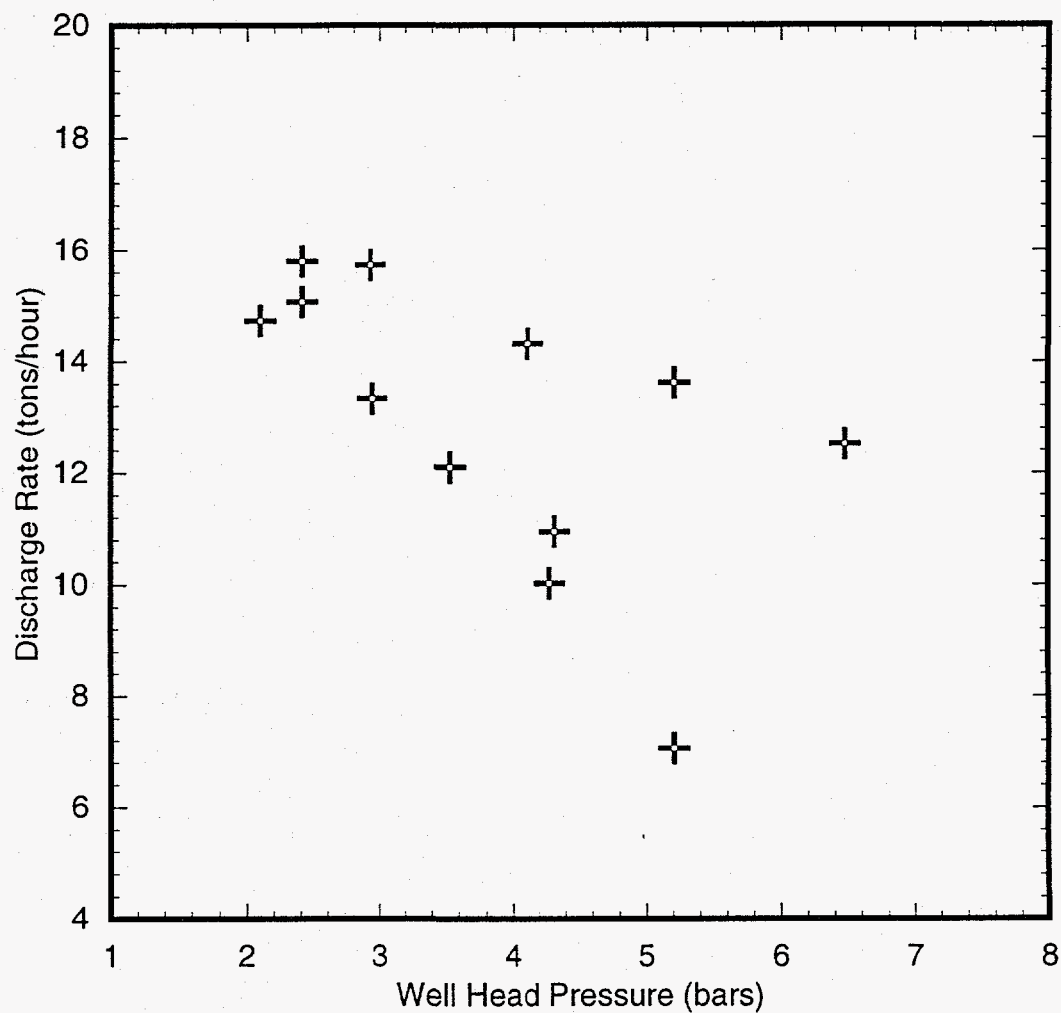


Figure 5.23. Discharge rate versus wellhead pressure for slim hole S-3 (July and October 1983). The discharge rate for S-3 fluctuates with a cycle time of ~10 minutes (see Section 5.1).

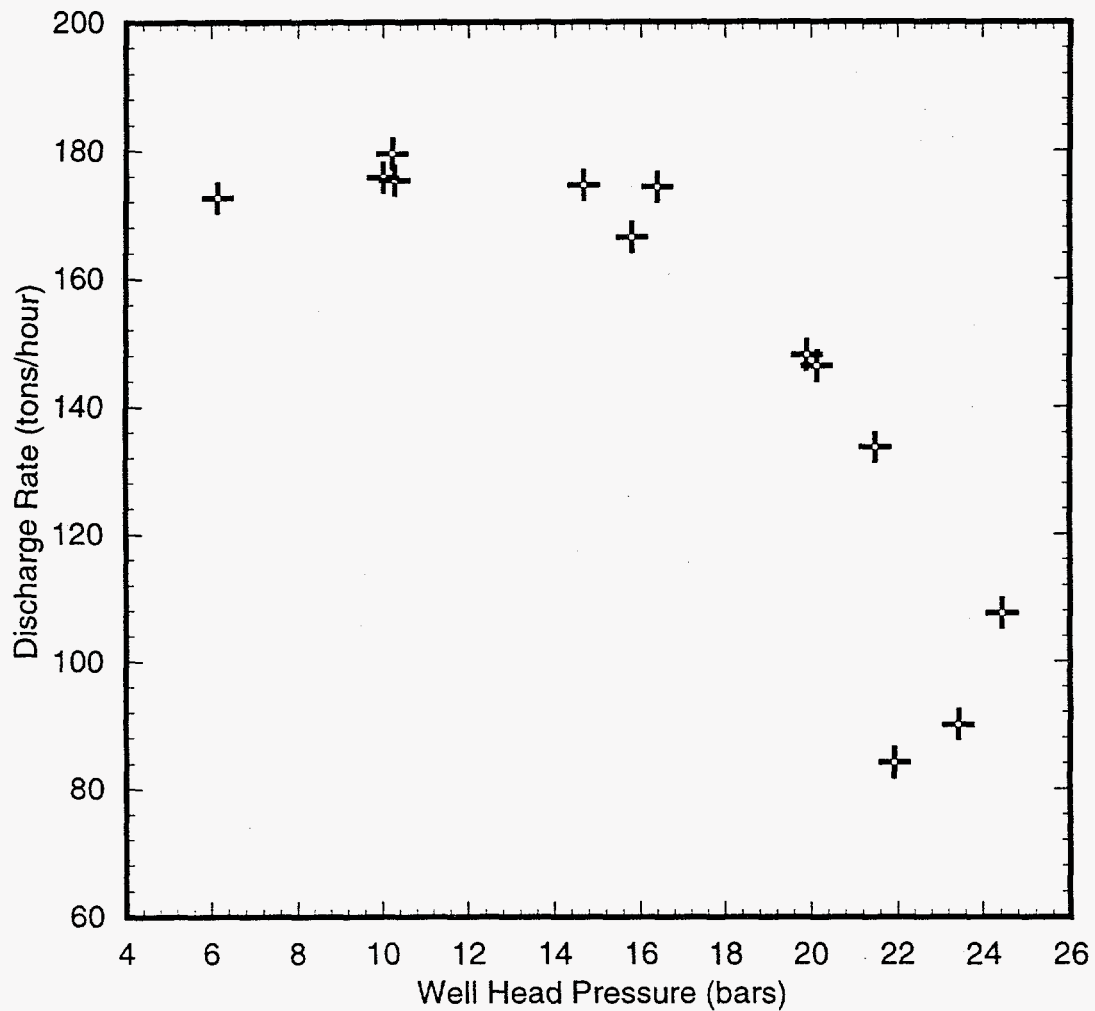


Figure 5.24. Discharge rate versus wellhead pressure for production well S-4 (1984, 1985, 1986, and 1988).

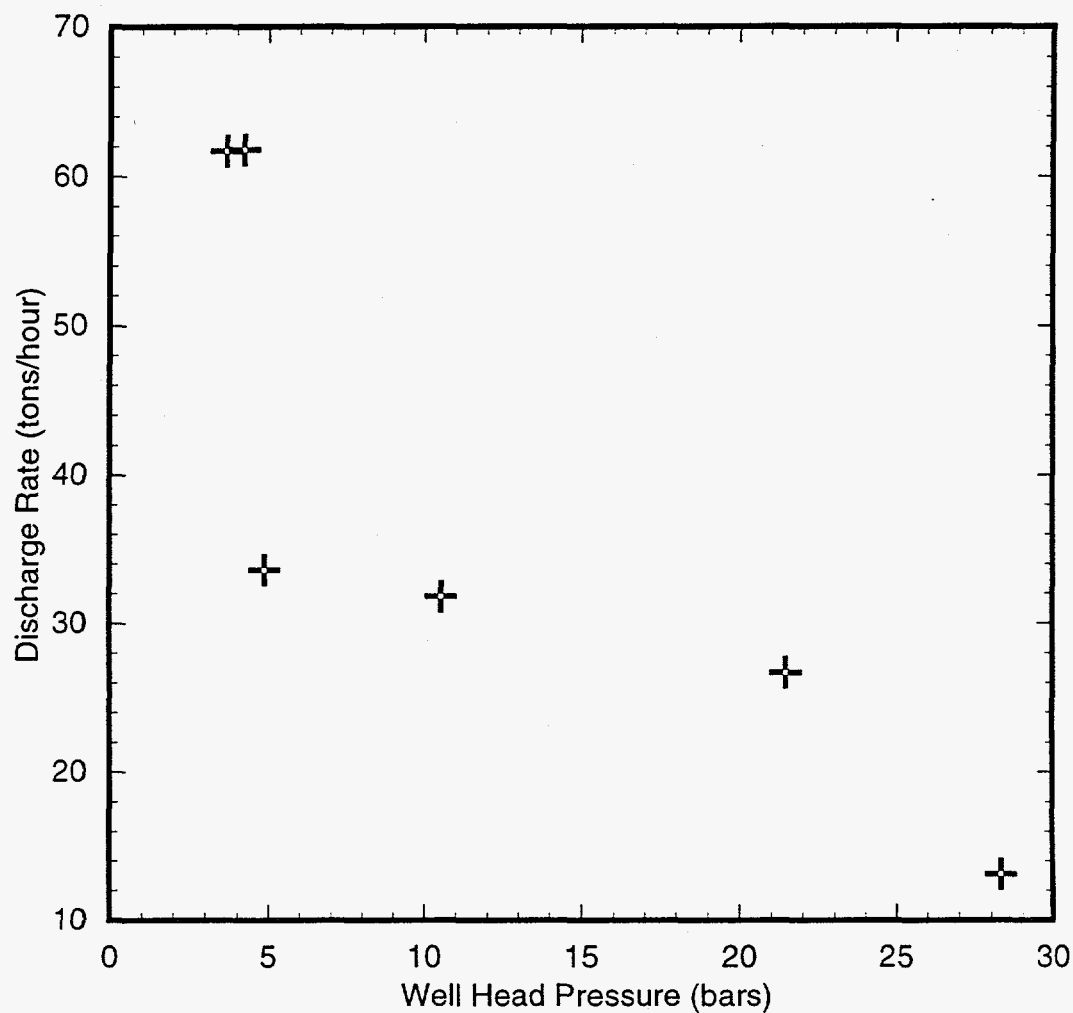


Figure 5.25. Discharge rate versus wellhead pressure for production well SA-1 (November 1988 and August 1989). The two highest discharge rates (~62 tons/hour) represent the August 1989 data.

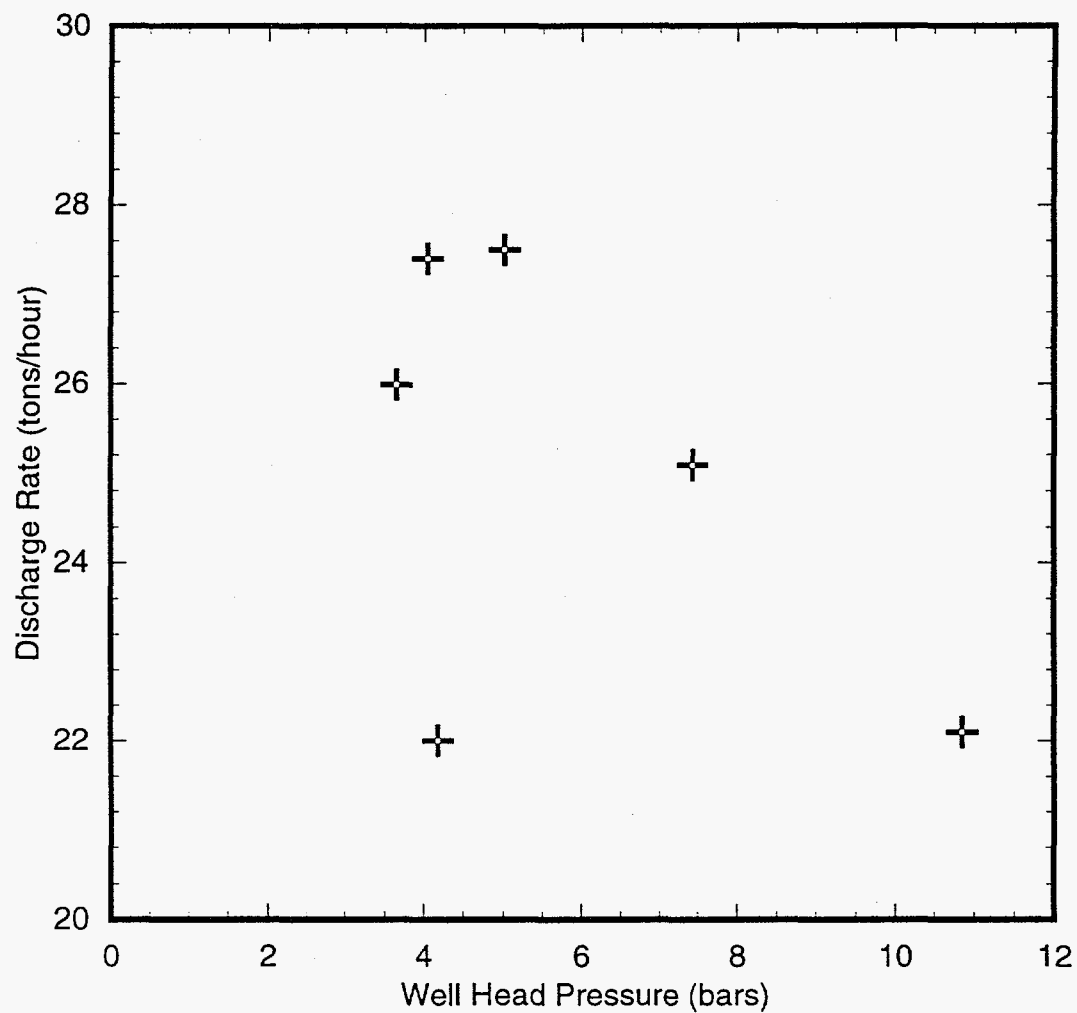


Figure 5.26. Discharge rate versus wellhead pressure for production well SA-2 (November 1988 and August 1989).

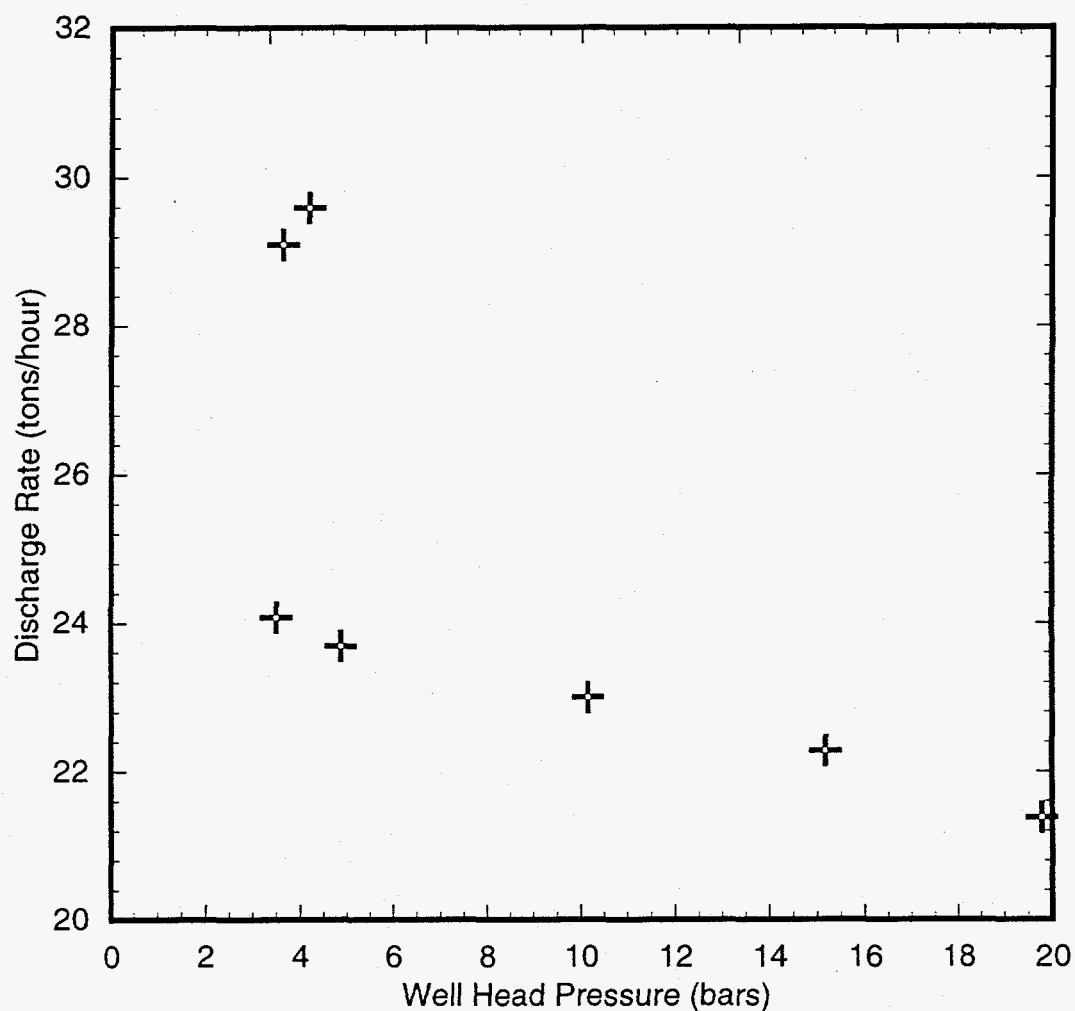


Figure 5.27. Discharge rate versus wellhead pressure for production well SA-4 (November 1988 and August 1989). The two highest discharge rates (29–30 tons/hour) represent the August 1989 data.

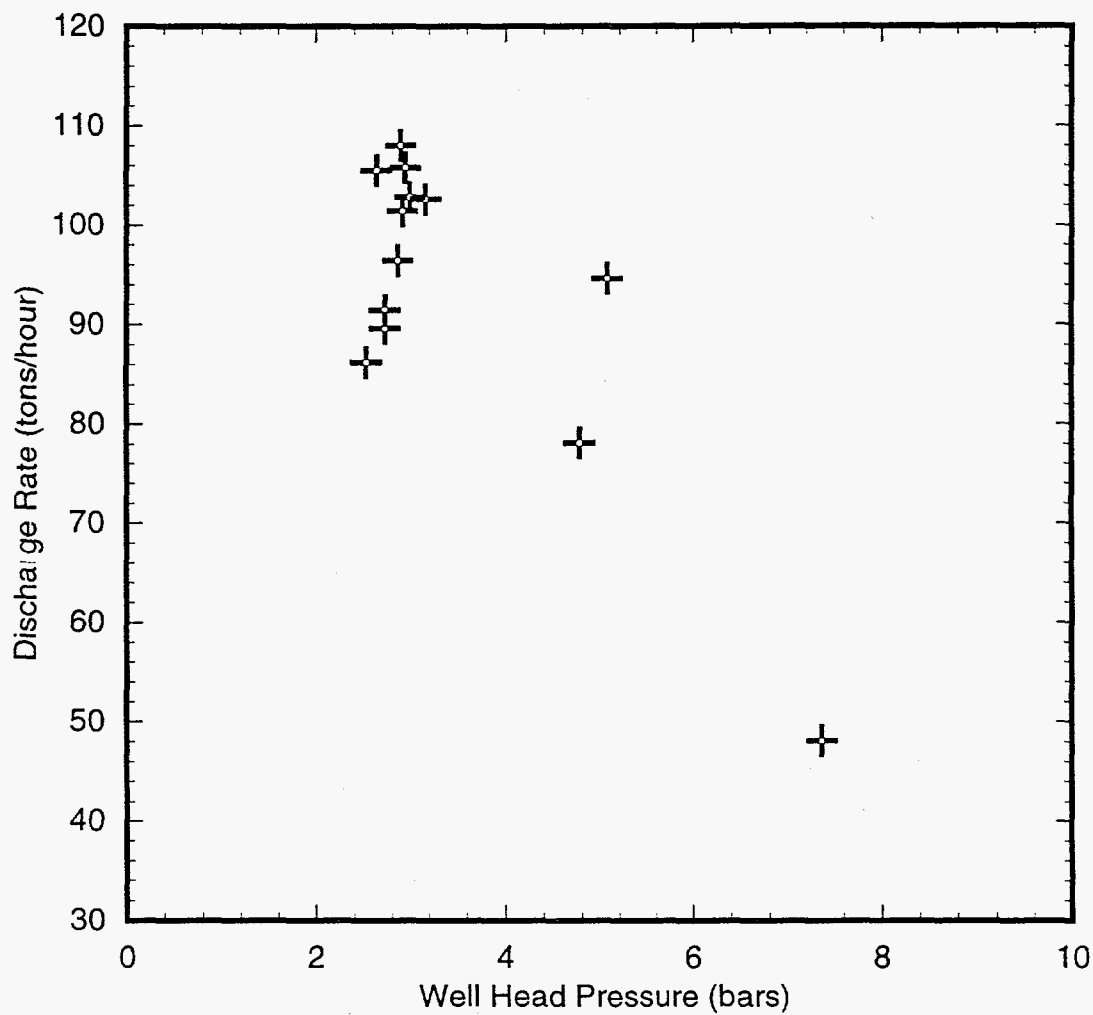


Figure 5.28. Discharge rate versus wellhead pressure for production well SB-1 (July 1989–December 1989).

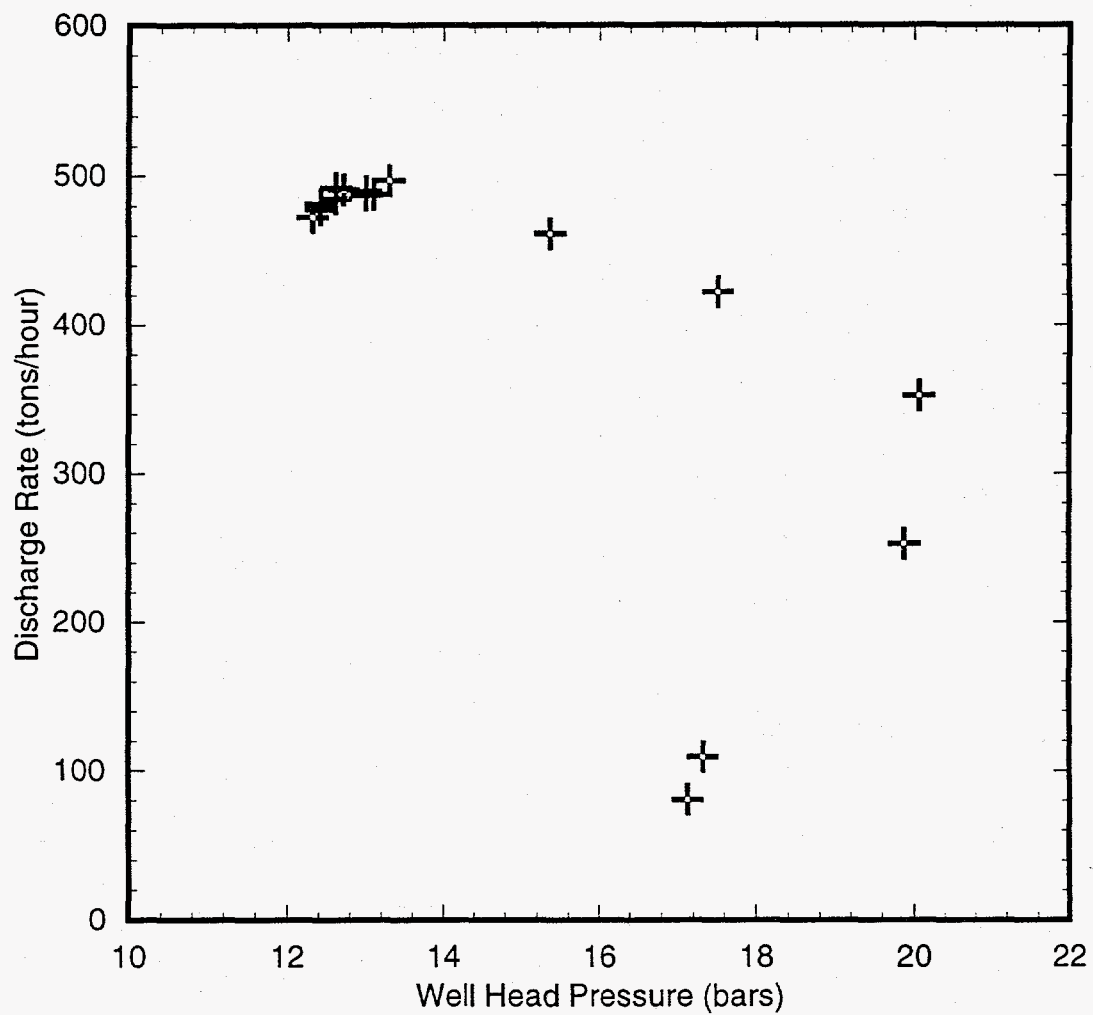
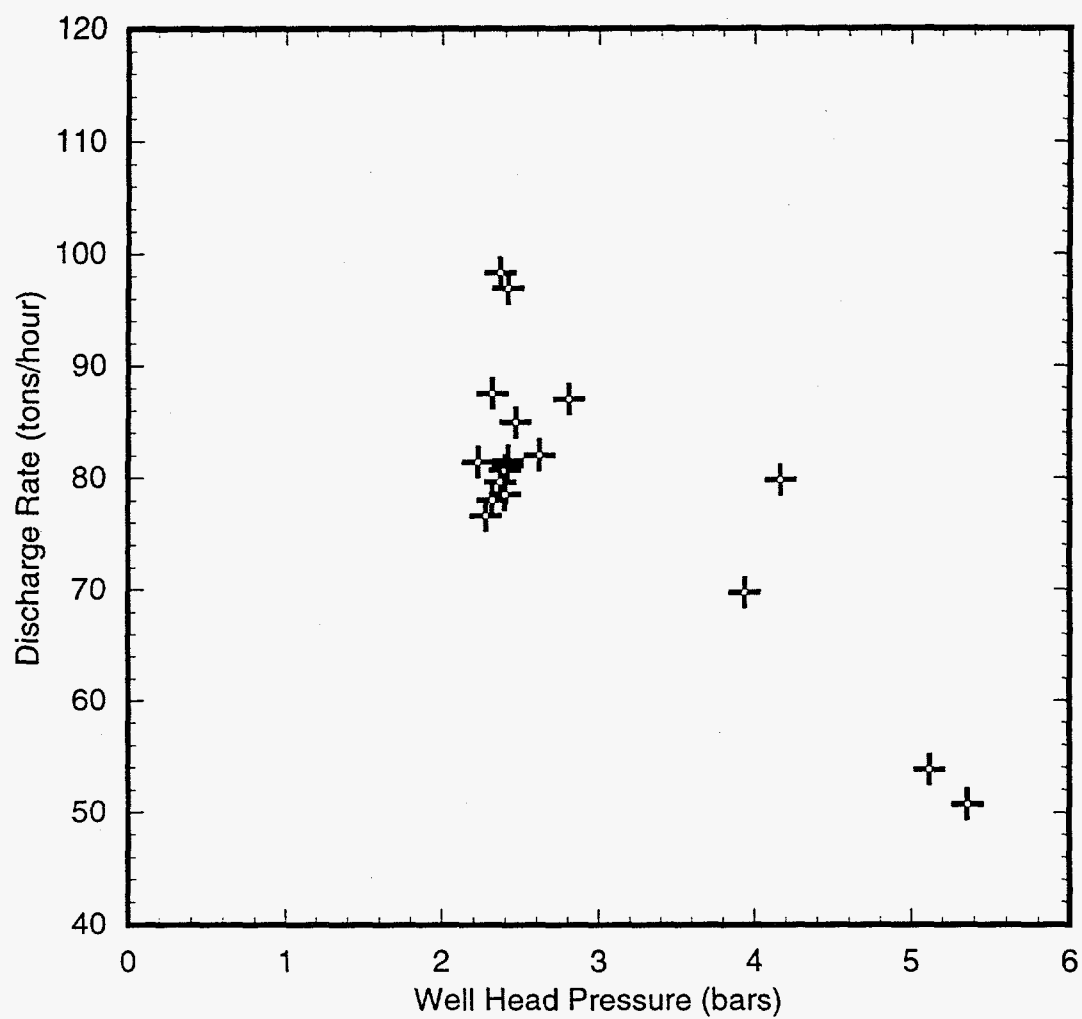


Figure 5.29. Discharge rate versus wellhead pressure for production well SC-1 (1988 and 1989).



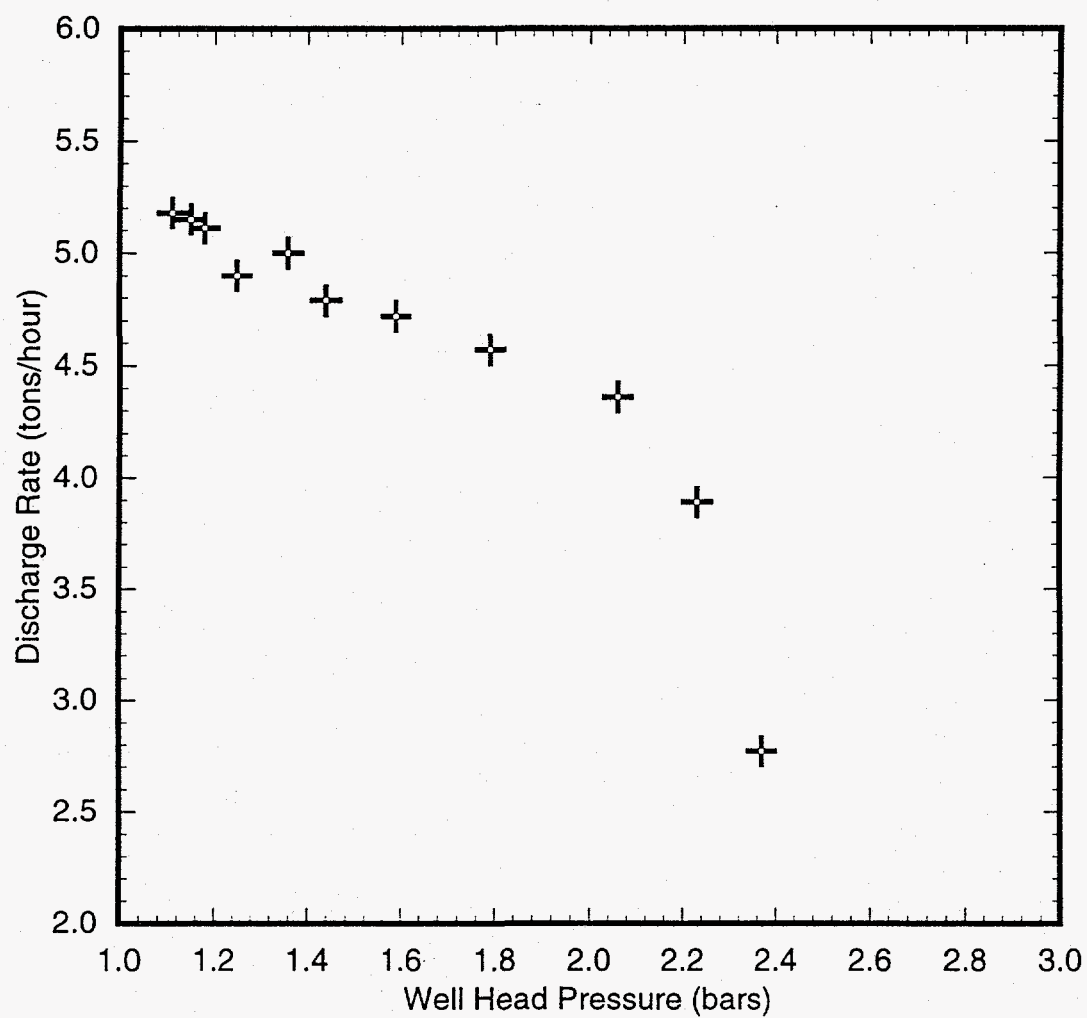


Figure 5.31. Discharge rate versus wellhead pressure for intermediate depth (drilled depth = 803 m) slim hole 52E-SM-2 (September 23, 1978).

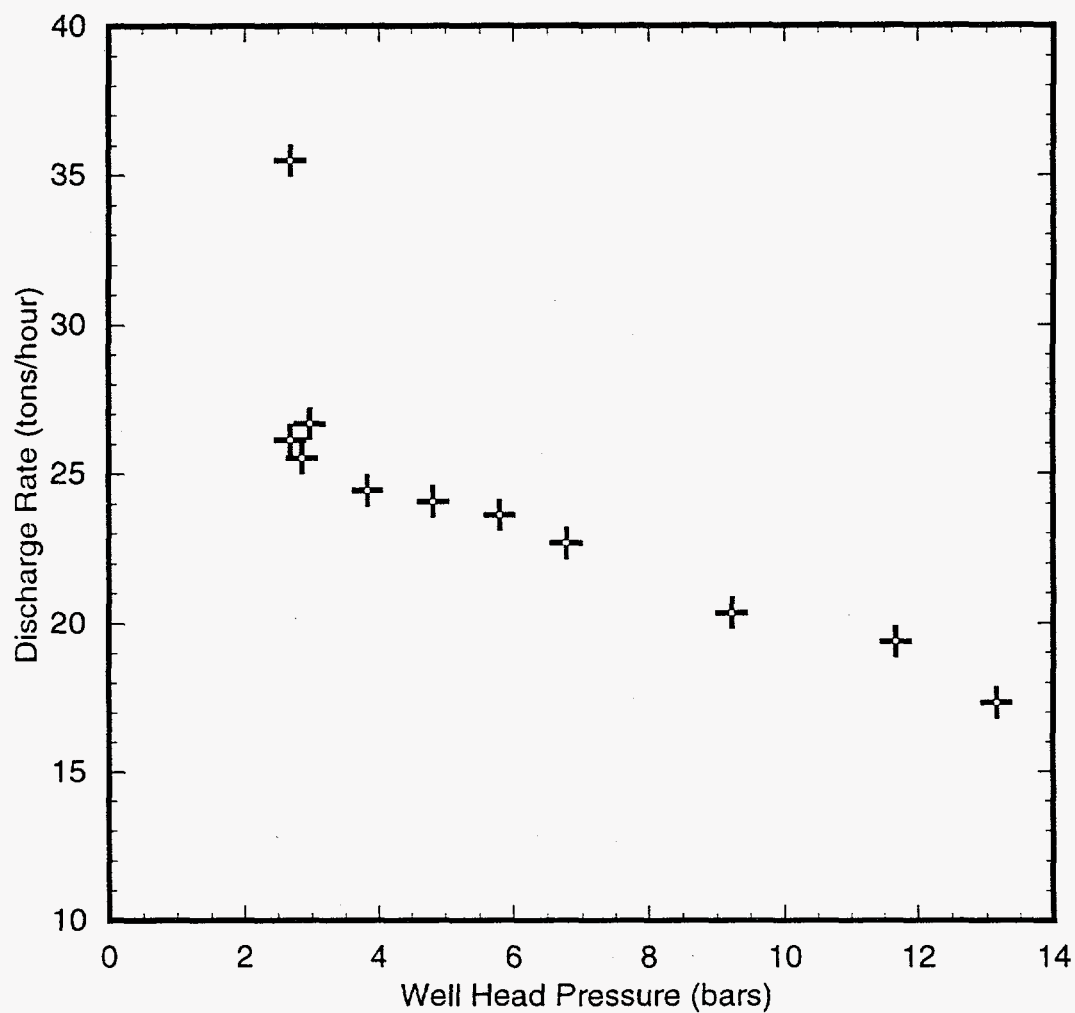


Figure 5.32. Discharge rate versus wellhead pressure for slim hole 52E-SM-2 (final completion) (October and November 1978).

52E-SM-2 causes *in situ* boiling; final completions of these slim holes discharge fluid with an enthalpy equal to that of liquid water in the reservoir. In an attempt to stimulate well productivity, cold river water was injected into wells S-4, SA-1, SA-2, SA-4 and SB-1 in April and May 1989. Cold water injection was ineffective in raising the productivity of wells S-4 and SA-2. Production from well SA-1 nearly doubled and that from SA-4 increased by about 25 percent. In as much as SB-1 was not discharged prior to cold river water injection, it is impossible to evaluate the efficacy of cold water injection for this well.

The measured maximum mass discharge rates for the various Sumikawa boreholes are presented in Table 5.4. It is apparent from Table 5.4 that the

maximum discharge for Sumikawa production wells varies over a wide range (from 28 tons/hour for SA-2 to 490 tons/hour for SC-1). Even for wells with liquid feeds and/or wells with limited *in situ* boiling, the discharge rate varies widely (from < 100 tons/hour for SD-1 to 490 tons/hour for SC-1). This large variation in discharge rates underscores the heterogeneous character of formation permeability at Sumikawa.

5.4 Effect of Borehole Diameter on Discharge Rate

Discharge characteristics of a geothermal borehole are principally controlled by (1) pressure losses associated with flow in reservoir rocks, and

Table 5-4. Measured maximum discharge rates for various Sumikawa boreholes.

Borehole Name	Final Diameter (mm)	Feedzone Depth (m TVD)	Measured Discharge Rate (T/hour)	Remarks
S-1	143	436	35	Produces only steam
S-2	101	900	4.1	Original hole; hole depth = 904.6 m <i>In situ</i> boiling
S-2	101	940	52	Liquid feed, redrilled hole
S-3	101	700	16	Liquid feed
S-4	159	1520	180	Limited <i>in situ</i> boiling
SA-1	216	1800	62	<i>In situ</i> boiling; produces mostly steam
SA-2	216	1450	28	<i>In situ</i> boiling; produces mostly steam
SA-4	216	1240	30	<i>In situ</i> boiling; produces steam
SB-1	216	1600	105	Liquid feed
SC-1	216	2310	490	Liquid feeds
SD-1	216	1200	100	Limited <i>in situ</i> boiling
52E-SM-2	101	550	5.1	Intermediate depth; hole depth = 803 m <i>In situ</i> boiling
52E-SM-2	79	980	27	Liquid feed, final completion

(2) pipe friction and heat losses in the wellbore. At Sumikawa, pressure losses in the reservoir constitute the bulk of pressure losses in boreholes for which discharge is accompanied by *in situ* boiling. Even for boreholes with liquid conditions at the feedzone depth, the pressure loss in the formation exceeds 10 bars (see Table 5.2 for boreholes S-2 and SC-1). This situation is quite different from that prevailing in the case of the Oguni Geothermal Field. At Oguni, the formation permeability is sufficiently high such that the pressure losses in the reservoir are insignificant compared to pressure losses in the borehole. The discharge behavior of an Oguni borehole is principally determined by pipe friction and heat losses in the wellbore. Pressure losses in the formation cannot, however, be neglected in the case of Sumikawa boreholes.

Pritchett (1993) employed numerical simulation to investigate the fluid-carrying capacity of boreholes of varying size. In the work by Pritchett (1993), the pressure losses in the formation were assumed to be negligible. Furthermore, the feedzone was assumed to contain single-phase liquid. Based on numerical simulations, Pritchett (1993) suggests that the maximum discharge rate M_{\max} will increase at a rate somewhat greater than the square of borehole diameter.

$$M_{\max} = M_o (d/d_o)^{2+n}, \quad n \geq 0$$

where M_o is the actual borehole discharge rate, and d and d_o are the internal borehole diameters (mm). The exact value of n will most likely vary with feedzone conditions (depth, pressure, enthalpy, and gas content). For the conditions assumed by Pritchett (depth = 1500 m, pressure 80 bars, single phase liquid at 250°C, uniform borehole diameter), n is approximately equal to 0.56. The conditions assumed in Pritchett's work do not hold for Sumikawa boreholes. There is a need to extend

Pritchett's work to investigate the effects of pressure losses in the reservoir and of *in situ* boiling on the flow capacity of geothermal boreholes.

The "area-scaled discharge rate" M^* is defined as follows:

$$M^* = M_o (d/d_o)^2$$

The "area scaled" and "scaled maximum ($n = 0.56$)" discharge rates for the Sumikawa slim holes are compared with measured discharge rates from large-diameter Sumikawa wells in Table 5.5. The discharge rates for wells SB-1 (liquid feed) and SD-1 (limited boiling) are approximately equal to the scaled maximum discharge rate for slim hole S-3. The discharge rates for wells SB-1, SD-1 and S-3 (scaled maximum discharge rate) are unusually small for wells with liquid feedzones; the discharge rate in this case is limited by low formation permeability and not by pressure losses in the borehole. The scaled maximum discharge rates for slim holes S-2 and 52E-SM-2 (liquid feeds) provide an adequate prediction for discharge from well S-4 (limited *in situ* boiling). The measured discharge rate for well SC-1 (liquid feeds), however, exceeds the scaled maximum discharge rate for slim holes S-2 and 52 E-SM-2 by about 25 percent. Well SC-1 is completed with 13 3/8 inch casing (internal diameter = 315 mm) above a depth of ~960 meters. The large diameter for the upper section of SC-1 is most likely responsible for the enormous discharge capacity of SC-1 (see Garg and Combs, 1997). The maximum discharge (scaled to a nominal 216 mm diameter) rates for Sumikawa boreholes with little or no *in situ* boiling (52E-SM-2, S-2, S-3, SB-1, SC-1, S-4, SD-1) range from 100 tons/hour (well SD-1) to 490 tons/hour (well SC-1). The comparable range for Oguni wells extends from 227 ton/hour (slim hole GH-7) to 488 ton/hour (slim hole GH-8). The upper limit for the

Table 5-5. Measured and predicted discharge rates for Sumikawa boreholes.

Borehole Name	Final Diameter (mm)	Measured Discharge Rate (tons/hour)	Area-Scaled Discharge* (tons/hour)	Scaled Maximum Discharge** (tons/hour)	Remarks
(A) Boreholes with liquid feeds and no <i>in situ</i> boiling					
52-E-SM-2	79	27	202	355	Final completion
S-2	101	52	238	364	Final completion
S-3	101	16	73	112	
SB-1	216	105			
SC-1	216	490			
(B) Boreholes with limited <i>in situ</i> boiling					
S-4	159	180	332	394	
SD-1	216	100			
(C) Boreholes with extensive <i>in situ</i> boiling					
52E-SM-2	101	5.1	23	36	Intermediate depth
S-2	101	4.1	19	29	Original hole
S-1	143	35	80	101	
SA-1	216	62			
SA-2	216	28			
SA-4	216	30			

* Area Scaled Discharge Rate = Measured Discharge Rate \times (216/well dia. in mm)²

** Scaled Maximum Discharge Rate = Measured Discharge Rate \times (216/well dia. in mm)^{2.56}

discharge rates is about the same for both the Sumikawa and Oguni boreholes. The Sumikawa boreholes do, however, display considerably more variability in discharge rates than the Oguni boreholes. In any event, the above-discussed data for Sumikawa boreholes taken in conjunction with Oguni data (Garg, *et al.*, 1994b), imply that the "scaled-maximum discharge rate" provides a reasonable first prediction of the discharge performance of large-diameter geothermal wells (with little or no *in situ* boiling).

The measured maximum discharge rates for Sumikawa boreholes with extensive *in situ* boiling are substantially lower than for boreholes with liquid feedzones. The average scaled maximum

discharge rate for slim holes 52E-SM-2, S-2, and S-1 is 55 tons/hour. By comparison, the average measured discharge rate for production wells SA-1, SA-2 and SA-4 is 40 tons/hour. The latter value for discharge rate (40 tons/hour) is not too different from that for Oguni well GH-15 (36 tons/hour). Oguni slim hole HH-2 has a scaled maximum discharge rate of 72 tons/hour. Based upon the available data from Oguni and Sumikawa boreholes (four slim holes, four large-diameter wells) with extensive *in situ* boiling, it appears that the "scaled maximum discharge rate" provides too high a prediction for the discharge rate of large-diameter wells. In all likelihood, the scaling rule ($n = 0.56$) derived for boreholes with liquid feeds and with little or no pressure loss in the formation, is not

applicable to boreholes with two-phase feeds. Additional theoretical work is needed to examine the scalability (or lack thereof) of discharge data from slim holes to predict the performance of large-diameter wells.

5.5 Summary

Discharge and injection data from slim holes and large-diameter wells at the Sumikawa Geothermal Field, Japan, were examined in an effort to establish relationships (1) between productivity of slim holes and large-diameter wells, (2) between injectivity and productivity indices of slim holes

and large-diameter wells, and (3) between productivity/injectivity indices and borehole diameter. The injectivity indices for Sumikawa boreholes do not depend in any systematic manner on the borehole diameter as was the case with the Oguni boreholes. Secondly, the productivity and injectivity indices for the Sumikawa boreholes with liquid feed zones are equal to first order as is the case with the Oguni boreholes. Finally, the Sumikawa borehole data imply that the "scaled-maximum discharge rate" provides a reasonable prediction of the production rate of large-diameter geothermal wells based on discharge data from slim holes.

6 Analysis of Pressure Transient Data

MMC has performed several single-well pressure drawdown/buildup and multiple-well pressure interference tests in the Sumikawa Geothermal Field. These pressure transient tests have helped in clarifying the permeability structure of the Sumikawa Geothermal Field. Interference tests have indicated the presence of (1) a high permeability north-south channel in the altered andesite layer, and (2) moderately high transmissivity dacitic layers in the "marine/volcanic" complex formation. In addition, it appears that the deep "granodiorite" reservoir penetrated by well SC-1 is isolated from the overlying altered andesite reservoir. The "altered andesite" and the "granodiorite" formations contain the principal geothermal aquifers at Sumikawa. Because of the low vertical permeability of the interbedded black shales, MMC plans to inject waste brine into the permeable dacitic layers in the "marine/volcanic complex" formation.

Analyses of Sumikawa pressure transient data obtained prior to mid-1990 have previously been presented by Pritchett, *et al.* (1989), Garg, *et al.* (1991, 1995) and Ishido, *et al.* (1992). Identification of the "altered andesite" formation as a high permeability reservoir is in large part based on the interpretation of two pressure interference tests (1986 and 1989 tests) between wells S-4 and N60-KY-1. A new interpretation of the latter pressure interference data is presented in Section 6.1.

In April and May 1989, MMC injected cold water into several wells (SA-1, SA-2, SA-4, S-4, SB-1, SB-2 and SB-3). During the injection test, several shutin wells (KY-1, S-3, S-4, SC-1,

and SD-1) were equipped with downhole capillary-tube pressure gauges. No definite evidence of pressure interference was found in the records obtained from wells S-3, S-4 or SC-1. Well SD-1 exhibited a pressure response to injection into well SB-3. Slim hole KY-1 responded to injection into wells S-4, SB-1 and SB-2. The pressure interference in KY-1 resulting from injection into S-4 is discussed in Section 6.1. The pressure changes associated with injection into wells SB-1, SB-2 and SB-3 are considered in Section 6.2.

Well SC-1 is the most prolific producer at Sumikawa. Pressure transient data are available from two injection tests and three discharge tests; these pressure data are discussed in subsection 6.3.

Maxwell's well test program DIAGNS (Alexander, *et al.*, 1992) was used to analyze the pressure transient data considered in Sections 6.1 - 6.3. DIAGNS is a workstation-based system for examination, processing, analysis, interpretation and inversion of well test data. For the present application, only the "INVERT" module of DIAGNS was required. The inversion module (INVERT) performs nonlinear least squares estimation of reservoir model parameters (*e.g.*, permeability-thickness, storage, skin, *etc.*) for a variety of mathematical models (*e.g.*, line-source, point-source, Warren-Root and MINC double porosity models, *etc.*). Confidence bounds, correlation and covariance matrices are also estimated to provide guidance in evaluating the confidence in and suitability of model parameters.

6.1 Wells S-4 and KY-1

Slim hole N60-KY-1 is cased and cemented to 1001 meters depth (-10 m ASL); uncemented slotted liner is present from that point to 1604 meters depth (-613 m ASL). Only two mud loss zones were encountered in the uncemented part of the hole; at -169 m ASL and at -571 m ASL. The deeper of these mud loss zones (-571 m ASL) is in the "altered andesite" formation; the shallow mud loss zone (at -169 m ASL) is contained in the "marine/volcanic" complex formation. Well S-4 was drilled vertically to a total depth of 1552 m ASL (-445 m ASL); the bottom of the 7-inch casing was set at 1071 meters (36 m ASL), and an open hole completion was used below this depth. The major feed-point for well S-4 is located at -413 m ASL in the "altered andesite" formation. The horizontal distance between S-4 and N60-KY-1 is about 1176 meters. It is highly likely that S-4 and N60-KY-1 communicate with each other through the altered andesites.

In the fall of 1986, well S-4 was discharged for approximately three months (September 2, 1986 to November 29, 1986); separated water (from the S-4 discharge stream) was injected into nearby relatively shallow slim hole S-2 (feed-zone depth = 940 meters = 131 m ASL). Four observation boreholes (O-5T, S-3, N60-KY-1 and SD-1) were equipped with capillary-tube pressure gauges. No pressure measurements were, however, made in either the production (S-4) or the injection boreholes. No pressure signal attributable to the discharge (or injection) of well S-4 (slim hole S-2) was seen in boreholes O-5T, S-3 and SD-1. On the other hand, a clear response associated with the discharge of S-4 was recorded in N60-KY-1; the overall amplitude of the pressure signal in N60-KY-1 exceeded 3 bars. Because of the low vertical permeability of the black shales, it is unlikely that injection into S-2 is in

any way responsible for the observed pressure signal in N60-KY-1. It is important to note here that the pressure in N60-KY-1 started to decline within a couple of hours after the initiation of discharge from well S-4.

Starting at 19:00 hours on May 16, 1989, cold river water was intermittently injected into well S-4 until 14:00 hours on May 19, 1989. Borehole N60-KY-1 was equipped with a capillary-tube type pressure gauge during the latter injection test. N60-KY-1 responded quickly (within a couple of hours) to each change in injection rate.

Pritchett, *et al.* (1989) analyzed the pressure response recorded in N60-KY-1 due to the 1986 discharge of well S-4. These authors postulated the presence of a north-south oriented permeable horizontal "channel" of constant cross-section area and uniform permeability; the feedpoints of S-4 and N60-KY-1 were assumed to lie within the permeable channel. The east, west, north, upper and lower boundaries of the channel are impermeable. To the south, the channel ends in a constant pressure boundary (presumably representing the influence of a two-phase region in the reservoir). Minimization of the deviations between measurements and computed pressures was used to infer the following parameter values:

- Channel cross-section area: 0.51 km²
- North-south permeability: 195 millidarcies
- Distance to northern (impermeable) boundary: 1.44 km north of N60-KY-1
- Distance to southern (constant pressure) boundary: 9.86 km south of S-4

Since the altered andesite layer is about 500 meters in thickness, the channel width (*i.e.*, east-west extent) is around 1 km.

The "channel model" outlined above, however, does a poor job of reproducing the high frequency pressure response recorded in N60-KY-1 during the 1989 injection test of well S-4. Garg, *et al.* (1991) discuss an alternative "anisotropic line-source" model for the 1986 and 1989 tests. The "channel model" assumes that the east-west permeability is sufficiently large such that the reservoir behaves in an essentially one-dimensional manner; by way of contrast, Garg, *et al.* (1991) require the east-west permeability to be much smaller than the north-south permeability. With the exception of the east-west permeability, the "anisotropic line-source model" is similar to the "channel model" as regards to reservoir cross-section area and the distances to the northern and southern boundaries.

Ishido, *et al.* (1992) presented a "double porosity channel model" to reproduce the 1986 and 1989 tests. The "double porosity channel model" has the same geometry, boundary conditions and global properties (transmissivity and storativity) as the "channel model" reported by Pritchett, *et al.* (1989). Ishido, *et al.*, attributed the lack of good agreement between the short term 1989 injection test and the "original channel model" to the latter's porous medium assumption. (The use of a porous medium representation for fractured rocks is tantamount to assuming that pressures equilibrate instantaneously between the high permeability "fracture zone" and the low permeability "country rock".) A MINC representation (Pruess and Narasimhan, 1985) was invoked by Ishido, *et al.* (1992) to represent the fractured reservoir behavior.

The pressure responses computed by the "anisotropic line-source model" (Garg, *et al.*, 1991) and by the "double porosity channel model" (Ishido, *et al.*, 1992) for both the 1986 and 1989 appear to agree reasonably well with the pressure measurements. Both Garg, *et al.*

(1991) and Ishido, *et al.* (1992) used an "effective discharge-rate history" for S-4 (1986 test) originally derived by Pritchett, *et al.* (1989). It is significant that the "effective discharge rate history" for S-4 (1986 test) does not strictly speaking, represent measured values; Pritchett, *et al.* (1989) invoked a variety of assumptions to derive this "effective discharge-rate history". In the following, we will reconsider the 1986 discharge rates for S-4 and present an alternate interpretation. This alternate interpretation of discharge data is in turn used to arrive at a new reservoir model.

6.1.1 Discharge Rate History (1986) for Well S-4

Well S-4 discharge was initiated at 11:20 hours LT on September 2, 1986, and ended at 16:30 hours LT on November 3, 1986. The flow rate measurements performed during the S-4 discharge are summarized in Table 6.1. Apparently, no measurements of water discharge rate were made between September 27, 1986 and November 2, 1986, which represents more than half the discharge interval. Despite these missing data, the pattern for the total discharge rate (water + steam) is quite clear. At the start of the test, the discharge rate was about 50 kg/s. Within a day, the flow rate declined to ~ 42 kg/s; thereafter, the flow rate remained more or less constant for about a week. Around September 13, 1986, the flow rate began to increase slowly, and reached the initial value (~ 50 kg/s) just prior to shutin on November 3, 1986.

Although no downhole pressure measurements in well S-4 were made during the 1986 discharge test, it is certain that two-phase (water/steam) boiling flow was induced locally in the reservoir adjacent to the S-4 feedpoint by the pressure reduction associated with the discharge.

Table 6.1. Measured discharge rates (1986) from well S-4.

Date	Steam Discharge	Water Discharge	Total Discharge
02 September 1986	32 kg/s	18 kg/s	50 kg/s
03 September 1986	28 kg/s	14 kg/s	42 kg/s
05 September 1986	27 kg/s	15 kg/s	42 kg/s
08 September 1986	26 kg/s	16 kg/s	42 kg/s
13 September 1986	26 kg/s	18 kg/s	44 kg/s
20 September 1986	26 kg/s	20 kg/s	46 kg/s
26 September 1986	27 kg/s	20 kg/s	47 kg/s
30 September 1986	26 kg/s	?	?
09 October 1986	26 kg/s	?	?
18 October 1986	26 kg/s	?	?
27 October 1986	26 kg/s	?	?
03 November 1986	26 kg/s	24 kg/s	50 kg/s

Note: Well S-4 discharge began 02 September at 11:20, and ended 03 November at 16:30

The principal feedzone for S-4 lies at a depth of 1520 meters. The stable feedzone pressure and temperature are estimated to be 93 (± 1) bars and (295–300)°C, respectively. The saturation pressure at which water will boil at (295–300)°C is (80–86) bars. Thus, a pressure reduction of (7–13) bars at the feedzone will result in *in situ* boiling. The productivity/injectivity index for S-4 is of the order of 1 kg/s-bar (Section 5); in other words, the pressure drop for a discharge rate of 50 kg/s is ~ 50 bars. It is thus likely that *in situ* boiling occurred more or less simultaneously with the initiation of discharge from S-4 on September 2, 1986. Pritchett, *et al.* (1989) assumed that *in situ* boiling did not start until September 7, 1986 (*i.e.*, five days after the start of S-4 discharge test). The argument advanced by Pritchett, *et al.*, (a decrease in the pressure decline rate in N60-KY-1 around September 7) in support of a delayed *in situ* boiling is rather tenuous. We maintain that *in situ* boiling started almost im-

mediately after the start of discharge from well S-4.

The two-phase region created during the S-4 discharge test was very likely of limited extent. The average temperature in the region between S-4 and N60-KY-1 is about 250°C. To boil water at 250°C would require a pressure reduction exceeding 50 bars, and only 3 bars reduction was observed at N60-KY-1. Therefore, it is likely that the flow between S-4 and N60-KY-1 was single-phase during the discharge test except for a two-phase region immediately surrounding the S-4 feedpoint. Garg and Pritchett (1988) discuss methods for analyzing pressure interference data from a hot water geothermal reservoir which evolves into a two-phase system as a result of fluid production, and in which the observation well remains in the single-phase (liquid) part of the reservoir. According to Garg and Pritchett (1988), single-phase solutions may

be applied for interference test interpretation provided that the discharge rate history used in the analysis is suitably modified to reflect the influence of the two-phase zone. The "effective discharge rate" for use in analysis is only a fraction of the actual (or measured) discharge rate. Estimation of the "effective discharge rate" requires detailed downhole feedpoint pressure histories and continuous measurements of discharge data in the production well; such measurements were not made during the 1986 discharge test.

Pritchett, *et al* (1989) used the following procedure to estimate the "effective discharge rate history" for well S-4 after September 7, 1986 (*i.e.*, after the presumed start of *in situ* boiling). Shortly after the start of discharge of S-4, the pressures in N60-KY-1 started declining at a rate of ~ 80 bars/year. After the S-4 discharge was stopped on November 3, 1986, the pressures (in N60-KY-1) began to recover initially at a rate of ~ 40 bars/year (Figure 6.1). Linear superposition theory implies that the change in slope of the pressure history (-80 bars/year) at the onset of discharge should bear the same relation to the causative change in discharge rate (0 to 50 kg/s) that the change in slope at shutin (from -8 bars/year to +40 bars/year = 48 bars/year) bears to the relevant change in discharge rate, *i.e.*,

$$\frac{\dot{M}^* - \dot{M}^{**}}{\dot{M}_o} = \frac{48}{80} = 0.6, \quad (6.1)$$

where

\dot{M}_o = effective discharge rate at the start of discharge test,

\dot{M}^* = effective discharge rate prior to shutin,

\dot{M}^{**} = after flow rate.

The afterflow \dot{M}^{**} will usually be a small fraction of the discharge rate. It may, however, persist for a long period of time, until the entire

steam zone has condensed away. Assuming that \dot{M}_o and \dot{M}^{**} equal 50 kg/s and 4 kg/s respectively (Pritchett, *et al.*, 1989), \dot{M}^* was estimated to be ~ 34 kg/s. The "effective discharge rate" for well S-4 utilized by Pritchett, *et al.* (1989) in their analysis of pressure interference response is given in Table 6.2.

Table 6.2. Effective discharge-rate history for well S-4 used by Pritchett, *et al.* (1989).

Time Interval			\dot{M}_e
08/04	20:00 to 09/02	11:20	0 kg/s
09/02	11:20 to 09/03	12:00	50 kg/s
09/03	12:00 to 09/07	00:00	42 kg/s
09/07	00:00 to 11/03	16:30	34 kg/s
11/03	16:30 to 11/29	09:00	4 kg/s

In so far as we believe that boiling started immediately after the initiation of discharge from S-4, it is unlikely that \dot{M}_o (*i.e.*, initial effective discharge rate) equals 50 kg/s (= total discharge rate); it is rather likely that \dot{M}_o is substantially smaller than 50 kg/s. In the next section, we discuss a possible approach to the determination of \dot{M}_o . Perhaps, it is worth emphasizing here that we do not object to the use of Equation (6.1) by Pritchett, *et al.* (1989). We do not, however, accept the hypothesis that *in situ* boiling did not start until September 7, 1986.

6.1.2 Determination of Initial Effective Discharge Rate \dot{M}_o for Well S-4 (1986 test)

In May 1989, cold water was injected intermittently into well S-4; the injection rate history is given in Table 6.3. Injection rates are quoted in cubic meters per second; for present

Continued on page 6-7

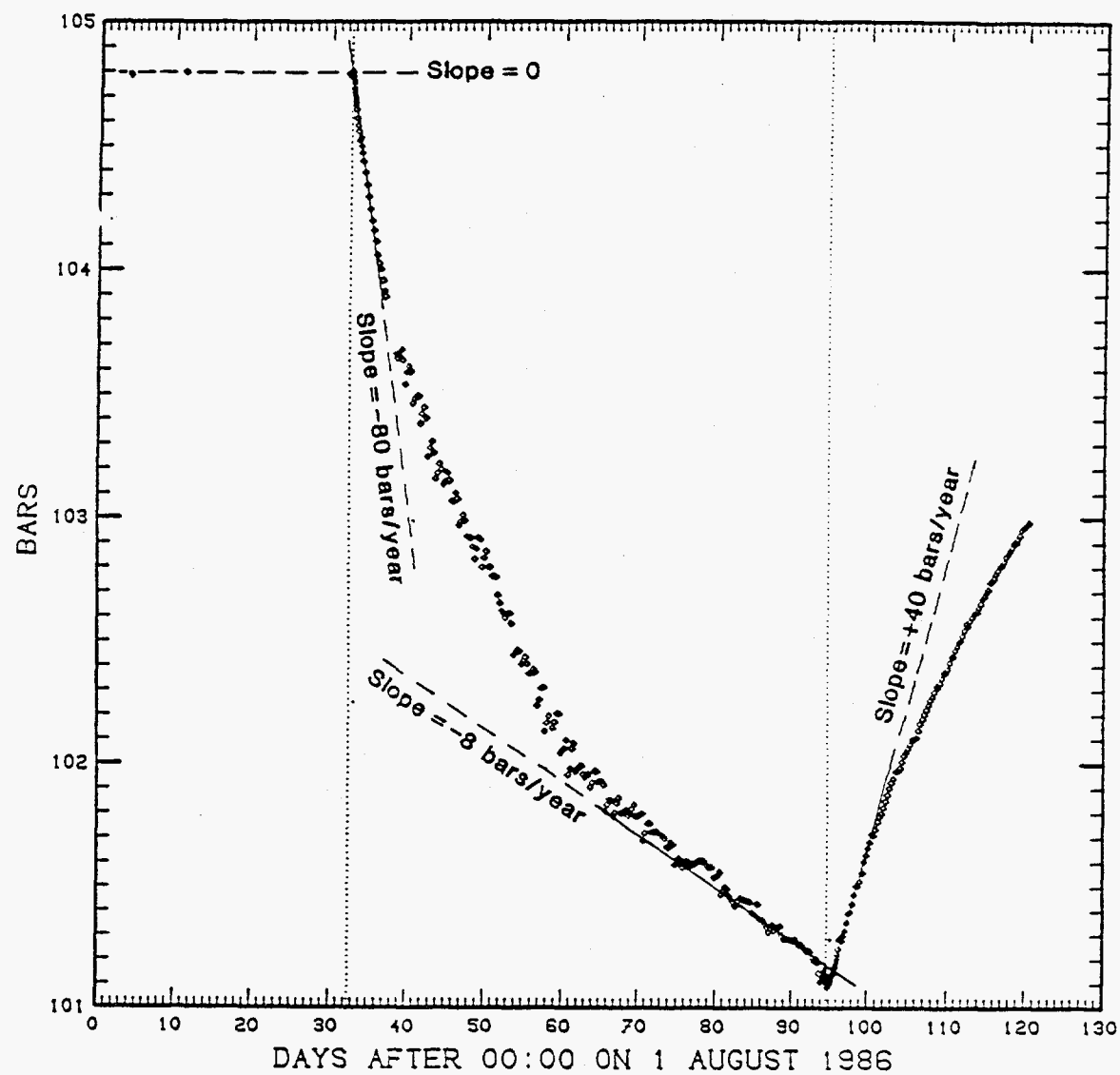


Figure 6.1. Measured pressure interference signal in well N60-KY-1 (1986). Pressures have been adjusted for gaps/offsets in measurements.

Table 6.3. Flow rate history for cold water injection into well S-4 (May 1989). All times are in hours since 00:00 hours LT on March 1, 1989.

Time Interval (Hours)			\dot{M}_{inj} (m ³ /s)
1843.0	–	1850.0	0.1139
1850.0	–	1865.933	0.
1865.933	–	1876.0	0.1230
1876.0	–	1889.167	0.
1889.167	–	1900.0	0.1214
1900.0	–	1904.0	0.0191
1904.0	–	1906.0	0.0339
1906.0	–	1908.0	0.0689
1908.0	–	1912.0	0.0970
1912.0	–		0.

purposes it suffices to assume that 1 m³/s equals 1000 kg/s. The measured pressure response in N60-KY-1 is shown in Figure 6.2. Each change in S-4 flow rate produces a distinct pressure response in N60-KY-1; the lag time between flow rate and discernible pressure changes is between 1 and 2 hours. From 1843 to 1850 hours, the injection rate into S-4 was about 114 kg/s. The pre-injection pressure in N60-KY-1 was 71.629 bars. The pressure in N60-KY-1 did not start increasing until some time after 1844 (*i.e.*, 1 hour after the start of injection) hours (Figure 6.2). Between 1844 and 1851 hours, the pressure increased to 71.939 bars; this corresponds to a pressure change (Δp) of 0.31 bars.

Garg and Pritchett (1990) present an approximate analytic solution for cold water injection into a single-phase hot water reservoir. Beyond the cold front surrounding the injection well, the pressure response is determined by the

kinematic viscosity of the *in situ* fluid. This means that the pressure response of well N60-KY-1 to injection into S-4 should be computed using *in situ* fluid properties (viscosity, density, compressibility, *etc.*). Stated somewhat differently, temperature of the injected fluid is irrelevant as far as the pressure response of N60-KY-1 is concerned. The latter result together with linear superposition theory implies that the pressure change in N60-KY-1 should bear the same relation to injection rate (1989 test) and to effective discharge rate (1986 test). Prior to the start of the 1986 discharge test (at 11:20 hours on September 2, 1986), the pressure in N60-KY-1 was 104.796 bars; by 19:20 hours on September 2, 1986 (*i.e.*, 8 hours after the start of discharge test), the pressure in N60-KY-1 had declined to 104.710 bars resulting in a pressure change (Δp) of 0.086 bars. Given the amplitudes of pressure changes over comparable time periods (8 hours after the start of discharge/injection) during the 1986 discharge (0.086 bars) and 1989 injection (0.310 bars) tests, and the injection rate (114 kg/s) for the 1989 test, the effective discharge rate \dot{M}_o for the early part of the 1986 test can be computed as follows:

$$\dot{M}_o = \frac{114 \times 0.086}{0.310} \approx 30 \text{ kg/s.}$$

The initial effective discharge rate \dot{M}_o is thus 60 percent of the measured total discharge rate (50 kg/s) on September 2, 1986.

In as much as the total discharge rate during the 1986 test varied considerably, it is likely that the "effective discharge rate" also underwent changes. Equation (6.1) implies that the change in effective discharge rate at shutin on November 3, 1986 was about 0.6 \dot{M}_o (~ 18 kg/s). Variations in the effective discharge rate prior to shutin (or the afterflow rate after shutin) cannot, how-

Continued on page 6-9

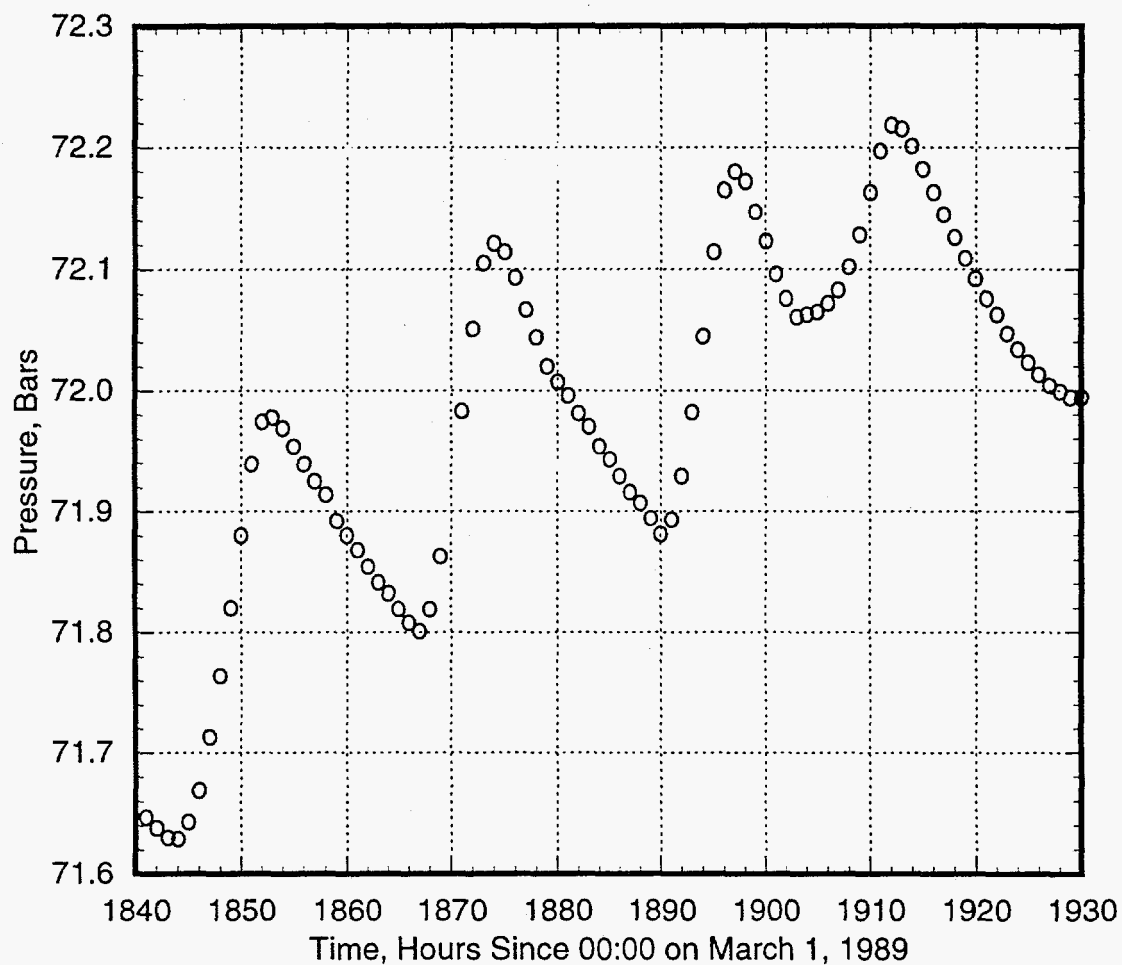


Figure 6.2. Measured pressure interference signal in N60-KY-1 due to injection into well S-4 (May 1989). All times are in hours since 00:00 hours LT on March 1, 1989.

ever, be determined from the available data. Stated somewhat differently, we regard the effective discharge rate history for S-4 (1986 test) to be unknown. In the following, we will consider several reasonable effective discharge rate histories for S-4, and examine the effect of such discharge rate variations on the computed formation parameters.

6.1.3 Analysis of 1989 Interference Test

The pressure interference response recorded in N60-KY-1 during the 1989 test was modeled using the line-source model. Both S-4 and N60-KY-1 are assumed to fully penetrate an infinite reservoir. The 1989 test data can be fitted adequately without invoking the existence of any boundaries. The average reservoir temperature in the region occupied by S-4 and N60-KY-1 is about 250°C. Dynamic viscosity and density for liquid water at a temperature of 250°C are approximately 10^{-4} Pa-s and 800 kg/m³, respectively. In the process of modeling the pressure interference data, the initial pressure p_i was kept fixed at 71.629 bars. The only unknown parameters in the model are permeability-thickness kh and storage ϕch . Two different analyses were performed using pressure/flow rate data for (1) first injection/fall-off cycle ($t = 1843$ – 1866 hours), and (2) complete 1989 injection test ($t = 1843$ – 1930 hours). The unknown parameters kh and ϕch were varied to obtain the best possible match between the measured and computed pressures (Figures 6.3 and 6.4). The final model parameters are:

(i) First injection/fall-off cycle

$$\begin{aligned} kh &= 16.3 \text{ darcy-m} \\ \phi ch &= 8.45 \times 10^{-9} \text{ m/Pa} \end{aligned}$$

(ii) Complete injection test

$$\begin{aligned} kh &= 14.8 \text{ darcy-m} \\ \phi ch &= 7.89 \times 10^{-9} \text{ m/Pa} \end{aligned}$$

To evaluate the robustness of the inferred model parameters, it is useful to examine the sensitivity of the mathematical fit to variations in model parameters (kh , ϕch). Variation of the normalized sum of squares of residuals

$$\frac{\sum [P_{\text{measured}} - P_{\text{computed}}(kh, \phi ch)]^2}{\sum [P_{\text{measured}} - P_{\text{best fit}}]^2}$$

with kh and ϕch is shown in Figures 6.5 and 6.6. It is reasonable to assume that all acceptable parameter values are enclosed by the contour labeled 2 in Figures 6.5 and 6.6. Therefore, it follows that the two sets of parameter values obtained from the two separate analyses described above are compatible with each other. Thus, the best estimates for formation kh and jch from the 1989 data are 15.6 (± 0.8) darcy-m and 8.2 (± 0.3) 10^{-9} m/Pa, respectively.

In an effort to evaluate the appropriateness of the line-source model, additional analyses of 1989 pressure data were performed using several other mathematical models (e.g., finite wellbore line-source model, Warren-Root and MINC/gradient flow double porosity models). No significant improvement (over the line-source model) in fit to pressure data was obtained. We, therefore, conclude that the line-source model provides the proper framework for analyzing the 1989 pressure interference test between S-4 and N60-KY-1.

6.1.4 1986 Pressure Interference Test: Early Response

In this section, we will consider the pressure response recorded in N60-KY-1 during the

Continued on page 6-14

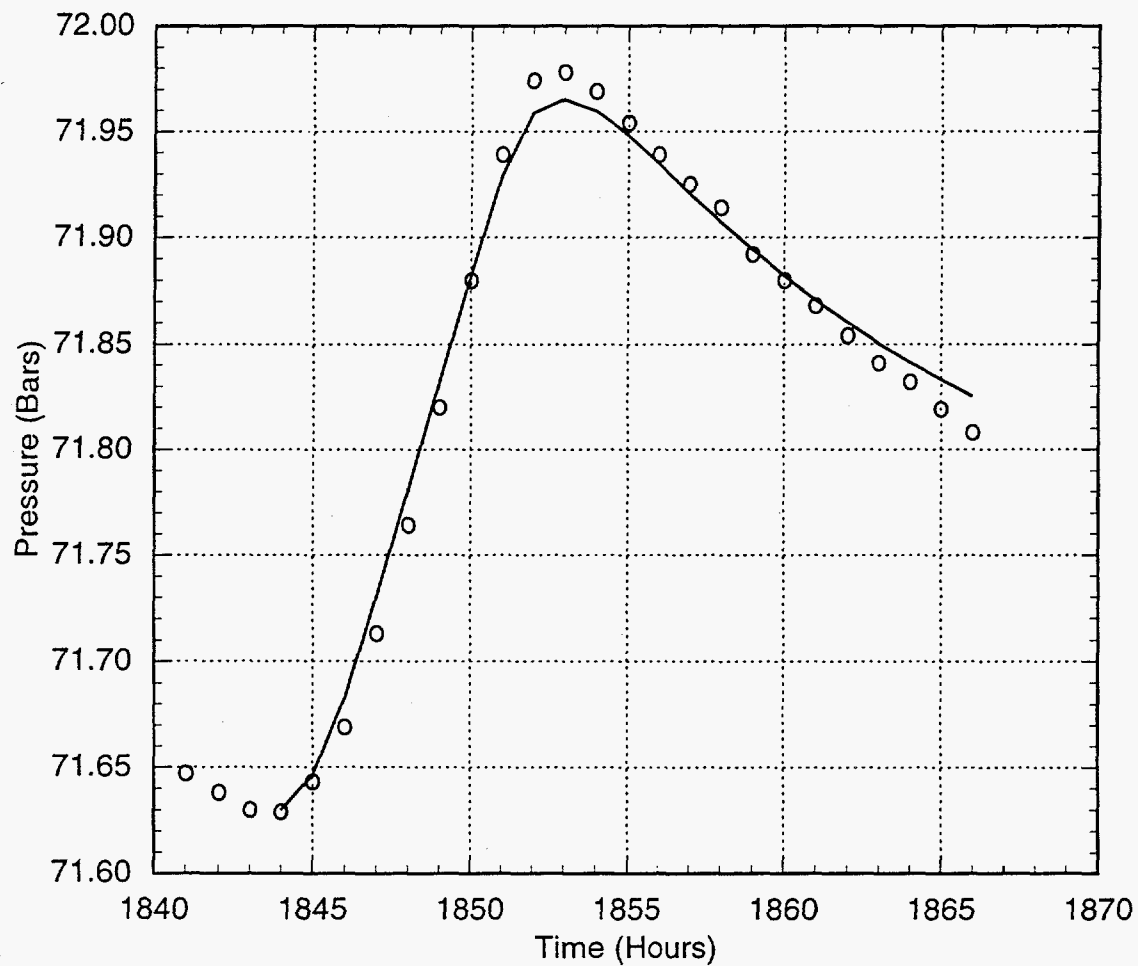


Figure 6.3. Comparison between measured (o) and computed (—) pressures in N60-KY-1 for the first injection/fall-off cycle. All times are in hours since 00:00 hours LT on March 1, 1989.

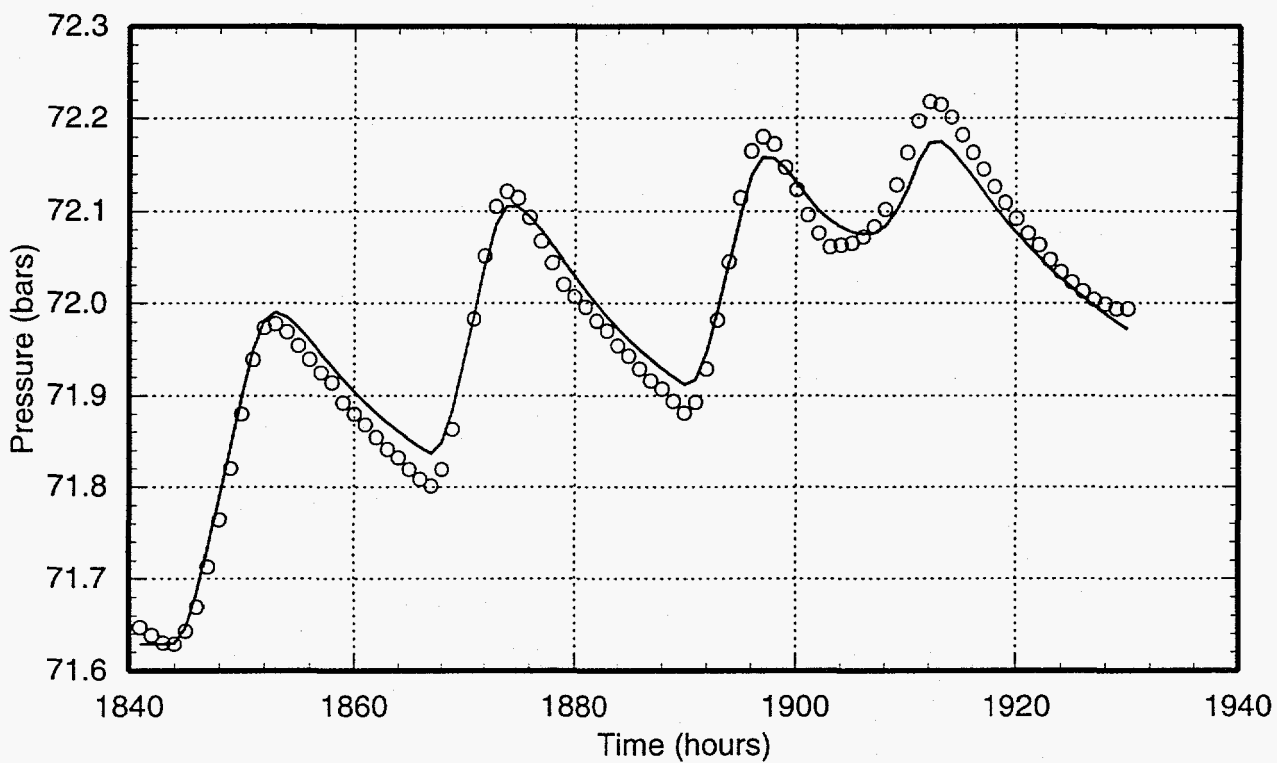


Figure 6.4. Comparison between measured (o) and computed (–) pressures in N60-KY-1 during the 1989 test. All times are in hours since 00:00 hours LT on March 1, 1989.

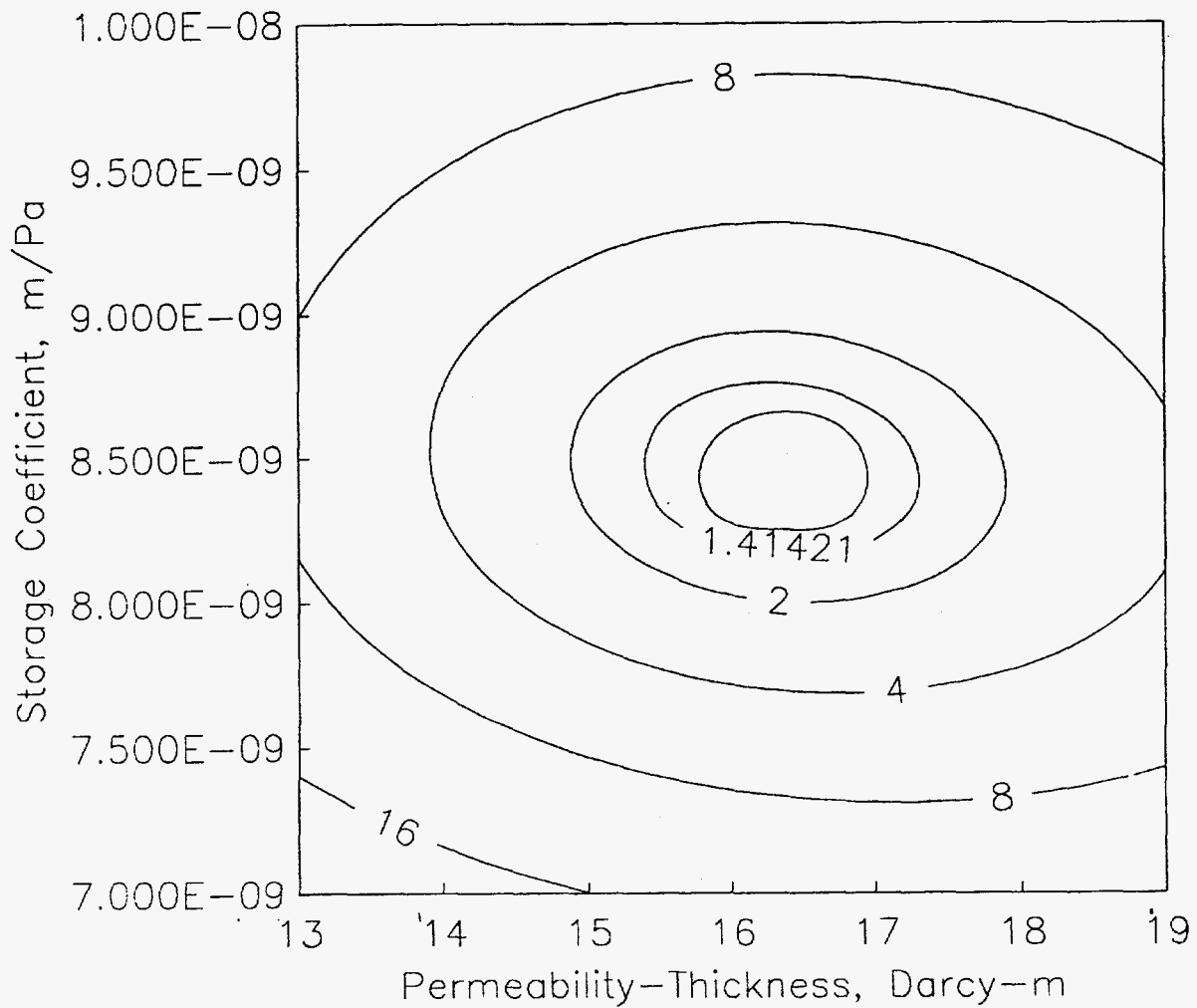


Figure 6.5. Variation of normalized (normalized with respect to the optimum fit) sum of squares of residuals with kh and ϕch for the pressure interference response of N60-KY-1 (first injection cycle, May 1989). Contour levels are 1.19, 1.41, 2, 4, 8 and 16.

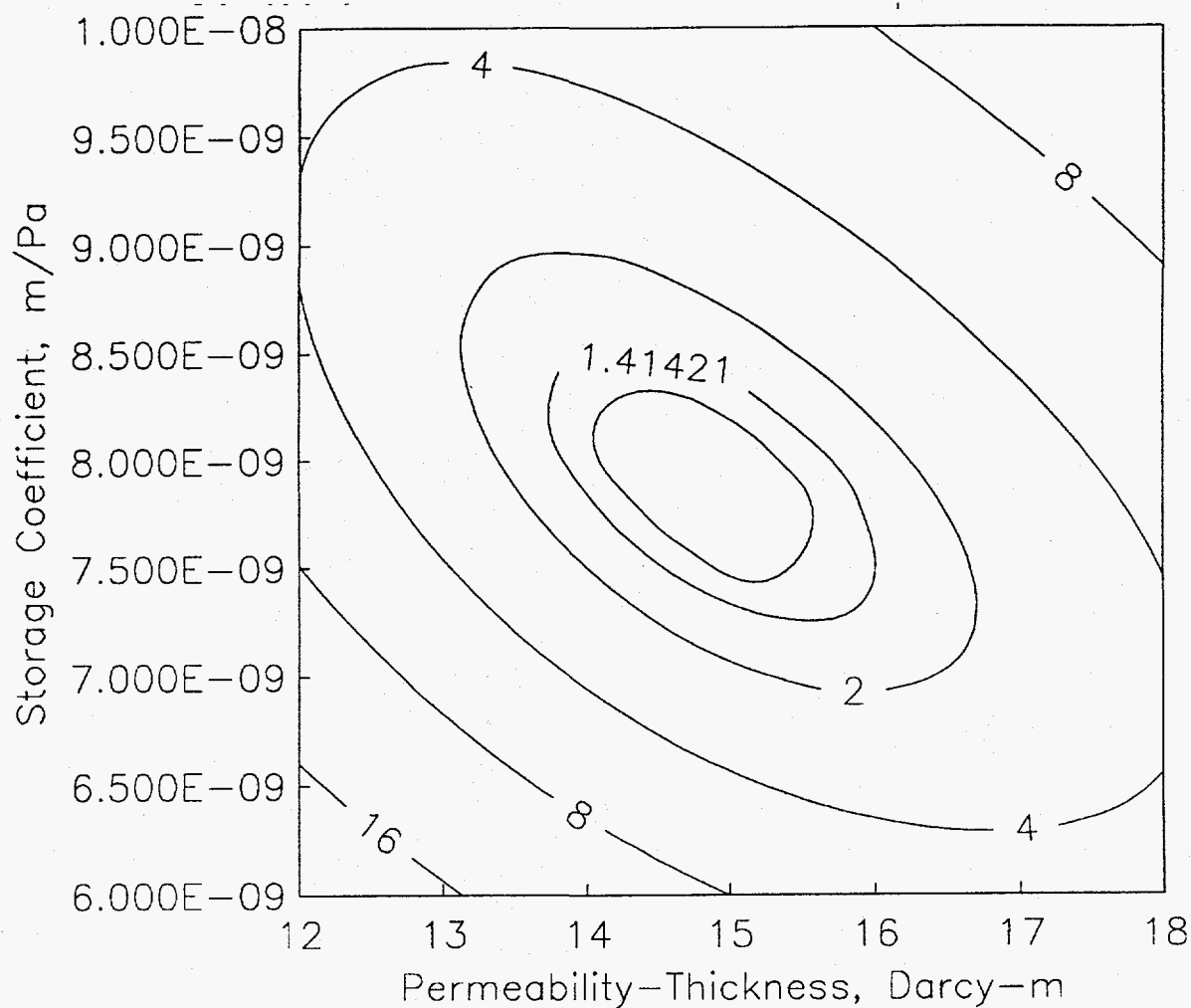


Figure 6.6. Variation of normalized (normalized with respect to the optimum fit) sum of squares of residuals with kh and ϕch for the pressure interference response of N60-KY-1 (complete injection test, May 1989). Contour levels are 1.19, 1.41, 2, 4, 8 and 16.

first 24 hours of the 1986 discharge test. Our choice of the time interval (*i.e.*, the time interval between the start of discharge test at 11:20 hours on September 2 to 12:00 hours on September 3) is dictated by the following considerations. The duration of the first injection/fall-off cycle during the 1989 injection test was approximately 24 hours. To meaningfully compare the formation parameters inferred from the 1986 and 1989 tests, it is essential to consider similar time periods for the two tests. Analysis of 1989 pressure interference data for the first injection/fall-off cycle did not indicate the presence of any boundaries; it is, therefore, likely that the early portion of 1986 test data is most diagnostic of formation properties. Finally, we note that except for the early part of the flow test, the "effective discharge-rate" history for the 1986 test is not well characterized.

Like the 1989 test, the pressure interference response observed in N60-KY-1 during the 1986 test was modeled using the line-source solution. As before, both S-4 and N60-KY-1 are assumed to fully penetrate an infinite aquifer. The initial pressure p_i was kept fixed at 104.796 bars. (Note that the pressure gauge was set at different depths in the 1986 and the 1989 tests.) The *in situ* dynamic viscosity and density for the liquid were taken to be 10^{-4} Pa-s and 800 kg/m^3 , respectively. The effective discharge rate for S-4 (see Section 6.1.1) was assumed to remain constant ($=30 \text{ kg/s}$) for the first 24 hours of the discharge test. Minimization of the deviations between the measured and computed pressures gave the following values for the unknown model parameters (kh , ϕch):

$$\begin{aligned} kh &= 12.9 \text{ darcy-m} \\ \phi ch &= 7.32 \times 10^{-9} \text{ m/Pa} \end{aligned}$$

The measured and computed pressures (Figure 6.7) are in excellent agreement. The variation of the normalized sum of squares of residu-

als with variations in kh and ϕch is shown in Figure 6.8. A comparison between Figures 6.5 and 6.8 shows that the kh values inferred for the 1986 and 1989 tests are consistent with each other; the ϕch value obtained from the 1986 test is slightly lower than that implied by the 1989 test. In the latter connection, we note that the "effective discharge rate" for the 1986 test (30 kg/s) is not very precise; variations of the order of 10 to 20 percent in the "effective discharge rate" cannot be ruled out. A second calculation was accordingly run using an effective discharge rate of 33 kg/s (*i.e.*, increasing the effective discharge rate by 10 percent); this analysis resulted in a 10% increase in the inferred values for kh (14.2 darcy-m) and ϕch ($8.05 \times 10^{-9} \text{ m/Pa}$). The latter result implies that for the 1986 test, both kh and ϕch scale linearly with the effective discharge rate. Considering the range of uncertainty for the 1986 effective discharge rate, it is reasonable to conclude that the model parameters (kh , ϕch) obtained from the 1986 and 1989 tests are consistent.

6.1.5 1986 Pressure Interference Test: Late Time Response

The uncertainties associated with the S-4 effective discharge rate make it impossible to obtain a unique interpretation of the observed pressure interference signal in N60-KY-1. In this subsection, we will examine the effect of uncertainties in the effective discharge rate on the inferred formation parameters. To provide a comparison with the previous work of Pritchett, *et al.* (1989), the effective discharge rate for the base case (case 1) was assumed to be 60 percent of that used (Table 6.2) by Pritchett, *et al.* (1989). The line-source solution was used to fit the pressure response in N60-KY-1. The best fit was obtained by assuming that the aquifer penetrated by S-4 and N60-KY-1 is bound by impermeable bound-

Continued on page 6-17

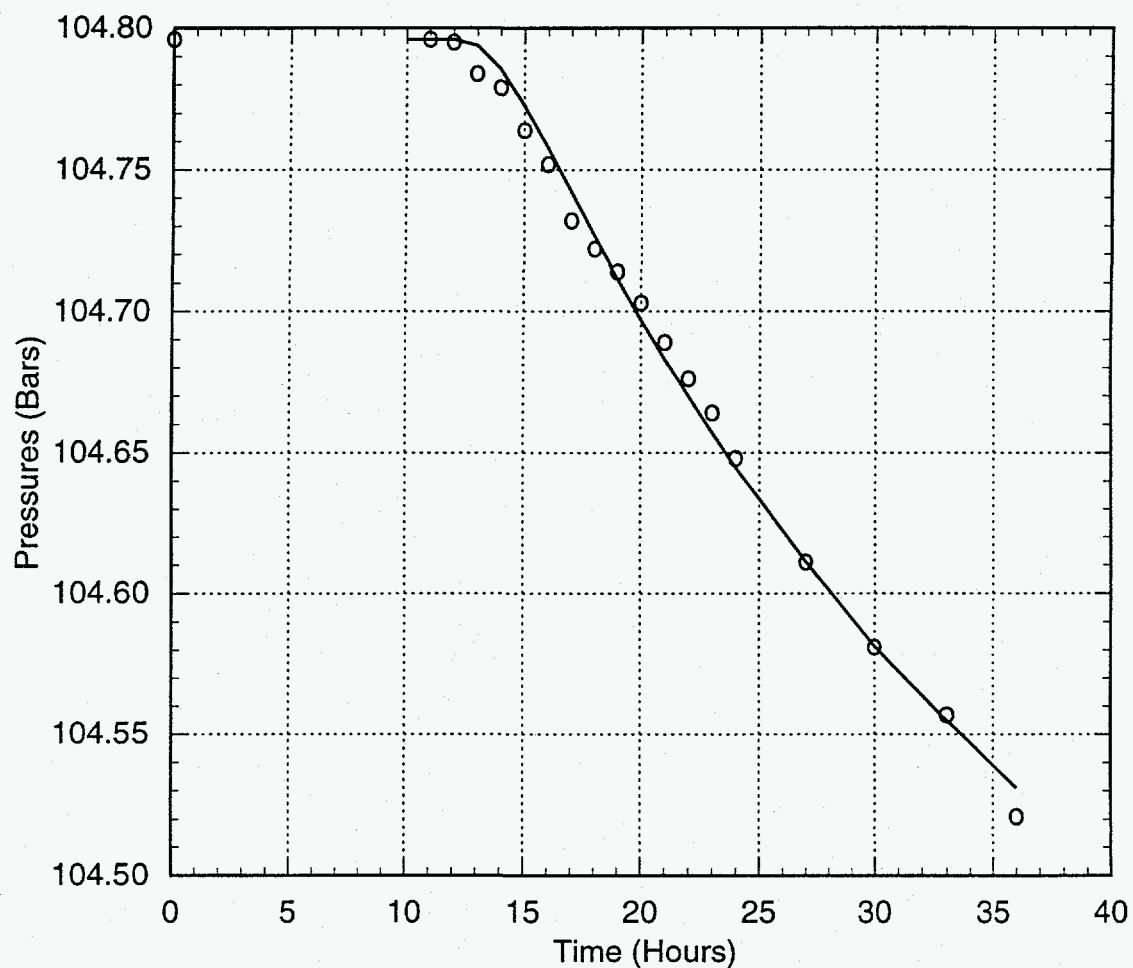


Figure 6.7. Comparison between measured (o) and computed (—) pressures in N60-KY-1 during the early part (*i.e.*, first 24 hours) of the 1986 test. All times are in hours since 00:00 hours LT on September 2, 1986.

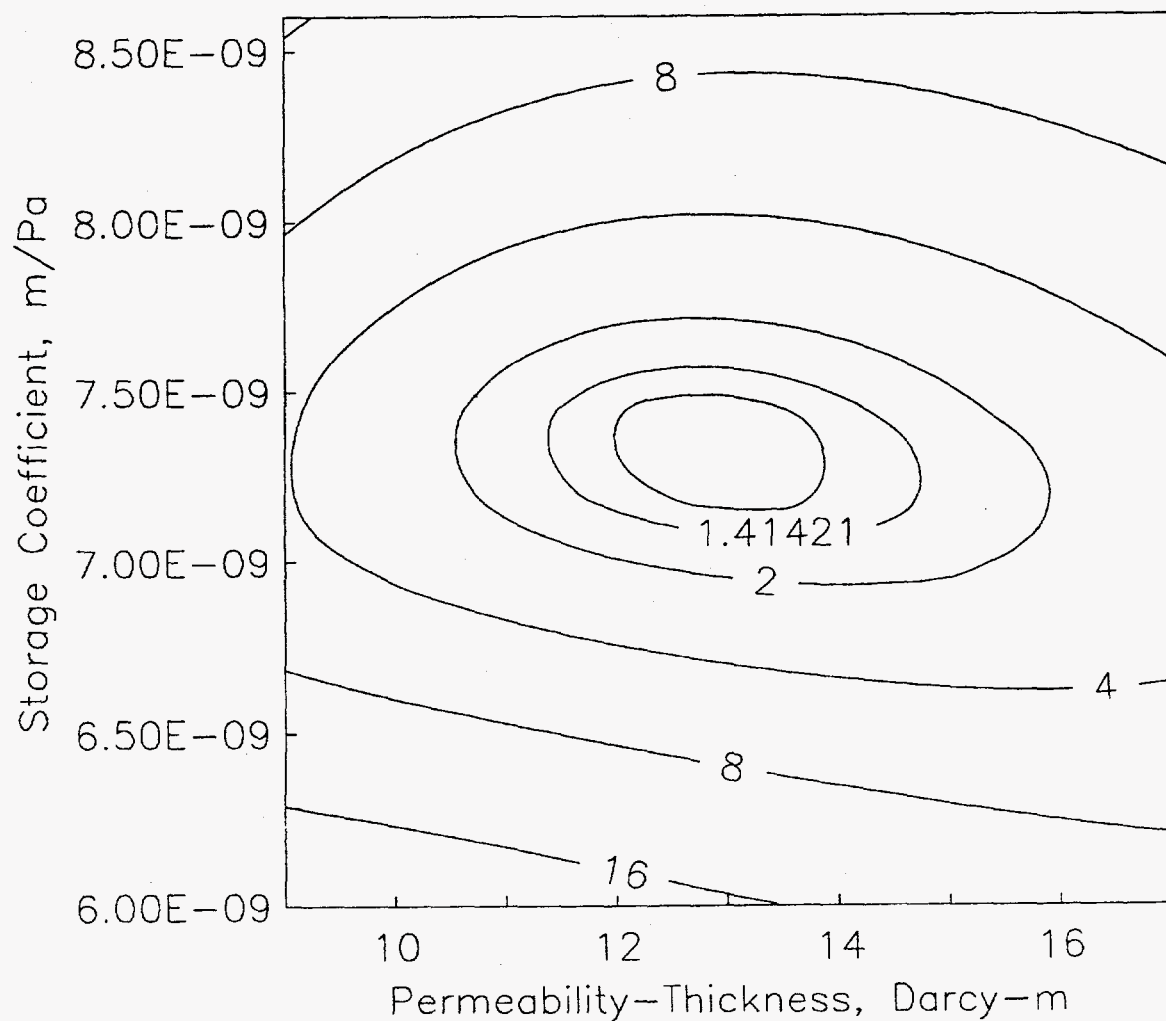


Figure 6.8. Variation of normalized (normalized with respect to the optimum fit) sum of squares of residuals with kh and qch for the early part of the 1986 test. Contour levels are 1.19, 1.41, 2, 4, 8 and 16.

Table 6.4. Formation parameters inferred using different effective discharge rate histories for well S-4 (1986 test).

	Case 1	Case 2	Case 3	Case 4	Case 5
Permeability-thickness kh (darcy-m)	13.5	13.5	13.5	9.7	13.8
ϕch storage (m/Pa)	8.1×10^{-9}	8.7×10^{-9}	8.5×10^{-9}	8.2×10^{-9}	8.0×10^{-9}
Distance to western impermeable boundary (km east of N60-KY-1)	1.77	2.08	4.31	10.0	1.88
Distance to eastern impermeable boundary (km east of N60-KY-1)	2.00	2.32	1.87	1.61	2.06
Distance to northern impermeable boundary (km north of N60-KY-1)	1.19	1.55	0.95	1.07	1.61
Distance to southern constant pressure boundary (km south of N60-KY-1)	9.43	6.87	10.1	No boundary	10.5

aries to the east, the west and the north; to the south, a constant pressure boundary (presumably reflecting the presence of a two-phase zone) terminates the aquifer. The formation parameters inferred for case 1 are given in Table 6.4. The computed pressure history for N60-KY-1 is in good agreement with the measurements (Figure 6.9). The east-west width (w) of the permeable aquifer is about 3.8 km; thus, kA ($= khw$) is estimated to be ~ 51 mdarcy-km². The latter value for kA is approximately 50 percent of that (~ 99 mdarcy-km²) obtained by Pritchett, *et al.* (1989). Pritchett, *et al.* assumed the formation porosity ϕ and compressibility c to be 0.05 and 1.7×10^{-9} Pa⁻¹, respectively; with A equal to 0.51 km², the areal storage (ϕcA) calculated by Pritchett, *et al.* is $\sim 4.3 \times 10^{-5}$ m² Pa⁻¹. The areal storage ϕcA ($= \phi chw$) obtained from the present in-

terpretation ($\sim 3.1 \times 10^{-5}$ m² Pa⁻¹) is about 70 percent of that given by Pritchett, *et al.* Recalling that the effective discharge rates used for the present interpretation are only 60 percent of those employed by Pritchett, *et al.* (1989), we conclude that the formation parameters (*i.e.*, kA , ϕcA) obtained from the two interpretations are similar.

To assess the impact of uncertainties in the effective discharge rate history for S-4 on the inferred formation parameters, four additional effective discharge rate histories (cases 2 through 5, Table 6.5) were considered. In all cases, the initial effective discharge rate was kept at 30 kg/s; furthermore, the jump in discharge rate at the moment of shutin (1504.5 hours, Table 6.5) was taken to be 18 kg/s (see Section 6.1.2). The discharge rate history for case 2 is the simplest; both

Continued on page 6-20

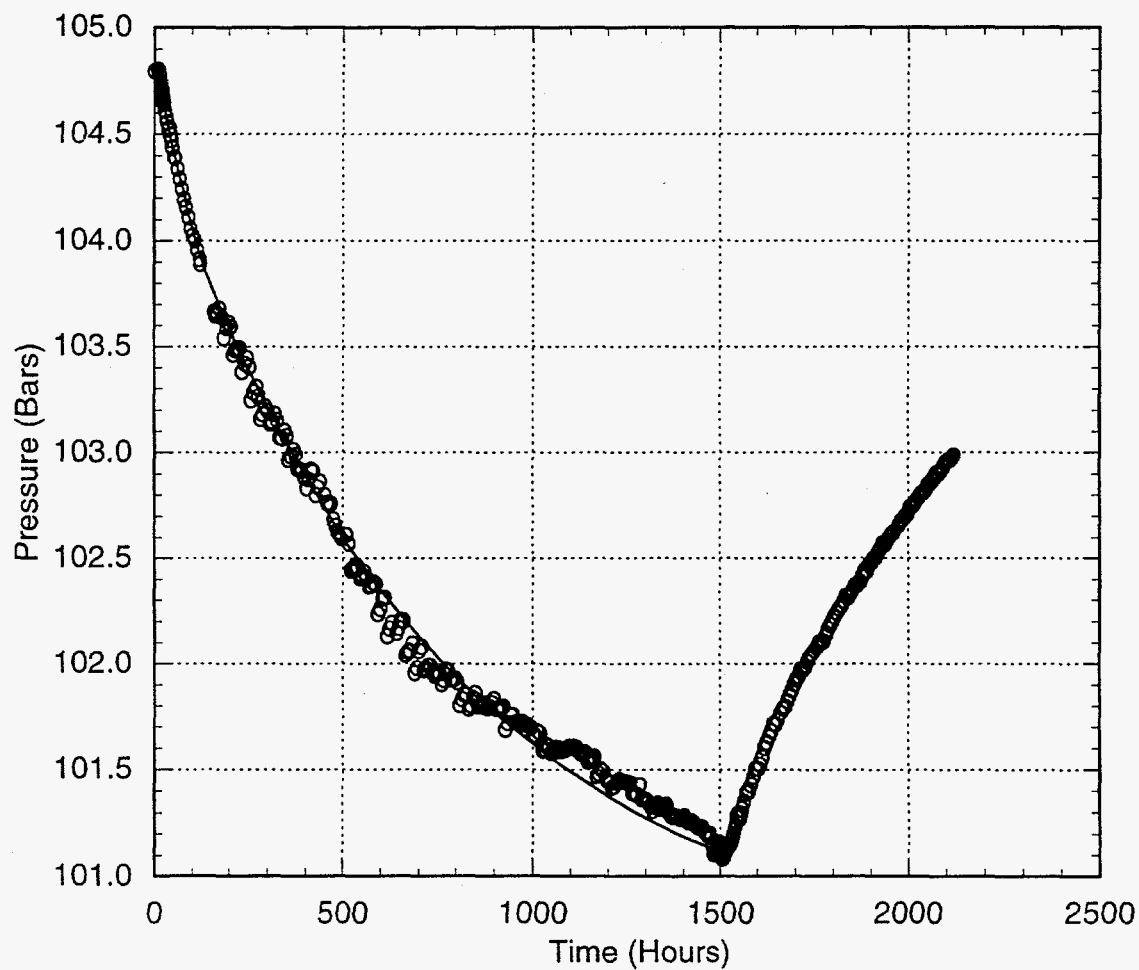


Figure 6.9. Comparison between measured (o) and computed (—) pressures in N60-KY-1 during the 1986 test (case 1). Effective discharge rate history for S-4 is assumed to be identical (apart from a multiplicative factor of 0.6) to that used by Pritchett, *et al.* (1989). All times are in hours since 00:00 hours LT on September 2, 1986.

Table 6.5. Assumed effective discharge rate history for well S-4 (1986 test) for cases 2, 3, 4, and 5. All times are in hours since 00:00 hours LT on September 2, 1986.

	Time Interval (Hours)	\dot{M}_e (kg/s)
Case 2	0.00 – 11.33	0.0
	11.333 – 1504.5	30.0
	1504.5 –	12.0
Case 3	0.00 – 11.333	0.0
	11.333 – 1504.5	30.0
	1504.5 – 1600.0	12.0
	1600.0 – 1700.0	6.0
	1700.0 – 1800.0	3.0
	1800.0 –	1.5
Case 4	0.00 – 11.333	0.0
	11.333 – 36.0	30.0
	36.0 – 276.0	25.2
	276.0 – 444.0	26.4
	444.0 – 588.0	27.6
	588.0 – 684.0	28.2
	684.0 – 1504.5	30.0
	1504.5 – 1600.0	12.0
	1600.0 – 1700.0	6.0
	1700.0 – 1800.0	3.0
	1800.0 –	1.5
Case 5	0.0 – 11.333	0.0
	11.333 – 36.0	30.0
	36.0 – 500.0	25.0
	500.0 – 1504.5	20.0
	1504.5 – 1600.0	2.0
	1600.0 – 1800.0	1.0
	1800.0 –	0.0

the discharge rate and the afterflow rate were assumed to be simple constants. Apart from a gradual reduction in the afterflow rate, the discharge rate history for case 3 is identical with that for case 2. In case 4, the discharge rates prior to shutin were varied in direct proportion to the measured discharge rates (Table 6.1). It is possible (perhaps even likely) that the ratio between the measured and effective discharge rates did not remain constant during the 1986 test; for case 5, the effective discharge rate (as a fraction of the measured discharge rate) was assumed to decline with time.

The formation parameters inferred for cases 2 through 5 are given in Table 6.4. With the exception of case 2, the computed pressures are in good agreement with measurements (Figures 6.10–6.13). The formation permeability-thickness and storage parameters do not differ significantly (an exception is kh value for case 4) from case-to-case (see Table 6.4). Unfortunately, the inferred distances to different boundaries vary significantly between the different cases. Stated somewhat differently, the boundary distances are very sensitive to the assumed variations in the effective discharge rate history for well S-4. It is thus clear that the available data do not permit a unique interpretation of the measured pressure interference signal in N60-KY-1. While the formation thickness and storage are well constrained from both the 1986 and 1989 tests, the distances to the various boundaries (or even the presence of boundaries) are much less certain.

6.1.6 Structural Interpretation

The feedpoints of both S-4 and N60-KY-1 are located within a deep altered andesite layer. Above this layer lies a thick formation consisting of alternating marine sediments (black shales) and dacite volcanic flows; because of the

presence of shales, it is likely that the average vertical permeability is rather low. Below the andesite layer, a crystalline granitic layer (granodiorite formation) is to be found. Sumikawa wells SA-1 (feedzone depth = 1800 m TVD) and SC-1 (principal feedzone depth = 2310 m TVD; other feedzones are at 1950–1970 m TVD, 2030–2050 m TVD, 2120–2130 m TVD, 2230–2250 m TVD) produce from the granodiorite layer. Since no pressure interference has been observed between wells S-4, SA-1 and SC-1, it is likely that the granodiorite formation has poor vertical permeability.

The thickness of the andesite layer sandwiched between the “marine/volcanic complex” and the “granodiorite” formations is about 500 meters. It is not known at this time if significant permeability is present over the entire thickness of the altered andesite layer. Assuming that the andesite layer is permeable over its entire thickness, Pritchett, *et al.* (1989) estimated the east-west width of the permeable channel (in the altered andesite layer) to be about 1 km (see Figure 6.14). The granodiorite formation appears to rise abruptly ~ 0.7 km west of well S-4; this geologic discontinuity was assumed to constitute the western boundary of the permeable channel (Pritchett, *et al.*, 1989). Pritchett, *et al.* postulated that another north-south vertical barrier is present ~ 0.2 to 0.3 km east of well S-4. This eastern flow barrier presumably lies between wells S-4, S-3, N60-KY-1 and 50-HM-3 (to the west) and wells S-2, S-1, SD-1 and Y-2T (to the east). Based on the results presented in Section 6.1.5, it is suggested that the east-west extent of the permeable channel is considerably larger than 1 km. Stated somewhat differently, it is likely that no barrier separates wells S-4, S-3, N60-KY-1 and 50-HM-3 (to the west) and wells S-2, S-1, SD-1 and Y-2T (to the east). In the latter connection, we note that a tracer was injected into well SD-1 on June 17, 1991; within a couple of

Continued on page 6-26

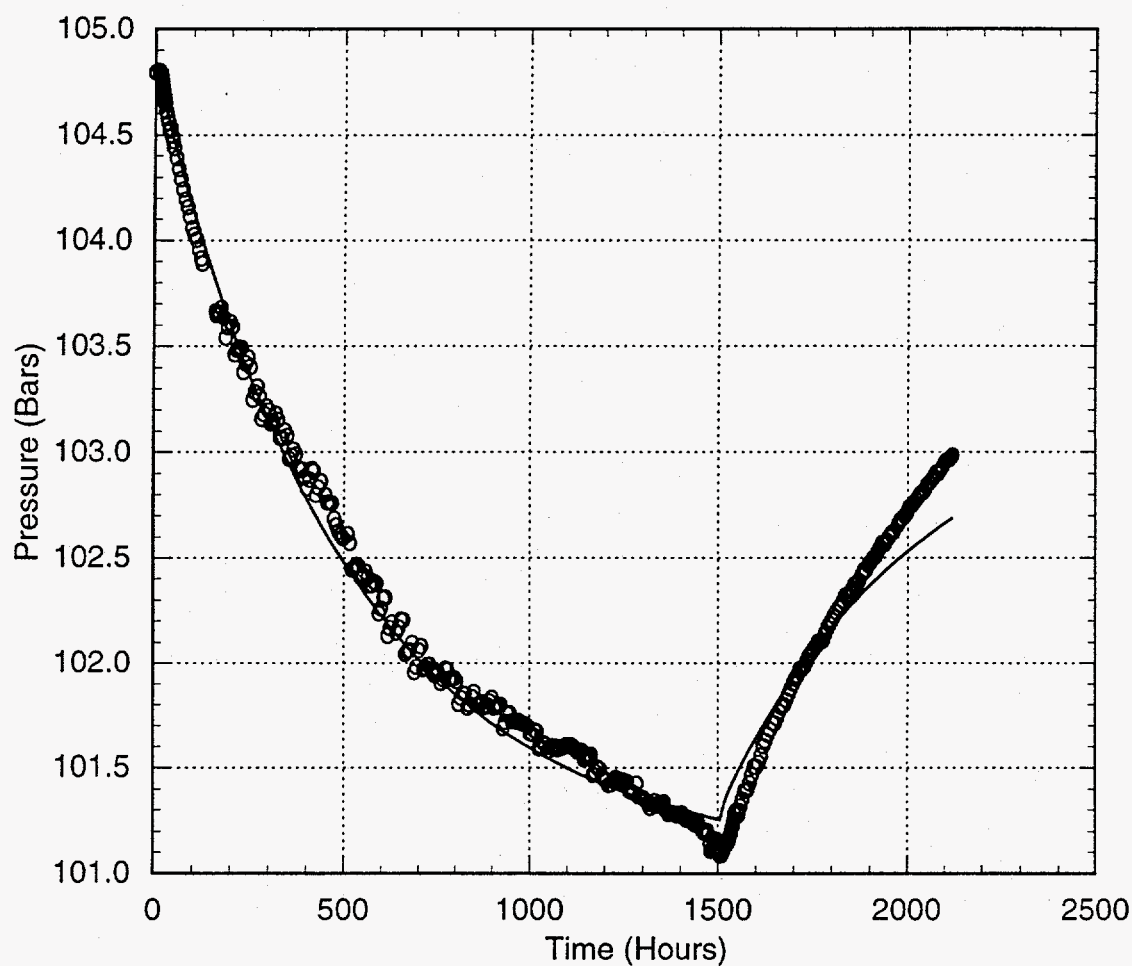


Figure 6.10. Comparison between measured (o) and computed (—) pressures in N60-KY-1 during the 1986 test (case 2). Effective discharge rate history for S-4 (case 2) is given in Table 6.5. All times are in hours since 00:00 hours LT on September 2, 1986.

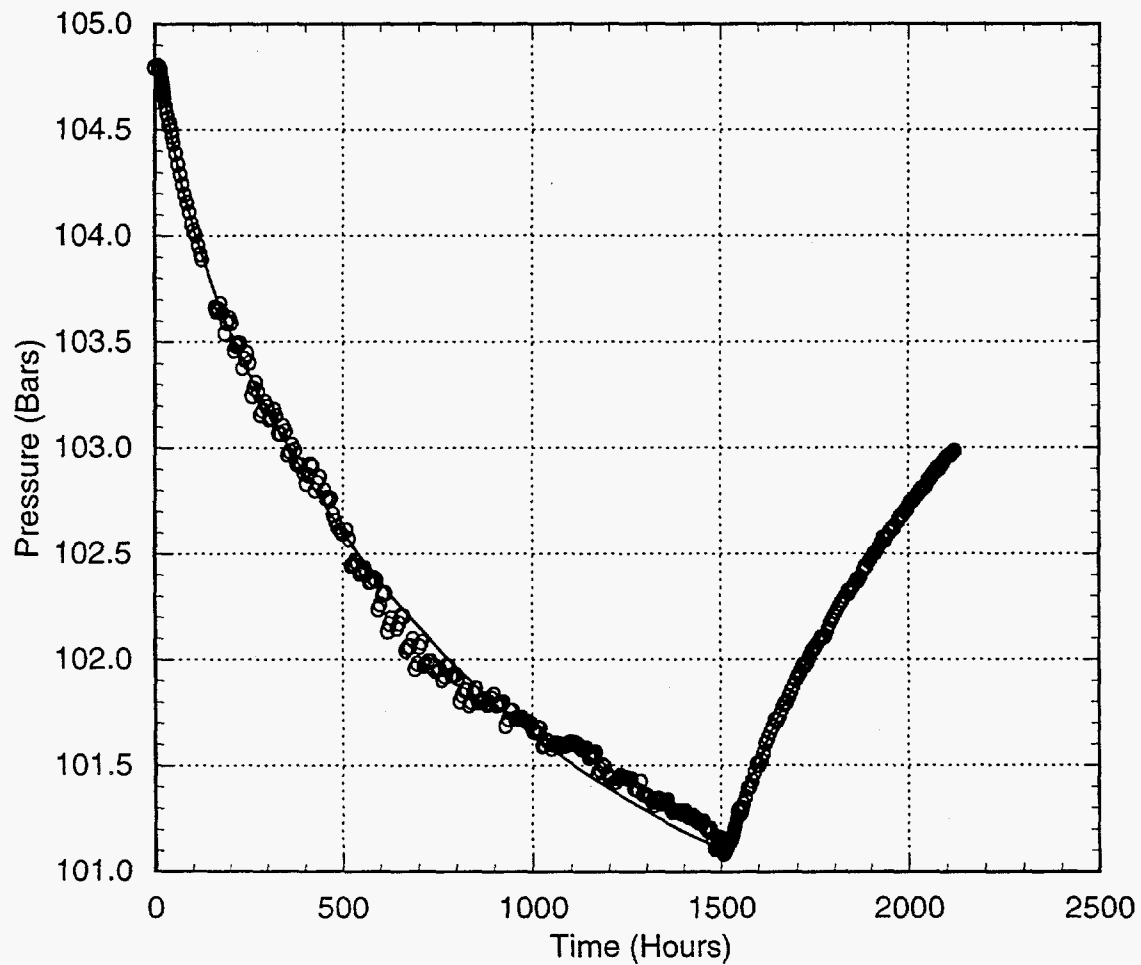


Figure 6.11. Comparison between measured (o) and computed (—) pressures in N60-KY-1 during the 1986 test (case 3). Effective discharge rate history for S-4 (case 3) is given in Table 6.5. All times are in hours since 00:00 hours LT on September 2, 1986.

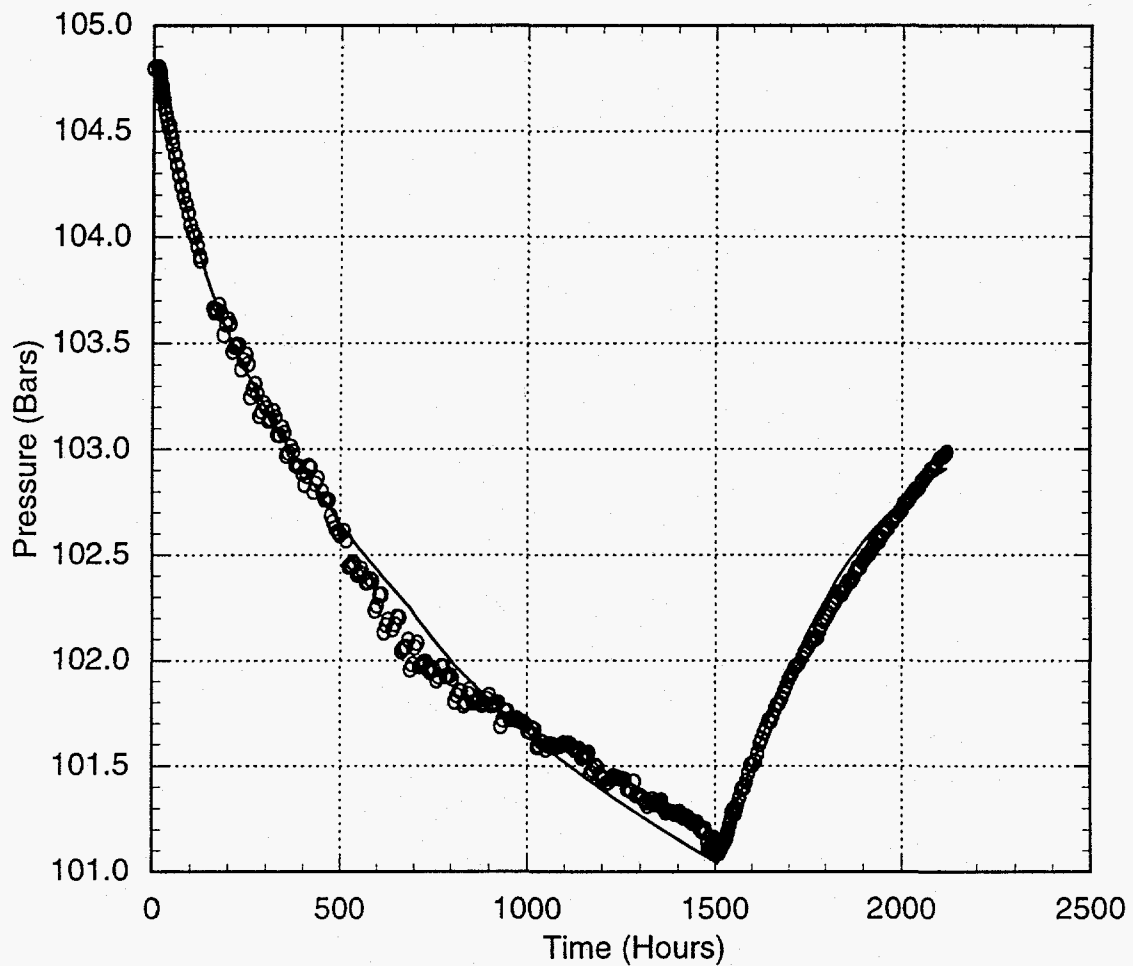


Figure 6.12. Comparison between measured (o) and computed (—) pressures in N60-KY-1 during the 1986 test (case 4). Effective discharge rate history for S-4 (case 4) is given in Table 6.5. All times are in hours since 00:00 hours LT on September 2, 1986.

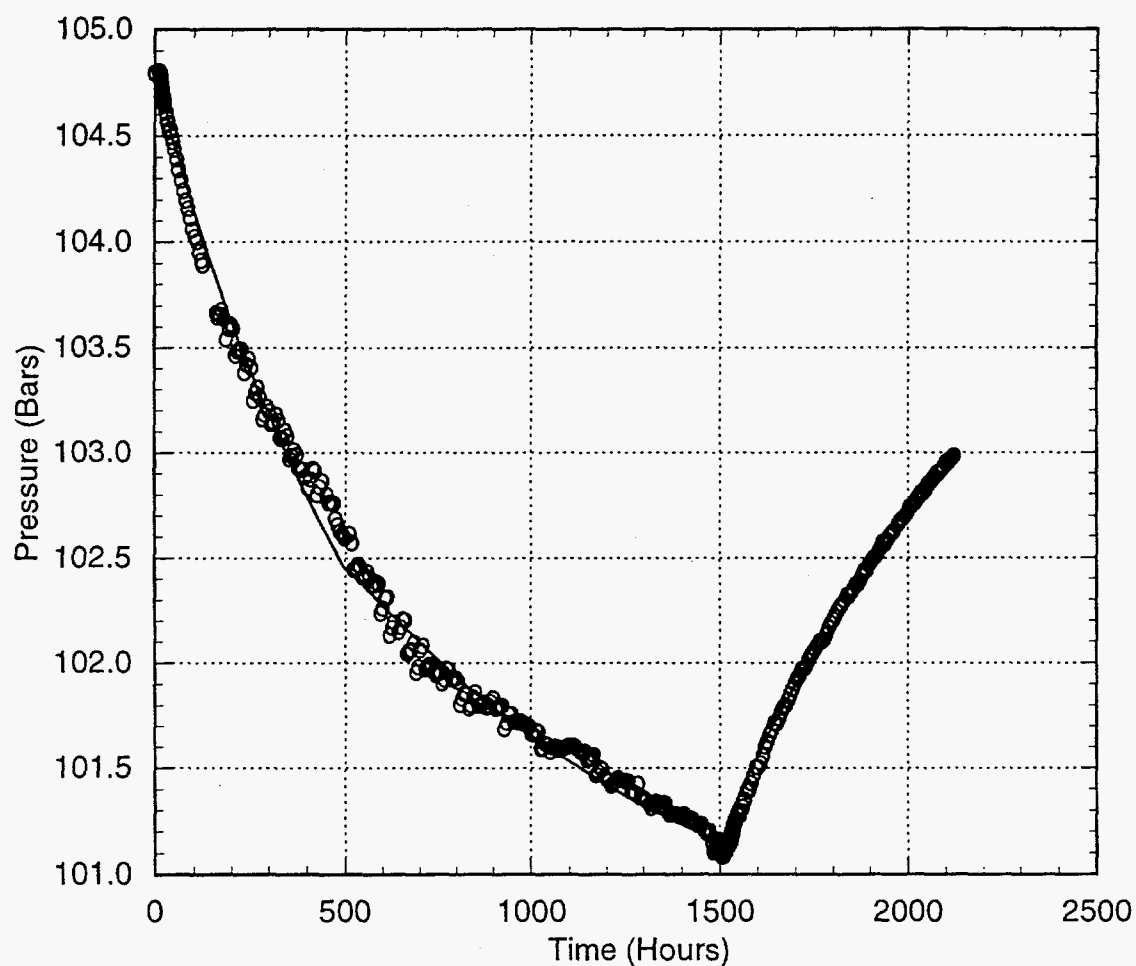


Figure 6.13. Comparison between measured (o) and computed (—) pressures in N60-KY-1 during the 1986 test (case 5). Effective discharge rate history for S-4 (case 5) is given in Table 6.5. All times are in hours since 00:00 hours LT on September 2, 1986.

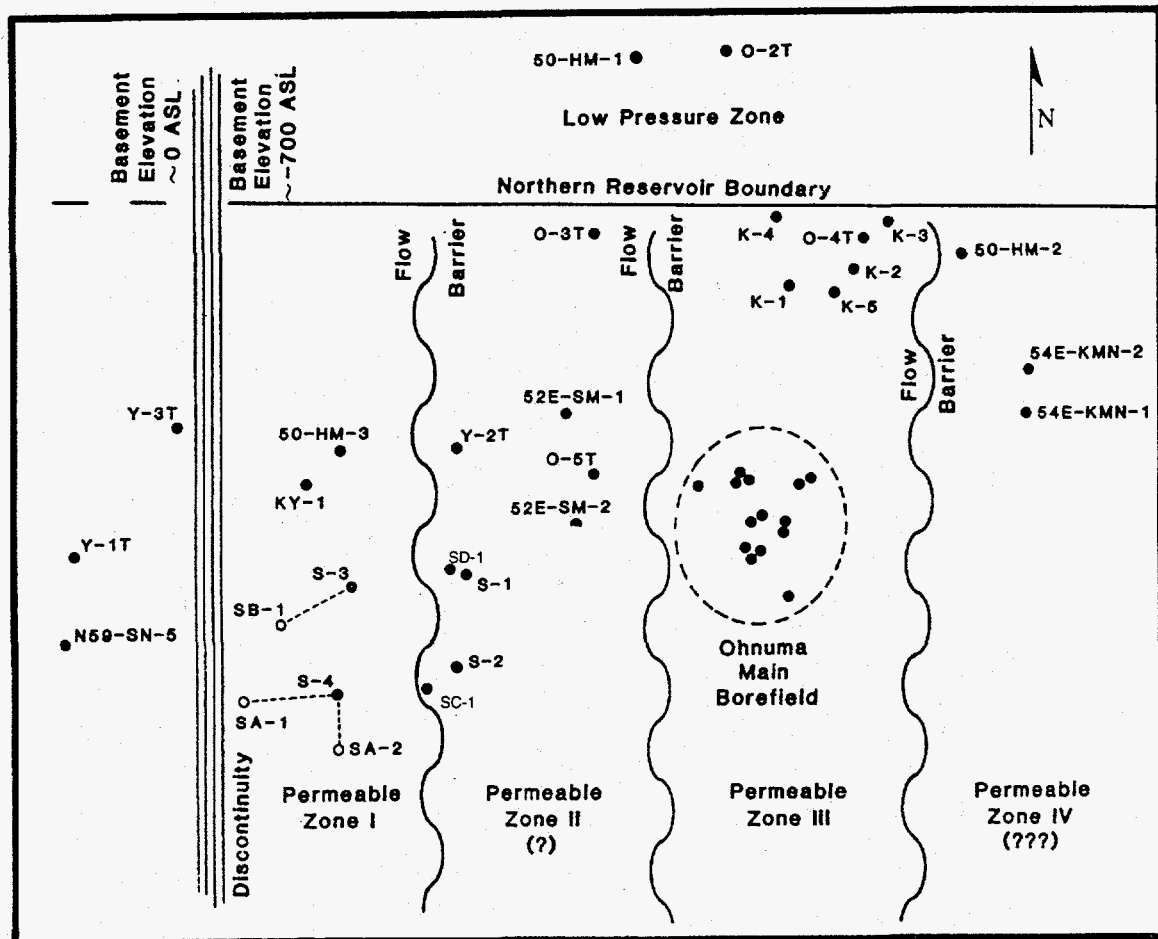


Figure 6.14. Estimated locations according to Pritchett, *et al.* (1989) of deep permeable channels in Sumikawa/Ohnuma area. Interpretations presented in this report suggest that there is no barrier between permeable zones I and II.

days, the tracer was recovered in well S-4. The latter result clearly implies a permeable connection between wells S-4 and SD-1. The non-response of SD-1 during the 1986 test of S-4 must thus be ascribed to causes other than the lack of a permeable connection between the two wells. Perhaps the internal flow in SD-1 masked the pressure interference associated with the discharge of S-4.

The feedzones for wells SA-2 (feedzone depth: 1450 m TVD), SA-4 (feedzone depth: 1240 m TVD) and SB-1 (feedzone depth = 1600 m TVD) presumably lie in the permeable layer intercepted by N60-KY-1 and S-4. In an effort to improve the productivity and injectivity of wells, MMC injected cold river water into wells S-4, SA-2, SA-4 and SB-1 in April and May 1989. As already noted, injection into well S-4 produced a pressure interference signal in N60-KY-1. Injection into SB-1 also resulted in a pressure disturbance in N60-KY-1. Unlike wells S-4 and SB-1, injection into wells SA-2 and SA-4 did not result in any discernible pressure response in N60-KY-1. Two possibilities exist. It may be that the feedzones for SA-2 and SA-4 are somehow disconnected from the permeable channel intersected by S-4, SB-1, and N60-KY-1. The more likely possibility is that two-phase conditions are prevalent at the feedzones for SA-2 and SA-4; injection into a two-phase zone will not produce a pressure disturbance in a distant well such as N60-KY-1.

The presence of an impermeable boundary to the north of N60-KY-1 is implied by the analyses shown in Table 6.4; this result is in accord with the earlier interpretation by Pritchett, *et al.* (1989). The distance to this northern boundary is of the order of 1 km north of well N60-KY-1. The northern boundary is probably associated with the dacitic dike along the Kumazawa river.

Analyses of 1986 test data (Table 6.4; Pritchett *et al.*, 1989) suggest the presence of a constant-pressure boundary to the south of well S-4. It is, however, unlikely that this constant pressure is located as far south (*i.e.*, 6 to 10 km south of well S-4) as that implied by the results given in Table 6.4. The explanation for this peculiar result is intrinsic in the linear character of the flow model. More specifically, it was assumed that the reservoir contains single-phase liquid. In reality, two-phase conditions prevail under undisturbed conditions a short distance (~ 1 km) south of well S-4. This suggests that the actual location of the constant pressure southern boundary is quite close to well S-4. Unfortunately, uncertainties in the effective discharge rate history for well S-4 (1986 test) preclude a precise determination of the distances to the various reservoir boundaries.

The high north-south permeability ($kh > 10$ darcy-m) inferred for the altered andesite formation would tend to explain the apparent uniformity of pressures at depth in the Sumikawa area, and also accounts for the extremely rapid response of N60-KY-1 to the S-4 discharge/injection. Both S-4 and N60-KY-1 were injection tested shortly after drilling and well completion. While these tests implied good injectivity for S-4, the apparent injectivity for N60-KY-1 is very small (Section 5). If N60-KY-1 intersects a high permeability reservoir, then the cold water injectivity should be good.

Two explanations are possible for the poor injectivity of N60-KY-1. The borehole was tested shortly after well completion; it is possible that fractures were laden with drilling mud and cuttings at the time of the injection test. Drilling mud/cuttings reduce only the near well permeability (and hence borehole injectivity); far field permeability is not affected.

The second explanation for the poor injectivity of N60-KY-1 involves the character of formation permeability at Sumikawa. The observed high regional permeability is probably due to a series of large parallel north-south fractures in the altered andesite formation. Superimposed upon this major fracture network is a second fracture network consisting of a very large number of relatively low-permeability minor fractures which are oriented in a more or less isotropic fashion. The major fractures serve to transmit pressure signals over long distances, but the minor fractures provide pressure communication among the major fractures and between the major fractures and the wells. Evidently, while well S-4 is directly connected to the major fracture network, the coupling with N60-KY-1 is poor—sufficient to transmit pressure signals quickly from a nearby major fracture, but insufficient to permit high fluid injection rates. It is significant that numerous regions of lost-circulation were encountered while drilling the southern (S-series) wells, but that farther north (where temperatures are lower) the fractures frequently appear to be sealed with vein materials. Such self-sealing would presumably act mainly to inhibit flow in the minor fracture network, and may be responsible for the poor injectivity of N60-KY-1.

6.2 1989 Injection Test

In April and May 1989, MMC injected cold water into several wells (SA-1, SA-2, SA-4, S-4, SB-1, SB-2 and SB-3); the detailed injection rate history is given in Table D.1. The flow rates listed in Table D.1 are the average flow rates for the time interval(s); in actuality, the flow rates may have fluctuated quite a bit around the average value(s). During the injection period, several shutin wells (KY-1, S-3, S-4, SC-1, and SD-1) were equipped with downhole capillary-tube pressure gauges. No definite evidence of pres-

sure interference was found in the records obtained from wells S-3, S-4 or SC-1. Well SD-1 exhibited a pressure response to injection into well SB-3. The pressure signal recorded in well KY-1 during April and May 1989 is shown in Figure 6.15. The pressure record (Figure 6.15) shows significant oscillations even prior to the start of injection at ~ 1098 hours (April 16, 1989). Besides the fictitious oscillations, the pressure record contains a number of gaps and apparently discontinuous shifts in pressure. Despite these difficulties with the KY-1 pressure record, it is possible to identify pressure changes attributable to injection into wells S-4, SB-1 and SB-2. The pressure interference in KY-1 resulting from injection into S-4 is discussed in Section 6.2. The pressure changes associated with injection into wells SB-1, SB-2 and SB-3 are considered in this section.

6.2.1 Wells KY-1 and SB-1

Slim hole N60-KY-1 is cased and cemented to 1001 meters depth (–10 m ASL); uncemented slotted liner is present from that point to 1604 meters depth (–613 m ASL). Only two mud loss zones were encountered in the uncemented part of the hole; at –169 m ASL and at –571 m ASL. The deeper of these mud loss zones (–571 m ASL) is in the “altered andesite” formation; the shallow mud loss zone (at –169 m ASL) is contained in the “marine/volcanic” complex formation. Well SB-1 is cased and cemented to a vertical depth of ~ 1062 meters (~ –13 m ASL), and an open hole completion was used below this depth. The principal feedzone for SB-1 is located at 1600 m TVD (~ –551 m ASL) in the “altered andesite” formation. The horizontal distance between the feedzones for SB-1 and N60-KY-1 (altered andesites) is ~ 689 meters. It is likely that SB-1 and N60-KY-1 communicate with each other through the altered andesites.

Continued on page 6-29

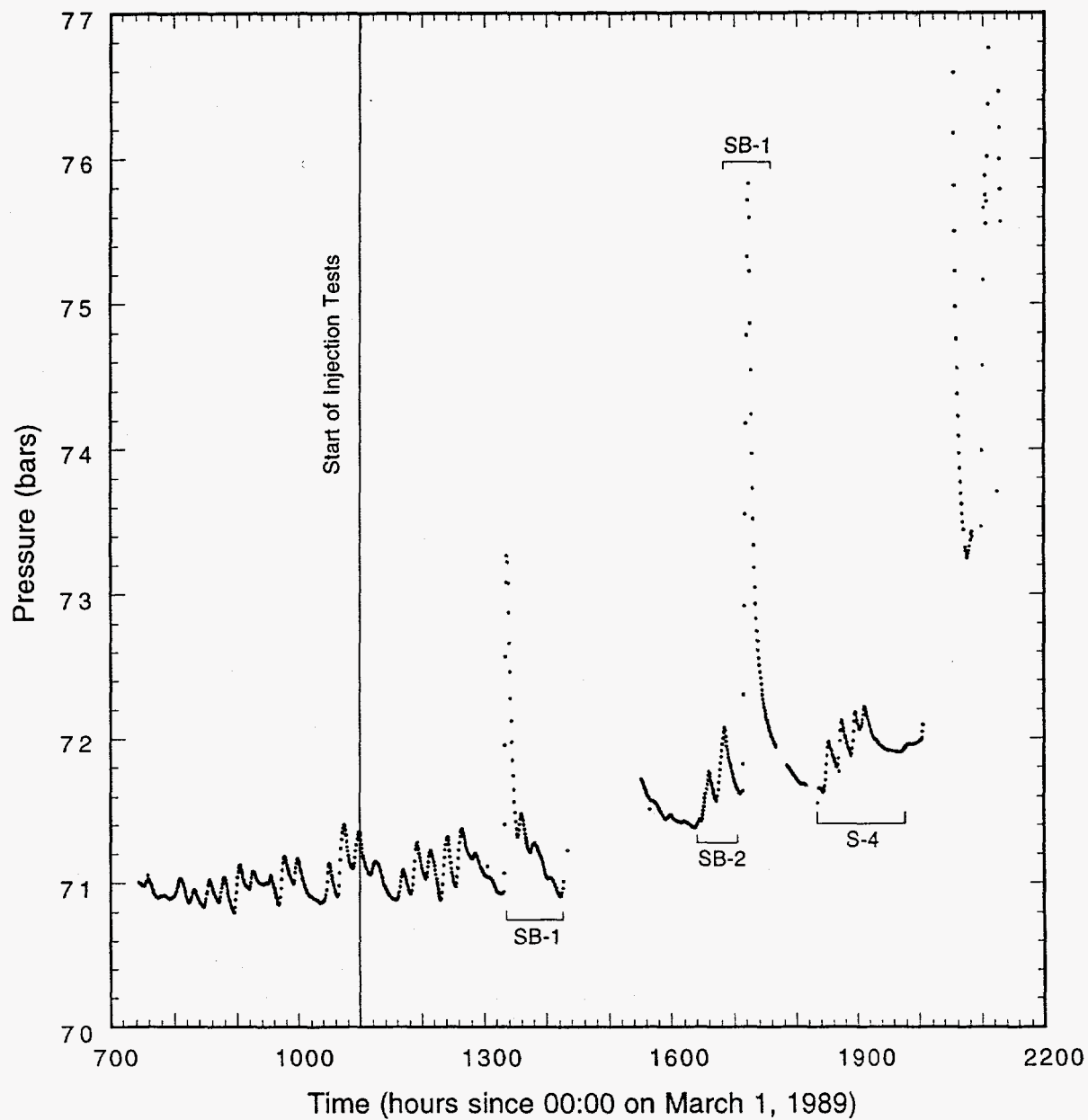


Figure 6-15. Measured pressure response in KY-1 during April and May 1989. Also indicated are the pressure responses believed to be associated with injection into wells S-4, SB-1, and SB-2.

Because of gaps in the recorded pressure response for well KY-1, it was possible to clearly identify pressure interference from only two episodes (April 25, 1989 and May 11, 1989) of cold water injection into well SB-1 (see Figures 6.16 and 6.17). In each case, the signal strength at well KY-1 was extremely high (several bars) despite the relatively small quantity of fluid injected into well SB-1 and despite the large separation between the well feedpoints. This suggests that the aquifer volume involved is very small. As established by the interpretation of the pressure interference tests between wells KY-1 and S-4 (Section 6.1), the "altered andesite" formation is very permeable, and the cross-section area of the channel is substantial. This permeability is presumably due to the presence of a system of fractures (probably oriented approximately north-south); although well S-4 intersected only one of these fractures at its primary feedpoint, the frequent intersections of the individual fractures within the channel served to distribute the pressure signal from S-4 throughout the entire fracture network in the formation such that the apparent cross-section area and aquifer volume were substantial. In the case of well SB-1, however, the very high ratio of pressure disturbance to injection flowrate suggest that only a limited part of the fracture network was accessed by the pressure disturbance before it was felt at KY-1. For example, it is possible that SB-1 injects fluid into a single fracture which either intersects KY-1 or passes very near the KY-1 feedpoint; this fracture presumably eventually intersects the remainder of the fracture network, but only at considerable distance.

This "semi-connected" fracture concept formed the basis of our model of the response of KY-1 to injection into SB-1. Well SB-1 was treated as a line-source, and a constant pressure boundary was used to represent the location at

which the individual fracture stimulated by well SB-1 becomes connected to the rest of the fracture network within the altered andesite layer. The effective transmissivity of the entire andesite layer is virtually infinite compared to that of a single fracture. A single interference signal cannot uniquely establish the orientation of the "infinite thickness" or "constant pressure" boundary; it was arbitrarily assumed that the constant pressure boundary is located south of KY-1. The reservoir temperature in the region between SB-1 and KY-1 is $\sim 250^\circ\text{C}$; thus, the *in situ* fluid viscosity and density are 10^{-4} Pa-s and 800 kg/m^3 .

As a result of numerical experimentation, the unknown parameters in the model were taken to be (1) formation pressure, p_i , (2) permeability-thickness product, kh , (3) diffusivity, $k/\phi c$, and (4) distance to the constant pressure boundary, Y . Minimization of error led to the following values for the free parameters in the model:

1. Injection test of April 25, 1989

Initial pressure, $p_i = 70.886$ bars
 Permeability-Thickness, $kh = 0.047$ darcy-m
 Diffusivity, $k/\phi c = 4.21 \times 10^8$ darcy-Pa
 Distance to Boundary, $Y = 707.5$ m

2. Injection test of May 11, 1989

Initial Pressure, $p_i = 71.702$ bars
 Permeability-Thickness, $kh = 0.168$ darcy-m
 Diffusivity, $k/\phi c = 4.22 \times 10^8$ darcy-Pa
 Distance to Boundary, $Y = 725.1$ m

The above two tests yields essentially the same value for diffusivity. The computed distances to the boundary are within 20 m of each other. The formation permeability-thickness values, however, differ by more than a factor of three (3). To understand the reasons for the latter, it is useful to examine the sensitivity of the mathematical fit to variations in model parameters (kh ,

Continued on page 6-32

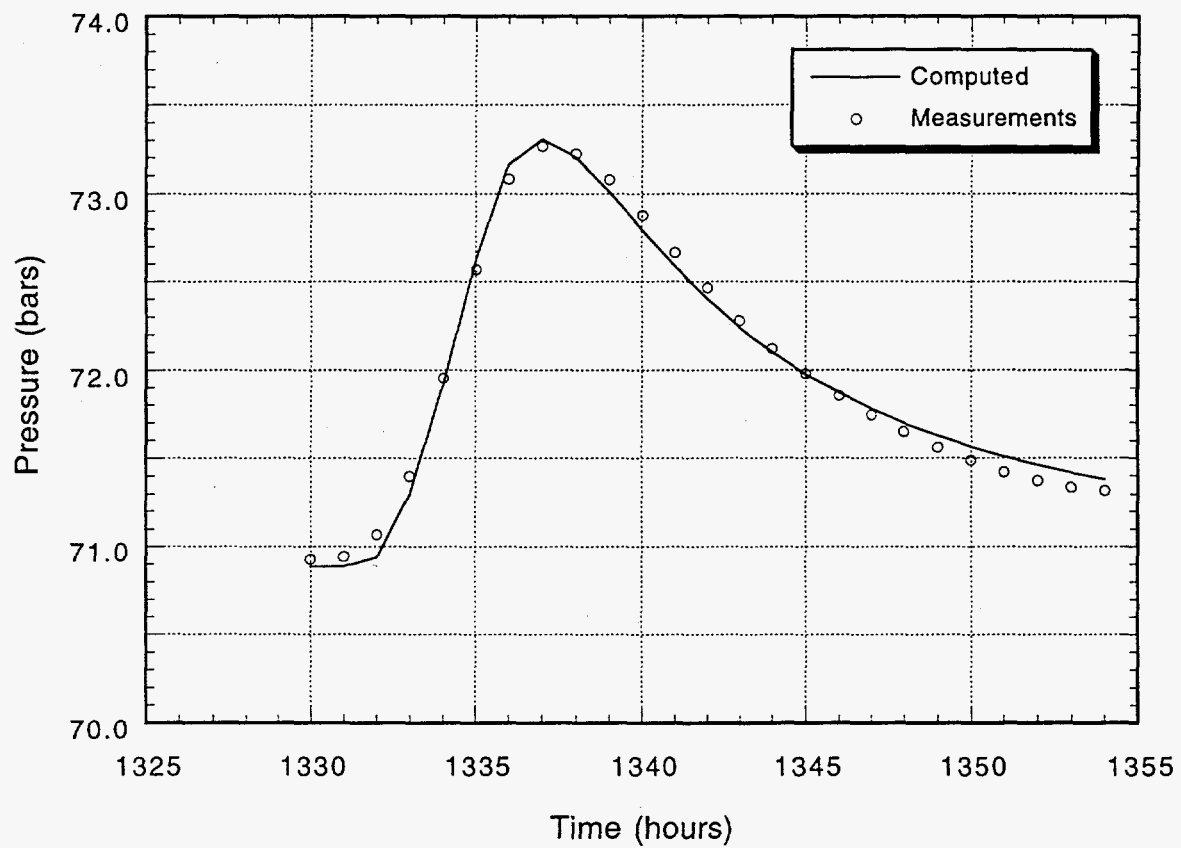


Figure 6-16. Comparison of pressure measurements in KY-1 with computed response due to cold water injection into SB-1 during the time interval from 10:25 hours ($t = 1330.417$ hours) on April 25, 1989 to 14:00 hours ($t = 1334$ hours) on April 25, 1989.

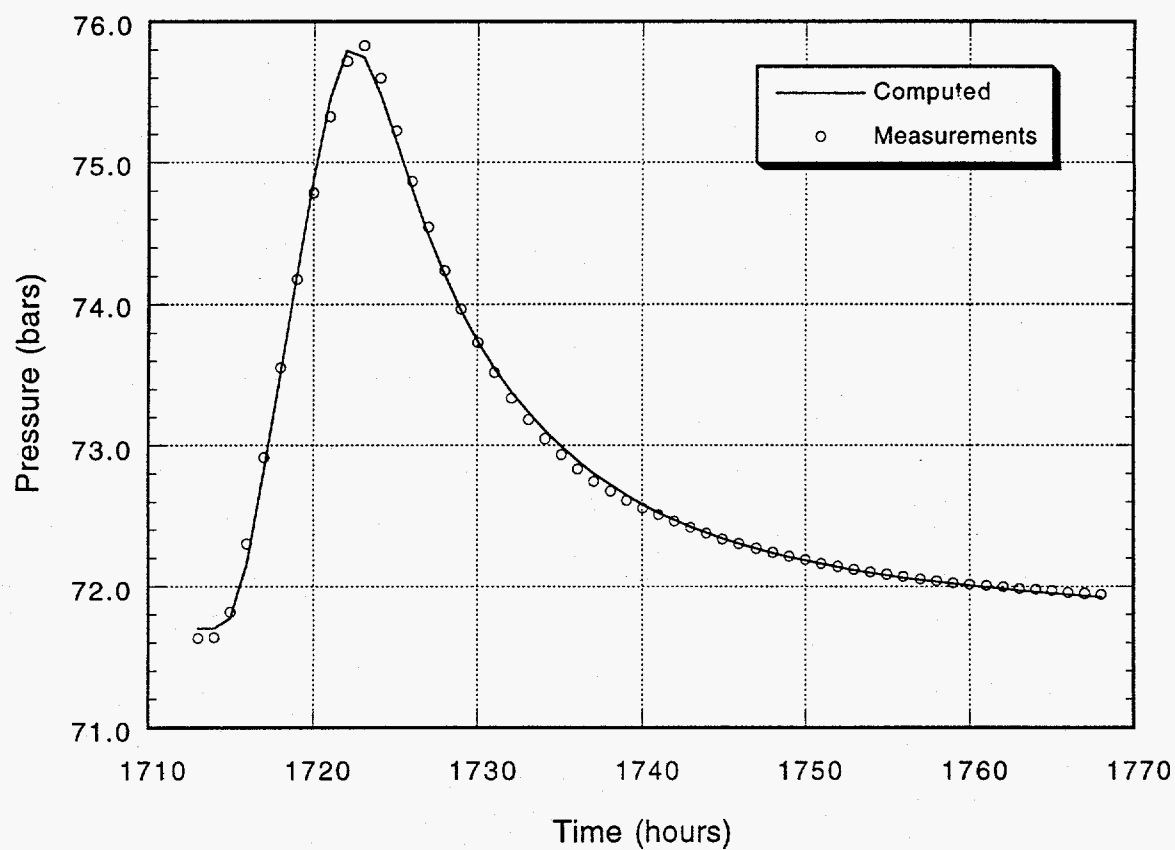


Figure 6-17. Comparison of pressure measurements in KY-1 with computed response due to cold water injection in to SB-1 during the time interval from 09:16 hours ($t = 1713.267$ hours) on May 11, 1989 to 15:50 hours ($t = 1719.833$ hours) on May 11, 1989.

Y). Variation of the normalized sum of squares of residuals

$$\frac{\sum [P_{\text{measured}} - P_{\text{computed}}(p_i, kh, k / \phi c, Y)]^2}{\sum [P_{\text{measured}} - P_{\text{best fit}}]^2}$$

with kh and Y is shown in Figures 6.18 and 6.19, respectively. It is reasonable to assume that all acceptable parameter values are enclosed by the contour labeled 2 in Figures 6.18 and 6.19. Apparently, kh and Y are highly correlated; small variation in Y lead to large variations in kh . Thus, it follows that the two values of kh obtained from the two injection tests are compatible with each other. The best estimate for kh is given by the average of two kh values, and is ~ 0.1 darcy-m.

The formation diffusivity $k/\phi c$ is $\sim 4.2 \times 10^8$ m/Pa. With $kh \sim 0.1$ darcy-m, the formation storage ϕch becomes $\sim 2.4 \times 10^{-10}$ m/Pa. Assuming that formation porosity ϕ and compressibility c are 0.05 and 1.7×10^{-9} Pa $^{-1}$, respectively, the formation thickness h is computed to be ~ 2.8 meters. Not surprisingly, the implied aquifer thickness is very small, and our speculation that the connection between SB-1 and N60-KY-1 consists of a single fracture appears to be correct.

6.2.2 Wells KY-1 and SB-2

Well SB-2 is cased and cemented to a vertical depth of ~ 678 meters, and an open hole completion was used below this depth. The principal feedzone for SB-2 is located at 1270 m TVD (~ -221 m ASL). The upper feedzone for N60-KY-1 is situated at -169 m ASL. The feedzones for both SB-2 and KY-1 are located in a dacite layer within the "marine/volcanic com-

plex" formation. The horizontal distance between the SB-2 and KY-1 feedzones is ~ 270 meters; well SB-2 is strongly deviated towards KY-1. The interwell temperature is about 220°C ; thus, the *in situ* fluid viscosity and density are 1.2×10^{-4} Pa-s and 840 kg/m 3 .

The recorded KY-1 pressure signal shows influence of cold water injection into well SB-2 on May 8 and May 9, 1989 (see Figure 6.20). The classical line-source model was used to fit the pressure response of KY-1 to injection into SB-2. The unknown parameters in the model are (1) initial pressure, p_i , (2) permeability-thickness, kh and storage, ϕch . Minimization of deviations between the calculated and observed pressures (Figure 6.20) gave the following values for the unknown parameters:

Initial Pressure, $p_i = 71.386$ bars
Permeability-Thickness, $kh = 18.7$ darcy-m
Storage, $\phi ch = 1.00 \times 10^{-7}$ m/Pa

It is significant that the provision of a pressure (or closed) boundary does not lead to an improved fit. The sensitivity of the mathematical fit to variations in kh and ϕch is illustrated in Figure 6.21. Both kh and ϕch are well constrained. Assuming that the formation porosity ϕ and compressibility c are 0.15 and 1.2×10^{-9} m/Pa, the computed storage (ϕch) yields a formation thickness of ~ 560 meters. It is unlikely that the dacite layer intercepted by SB-2 and KY-1 is 560 meters thick. The more likely possibility is that the latter dacite layer is connected to other permeable dacite bodies within the "marine/volcanic complex" formation. The black shales in the "marine/volcanic complex" formation impede the vertical flow of fluids, and the formation has poor vertical permeability. The horizontal permeability is, however, governed by the connectivity between dacite units. The "marine/volcanic complex" formation may be com-

Continued on page 6-37

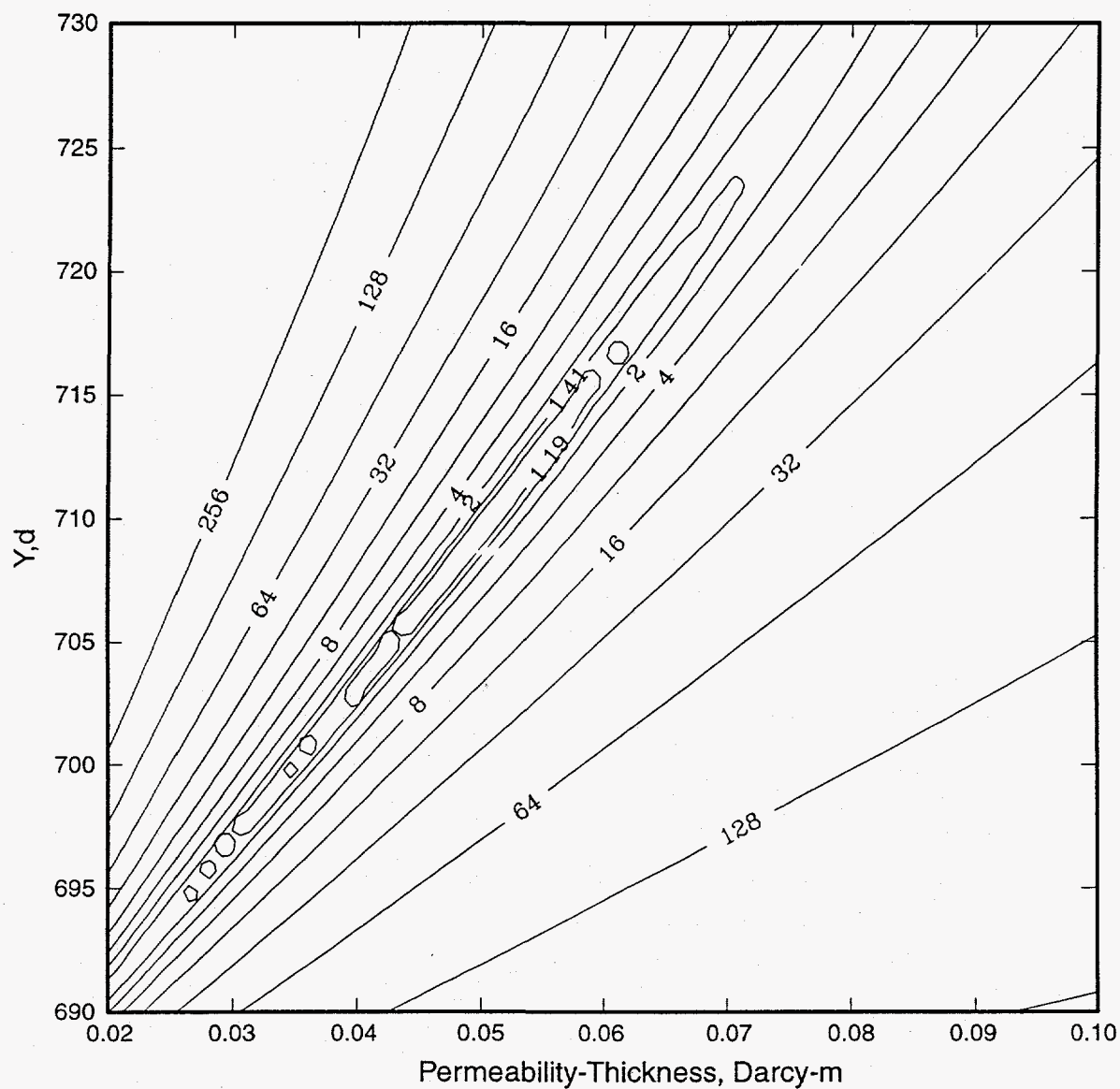


Figure 6.18. Variation of normalized sum of squares of residuals with kh and Y for the pressure response of N60-KY-1 (injection test of April 25, 1989). Contour levels are 1.19, 1.41, 2, 4, 8, 16, 32, 64, 128 and 256.

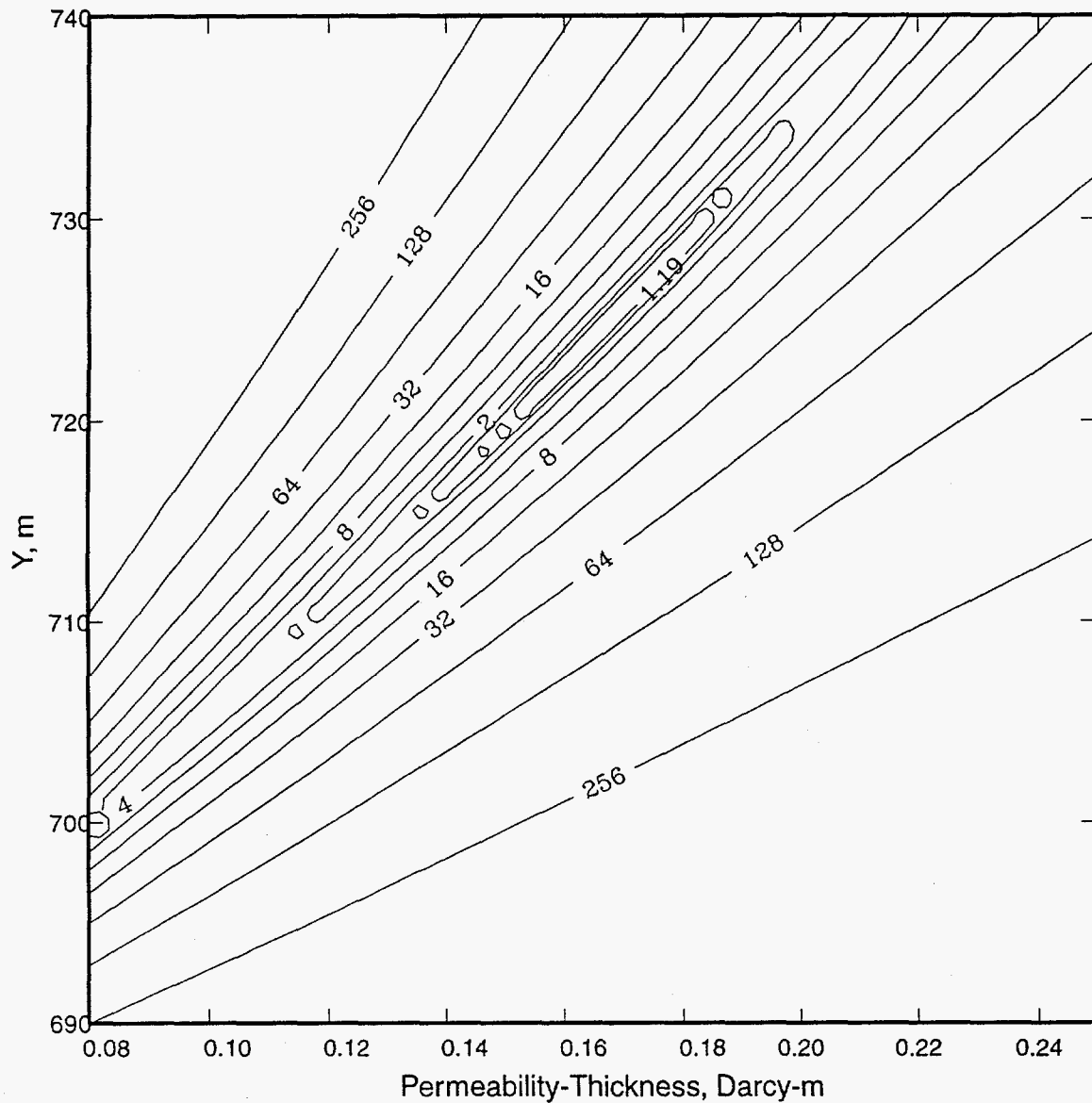


Figure 6.19. Variation of normalized sum of squares of residuals with kh and Y for the pressure response of N60-KY-1 (injection test of May 11, 1989). Contour levels are 1.19, 1.41, 2, 4, 8, 16, 32, 64, 128 and 256.

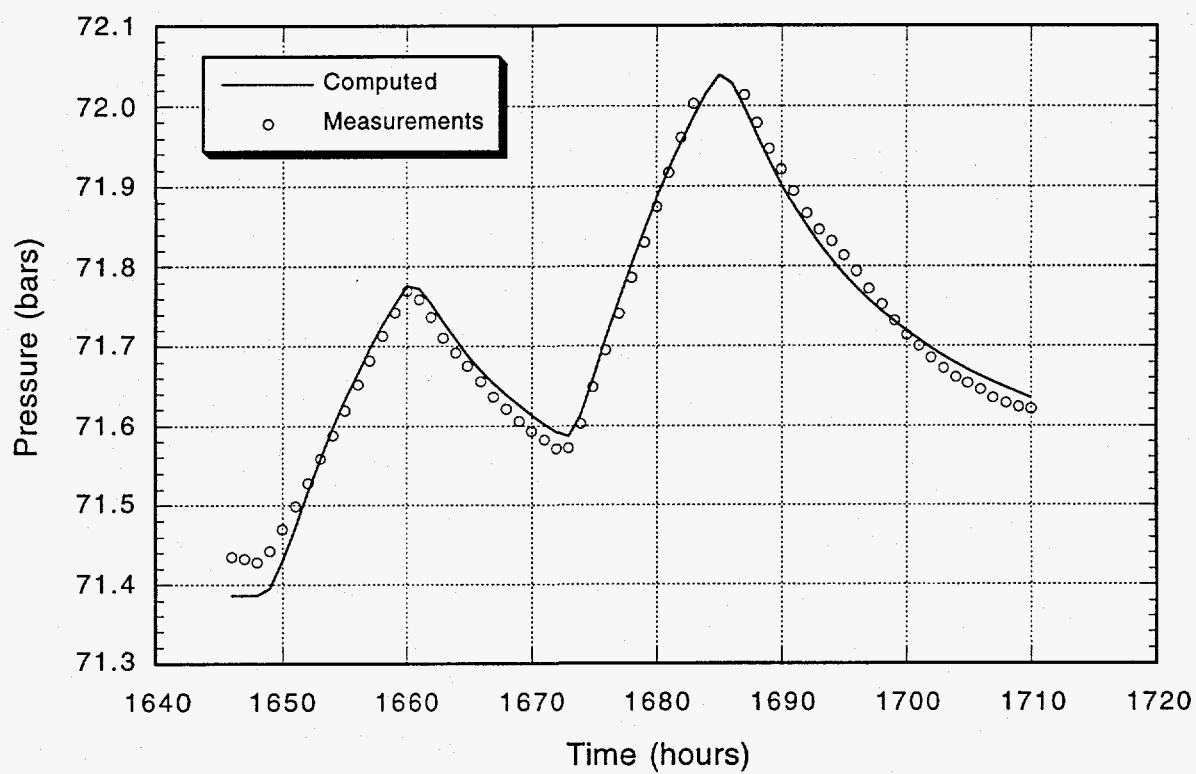


Figure 6.20. Comparison of pressure measurements in KY-1 with computed response due to cold water injection into well SB-2 on May 8 and May 9, 1989.

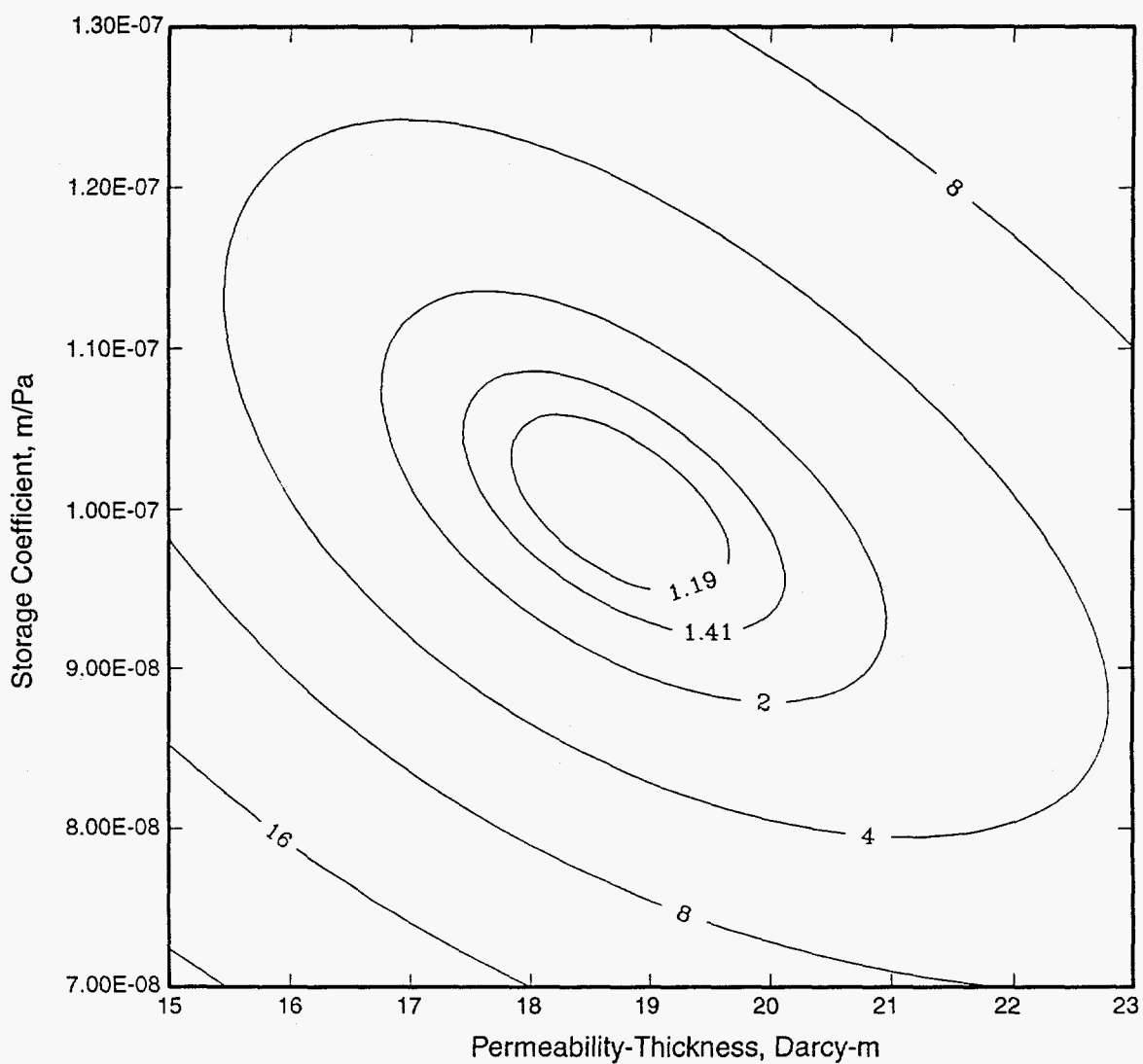


Figure 6.21. Variation of the normalized sum of squares of residuals with kh and ϕch for the pressure response of N60-KY-1 (injection test of May 8–9, 1989). Contour levels are 1.19, 1.41, 2, 4, 8, 16, and 32.

pared to a naturally fractured formation with most of the fractures aligned in the horizontal direction.

6.2.3 Wells SD-1 and SB-3

Well SD-1 is cemented and cased to 707 m MD ($\sim +309$ m ASL); and a 7-inch slotted/blank uncemented liner is present from that point to 1704 m MD (~ 1687 m TVD = -671 m ASL). In the uncased part of the hole, well SD-1 encountered feedzones at 800–900 m MD, 1040–1060 m MD, 1300–1360 m MD, 1450–1490 m MD, and 1530–1570 m MD. The top two feedzones are in the “marine/volcanic complex” formation; the remaining feedzones penetrate the “altered andesite” layer. During cold water injection tests in April and May 1989, downhole pressures in well SD-1 were monitored with a gauge (gauge depth = 800 m) of the capillary tube type. It appears that well SD-1 responds to cold water injection into well SB-3. The major feedzone for well SB-3 is located at 249 to 89 m ASL in the “marine/volcanic complex” formation. Presumably, wells SD-1 and SB-3 communicate through a dacite layer in the “marine/volcanic complex”. The horizontal distance between the SB-3 and SD-1 feedzones (feedzone at 800–900 m MD) is ~ 413 meters, and the interfeedzone temperature is $\sim 220^\circ\text{C}$. Thus, the *in situ* fluid density and viscosity are ~ 840 kg/m³ and 1.2×10^{-4} Pa-s, respectively.

The downhole pressures recorded in well SD-1 during April and May 1989 are displayed in Figure 6.22. The pressure data are oscillatory (oscillation amplitude ~ 0.2 bars) and contain a number of gaps. Despite these obvious shortcomings of the pressure record, it is clear that well SD-1 responds to cold water injection into well SB-3 from May 19 to May 23, 1989 ($t = 1912$ to 2072 hours, Table D.1). The amplitude of the pressure response is ~ 3 bars.

To analyze the pressure interference response of well SD-1, it is assumed that well SB-3 can be treated as a classical line-source. The unknown model parameters are (1) initial formation pressure, p_i , (2) permeability-thickness, kh , and (3) storage, ϕch . Minimization of error gives the following values for the model parameters.

Initial Formation Pressure, $p_i = 44.01$ bars
Permeability-Thickness, $kh = 3.08$ darcy-m
Storage, $\phi ch = 3.98 \times 10^{-8}$ m/Pa

The computed pressure response is compared with the measurements in Figure 6.22. Considering the data quality, the agreement is satisfactory. Inclusion of a pressure (or no flow) boundary does not result in an improved fit; this implies that the aquifer penetrated by SD-1 and SB-3 is quite extensive in the horizontal direction. The variation of the normalized sum of squares of residuals with kh and ϕch is plotted in Figure 6.23; it appears that both kh and ϕch are well constrained.

The permeability-thickness, kh and storage, ϕch inferred from the SD-1/SB-3 interference test are substantially smaller than those obtained from the KY-1/SB-2 interference test. The feedzones for KY-1 and SB-2 are significantly deeper than those for wells SD-1 and SB-3. As remarked elsewhere, the vertical permeability for the “marine/volcanic complex” formation is poor. It is therefore possible that the dacite aquifers penetrated by KY-1/SB-2 and SD-1/SB-3 are poorly connected.

6.3 Pressure Transient Tests for Well SC-1

Sumikawa well SC-1 is cased and cemented (13-³/₈ inch casing to ~ 1018 m TVD, and 9-⁵/₈ inch casing from ~ 961 m TVD to ~ 1799 m TVD) to a depth of ~ 1799 meters; an 8-¹/₂ inch open hole (lined with a 7-inch slotted liner)

Continued on page 6-40

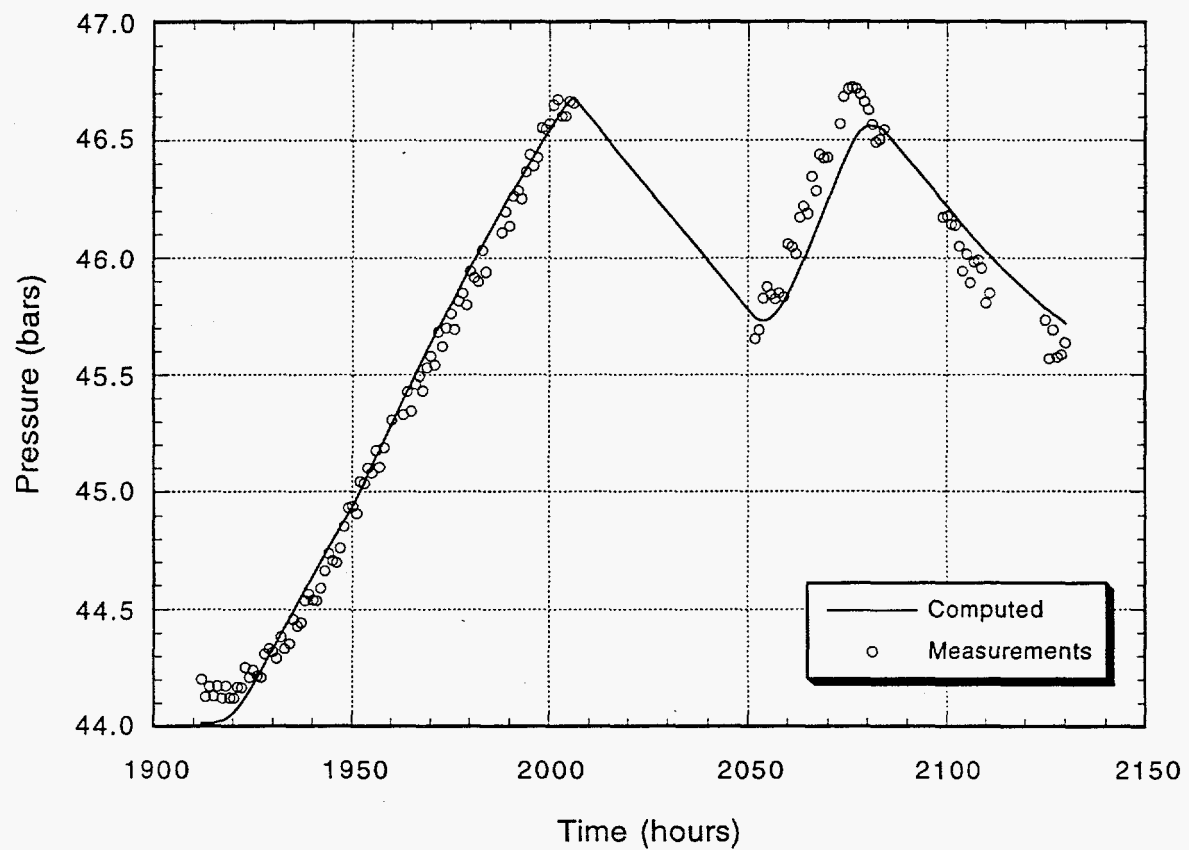


Figure 6.22. Pressure interference response of well SD-1 due to cold water injection into well SB-3 during May 1989.

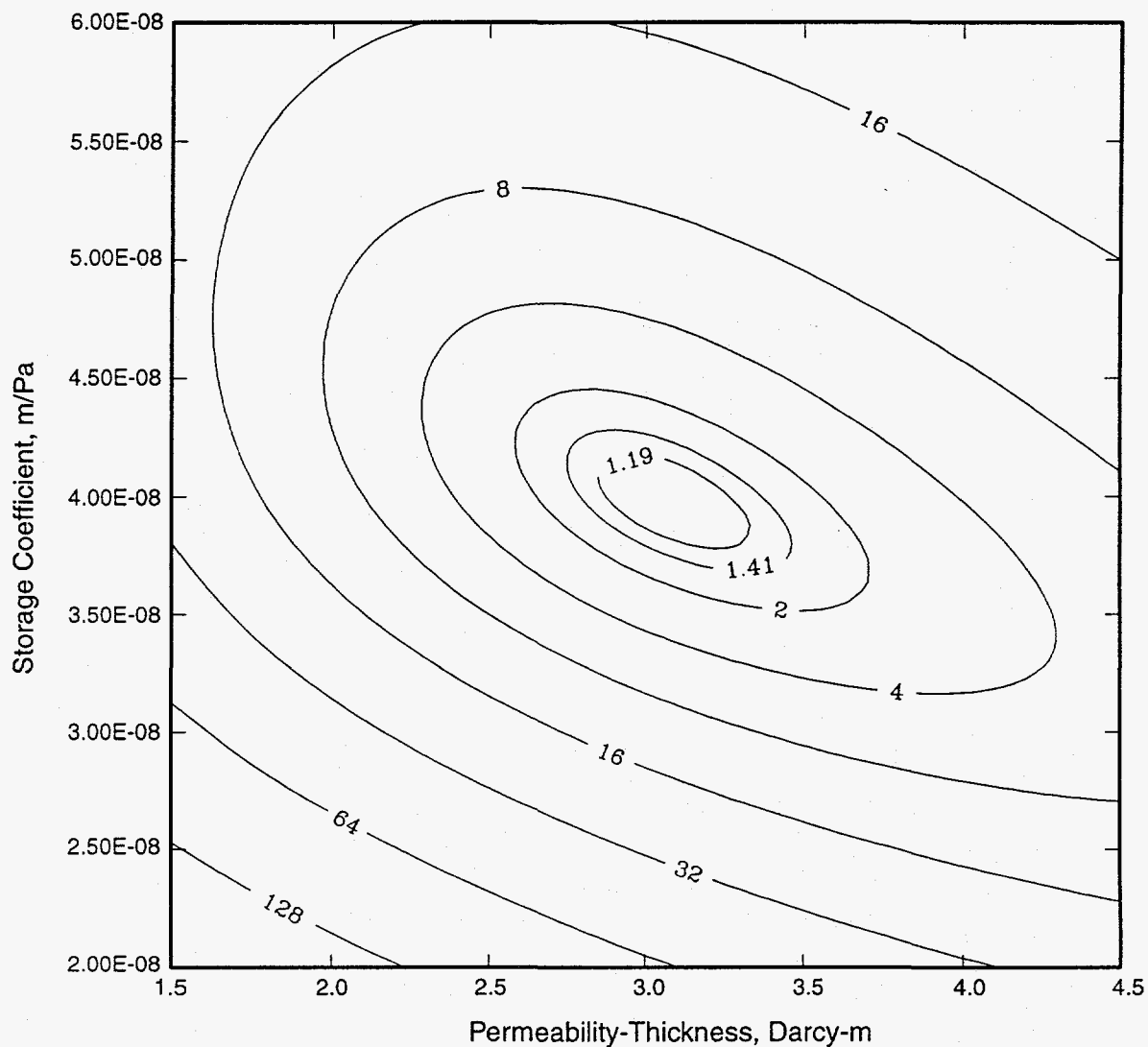


Figure 6.23. Variations of the normalized sum of squares of residuals with kh and ϕch for the pressure response of well SD-1 due to injection into SB-3 (May 1989). Contour levels are 1.19, 1.41, 2, 4, 8, 16, 32, 64, and 128.

completion is used below ~ 1799 meters. Well SC-1 has fluid entries at 1947–1967 m TVD, 2026–2046 m TVD, 2114–2124 m TVD, 2222–2242 m TVD, and 2310 m TVD. The upper two entries for SC-1 are in the “marine/volcanic complex” formation, and the bottom three entries are in the “granodiorite” formation. The well derives over 60 percent of its total discharge from the fluid entry at 2310 m TVD. With the exception of well SA-1 (feedzone at ~ 1790 m TVD), SC-1 is the only Sumikawa well that taps the “granodiorite” formation. Available pressure transient data do not indicate any pressure communication between SC-1 and other Sumikawa boreholes. The lack of pressure communication may be because of the depth of fluid entries for well SC-1. All the fluid entries for SC-1 are significantly deeper than the feedzones for other Sumikawa wells. As remarked elsewhere in this report, the vertical permeabilities at Sumikawa are generally poor.

Five documented pressure-transient experiments have been carried out on well SC-1. First, on 15 November 1987 (shortly after the well was completed), a cold-water injection test of 2.75 hours duration was conducted, with a downhole gauge at 2300 meters depth which recorded the recovery of pressure for three hours after injection ceased. Seven months later, on 7 June 1988, a similar injection test was performed of even shorter duration (2.08 hours) and subsequent downhole pressure recovery was recorded for 1.5 hours. Later in 1988, two discharge tests were conducted. Discharge first began on 30 September and ceased on 9 October; a downhole pressure gauge at 2315 m vertical depth recorded pressures during the latter part of the discharge interval, and during the subsequent pressure buildup phase for about five days after shutin. Then, on 17 October 1988 discharge was initiated again and continued until 15 November.

Unfortunately, during this second 1988 discharge test, it proved impossible to place the pressure gauge at 2315 m depth. Owing to the presence of a chemical sampler which had become lodged downhole, the pressure recordings for this test were made at only 971 meters depth. Pressure records were obtained from 14 November 1988 (just prior to shutin) to 7 December 1988. Finally, as noted above, a third discharge test was conducted from 6 October 1989 to 28 November 1989; pressures were recorded at 2315 meters vertical depth from 26 October 1989 to 25 December 1989.

The pressure records from the various tests of well SC-1 were analyzed using both the line-source (finite wellbore radius) and the spherical source models. The two models yield similar fits between measurements and computed pressures. For geothermal well tests, the formation thickness is usually an unknown. Based on core tests, the granodiorite/diorites have a porosity ϕ of 0.02. The formation compressibility (rock plus fluid) c is assumed to be $1.5 \times 10^{-9} \text{ Pa}^{-1}$. For all our analyses of SC-1 pressure transient data, ϕc was taken to be $3 \times 10^{-11} \text{ Pa}^{-1}$. Using the spherical source model, the best fit to the buildup data for the 1989 discharge test gave a formation thickness of ~ 420 meters (This result is discussed in detail later on.); this implies that the storage ϕch is $\sim 1.3 \times 10^{-8} \text{ m/Pa}$. Although several analyses were performed while keeping ϕch as an unknown parameter (line-source model), in the following discussion we will only present results obtained by holding ϕch fixed. Because many of the model parameters are strongly correlated with ϕch , keeping ϕch as an unknown in the modeling process does not always lead to a better agreement between the measured and calculated pressures.

Analyses of pressure transient data from the existing tests yield inconsistent estimates for reservoir parameters. In the following, we review all available pressure transient data for well SC-1. Explanations are offered for the inconsistent parameter estimates.

The November 1987 Injection Test

The first injection test (15 November 1987) was a multi-rate test; cold water was injected at various rates for 165 minutes (2.75 hours). The pressure gauge was located at 2290 m TVD (2300 m MD); pressures were recorded from $t = 10$ minutes to $t = 345$ minutes (see Figure 6.24).

Because of the apparent variation of the injectivity index with the injection rate, it was decided to match only the fall-off pressure history. The line-source model (finite wellbore) was used to match the fall-off response. The unknown parameters in the model were assumed to be (1) initial pressure, p_i , (2) permeability-thickness, kh , (3) skin, s , and (4) wellbore storage, C . As mentioned earlier, the formation storage (ϕch) was kept fixed at 1.3×10^{-8} m/Pa. Minimization of deviations between the computed and measured fall-off pressures gave the following values for the unknown parameters:

Initial Formation Pressure, $p_i = 148.0$ bars
Permeability-Thickness, $kh = 18.7$ darcy-m
Skin, $s = 12.7$
Wellbore Storage, $C = 1.55 \times 10^{-5}$ m³/Pa

The computed results are in excellent agreement with the fall-off data (see Figure 6.25). Except for the pressure data corresponding to injection at the highest rate, the mathematical model also yields an adequate fit to pressure buildup data. This is significant in that pressure buildup data were not used for estimating the unknown model parameters.

The June 1988 Injection Test

The second injection test carried out on well SC-1 (June 7, 1988) was even shorter in duration (125 minutes) and involved a constant injection rate (60 kg/s; about 220 tons/hour). The downhole pressure gauge was initially placed at a depth of 2340 m MD (~ 2329 m TVD). Downhole pressures were recorded from $t = 0$ to $t = 61$ minutes, and from $t = 119$ minutes to $t = 225$ minutes (Figure 6.26). Between $t = 61$ minutes and $t = 119$ minutes, the tool was moved up and down the hole to perform a flowing PTS survey. It appears that the final tool depth after the PTS survey ($t > 119$ minutes) was different from its location prior to the survey ($t < 61$ minutes).

We used the same line-source model (finite wellbore) to try to fit the results of the 1988 injection test as was used for the 1987 test (above). The free parameters were taken to be (1) initial pressure, p_i , (2) permeability-thickness, kh , (3) skin, s , and (4) wellbore storage, C . Parameters obtained by error minimization are:

Initial Formation Pressure, $p_i = 153.5$ bars
Permeability-Thickness, $kh = 5.9$ darcy-m
Skin, $s = -2.3$
Wellbore Storage, $C = 1.92 \times 10^{-5}$ m³/Pa

The above formation pressure value is about 1.8 bars greater than the value recorded prior to the test at 2329 m TVD; we conclude that the gauge depth after the completion of the PTS survey was somewhat deeper.

The mathematical fit is in adequate agreement with the fall-off data from the second injection test (Figure 6.27). Unfortunately, the model parameters derived from the 1987 and 1988 injection tests are quite disparate; we shall return to this question later on.

Continued on page 6-46

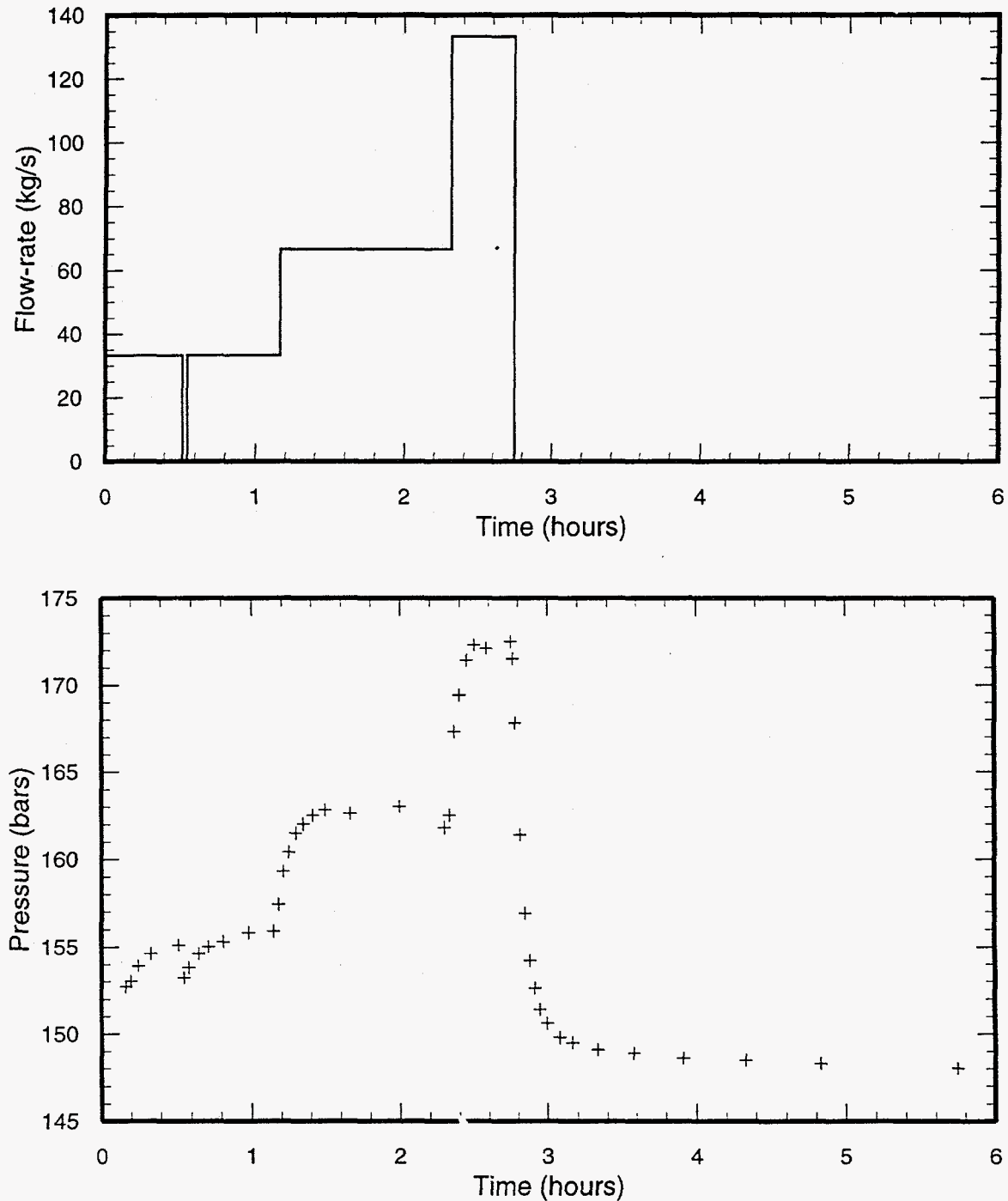


Figure 6.24. Injection Rate (upper panel) and downhole pressure (depth = 2290 m TVD) history for the November 15, 1987 injection test of well SC-1. All times are since the start of the injection test.

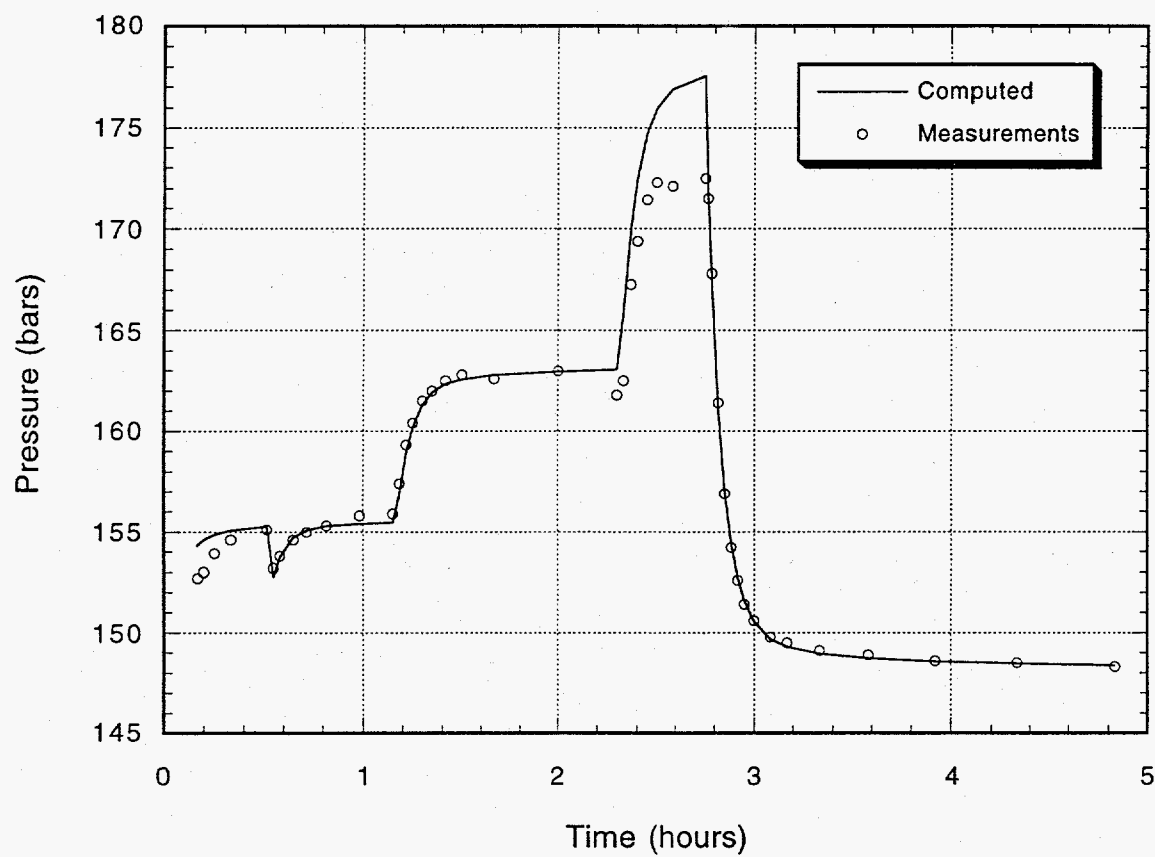


Figure 6.25. Comparison of computed and observed downhole pressures for the November 15, 1987 injection test of well SC-1.

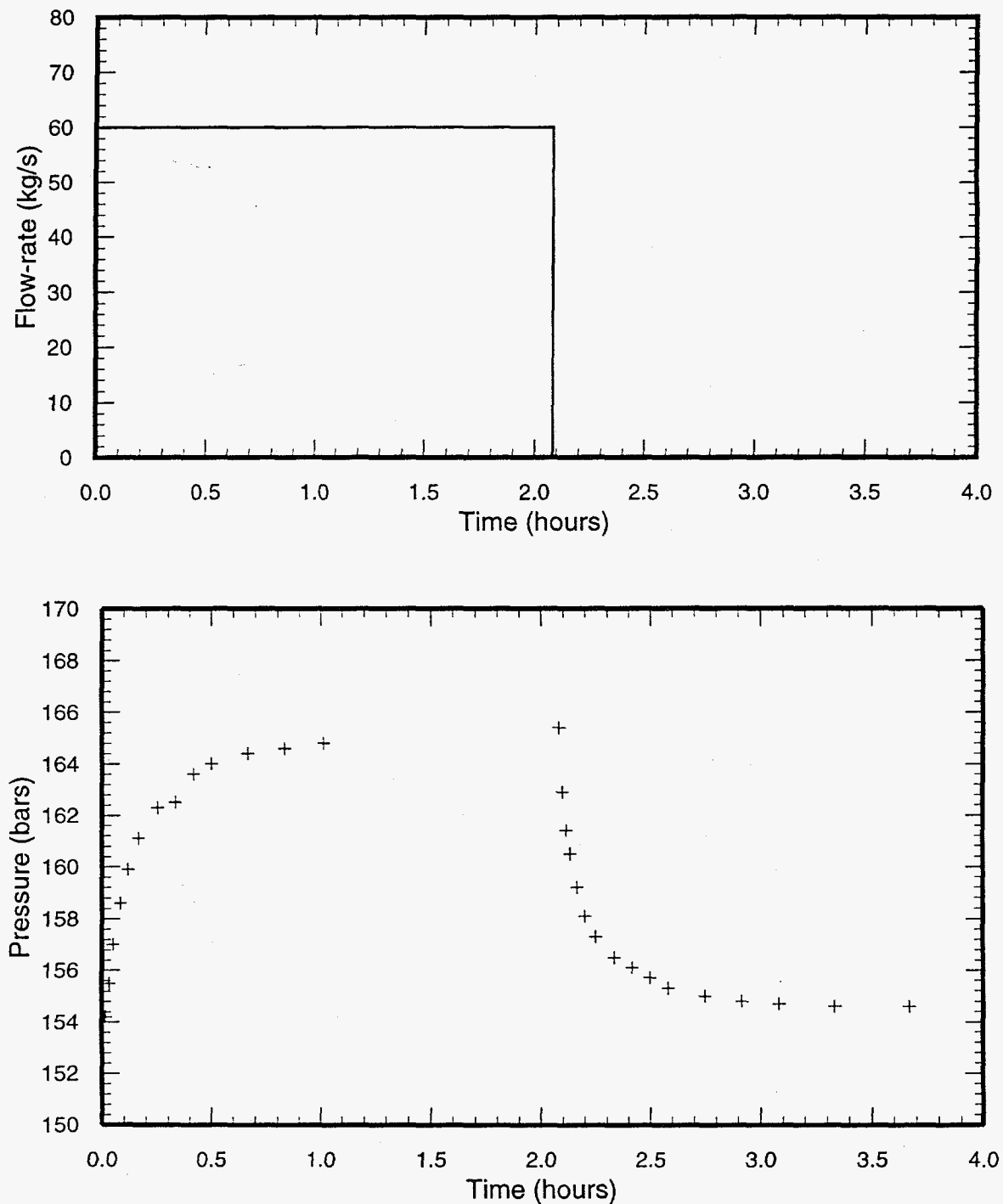


Figure 6.26. Injection rate (upper panel) and downhole pressure (lower panel) history for the June 7, 1988 injection test of well SC-1. All times are since the start of the injection test.

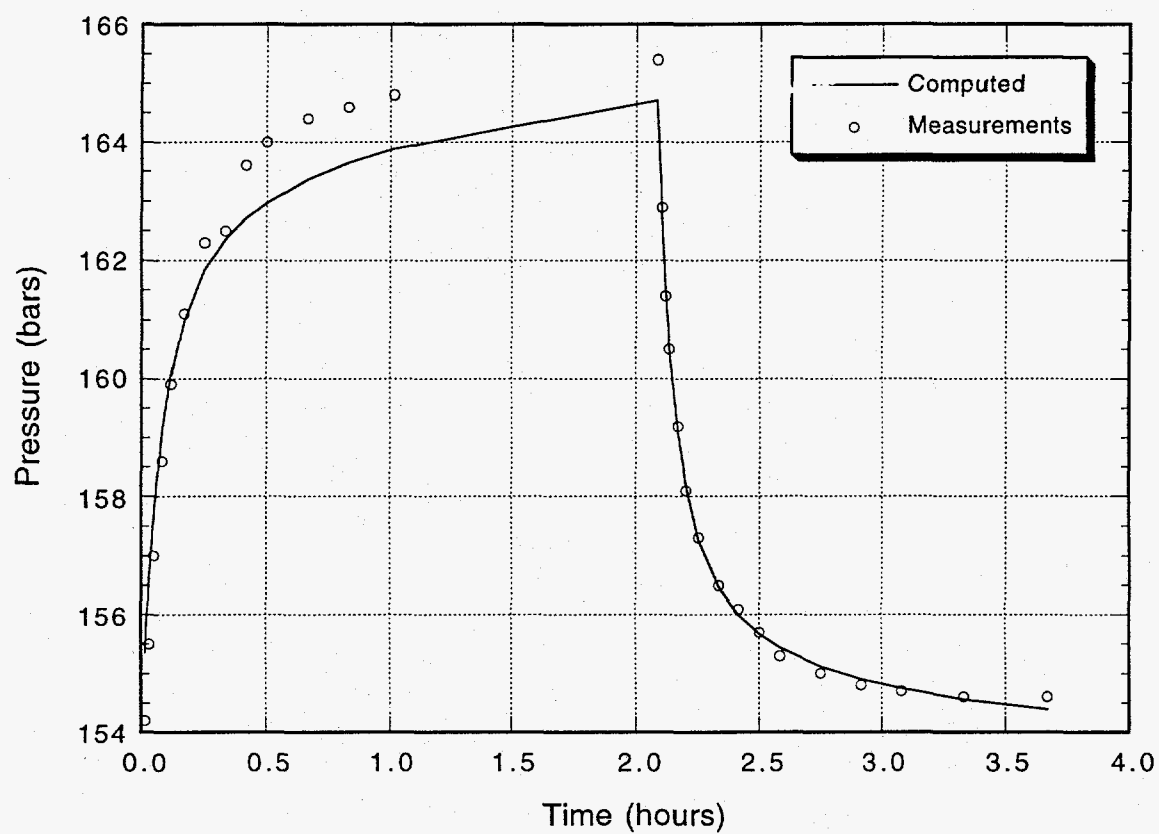


Figure 6.27. Comparison of computed and observed downhole pressures for the June 7, 1988 injection test of well SC-1.

The First 1988 Discharge Test

The first discharge test of Sumikawa well SC-1 took place between September 30, 1988 and October 9, 1988. The discharge rate history (based on data reported by MMC) for this test is illustrated in Figure 6.28. Downhole pressures recorded with a capillary-tube type gauge located at 2315 m TVD (2325 m MD) during the latter part of the discharge period, and during the subsequent shutin period are also shown in Figure 6.28.

The pressure transient data for the discharge test were modeled using the line-source (finite wellbore) model. The best agreement between the computed and measured pressures was obtained by assuming the presence of two lateral boundaries (perpendicular to each other), at distances X_B and Y_B from the well. The free parameters involved in the error minimization process were: (1) initial pressure, p_i , (2) permeability-thickness, kh , (3) skin, s , (4) wellbore storage, C , and (5) distances to the boundaries, X_B and Y_B . The results of error minimization are:

Initial Formation Pressure, $p_i = 148.7$ bars
 Permeability-Thickness, $kh = 57.1$ darcy-m
 Skin, $s = 17.2$
 Wellbore Storage, $C = 4.52 \times 10^{-5}$ m³/Pa
 Distance to Boundary, $X_B = 1310$ meters
 Distance to Boundary, $Y_B = 1450$ meters

The measured pressure history is compared with the computed pressures in Figure 6.29; the agreement is excellent. Unfortunately, the model parameters inferred from the first discharge test of SC-1 exhibit disturbing inconsistencies with data from other pressure transient tests of well SC-1.

The Second 1988 Discharge Test

The second 1988 SN-7D discharge test lasted 22 days, and involved significantly greater discharge rates than the first test. Unfortunately, as noted earlier, a chemical sampler became lodged in the well at an intermediate depth during the test, which precluded stationing the pressure gauge near the well's feedpoint. Instead, the gauge was installed at a much shallower location (971 meters depth), just prior to shutin. The discharge rates and the pressure record for the second 1988 discharge test are shown in Figure 6.30. The periodic fluctuations appear to be thermal effects arising from well "cycling" between the various feedzones and may not be present at ~2300 meters depth.

According to shutin temperature surveys for well SC-1, the stable temperature at 971 m TVD is at least 260°C. The saturation pressure for water at 260°C is ~ 47 bars. Since the flowing pressure prior to shutin at 971 m TVD was ~ 38 bars, it would appear that two-phase conditions prevailed at the gauge depth during the second discharge test. The pressure at 971 m TVD remained below 47 bars for ~ 15 hours after the discharge test was stopped at 12:00 LT on November 15, 1988. Because of the presence of two-phase conditions at the gauge depth for small shutin times, we do not assign any significance to the skin and wellbore storage values inferred from the mathematical fit (see below).

The line-source model (finite wellbore) was used to fit the pressure buildup data ($t > 699$ hours; well was shutin at $t = 698$ hours). As for the first discharge test, the best fit was obtained by incorporating two lateral boundaries (perpendicular to each other) in the mathematical model. The unknown parameters were assumed to be (1) initial pressure, p_i , (2) permeability-thickness,

Continued on page 6-50

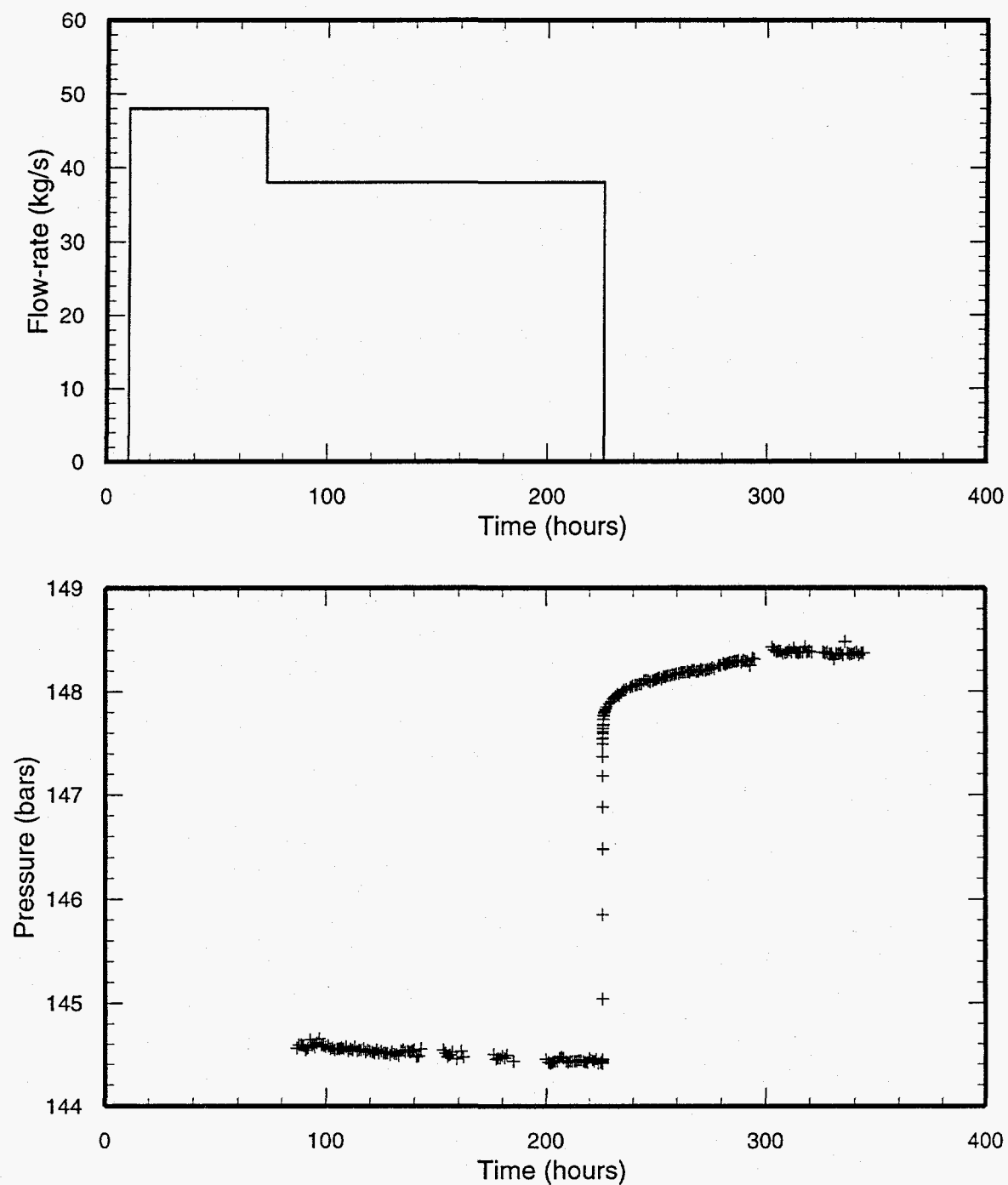


Figure 6.28. Discharge rate (upper panel) and downhole pressures (lower panel) recorded during the first 1988 discharge test of SC-1. All times are in hours since 00:00 LT on September 30, 1988.

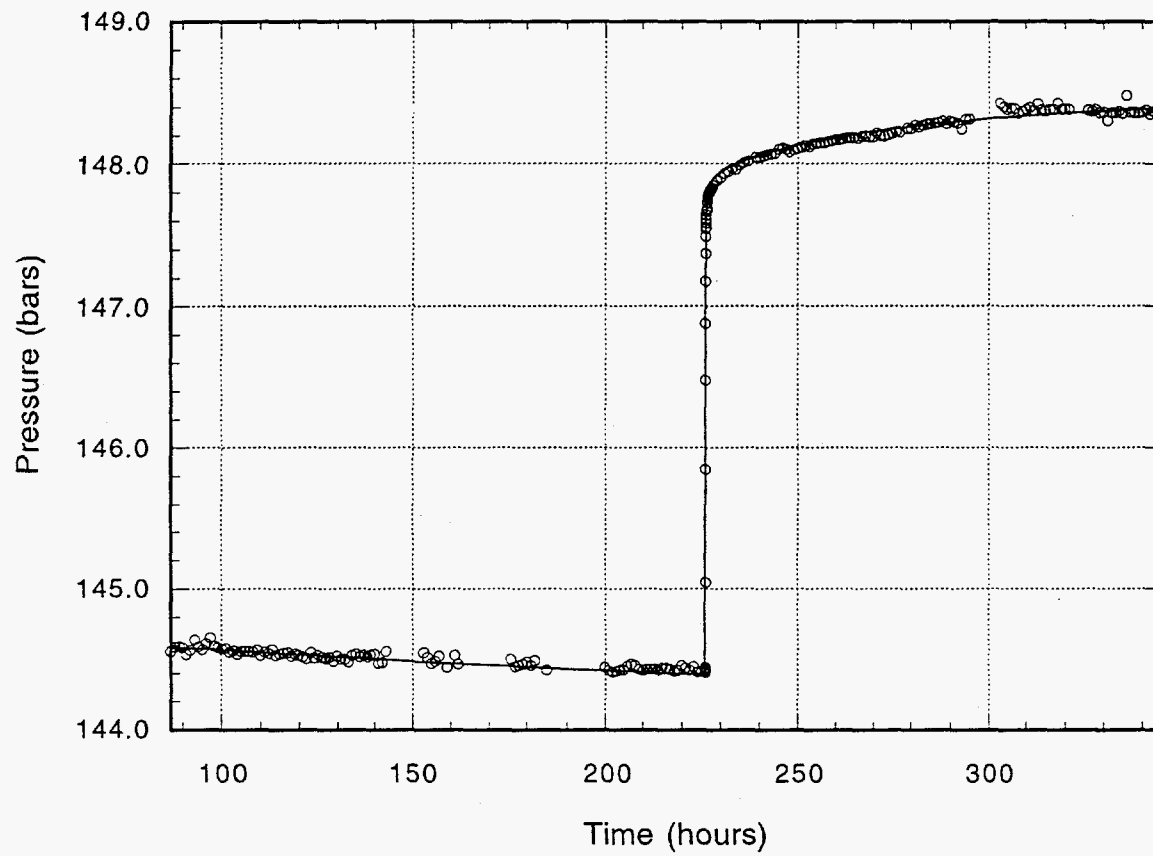


Figure 6.29. Comparison of computed and measured pressures for the first 1988 discharge test of SC-1.

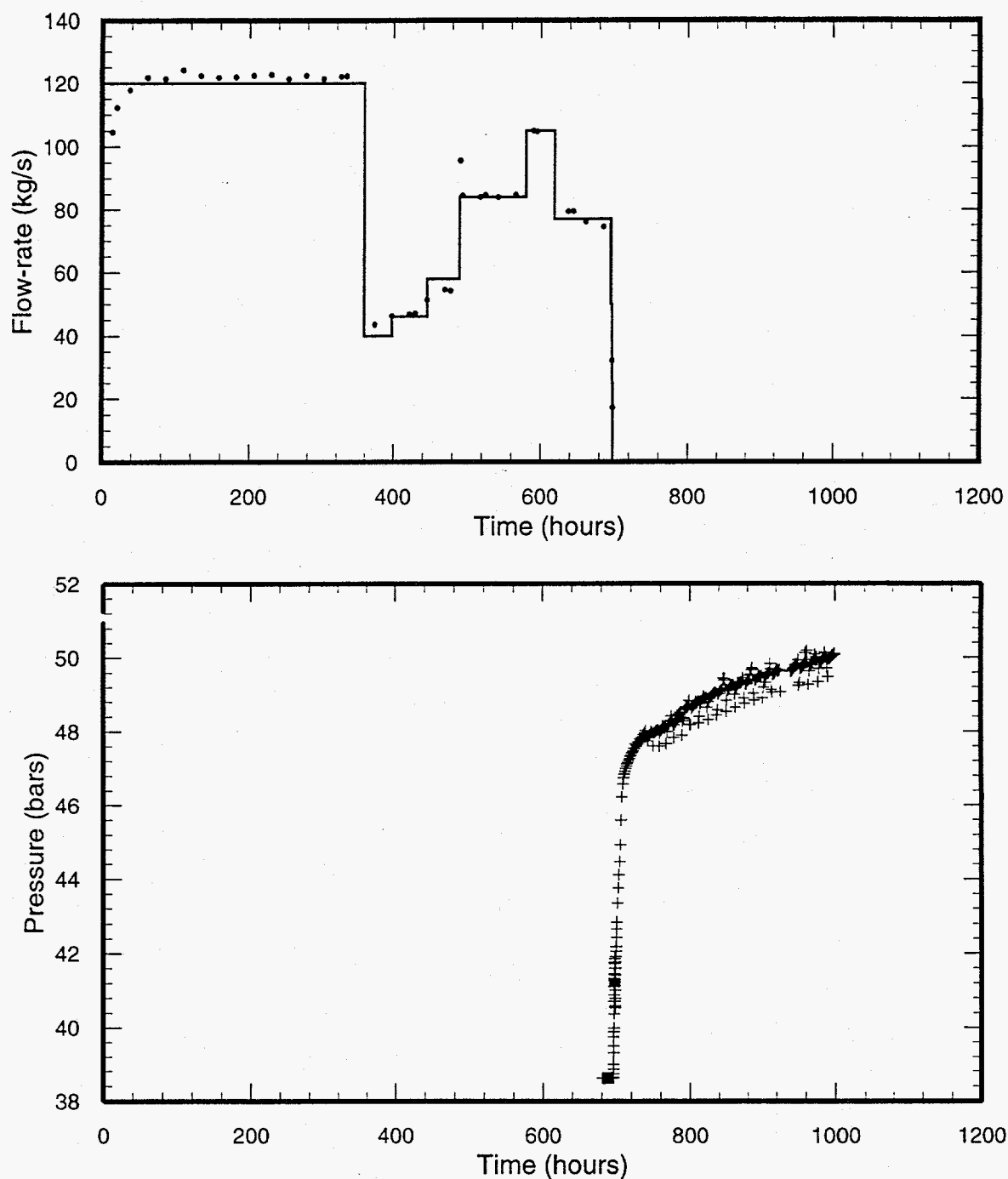


Figure 6.30. The upper panel shows the discharge rates (•) reported by MMC for the second 1988 discharge test; the solid line (upper panel) is the approximate discharge history used for pressure transient calculations. The pressures recorded by a capillary type gauge at 971 m TVD are shown in the lower panel. All times are since the start of the discharge test at 10:00 LT on October 17, 1988.

kh , (3) skin, s , (4) wellbore storage, C , and (5) distances to the two boundaries, X_B and Y_B . Minimization of errors gave the following values for the model parameters:

Initial Pressure, $p_i = 52.4$ bars
 Permeability-Thickness, $kh = 16.1$ darcy-m
 Skin, $s = -0.3$
 Wellbore Storage, $C = 2.18 \times 10^{-3} \text{ m}^3/\text{Pa}$
 Distance to Boundary, $X_B = 1660$ meters
 Distance to Boundary, $Y_B = 1660$ meters

The measured pressure values are compared with calculated pressures in Figure 6.31; the agreement is quite good.

The 1989 Discharge Test

The discharge rate data for well SC-1, as reported by MMC for the 1989 discharge test are shown in Figure 6.32. For pressure transient analyses purposes, the actual discharge rate history was approximated as a series of step-rate changes (Figure 6.32). The pressure transient response during the latter part of the 1989 discharge test and during the subsequent pressure buildup was recorded with a capillary tube type pressure gauge located at 2315 m TVD. The measured pressure series was filtered to eliminate short wave length fluctuations in the data; the filtered pressures are illustrated in Figure 6.32. To simplify pressure transient analysis, it was decided to consider only a limited subset of pressure drawdown data. More specifically, only pressure data obtained from $t \sim 825$ hours to $t \sim 1200$ hours (discharge rate ~ 130 to 140 kg/s) are considered. Additionally, the filtered pressure data (Figure 6.32) were sampled to retain a manageable number (< 100) of pressure values.

For geothermal wells with a long section of open borehole, the appropriate value for forma-

tion thickness (and hence storage) is usually an unknown. To determine the formation thickness (and storage), an initial analysis was performed using the finite-spherical source model to fit the pressure buildup data for the 1989 discharge test. The SC-1 feedpoint is assumed to be located midway between an aquifer of finite height (h). Stated somewhat differently, the feedzone is taken to be equidistant ($\pm 0.5 h$) from an upper and a lower boundary. The formation porosity-compressibility product (ϕc) was kept fixed at $3 \times 10^{-11} \text{ Pa}^{-1}$. The unknown parameters in the model are (1) initial pressure, p_i , (2) spherical permeability, k , (3) effective spherical wellbore radius, r_{sw} , (4) wellbore storage, C , and (5) formation thickness, h . Minimization of deviations between the measured and computed pressures gave the following values for the unknown parameters:

Initial Pressure, $p_i = 147.0$ bars
 Spherical Permeability, $k = 16.6$ millidarcy
 Effective Spherical Well Radius, $r_{sw} = 14.0$ m
 Wellbore Storage, $C = 5.0 \times 10^{-6} \text{ m}^3/\text{Pa}$
 Formation Thickness, $h = 420$ m

The computed results are compared with the pressure measurements in Figure 6.33; the agreement is satisfactory. With a formation thickness (h) of 420 meters, the storage (ϕch) is $\sim 1.3 \times 10^{-8} \text{ m}^3/\text{Pa}$. The latter value for storage was used for fitting all other pressure transient tests of well SC-1.

Several additional analyses were performed for the 1989 test. Best match between the measured and computed drawdown/buildup pressures was obtained using the line-source (finite wellbore) model with a single boundary. The storage ϕch was kept fixed at $1.3 \times 10^{-8} \text{ m}^3/\text{Pa}$. The unknown parameters in the model were assumed to be (1) initial pressure, p_i , (2) permeability-thickness, kh , (3) skin, s , (4) wellbore storage, C and (5) distance to boundary, X_B . Minimization

Continued on page 6-54

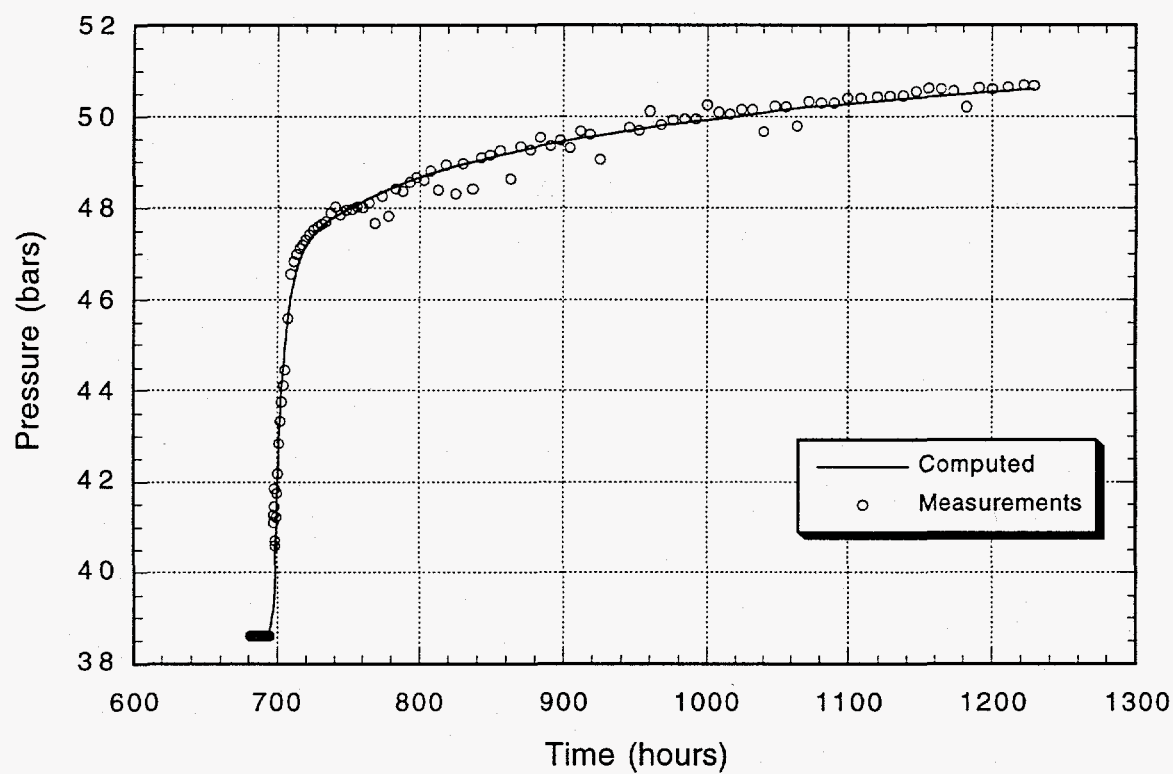


Figure 6.31. Comparison of measured (o) and computed (—) pressures for the second 1988 discharge test of well SC-1.

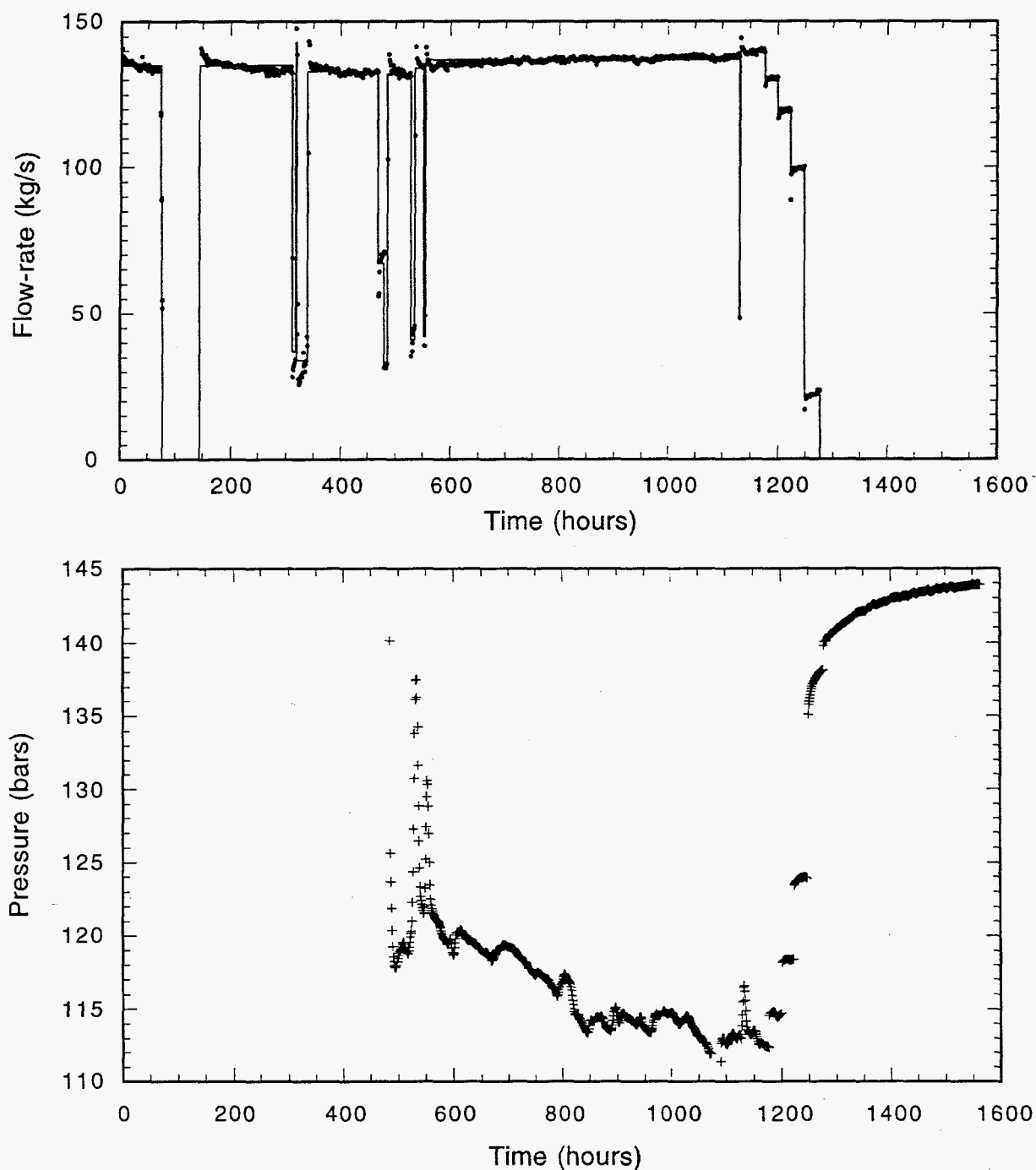


Figure 6.32. The upper panel shows the discharge rates (•) reported by MMC for the 1989 discharge test (09:10 LT October 6, 1989–13:10 LT November 28, 1989); the solid line (upper panel) is the approximate discharge history used for pressure transient analysis. The pressures recorded by a capillary type gauge at 2315 m TVD are shown in the lower panel. All times are since the start of the discharge test at 09:10 LT on October 6, 1989.

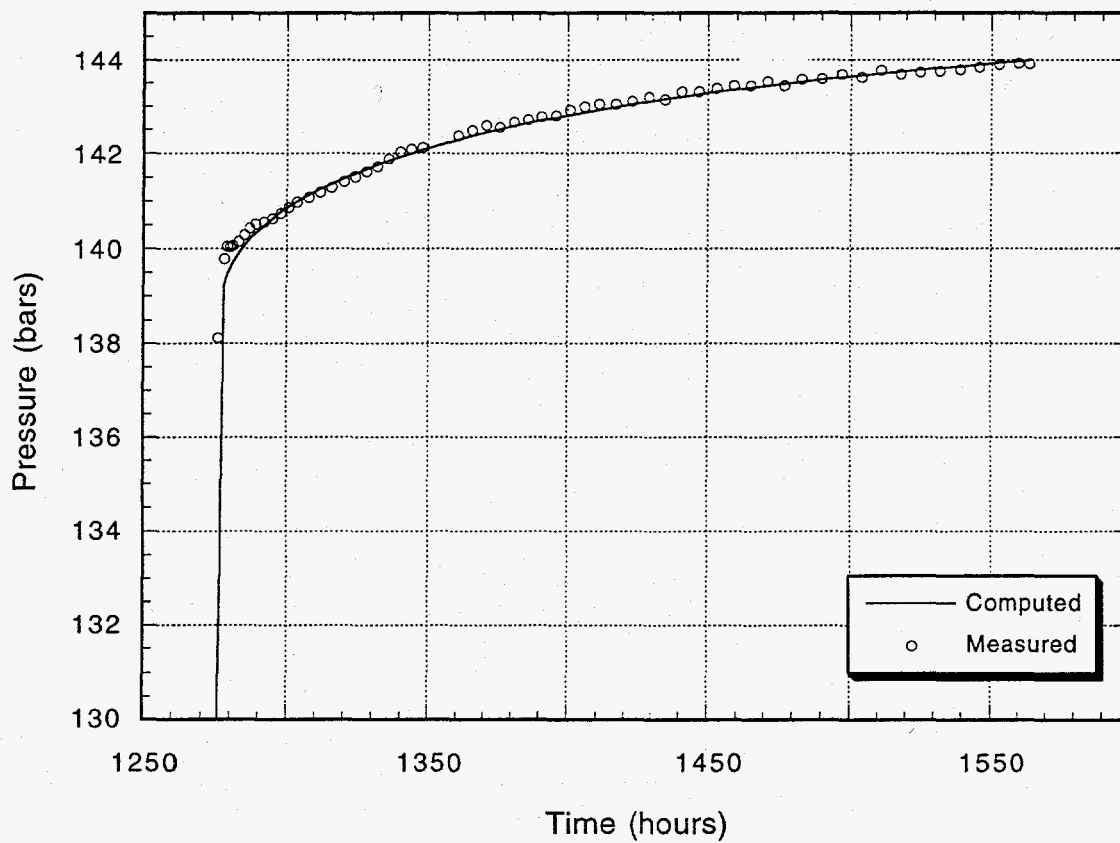


Figure 6.33. Comparison of computed (using spherical source model) and measured buildup pressures for the 1989 discharge test of well SC-1.

of errors gave the following values for the unknown parameters:

Initial Pressure, $p_i = 148.4$ bars
 Permeability-Thickness, $kh = 9.1$ darcy-m
 Skin, $s = -0.57$
 Wellbore Storage, $C = 7.4 \times 10^{-5}$ m³/Pa
 Distance to Boundary, $X_b = 1490$ m

The computed pressures are compared with the measurements in Figure 6.34; the agreement is quite good.

Evaluation of Model Results

The formation parameters inferred from the two short-term injection tests and three discharge tests are compared in Table 6.6. A large variation in formation parameters is indicated from test-to-test. While parameters inferred from the two short-term injection tests are not expected to be reliable, the substantial difference in “ kh ” values obtained from the three discharge tests is especially troubling. The permeability-thickness value obtained from the first 1988 discharge test exceeds by factors between 2.8 and 6.3 the “ kh ” values for the other two discharge tests. Clearly, something is wrong with the results obtained from the first discharge test. Several candidate hypotheses were evaluated in an attempt to explain these discrepancies. For a time, it was thought that the discharge rate from the first 1988 test had been erroneously reported (for example, that perhaps only one of the two available weir boxes had been in use instead of both, resulting in an error of a factor of two in the reported flow rates). MMC insists that this is not the case. The following hypothesis is offered as a likely explanation.

Suppose that, during the first 1988 discharge test, the downhole chamber filled completely with water prior to the shut-in of the well. If this

was the case, then the pressure data illustrated in Figure 6.28 were collected when the water level had risen up into the capillary tubing itself. Under these conditions, it is easy to show that the *indicated* pressure (p_I) disturbance recorded by the surface transducer will differ from the *true* pressure (p) disturbance by:

$$\frac{dp_I}{dp} = \frac{p_I}{(p_I + \rho g L)}$$

where ρ is the density of the water surrounding the downhole chamber, g is the acceleration due to gravity, and L is the total capillary tube length. For the present case, taking the density of water to be 810 kg/m³ (appropriate for 245°C, the approximate temperature of the deepest feedzone for SC-1), taking the total length of capillary tubing (including that on the drum at the surface) as 2.45 km as reported by MMC, and taking a “typical” value of p_I to be 140 bars, there follows:

$$\frac{dp_I}{dp} = 0.4$$

This means that, if the above hypothesis is correct, the downhole pressure disturbances during the first 1988 discharge test were actually ~ 2.5 times greater than measured by the surface transducer.

Because of the uncertainties associated with the pressure signal for the first 1988 discharge test, and the shallow gauge location during the second 1988 discharge test, the formation parameters inferred from these two tests may not be reliable. Accordingly, the best available estimate for formation parameters is provided by the analysis of the 1989 discharge test. However, at this stage it would be foolhardy to claim that the formation properties for the reservoir intercepted by well SC-1 are well characterized. Additional pressure transient test data for well SC-1 are required to resolve the uncertainties and ambiguities raised by the available test data.

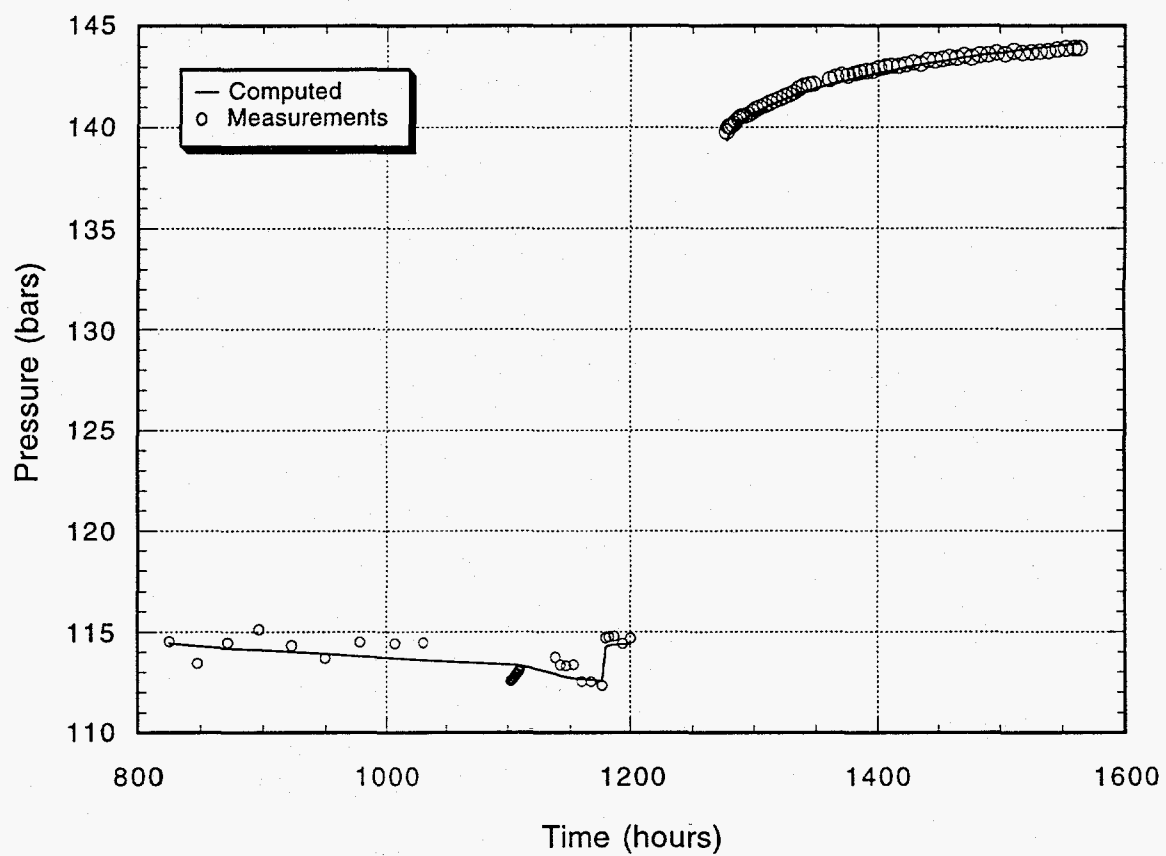


Figure 6.34. Comparison between measured (o) and computed (—) drawdown/buildup pressures for the 1989 discharge test of well SC-1.

Table 6.6. Formation parameters inferred from various pressure transient tests of well SC-1.

PARAMETER	TEST				
	November 1987 Injection Test	June 1988 Injection Test	First 1988 Discharge Test	Second 1988 Discharge Test	1989 Discharge Test
Nominal Gauge Depth (m TVD)	2290	2329	2315	971	2315
Initial Pressure (bars)	148.0	153.5	148.7	52.4	148.4
Permeability-Thickness, kh (Darcy-m)	18.7	5.9	57.1	16.1	9.1
Skin, s	12.7	-2.3	17.2	-0.3	-0.6
Wellbore Storage, C (m ³ /Pa)	1.6×10^{-5}	1.9×10^{-5}	4.5×10^{-5}	2.2×10^{-3}	7.4×10^{-5}
Distance to First Boundary	NA	NA	1310	1660	1490
Distance to Second Boundary	NA	NA	1450	1660	NA

NA = Not Applicable

7 A Conceptual Model of the Sumikawa Geothermal Field

A conceptual model may be defined as a descriptive model that encompasses the essential physical processes operating in a geothermal system. Alternatively, a conceptual model may be thought of as a means of visualizing the flow pattern(s) in the system. In any event, a conceptual model is a prerequisite for developing detailed quantitative models of the geothermal reservoir. The main elements of a hydrothermal system (White, 1961) are shown, in schematic manner, in Figure 7.1. Surface water (rainwater, snow, etc.) is the principal source of recharge water. Part of this recharge (A), supplies the shallow (and cold) groundwater aquifers, and since the recharge water is cooler (and denser) than the deeper fluid, part will flow down permeable faults (B). The downward flowing cold water will be heated within some "heating volume" as it approaches the deep heat source (magma body?) and will mix with some amount of altered magmatic fluid. Some of the heated fluid mass will then convect upward along permeable faults (C). As the fluid rises vertically, it will depressurize and may boil. Most of the upwelling fluid will likely either flow laterally into the geothermal reservoir or be forced laterally by the relatively impermeable geothermal reservoir cap (D), but some will leak across the cap into the shallow aquifer (E). Some of the reservoir fluid, (F), may also exit at the ground surface and produce surface manifestations such as hot springs and fumaroles. Finally, part of the fluid leaving the heating volume will also be pushed laterally, (G). All the elements of this idealized model need not be present in a real hydrothermal system. Many variations are

possible. The low permeability cap is often either absent or provides a less than perfect barrier to fluid flow. In many places (e.g., Imperial Valley Geothermal Fields, U.S.A.), surface manifestations such as hot springs/fumaroles are nonexistent. Also, nonmeteoric waters (e.g., sea water and magmatic water) are present in many hydrothermal systems.

A geothermal reservoir may contain either single-phase fluid or a two-phase mixture of liquid and steam. In either case, the geothermal system is driven by an upflow of fluid from depth. The two-phase systems are created by the depressurization of this upflowing fluid, and its boiling at some depth. The fluid upflow is two-phase at exploitable depths. In mountainous terrain, steam will rise vertically to create a vapor zone and steam-heated surface discharges (fumaroles, acidic hot springs, etc.), and liquid will flow away horizontally to eventual discharge as chloride springs. This basic model holds for many two-phase geothermal systems (e.g., Baca, New Mexico, U.S.A.; Sumikawa, Japan).

The idealized model(s) described above provides a convenient point of departure for data synthesis and for the development of specific conceptual models. To be useful for detailed quantitative modeling, a conceptual model should encompass a description of (1) source fluid(s) (i.e., meteoric, sea water, magmatic), (2) fluid state (pressure, temperature, salinity, gas content, etc.), (3) the permeability structure, (4) the thermal and hydraulic boundaries of the system, (5) the

Continues on page 7-3

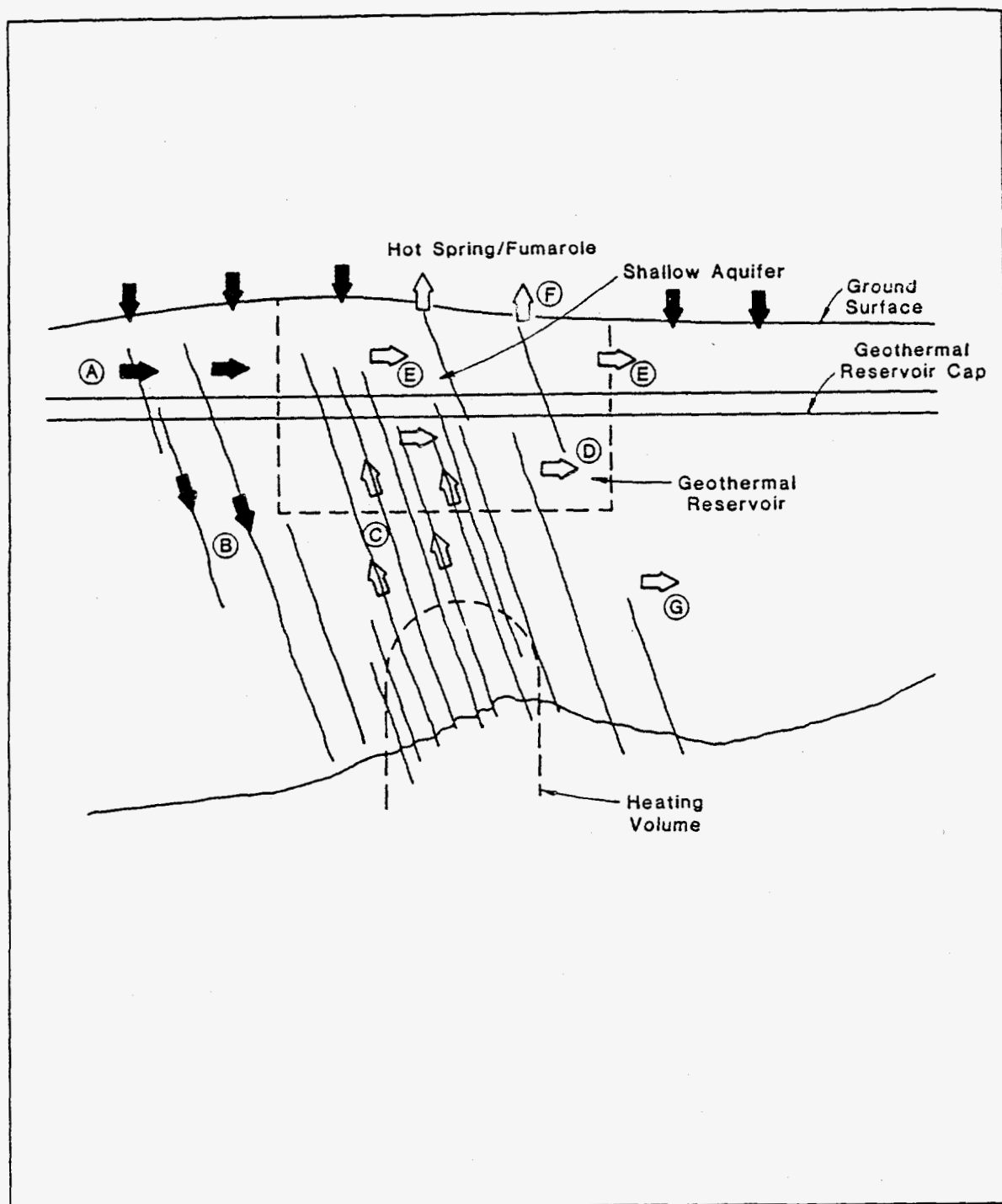


Figure 7.1. Schematic diagram of a hydrothermal system.

deep heat source, and (6) the evolution of the geothermal system to its present state. More often than not, little or no information is available concerning the deep heat source, the region of downflow (recharge zone), and the hydraulic boundaries of the system (at least prior to large scale exploitation of the geothermal reservoir), and it is necessary to invoke a variety of hypothesis regarding these elements of the geothermal system. As far as possible, the conceptual model should be based on field measurements. In the following sections, we will outline a conceptual model for the Sumikawa Geothermal Field.

7.1 Fluid State

7.1.1 Reservoir Pressures

The reservoir pressures identified from an analysis of various wells may be synthesized to yield the subsurface pressure distribution in the geothermal reservoir. For a reservoir with good horizontal and vertical permeabilities, feed point pressure should depend only upon feed point depth (measured from a common datum), i.e.

$$P = P_o + az \quad (7.1)$$

where z denotes the feedpoint depth below some common datum (sea-level, for example), and a and P_o are constants.

A least-squares procedure was employed to fit the feedzone pressures for the various Sumikawa wells (Section 4) to Equation (7.1). The results of the least-squares fit are:

$$P = 61.088 - 0.07440 Z \quad (7.2)$$

where P is in bars (absolute) and Z is in mASL (meters above sea level).

Pressure data for wells SA-2 and SA-4 were not included in the mathematical fit. The root-mean-square error of the above fit is 1.66 bars. As can be seen from Figure 7.2, the mathematical fit agrees closely with all of the pressure data used to derive the fit. Feedzone pressures for wells SA-2 and SA-4 differ substantially ($\sim 9 \pm 0.6$ bars) from the mathematical fit. Although there is some uncertainty concerning the SA-2 and SA-4 feedzone pressures, the latter result suggests that these wells may be poorly connected to the permeable region at Sumikawa. Discharge from these wells is accompanied by *in situ* boiling and a large pressure drop. Clearly, wells SA-2 and SA-4 are located in a low permeability zone.

The vertical pressure gradient at Sumikawa is 7.440 kPa/m, and corresponds to a hydrostatic gradient at $\sim 275^\circ\text{C}$. This implies fluid upflow in regions of the reservoir where temperature exceeds 275°C . The reservoir pressure extrapolates to atmospheric pressure (~ 0.9 bars) at $Z = 809$ mASL. The nominal piezometric surface for the Sumikawa reservoir thus lies at ~ 809 mASL.

As part of a heat-flow survey of the Sumikawa/Ohnuma area, a number of shallow (80 meter) heat flow holes were drilled over a 20 square kilometer area. Of the 32 such wells for which records are available, standing water was present above bottomhole in all but two. It therefore appears that the water table lies generally above 80 meters depth in the area.

The locations of the various heat flow holes are shown in Figure 7.3. Also shown, for reference, are the positions of a number of the deeper wells in the area, and the location of the Ohnuma power station. The wells are seen to be reasonably uniformly distributed over the area. For each of the 32 heat flow holes, the depth of the standing

Continues on page 7-6

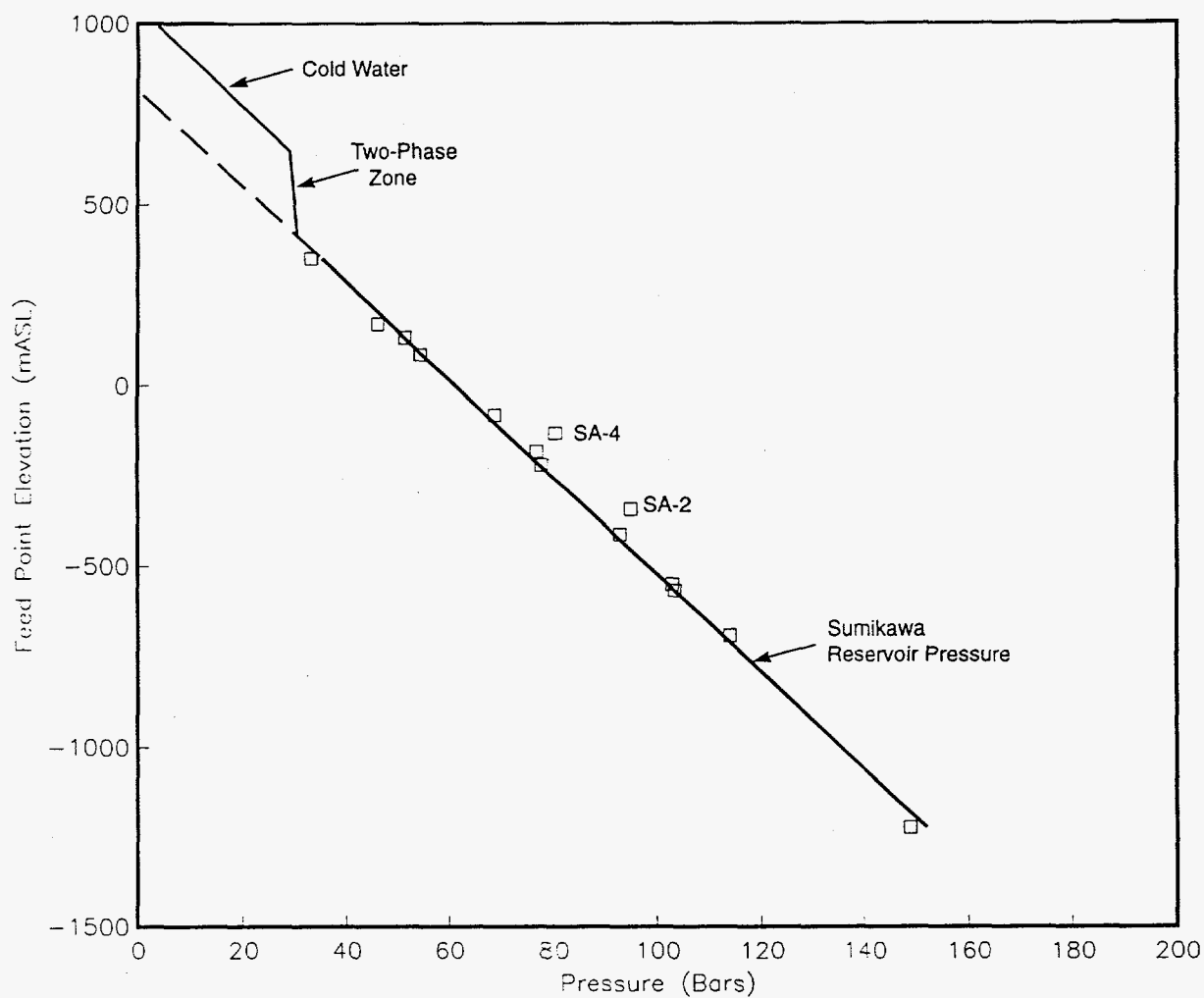


Figure 7.2. Sumikawa reservoir pressures. Wells SA-2 and SA-4 were not included in the mathematical fit to the feedzone pressures (solid and dashed straight line). The locations of the two phase zone and the shallow cold water reservoir are only schematic.

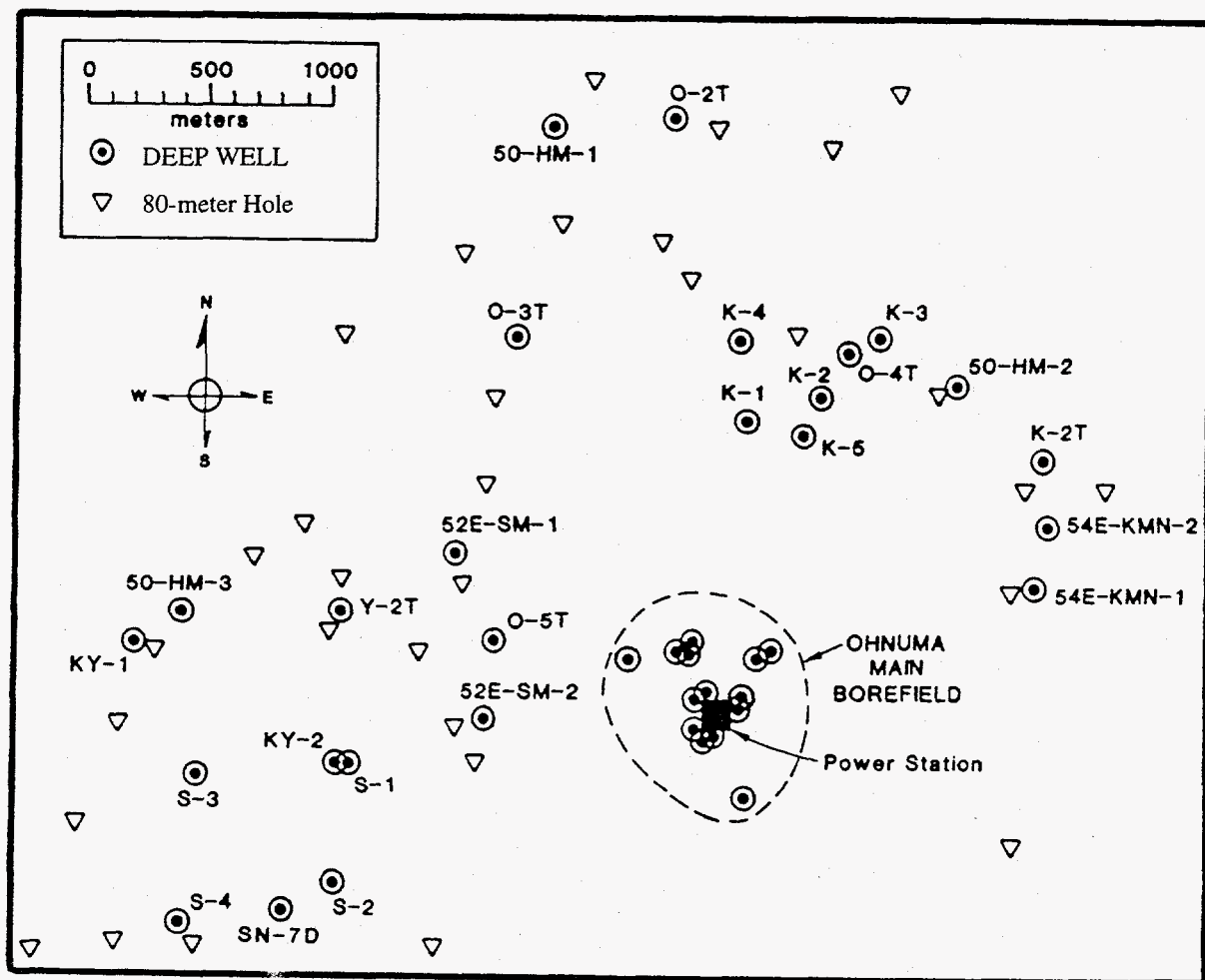


Figure 7.3. Locations of 80-meter heat flow holes in Sumikawa/Ohnuma area.

water level, sorted in order of increasing wellhead elevation above sea level, is given in Table 7.1. There is a substantial scatter in the stable water depths, and there appears to be very little correlation between standing water depth and ground surface elevation. It seems fair to conclude that the water level in an 80-meter hole in the Sumikawa/Ohnuma area will, on the average, be about 45 meters downhole, with a standard deviation of plus or minus 21 meters.

The average ground surface elevation in the vicinity of S-series wells is ~1060 mASL. The water table in this area is presumably located on average at ~1015 mASL. The nominal piezometric surface extrapolated from a fit to feedzone pressures lies about 200 meters below the local water

table. The discrepancy between the positions of the nominal piezometric surface for the deep reservoir and that for the shallow ground water aquifer is most likely due to the presence of a two-phase zone (see Figure 7.2 for a schematic representation of the shallow cold water aquifer and the two-phase zone at Sumikawa). The two-phase zone has a subhydrostatic gradient, and separates the deeper hot water reservoir from the shallow cold water equifer.

In the general neighborhood of the S-series wells, the region of subhydrostatic pressure gradient begins at least as deep as +300 m ASL. The lake sediment layer (which appears to serve as a relatively impermeable caprock for this part of the reservoir) extends no deeper than about +600 m

Table 7.1. Depths of standing water in 80-meter heat flow holes.

GSE	SW D	GSE	SW D	GSE	SW D	GSE	SW D
580	28	740	75	870	19	960	29
680	35	770	42	900	15	980	43
680	77	770	44	910	17	990	60
700	9	810	48	910	37	1000	11
700	30	820	80*	920	20	1060	42
700	68	830	67	930	36	1100	80*
740	30	840	40	940	59	1130	44
740	35	860	67	950	62	1130	73

*Well was dry.

Average ground surface elevation = 863.8 meters ASL

Average standing water depth = 44.4 meters

One standard deviation in water depth = 21.4 meters

"GSE" = ground surface elevation in meters, ASL.

"SW D" = stable standing water depth in well, meters.

ASL in this vicinity. Thus, the intervening volume probably contains a two-phase flow region, with a recirculating mixture of water and steam trapped between the sedimentary caprock above and a hot compressed-liquid layer below. The depth of the bottom of this two-phase region probably depends upon position and increases as one moves southward toward the Mt. Yake volcano. It should be realized that the depth of onset of the subhydrostatic pressure gradient (~300 m ASL) only establishes an upward bound on the extent of the two-phase region—the actual boiling interface depth depends on temperature and could be much deeper. A subhydrostatic gradient merely indicates that the steam phase occupies most of the fluid volume so that the liquid phase has become essentially immobile. Two-phase flow with high liquid content relative to steam will be characterized by a liquid-hydrostatic pressure gradient, just like a single-phase liquid region. Above the sedimentary caprock, the distributions of underground pressure resemble cold-water hydrostatic columns suspended from a water table (one-atmosphere surface) which lies only a short distance below the local ground surface.

The average permeability of the lake sediment caprock itself must be exceedingly low. The vertical pressure gradient across this layer is much less than hydrostatic, as noted above. Under these circumstances, cold water from the shallow volcanic layer above will flow downward, cool the reservoir, and extinguish the underlying two-phase flow zone unless the permeability (k) of the caprock layer satisfies:

$$k \ll (K \times v) / (\rho \times g \times c_{vf} \times H) \quad (7.3)$$

This expression may be derived by requiring that the average upward conductive heat flux across the caprock layer:

$$\text{Conductive flux} = K \times (T_{\text{lower}} - T_{\text{upper}}) / H$$

be vastly greater than the downward convective cooling flux from above for zero vertical pressure gradient:

$$\text{Convective flux} = k \times c_{vf} \times \rho \times g \times (T_{\text{lower}} - T_{\text{upper}}) / v$$

where T_{upper} is the cold-water temperature in the upper zone above the caprock and T_{lower} is the underlying reservoir temperature. Taking the following typical values:

K (thermal conductivity)	$= 2 \text{ W/m} \cdot ^\circ\text{C}$
v (fluid kinematic viscosity)	$= 2 \times 10^{-7} \text{ m}^2/\text{s} \text{ (150}^\circ\text{C)}$
ρ (fluid density)	$= 920 \text{ kg/m}^3 \text{ (150}^\circ\text{C)}$
g (gravity acceleration)	$= 9.8 \text{ m/s}^2$
c_{vf} (fluid heat capacity)	$= 4300 \text{ J/kg} \cdot ^\circ\text{C} \text{ (150}^\circ\text{C)}$
H (caprock thickness)	$= 200 \text{ m}$

we obtain for the lake sediment permeability:

$$k \ll 5 \times 10^{-17} \text{ m}^2 (= 0.05 \text{ millidarcies}).$$

7.1.2 Reservoir Temperature

At Sumikawa, underground temperatures are highest to the south and decline to the north and northwest. The estimated temperatures at sea level (~700-1100 m depth) in the area (based mainly on temperature surveys in shut-in boreholes are shown in Figure 7.4. The highest temperature so far measured in the field is at the bottom of well SA-2 (320°C at 840 below sea level); this is also the southernmost deep borehole at Sumikawa.

Temperatures are significantly higher at Sumikawa (near the S-series boreholes) than at the nearby operating Ohnuma borefield. Generally speaking, temperatures appear to increase mono-

Continues on page 7-9

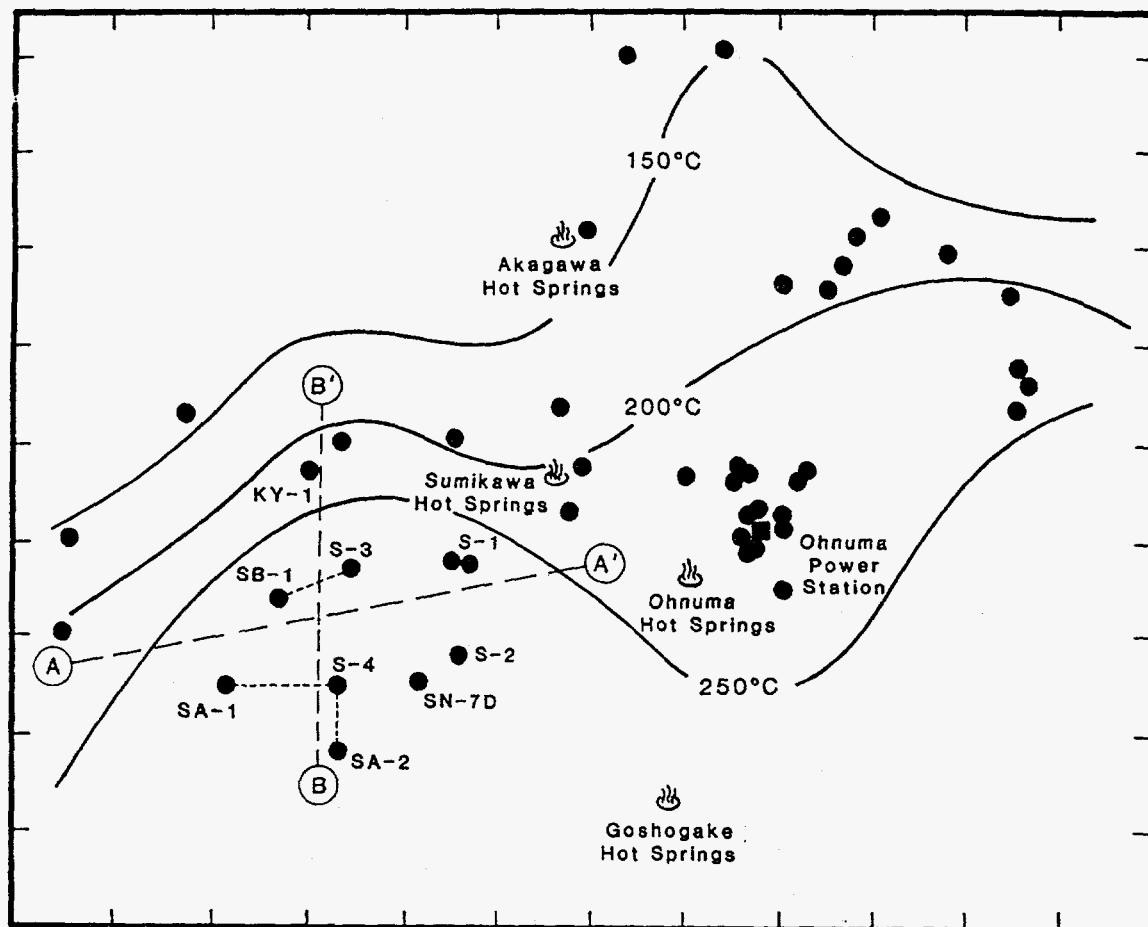


Figure 7.4. Temperatures at sea-level elevation in the Sumikawa/Ohnuma area (adapted from Kubota, 1988).

tonically with depth. Temperature inversions have, however, been observed in two boreholes (SC-1 and SD-1). Well SC-1 is located between wells S-2 (to the east) and S-4 (to the west); the maximum temperature ($\sim 310^{\circ}\text{C}$) occurs at $\sim 650 (\pm 150)$ meters below sea level. Well SD-1 is located ~ 500 meters to the north of well SC-1; a temperature inversion in SD-1 is present at about $400 (\pm 50)$ meters below sea level. The temperature inversions in wells SC-1 and SD-1 indicate fluid flow to the north and to the east.

The existence of a positive self-potential anomaly in the neighborhood of the S-series boreholes (Ishido, et al., 1987) is indicative of the presence of upwelling deep hot water in the vicinity. The upwelling hot water flows laterally to the north and to the east of pad A (drilling pad for wells S-4, SA-1, SA-2 and SA-4). Observed surface manifestations of hot-water upflow (hot springs) are generally located along a north-south axis (east of S-series wells) lying between Sumikawa and Ohnuma. Most of these springs are acid SO_4 indicating vertical upflow of steam from boiling liquid. The relatively low temperatures encountered to the north and west of the Sumikawa may be indicative of downward flux of cold water in these areas (see also Kubota, 1988).

7.1.3 Fluid Chemistry

The Sumikawa reservoir fluid is of low salinity. The chlorinity ranges from 100 mg/kg to 600 mg/kg. The noncondensable gas content is also very small, typically $< 0.1\%$ by volume of the produced steam. Thus, for many reservoir engineering purposes, the Sumikawa reservoir fluid can be treated as pure water.

From a geochemical viewpoint, the Sumikawa reservoir fluid is unusually inhomogeneous. The geochemical temperatures span a wide range (200 to 300°C), and the Cl/B (usually considered non-reactive constituents) ratio varies from 5 to 1.5. In addition, $\text{Cl}/(\text{HCO}_3 + \text{SO}_4)$, $\text{Mg}/(\text{Na}+\text{K})$, and enthalpy values exhibit a wide variation. The diversity in chemical compositions suggests that the Sumikawa geothermal system is relatively young (see also Section 7.4), and that little mixing has occurred within the reservoir.

At Sumikawa, the reservoir fluids are mainly of the NaCl type with a near neutral pH. Acidic fluids were, however, encountered in wells S-2 and SA-2. Well SA-2 is the southernmost borehole at Sumikawa. The $\text{Ar-N}_2\text{-He}$ data for SA-2 indicates strong magmatic influence. Mt. Yake is located approximately 1 km south of SA-2. The Tamagawa hot spring on the west slope of Mt. Yake produces partially altered and diluted volcanic fluid. It is, therefore, reasonable to conclude that acidic fluids in SA-2 have a volcanic origin. While the surface oxidation of H_2S cannot be ruled out as the major source of acidity in S-2 waters, the relatively high Cl in S-2 indicates magmatic influence.

The enthalpy-chloride diagram suggests a parent water at 345°C with about 250 mg/kg chloride. With the exception of S-2 waters, the Sumikawa waters can be produced by boiling and dilution from this parent water. The S-2 waters are much higher in chloride than other Sumikawa waters, and may contain a magmatic component that has not been fully diluted and neutralized.

7.2 Heat Source

The temperatures at Sumikawa generally increase in a southward direction towards Mt. Yake.

The highest temperature ($\sim 320^{\circ}\text{C}$) was recorded in the southernmost deep borehole SA-2. Well SA-2 is located approximately 1 km north of Mt. Yake. As remarked earlier, SA-2 fluids exhibit a distinct magmatic component. Along with temperature, both the chloride and isotopic ($\delta^{18}\text{O}$) values increase to the south. These data indicate that the heat source for the Sumikawa geothermal field lies under Mt. Yake. High temperature and isotopically heavy concentrated brine rises vertically from the upflow zone under Mt. Yake, flows to the north and northeast and gets diluted by meteoric water. The total thermal output of hot springs, thermal seepages into rivers and conductive heat flux at Sumikawa is estimated to be about 70 MW (Section 2). This value provides a lower bound on the heat content of the high temperature recharge fluid from the Mt. Yake upflow zone.

7.3 Formation Permeability and Hydraulic Boundaries

MMC has performed both single-well and multiple-well pressure transient tests. These pressure transient tests have been invaluable for delineating the permeability structure at Sumikawa (Section 6). The vertical permeabilities at Sumikawa are small in comparison with horizontal permeabilities. Permeability in the field is due primarily to the pervasive network of fractures. Both the volcanic and sedimentary country rocks between the fractures appear to be essentially impermeable. The lake sediments are nearly impermeable and act as a caprock for the underlying geothermal reservoirs.

The fluid production at Sumikawa is mainly derived from two geothermal aquifers within the "altered andesite" and the deeper "granodiorite" formations. The shallower of these two reservoirs

(in the andesite formation) is usually encountered between 1000 and 1800 meters depth, and has been penetrated by several wells. The transmissivity for the altered andesite reservoir is ~ 13 darcy-meters (Section 6.1). At present, only well SC-1 produces a substantial quantity of hot fluid from a permeable horizon in the "granodiorite" formation. Pressure transient data for well SC-1 indicate a transmissivity of ~ 9 darcy-meters (Section 6.3). The "marine-volcanic complex" formation contains one or more permeable dacite layers. Because of its low vertical permeability, the "marine-volcanic complex" formation will be used for injecting waste brine. The dacite layers sandwiched between black shales have moderate to good transmissivity (Section 6.2).

The pressure interference data for wells S-4 and N60-KY-1 indicate the presence of impermeably hydraulic boundaries to the west and the north of the S-series wells. The western boundary is most likely associated with the abrupt rise of granodiorite formation to the west of well S-4. The presence of the western boundary is also implied by gravity and electrical data (Section 2). The northern boundary is probably associated with the dacitic dike along the Kumazawa river.

Both the pressure interference data for wells S-4 and N60-KY-1, and the stable feedzone pressure data imply the presence of a permeable barrier between the Sumikawa and Ohnuma fields. Ohnuma geothermal field has been in production since 1973. Since the start of production at Ohnuma, the pressures at Ohnuma have fallen by over 10 bars. The stable feedzone pressures (pre-1990) at Sumikawa are, however, in close agreement with pre-1973 Ohnuma pressures. This implies the pressures of a low permeability zone between the two reservoirs (Pritchett, et al., 1990).

As noted earlier, the Sumikawa geothermal field receives fluid recharge from the south. Although the geothermal system is open to the south, the low productivity of wells SA-1, SA-2 and SA-4 suggests that the formation permeability is small. The feedzone pressures for wells SA-2 and SA-4 are at present not well characterized. Available pressure data indicate that feedzone pressures for wells SA-2 and SA-4 are considerably higher than those for other Sumikawa wells, and imply that these wells are poorly connected to the rest of the geothermal field.

7.4 Evolution of Sumikawa Geothermal System

Geothermal systems prior to exploitation are sometimes treated as steady-state systems. This is true in only a very narrow sense in that the physical processes occurring in a geothermal system over a 10-50 year time-scale are more or less stationary. Over a longer time-scale (10^3 - 10^5 years), these systems do undergo transformations.

Available estimates of lifetimes for specific geothermal systems run as high as 3 million years (Grant, et al., 1982). Simulations of transient convection processes associated with the initiation of convection due to single magma intrusions show that the time to reach steady-state is about 10^4 years (see e.g., Garg and Kassoy, 1981). This implies that a single magma source cannot supply the heat required to maintain a geothermal system; the magma body responsible for geothermal activity must itself be in convective contact with a still deeper magma source.

From a modeling point of view, it is useful to know if a given geothermal system is heating up or cooling down. Comparison of present-day reservoir temperatures with those derived from fluid in-

clusions and alteration mineralogy may be used to establish the present stage (heating up or cooling down) in the life of a geothermal reservoir. The homogenization temperatures of fluid inclusions found during drilling of various wells in the Sumikawa area are shown in Figure 7.5. Most of these "homogenization temperatures" do not exceed the present temperature in the system. This implies that the system is heating up (not cooling down), and is accordingly young. The latter conclusion is also supported by the unusually inhomogeneous reservoir fluids at Sumikawa (Section 7.1.3).

7.5 Concluding Remarks

The principal purpose of this case study of the Sumikawa geothermal field is to document and to evaluate the use of drilling logs, surface and downhole geophysical measurements, chemical analyses, and pressure transient data for the assessment of a high temperature volcanic geothermal field. Reservoir assessment may be defined as the prediction of the quantity and quality of fluid that may be withdrawn from a given geothermal field. A computer based numerical model is usually required for making detailed predictions regarding the response of a geothermal system to exploitation. A physically viable conceptual model is a necessary prerequisite for the development of detailed three-dimensional numerical models.

The conceptual model of the Sumikawa geothermal field presented herein was developed by utilizing all available pre-exploitation data. This model may be used as a point of departure for developing numerical models of the Sumikawa geothermal field. As discussed elsewhere in this report, surface geological surveys, chemical analyses, drilling data and pressure transient measurements were found most useful for formulating the

Continues on page 7-13

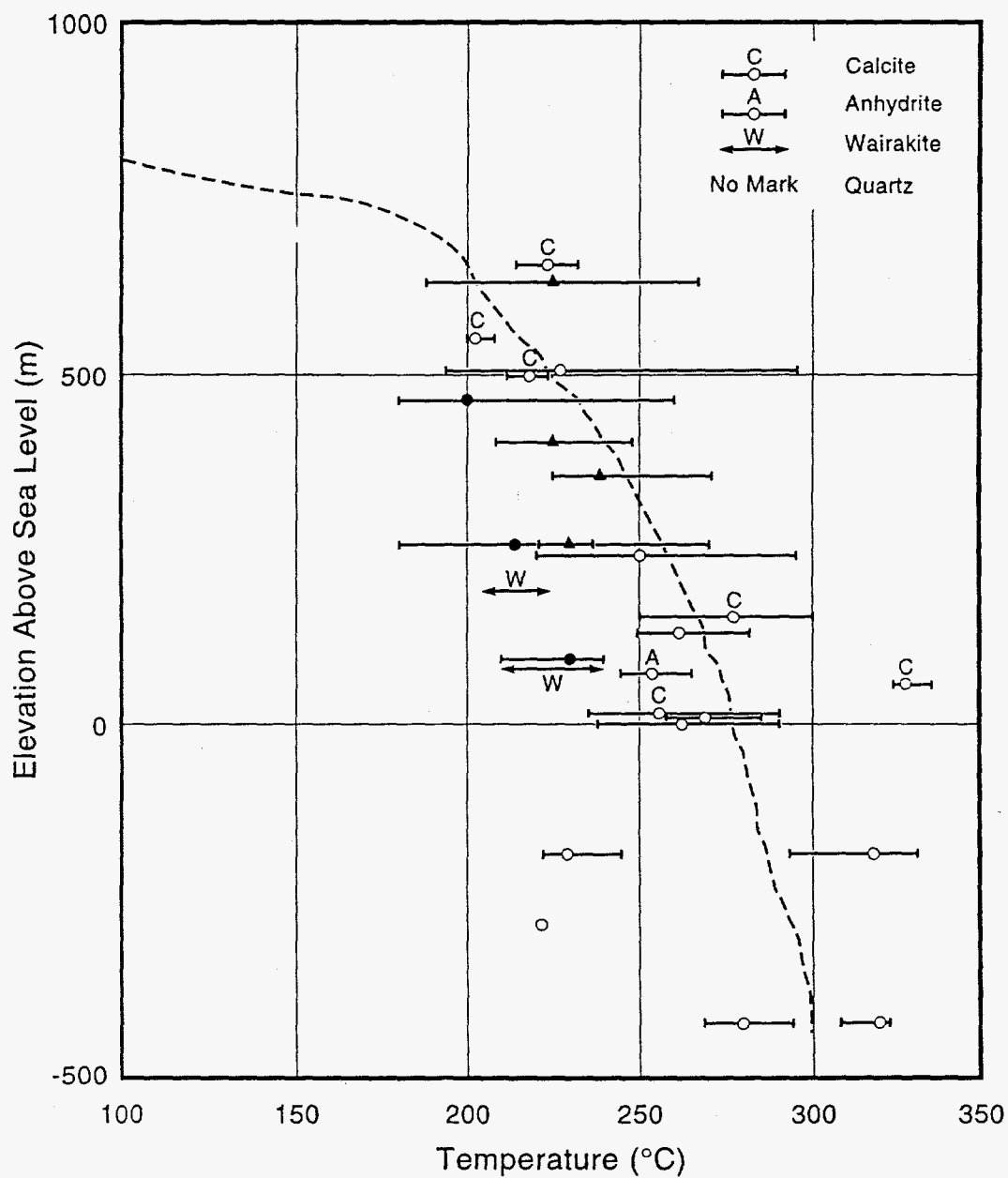


Figure 7.5. Comparison of fluid inclusion temperatures with measured temperatures in (dashed line) Sumikawa Well S-4 (from MMC, 1985).

Sumikawa conceptual model. For various reasons, geophysical measurements such as gravity, seismic and electric surveys have proven to be of limited value at Sumikawa. It would be, however, foolhardy to generalize the Sumikawa experience. Each geothermal prospect represents a unique combination of geological, hydrological, geochemical, geophysical, financial and cultural characteristics. One set of geological and geophysical exploration and reservoir assessment techniques will not suffice in all situations.

8 References

- Alexander, J. H., T. G. Barker, S. K. Garg, K. L. McLaughlin, L. A. Owusu and J. W. Pritchett (1992), "Geothermal Well Test Analysis Software," S-Cubed, La Jolla, California, Report No. SSS-FR-92-13516, September.
- Arnórsson, S., E. Gunnlaugsson and H. Svavarsson (1983), "The Chemistry of Geothermal Waters in Iceland. III. Chemical Geothermometry in Geothermal Investigations," *Geochimica et Cosmochimica Acta*, Vol. 47, pp. 567-577.
- Arnórsson, S., S. Sigurdsson and H. Svavarsson (1982), "The Chemistry of Geothermal Waters, Iceland. I. Calculation of Aqueous Speciation from 0° to 370° C: *Geochimica et Cosmochimica Acta*, Vol. 46, pp. 1513-1532.
- D'Amore, F. and R. Celati (1983), "Methodology for Calculating Steam Quality in Geothermal Reservoirs," *Geothermics*, Vol. 12, No. 2-3, pp. 129-140.
- D'Amore, F. and C. Panichi (1980), "Evaluation of Deep Temperatures of Hydrothermal Systems by a New Gas Geothermometer," *Geochimica et Cosmochimica Acta*, Vol. 44, pp. 549-556.
- D'Amore, F. and A. H. Truesdell (1985), "Calculation of geothermal reservoir temperatures and steam fractions from gas compositions," *Geothermal Res. Council Trans.*, Vol. 9, part 1, pp. 305-310.
- Ellis, A.J., (1970), "Quantitative interpretation of chemical characteristics of hydrothermal systems," *Geothermics*, Vol. 2, pp. 516-528.
- Fournier, R. O. (1977) "Chemical Geothermometers and Mixing Models for Geothermal Systems," *Geothermics*, Vol. 5, pp. 41-50.
- Fournier, R. O. (1979), "A Revised Equation for the Na/K Geothermometer," *Geothermal Resources Council Transactions*, Vol. 3, pp. 221-224.
- Fournier, R.O. and R. W. Potter (1982), "A Revised and Expanded Silica (Quartz) Geothermometer," *Geothermal Resources Council Bulletin*, Vol. 11, pp. 3-9.
- Fournier, R. O. and A. H. Truesdell (1973), "An Empirical Na/K/Ca Geothermometer for Natural Waters," *Geochimica et Cosmochimica Acta*, Vol. 37, pp. 1255-1275.
- Garg, S. K. (1996), "An Overview of the Case Studies of the Coso, Roosevelt Hot Springs, and Sumikawa Geothermal Fields," *Proceedings U.S. Department of Energy Program Review XIV*, Berkeley, California, April 8-10, pp. 79-87.

- Garg, S. K. and J. Combs (1995), "Production/Injection Characteristics of Slim Holes and Large-Diameter Wells at the Sumikawa Geothermal Field, Japan," *Proceedings Twentieth Workshop on Geothermal Reservoir Engineering*, Stanford University, Stanford, California, January 24-26, pp. 31-39.
- Garg, S.K. and J. Combs (1997), "Use of Slim Holes with Liquid Feedzones for Geothermal Reservoir Assessment," *Geothermics*, vol. 26, pp.153-178.
- Garg, S. K. and D. R. Kassoy (1981), "Convective Heat and Mass Transfer in Hydrothermal Systems," in *Geothermal Systems: Principles and Case Histories* (Eds. L. Rybach and L. J. P. Muffler), Wiley, New York, pp 37-76.
- Garg, S. K. and L. A. Owusu (1996), "Analysis of Pressure Interference Tests for Well S-4 and Slim Hole KY-1: Sumikawa Geothermal Field, Japan," *Proceedings Twenty-First Workshop on Geothermal Reservoir Engineering*, Stanford University, Stanford, California, January 22-24, pp. 449-459.
- Garg, S. K. and J. W. Pritchett (1988), "Pressure Interference Data Analysis for Two-Phase (Water/Steam) Geothermal Reservoirs," *Water Resources Research*, Vol. 24, pp. 843-852.
- Garg, S. K. and J. W. Pritchett (1990), "Cold Water Injection into Single- and Two-Phase Geothermal Reservoirs," *Water Resources Research*, Vol. 26, pp. 331-338.
- Garg, S. K., J. W. Pritchett, K. Ariki, and Y. Kawano (1991), "Pressure-Interference Testing of the Sumikawa Geothermal Field," *Proceedings Sixteenth Workshop on Geothermal Reservoir Engineering*, Stanford University, Stanford, California, January 23-25, pp. 221-229.
- Garg, S. K., J. Combs, J. W. Pritchett, J. L. Stevens, and L. Luu (1994a), "Development of a Geothermal Resource in a Fractured Volcanic Formation: Case Study of the Sumikawa Geothermal Field, Japan (FY 1993)," Report SSS-DTR-94-14778, S-Cubed, La Jolla, California.
- Garg, S.K., J. Combs and M. Abe (1994b), "A Study of Production/Injection Data from Slim Holes and Production Wells at the Oguni Geothermal Field, Japan," Report No. SSS-TR-94-14464, S-Cubed, La Jolla, California.
- Garg, S. K., J. W. Pritchett, A. H. Truesdell and J. L. Stevens (1995), "Development of a Geothermal Resource in a Fractured Volcanic Formation: Case Study of the Sumikawa Geothermal Field, Japan (FY 1994)," Report SSS-DTR-95-14956, S-Cubed, La Jolla, California.
- Garg, S. K., J. W. Pritchett, A. H. Truesdell and J. L. Stevens (1996), "Development of a Geothermal Resource in a Fractured Volcanic Formation: Case Study of the Sumikawa Geothermal Field, Japan (FY 1995)," Report SSS-DTR-96-15423, S-Cubed, La Jolla, California.

- Giggenbach, W. F. (1980), "Geothermal Gas Equilibria," *Geochimica et Cosmochimica Acta*, Vol. 44, pp. 2021-2032.
- Giggenbach, W. F. (1988), "Geothermal solute equilibria. Derivation of Na-K-Ca-Mg geothermometers," *Geochimica et Cosmochimica Acta*, Vol. 52, pp. 2749-2765.
- Giggenbach, W. F. (1991), "Chemical techniques in geothermal exploration," *Chapter 5 in Application of Geochemistry in Geothermal Reservoir Development*. F. D'Amore, ed., UNITAR/UNDP, Rome, Italy, pp. 119-144.
- Grant, M. A., I. G. Donaldson and P. F. Bixley (1982), *Geothermal Reservoir Engineering*, Academic Press, New York.
- Hadgu, T., R. W. Zimmermann and G. S. Bodvarsson (1994), "Theoretical Studies of Flowrates from Slim Holes and Production-Size Geothermal Wells," *Proceedings Nineteenth Workshop on Geothermal Reservoir Engineering*, Stanford University, Stanford, California, January 18-20, pp. 253-260.
- Henley, R. W. and A. H. Truesdell, P. B. Barton, Jr. and J. A. Whitney (1984), "Fluid-Mineral Equilibria in Hydrothermal Systems," *Reviews in Economic Geology*, Vol. 1, Society of Economic Geologists, El Paso, Texas.
- Ishido, T., T. Kikuchi and M. Sugihara (1987), "The Electrokinetic Mechanism of Hydrothermal Circulation-Related and Production-Induced Self Potentials," *Proceedings Twelfth Workshop on Geothermal Reservoir Engineering*, Stanford University, Stanford, California, January 20-22, pp. 285-290.
- Ishido, T., T. Kikuchi, Y. Yano, Y. Miyazaki, S. Nakao, and K. Hatakeyama (1992), "Analysis of Pressure Transient Data from the Sumikawa Geothermal Field," *Proceedings Seventeenth Workshop on Geothermal Reservoir Engineering*, Stanford University, Stanford, California, January 29-31, pp. 181-186.
- Ito, J., Y. Kubota and M. Kurosawa (1977), "On the Geothermal Water Flow of the Ohnuma Geothermal Reservoir," *Journal of the Japan Geothermal Energy Association*, Vol. 14, No. 3 (Ser. No. 54).
- KRTA Limited (1985), "Sumikawa Geothermal Reservoir Study," submitted to Mitsubishi Metal Corporation, Report No. P2597, April.
- Kubota, Y. (1988), "Natural Convection System at the Ohnuma-Sumikawa Geothermal Field, Northeast Japan," *Proceedings Tenth New Zealand Geothermal Workshop*, Auckland, New Zealand, pp. 73-78.

- MMC (1985), "Tables and Figures Concerning the Sumikawa Geothermal Area," Mitsubishi Metal Corporation, Tokyo, Japan.
- MMC (1986), "Report on Data Analysis at the Sumikawa Area," Mitsubishi Metal Corporation, Tokyo, Japan.
- MMC (1987), "Report on Data Analysis at the Sumikawa Area," Mitsubishi Metal Corporation, Tokyo, Japan.
- MMC (1988), "Report on Data Analysis at the Sumikawa Area," Mitsubishi Metal Corporation, Tokyo, Japan.
- MMC (1989), "Report on Data Analysis at the Sumikawa Area," Mitsubishi Metal Corporation, Tokyo, Japan.
- Matsuo, S., J. Ohsaka, J. Hirabayashi, T. Ozawa and K. Kimishima (1982), "Chemical Nature of Volcanic Gases of Usu Volcano in Japan," *Bull. Volcanol.* vol. 45, pp. 261-264.
- NEDO (1985), "Geothermal Energy Survey and Technology," FY 1984 Annual Report, Report No. NEDO-OS-8506, New Energy and Industrial Technology Development Organization, Tokyo, Japan.
- Nieva, D. and R. Nieva (1987), "Developments in geothermal energy in Mexico, part 12. A cationic geothermometer for prospecting of geothermal resources," *Heat Recovery Systems Chapter 7*, pp. 243-258.
- Ogawa, Y., T. Uchida, T. Kikuchi and I. Sato (1986), "Magnetotelluric Survey in Sengan Geothermal Area, Preprint, Geological Survey, Tsukuba, Japan.
- Pritchett, J.W. (1993), "Preliminary Study of Discharge Characteristics of Slim Holes Compared to Production Wells in Liquid-Dominated Geothermal Reservoirs," *Proceedings Eighteenth Workshop on Geothermal Reservoir Engineering*, Stanford University, Stanford, California, January 26-28, pp. 181-187.
- Pritchett, J. W., S. K. Garg, H. Maki and Y. Kubota (1989), "Hydrology of the Sumikawa Geothermal Prospect, Japan," *Proceedings Fourteenth Workshop on Geothermal Reservoir Engineering*, Stanford University, Stanford, California, January 24-26, pp. 61-66.
- Pritchett, J. W., S. K. Garg, T. G. Barker and A. H. Truesdell (1990), Case Study of a Two-Phase Reservoir, Sumikawa Geothermal Field (Phase 5)," Report Number SSS-FR-90-11401, S-Cubed, La Jolla, California.
- Pruess, K. and T.N. Narasimhan (1985), "A Practical Method for Modeling Fluid and Heat Flow in Fractured Porous Media," *SPE Journal*, vol. 25, pp. 14-26.

- Sakai, H. and O. Matsubaya (1977), "Stable Isotope Studies of Japanese Geothermal Systems," *Geothermics*, Vol. 5, pp. 97-124.
- Stevens, J. L., S. K. Garg, L. Luu, T. G. Barker, J. W. Pritchett, A. H. Truesdell, and L. Quijano (1992), "GEOSYS: An X/Motif-based system for analysis and management of geothermal data," *Geothermal Resource Council Transactions*, Vol. 16, pp. 663-664.
- Truesdell, A. H. (1975), "Summary of Section III—Geochemical Techniques in Exploration," *Second United Nations Symposium on the Development and Use of Geothermal Resources, San Francisco*, Vol. 1, pp. liii-1xxix.
- Truesdell, A. H., J. R. Haizlip, H. Armannsson, F. D'Amore (1989), "Origin and Transport of Chloride in Superheated Steam," *Geothermics*, Vol. 18, pp. 295-304.
- Truesdell, A., A. Mañon, L. Quijano, T. Coplen, and M. Lippmann (1992), "Boiling and Condensation Processes in the Cerro Prieto Beta Reservoir under Exploitation," *Proceedings Seventeenth Workshop on Geothermal Reservoir Engineering*, Stanford University, Stanford, California, January 29-31, pp. 205-214.
- Uchida, T. (1995), "Resistivity Structure of Sumikawa Geothermal Field, Northeastern Japan, obtained from Magnetotelluric Data," *Proceedings World Geothermal Congress*, Florence, Italy, pp. 921-925.
- Uchida, T., Y. Ogawa and T. Kikuchi (1986), "Resistivity Structure of the North-West Part of the Sengan Geothermal Area in North-East Japan Inferred from the Two-Dimensional Interpretation of Schlumberger Sounding," supplied by New Energy and Industrial Technology Development Organization (NEDO), Tokyo, Japan.
- Ueda, A., Y. Kubota, H. Katoh, K. Hatakeyama and O. Matsubaya (1991), "Geochemical Characteristics of the Sumikawa Geothermal System, Northeast Japan," *Geochemical Journal (Japan)*, Vol. 25, No. 4, pp. 223-244.

Appendix A

Tables of Geochemical Data

Table A.1. Physical data, sampling dates and measured production fluid enthalpy for Sumikawa wells.
Data from MMC.

Well	Date completed	TVD, m	Bottom of Casing TVD, m	Tmax at TVD, m °C	Production Zones, TVD, m	Sampling Dates, (water and steam samples)	Enthalpy, kJ/kg
S-1	11/81	448	305	225@448	--	11/81 (2s) 4/82 (5s)	2670
S-2	5/82 10/82	903 1065	703 703	-- 245@940	-- --	7/82 (8w, 3s) 11/82 (5w, 3s) 5/83 (3w, 1s)	2300 1090
S-3	6/83	805	601	236@620	650-750	7/83-8/83 (11w, 4s) 10/83-1/84 (15w, 4s)	1090±40
S-4	11/83	1552	1071	300@1550	1200-1400?	7/84-11/84 (17w, 4s) 8/85-11/85 (17w, 3s) 7/86-11/86 (14w, 3s) 10/88-11/88 (9w, 4s) 6/89-11/89 (7w, 8s)	1340-1840
SA-1	10/86	1832	1056	305@1830	~1800	10/88-11/88 (6w, 8s) 6/89-11/89 (7w, 8s)	2090?
SA-2	11/86	1943	1061	317@1940	~1450	6/89-12/89 (10w, 18s)	
SA-4	5/88	1739	1130	300@1735	920, 1240	10/88-11/88 (5w, 4s) 6/89-9/89 (2w, 9s)	2760±
SB-1	10/87	2006	1062	300@2000	~1550	6/89-11/89 (7w, 10s)	1090-1260
SC-1	11/87	2472	1799	310@1850	--	8/88-11-88 (12w, 4s) 10/89-11/89 (4w, 10s)	1130-1260
SD-1	10/86	1691	707	250@1560	--	8/89-11-89 (5w, 13s)	1000-1130
SM-2	10/78	1001	803	--	--	9/78-10/79 (12w, 0s?)	1000-1170

Table A.2. Sumikawa and Ohnuma well water analyses.

Chemical compositions of water flashed to one atmosphere (0.9 bar abs) from well discharges of the Sumikawa geothermal field with selected analyses of waters from the Ohnuma field. Analyses are in mg/kg. Other units are bars (gauge), tons/hr, kilojoules/kilogram, and pH units. Condensate analyses are indicated by "C" following the well name. All data are from MMC (1985, 1990).

Well	Date	WHP	Fstm	Fwat	Enth	pH	Na	K	Ca	Mg	Fe	HCO3	Cl	SO4	I	B	SiO2	As	Li	F	Br	Al
O-10R	83/05/21	1.57	29.2	60.5	1140	7.2	418	51.4	5.2	3.1	0.12	53.9	561	190	-	202	506	17.1	-	-	-	-
O-1R	69/11/17	-	27	70	1030	2.4	385	67.5	23.3	29	53.1	0.1	511	702	-	-	551	-	-	-	-	-
O-2R	71/02/09	0.49	2.5	11.5	808	3.1	-	-	30.3	13.6	57.6	-	536	462	-	-	533	-	-	-	-	-
O-3Ra	70/07/27	2.3	36	141	864	8.2	-	-	18.3	0.48	0.16	-	373	154	-	-	416	10.3	-	-	-	-
O-3Rb	70/08/26	0.294	7	26	884	7.8	-	-	14.7	0.7	0.05	-	418	173	-	-	460	10.6	-	-	-	-
O-3Rba	74/05/10	0.784	23	68.2	975	8.2	317	41.6	6.13	8.73	0.34	69.2	405	143	0.144	139	435	8.07	-	-	-	-
O-5R	71/12/27	1.47	26	62	1070	8.1	339	49.4	13.2	4.13	0.09	66.5	472	212	-	133	435	10.3	-	-	-	-
O-6R	72/12/28	1.32	29	90	956	8.2	277	42.6	12.5	2.49	0.08	82.7	423	141	-	83.4	426	9.64	-	-	-	-
O-6T	71/10/13	0.98	1.53	5.63	888	5.9	374	60.4	16	2.9	4.5	-	578	305	-	-	441	-	-	-	-	-
O-8R	76/10/20	0.833	19.6	66	922	7.5	489	59	3.8	4.7	0.4	67.4	646	215	0.49	158	491	9.96	-	-	-	-
S-1C	81/11/23	7.74	-	-	2670	5.5	2	0.4	3.5	1.5	0.08	77.2	4.1	20.4	-	<5	4.5	0.01	-	-	-	-
S-1C	81/11/27	7.74	-	-	2670	5.3	1.8	0.2	18.9	1.5	0.18	110	6.1	8	-	<5	11.5	0.01	-	-	-	-
S-1C	82/04/26	7.15	34.7	0.0	2670	5.7	0.8	0.0	0.4	0.2	0.04	22.7	2	<1	-	1.8	<1	-	-	-	-	-
S-1C	82/04/27	7.45	35.7	0.0	2670	5.1	1	0.0	0.6	0.4	-	15.9	3.1	-	-	-	-	-	-	-	-	-
S-1C	82/04/28	7.25	-	-	2670	5.6	0.8	0.0	0.7	0.3	-	13.5	2.2	<1	-	2	<1	-	-	-	-	-
S-1C	82/04/29	7.74	34.4	0.0	2670	5.2	0.7	0.0	0.5	0.5	0.04	17.2	3.1	<1	-	2	<1	-	-	-	-	-
S-2	82/07/06	-	-	-	-	7.88	440	51.6	11.6	7.05	7.92	343	323	281	-	57	525	4.27	-	-	-	-
S-2	82/07/07	-	-	-	-	7.86	578	69.6	9.22	5.59	14.8	337	399	423	-	101	488	7.4	-	-	-	-
S-2	82/07/08	-	3.45	0.62	2320	7.82	1080	146	17.6	10.7	25.9	398	862	950	-	184	485	13.6	-	-	-	-
S-2	82/07/09	-	3.5	0.6	2340	7.2	715	94	30.1	18.2	5.75	208	598	613	-	142	661	10.8	-	-	-	-
S-2	82/07/10	-	3.21	0.75	2240	7.72	735	98.4	24	14.6	4.02	221	664	655	-	171	691	13.2	-	-	-	-
S-2	82/07/11	-	-	-	-	5.9	668	98.4	16	9.72	13.5	184	628	637	-	145	633	13.6	-	-	-	-
S-2	82/07/12	-	3.2	0.85	2190	5.52	732	99	20.4	12.4	8.23	147	660	704	-	159	664	12.3	-	-	-	-
S-2	82/07/13	-	-	-	-	5.48	842	110	26.1	15.8	12.7	159	780	762	-	146	686	15.1	-	-	-	-
S-2	82/11/02	-	-	-	-	2.8	269	77	16	48.7	291	0.00	246	1190	-	23.3	537	0.472	-	-	-	-
S-2	82/11/03	3.14	15.5	38.4	1060	2.8	308	84	13.6	60.8	307	0.00	294	1310	-	31.3	528	1890	-	-	-	-
S-2	82/11/09	-	-	-	-	2.78	360	89.6	44.9	67.3	345	0.00	396	1480	-	40.8	584	2.64	-	-	-	-
S-2	82/11/10	-	-	-	-	2.62	426	93	49.7	94.7	462	0.00	509	1720	-	51.8	594	2.79	-	-	-	-
S-2	82/11/11	3.14	15.1	33.1	1110	2.61	458	99	45.7	104	474	0.00	544	1790	-	55.8	592	1.12	-	-	-	-
S-2	82/11/11	3.14	15.5	38.4	1060	2.6	458	99	45.7	104	474	-	544	1790	-	55.8	592	1.12	-	-	-	-
S-2	83/05/13	-	-	-	-	2.74	592	94	2.12	91.6	543	0.00	776	2090	-	64	581	2.09	-	-	-	-
S-2	83/05/14	4.41	-	-	-	2.68	605	94.4	8.81	97.1	546	0.00	764	2050	-	70	591	3.62	-	-	-	-
S-2	83/05/16	-	-	-	-	2.61	655	103	8.5	97.2	606	0.00	867	2190	-	83	641	8.66	-	-	-	-
S-3	83/07/10	-	-	-	-	8.8	139	24.2	2.32	3.91	0.13	134	85.9	120	<0.01	28.1	471	2.27	-	-	-	-
S-3	83/07/08	-	-	-	-	8.68	148	24.8	6.85	1.87	0.27	148	93.2	104	<0.1	41	471	2.45	-	-	-	-
S-3	83/07/09	1.96	3.8	17.5	808	8.8	134	24.2	2.08	4.44	0.26	121	80.5	128	<0.01	27.2	457	1.65	-	-	-	-
S-3	83/07/11	-	-	-	-	8.8	128	22	5.17	2.57	0.37	119	59.6	109	<0.01	23.4	423	1.69	-	-	-	-
S-3	83/07/13	-	-	-	-	8.86	138	23	5.37	3.87	0.29	107	85	106	<0.01	25	519	1.98	-	-	-	-
S-3	83/07/14	1.52	5.3	9.8	1200	8.96	128	21.6	4.41	3.82	0.39	119	44.6	105	<0.01	23	468	1.13	-	-	-	-

Table A.2. Sumikawa and Ohnuma well water analyses (continued).

Well	Date	WHP	Fstm	Fwat	Enth	pH	Na	K	Ca	Mg	Fe	HCO3	Cl	SO4	I	B	SiO2	As	Li	F	Br	Al
S-3	83/07/20	-	-	-	-	8.62	160	25.6	3.37	3.79	0.05	149	100	107	<0.01	44	493	3.58	-	-	-	-
S-3	83/07/25	-	-	-	-	8.72	161	26.4	3.09	3.6	0.06	165	95.9	105	<0.01	44	476	3.38	-	-	-	-
S-3	83/07/28	0.98	3.3	7.8	1080	8.51	162	28	4.81	3.4	0.13	140	124	87.9	<0.01	55	485	3.31	-	-	-	-
S-3	83/08/03	-	-	-	-	8.32	166	30	5.61	2.92	0.08	149	147	99.2	0.038	62	480	5.18	-	-	-	-
S-3	83/08/08	1.37	3.1	7.1	1090	8.34	165	29.6	4.81	2.97	0.06	152	144	94.7	0.036	64	479	4.91	-	-	-	-
S-3	83/10/19	-	-	-	-	8.92	171	25.6	1.76	1.39	0.49	220	34.2	161	<0.01	14.5	332	0.55	-	-	-	-
S-3	83/10/20	1.43	4.6	12.4	1020	8.78	188	27.6	1.96	3.62	0.25	190	79.5	170	<0.01	33.2	443	2.13	-	-	-	-
S-3	83/10/21	-	-	-	-	8.68	173	30	1.56	2.48	0.16	160	90.4	146	<0.01	38.6	441	2.6	-	-	-	-
S-3	83/10/22	1.21	4.1	10.6	1040	8.7	168	27.6	4.06	1.68	0.08	162	100	126	0.018	41.7	442	2.36	-	-	-	-
S-3	83/10/24	-	-	-	-	8.52	160	26	0.8	4.42	0.07	131	110	123	0.018	47	443	3.11	-	-	-	-
S-3	83/10/27	2.06	3.4	6.9	1150	8.66	166	27	2.69	3.11	0.11	162	104	121	<0.01	46.5	469	2.99	-	-	-	-
S-3	83/10/29	-	-	-	-	8.52	170	25	1.8	3.04	0.07	155	120	109	0.034	51.7	479	3.32	-	-	-	-
S-3	83/10/31	-	-	-	-	8.5	170	25.6	4.73	0.49	0.1	133	138	97.3	0.03	56	482	3.26	-	-	-	-
S-3	83/11/02	-	-	-	-	8.66	160	24.4	4.41	1.12	0.1	154	109	99.4	0.023	48	467	3.14	-	-	-	-
S-3	83/11/05	-	-	-	-	8.54	185	28	1.2	3.35	0.08	153	149	104	0.03	64	482	4.02	-	-	-	-
S-3	83/11/10	0.98	3.1	7.6	1060	8.48	180	27.6	3.97	0.9	0.09	134	155	90.6	0.034	66	547	4.39	-	-	-	-
S-3	83/11/25	0.784	3.1	7.6	1060	8.4	186	29	1.8	3.79	0.09	135	165	84.2	-	74	536	4.88	-	-	-	-
S-3	83/12/26	-	-	-	-	8.38	180	30.8	0.4	3.33	0.08	166	148	80.9	0.034	84	476	4.27	-	-	-	-
S-3	84/01/14	-	-	-	-	8.36	204	32.4	0.4	3.92	0.09	155	182	78.8	0.044	80	528	4.5	-	-	-	-
S-3	84/01/28	-	-	-	-	8.2	215	33.6	0.4	4.06	0.07	128	189	78.2	0.036	78	549	8.21	-	-	-	-
S-4	84/07/05	-	117	42.3	2070	6.2	318	77	0.12	0.4	3.45	17.1	524	72.5	-	242	1230	17.1	-	-	-	-
S-4	84/07/06	7.84	79.3	35.5	1970	6.9	290	62	0.41	0.48	0.2	42.9	463	82.5	0.08	216	1160	13.3	-	-	-	-
S-4	84/07/07	-	-	-	-	6.9	310	67.6	0.12	0.4	0.47	32.3	438	82.5	0.09	211	1070	16.6	-	-	-	-
S-4	84/07/10	7.84	76.5	42	1870	7.1	295	66.4	0.1	0.32	0.09	37.8	394	88.5	0.08	191	975	15.1	-	-	-	-
S-4	84/07/12	-	-	-	-	7.2	288	66.4	0.1	0.24	0.09	47.6	356	95.7	0.09	189	1020	14.5	-	-	-	-
S-4	84/07/17	7.64	70.8	53.1	1700	7.3	288	59	0.6	0.29	0.07	52.7	332	96.5	0.07	65	1080	13.4	-	-	-	-
S-4	84/07/25	8.04	81.7	54.1	1770	7.4	270	56.4	0.6	0.34	0.07	64.3	298	101	0.07	155	998	13.3	-	-	-	-
S-4	84/08/05	8.53	82.9	52.5	1790	7.6	245	58	0.32	0.78	0.08	69.2	301	107	0.07	149	965	12.5	-	-	-	-
S-4	84/08/30	9.02	92.7	67.2	1720	7.4	280	62.4	0.4	0.89	0.09	54.5	376	89.9	0.08	165	1000	13.2	-	-	-	-
S-4	84/09/03	8.13	86.2	63.5	1710	7.5	280	57.6	0.16	2.19	0.13	59.8	348	103	0.07	156	972	12.3	-	-	-	-
S-4	84/09/07	8.04	85.5	64.2	1700	7.6	266	56.8	0.2	2.04	0.1	67.7	341	107	0.07	151	956	11.1	-	-	-	-
S-4	84/09/12	8.13	85.5	63.8	1700	7.6	262	55.2	0.16	2.53	0.12	72	295	109	0.07	145	965	12	-	-	-	-
S-4	84/09/22	8.33	85.5	65.5	1690	7.8	296	59.6	0.2	1.87	0.11	78.7	314	111	0.08	150	968	13.1	-	-	-	-
S-4	84/10/03	8.43	85.7	59.5	1740	7.8	302	56	0.16	2.09	0.1	78.7	314	112	0.08	150	932	12.5	-	-	-	-
S-4	84/10/17	8.33	87.3	75.5	1620	7.9	266	55.2	0.16	1.82	0.15	84.2	328	109	0.07	133	934	12.5	-	-	-	-
S-4	84/10/30	8.43	87.2	74.4	1630	7.9	275	54	0.12	2.14	0.07	86.7	299	107	0.06	132	933	12.8	-	-	-	-
S-4	84/11/06	8.43	88.1	76.6	1620	7.6	250	52	0.12	2.19	0.09	87.3	316	109	0.06	133	935	10.9	-	-	-	-
S-4	85/08/26	10.8	101	54.5	1870	6.3	278	66.4	3.08	0.44	0.82	18.4	418	87.7	0.132	191	1010	15.5	-	-	-	-
S-4	85/08/27	10	94.6	31.5	2100	7.2	272	62.4	1.6	0.06	0.13	53.9	398	88.1	0.073	181	989	14.5	-	-	-	-
S-4	85/08/28	9.41	92.1	40.2	1980	7.3	268	62.2	1.82	0.06	0.08	55.7	385	91.6	0.069	172	980	13.9	-	-	-	-
S-4	85/08/30	9.11	89.7	42.2	1950	7.4	265	59.6	1.86	0.03	0.05	66.1	361	95.9	0.062	159	951	12.8	-	-	-	-
S-4	85/09/02	-	-	-	-	7.5	255	56.4	1.96	0.03	0.04	70.4	335	102	0.065	149	937	11.4	-	-	-	-
S-4	85/09/04	9.7	91.9	64.5	1730	7.5	248	56	1.95	0.03	0.03	72.3	327	103	0.058	141	922	11.2	-	-	-	-
S-4	85/09/09	9.21	89.1	65.5	1710	7.6	243	51.6	2.09	0.02	0.02	79	304	110	0.058	134	922	10.1	-	-	-	-
S-4	85/09/14	9.21	88.9	66.9	1700	7.6	240	51.4	2.25	0.02	0.02	82.1	293	112	0.058	130	911	9.89	-	-	-	-
S-4	85/09/21	9.21	89.7	74.1	1640	7.7	250	52.2	2.44	0.01	0.01	85.7	294	113	0.072	126	913	9.6	-	-	-	-
S-4	85/09/28	9.31	90.3	76.5	1630	7.7	252	52	2.44	0.02	0.01	85.7	286	117	0.07	122	895	9.4	-	-	-	-
S-4	85/10/05	9.21	90.5	80.4	1600	7.7	249	51.6	2.6	0.01	0.02	91.3	287	116	0.068	121	885	9.27	-	-	-	-
S-4	85/10/10	9.41	90.8	81.1	1600	7.7	248	51.6	2.5	0.02	0.02	94.9	290	116	0.065	119	884	9.3	-	-	-	-
S-4	85/10/19	9.9	91.1	81.5	1600	7.6	251	51.6	2.63	0.02	0.02	104	291	116	0.066	118	890	8.87	-	-	-	-
S-4	85/10/26	9.7	91.3	85.1	1580	7.7	250	51	2.69	0.01	0.04	101	290	115	0.066	117	871	8.83	-	-	-	-

Table A.2. Sumikawa and Ohnuma well water analyses (continued).

Well	Date	WHP	Fstn	Fwat	Enth	pH	Na	K	Ca	Mg	Fe	HCO3	Cl	SO4	I	B	SiO2	As	Li	F	Br	Al
S-4	85/11/02	-	91.2	80.4	1610	7.6	250	50.4	2.51	0.01	0.01	101	282	112	0.069	113	826	8.85	-	-	-	-
S-4	85/11/12	9.9	91.8	84.4	1580	7.6	245	50.4	2.7	0.01	0.00	105	279	113	0.065	114	859	8.74	-	-	-	-
S-4	85/11/16	10	91.8	84	1590	7.7	245	51.6	2.69	0.01	0.01	105	280	113	0.069	114	860	8.55	-	-	-	-
S-4	86/07/17	-	-	-	-	6.7	284	65	3.28	0.33	1.78	23.2	391	83.3	0.058	182	1070	14.5	-	-	-	-
S-4	86/07/18	11.4	101	48.1	1940	7.5	270	58	4.95	0.05	0.09	69.6	350	99.4	0.058	167	917	14.6	-	-	-	-
S-4	86/09/02	12.6	-	-	-	5.3	260	64.8	4.23	0.16	3.46	6.7	430	83.6	-	186	891	14.6	-	-	-	-
S-4	86/09/03	10.9	101	51.4	1900	7.6	264	58.4	1.46	0.03	0.08	60.4	350	97.8	0.031	170	896	12.8	-	-	-	-
S-4	86/09/05	10.7	95.9	54.2	1850	7.7	258	57	1.56	0.03	0.05	70.8	323	103	0.031	164	920	10.8	-	-	-	-
S-4	86/09/06	-	94	57	1810	7.8	238	52.4	1.55	0.04	0.05	82.4	309	111	0.042	169	820	10.9	-	-	-	-
S-4	86/09/13	10.2	93.2	63.5	1750	7.5	237	49.6	1.6	0.02	0.05	72	278	121	0.036	124	866	9.55	-	-	-	-
S-4	86/09/20	10.2	93.3	71	1690	7.9	238	50	1.7	0.02	0.09	91.5	266	120	0.04	163	856	7.57	-	-	-	-
S-4	86/09/26	10.2	95.5	72.3	1690	7.9	238	46.8	2.3	-	0.09	92.1	260	123	0.04	160	879	9.3	-	-	-	-
S-4	86/10/09	10.2	93.1	-	-	8	232	47.6	2.02	-	0.17	98.2	266	123	0.042	161	910	8.07	-	-	-	-
S-4	86/10/10	10.2	93.4	-	-	8	237	47.6	2.08	0.04	0.05	97.6	266	123	0.04	151	811	9.08	-	-	-	-
S-4	86/10/11	10.2	94.4	-	-	8	248	45.6	2.21	0.01	0.09	103	246	121	0.043	131	897	9.6	-	-	-	-
S-4	86/11/01	10.2	-	-	-	8	238	46	2.3	0.01	0.09	103	266	118	0.041	132	841	9.37	-	-	-	-
S-4	86/11/03	10.2	93.7	85.9	1590	8	240	47.4	2.37	0.00	0.09	101	256	119	0.045	126	842	8.95	-	-	-	-
S-4	88/10/25	-	-	-	-	6.3	250	61.6	14.8	17.7	9.5	19.4	396	133	-	-	1130	8.8	-	-	-	-
S-4	88/10/31	4.51	63	-	-	6.6	202	47.2	0.4	20.6	2.7	56.8	284	78.6	0.043	116	804	8.62	-	-	-	-
S-4C	88/11/05	5.86	-	-	-	5.3	0.3	0.2	0.3	0.0	0.2	30.6	2	6.2	-	<5	<2	0.08	-	-	-	-
S-4	88/11/13	3.82	-	-	-	7.8	224	50.8	0.6	0.1	0.1	93.6	248	123	0.05	124	866	9.01	-	-	-	-
S-4C	88/11/13	2.43	-	-	-	5.7	0.0	0.2	0.4	0.0	0.1	12.5	1.6	0.0	0.000	<5	<2	0.01	-	-	-	-
S-4	88/11/22	5.49	-	-	-	7.7	256	52	0.7	0.8	0.3	105	298	127	0.056	136	876	9.58	-	-	-	-
S-4C	88/11/22	5.47	-	-	-	5.5	0.6	0.6	1.1	0.1	0.5	29.3	2.6	0.2	-	<5	<2	0.07	-	-	-	-
S-4	88/11/24	5.49	76.4	96.5	1400	7.3	174	31.2	0.3	0.2	0.7	44.9	213	89.5	-	101	584	13.5	-	-	-	-
S-4C	88/11/24	5.47	62.6	110	1230	5.1	0.1	0.1	0.2	0.1	0.3	9.4	6.1	3.1	-	<2	5	0.01	-	-	-	-
S-4	89/06/10	4.98	-	-	-	7.1	187	36	7.4	0.02	0.2	21.2	173	187	0.05	70	773	5.56	0.67	3.7	0.9	2.1
S-4	89/06/28	3.52	-	-	-	8	224	44.2	3.1	<0.01	<0.1	80.1	221	127	0.06	89	810	7.61	0.66	4.5	1	2.5
S-4	89/07/27	3.75	-	-	-	7.8	249	48	1.8	0.02	<0.1	91	288	128	0.06	104	825	8.18	0.69	4.9	0.9	2.3
S-4	89/08/31	3.78	-	-	-	7.7	273	53	2.6	0.01	<0.1	88.8	323	135	0.12	133	833	8.54	0.71	4.9	0.8	2.3
S-4	89/09/30	4.07	-	-	-	7.8	286	53	2.8	0.02	<0.1	91.8	336	133	0.08	142	797	6.12	0.7	4.74	1.2	2.2
S-4	89/10/28	-	-	-	-	7.9	296	56	2.5	0.02	<0.1	89.4	379	138	0.09	160	787	8.08	0.77	4.7	0.9	2.2
S-4	89/11/15	4.94	-	-	-	7.7	331	59.5	2.1	0.03	<0.1	74.5	421	132	0.09	194	767	7.61	0.82	4.5	1	1.8
SA-1	88/10/22	-	-	-	-	7.4	122	38.8	62.5	3.4	12.8	68.7	195	163	-	-	740	0.37	-	-	-	-
SA-1C	88/11/04	5	-	-	-	4.3	0.1	0.0	0.3	0.0	0.1	0.0	2	4.1	0.000	<5	<2	0.02	-	-	-	-
SA-1	88/11/18	-	-	-	-	6.6	560	129	6.4	6.2	6.5	44.9	889	104	0.151	624	1390	40.6	-	-	-	-
SA-1C	88/11/18	-	-	-	-	4.7	1.2	0.8	0.4	0.1	0.1	9.4	2	0.6	0.000	<5	<2	0.06	-	-	-	-
SA-1C	88/11/22	3.92	-	-	-	5	0.0	0.2	0.5	1.2	0.2	8.7	2.6	1	-	<5	<2	0.01	-	-	-	-
SA-1	88/11/25	4.31	28.5	5.1	2330	5.8	370	86.4	1.2	4.7	4.2	14.4	593	67.5	0.065	444	926	30.2	-	-	-	-
SA-1	89/06/04	3.69	-	-	-	8.2	119	27.4	20.1	0.11	<0.1	60.7	102	139	0.03	40	692	2.94	0.71	2.2	0.9	0.8
SA-1	89/06/26	3.89	-	-	-	6.8	347	76	15.3	0.05	0.2	35.2	554	121	0.08	316	1100	24.2	1.84	3.5	1.1	1
SA-1	89/07/28	2.73	-	-	-	6.5	440	96	13.3	0.05	0.3	34.6	730	85.8	0.1	430	1230	32.5	2.22	4.2	0.9	0.8
SA-1	89/08/31	2.84	-	-	-	6.4	551	120	13.3	0.04	0.2	42.3	908	98.1	0.01	596	1370	43.9	2.86	4.5	0.9	0.7
SA-1	89/09/30	3.38	-	-	-	6.5	532	118	11.9	0.04	0.2	41.7	890	95.3	0.13	585	1360	44.9	2.74	4.2	1.5	0.7
SA-1	89/10/28	-	-	-	-	6.7	522	116	14.8	0.06	0.3	53.7	856	100	0.12	612	1350	43.7	2.77	4.4	1.1	0.5
SA-1	99/11/16	4.5	-	-	-	6.8	536	116	20	0.07	1.1	65.6	840	107	0.1	766	1300	46.5	2.8	5	1.4	0.2

Table A.2. Sumikawa and Ohnuma well water analyses (continued).

Well	Date	WHP	Fstn	Fwat	Enth	pH	Na	K	Ca	Mg	Fe	HCO3	Cl	SO4	I	B	SiO2	As	Li	F	Br	Al
SA-2	89/06/21	1.48	-	-	-	8	516	116	132	7.46	<0.1	63.7	1050	118	0.16	24	517	4.89	2.35	1.2	0.8	0.2
SA-2	89/06/30	12.5	-	-	-	8	488	113	74	0.67	0.1	60.6	962	30.5	0.15	29	605	6.09	2.56	1.2	1	0.2
SA-2	89/07/03	7.78	38.1	10.1	2200	6.1	1030	233	397	1.49	2.1	19.4	2270	390	0.44	81	669	12.5	5.6	3.3	<0.5	0.3
SA-2	89/07/08	12.8	-	-	-	5.8	2400	520	1090	4.33	6.8	39.4	4880	1000	0.71	442	482	29.6	12.7	5.2	2.2	0.4
SA-2	89/07/27	2.72	-	-	-	3.4	123	79.5	92.5	1.47	2.4	0.0	457	32.9	0.15	204	20	0.87	2.01	0.2	<0.5	0.1
SA-2C	89/08/30	2.87	-	-	-	3.9	<0.1	<0.2	<0.1	0.04	-	<1	3.6	<1	-	-	<2	0.04	-	-	-	-
SA-2	89/09/29	3.38	-	-	-	3.4	206	172	132	2.08	104	<1	862	43	0.66	765	12	0.31	3.81	0.81	1.4	<0.1
SA-2	89/10/27	-	-	-	-	3.7	1500	89	57.7	0.77	118	<1	2730	33.3	0.42	873	12	0.71	1.85	1.5	<0.5	<0.1
SA-2	89/11/15	4.71	-	-	-	3.3	11.1	3	2.1	0.07	1	<1	25.9	23.7	<0.01	82	26	0.13	0.05	0.3	<0.5	<0.1
SA-2C	89/12/01	-	-	-	-	3.5	0.155	338	376	7.9	3460	<1	8030	147	-	3140	221	1.34	7.75	9.1	2.4	0.2
SA-4C	88/10/30	4.21	22	-	2670	4.2	10.8	0.8	0.4	1.7	0.4	0.0	4.1	0.6	-	-	<6	0.22	-	-	-	-
SA-4C	88/11/05	5.1	-	-	-	3.8	0.1	0.0	0.2	0.0	0.0	0.0	1.6	4.1	-	<5	<2	0.02	-	-	-	-
SA-4C	88/11/13	2.45	-	-	-	5.7	1.3	0.8	0.3	0.1	0.1	6.2	2.4	2	-	<5	<2	0.07	-	-	-	-
SA-4C	88/11/22	4.12	-	-	-	5.1	0.3	0.6	1.6	0.4	1.5	11.2	3.4	0.6	-	<5	<2	0.01	-	-	-	-
SA-4C	88/11/27	4.12	23.7	-	2670	4.2	0.8	0.5	0.2	0.1	0.6	0.0	6.1	1.2	-	18	5	0.49	-	-	-	-
SA-4	89/06/05	2.95	29.8	-	2670	9	121	31.8	18.4	0.18	0.2	136	71	126	<0.01	15	585	0.82	-	2.3	4.5	1.6
SA-4C	89/06/27	4.95	-	-	-	7	13.3	3.2	2.3	0.04	0.4	18.2	5.9	11.3	<0.01	48	16	1.1	-	0.4	<0.5	0.1
SA-4C	89/07/28	2.63	-	-	-	4.3	0.4	0.2	<0.1	0.01	-	<1	4.3	<1	-	-	<2	<0.01	-	-	-	-
SA-4C	89/08/31	13.9	-	-	-	4.3	0.5	<0.2	<0.1	<0.01	-	<1	3.8	<1	-	-	<2	<0.01	-	-	-	-
SA-4C	89/09/29	3.53	-	-	-	4.6	<0.2	<0.2	<0.1	<0.01	-	<1	3.3	<1	-	-	<2	0.02	-	-	-	-
SA-4C	89/10/27	3.44	-	-	-	3.7	0.5	0.4	<0.1	<0.01	-	<1	3.1	<1	-	-	<2	0.01	-	-	-	-
SA-4C	89/11/15	4.52	-	-	-	4.2	4.3	0.6	<0.1	<0.01	-	<1	4.6	2.1	-	-	0.09	<2	-	-	-	-
SB-1	89/06/15	0.49	7.8	42.9	752	8.8	128	20.8	31.1	0.02	<0.1	129	84	149	0.03	30	381	2.1	-	2.6	1.6	0.2
SB-1	89/07/01	0.323	7.4	41.1	749	8.5	161	24.8	15.3	0.04	<0.1	113	158	118	0.03	51	439	3.96	-	3.1	1	0.4
SB-1	89/07/13	1.72	30	71.2	1080	8.2	229	35.2	9.9	0.02	<0.1	68.5	244	113	0.04	83	589	5.53	-	4.1	1.1	1.1
SB-1	89/08/08	2.06	37.2	68.3	1200	8	248	44	6.4	0.04	<0.1	131	296	126	0.06	107	627	6.14	-	4.3	1.2	1.1
SB-1	89/09/16	2.11	35.5	68.3	1180	7.9	280	47.4	7	0.02	<0.1	136	325	130	0.08	135	646	8.26	-	4.9	<0.5	1.3
SB-1	89/10/20	1.94	34.2	59.8	1230	8	305	49.8	7.6	0.03	<0.1	133	375	137	0.1	161	639	7.19	-	4.8	0.7	1.2
SB-1	89/11/16	1.86	33.2	54.6	1260	7.9	357	56.8	7.5	0.03	<0.1	128	440	134	0.1	197	676	7.13	-	4.7	0.8	1.2
SC-1	88/8/11	12.7	-	-	-	6.7	348	45.6	1.6	7	3.1	28.7	452	137	-	195	970	14.3	-	-	-	-
SC-1	88/10/01	19.9	46.2	98.5	1130	6.7	324	45.2	0.8	0.5	0.1	25	440	114	0.088	168	837	14.3	-	-	-	-
SC-1	88/10/06	19.3	41.8	90.1	1120	6.8	322	46	0.8	0.4	0.0	31.2	440	111	0.086	166	825	14	-	-	-	-
SC-1C	88/10/06	19.3	41.8	90.1	1120	6.4	0.4	0.2	0.5	0.1	0.1	23.7	2.7	8	-	<5	3	0.01	-	-	-	-
SC-1	88/10/19	12.3	150	293	1170	6.9	314	42.4	0.8	0.4	0.0	34.3	465	114	0.098	166	819	14.6	-	-	-	-
SC-1C	88/10/19	12.3	150	293	1170	6.9	0.2	0.0	0.6	0.4	0.1	12.5	2	1.6	-	<5	<1	0.01	-	-	-	-
SC-1C	88/10/29	12.5	155	293	1190	6	1.8	0.2	0.4	0.1	0.1	12.5	3.2	0.6	-	<5	3	0.03	-	-	-	-
SC-1	88/10/29	12.5	155	293	1190	7.1	314	46	0.6	0.9	0.1	43.7	459	92	0.098	167	810	13.5	-	-	-	-
SC-1	88/11/09	18.8	107	201	1190	7.1	310	52.4	0.4	0.5	0.2	45.6	446	101	0.095	167	810	13.5	-	-	-	-
SC-1C	88/11/09	18.8	107	201	1190	5.7	1.5	0.8	0.4	0.1	0.1	9.4	2.8	13.1	-	<5	<2	0.02	-	-	-	-
SC-1	88/11/10	-	-	-	-	6.4	220	35.6	7.2	5.4	0.6	59.9	308	70.8	0.047	112	537	8.49	-	-	-	-
SC-1	88/11/14	19.4	88.1	191	1120	7.3	312	53.2	0.6	1	0.0	49.9	442	101	0.092	169	850	13.7	-	-	-	-
SC-1	89/10/09	16.8	131	274	1140	7.8	322	48.8	4	0.03	0.2	41.7	457	102	0.1	156	828	14.3	0.83	3.7	0.7	2.6
SC-1	89/10/15	11.6	157	310	1160	7.4	321	48.7	3.6	0.03	<0.1	48.5	454	87.5	0.09	158	828	14.3	0.82	3.66	0.6	2.6
SC-1	89/10/21	11.6	187	309	1260	7.4	-	-	-	-	-	-	450	-	-	-	-	-	-	-	-	-
SC-1	89/11/16	12.2	183	305	1250	7.4	320	51.6	3.1	0.03	0.1	54.8	456	90.3	0.09	181	825	14.6	0.89	3.5	0.6	2.6
SD-1	89/08/09	1.62	26.9	71.5	1020	8.2	220	34.6	9.2	0.16	0.3	60.7	198	158	0.04	86	582	5.15	0.68	3.8	0.9	1.1
SD-1	89/08/21	1.47	22.4	65	984	8.1	229	38.2	9.8	0.03	0.1	154	216	167	0.05	88	568	5.42	0.7	3.9	0.5	0.9
SD-1	89/09/16	1.42	21.8	56	1040	8	241	39.4	10.1	0.02	<0.1	120	243	161	0.06	95	554	6.43	0.61	4.9	<0.5	1.3
SD-1	89/10/20	1.57	26	55.1	1130	8.1	241	40	10.1	0.03	<0.1	116	267	159	0.07	105	576	4.32	0.69	4	0.5	1
SD-1	89/11/16	1.57	26.5	54.3	1150	8	268	45.1	9.7	0.04	<0.1	104	298	160	0.07	127	606	5.76	0.82	3.9	1	1

Table A.2. Sumikawa and Ohnuma well water analyses (concluded).

Well	Date	WHP	Fstm	Fwat	Enth	pH	Na	K	Ca	Mg	Fe	HCO ₃	Cl	SO ₄	I	B	SiO ₂	As	Li	F	Br	Al
SM-2	78/09/25	0.206	1.7	3.5	1140	8.3	356	31	9	6	0.8	141	265	242	-	70	443	7.73	-	-	-	-
SM-2	78/10/25	-	7.7	27.8	895	7.77	312	53.6	-	2.17	0.19	72.3	409	93.4	0.098	204	201	14.1	-	-	-	-
SM-2	78/11/06	-	7.27	19.4	1020	7.74	308	58.4	-	1.81	0.16	61.2	429	96.7	0.102	164	695	15.6	-	-	-	-
SM-2	78/11/17	-	6.88	18.7	1010	7.71	323	62.4	-	2.77	0.18	59.4	457	105	0.104	172	723	17.1	-	-	-	-
SM-2	78/11/17	1.76	7.9	19.4	1060	7.7	323	62.4	-	2.8	0.2	59.4	457	105	0.1	172	723	17.1	-	-	-	-
SM-2	79/01/23	-	6.88	12.1	1220	7.42	352	62	-	5.79	0.2	62.5	459	106	0.105	169	622	19.9	-	-	-	-
SM-2	79/03/10	-	-	-	-	7.55	350	59	-	3.74	0.21	57.6	486	109	0.108	160	663	16.1	-	-	-	-
SM-2	79/04/10	-	-	-	-	7.52	355	59.6	-	3.02	0.2	59.4	476	110	0.108	165	645	17.2	-	-	-	-
SM-2	79/05/10	-	-	-	-	7.5	352	62	-	3.96	0.2	52.7	476	103	0.11	180	656	15.9	-	-	-	-
SM-2	79/06/10	-	-	-	-	7.42	501	59	-	3.55	0.2	61.9	484	108	0.12	170	673	16.8	-	-	-	-
SM-2	79/08/10	-	6.77	13.7	1150	7.62	368	59.6	-	3.69	0.2	64.9	499	102	0.115	158	619	17.4	-	-	-	-
SM-2	79/09/10	-	-	-	-	7.67	350	58.4	-	4.51	0.09	61.2	479	107	0.108	166	660	16.6	-	-	-	-
SM-2	79/10/10	-	6.88	13.2	1180	7.73	360	59.2	-	4.51	0.13	58.2	436	102	0.11	178	639	15.1	-	-	-	-

Table A.3. Composition of Sumikawa and Ohnuma steam.

Well	Date	WHP	Fstm	Fwat	Ysep	G/S	CO2	H2S	H2	CH4	N2	O2	Ar	He	Ne	TDP
O-1R	69/11/21	-	7.5	19.4	0.278	0.0002	50	18.7	24.9	-	-	0.2	-	-	-	-
O-3Ra	70/11/19	2.35	10	39.2	0.203	0.0002	77.1	15.1	-	-	-	2.3	-	-	-	-
O-3Ra	87/08/25	-	-	-	-	0.0007	37.8	12	0.176	0.16	48	0.031	0.65	0.004	0.0006	187
O-3Rb	74/12/20	0.8	6.39	18.9	0.252	0.0009	74.6	6.8	0.223	0.093	18	-	-	-	-	173
O-3Rb	87/08/24	-	-	-	-	0.0007	58.8	9.2	1.57	0.2	28	0.95	0.37	0.00038	0.00038	223
O-5R	74/12/20	1.5	7.22	17.2	0.295	0.0011	43.7	4.5	2.49	0.41	49	-	-	-	-	228
O-5R	87/08/25	-	-	-	-	0.0005	52.7	14.6	0.216	0.13	30	1.4	0.39	0.00036	0.00056	187
O-6R	74/12/20	1.35	8.06	25	0.244	0.0008	71.8	6.9	0.17	0.064	21	-	-	-	-	171
O-6R	87/08/24	-	-	-	-	0.0006	44.9	7.6	0.121	0.13	45	0.48	0.59	0.00033	0.00062	172
O-6T	71/10/12	1	0.43	1.56	0.216	0.0004	71.8	4.09	-	-	-	1.1	-	-	-	-
O-8R	77/06/06	0.85	5.44	18.3	0.229	0.0003	52.3	7.08	-	-	-	-	-	-	-	-
O-10R	83/05/21	1.6	8.11	16.8	0.375	0.0002	37.6	32.3	0.421	0.18	29	0.24	0.42	-	-	219
S-1	81/11/23	-	-	-	1	0.00077	72.2	27.8	-	-	-	-	-	-	-	-
S-1	81/11/27	-	-	-	1	0.00077	67.6	32.4	-	-	-	-	-	-	-	-
S-1	82/04/26	-	-	-	1	0.00069	74.6	20.9	1.34	0.0043	3.2	-	0.0043	-	-	257
S-1	82/04/27	-	-	-	1	0.0005	67.9	24.1	2.91	0.14	4.9	-	0.061	-	-	251
S-1	82/04/28	-	-	-	1	0.0009	81.8	12.1	3.39	0.18	2.5	-	0.045	-	-	237
S-1	82/04/29	7.9	9.56	0.0	1	0.0008	77.7	13.8	2.01	0.058	5.1	1.1	0.073	-	-	237
S-2	82/07/07	-	-	-	0.837	0.00046	84.4	6.53	1.87	0.61	6.3	-	0.22	-	-	203
S-2	82/07/09	0	0.97	0.17	0.851	0.0007	74.7	9.9	2.16	0.49	9.9	1.8	0.15	-	-	217
S-2	82/11/03	-	-	-	0.289	0.00035	11.9	1.74	30.7	0.58	54	-	0.93	-	-	339
S-2	82/11/11	3.2	4.31	10.7	0.288	0.0012	12.8	7.08	46.5	0.32	29	0.48	0.64	-	-	392
S-2	83/05/14	-	-	-	0.307	8.8E-05	34.9	19.1	29.8	0.34	15	-	0.34	-	-	343
S-3	83/07/09	-	-	-	0.263	0.00025	48.3	5.73	2.09	0.41	43	-	0.61	-	-	224
S-3	83/07/14	-	-	-	0.365	0.00029	67.5	10.4	2.16	0.42	19	-	0.42	-	-	222
S-3	83/07/28	-	-	-	0.289	0.00013	77.6	14	2.33	0.39	5.4	-	0.23	-	-	224
S-3	83/08/08	-	-	-	0.302	0.00036	86.2	10.8	0.776	0.86	1.2	-	0.11	-	-	185
S-3	83/10/20	-	-	-	0.276	0.00042	88.4	8.03	2.03	0.71	0.4	-	0.47	-	-	205
S-3	83/10/22	-	-	-	0.285	0.00077	58.7	5.96	3.28	0.41	31	-	0.45	-	-	230
S-3	83/10/27	-	-	-	0.333	0.0015	83	7.15	0.107	0.21	9.1	-	0.38	-	-	151
S-3	83/11/10	1	0.86	2.11	0.29	0.0008	49.7	25.9	-	-	19	5.2	0.22	-	-	-
S-4	84/07/12	-	-	-	0.479	0.00018	61.2	19.8	6.23	0.44	12	-	0.27	-	-	263
S-4	84/09/12	-	-	-	0.463	0.00022	64.7	11.8	14.2	0.5	8.6	-	0.23	-	-	277
S-4	84/10/17	-	-	-	0.426	0.00023	66.1	33.9	-	-	-	-	-	-	-	-
S-4	84/10/30	8.6	24.5	21.3	0.535	0.0005	59.9	29.3	4.82	0.26	5.5	0.11	0.086	-	-	268
S-4	85/09/14	8.5	24.7	18.6	0.571	0.0002	60.4	14.8	0.819	0.05	19	4.8	0.22	0.00012	0.00042	223
S-4	85/10/10	8.7	25.2	22.5	0.528	0.0002	52.6	13.4	12.1	0.92	20	0.14	0.32	0.00085	-	276
S-4	85/11/12	9.2	25.5	23.4	0.521	0.0002	45	30.8	8.66	0.65	14	0.22	0.23	0.00056	-	288
S-4	86/09/26	9.5	26.5	20.1	0.569	0.0006	74.8	21.5	1.38	0.084	2.2	-	0.043	6.6E-05	-	231
S-4	86/11/01	9.5	26	23.9	0.521	0.0006	79.7	16.3	1.36	0.12	2.4	-	0.056	0.0002	-	222
S-4	88/11/05	5.98	-	-	-	0.00368	52.4	30.6	5.48	0.34	11	0.1	0.16	0.00054	-	274

Table A.3. Composition of Sumikawa and Ohnuma steam (continued).

Well	Date	WHP	Fstm	Fwat	Ysep	G/S	CO2	H2S	H2	CH4	N2	O2	Ar	He	Ne	TDP
S-4	88/11/13	3.93	-	-	-	0.00266	46.8	33.3	4.81	0.58	14	0.17	0.22	0.00099	0.00075	270
S-4	88/11/22	5.58	-	-	-	0.00697	46.6	43.2	-	-	-	-	-	-	-	-
S-4	88/11/24	5.58	17.4	30.6	0.363	0.00031	21.7	55.1	-	-	-	-	-	-	-	-
S-4	89/06/17	4.32	-	-	-	0.00012	12.7	64.2	2	0.37	21	0.5	0.27	0.00085	0.0003	307
S-4	89/06/28	3.59	-	-	-	0.00039	15.8	81.2	0.394	0.058	2.6	0.043	0.036	9.4E-05	3.0E-05	269
S-4	89/07/27	3.83	-	-	-	0.00012	57.3	19.5	3.41	0.42	19	0.21	0.24	0.00046	0.0003	248
S-4	89/07/27	3.96	-	-	-	0.00012	52.6	19.5	4.16	0.52	23	0.26	0.29	0.00056	0.00036	255
S-4	89/08/10	3.79	-	-	-	0.00011	18.2	61.8	0.00038	0.2	17	0.58	0.23	0.0002	1.7	104
S-4	89/08/10	3.92	-	-	-	0.00011	18.2	61.8	1.68	0.2	17	0.52	0.23	0.00038	0.0002	293
S-4	89/08/31	3.99	-	-	-	0.00065	7.2	4.6	2.53	0.34	74	10	0.89	0.00088	0.0016	294
S-4	89/09/30	4.29	-	-	-	0.00012	33.9	41.7	2	0.26	22	0.15	0.28	0.00037	0.00037	266
SA-1	88/06/17	3.33	-	-	-	0.00018	13.9	70.1	0.691	0.02	13	3	0.15	0.00013	0.00021	302
SA-1	88/06/26	3.97	-	-	-	0.0002	38.2	51.5	3.58	0.089	5.9	0.8	0.072	0.00026	4.1E-05	296
SA-1	88/07/28	2.79	-	-	-	0.00026	43.4	40	10.1	0.23	5.8	-	0.069	0.00063	-	311
SA-1	88/08/31	2.9	-	-	-	0.00068	30.4	64.6	-	-	-	-	-	-	-	-
SA-1	88/11/04	5.08	-	-	-	0.00131	14.3	70.8	2.54	0.07	12	0.061	0.15	0.00024	0.00073	333
SA-1	88/11/18	2.27	-	-	-	0.00126	13	77.3	6.36	0.11	2.5	0.23	0.051	0.00031	-	371
SA-1	88/11/22	4.03	-	-	-	0.00133	16.1	73.8	-	-	-	-	-	-	-	-
SA-1	88/11/25	4.24	6.8	1.8	0.791	0.00032	17.2	74.5	-	-	-	-	-	-	-	-
SA-1	89/06/01	4	6.4	-	-	0.00146	38.4	0.3	0.207	0.046	62	0.44	0.82	0.00037	0.002	160
SA-1	89/06/03	3.38	5.7	32.5	0.149	0.00102	32	2.4	1.38	0.21	63	0.17	0.9	0.0059	0.0011	220
SA-1	89/06/05	3.18	9.9	-	-	0.00035	44.8	5.1	3.52	0.22	46	0.26	0.69	0.00055	0.00085	244
SA-1	89/06/26	4.1	12	2.9	0.805	0.0002	28.2	51.5	3.57	0.089	5.9	0.8	0.072	0.00026	4.1E-05	308
SA-1	89/07/28	2.88	-	-	-	0.00026	43.4	40	10.1	0.23	5.8	-	0.069	0.00063	-	311
SA-1	89/08/08	19.6	9.6	2.3	0.807	0.00125	26.7	67	4.47	0.084	1.9	-	0.038	9.5E-05	-	324
SA-1	89/08/31	3	-	-	-	0.00068	30.4	64.6	3.15	0.067	1.5	0.15	0.023	0.0002	-	308
SA-1	89/09/30	3.56	-	-	-	0.0004	36.6	55.2	0.484	0.06	6.4	1.5	0.061	4.1E-05	-	241
SA-2	88/06/23	4.54	-	-	-	0.0002	12.9	64	10.6	0.26	11	0.36	0.14	0.00074	-	377
SA-2	88/07/03	7.94	-	-	-	0.00069	57.1	29.3	1.35	0.053	12	0.73	0.14	0.00072	0.00014	247
SA-2	88/07/27	2.78	-	-	-	0.00305	65.1	20.2	4.26	0.14	10	-	0.088	0.0019	-	261
SA-2	88/08/30	8	-	-	-	0.00458	74.2	21.3	0.00062	0.03	2.6	0.22	0.016	-	1.6	89.
SA-2	88/11/04	5.08	-	-	-	0.00659	77.1	16.8	3.11	0.022	2.7	0.066	0.014	0.001	-	262
SA-2	88/11/18	2.27	-	-	-	0.00719	78.7	18.8	1.25	0.058	1.2	0.037	0.0046	0.00046	-	228
SA-2	88/11/22	4.03	-	-	-	0.00895	78.6	18.8	-	-	-	-	-	-	-	-
SA-2	88/11/26	4.24	7.6	-	-	0.00469	76.3	20.9	-	-	-	-	-	-	-	-
SA-2	89/06/23	4.69	-	-	-	0.0002	12.9	64	10.6	0.26	11	0.37	0.14	0.00074	-	377
SA-2	89/07/03	8.2	10.6	2.81	0.791	0.00069	57.1	29.3	1.36	0.053	12	0.74	0.14	0.00072	0.00014	247
SA-2	89/07/28	2.87	-	-	-	0.00305	65.2	20.2	4.26	0.14	10	-	0.088	0.0019	-	261
SA-2	89/08/09	0.6	7.9	0.0	1	0.00604	64.3	34.2	0.402	0.0092	1	0.016	0.0098	0.00013	-	228
SA-2	89/08/18	2.88	-	-	-	0.0058	87.9	5.9	2.44	0.051	3.7	-	0.019	0.00098	-	228
SA-2	89/08/24	3.05	-	-	-	0.0082	79.9	16.3	1.11	0.023	2.4	0.28	0.019	0.00044	-	231
SA-2	89/08/30	3.03	-	-	-	0.00458	74.2	21.3	1.65	0.03	2.6	0.22	0.017	0.00063	-	245
SA-2	89/09/10	3.51	-	-	-	0.00423	71.1	15.1	5.49	0.1	7.6	0.3	0.031	0.0022	-	265
SA-2	89/09/19	4.49	-	-	-	0.00465	78.1	17.2	2.34	0.033	2.4	-	0.0086	0.00083	-	249
SA-2	89/09/29	3.56	-	-	-	0.00417	81.1	15.9	1.44	0.019	1.5	0.009	0.023	0.0005	-	239

Table A.3. Composition of Sumikawa and Ohnuma steam (continued).

Well	Date	WHP	Fstm	Fwat	Ysep	G/S	CO2	H2S	H2	CH4	N2	O2	Ar	He	Ne	TDP
SA-4	88/11/05	5.16	-	-	1	0.0135	64.8	23.3	4.6	0.4	6.7	0.14	0.22	0.00082	-	256
SA-4	88/11/13	2.48	-	-	1	0.0136	69.9	22.2	3.29	0.25	4.2	0.077	0.066	0.0006	-	247
SA-4	88/11/22	4.24	-	-	1	0.0019	59.5	33	3.09	0.25	4	0.089	0.06	0.00049	-	257
SA-4	88/11/27	4.24	6.58	-	1	0.00166	53.1	40.5	1.97	0.16	3.9	0.21	0.077	0.00041	-	255
SA-4	89/06/05	3.11	8.3	-	1	0.00032	61.7	0.6	1.74	0.26	35	0.11	0.5	0.00075	0.00075	189
SA-4	89/06/17	3.33	-	-	1	0.00104	47.9	35.8	3.36	0.33	12	0.76	0.16	0.00082	9.8E-05	265
SA-4	89/06/27	5.22	-	-	1	0.0012	53.1	37.9	2.87	0.28	5.7	-	0.082	0.00027	6.3E-05	259
SA-4	89/07/28	2.77	-	-	1	0.00069	15.9	69.5	5.75	0.5	8.2	-	0.042	0.001	-	334
SA-4	89/08/10	2.63	-	-	1	0.0031	52.8	42	1.93	0.15	2.8	0.14	0.039	0.0002	2.6E-05	255
SA-4	89/08/30	3.97	-	-	1	0.00149	44.5	44.6	3.66	0.25	6.3	0.71	0.08	0.00061	-	277
SA-4	89/08/31	14.2	-	-	1	0.00149	44.5	44.9	0.00061	0.25	6.3	0.71	0.08	-	3.7	92.
SA-4	89/09/10	3.41	-	-	1	0.00133	66.3	26.3	3.86	0.2	3.4	-	0.061	0.00052	-	258
SA-4	89/09/29	3.72	-	-	1	0.00131	64.7	28.1	3.6	0.13	3.6	-	0.055	0.00054	-	262
SB-1	89/06/19	0.21	1.6	9.2	0.148	0.00229	18.6	1.32	0.202	0.15	80	0.39	1	0.0074	0.0012	185
SB-1	89/07/01	0.34	2.2	11.4	0.162	0.00086	30.5	6.8	0.328	0.25	62	0.44	0.82	0.0063	0.00082	197
SB-1	89/07/13	1.81	8.9	19.9	0.309	0.00035	33.6	32.8	1.55	0.4	32	0.22	0.47	0.0044	0.00044	251
SB-1	89/07/20	1.92	9.4	19.9	0.321	0.00039	32.3	47.8	0.66	0.3	20	0.12	0.36	0.002	0.00038	236
SB-1	89/07/25	2.07	9.8	20.5	0.323	0.00032	36.8	40.8	0.5	0.3	21	0.56	0.29	0.0017	0.00034	223
SB-1	89/08/08	2.17	10.3	19	0.352	0.00043	33.2	26.4	0.358	0.29	38	0.19	0.52	0.0012	0.00048	212
SB-1	89/08/22	2.22	10.6	19.3	0.355	0.00075	40.1	17.8	0.695	0.32	40	0.23	0.59	0.00093	0.00063	218
SB-1	89/09/08	2.27	10	18.7	0.348	0.00038	38.3	26.1	0.394	0.36	34	1.3	0.43	0.00075	0.001	209
SB-1	89/09/16	2.22	9.9	19	0.343	0.00036	40.1	30	0.434	0.36	26	1.4	0.38	0.00072	0.00045	211
SB-1	89/10/01	2.17	9.8	18.1	0.351	0.00064	18.8	32	0.274	0.29	44	3.2	0.71	0.00093	0.00079	225
SM-2	78/09/25	0.21	0.47	0.97	0.326	0.0005	79.1	11.3	-	-	-	-	-	-	-	-
SM-2	78/11/17	1.8	2.19	5.39	0.289	0.0003	48.4	49.9	-	-	-	-	-	-	-	-
SC-1	88/10/07	19.8	11.7	25.6	0.314	0.00456	7.65	1.65	-	-	-	-	-	-	-	-
SC-1	88/10/19	12.6	41.6	81.5	0.338	0.0017	19	4.42	0.704	0.21	74	0.18	0.93	0.00054	0.0012	226
SC-1	88/10/29	12.8	43	81.3	0.346	0.00082	26.7	12.9	0.47	0.28	58	0.5	0.71	0.0006	0.0014	217
SC-1	88/11/09	19.2	29.8	55.9	0.348	0.00074	22	16.3	0.447	0.23	59	0.22	0.73	0.00062	0.0011	226
SC-1	89/10/09	17.7	36.3	76	0.323	0.00067	25.1	16.3	-	-	-	-	-	-	-	-
SC-1	89/10/12	12.4	44.6	94	0.322	0.00066	24.1	17.4	-	-	-	-	-	-	-	-
SC-1	89/10/13	12.3	38.7	92.7	0.295	0.00068	35.1	19.8	-	-	-	-	-	-	-	-
SC-1	89/10/14	12.2	38.4	91.9	0.295	0.00073	42.1	15.6	-	-	-	-	-	-	-	-
SC-1	89/10/15	12.2	38.2	91.5	0.295	0.00083	39.5	13	-	-	-	-	-	-	-	-
SC-1	89/10/21	11.8	46.6	85.7	0.352	0.00084	26.1	16.5	0.637	0.47	51	3.7	0.67	0.0011	0.00086	224
SC-1	89/11/01	-	-	-	-	0.0007	27	23	0.86	0.44	43	3.7	0.51	0.0012	0.0007	236
SC-1	89/11/07	-	-	-	-	0.00082	32	15.2	1.18	0.46	45	4	0.62	0.0009	0.0014	233
SC-1	89/11/16	12.4	50.9	84.4	0.376	0.00077	28.6	21.5	1.07	0.34	43	3.5	0.54	0.00075	0.0008	242
SC-1	89/11/27	-	-	-	-	0.00072	19	27.2	-	-	-	-	-	-	-	-

Table A.3. Composition of Sumikawa and Ohnuma steam (concluded).

Well	Date	WHIP	Fstm	Pwat.	Ysep	G/S	CO2	H2S	H2	CH4	N2	O2	Ar	He	Ne	TDP
SD-1	89/08/08	1.86	8.6	22.6	0.276	0.00067	38.5	51.1	0.559	0.17	9.3	0.14	0.1	0.00086	0.0001	232
SD-1	89/08/09	1.7	7.5	19.9	0.274	0.00075	42.2	50.5	0.847	0.19	6	0.1	0.12	0.00057	5.8E-05	240
SD-1	89/08/10	1.65	7.3	19.6	0.271	0.00057	32.6	62.8	0.764	0.14	3.5	-	0.046	0.00081	1.8E-05	251
SD-1	89/08/15	1.65	7.1	18.8	0.274	0.00033	46.7	45	1.38	0.21	6.4	0.44	0.071	0.0018	-	248
SD-1	89/08/21	1.55	6.2	18.1	0.255	0.00048	45.4	44	1.67	0.22	8.1	0.51	0.11	0.0019	-	253
SD-1	89/08/25	3.49	5.6	16.5	0.253	0.00133	49.9	43	1.53	0.19	9	0.76	0.11	0.001	0.00011	249
SD-1	89/09/08	1.55	6.6	16.5	0.286	0.00063	43.9	40.1	1.77	0.3	13	0.22	0.2	0.0017	-	252
SD-1	89/09/16	1.5	6.1	15.6	0.281	0.00109	47.4	20.8	4.04	0.66	25	1	0.37	0.0048	0.00016	256
SD-1	89/10/01	1.6	6.9	15.6	0.307	0.00127	51.4	32.8	1.99	0.26	13	0.72	0.15	0.0015	0.0012	248
SD-1	89/10/12	-	-	-	-	0.00112	45.5	39.8	1.6	0.23	12	0.59	0.14	0.001	0.00012	250
SD-1	89/10/20	1.6	7.22	15.3	0.321	0.00113	34.7	16	4.98	0.72	41	1	0.59	0.0021	0.00059	268
SD-1	89/10/31	-	-	-	-	0.00127	31.9	35.2	2.94	0.44	28	0.44	0.34	0.0012	0.00036	272
SD-1	89/11/16	1.6	7.36	15.1	0.328	0.00089	34.6	40.6	1.9	0.27	22	0.42	0.3	0.00052	0.00032	263

Table A.4. Oxygen and hydrogen isotope analyses of fluids from wells and springs. Units are permil SMOW and tritium units. Abbreviations are wat, separated water; stm, separated steam; and td, total discharge.

Source	Date	dDwat	dOwat	dDstm	dOstm	dDtd	dOtd	Trit
S-1	82/04/26	-	-	-71.8	-10.27	-71.8	-10.27	-
S-1	82/04/27	-	-	-72.3	-10.16	-72.3	-10.16	-
S-1	82/04/28	-	-	-72.3	-10.32	-72.3	-10.32	-
S-2	82/07/07	-51.6	-6.12	-81.6	-12.50	-	-	-
S-2	82/07/08	-47.3	-5.95	-	-	-	-	-
S-2	82/07/09	-48.3	-5.75	-78.4	-12.00	-73.4	-10.96	-
S-2	82/07/10	-49.3	-5.91	-	-	-	-	-
S-2	82/07/12	-48.5	-5.70	-	-	-	-	-
S-2	82/07/13	-48.1	-5.84	-	-	-	-	-
S-2	82/11/03	-61.8	-9.45	-87.5	-14.63	-69.1	-10.93	-
S-2	82/11/09	-61.0	-9.27	-	-	-	-	-
S-2	82/11/11	-60.5	-9.10	-64.3	-9.45	-61.6	-9.21	-
S-3	83/07/09	-62.7	-9.17	-79.4	-12.18	-65.9	-9.75	-
S-3	83/07/14	-62.6	-8.96	-79.1	-12.23	-68.5	-10.14	-
S-3	83/07/28	-65.6	-8.82	-89.7	-13.77	-72.5	-10.23	-
S-3	83/08/08	-64.1	-8.65	-89.6	-13.45	-71.7	-10.08	-
S-4	83/11/29	-57.8	-6.8	-71.7	-11.1	-68.2	-10.01	-
S-4	84/07/12	-58.2	-6.8	-81.1	-11.7	-72.2	-9.80	-
S-4	84/09/12	-61.5	-7.0	-83.5	-12.0	-73.8	-9.80	-
S-4	84/10/17	-61.5	-7.4	-91.4	-13.7	-76.4	-10.53	-
S-4	84/10/30	-63.1	-7.5	-95.1	-14.8	-78.5	-11.00	-
S-4	85/09/14	-59.4	-7.07	-82.3	-11.96	-72.47	-9.86	-
S-4	85/10/09	-62.0	-7.36	-70.7	-9.76	-66.58	-8.62	-
S-4	85/11/10	-61.7	-7.45	-77.6	-11.42	-69.99	-9.52	-
S-4	86/09/26	-60.8	-7.4	-85.1	-12.9	-74.6	-10.5	-
S-4	86/11/01	-58.6	-7.5	-88.8	-13.6	-74.4	-10.7	-
S-4	88/11/05	-	-	-	-	-	-	0.27
S-4	88/11/13	-63.7	-7.7	-89.3	-14.8	-	-	0.52
S-4	88/11/22	-66.7	-7.7	-106.2	-17.0	-	-	-
S-4	88/11/24	-63.9	-8.7	-77.9	-10.9	-71.7	-9.9	<0.28
S-4	89/06/28	-	-	-	-	-	-	1.30
S-4	89/07/27	-61.8	-7.7	-81.7	-12.1	-68.6	-9.2	1.0
S-4	89/09/30	-55.2	-7.4	-80.3	-12.3	-63.2	-9.0	<0.27
S-4	89/11/15	-57.7	-7.5	-79.6	-11.7	-63.6	-8.6	0.41
SA-1	88/11/04	-	-	-	-	-	-	0.34
SA-1	88/11/18	-45.5	-5.4	-92.9	-14.0	-	-	0.30
SA-1	88/11/22	-60.7	-6.1	-94.3	-14.4	-	-	0.55
SA-1	88/11/25	-64.0	-6.8	-79.1	-10.1	-76.8	-9.6	-
SA-1	89/06/27	-	-	-	-	-	-	1.50
SA-1	89/07/28	-58.1	-6.3	-77.5	-10.8	-74.4	-10.1	-
SA-1	89/09/30	-55.5	-6.5	-75.7	-10.8	-73.3	-10.3	0.37
SA-1	89/11/16	-56.2	-6.9	-81.8	-11.8	-78.7	-11.0	<0.24
SA-2	88/11/04	-	-	-66.1	-6.7	-	-	1.3
SA-2	88/11/14	-	-	-74.8	-6.7	-	-	0.76
SA-2	88/11/22	-	-	-75.7	-10.1	-	-	<0.28
SA-2	88/11/26	-	-	-72.9	-8.7	-	-	-
SA-2	89/07/03	-	-	-	-	-	-	5.20
SA-2	89/07/27	-41.1	-4.8	-70.8	-10.4	-	-	3.4
SA-2	89/09/24	-	-	-65.3	-9.5	-	-	-
SA-2	89/09/29	-	-	-	-	-	-	0.87
SA-2	89/11/15	-	-	-66.8	-9.9	-	-	0.57

Table A.4. Oxygen and hydrogen isotope analyses of fluids from wells and springs. Units are permil SMOW and tritium units. Abbreviations are wat, separated water; stm, separated steam; and td, total discharge (concluded).

Source	Date	dDwat	dOwat	dDstm	dOstm	dDttd	dOttd	Trit
SA-4	88/11/05	-	-	-93.2	-14.8	-	-	<0.26
SA-4	88/11/14	-	-	-87.7	-13.2	-	-	<0.27
SA-4	88/11/22	-	-	-81.0	-12.2	-	-	<0.27
SA-4	88/11/27	-	-	-72.8	-10.4	-	-	-
SA-4	89/06/17	-	-	-	-	-	-	6.80
SA-4	89/06/27	-	-	-	-	-	-	2.50
SA-4	89/07/28	-	-	-73.0	-11.1	-	-	1.4
SA-4	89/09/29	-	-	-70.2	-11.4	-	-	0.53
SA-4	89/11/15	-	-	-64.3	-11.4	-	-	<0.24
SB-1	89/07/01	-	-9.30	-	-14.50	-	-	3.3
SB-1	89/07/13	-	-8.07	-	-13.07	-	-	-
SB-1	89/07/13	-62.0	-8.1	-87.6	-13.1	-65.8	-8.9	-
SB-1	89/07/20	-	-8.26	-	-13.05	-	-	-
SB-1	89/07/25	-	-8.09	-	-13.01	-	-	-
SB-1	89/08/08	-	-7.48	-	-13.42	-	-	-
SB-1	89/09/16	-55.5	-7.4	-83.4	-12.2	-65.0	-9.0	0.77
SB-1	89/11/16	-53.6	-7.1	-79.7	-12.6	-63.5	-9.2	0.49
SC-1	88/10/19	-61.7	-7.8	-69.6	-10.3	-64.4	-8.6	0.71
SC-1	88/10/29	-63.7	-7.7	-83.6	-11.4	-70.6	-9.1	0.39
SC-1	88/11/09	-67.8	-7.9	-86.9	-11.4	-74.4	-9.1	0.39
SC-1	89/10/15	-63.1	-7.6	-70.4	-10.7	-65.8	-8.7	<0.24
SC-1	89/11/06	-	-	-	-	-	-	<0.25
SD-1	89/08/21	-62.1	-7.6	-88.5	-12.3	-69.0	-8.8	0.39
SD-1	89/09/16	-62.0	-7.7	-83.1	-12.1	-67.9	-8.9	0.36
SD-1	89/10/21	-57.3	-7.7	-83.2	-12.1	-65.6	-9.1	0.54
SD-1	89/11/16	-56.3	-7.6	-82.1	-12.4	-64.8	-9.2	0.59

Table A.5. Aquifer liquid temperatures, enthalpy values, and chloride concentrations. Units are kilojoules per kilogram, degrees Celsius and milligrams per kilogram.

Well	Date	Enth	Cl	TQA	T13	TNK-WE	TNK-F	ETQA	ET13	CTQA	CT13	CE
S-2	82/07/12	2190	660	250	228	223	244	1090	978	461	493	139
S-2	82/07/13	-	780	253	226	219	241	1100	971	540	585	-
S-2	82/11/02	-	246	234	260	338	328	1010	1130	181	167	-
S-2	82/11/03	1060	294	233	261	329	321	1000	1140	216	198	209
S-2	82/11/09	-	396	240	244	312	310	1040	1060	285	282	-
S-2	82/11/10	-	509	242	238	290	295	1050	1030	365	369	-
S-2	82/11/11	1110	544	242	240	289	293	1040	1040	390	392	374
S-2	83/05/13	-	776	240	260	243	260	1040	1140	559	525	-
S-2	83/05/14	-	764	241	242	241	258	1040	1050	548	546	-
S-2	83/05/16	-	867	248	245	242	259	1070	1060	611	615	-
S-3	83/07/10	-	85.3	225	232	257	270	965	998	64.6	63.4	-
S-3	83/07/08	-	93.2	225	219	251	266	964	937	70.1	71.2	-
S-3	83/07/09	808	80.5	222	235	261	274	955	1010	60.9	58.9	66.1
S-3	83/07/11	-	59.6	217	220	255	269	929	945	45.8	45.3	-
S-3	83/07/13	-	85	232	220	251	265	998	942	62.7	64.8	-
S-3	83/07/14	1200	44.6	224	221	252	267	963	947	33.6	33.9	29
S-3	83/07/20	-	100	228	225	244	261	980	967	74.6	75.1	-
S-3	83/07/25	-	95.9	225	228	248	263	968	979	72	71.5	-
S-3	83/07/28	1080	124	227	226	255	269	974	973	92.6	92.7	87
S-3	83/08/03	-	147	226	228	262	274	971	982	110	110	-
S-3	83/08/08	1090	144	226	229	260	273	970	987	108	107	100
S-3	83/10/19	-	34.2	201	229	236	254	856	986	27.4	25.4	-
S-3	83/10/20	1020	79.5	220	229	233	253	945	985	60.5	59.1	58
S-3	83/10/21	-	90.4	220	241	256	270	943	1040	68.9	64.9	-
S-3	83/10/22	1040	100	220	226	248	264	944	971	76.4	75.2	72.3
S-3	83/10/24	-	110	220	242	247	263	945	1050	83.4	78.4	-
S-3	83/10/27	1150	104	224	229	247	263	963	987	78.6	77.5	69.9
S-3	83/10/29	-	120	226	228	233	252	970	979	89.8	89.3	-
S-3	83/10/31	-	138	226	219	236	255	972	938	103	106	-
S-3	83/11/02	-	109	224	219	238	256	962	939	82	83.1	-
S-3	83/11/05	-	149	226	236	237	255	972	1020	112	109	-
S-3	83/11/10	1060	155	236	223	239	257	1020	958	113	117	110
S-3	83/11/25	1060	165	234	234	241	258	1010	1010	121	121	117
S-3	83/12/26	-	148	225	257	254	268	968	1120	111	101	-
S-3	84/01/14	-	182	233	255	243	260	1000	1110	134	125	-
S-3	84/01/28	-	189	236	255	241	259	1020	1110	138	130	-
S-4	84/07/05	-	524	305	318	308	307	1370	1450	300	282	-
S-4	84/07/06	1720	463	300	287	287	292	1340	1270	271	286	195
S-4	84/07/07	-	438	292	308	290	294	1300	1390	265	247	-
S-4	84/07/10	1620	394	283	312	295	298	1250	1410	246	218	183
S-4	84/07/12	-	356	287	313	299	301	1270	1420	219	196	-
S-4	84/07/17	1450	332	293	278	280	287	1300	1220	200	211	179
S-4	84/07/25	1520	298	285	278	283	290	1260	1220	185	190	152
S-4	84/08/05	1540	301	282	294	304	304	1250	1310	189	181	150
S-4	84/08/30	1470	376	286	290	294	297	1270	1290	233	230	200
S-4	84/09/03	1460	348	283	296	281	288	1250	1320	218	207	186
S-4	84/09/07	1450	341	281	294	287	292	1240	1310	215	205	184
S-4	84/09/12	1450	295	282	296	285	290	1250	1320	185	176	159
S-4	84/09/22	1440	314	283	292	278	285	1250	1300	197	190	171
S-4	84/10/03	1490	314	279	289	265	276	1230	1280	199	192	163
S-4	84/10/17	1370	328	279	295	282	289	1230	1320	208	196	189
S-4	84/10/30	1380	299	279	295	274	283	1230	1320	190	179	171
S-4	84/11/06	1360	316	279	297	283	289	1230	1330	200	187	182
S-4	85/08/26	1620	418	287	268	305	305	1270	1170	258	276	193
S-4	85/08/27	1850	398	285	272	299	300	1260	1200	248	259	143
S-4	85/08/28	1730	385	284	271	300	302	1260	1190	240	251	160
S-4	85/08/30	1690	361	281	268	295	298	1240	1180	228	238	155
S-4	85/09/02	-	335	280	265	293	296	1230	1160	212	223	-
S-4	85/09/04	1480	327	278	266	296	298	1230	1170	208	217	171
S-4	85/09/09	1460	304	278	260	286	291	1230	1140	194	206	163

Table A.5. Aquifer liquid temperatures, enthalpy values, and chloride concentrations. Units are kilojoules per kilogram, degrees Celsius and milligrams per kilogram (continued).

Well	Date	Enth	Cl	TOA	T13	TNK-WE	TNK-F	ETOA	ET13	CTOA	CT13	CE
S-4	85/09/14	1450	293	277	260	287	292	1220	1130	187	199	158
S-4	85/09/21	1390	294	277	258	283	289	1220	1120	188	201	166
S-4	85/09/28	1380	286	276	257	282	288	1210	1120	184	196	163
S-4	85/10/05	1350	287	275	256	282	289	1210	1120	185	197	167
S-4	85/10/10	1350	290	274	257	283	289	1210	1120	187	198	169
S-4	85/10/19	1350	291	275	256	281	288	1210	1110	187	200	170
S-4	85/10/26	1330	290	273	255	280	287	1200	1110	188	200	172
S-4	85/11/02	1360	282	268	255	278	286	1180	1110	186	194	163
S-4	85/11/12	1330	279	272	255	281	288	1190	1110	182	192	165
S-4	85/11/16	1340	280	272	257	285	290	1190	1120	182	192	165
S-4	86/07/17	-	391	292	264	298	300	1300	1150	236	261	-
S-4	86/07/18	1690	350	278	253	288	293	1220	1100	223	243	151
S-4	86/09/02	-	430	275	265	313	310	1210	1160	277	287	-
S-4	86/09/03	1650	350	276	270	293	296	1210	1180	225	229	157
S-4	86/09/05	1600	323	278	268	292	296	1230	1180	206	213	152
S-4	86/09/06	1560	309	268	266	292	296	1170	1160	204	205	151
S-4	86/09/13	1500	278	273	262	284	290	1200	1140	181	187	144
S-4	86/09/20	1440	266	272	261	284	290	1190	1140	173	179	144
S-4	86/09/26	1440	260	274	253	274	283	1200	1100	168	180	141
S-4	86/10/09	1440	266	277	257	281	288	1220	1120	170	182	144
S-4	86/10/10	1440	266	267	255	277	285	1170	1110	176	183	144
S-4	86/10/11	1440	246	276	249	264	275	1210	1080	158	172	134
S-4	86/11/01	1440	266	270	252	271	281	1180	1090	174	185	144
S-4	86/11/03	1330	256	270	253	275	283	1180	1100	168	177	151
S-4	88/10/25	-	396	297	248	311	309	1330	1070	234	279	-
S-4	88/10/31	1260	284	266	284	302	302	1170	1260	189	177	176
S-4	88/11/13	1260	248	273	279	297	299	1200	1230	161	157	154
S-4	88/11/22	1260	298	274	272	279	286	1200	1190	193	194	185
S-4	88/11/24	1260	213	240	263	260	273	1040	1150	153	143	133
S-4	89/06/10	13800	173	263	232	271	280	1150	999	116	128	-
S-4	89/06/28	1310	221	267	248	275	283	1170	1080	146	156	133
S-4	89/07/27	1380	288	268	255	271	281	1180	1110	190	198	164
S-4	89/08/31	1370	323	269	254	272	281	1180	1100	212	223	185
S-4	89/09/30	1310	336	265	251	265	276	1160	1090	224	235	202
S-4	89/10/28	-	379	264	254	268	279	1160	1110	253	262	-
S-4	89/11/15	1260	421	262	255	261	273	1150	1110	283	290	261
SA-1	88/10/22	-	195	259	232	358	341	1130	1000	132	144	-
SA-1	88/11/18	-	889	320	273	299	301	1460	1200	475	576	-
SA-1	88/11/25	2330	593	279	286	302	302	1230	1270	377	367	89
SA-1	89/06/04	2410	102	254	223	299	301	1100	957	70.5	77.1	11.8
SA-1	89/06/26	2350	554	295	247	291	295	1310	1070	331	391	77.5
SA-1	89/07/28	2420	730	305	254	290	294	1370	1100	418	504	80.6
SA-1	89/08/31	2430	908	318	259	290	294	1450	1130	490	616	96.8
SA-1	89/09/30	2260	890	317	261	293	296	1440	1140	483	601	161
SA-1	89/10/28	-	856	316	258	293	297	1430	1130	466	583	-
SA-1	89/11/16	2370	840	311	253	289	294	1410	1100	468	582	113
SA-2	89/06/21	2730	1050	231	233	295	298	996	1000	775	772	-25.7
SA-2	89/06/30	2700	962	243	240	300	301	1050	1040	687	692	-14.7
SA-2	89/07/03	2720	2270	251	237	296	299	1090	1020	1580	1650	-47.2
SA-2	89/07/08	2700	4880	226	241	289	294	972	1040	3660	3500	-74.4
SA-2	89/07/27	2730	457	66	280	544	455	276	1240	483	289	-11.2
SA-2	89/09/29	2730	862	47.3	311	641	506	198	1410	940	479	-21.1
SA-2	89/10/27	-	2730	47.3	182	137	176	198	772	2980	2290	-
SA-2	89/11/15	2730	25.9	75.9	207	327	320	318	884	26.9	20.4	-0.634
SA-4	89/06/05	-	71	241	233	322	317	1040	1000	51.1	52.2	-
SB-1	89/06/15	758	84	210	198	247	263	897	845	65.7	67.6	70.9
SB-1	89/07/01	758	158	220	207	239	257	942	883	121	125	133
SB-1	89/07/13	1080	244	241	219	239	257	1040	937	175	187	171
SB-1	89/08/08	1200	296	246	235	259	272	1070	1010	210	217	192
SB-1	89/09/16	1180	325	248	233	252	267	1080	1000	228	239	214
SB-1	89/10/20	1230	375	247	232	247	263	1070	998	264	277	239
SB-1	89/11/16	-	440	252	234	244	260	1090	1010	306	323	-

Table A.5. Aquifer liquid temperatures, enthalpy values, and chloride concentrations. Units are kilojoules per kilogram, degrees Celsius and milligrams per kilogram (concluded)

Well	Date	Enth	Cl	TQA	T13	TNK-WE	TNK-F	ETQA	ET13	CTQA	CT13	CE
SC-1	88/8/11	-	452	283	237	219	241	1250	1020	283	328	-
SC-1	88/10/01	1130	440	270	248	226	247	1180	1080	289	309	300
SC-1	88/10/06	1120	440	268	250	229	250	1180	1080	290	308	301
SC-1	88/10/19	1170	465	268	245	222	244	1170	1060	307	330	307
SC-1	88/10/29	1190	459	267	254	233	252	1170	1110	304	317	300
SC-1	88/11/09	1190	446	267	270	252	267	1170	1180	296	292	291
SC-1	88/11/10	-	308	234	224	246	262	1010	964	226	232	-
SC-1	88/11/14	1120	442	271	266	253	267	1190	1160	289	294	302
SC-1	89/10/09	1140	457	269	235	237	255	1180	1010	301	334	309
SC-1	89/10/15	1230	454	269	236	237	256	1180	1020	299	331	288
SC-1	89/11/16	1260	456	268	242	246	262	1180	1050	301	326	284
SD-1	89/08/09	1020	198	240	220	242	259	1040	943	143	151	144
SD-1	89/08/21	986	216	238	224	250	265	1030	962	156	163	161
SD-1	89/09/16	1040	243	236	223	247	263	1020	959	177	183	175
SD-1	89/10/20	1130	267	239	224	249	265	1030	964	193	201	181
SD-1	89/11/16	1150	298	243	228	251	266	1050	981	213	222	200
SM-2	78/09/25	1140	265	220	194	173	205	945	825	202	216	178
SM-2	78/10/25	895	409	170	-	254	268	721	-0.02	352	-	320
SM-2	78/11/06	1020	429	254	-	269	279	1110	-	296	-	312
SM-2	78/11/17	1010	457	257	-	271	281	1120	-	313	-	334
SM-2	78/11/17	1060	457	257	-	271	281	1120	-	312	-	325
SM-2	79/01/23	1230	459	245	-	258	271	1060	-	326	-	293
SM-2	79/03/10	-	486	250	-	252	266	1090	-	340	-	-
SM-2	79/04/10	-	476	248	-	251	266	1080	-	335	-	-
SM-2	79/05/10	-	476	249	-	258	271	1080	-	333	-	-
SM-2	79/06/10	-	484	252	-	206	231	1090	-	337	-	-
SM-2	79/08/10	1150	499	245	-	246	262	1060	-	354	-	334
SM-2	79/09/10	-	479	250	-	250	265	1090	-	335	-	-
SM-2	79/10/10	1180	436	247	-	248	264	1070	-	307	-	287

Note:

Symbols: Enth, total discharge enthalpy calculated from flows of water and steam at one atmosphere abs. (in kJ/kg); TQA, quartz (silica) saturation geothermometer calculated assuming all cooling from steam loss (Fournier and Potter, 1982); T13, Na-K-Ca geothermometer with $\beta = 1/3$ (Fournier and Truesdell, 1973); TNK-W, Na-K geothermometer from White and Ellis (Truesdell, 1975); TNK-F Na-K geothermometer from Fournier (Fournier, 1979); ETQA and ET13, enthalpy (kJ/kg) of aquifer liquid calculated assuming steam-saturated aquifer liquid temperatures indicated by TQA and T13; CTQA and CT13, calculated aquifer liquid chloride concentrations (in mg/kg) by methods in Henley, *et al.* (1984); CE, total discharge chloride concentrations calculated from total discharge enthalpy.

Table A.6. 1989 cold-water injection into Sumikawa wells.

Well	Dates	Cumulative Volume Injected (m³)
SA-1	4/15-5/16	19,430
SA-2	4/16-5/17	29,680
SA-4	4/17-5/18	27,530
S-4	5/16-5/19	9,380
SB-1	4/25-5/29	16,830
SB-2	4/29-5/30	20,000
SB-3	4/25-5/31	30,070

Table A.7. Partial analyses made by MMC in 1989 after the injection of cold water (data from MMC). Units are Flows, tons/hour; pH, pH units; Cl, mg/kg; Conductivity, mS/cm²; Cumulative Flow, 1000 t/h. The pressure of separation is not specified.

Flows (t/hr)					Chloride in Water	Electrical Conductivity	Chloride in Total Discharge	Cumulative Flow
Well	Date	Steam	Water	pH				
S-4	89/06/10	29.0	120.8	7.1	173	1090	140	1.93
S-4	89/08/12	31.9	121.9	7.9	183	1070	145	9.25
S-4	89/06/17	43.9	120.7	8.1	197	1130	144	28.6
S-4	89/08/23	50.2	122.5	8.0	229	1210	182	52.8
S-4	89/06/28	53.2	121.9	8.0	221	1250	154	71.3
S-4	89/07/19	63.0	121.8	7.8	285	1380	188	109.9
S-4	89/07/27	60.0	118.9	7.8	288	1430	191	143.7
S-4	89/08/31	55.3	108.8	7.7	323	1570	214	241.9
S-4	89/09/30	53.0	112.3	7.8	336	1640	228	342.1
S-4	89/10/28	50.4	115.1	7.9	379	1760	264	439.0
S-4	89/11/15	44.8	122.5	7.7	421	1870	308	511.0
SA-1	89/06/01	18.0	116.9	-	146	-	128	0.66
SA-1	89/06/02	14.8	112.9	-	138	-	122	3.70
SA-1	89/06/04	18.0	94.8	8.0	102	790	85.7	9.21
SA-1	89/06/09	40.9	53.6	7.4	202	992	115	21.67
SA-1	89/06/12	47.1	45.9	7.2	343	1420	169	28.36
SA-1	89/06/17	50.0	33.2	7.0	475	1820	190	38.88
SA-1	89/06/23	46.8	18.0	6.8	532	2020	148	49.26
SA-1	89/06/20	44.9	10.3	6.8	554	2140	103	53.40
SA-1	89/07/04	-	-	6.9	455	1760	-	61.50
SA-1	89/07/19	41.0	10.4	6.7	561	2110	114	65.24
SA-1	89/07/28	41.2	8.0	6.5	730	2640	119	75.79
SA-1	89/08/31	38.0	8.9	6.4	908	3270	140	92.05
SA-1	89/09/30	49.6	6.8	6.5	890	3280	107	133.3
SA-1	89/10/28	53.8	7.1	6.7	858	3170	99.8	167.7
SA-1	89/11/16	51.6	7.1	6.8	840	3150	102	196.2

Table A.7. Partial analyses made by MMC in 1989 after the injection of cold water (data from MMC). Units are Flows, tons/hour; pH, pH units; Cl, mg/kg; Conductivity, mS/cm²; Cumulative Flow, 1000 t/h. The pressure of separation is not specified (continued).

Flows (t/hr)					Chloride in Water	Electrical Conductivity	Chloride in Total Discharge	Cumulative Flow
Well	Date	Steam	Water	pH				
SA-2	89/06/07	-	-	7.3	1200	4390	-	-
SA-2	89/06/17	-	-	7.7	1360	4700	-	-
SA-2	89/06/19	-	-	7.9	1210	4240	-	-
SA-2	89/06/21	-	-	8.0	1060	3710	-	-
SA-2	89/06/28	-	-	8.0	680	2940	-	-
SA-2	89/06/30	-	-	8.0	962	3260	-	-
SA-2	89/07/01	-	-	7.7	1270	4150	-	-
SA-2	89/07/03	-	-	6.1	2270	7360	-	-
SA-2	89/07/04	39.6	8.2	5.5	2030	6680	348	0.57
SA-2	89/07/05	-	-	5.6	2590	8150	-	1.05
SA-2	89/07/06	-	-	4.3	3520	10700	-	1.23
SA-2	89/07/07	-	-	4.8	2140	6590	-	-
SA-2	89/07/08	-	-	5.8	4880	15100	-	-
SA-2	89/07/19	-	-	4.1	3080	9420	-	1.66
SA-2	89/07/22	35.0	1.1	4.3	7380	20000	225	4.34
SA-2	89/07/27	30.6	0.0	3.4	457	1700	-	8.13
SA-2	89/08/24	21.9	0.0	3.7	34.9	274	-	17.8
SA-2	89/09/30	20.4	0.0	3.4	862	3150	-	34.3
SA-2	89/10/27	16.7	0.0	3.7	2730	8570	-	45.6
SA-2	89/11/15	13.1	0.0	3.3	25.9	248	-	52.8
SA-2	89/12/01	13.3	0.0	3.5	8030	20800	-	55.3
SA-4	89/06/05	23.0	82.4	9.0	71	749	51.9	3.14
SA-4	89/06/09	33.9	42.3	8.4	84	740	46.6	10.9
SA-4	89/08/12	35.1	33.2	8.4	93	834	45.2	16.0
SA-4	89/06/17	37.4	14.0	7.9	113	847	30.8	23.2
SA-4	89/06/23	33.6	0.0	7.5	133	82	-	28.6
SA-4	89/06/27	30.0	0.0	7.0	5.9	102	-	31.4
SB-1	89/06/15	7.8	42.9	8.8	82	804	69	0.203
SB-1	89/06/19	4.4	29.7	8.8	80.9	803	70	0.438
SB-1	89/06/30	6.8	41.1	8.5	129	912	111	1.18
SB-1	89/07/01	7.4	41.1	8.5	158	936	134	2.35
SB-1	89/07/03	11.9	52.8	8.4	179	1030	146	5.36
SB-1	89/07/04	14.5	58.7	8.4	184	1040	131	7.12
SB-1	89/07/06	19.2	62.9	8.4	179	1080	137	10.9
SB-1	89/07/10	27.1	71.7	8.2	227	1190	165	19.9

Table A.7. Partial analyses made by MMC in 1989 after the injection of cold water (data from MMC). Units are Flows, tons/hour; pH, pH units; Cl, mg/kg; Conductivity, mS/cm²; Cumulative Flow, 1000 t/h. The pressure of separation is not specified (concluded).

Well	Date	Flows (t/hr)		pH	Chloride in Water	Electrical Conductivity	Chloride in Total Discharge	Cumulative Flow
		Steam	Water					
SB-1	89/07/13	30.6	71.2	8.2	244	1230	171	27.3
SB-1	89/07/17	32.7	72.8	8.2	236	1260	163	37.4
SB-1	89/07/20	33.9	71.7	8.2	230	1260	156	45.0
SB-1	89/07/25	35.2	73.9	8.1	264	1370	179	58.0
SB-1	89/07/31	36.3	71.7	8.1	278	1440	185	73.4
SB-1	89/08/08	37.2	68.3	8.0	296	1500	192	94.0
SB-1	89/08/14	37.3	70.5	8.0	307	1530	201	109
SB-1	89/08/22	38.1	69.4	8.0	312	1550	201	130
SB-1	89/09/08	35.8	68.3	7.9	321	1620	211	163
SB-1	89/09/16	35.5	68.3	7.9	325	1640	214	183
SB-1	89/10/20	34.2	59.8	9.0	375	1850	239	264
SB-1	89/11/16	33.2	54.6	7.9	440	1990	274	323
SC-1	89/10/09	130.5	273.7	7.3	457	1960	309	38.0
SC-1	89/10/15	156.7	310.1	7.4	454	1950	302	77.0
SC-1	89/10/21	167.7	308.5	7.4	450	1860	292	136
SC-1	89/11/16	183.3	306.1	7.4	456	1860	285	428
SD-1	89/08/08	30.8	81.2	8.2	194	1220	141	1.38
SD-1	89/08/09	26.9	71.5	8.2	198	1250	145	3.74
SD-1	89/08/11	26.5	69.6	8.1	205	1290	148	9.37
SD-1	89/08/14	25.7	70.6	8.1	215	1310	158	15.3
SD-1	89/08/16	26.0	66.8	8.1	219	1330	158	19.7
SD-1	89/08/18	25.8	65.9	8.1	224	1350	160	24.1
SD-1	89/08/21	22.4	65.0	8.1	216	1340	160	30.5
SD-1	89/08/25	20.3	59.5	8.1	224	1370	167	38.3
SD-1	89/09/08	23.8	59.5	8.0	235	1380	175	67.6
SD-1	89/09/16	21.8	56.0	8.0	243	1420	175	83.6
SD-1	89/10/02	25.0	55.1	8.0	247	1440	170	114
SD-1	89/10/20	26.0	55.1	8.1	267	1490	181	149
SD-1	89/11/16	26.5	54.3	8.0	298	1550	200	201

Table A.8. Calculated reservoir temperatures of Sumikawa and Ohnuma well waters using Silica, Na-K-Ca, and various Na/K geothermometer equations. See footnote for sources. Temperatures in degrees Celsius.

Well	Date	TQA	T13	TNK-WE	TNK-F	TNK-A	TNK-N	TNK-G	TKMg
O-1R	69/11/17	236	229	257	270	260	256	281	102
O-2R	71/02/09	234	-	-	-	-	-	-	-
O-3Rb	70/08/26	223	-	-	-	-	-	-	-
O-3Rb	74/05/10	219	220	219	241	224	228	255	105
O-5R	71/12/27	219	220	232	252	237	238	264	121
O-6R	72/12/28	217	220	239	257	243	243	269	125
O-6T	71/10/13	220	227	246	262	250	248	274	133
O-8R	76/10/20	228	230	209	234	215	220	248	125
O-10R	83/05/21	230	224	211	235	217	222	249	127
S-1C	81/11/23	15.5	155	277	285	278	270	294	22.4
S-1C	81/11/27	45.8	115	199	226	206	213	241	10.9
S-2	82/07/06	232	213	205	231	212	218	245	115
S-2	82/07/07	227	223	208	233	215	220	248	127
S-2	82/07/08	227	238	222	244	228	231	258	141
S-2	82/07/09	250	221	219	242	225	228	255	118
S-2	82/07/10	254	225	221	243	227	230	257	123
S-2	82/07/11	247	234	233	253	238	239	265	130
S-2	82/07/12	250	228	223	244	228	231	258	126
S-2	82/07/13	253	226	218	241	224	227	255	125
S-2	82/11/02	234	260	338	327	334	312	333	98.5
S-2	82/11/03	233	261	329	321	326	306	327	97.9
S-2	82/11/09	240	244	312	310	311	295	317	98.3
S-2	82/11/10	242	238	290	295	291	280	303	94.7
S-2	82/11/11	241	240	289	293	289	279	302	95.1
S-2	83/05/13	240	260	243	260	247	246	272	95.4
S-2	83/05/14	241	242	241	258	245	244	271	94.7
S-2	83/05/16	248	245	242	259	246	245	271	97.1
S-3	83/07/08	225	219	251	266	254	251	277	113
S-3	83/07/09	222	234	261	273	264	259	284	99.6
S-3	83/07/10	225	232	256	270	259	255	281	101
S-3	83/07/11	217	220	254	268	258	254	280	105
S-3	83/07/13	232	219	250	265	254	251	277	100
S-3	83/07/14	224	221	252	266	255	252	278	98.6
S-3	83/07/20	228	225	244	261	248	247	273	103
S-3	83/07/25	225	228	248	263	252	249	275	105
S-3	83/07/28	227	226	255	269	258	255	280	107
S-3	83/08/03	226	228	262	274	264	259	284	112
S-3	83/08/08	226	229	260	273	263	258	284	111
S-3	83/10/19	201	229	236	254	240	240	267	118

Table A.8. Calculated reservoir temperatures of Sumikawa and Ohnuma well waters using Silica, Na-K-Ca, and various Na/K geothermometer equations. See footnote for sources. Temperatures in degrees Celsius (continued).

Well	Date	TQA	T13	TNK-WE	TNK-F	TNK-A	TNK-N	TNK-G	TKMg
S-3	83/10/20	220	229	233	252	238	238	265	106
S-3	83/10/21	220	241	256	269	259	255	280	114
S-3	83/10/22	220	226	248	264	252	249	275	117
S-3	83/10/24	220	242	247	262	250	248	274	102
S-3	83/10/27	224	229	247	263	250	248	274	108
S-3	83/10/29	226	228	233	252	238	239	265	106
S-3	83/10/31	226	219	236	255	241	241	267	134
S-3	83/11/02	224	219	238	256	242	242	268	120
S-3	83/11/05	226	236	237	255	241	241	268	108
S-3	83/11/10	235	223	239	257	243	243	269	127
S-3	83/11/25	234	234	241	258	245	244	270	107
S-3	83/12/26	225	257	254	268	257	254	279	110
S-3	84/01/14	233	255	243	260	247	246	272	110
S-3	84/01/28	236	255	241	259	245	244	271	110
S-4	84/07/05	305	318	308	307	307	292	314	178
S-4	84/07/06	300	287	287	292	288	277	301	166
S-4	84/07/07	292	308	290	294	291	280	303	173
S-4	84/07/10	283	312	295	298	296	283	307	176
S-4	84/07/12	287	313	299	301	299	286	309	182
S-4	84/07/17	293	278	280	287	282	273	297	174
S-4	84/07/25	285	278	283	289	285	275	299	169
S-4	84/08/05	282	294	304	304	303	289	312	154
S-4	84/08/30	286	289	294	297	294	282	306	155
S-4	84/09/03	283	296	281	288	282	273	297	136
S-4	84/09/07	281	294	287	292	288	277	301	137
S-4	84/09/12	282	296	285	290	286	276	300	133
S-4	84/09/22	283	292	278	285	279	271	295	140
S-4	84/10/03	279	289	265	276	268	262	287	136
S-4	84/10/17	279	295	282	289	284	274	298	138
S-4	84/10/30	279	295	274	283	276	268	293	135
S-4	84/11/06	279	297	283	289	284	274	298	133
S-4	85/08/26	286	268	305	305	305	290	313	170
S-4	85/08/27	284	272	299	300	298	285	309	209
S-4	85/08/28	284	271	300	302	300	287	310	209
S-4	85/08/30	281	268	295	298	295	283	306	224
S-4	85/09/02	280	265	293	296	293	281	305	221
S-4	85/09/04	278	266	296	298	296	284	307	221
S-4	85/09/09	278	260	286	291	287	277	301	227
S-4	85/09/14	277	260	287	292	288	278	301	226
S-4	85/09/21	277	258	283	289	284	275	299	245
S-4	85/09/28	275	257	281	288	283	273	298	227
S-4	85/10/05	274	256	282	289	283	274	298	244

Table A.8. Calculated reservoir temperatures of Sumikawa and Ohnuma well waters using Silica, Na-K-Ca, and various Na/K geothermometer equations. See footnote for sources. Temperatures in degrees Celsius (continued).

Well	Date	TQA	T13	TNK-WE	TNK-F	TNK-A	TNK-N	TNK-G	TKMg
S-4	85/10/10	274	257	283	289	284	274	298	227
S-4	85/10/19	275	256	281	288	282	273	297	227
S-4	85/10/26	273	255	280	287	281	272	296	244
S-4	85/11/02	268	255	278	285	279	271	295	243
S-4	85/11/12	272	255	281	288	282	273	297	243
S-4	85/11/16	272	257	285	290	286	276	300	244
S-4	86/07/17	292	264	298	300	298	285	308	175
S-4	86/07/18	278	253	288	293	289	278	302	210
S-4	86/09/02	275	265	313	310	311	295	317	190
S-4	86/09/03	276	270	293	296	293	281	305	223
S-4	86/09/05	278	268	292	296	293	281	305	222
S-4	86/09/06	268	266	292	295	292	281	304	211
S-4	86/09/20	272	261	284	290	285	275	299	225
S-4	86/09/26	274	253	274	283	276	268	293	-
S-4	86/10/09	277	257	281	287	282	273	297	-
S-4	86/10/10	267	255	277	285	279	270	295	206
S-4	86/10/11	276	249	264	275	267	261	286	238
S-4	86/11/01	270	251	271	281	273	266	291	238
S-4	86/11/03	270	253	275	283	277	269	293	0
S-4	88/10/25	297	248	311	309	309	294	316	106
S-4	88/10/31	266	284	302	302	301	287	311	96.9
S-4	88/11/13	273	279	297	299	297	284	307	189
S-4	88/11/22	274	272	279	286	280	272	296	150
S-4	88/11/24	240	263	260	273	263	258	284	157
S-4	89/06/10	263	232	271	280	273	266	291	209
S-4	89/06/28	267	248	275	283	276	269	293	-
S-4	89/07/27	268	255	271	281	273	266	291	223
S-4	89/08/31	269	254	272	281	274	267	291	246
S-4	89/09/30	265	251	265	276	268	262	287	228
S-4	89/10/28	264	254	268	279	271	264	289	231
S-4	89/11/15	262	255	261	273	264	259	284	224
S-4C	88/11/05	-	208	555	460	525	443	449	-
S-4C	88/11/22	-	235	725	547	666	528	521	56.1
S-4C	88/11/24	18.2	215	725	547	666	528	521	21.8
SA-1	88/10/22	259	232	358	341	353	326	345	117
SA-1	88/11/18	320	273	299	301	299	286	309	146
SA-1	88/11/25	279	286	301	302	301	287	310	137
SA-1	89/06/04	254	223	299	301	299	286	309	163
SA-1	89/06/26	295	247	291	295	291	280	304	223
SA-1	89/07/28	305	254	290	294	291	280	303	235
SA-1	89/08/31	318	259	290	294	291	279	303	252

Table A.8. Calculated reservoir temperatures of Sumikawa and Ohnuma well waters using Silica, Na-K-Ca, and various Na/K geothermometer equations. See footnote for sources. Temperatures in degrees Celsius (continued).

Well	Date	TQA	T13	TNK-WE	TNK-F	TNK-A	TNK-N	TNK-G	TKMg
SA-1	89/09/30	317	261	293	296	293	282	305	251
SA-1	89/10/28	316	258	293	297	294	282	305	240
SA-1	89/11/16	311	253	289	294	290	279	302	236
SA-1C	88/11/18	-	235	555	460	525	443	449	62.4
SA-2	89/06/21	231	233	295	298	295	283	306	139
SA-2	89/06/30	243	240	300	301	300	286	310	183
SA-2	89/07/03	251	236	296	299	296	284	307	197
SA-2	89/07/08	226	241	289	294	290	279	303	209
SA-2	89/07/27	66	280	544	454	516	437	444	154
SA-2	89/09/29	47.3	311	641	506	598	488	487	177
SA-2	89/10/27	47.3	182	137	176	147	164	194	171
SA-2	89/11/15	75.9	207	327	320	324	305	326	99.3
SA-2C	89/12/01	176	2910	-618	-929	-671	-904	-1150	177
SA-4	89/06/05	241	233	322	317	320	301	323	159
SA-4C	88/10/30	-	152	157	193	166	180	209	33.6
SA-4C	88/11/13	-	235	528	445	502	428	436	62.4
SA-4C	88/11/22	-	264	1260	756	1080	735	686	41.9
SA-4C	88/11/27	18.2	229	533	448	506	431	438	52.3
SA-4C	89/06/27	57.7	203	307	306	306	291	314	109
SA-4C	89/07/28	-	-	465	409	448	392	405	57.2
SA-4C	89/10/27	-	-	624	497	583	479	479	-
SA-4C	89/11/15	-	-	226	247	232	233	260	-
SB-1	89/06/15	210	198	247	262	250	248	274	186
SB-1	89/07/01	220	207	239	257	244	243	269	179
SB-1	89/07/13	241	218	239	257	243	243	269	208
SB-1	89/08/08	246	234	259	272	262	257	283	203
SB-1	89/09/16	248	233	252	267	256	252	278	222
SB-1	89/10/20	247	232	247	263	251	249	275	215
SB-1	89/11/16	252	234	244	260	248	246	272	221
SC-1	88/8/11	283	237	219	241	224	228	255	111
SC-1	88/10/01	270	248	226	247	232	233	260	153
SC-1	88/10/06	268	250	229	250	234	236	262	158
SC-1	88/10/19	268	245	222	244	228	230	257	155
SC-1	88/10/29	267	254	233	252	237	238	265	144
SC-1	88/11/09	267	270	252	267	255	252	278	159
SC-1	88/11/10	234	224	246	262	250	248	274	108
SC-1	88/11/14	271	266	253	267	257	253	279	147
SC-1	89/10/09	269	235	237	255	242	241	268	214

Table A.8. Calculated reservoir temperatures of Sumikawa and Ohnuma well waters using Silica, Na-K-Ca, and various Na/K geothermometer equations. See footnote for sources. Temperatures in degrees Celsius (continued).

Well	Date	TQA	T13	TNK-WE	TNK-F	TNK-A	TNK-N	TNK-G	TKMg
SC-1	89/10/15	269	236	237	256	242	242	268	214
SC-1	89/11/16	268	242	245	262	249	248	274	217
SC-1C	88/10/06	7.47	192	465	409	448	392	405	34.2
SC-1C	88/10/29	7.47	143	199	226	206	213	241	34.2
SC-1C	88/11/09	-	225	484	420	464	403	414	62.4
SD-1	89/08/09	240	220	242	259	246	245	271	165
SD-1	89/08/21	238	224	250	265	254	251	277	203
SD-1	89/09/16	236	223	247	263	251	249	275	214
SD-1	89/10/20	239	224	249	265	253	250	276	205
SD-1	89/11/16	243	228	251	266	255	252	278	204
SM-2	78/09/25	220	194	173	205	181	192	221	102
SM-2	78/10/25	170	-	254	268	258	254	280	134
SM-2	78/11/06	254	-	269	279	271	264	289	140
SM-2	78/11/17	257	-	271	281	273	266	291	135
SM-2	79/01/23	245	-	258	271	261	257	282	123
SM-2	79/03/10	250	-	252	266	255	252	278	128
SM-2	79/04/10	248	-	251	266	255	252	277	132
SM-2	79/05/10	249	-	258	271	261	257	282	129
SM-2	79/06/10	251	-	206	231	212	218	246	129
SM-2	79/08/10	245	-	246	262	250	248	274	129
SM-2	79/09/10	250	-	250	265	254	251	277	125
SM-2	79/10/10	247	-	248	264	252	250	275	126

The geothermometer equations used in this table are: TQA, quartz saturation equation with adiabatic cooling (Fournier and Potter, 1982); T13, Na-K-Ca equation with $\beta = 1/3$ (Fournier and Truesdell, 1973); TNK-WE, Na/K equation with data from D. White and J. Ellis (Truesdell, 1975); TNK-F, Na/K equation from Fournier (1979); TNK-A, Na/K equation from Arnorsson et al. (1983); TNK-N, Na/K equation from Nieva and Nieva (1987); TNK-G, Na/K equation from Giggenbach (1988); TKMg, K-Mg equation from Giggenbach (ob. cit.).

Table A.9. Further explanation of the WATCH output.

The printout from WATCH seems confusing, but the information is clearly presented and helps in understanding the calculations of deep water chemistry and mineral saturation. Starting at the top of Table A.9a, the input data is mirrored and the anion-cation balance is calculated. This provides a check on the accuracy of analytical data and data entry. The next section shows the reservoir water and steam composition in weight percent, reservoir ion balance and the gas partial pressures. With this data samples collected downhole or at different separator pressures can be compared. The gas partial pressures are needed for some mineral stability diagrams. Under this are oxidation ("redox" or Eh) potentials in volts calculated from analyses of redox-sensitive constituents. This data is used to calculate the reservoir concentrations of ferric and ferrous ions and saturation with Fe minerals.

Activity coefficients and concentrations of chemical species in deep water are useful for relating water compositions to mineral stabilities using "activity-activity" diagrams (activity = activity coefficient concentration), such as the K^+/H^+ vs Na^+/H^+ diagram where solution activity values can be compared with the stability fields of microcline, muscovite, kaolinite and albite. Finally the program calculates saturation with a set of minerals that may occur in the original rock or as alteration products. This data is presented as logarithms of equilibrium ("theoretical") and observed ("calculated") ion products for mineral solution. If these values are equal, the mineral is exactly saturated. If the equilibrium ion product is larger then the mineral is undersaturated; if it is smaller, the mineral is supersaturated.

In practice the quantities are seldom exactly equal (unless set that way to calculate the concentration of aluminium ion) and agreement within 0.1 to 0.5 log unit may indicate probable saturation. On the other hand, an ion product difference of more than one log unit indicates undersaturation or supersaturation. Some minerals in the list (e.g. wollastonite) are almost never in true equilibrium in geothermal waters because they are formed only at much higher temperatures and react so slowly that they may be considered inert, but other minerals may be in equilibrium at a different pH or gas partial pressure. At equilibrium (in undisturbed reservoirs) mineral pairs control reservoir chemistry (as K-feldspar and mica control K^+/H^+ ratio). However in exploited fields, induced boiling or fluid inflow and mixing may cause gas pressures or pH to change so rapidly that these minerals do not dissolve or precipitate rapidly enough to maintain constant conditions.

Note that when calculating equilibria of aluminosilicate minerals, it is necessary to use the concentration of aluminum ions in solution. When Al has not been analyzed, it is possible to arrive at this information by assuming that a particular aluminosilicate mineral is exactly saturated. For Sumikawa, we have chosen microcline (K-feldspar) as exactly saturated, and an Al+3 concentration, that produced exact microcline saturation was chosen.

Table A.9a. WATCH results for Ohnuma well O-6T. Note that the measured total enthalpy (958 kJ/kg) and the reference temperature (220.3C from quartz solubility) indicate only 0.7% steam in the reservoir. The oxidation potential (0.4 V. calculated from H2S and H2) is relatively oxidizing and the pH is relatively low (5.8). Mineral solubility calculations (using Al⁺⁺⁺ based on assumed microcline saturation) show anhydrite, laumontite, wairakite, albite, analcime goethite, prehnite and zoisite saturation with pyrrhotite, epidote, and K-montmorillonite possibly saturated. Notably calcite and muscovite are not saturated. Calculations using Al based on adularia show most aluminosilicates supersaturated.

Water sample (mg/kg)		Steam sample			
pH/deg.C	5.90/ 20.0	Gas (volume %)		Reference temperature	deg.C : 220.3
CO2	.00	CO2	71.80		
H2S	.00	H2S	4.09	Sampling pressure	bar abs. : 1.0
NH3	.00	NH3	.00	Discharge enthalpy	kJ/kg : 958.
B	374.00	H2	.42	Discharge	kg/s : .0
SiO2	441.00	O2	1.10	Steam fraction at collection	: .2388
Na	374.00	CH4	.00		
K	60.40	N2	.00	Measured temperature	deg.C : .0
Mg	2.900				
Ca	16.00	Liters gas per kg			
F	.000	condensate/deg.C	.50/20.0	Condensate (mg/kg)	
Cl	578.00			pH/deg.C	.00/ .0
SO4	305.00	Total steam (mg/kg)		CO2	.00
Al	.134	CO2	.00	H2S	.00
Fe	4.500	H2S	.00	NH3	.00
TDS	.00	NH3	.00	Na	.00

Ionic strength = .02425

Ionic balance : Cations (mol.eq.) = .01882823 Anions (mol.eq.) = .02248245 Diff (%) = -17.69

Deep water components (mg/kg)		Deep steam (mg/kg)		Gas pressures (bara)	
B	286.70	CO2	51.28	CO2	15136.65
SiO2	338.06	H2S	4.26	H2S	383.68
Na	286.70	NH3	.00	NH3	.00
K	46.30	H2	.00	H2	5.55
Mg	2.223	O2	.16	O2	227.09
Ca	12.27	CH4	.00	CH4	.00
F	.000	N2	.00	N2	.00
Cl	443.08			H2O	.233E+02
SO4	233.81			Total	.235E+02
Al	.1027				
Fe	3.4496				
TDS	.00	Aquifer steam fraction =	.0070		

Ionic strength = .01705

1000/T (Kelvin) = 2.03

Ionic balance : Cations (mol.eq.) = .01359068 Anions (mol.eq.) = .01654254 Diff(%) = -19.59

Oxidation potential (volts): Eh H2S= -.407 Eh CH4= 99.999 Eh H2= -.430 Eh NH3= 99.999

Table A.9a. WATCH results for Ohnuma well O-6T. Note that the measured total enthalpy (958 kJ/kg) and the reference temperature (220.3C from quartz solubility) indicate only 0.7% steam in the reservoir. The oxidation potential (0.4 V. calculated from H₂S and H₂) is relatively oxidizing and the pH is relatively low (5.8). Mineral solubility calculations (using Al⁺⁺⁺ based on assumed microcline saturation) show anhydrite, laumontite, wairakite, albite, analcime goethite, prehnite and zoisite saturation with pyrrhotite, epidote, and K-montmoril-lonite possibly saturated. Notably calcite and muscovite are not saturated. Calculations using Al based on adularia show most aluminosilicates supersaturated (continued).

Chemical geothermometers (degrees C)

Quartz 220.3 (Fournier & Potter, GRC Bulletin, pp. 3-12, Nov. 1982)

Chalcedony 204.3 (Fournier, Geothermics, vol. 5, pp. 41-50, 1977)

Na/K 246.1 (Arnorsson et al., Geochim. Cosmochim. Acta, vol. 47, pp. 567-577, 1983)

Activity coefficients in deep water

H+	.832	KSO ₄ -	.812	Fe ⁺⁺	.445	FeCl ⁺	.802
OH-	.799	F-	.799	Fe ⁺⁺⁺	.195	Al ⁺⁺⁺	.195
H ₃ SiO ₄ -	.802	Cl-	.795	FeOH ⁺	.809	AlOH ⁺⁺	.437
H ₂ SiO ₄ --	.437	Na ⁺	.802	Fe(OH) ₃ -	.809	Al(OH) ₂ ⁺	.812
H ₂ BO ₃ -	.791	K ⁺	.795	Fe(OH) ₄ --	.431	Al(OH) ₄ -	.806
HCO ₃ -	.802	Ca ⁺⁺	.445	Fe(OH) ⁺⁺	.431	AlSO ₄ ⁺	.806
CO ₃ --	.424	Mg ⁺⁺	.471	Fe(OH) ₂ ⁺	.812	Al(SO ₄) ₂ -	.806
HS-	.799	CaHCO ₃ ⁺	.816	Fe(OH) ₄ -	.812	AlF ⁺⁺	.437
S--	.431	MgHCO ₃ ⁺	.802	FeSO ₄ ⁺	.809	AlF ₂ ⁺	.812
HSO ₄ -	.806	CaOH ⁺	.816	FeCl ⁺⁺	.431	AlF ₄ -	.806
SO ₄ --	.417	MgOH ⁺	.819	FeCl ₂ ⁺	.809	AlF ₅ --	.424
NaSO ₄ -	.812	NH ₄ ⁺	.791	FeCl ₄ -	.802	AlF ₆ ---	.145

Chemical species in deep water - ppm and log mole

Deep water pH is 5.859

H+	.00	-5.780	Mg ⁺⁺	.51	-4.675	Fe(OH) ₃	3.92	-4.435
OH-	.11	-5.195	NaCl	5.16	-4.054	Fe(OH) ₄ -	3.01	-4.614
H ₄ SiO ₄	540.08	-2.250	KCl	.38	-5.296	FeCl ⁺	.01	-7.005
H ₃ SiO ₄ -	.60	-5.201	NaSO ₄ -	22.78	-3.718	FeCl ₂	.00	-12.137
H ₂ SiO ₄ --	.00	-10.305	KSO ₄ -	13.79	-3.991	FeCl ⁺⁺	.00	-17.505
NaH ₃ SiO ₄	.09	-6.099	CaSO ₄	22.50	-3.782	FeCl ₂ ⁺	.00	-18.947
H ₃ BO ₃	1638.39	-1.577	MgSO ₄	8.43	-4.155	FeCl ₃	.00	-21.204
H ₂ BO ₃ -	1.41	-4.634	CaCO ₃	.00	-7.888	FeCl ₄ -	.00	-23.829
H ₂ CO ₃	69.15	-2.953	MgCO ₃	.00	-9.816	FeSO ₄	.01	-7.092
HCO ₃ -	2.88	-4.327	CaHCO ₃ ⁺	.32	-5.505	FeSO ₄ ⁺	.00	-16.375
CO ₃ --	.00	-9.079	MgHCO ₃ ⁺	.00	-7.445	Al ⁺⁺⁺	.00	-19.657
H ₂ S	3.98	-3.932	CaOH ⁺	.00	-7.096	AlOH	.00	-13.353
HS-	.27	-5.088	MgOH ⁺	.01	-6.634	Al(OH) ₂ ⁺	.00	-7.829
S--	.00	-14.075	NH ₄ OH	.00	.000	Al(OH) ₃	.30	-5.422
H ₂ SO ₄	.00	-10.924	NH ₄ ⁺	.00	.000	Al(OH) ₄ -	.00	-8.104
HSO ₄ -	7.97	-4.086	Fe ⁺⁺	.01	-6.619	AlSO ₄ ⁺	.00	-18.586
SO ₄ --	175.13	-2.739	Fe ⁺⁺⁺	.00	-20.672	Al(SO ₄) ₂ -	.00	-19.007
HF	.00	.000	FeOH ⁺	.02	-6.577	AlF ⁺⁺	.00	.000
F-	.00	.000	Fe(OH) ₂	.00	-7.622	AlF ₂ ⁺	.00	.000
Cl-	439.77	-1.906	Fe(OH) ₃ -	.00	-9.396	AlF ₃	.00	.000
Na ⁺	280.25	-1.914	Fe(OH) ₄ --	.00	-15.463	AlF ₄ -	.00	.000
K ⁺	42.12	-2.968	Fe(OH) ⁺⁺	.00	-13.359	AlF ₅ --	.00	.000
Ca ⁺⁺	5.51	-3.862	Fe(OH) ₂ ⁺	.00	-7.420	AlF ₆ ---	.00	.000

Table A.9a. WATCH results for Ohnuma well O-6T. Note that the measured total enthalpy (958 kJ/kg) and the reference temperature (220.3C from quartz solubility) indicate only 0.7% steam in the reservoir. The oxidation potential (0.4 V. calculated from H₂S and H₂) is relatively oxidizing and the pH is relatively low (5.8). Mineral solubility calculations (using Al⁺⁺⁺ based on assumed microcline saturation) show anhydrite, laumontite, wairakite, albite, analcime goethite, prehnite and zoisite saturation with pyrrhotite, epidote, and K-montmorillonite possibly saturated. Notably calcite and muscovite are not saturated. Calculations using Al based on adularia show most aluminosilicates supersaturated (continued).

Log solubility products of minerals in deep water (Al based on microcline)

	Theor.	Calc.		Theor	Calc.		Theor.	Calc.
Adularia	-14.569	-15.332	Albite, low	-14.092	-14.274	Analcime	-11.557	-12.023
Anhydrite	-7.566	-7.333	Calcite	-12.019	-13.665	Chalcedony	-2.121	-2.250
Mg-Chlorite	-82.811	-85.128	Fluorite	-10.807	99.999	Goethite	.680	.588
Laumontite	-24.507	-24.241	Microcline	-15.332	-15.332	Magnetite	-19.724	-16.381
Ca-Montmor.	-72.841	-67.393	K-Montmor.	-34.280	-34.657	Mg-Montmor.	-74.319	-68.182
Na-Montmor.	-34.536	-33.600	Muscovite	-17.924	-15.773	Prehnite	-36.489	-36.789
Pyrrhotite	-37.514	-38.153	Pyrite	-62.418	-46.814	Quartz	-2.249	-2.250
Wairakite	-24.095	-24.241	Wollastonite	8.003	5.255	Zoisite	-36.789	-37.010
Epidote	-36.981	-36.202	Marcasite	-44.640	-46.814	Talc	9.765	11.149
Chrysotile	16.301	15.649	Sil. amorph.	-1.740	-2.250			

Table A.9b. WATCH results for Ohnuma well O-10R. The measured enthalpy and quartz temperature indicate 9% reservoir steam. Note that the calculated reservoir gas pressures are much lower than those for well O-6T because there is less gas in the total fluid and more vapor space to put it in. The fluid is more alkaline and more reducing (pH 7.2, Eh 0.62+/-0.4 V.) than well O-6T fluid. Mineral saturation calculations (based on microcline) show that albite, laumontite, wairakite, anhydrite, epidote and muscovite are nearly saturated and calcite and zoisite are somewhat less so. Wolastonite appears possibly saturated but this is a coincidence.

Water sample (mg/kg)		Steam sample		
pH/deg.C	7.20/ 20.0	Gas (volume %)		Reference temperature deg.C : 227.8
CO2	39.00	CO2	37.60	
H2S	.00	H2S	32.30	Sampling pressure bar abs. : 1.0
NH3	.00	NH3	.00	Discharge enthalpy kJ/kg : 1140.
B	202.00	H2	.42	Discharge kg/s : .0
SiO2	506.00	O2	.24	Steam fraction at collection : .3194
Na	418.00	CH4	.18	
K	51.40	N2	28.60	Measured temperature deg.C : .0
Mg	3.100			
Ca	5.20	Liters gas per kg		
F	.000	condensate/deg.C	.25/20.0	Condensate (mg/kg)
Cl	561.00			pH/deg.C .00/ .0
SO4	190.00	Total steam (mg/kg)		CO2 .00
Al	.150	CO2	.00	H2S .00
Fe	.120	H2S	.00	NH3 .00
TDS	2580.00	NH3	.00	Na .00

Ionic strength = .02245

Ionic balance : Cations (mol.eq.) = .01992661 Anions (mol.eq.) = .02065779 Diff (%) = -3.60

Deep water components (mg/kg)				Deep steam (mg/kg)		Gas pressures (bara)	
B	150.71	CO2	5.81	CO2	867.36	CO2	.954E-02
SiO2	377.52	H2S	8.87	H2S	323.99	H2S	.460E-02
Na	311.86	NH3	.00	NH3	.00	NH3	.000E+00
K	38.35	H2	.00	H2	.32	H2	.762E-04
Mg	2.313	O2	.00	O2	2.88	O2	.435E-04
Ca	3.88	CH4	.00	CH4	1.09	CH4	.328E-04
F	.000	N2	.18	N2	300.89	N2	.520E-02
Cl	418.55					H2O	.269E+02
SO4	141.76					Total	.269E+02
Al	.1121						
Fe	.0895						
TDS	1924.88	Aquifer steam fraction =		.0878			

Ionic strength = .01588

1000/T (Kelvin) = 2.00

Ionic balance : Cations (mol.eq.) = .01437116 Anions (mol.eq.) = .01492831 Difference (%) = -3.80

Oxidation potential (volts) : Eh H2S= -.582 Eh CH4= -.621 Eh H2= -.508 Eh NH3= 99.999

Table A.9b. WATCH results for Ohnuma well O-10R. The measured enthalpy and quartz temperature indicate 9% reservoir steam. Note that the calculated reservoir gas pressures are much lower than those for well O-6T because there is less gas in the total fluid and more vapor space to put it in. The fluid is more alkaline and more reducing (pH 7.2, Eh 0.62±0.4 V.) than well O-6T fluid. Mineral saturation calculations (based on microcline) show that albite, laumontite, wairakite, anhydrite, epidote and muscovite are nearly saturated and calcite and zoisite are somewhat less so. Wolastonite appears possibly saturated but this is a coincidence (continued).

Chemical geothermometers (degrees C)

Quartz 227.8 (Fournier & Potter, GRC Bulletin, pp. 3-12, Nov. 1982)

Chalcedony 212.9 (Fournier, Geothermics, vol. 5, pp. 41-50, 1977)

Na/K 218.4 (Amorsson et al., Geochim. Cosmochim. Acta, vol. 47, pp. 567-577, 1983)

Activity coefficients in deep water

H+	.833	KSO4-	.813	Fe++	.446	FeCl+	.803
OH-	.800	F-	.800	Fe+++	.195	Al+++	.195
H3SiO4-	.803	Cl-	.796	FeOH+	.810	AlOH++	.438
H2SiO4--	.438	Na+	.803	Fe(OH)3-	.810	Al(OH)2+	.813
H2BO3-	.792	K+	.796	Fe(OH)4--	.432	Al(OH)4-	.807
HCO3-	.803	Ca++	.446	Fe(OH)++	.432	AlSO4+	.807
CO3--	.425	Mg++	.471	Fe(OH)2+	.813	Al(SO4)2-	.807
HS-	.800	CaHCO3+	.816	Fe(OH)4-	.813	AlF++	.438
S--	.432	MgHCO3+	.803	FeSO4+	.810	AlF2+	.813
HSO4-	.807	CaOH+	.816	FeCl++	.432	AlF4-	.807
SO4--	.418	MgOH+	.819	FeCl2+	.810	AlF5--	.425
NaSO4-	.813	NH4+	.792	FeCl4-	.803	AlF6---	.147

Chemical species in deep water - ppm and log mole

Deep water pH is 7.170

H+	.00	-7.091	Mg++	.63	-4.583	Fe(OH)3	.01	-6.998
OH-	2.38	-3.854	NaCl	5.99	-3.989	Fe(OH)4-	.19	-5.823
H4SiO4	589.75	-2.212	KCl	.35	-5.331	FeCl+	.00	-12.298
H3SiO4-	12.25	-3.890	NaSO4-	17.58	-3.831	FeCl2	.00	-17.107
H2SiO4--	.00	-7.733	KSO4-	8.58	-4.197	FeCl++	.00	-24.322
NaH3SiO4	2.16	-4.737	CaSO4	6.11	-4.348	FeCl2+	.00	-25.776
H3BO3	847.44	-1.863	MgSO4	7.36	-4.214	FeCl3	.00	-28.030
H2BO3-	14.35	-3.627	CaCO3	.01	-6.902	FeCl4-	.00	-30.645
H2CO3	4.70	-4.120	MgCO3	.00	-8.336	FeSO4	.00	-12.563
HCO3-	3.32	-4.264	CaHCO3+	.15	-5.823	FeSO4+	.00	-23.350
CO3--	.00	-7.781	MgHCO3+	.00	-7.249	Al+++	.00	-24.026
H2S	4.01	-3.930	CaOH+	.04	-6.143	AlOH++	.00	-16.207
HS-	4.72	-3.846	MgOH+	.32	-5.107	Al(OH)2+	.00	-9.186
S--	.00	-11.478	NH4OH	.00	.000	Al(OH)3	.31	-5.394
H2SO4	.00	-13.574	NH4+	.00	.000	Al(OH)4-	.01	-6.923
HSO4-	.33	-5.474	Fe++	.00	-11.943	AlSO4+	.00	-23.057
SO4--	110.97	-2.937	Fe+++	.00	-27.638	Al(SO4)2-	.00	-23.628
HF	.00	.000	FeOH+	.00	-10.498	AlF++	.00	.000
F-	.00	.000	Fe(OH)2	.00	-10.117	AlF2+	.00	.000
Cl-	414.76	-1.932	Fe(OH)3-	.00	-10.439	AlF3	.00	.000
Na+	305.70	-1.876	Fe(OH)4--	.00	-15.194	AlF4-	.00	.000
K+	35.69	-3.040	Fe(OH)++	.00	-18.847	AlF5--	.00	.000
Ca++	1.99	-4.305	Fe(OH)2+	.00	-11.410	AlF6---	.00	.000

Table A.9b. WATCH results for Ohnuma well O-10R. The measured enthalpy and quartz temperature indicate 9% reservoir steam. Note that the calculated reservoir gas pressures are much lower than those for well O-6T because there is less gas in the total fluid and more vapor space to put it in. The fluid is more alkaline and more reducing (pH 7.2, Eh 0.62+/-0.4 V.) than well O-6T fluid. Mineral saturation calculations (based on microcline) show that albite, laumontite, wairakite, anhydrite, epidote and muscovite are nearly saturated and calcite and zoisite are somewhat less so. Wolastonite appears possibly saturated but this is a coincidence (continued).

Log solubility products of minerals in deep water (based on microcline)

	Theor.	Calc.		Theor.	Calc.		Theor.	Calc.
Adularia	-14.512	-15.250	Albite, low	-14.044	-14.082	Analcime	-11.538	-11.870
Anhydrite	-7.701	-7.971	Calcite	-12.206	-12.808	Chalcedony	-2.088	-2.212
Mg-Chlorite	-83.290	-73.742	Fluorite	-10.843	99.999	Goethite	1.073	-1.963
Laumontite	-24.502	-24.453	Microcline	-15.250	-15.250	Magnetite	-19.030	-24.120
Ca-Montmor.	-72.737	-82.557	K-Montmor.	-34.179	-42.089	Mg-Montmor.	-74.223	-82.811
Na-Montmor.	-34.442	-40.922	Muscovite	-17.891	-18.297	Prehnite	-36.673	-34.798
Pyrrhotite	-33.390	-55.653	Pyrite	-57.117	-70.060	Quartz	-2.212	-2.212
Wairakite	-24.191	-24.453	Wollastonite	7.867	7.472	Zoisite	-37.055	-36.322
Epidote	-36.996	-36.761	Marcasite	-39.605	-70.060	Talc	9.482	19.442
Chrysotile	15.952	23.866	Sil. amorph.	-1.718	-2.212			

Log solubility products of minerals in deep water (based on adularia)

	Theor.	Calc.		Theor.	Calc.		Theor.	Calc.
Adularia	-14.512	-14.512	Albite, low	-14.044	-13.344	Analcime	-11.538	-11.132
Anhydrite	-7.701	-7.971	Calcite	-12.206	-12.808	Chalcedony	-2.088	-2.212
Mg-Chlorite	-83.290	-72.266	Fluorite	-10.843	99.999	Goethite	1.073	-1.963
Laumontite	-24.502	-22.977	Microcline	-15.250	-14.512	Magnetite	-19.030	-24.120
Ca-Montmor.	-72.737	-72.225	K-Montmor.	-34.179	-36.923	Mg-Montmor.	-74.223	-72.479
Na-Montmor.	-34.442	-35.756	Muscovite	-17.891	-16.083	Prehnite	-36.673	-33.322
Pyrrhotite	-33.390	-55.653	Pyrite	-57.117	-70.060	Quartz	-2.212	-2.212
Wairakite	-24.191	-22.977	Wollastonite	7.867	7.472	Zoisite	-37.055	-34.108
Epidote	-36.996	-35.285	Marcasite	-39.605	-70.060	Talc	9.482	19.442
Chrysotile	15.952	23.866	Sil. amorph.	-1.718	-2.212			

Table A.9c. WATCH results for Sumikawa well S-2 in August 1982. Well S-2 fluid is particularly interesting because it became highly acid when the well was deepened in October 1982. Tables A.2 and A.3 show this change. In August 1982 the pH of separated water was 7.86 and the enthalpy and aquifer steam fraction were very high (2330 kJ/kg and 0.74 respectively). Other than having relatively high SO₄ (SO₄>Cl), Mg and Fe, the analysis is similar to other neutral Sumikawa production fluids. This water is (nearly) saturated with albite, undersaturated with anhydrite, laumontite, wairakite, analcime and muscovite, and supersaturated with calcite, epidote and zoisite.

Water sample (mg/kg)		Steam sample			
pH/deg.C	7.86/ 20.0	Gas (volume %)		Reference temperature	deg.C : 202.7
CO2	243.00	CO2	84.40		
H2S	.00	H2S	6.53	Sampling pressure	bar abs. : 1.0
NH3	.00	NH3	.00	Discharge enthalpy	kJ/kg : 2300.
B	101.00	H2	1.87	Discharge	kg/s : .0
SiO2	488.00	O2	.00	Steam fraction at collection	: .8153
Na	578.00	CH4	.61		
K	69.60	N2	6.33	Measured temperature	deg.C : .0
Mg	5.590				
Ca	9.22	Liters gas per kg			
F	4.000	condensate/deg.C	.57/20.0	Condensate (mg/kg)	
Cl	399.00			pH/deg.C	.00/ .0
SO4	423.00	Total steam (mg/kg)		CO2	.00
Al	.146	CO2	.00	H2S	.00
Fe	14.800	H2S	.00	NH3	.00
TDS	3110.00	NH3	.00	Na	.00
Ionic strength = .03173					
Ionic balance : Cations (mol.eq.) = .02802191 Anions (mol.eq.) = .02578524 Diff(%) = 8.31					
Deep water components (mg/kg)		Deep steam (mg/kg)		Gas pressures (bara)	
B	73.04	CO2	30.19	CO2	1013.38
SiO2	352.89	H2S	7.52	H2S	55.19
Na	417.97	NH3	.00	NH3	.00
K	50.33	H2	.00	H2	.98
Mg	4.042	O2	.00	O2	.00
Ca	6.67	CH4	.00	CH4	2.54
F	2.893	N2	.01	N2	46.00
Cl	288.53			H2O	.164E+02
SO4	305.89			Total	.165E+02
Al	.1053				
Fe	10.7025				
TDS	2248.97	Aquifer steam fraction = .7445			
Ionic strength = .02123 1000/T (Kelvin) = 2.10					
Ionic balance : Cation. (mol.eq.) = .01903740 Anions (mol.eq.) = .01802499 Diff(%) = 5.46					
Oxidation potential (volts) : Eh H2S= -.640 Eh CH4= -.668 Eh H2= -.587 Eh NH3= 99.99					

Table A.9c. WATCH results for Sumikawa well S-2 in August 1982. Well S-2 fluid is particularly interesting because it became highly acid when the well was deepened in October 1982. Tables A.2 and A.3 show this change. In August 1982 the pH of separated water was 7.86 and the enthalpy and aquifer steam fraction were very high (2330 kJ/kg and 0.74 respectively). Other than having relatively high SO₄ (SO₄>Cl), Mg and Fe, the analysis is similar to other neutral Sumikawa production fluids. This water is (nearly) saturated with albite, undersaturated with anhydrite, laumontite, wairakite, analcime and muscovite, and supersaturated with calcite, epidote and zoisite (continued).

Chemical geothermometers (degrees C)

Quartz 203.2 (Fournier & Potter, GRC Bulletin, pp. 3-12, Nov. 1982)

Chalcedony 184.6 (Fournier, Geothermics, vol. 5, pp. 41-50, 1977)

Na/K 214.9 (Arnorsson et al., Geochim. Cosmochim. Acta, vol. 47, pp. 567-577, 1983)

Activity coefficients in deep water

H+	.829	KSO ₄ -	.806	Fe++	.434	FeCl+	.796
OH-	.792	F-	.792	Fe+++	.188	Al+++	.188
H ₃ SiO ₄ -	.796	Cl-	.787	FeOH+	.803	AlOH++	.425
H ₂ SiO ₄ --	.425	Na+	.796	Fe(OH)3-	.803	Al(OH)2+	.806
H ₂ BO ₃ -	.783	K+	.787	Fe(OH)4--	.419	Al(OH)4-	.799
HCO ₃ -	.796	Ca++	.434	Fe(OH)++	.419	AlSO ₄ +	.799
CO ₃ --	.411	Mg++	.462	Fe(OH)2+	.806	Al(SO ₄)2-	.799
HS-	.792	CaHCO ₃ +	.810	Fe(OH)4-	.806	AlF++	.425
S--	.419	MgHCO ₃ +	.796	FeSO ₄ +	.803	AlF2+	.806
HSO ₄ -	.799	CaOH+	.810	FeCl++	.419	AlF4-	.799
SO ₄ --	.403	MgOH+	.814	FeCl2+	.803	AlF5--	.411
NaSO ₄ -	.806	NH ₄ +	.783	FeCl4-	.796	AlF6---	.136

Chemical species in deep water - ppm and log mole

Deep water pH is 8.136

H+	.00	-8.054	Mg++	.73	-4.524	Fe(OH)3	.21	-5.713
OH-	16.93	-3.002	NaCl	3.81	-4.185	Fe(OH)4-	23.49	-3.722
H ₄ SiO ₄	436.10	-2.343	KCl	.19	-5.591	FeCl+	.00	-11.586
H ₃ SiO ₄ -	108.48	-2.943	NaSO ₄ -	35.57	-3.525	FeCl2	.00	-17.763
H ₂ SiO ₄ --	.21	-5.659	KSO ₄ -	15.10	-3.952	FeCl++	.00	-25.098
NaH ₃ SiO ₄	22.79	-3.714	CaSO ₄	9.83	-4.141	FeCl2+	.00	-26.767
H ₃ BO ₃	353.42	-2.243	MgSO ₄	12.51	-3.983	FeCl3	.00	-29.282
H ₂ BO ₃ -	63.29	-2.983	CaCO ₃	1.08	-4.967	FeCl4-	.00	-32.179
H ₂ CO ₃	3.10	-4.301	MgCO ₃	.04	-6.326	FeSO ₄	.00	-11.319
HCO ₃ -	37.10	-3.216	CaHCO ₃ +	1.35	-4.876	FeSO ₄ +	.00	-23.671
CO ₃ --	.18	-5.519	MgHCO ₃ +	.04	-6.284	Al+++	.00	-25.647
H ₂ S	.38	-4.953	CaOH+	.25	-5.357	AlOH++	.00	-17.546
HS-	6.93	-3.679	MgOH+	1.30	-4.503	Al(OH)2+	.00	-10.186
S--	.00	-10.492	NH ₄ OH	.00	.000	Al(OH)3	.16	-5.682
H ₂ SO ₄	.00	-15.733	NH ₄ +	.00	.000	Al(OH)4-	.17	-5.740
HSO ₄ -	.03	-6.495	Fe++	.00	-10.867	AlSO ₄ +	.00	-24.661
SO ₄ --	249.50	-2.585	Fe+++	.00	-27.669	Al(SO ₄)2-	.00	-25.046
HF	.00	-7.168	FeOH+	.00	-8.777	AlF++	.00	-21.095
F-	2.89	-3.818	Fe(OH)2	.00	-7.828	AlF2+	.00	-18.149
Cl-	286.13	-2.093	Fe(OH)3-	.00	-7.664	AlF3	.00	-17.206
Na+	405.17	-1.754	Fe(OH)4--	.00	-11.466	AlF4-	.00	-18.151
K+	45.86	-2.931	Fe(OH)++	.00	-18.473	AlF5--	.00	-20.306
Ca++	2.63	-4.183	Fe(OH)2+	.00	-10.699	AlF6---	.00	-23.783

Table A.9c. WATCH results for Sumikawa well S-2 in August 1982. Well S-2 fluid is particularly interesting because it became highly acid when the well was deepened in October 1982. Tables A.2 and A.3 show this change. In August 1982 the pH of separated water was 7.86 and the enthalpy and aquifer steam fraction were very high (2330 kJ/kg and 0.74 respectively). Other than having relatively high SO₄ (SO₄>Cl), Mg and Fe, the analysis is similar to other neutral Sumikawa production fluids. This water is (nearly) saturated with albite, undersaturated with anhydrite, laumontite, wairakite, analcime and muscovite, and supersaturated with calcite, epidote and zoisite (continued).

Log solubility products of minerals in deep water (Al based on microcline)

	Theor.	Calc.		Theor.	Calc.		Theor.	Calc.
Adularia	-14.743	-15.570	Albite, low	-14.243	-14.389	Analcime	-11.633	-12.046
Anhydrite	-7.254	-7.525	Calcite	-11.590	-10.450	Chalcedony	-2.204	-2.343
Mg-Chlorite	-81.820	-67.168	Fluorite	-10.729	-12.384	Goethite	-.216	-.712
Laumontite	-24.583	-24.930	Microcline	-15.570	-15.570	Magnetite	-21.313	-18.861
Ca-Montmor.	-73.254	-95.939	K-Montmor.	-34.606	-48.731	Mg-Montmor.	-74.710	-96.253
Na-Montmor.	-34.842	-47.550	Muscovite	-18.046	-20.375	Prehnite	-36.139	-33.339
Pyrrhotite	-47.035	-53.500	Pyrite	-74.754	-76.762	Quartz	-2.344	-2.343
Wairakite	-23.922	-24.930	Wollastonite	8.335	9.383	Zoisite	-36.249	-35.742
Epidote	-37.223	-34.052	Marcasite	-56.320	-76.762	Talc	10.450	24.863
Chrysotile	17.150	29.550	Sil. amorph.	-1.795	-2.343			

Table A.9d. WATCH results for Sumikawa well S-2 in November. The fluid chemistry is very different from that collected 3 months earlier. The fluid is now only 2% reservoir steam. Gas in separated steam is about 2 times higher. Surface pH has dropped to 2.0 than in the earlier fluid (-0.44 vs -0.62 V.). In the earlier fluid, Na and K have decreased, but SO₄, Mg and Fe have increased. SO₄ is 308 ppm; B, 101 to 31 ppm; SO₄, 306 to 1310 ppm; Mg, 14 to 225 ppm may result from reaction of steam with rock. Geothermometer temperatures are higher, particularly for Na-K. The fluid is a mixture of neutral, high-Cl water with a minor amount of steam. The changes in fluid chemistry are reflected in the fact that the fluid is now supersaturated and calcite is very undersaturated. Albite and pyrrhotite are near saturation.

Water sample (mg/kg)		Steam sample		
pH/deg.C	2.80/ 20.0	Gas (volume %)		Reference
CO2	.00	CO2	.11.90	
H2S	.00	H2S	1.74	Sampling
NH3	.00	NH3	.00	Discharge
B	31.30	H2	30.70	Discharge
SiO2	528.00	O2	.00	Steam fr.
Na	308.00	CH4	.58	
K	84.00	N2	54.20	Measured
Mg	60.800			
Ca	13.60	Liters gas per kg		
F	.000	condensate/deg.C	.44/20.0	Condens.
Cl	294.00			pH/deg.C
SO4	1310.00	Total steam (mg/kg)		CO2
Al	.130	CO2	.00	H2S
Fe	307.000	H2S	.00	NH3
TDS	3880.00	NH3	.00	Na

Ionic strength = .04628

Ionic balance : Cations (mol.eq.) = .02942291 Anions (mol.eq.) = .02942291

Deep water components (mg/kg)				Deep steam (mg/kg)	
B	22.95	CO2	4.51	CO2	971.2
SiO2	387.15	H2S	1.22	H2S	80.6
Na	225.84	NH3	.00	NH3	.0
K	61.59	H2	.12	H2	132.0
Mg	44.581	O2	.00	O2	.0
Ca	9.97	CH4	.01	CH4	20.0
F	.000	N2	2.55	N2	3252.0
Cl	215.57				
SO4	960.54				
Al	.0951				
Fe	225.1030				
TDS	2844.95	Aquifer steam fraction = .0235			

Ionic strength = .02112

Ionic balance : Cations (mol.eq.) = .01105723 Anions (mol.eq.) = .01105723

Oxidation potential (volts) : Eh H2S= -.325 Eh CH4= -.325

Table A.9d. WATCH results for Sumikawa well S-2 in November 1982 just after deepening. The fluid is very different from that collected 3 months earlier. The enthalpy has dropped to 1060 kJ/kg with only 2% reservoir steam. Gas in separated steam is lower (0.44 vs 0.56) but gas pressures, about 2 times higher. Surface pH has dropped to 2.8 and oxidation potentials are much higher than in the earlier fluid (-0.44 vs -0.62 V.). In the flashed water Cl, Na and B concentrations have decreased, but SO₄, Mg and Fe have increased (changes: Cl, 399 to 294 ppm; Na, 578 to 308 ppm; B, 101 to 31 ppm; SO₄, 306 to 1310 ppm; and Mg, 5 to 60 ppm). The increase in Fe from 14 to 225 ppm may result from reaction of the acid waters with the iron casing. Geothermometer temperatures are higher, particularly Na/K. Apparently the earlier water was a mixture of neutral, high-Cl water with a minor amount of the acid SO₄ water found after deepening. The changes in fluid chemistry are reflected in the mineral saturations. Anhydrite is now supersaturated and calcite is very undersaturated, but (surprisingly) laumontite, wairakite, albite and pyrrhotite are near saturation (continued).

Chemical geothermometers (degrees C)

Quartz	232.1	(Fournier & Potter, GRC Bulletin, pp. 3-12, Nov. 1982)
Chalcedony	217.8	(Fournier, Geothermics, vol. 5, pp. 41-50, 1977)
Na/K	285.7	(Amorsson et al., Geochim. Cosmochim. Acta, vol. 47, pp. 567-577, 1983)

Activity coefficients in deep water

H+	.812	KSO ₄ -	.787	Fe++	.396	FeCl+	.776
OH-	.771	F-	.771	Fe+++	.157	Al+++	.157
H ₃ SiO ₄ -	.776	Cl-	.767	FeOH+	.784	AlOH++	.387
H ₂ SiO ₄ --	.387	Na+	.776	Fe(OH)3-	.784	Al(OH)2+	.787
H ₂ BO ₃ -	.762	K+	.767	Fe(OH)4--	.380	Al(OH)4-	.780
HCO ₃ -	.776	Ca++	.396	Fe(OH)++	.380	AlSO ₄ +	.780
CO ₃ --	.373	Mg++	.425	Fe(OH)2+	.787	Al(SO ₄)2-	.780
HS-	.771	CaHCO ₃ +	.792	Fe(OH)4-	.787	AlF++	.387
S--	.380	MgHCO ₃ +	.776	FeSO ₄ +	.784	AlF ₂ +	.787
HSO ₄ -	.780	CaOH+	.792	FeCl++	.380	AlF ₄ -	.780
SO ₄ --	.364	MgOH+	.796	FeCl ₂ +	.784	AlF ₅ --	.373
NaSO ₄ -	.787	NH ₄ +	.762	FeCl ₄ -	.776	AlF ₆ ---	.109

Table A.9d. WATCH results for Sumikawa well S-2 in November 1982 just after deepening. The fluid is very different from that collected 3 months earlier. The enthalpy has dropped to 1060 kJ/kg with only 2% reservoir steam. Gas in separated steam is lower (0.44 vs 0.56) but gas pressures, about 2 times higher. Surface pH has dropped to 2.8 and oxidation potentials are much higher than in the earlier fluid (-0.44 vs -0.62 V). In the flashed water Cl, Na and B concentrations have decreased, but SO₄, Mg and Fe have increased (changes: Cl, 399 to 294 ppm; Na, 578 to 308 ppm; B, 101 to 31 ppm; SO₄, 306 to 1310 ppm; and Mg, 5 to 60 ppm). The increase in Fe from 14 to 225 ppm may result from reaction of the acid waters with the iron casing. Geothermometer temperatures are higher, particularly Na/K. Apparently the earlier water was a mixture of neutral, high-Cl water with a minor amount of the acid SO₄ water found after deepening. The changes in fluid chemistry are reflected in the mineral saturations. Anhydrite is now supersaturated and calcite is very undersaturated, but (surprisingly) laumontite, wairakite, albite and pyrrhotite are near saturation (continued).

Chemical species in deep water - ppm and log mole

Deep water pH is 5.154

H+	.01	-5.064	Mg++	4.26	-3.756	Fe(OH)3	361.51	-2.471
OH-	.03	-5.825	NaCl	2.33	-4.399	Fe(OH)4-	69.19	-3.253
H4SiO4	619.15	-2.191	KCl	.25	-5.469	FeCl+	.66	-5.142
H3SiO4-	.12	-5.915	NaSO4-	55.25	-3.333	FeCl2	.00	-9.908
H2SiO4--	.00	-11.791	KSO4-	52.20	-3.413	FeCl++	.00	-14.314
NaH3SiO4	.01	-6.933	CaSO4	26.91	-3.704	FeCl2+	.00	-16.099
H3BO3	131.25	-2.673	MgSO4	199.55	-2.780	FeCl3	.00	-18.643
H2BO3-	.02	-6.456	CaCO3	.00	-10.873	FeCl4-	.00	-21.509
H2CO3	6.32	-3.992	MgCO3	.00	-11.531	FeSO4	4.59	-4.520
HCO3-	.04	-6.224	CaHCO3+	.00	-7.758	FeSO4+	.00	-12.461
CO3--	.00	-11.797	MgHCO3+	.00	-8.383	Al+++	.00	-18.448
H2S	1.20	-4.452	CaOH+	.00	-8.097	AlOH++	.00	-12.465
HS-	.01	-6.448	MgOH+	.03	-6.192	Al(OH)2+	.00	-7.300
S--	.00	-16.009	NH4OH	.00	.000	Al(OH)3	.27	-5.459
H2SO4	.00	-8.759	NH4+	.00	.000	Al(OH)4-	.00	-9.165
HSO4-	188.35	-2.712	Fe++	1.75	-4.504	AlSO4+	.00	-16.853
SO4--	511.33	-2.274	Fe+++	.00	-17.476	Al(SO4)2-	.00	-16.770
HF	.00	.000	FeOH+	.70	-5.018	AlF++	.00	.000
F-	.00	.000	Fe(OH)2	.03	-6.546	AlF2+	.00	.000
Cl-	213.78	-2.220	Fe(OH)3-	.00	-8.720	AlF3	.00	.000
Na+	214.25	-2.031	Fe(OH)4--	.00	-15.451	AlF4-	.00	.000
K+	46.36	-2.926	Fe(OH)++	.00	-10.557	AlF5--	.00	.000
Ca++	2.05	-4.292	Fe(OH)2+	.95	-4.977	AlF6---	.00	.000

Log solubility products of minerals in deep water (Al based on microcline)

	Theor.	Calc.		Theor.	Calc.		Theor.	Calc.
Adularia	-14.463	-15.175	Albite, low	-14.003	-14.275	Analcime	-11.527	-12.084
Anhydrite	-7.848	-7.406	Calcite	-12.410	-16.920	Chalcedony	-2.053	-2.191
Mg-Chlorite	-83.841	-85.833	Fluorite	-10.884	99.999	Goethite	1.505	2.581
Laumontite	-24.513	-24.579	Microcline	-15.175	-15.175	Magnetite	-18.273	-11.620
Ca-Montmor.	-72.663	-59.497	K-Montmor.	-34.091	-30.443	Mg-Montmor.	-74.155	-58.931
Na-Montmor.	-34.360	-29.543	Muscovite	-17.866	-14.422	Prehnite	-36.891	-38.957
Pyrrhotite	-28.918	-28.586	Pyrite	-51.391	-36.973	Quartz	-2.174	-2.191
Wairakite	-24.309	-24.579	Wollastonite	7.725	3.423	Zoisite	-37.364	-38.581
Epidote	-37.096	36.377	Marcasite	-34.159	-36.973	Talc	9.185	9.777
Chrysotile	15.585	14.159	Sil. amorph.	-1.695	-2.191			

Table A.9e. WATCH results for Sumikawa well S-3 83/07/28. S-3 water is relatively dilute and contains high $\text{HCO}_3+\text{SO}_4/\text{Cl}$ and $\text{Ca}+\text{Mg}/\text{Na}+\text{K}$ and is somewhat oxidizing (Eh 0.63 V.) compared to higher temperature Sumikawa waters suggesting that it is mixed with surface water. Saturation calculations show that it is saturated with albite, wairakite and calcite and fairly close to saturation with anhydrite, laumontite, analcite and muscovite. The proportion of $\text{HCO}_3+\text{SO}_4/\text{Cl}$ in S-3 waters has varied widely (Figure 3.37) and the low Cl waters may show near saturation with montmorillonite clays.

Water sample (mg/kg)		Steam sample					
pH/deg.C	8.51/ 20.0	Gas (volume %)		Reference temperature	deg.C : 226.6		
CO2	.00	CO2	77.60				
H2S	.00	H2S	14.00	Sampling pressure	bar abs. : 1.0		
NH3	.00	NH3	.00	Discharge enthalpy	kJ/kg : 1080.		
B	55.00	H2	2.33	Discharge	kg/s : .0		
SiO2	485.00	O2	.00	Steam fraction at collection	: .2610		
Na	162.00	CH4	.39				
K	28.00	N2	5.43	Measured temperature	deg.C : .0		
Mg	3.400						
Ca	4.81	Liters gas per kg					
F	.000	condensate/deg.C	.16/20.0	Condensate (mg/kg)			
Cl	124.00			pH/deg.C	.00/ .0		
SO4	87.90	Total steam (mg/kg)		CO2	.00		
Al	.208	CO2	.00	H2S	.00		
Fe	.090	H2S	.00	NH3	.00		
TDS	1310.00	NH3	.00	Na	.00		
Ionic strength = .00841							
Ionic balance : Cations (mol.eq.) = .00822505 Anions (mol.eq.) = .00632439 Diff(%) = 26.13							
Deep water components (mg/kg)		Deep steam (mg/kg)		Gas pressures (bara)			
B	43.14	CO2	8.18	CO2	891.92	CO2	.959E-02
SiO2	380.42	H2S	3.47	H2S	86.69	H2S	.120E-02
Na	127.07	NH3	.00	NH3	.00	NH3	.000E+00
K	21.96	H2	.00	H2	1.40	H2	.327E-03
Mg	2.667	O2	.00	O2	.00	O2	.807E-36
Ca	3.77	CH4	.00	CH4	1.86	CH4	.550E-04
F	.000	N2	.03	N2	45.22	N2	.764E-03
Cl	97.26					H2O	.263E+02
SO4	68.95					Total	.263E+02
Al	.1635						
Fe	.0706						
TDS	1027.54	Aquifer steam fraction = .0578					
Ionic strength = .00609				1000/T (Kelvin) = 2.00			
Ionic balance : Cations (mol.eq.) = .00618563				Anions (mol.eq.) = .00471571 Diff(%) = 26.97			
Oxidation potential (volts) : Eh H2S= -.613 Eh CH4= -.652 Eh H2= -.568 Eh NH3= 99.999							

Table A.9e. WATCH results for Sumikawa well S-3 83/07/28. S-3 water is relatively dilute and contains high $\text{HCO}_3+\text{SO}_4/\text{Cl}$ and $\text{Ca}+\text{Mg}/\text{Na}+\text{K}$ and is somewhat oxidizing (Eh 0.63 V.) compared to higher temperature Sumikawa waters suggesting that it is mixed with surface water. Saturation calculations show that it is saturated with albite, wairakite and calcite and fairly close to saturation with anhydrite, laumontite, analcite and muscovite. The proportion of $\text{HCO}_3+\text{SO}_4/\text{Cl}$ in S-3 waters has varied widely (Figure 3.37) and the low Cl waters may show near saturation with montmorillonite clays (continued).

Chemical geothermometers (degrees C)

Quartz	226.9	(Fournier & Potter, GRC Bulletin, pp. 3-12, Nov. 1982)
Chalcedony	211.8	(Fournier, Geothermics, vol. 5, pp. 41-50, 1977)
Na/K	258.4	(Arnorsson et al., Geochim. Cosmochim. Acta, vol. 47, pp. 567-577, 1983)

Activity coefficients in deep water

H+	.881	KSO4-	.871	Fe++	.581	FeCl+	.867
OH-	.865	F-	.865	Fe+++	.321	Al+++	.321
H3SiO4-	.867	Cl-	.863	FeOH+	.870	AlOH++	.576
H2SiO4--	.576	Na+	.867	Fe(OH)3-	.870	Al(OH)2+	.871
H2BO3-	.862	K+	.863	Fe(OH)4--	.573	Al(OH)4-	.868
HCO3-	.867	Ca++	.581	Fe(OH)++	.573	AlSO4+	.868
CO3--	.569	Mg++	.596	Fe(OH)2+	.871	Al(SO4)2-	.868
HS-	.865	CaHCO3+	.873	Fe(OH)4-	.871	AlF++	.576
S--	.573	MgHCO3+	.867	FeSO4+	.870	AlF2+	.871
HSO4-	.868	CaOH+	.873	FeCl++	.573	AlF4-	.868
SO4--	.565	MgOH+	.874	FeCl2+	.870	AlF5--	.569
NaSO4-	.871	NH4+	.862	FeCl4-	.867	AlF6---	.281

Chemical species in deep water - ppm and log mole

Deep water pH is 7.476

H+	.00	-7.421	Mg++	.74	-4.515	Fe(OH)3	.00	-7.357
OH-	4.40	-3.587	NaCl	.66	-4.948	Fe(OH)4-	.15	-5.914
H4SiO4	583.66	-2.217	KCl	.05	-6.133	FeCl+	.00	-13.801
H3SiO4-	23.05	-3.616	NaSO4-	4.66	-4.408	FeCl2	.00	-19.229
H2SiO4--	.01	-7.231	KSO4-	3.25	-4.619	FeCl++	.00	-26.270
NaH3SiO4	1.93	-4.786	CaSO4	5.13	-4.424	FeCl2+	.00	-28.230
H3BO3	239.05	-2.413	MgSO4	6.99	-4.236	FeCl3	.00	-31.055
H2BO3-	7.57	-3.905	CaCO3	.07	-6.165	FeCl4-	.00	-34.305
H2CO3	4.71	-4.120	MgCO3	.00	-7.544	FeSO4	.00	-13.622
HCO3-	6.42	-3.978	CaHCO3+	.38	-5.422	FeSO4+	.00	-24.797
CO3--	.00	-7.271	MgHCO3+	.01	-6.799	Al+++	.00	-24.933
H2S	1.04	-4.514	CaOH+	.10	-5.759	AlOH++	.00	-16.744
HS-	2.36	-4.147	MgOH+	.86	-4.679	Al(OH)2+	.00	-9.358
S--	.00	-11.569	NH4OH	.00	.000	Al(OH)3	.45	-5.242
H2SO4	.00	-14.398	NH4+	.00	.000	Al(OH)4-	.03	-6.472
HSO4-	.09	-6.017	Fe++	.00	-12.922	AlSO4+	.00	-23.980
SO4--	53.60	-3.253	Fe+++	.00	-29.055	Al(SO4)2-	.00	-24.745
HF	.00	.000	FeOH+	.00	-11.102	AlF++	.00	.000
F-	.00	.000	Fe(OH)2	.00	-10.404	AlF2+	.00	.000
Cl-	96.84	-2.564	Fe(OH)3--	.00	-10.473	AlF3	.00	.000
Na+	125.53	-2.263	Fe(OH)4--	.00	-15.014	AlF4-	.00	.000
K+	20.99	-3.270	Fe(OH)++	.00	-19.891	AlF5--	.00	.000
Ca++	2.01	-4.299	Fe(OH)2+	.00	-12.086	AlF6---	.00	.000

Table A.9e. WATCH results for Sumikawa well S-3 83/07/28. S-3 water is relatively dilute and contains high $\text{HCO}_3\text{+SO}_4/\text{Cl}$ and Ca+Mg/Na+K and is somewhat oxidizing (Eh 0.63 V.) compared to higher temperature Sumikawa waters suggesting that it is mixed with surface water. Saturation calculations show that it is saturated with albite, wairakite and calcite and fairly close to saturation with anhydrite, laumontite, analcite and muscovite. The proportion of $\text{HCO}_3\text{+SO}_4/\text{Cl}$ in S-3 waters has varied widely (Figure 3.37) and the low Cl waters may show near saturation with montmorillonite clays (continued).

Log solubility products of minerals in deep water (Al based on microcline)

	Theor.	Calc.		Theor.	Calc.		Theor.	Calc.
Adularia	-14.521	-15.263	Albite, low	-14.051	-14.254	Analcite	-11.541	-12.037
Anhydrite	-7.679	-8.036	Calcite	-12.176	-12.050	Chalcedony	-2.093	-2.217
Mg-Chlorite	-83.211	-70.106	Fluorite	-10.838	99.999	Goethite	1.010	-2.324
Laumontite	-24.502	-23.959	Microcline	-15.263	-15.263	Magnetite	-19.142	-25.106
Ca-Montmor.	-72.752	-83.407	K-Montmor.	-34.194	-42.770	Mg-Montmor.	-74.236	-83.612
Na-Montmor.	-34.456	-41.761	Muscovite	-17.895	-18.521	Prehnite	-36.642	-33.577
Pyrrhotite	-34.056	-63.018	Pyrite	-57.971	-82.507	Quartz	-2.218	-2.217
Wairakite	-24.175	-23.959	Wollastonite	7.889	8.200	Zoisite	-37.011	-35.206
Epidote	-36.988	-35.901	Marcasite	-40.417	-82.507	Talc	9.527	21.768
Chrysotile	16.008	26.202	Sil. amorph.	-1.722	-2.217			

Table A.9f. WATCH results for Sumikawa well S-4 85/09/17. S-4 fluid is typical of the high-temperature Sumikawa reservoir with compositions spanning those of wells SA-1, SA-2, SB-1, SC-1 and SM-2, in addition to some Ohnuma wells. The neutral pH, high SiO₂, low Mg and low Eh are also typical of high-temperature geothermal waters worldwide. Anhydrite, laumontite, wairakite, albite, analcite and calcite are saturated (all but wairakite and analcite within 0.2 log units) in addition to quartz and microcline which are assumed saturated.

Water sample (mg/kg)		Steam sample					
pH/deg.C	7.60/ 20.0	Gas (volume %)		Reference temperature	deg.C : 277.0		
CO2	59.00	CO2	60.40				
H2S	.00	H2S	14.80	Sampling pressure	bar abs. : 1.0		
NH3	.00	NH3	.00	Discharge enthalpy	kJ/kg : 1700.		
B	130.00	H2	.82	Discharge	kg/s : .0		
SiO2	911.00	O2	4.80	Steam fraction at collection	: .5427		
Na	240.00	CH4	.05				
K	51.40	N2	18.70	Measured temperature	deg.C : .0		
Mg	.020						
Ca	2.25	Liters gas per kg					
F	.000	condensate/deg.C	.25/20.0	Condensate (mg/kg)			
Cl	293.00			pH/deg.C	.00/ .0		
SO4	112.00	Total steam (mg/kg)		CO2	.00		
Al	.091	CO2	.00	H2S	.00		
Fe	.020	H2S	.00	NH3	.00		
TDS	2160.00	NH3		Na	.00		
Ionic strength = .01320							
Ionic balance : Cations (mol.eq.) = .01183549 Anions (mol.eq.) = .01216855 Diff(%) = -2.78							
Deep water components (mg/kg)		Deep steam (mg/kg)		Gas pressures (bara)			
B	85.72	CO2	9.60	CO2	555.35	CO2	.139E-01
SiO2	600.71	H2S	5.60	H2S	80.18	H2S	.260E-02
Na	158.26	NH3	.00	NH3	.00	NH3	.000E+00
K	33.89	H2	.00	H2	.30	H2	.166E-03
Mg	.013	O2	.10	O2	28.05	O2	.969E-03
Ca	1.48	CH4	.00	CH4	.15	CH4	.101E-04
F	.000	N2	.25	N2	95.84	N2	.378E-02
Cl	193.20					H2O	.613E+02
SO4	73.85					Total	.614E+02
Al	.0597						
Fe	.0132						
TDS	1424.30	Aquifer steam fraction = .3064					
Ionic strength = .00819						1000/T (Kelvin) = 1.82	
Ionic balance : Cations (mol.eq.) = .00749690						Anions (mol.eq.) = .00771754	
						Diff(%) = -2.90	
Oxidation potential (volts) : Eh H2S= -.711 Eh CH4= -.748 Eh H2= -.619 Eh NH3= 99.99							

Table A.9f. WATCH results for Sumikawa well S-4 85/09/17. S-4 fluid is typical of the high-temperature Sumikawa reservoir with compositions spanning those of wells SA-1, SA-2, SB-1, SC-1 and SM-2, in addition to some Ohnuma wells. The neutral pH, high SiO₂, low Mg and low Eh are also typical of high-temperature geothermal waters worldwide. Anhydrite, laumontite, wairakite, albite, analcite and calcite are saturated (all but wairakite and analcite within 0.2 log units) in addition to quartz and microcline which are assumed saturated (continued).

Chemical geothermometers (degrees C)

Quartz	277.7	(Fournier & Potter, GRC Bulletin, pp. 3-12, Nov. 1982)
Chalcedony	263.7	(Fournier, Geothermics, vol. 5, pp. 41-50, 1977)
Na/K	275.5	(Armorsson et al., Geochim. Cosmochim. Acta, vol. 47, pp. 567-577, 1983)

Activity coefficients in deep water

H+	.840	KSO4-	.825	Fe++	.469	FeCl+	.818
OH-	.815	F-	.815	Fe+++	.208	Al+++	.208
H3SiO4-	.818	Cl-	.813	FeOH+	.823	AlOH++	.463
H2SiO4--	.463	Na+	.818	Fe(OH)3-	.823	Al(OH)2+	.825
H2BO3-	.810	K+	.813	Fe(OH)4--	.458	Al(OH)4-	.820
HCO3-	.818	Ca++	.469	Fe(OH)++	.458	AlSO4+	.820
CO3--	.453	Mg++	.489	Fe(OH)2+	.825	Al(SO4)2-	.820
HS-	.815	CaHCO3+	.827	Fe(OH)4-	.825	AlF++	.463
S--	.458	MgHCO3+	.818	FeSO4+	.823	AlF2+	.825
HSO4-	.820	CaOH+	.827	FeCl++	.458	AlF4-	.820
SO4--	.447	MgOH+	.830	FeCl2+	.823	AlF5--	.453
NaSO4-	.825	NH4+	.810	FeCl4-	.818	AlF6---	.168

Chemical species in deep water - ppm and log mole

Deep water pH is 7.562

H+	.00	-7.486	Mg++	.00	-7.204	Fe(OH)3	.00	-8.430
OH-	7.36	-3.364	NaCl	5.05	-4.063	Fe(OH)4-	.03	-6.634
H4SiO4	937.12	-2.011	KCl	.42	-5.253	FeCl+	.00	-17.616
H3SiO4-	21.55	-3.645	NaSO4-	9.62	-4.092	FeCl2	.00	-20.699
H2SiO4--	.00	-7.503	KSO4-	12.14	-4.047	FeCl++	.00	-29.181
NaH3SiO4	2.45	-4.682	CaSO4	2.82	-4.684	FeCl2+	.00	-30.859
H3BO3	475.75	-2.114	MgSO4	.02	-6.822	FeCl3	.00	-33.262
H2BO3-	14.32	-3.628	CaCO3	.03	-6.592	FeCl4-	.00	-35.992
H2CO3	9.11	-3.833	MgCO3	.00	-10.358	FeSO4	.00	-17.809
HCO3-	4.25	-4.158	CaHCO3+	.13	-5.882	FeSO4+	.00	-28.031
CO3--	.00	-7.842	MgHCO3+	.00	-9.466	Al+++	.00	-28.515
H2S	3.07	-4.046	CaOH+	.08	-5.833	AlOH++	.00	-18.950
HS-	2.46	-4.129	MgOH+	.01	-6.483	Al(OH)2+	.00	-10.307
S--	.00	-11.122	NH4OH	.00	.000	Al(OH)3	.17	-5.657
H2SO4	.00	-13.555	NH4+	.00	.000	Al(OH)4-	.00	-7.981
HSO4-	.42	-5.361	Fe++	.00	-17.274	AlSO4+	.00	-27.144
SO4--	55.04	-3.242	Fe+++	.00	-33.357	Al(SO4)2-	.00	-27.666
HF	.00	.000	FeOH+	.00	-14.904	AlF++	.00	.000
F-	.00	.000	Fe(OH)2	.00	-13.431	AlF2+	.00	.000
Cl-	189.94	-2.271	Fe(OH)3-	.00	-12.509	AlF3	.00	.000
Na+	153.93	-2.174	Fe(OH)4--	.00	-16.983	AlF4-	.00	.000
K+	30.16	-3.113	Fe(OH)++	.00	-23.045	AlF5--	.00	.000
Ca++	.53	-4.876	Fe(OH)2+	.00	-13.976	AlF6---	.00	.000

Table A.9f. WATCH results for Sumikawa well S-4 85/09/17. S-4 fluid is typical of the high-temperature Sumikawa reservoir with compositions spanning those of wells SA-1, SA-2, SB-1, SC-1 and SM-2, in addition to some Ohnuma wells. The neutral pH, high SiO₂, low Mg and low Eh are also typical of high-temperature geothermal waters worldwide. Anhydrite, laumontite, wairakite, albite, analcite and calcite are saturated (all but wairakite and analcite within 0.2 log units) in addition to quartz and microcline which are assumed saturated (continued).

Log solubility products of minerals in deep water (Al based on microcline)

	Theor.	Calc.		Theor.	Calc.		Theor.	Calc.
Adularia	-14.374	-14.977	Albite, low	-13.947	-14.036	Analcite	-11.599	-12.024
Anhydrite	-8.611	-8.797	Calcite	-13.481	-13.391	Chalcedony	-1.891	-2.011
Mg-Chlorite	-87.175	-82.710	Fluorite	-11.109	99.999	Goethite	3.805	-3.265
Laumontite	-24.818	-24.731	Microcline	-14.977	-14.977	Magnetite	-14.275	-31.038
Ca-Montmor.	-72.576	-88.388	K-Montmor.	-33.813	-44.794	Mg-Montmor.	-74.083	-90.697
Na-Montmor.	-34.097	-43.853	Muscovite	-17.841	-19.553	Prehnite	-38.313	-34.831
Pyrrhotite	-5.596	-65.844	Pyrite	-21.879	-83.490	Quartz	-2.012	-2.011
Wairakite	-25.119	-24.731	Wollastonite	7.047	7.907	Zoisite	-39.262	-37.119
Epidote	-39.108	-38.096	Marcasite	-5.949	-83.490	Talc	7.748	14.782
Chrysotile	13.823	18.804	Sil. amorph.	-1.588	-2.011			

Table A.9g. WATCH results for Sumikawa well SA-1 89/06/21. SA-1 is a high-enthalpy well with an aquifer steam fraction of 0.63, and slightly lower values of pH (6.8) and Eh (0.67V). It has a high reservoir temperature, high Cl relative to SO₄ and HCO₃ and high B. This chemistry suggests both sedimentary (high B) and magmatic influence. Reservoir gas pressures are similar to those calculated for lower-enthalpy discharge fluids with higher gas concentrations. Although gas concentrations vary, gas pressures are constant in a reservoir at equilibrium. This water is in equilibrium with albite, slightly supersaturated with anhydrite and undersaturated with calcite.

Water sample (mg/kg)		Steam sample					
pH/deg.C	6.80/ 20.0	Gas (volume %)		Reference temperature	deg.C : 295.0		
CO2	25.00	CO2	28.20				
H2S	.00	H2S	51.50	Sampling pressure	bar abs. : 1.0		
NH3	.00	NH3	.00	Discharge enthalpy	kJ/kg : 2220.		
B	316.00	H2	3.57	Discharge	kg/s : .0		
SiO2	1100.00	O2	.80	Steam fraction at collection	: .7789		
Na	347.00	CH4	.09				
K	76.00	N2	5.86	Measured temperature	deg.C : .0		
Mg	.050						
Ca	15.30	Liters gas per kg					
F	.000	condensate/deg.C	.25/20.0	Condensate (mg/kg)			
Cl	554.00			pH/deg.C	.00/ .0		
SO4	121.00	Total steam (mg/kg)		CO2	.00		
Al	.063	CO2	.00	H2S	.00		
Fe	.200	H2S	.00	NH3	.00		
TDS	3840.00	NH3	.00	Na	.00		
Ionic strength = .01977							
Ionic balance : Cations (mol.eq.) = .01774763 Anions (mol.eq.) = .01862048 Diff(%) = -4.80							
Deep water components (mg/kg)		Deep steam (mg/kg)		Gas pressures (bara)			
B	186.67	CO2	3.17	CO2	167.47	CO2	.549E-02
SiO2	649.81	H2S	14.19	H2S	218.58	H2S	.925E-02
Na	204.99	NH3	.00	NH3	.00	NH3	.000E+00
K	44.90	H2	.00	H2	.93	H2	.664E-03
Mg	.030	O2	.02	O2	3.30	O2	.149E-03
Ca	9.04	CH4	.00	CH4	.19	CH4	.168E-04
F	.000	N2	.09	N2	21.18	N2	.109E-02
Cl	327.27					H2O	.800E+02
SO4	71.48					Total	.801E+02
Al	.0371						
Fe	.1181						
TDS	2268.44	Aquifer steam fraction = .6258					
Ionic strength = .01049						1000/T (Kelvin) = 1.76	
Ionic balance : Cations (mol.eq.) = .00971880						Anions (mol.eq.) = .01024452	
						Diff(%) = -5.27	
Oxidation potential (volts) : Eh H2S= -.666 Eh CH4= -.725 Eh H2= -.606 Eh NH3= 99.999							

Table A.9g. WATCH results for Sumikawa well SA-1 89/06/21. SA-1 is a high-enthalpy well with an aquifer steam fraction of 0.63, and slightly lower values of pH (6.8) and Eh (0.67V.). It has a high reservoir temperature, high Cl relative to SO₄ and HCO₃ and high B. This chemistry suggests both sedimentary (high B) and magmatic influence. Reservoir gas pressures are similar to those calculated for lower-enthalpy discharge fluids with higher gas concentrations. Although gas concentrations vary, gas pressures are constant in a reservoir at equilibrium. This water is in equilibrium with albite, slightly supersaturated with anhydrite and undersaturated with calcite (continued).

Chemical geothermometers (degrees C)

Quartz	293.0	(Fournier & Potter, GRC Bulletin, pp. 3-12, Nov. 1982)
Chalcedony	276.0	(Fournier, Geothermics, vol. 5, pp. 41-50, 1977)
Na/K	278.4	(Amorsson et al., Geochim. Cosmochim. Acta, vol. 47, pp. 567-577, 1983)

Activity coefficients in deep water

H+	.810	KSO4-	.789	Fe++	.396	FeCl+	.780
OH-	.777	F-	.777	Fe+++	.150	Al+++	.150
H3SiO4-	.780	Cl-	.773	FeOH+	.787	AlOH++	.388
H2SiO4--	.388	Na+	.780	Fe(OH)3-	.787	Al(OH)2+	.789
H2BO3-	.770	K+	.773	Fe(OH)4--	.383	Al(OH)4-	.784
HCO3-	.780	Ca++	.396	Fe(OH)++	.383	AlSO4+	.784
CO3--	.377	Mg++	.419	Fe(OH)2+	.789	Al(SO4)2-	.784
HS-	.777	CaHCO3+	.793	Fe(OH)4-	.789	AlF++	.388
S--	.383	MgHCO3+	.780	FeSO4+	.787	AlF2+	.789
HSO4-	.784	CaOH+	.793	FeCl++	.383	AlF4-	.784
SO4--	.371	MgOH+	.796	FeCl2+	.787	AlF5--	.377
NaSO4-	.789	NH4+	.770	FeCl4-	.780	AlF6---	.112

Chemical species in deep water - ppm and log mole

Deep water pH is 6.965

H+	.00	-6.874	Mg++	.01	-6.607	Fe(OH)3	.01	-6.970
OH-	1.90	-3.952	NaCl	19.39	-3.479	Fe(OH)4-	.25	-5.697
H4SiO4	1034.54	-1.968	KCl	1.37	-4.736	FeCl+	.00	-15.872
H3SiO4-	4.34	-4.340	NaSO4-	9.36	-4.105	FeCl2	.00	-18.110
H2SiO4--	.00	-8.908	KSO4-	16.33	-3.918	FeCl++	.00	-26.297
NaH3SiO4	.63	-5.276	CaSO4	16.26	-3.923	FeCl2+	.00	-27.801
H3BO3	1060.11	-1.766	MgSO4	.04	-6.436	FeCl3	.00	-29.962
H2BO3-	7.49	-3.910	CaCO3	.00	-7.412	FeCl4-	.00	-32.394
H2CO3	4.11	-4.179	MgCO3	.00	-11.565	FeSO4	.00	-16.489
HCO3-	.30	-5.302	CaHCO3+	.08	-6.086	FeSO4+	.00	-25.588
CO3--	.00	-9.741	MgHCO3+	.00	-9.972	Al+++	.00	-27.853
H2S	12.59	-3.432	CaOH+	.19	-5.469	AlOH++	.00	-18.466
HS-	1.55	-4.329	MgOH+	.02	-6.221	Al(OH)2+	.00	-10.042
S--	.00	-11.777	NH4OH	.00	.000	Al(OH)3	.11	-5.862
H2SO4	.00	-12.209	NH4+	.00	.000	Al(OH)4-	.00	-9.269
HSO4-	2.00	-4.686	Fe++	.00	-15.782	AlSO4+	.00	-26.581
SO4--	38.84	-3.393	Fe+++	.00	-31.059	Al(SO4)2-	.00	-27.207
HF	.00	.000	FeOH+	.00	-13.917	AlF++	.00	.000
F-	.00	.000	Fe(OH)2	.00	-12.841	AlF2+	.00	.000
Cl-	314.86	-2.052	Fe(OH)3-	.00	-12.220	AlF3	.00	.000
Na+	195.43	-2.071	Fe(OH)4--	.00	-17.322	AlF4-	.00	.000
K+	39.45	-2.996	Fe(OH)++	.00	-21.002	AlF5--	.00	.000
Ca++	4.08	-3.992	Fe(OH)2+	.00	-12.149	AlF6---	.00	.000

Table A.9g. WATCH results for Sumikawa well SA-1 89/06/21. SA-1 is a high-enthalpy well with an aquifer steam fraction of 0.63, and slightly lower values of pH (6.8) and Eh (0.67V.). It has a high reservoir temperature, high Cl relative to SO₄ and HCO₃ and high B. This chemistry suggests both sedimentary (high B) and magmatic influence. Reservoir gas pressures are similar to those calculated for lower-enthalpy discharge fluids with higher gas concentrations. Although gas concentrations vary, gas pressures are constant in a reservoir at equilibrium. This water is in equilibrium with albite, slightly supersaturated with anhydrite and undersaturated with calcite (continued).

Log solubility products of minerals in deep water (Al based on microcline)

	Theor.	Calc.		Theor.	Calc.		Theor.	Calc.
Adularia	-14.413	-14.979	Albite, low	-13.995	-14.050	Analcime	-11.693	-12.082
Anhydrite	-8.953	-8.219	Calcite	-13.966	-14.560	Chalcedony	-1.828	-1.968
Mg-Chlorite	-88.897	-85.261	Fluorite	-11.216	99.999	Goethite	4.868	-1.738
Laumontite	-25.070	-24.202	Microcline	-14.979	-14.979	Magnetite	-12.446	-27.784
Ca-Montmor.	-72.527	-82.496	K-Montmor.	-33.697	-42.158	Mg-Montmor.	-74.031	-85.087
Na-Montmor.	-33.980	-41.229	Muscovite	-17.849	-18.791	Prehnite	-39.084	-34.753
Pyrrhotite	4.936	-49.096	Pyrite	-8.697	-61.091	Quartz	-1.960	-1.968
Wairakite	-25.574	-24.202	Wollastonite	6.770	7.568	Zoisite	-40.251	-36.658
Epidote	-40.858	-36.491	Marcasite	6.715	-61.091	Talc	7.145	12.963
Chrysotile	13.090	16.899	Sil. amorph.	-1.545	-1.968			

Table A.9h. WATCH results for Sumikawa well SA-2 89/07/03. SA-2 is the well closest to Mt. Yake and shows magmatic influence. As with S-2, this well evolved from slightly alkaline (pH 8) to distinctly acid (pH 3.3) during a year of sampling. The sample chosen is early (pH 6.1) in this progression. Chloride in SA-2 discharge (and in the reservoir) is high and variable with almost no dissolved CO₂. The very low B/Cl and very high Cl/SO₄ ratios and the Ar-N₂-He gas concentration pattern also suggest strongly that this well fluid contains significant magmatic fluid. As for S-2, the water is supersaturated with anhydrite, undersaturated with calcite and approximately saturated with laumontite, wairakite, albite and muscovite.

Water sample (mg/kg)		Steam sample			
pH/deg.C	6.10/ 20.0	Gas (volume %)		Reference temperature	deg.C : 244.6
CO ₂	12.00	CO ₂			
		NH ₃	.00	Discharge enthalpy	kJ/kg : 2200.
B	81.00	H ₂	1.36	Discharge	kg/s : .0
SiO ₂	669.00	O ₂	.74	Steam fraction at collection	: .7714
Na	1030.00	CH ₄	.05		
K	233.00	N ₂	12.00	Measured temperature	deg.C : .0
Mg	397.000				
Ca	149.00	Liters gas per kg			
F	.000	condensate/deg.C	.86/20.0	Condensate (mg/kg)	
Cl	2270.00			pH/deg.C	.00/ .0
SO ₄	390.00	Total steam (mg/kg)		CO ₂	.00
Al	.047	CO ₂	.00	H ₂ S	.00
Fe	2.100	H ₂ S	.00	NH ₃	.00
TDS	4000.00	NH ₃	.00	Na	.00

Ionic strength = .10072

Ionic balance : Cations (mol.eq.) = .08839636 Anions (mol.eq.) = .06973521 Diff(%) = 23.60

Deep water components (mg/kg)				Deep steam (mg/kg)		Gas pressures (bara)	
B	53.62	CO ₂	6.72	CO ₂	1059.33	CO ₂	.157E-01
SiO ₂	442.85	H ₂ S	8.37	H ₂ S	416.26	H ₂ S	.798E-02
Na	681.82	NH ₃	.00	NH ₃	.00	NH ₃	.000E+00
K	154.24	H ₂	.00	H ₂	1.16	H ₂	.374E-03
Mg	262.797	O ₂	.01	O ₂	9.97	O ₂	.204E-03
Ca	98.63	CH ₄	.00	CH ₄	.36	CH ₄	.146E-04
F	.000	N ₂	.14	N ₂	141.53	N ₂	.330E-02
Cl	1502.64					H ₂ O	.363E+02
SO ₄	258.16					Total	.363E+02
Al	.0308						
Fe	1.3901						
TDS	2647.83	Aquifer steam fraction = .6546					

Ionic strength = .05928

1000/T (Kelvin) = 1.93

Ionic balance : Cations (mol.eq.) = .05430397 Anions (mol.eq.) = .04238228 Diff(%) = 24.66

Oxidation potential (volts) : Eh H₂S= -.496 Eh CH₄= -.545 Eh H₂= -.460 Eh NH₃= 99.999

Table A.9h. WATCH results for Sumikawa well SA-2 89/07/03. SA-2 is the well closest to Mt. Yake and shows magmatic influence. As with S-2, this well evolved from slightly alkaline (pH 8) to distinctly acid (pH 3.3) during a year of sampling. The sample chosen is early (pH 6.1) in this progression. Chloride in SA-2 discharge (and in the reservoir) is high and variable with almost no dissolved CO₂. The very low B/Cl and very high Cl/SO₄ ratios and the Ar-N₂-He gas concentration pattern also suggest strongly that this well fluid contains significant magmatic fluid. As for S-2, the water is supersaturated with anhydrite, undersaturated with calcite and approximately saturated with laumontite, wairakite, albite and muscovite.

Chemical geothermometers (degrees C)

Quartz	244.6	(Fournier & Potter, GRC Bulletin, pp. 3-12, Nov. 1982)
Chalcedony	231.5	(Fournier, Geothermics, vol. 5, pp. 41-50, 1977)
Na/K	288.5	(Amorsson et al., Geochim. Cosmochim. Acta, vol. 47, pp. 567-577, 1983)

Activity coefficients in deep water

H+	.744	KSO ₄ -	.698	Fe++	.253	FeCl+	.675
OH-	.666	F-	.666	Fe+++	.073	Al+++	.073
H ₃ SiO ₄ -	.675	Cl-	.656	FeOH+	.691	AlOH++	.240
H ₂ SiO ₄ --	.240	Na+	.675	Fe(OH)3-	.691	Al(OH)2+	.698
H ₂ BO ₃ -	.646	K+	.656	Fe(OH)4--	.232	Al(OH)4-	.683
HCO ₃ -	.675	Ca++	.253	Fe(OH)++	.232	AlSO ₄ +	.683
CO ₃ --	.221	Mg++	.292	Fe(OH)2+	.698	Al(SO ₄)2-	.683
HS-	.666	CaHCO ₃ +	.706	Fe(OH)4-	.698	AlF++	.240
S--	.232	MgHCO ₃ +	.675	FeSO ₄ +	.691	AlF2+	.698
HSO ₄ -	.683	CaOH+	.706	FeCl++	.232	AlF4-	.683
SO ₄ --	.210	MgOH+	.713	FeCl2+	.691	AlF5--	.221
NaSO ₄ -	.698	NH ₄ +	.646	FeCl4-	.675	AlF6---	.034

Chemical species in deep water - ppm and log mole

Deep water pH is 6.189

H+	.00	-6.061	Mg++	204.27	-2.076	Fe(OH)3	.82	-5.116
OH-	.34	-4.699	NaCl	44.38	-3.120	Fe(OH)4-	2.13	-4.764
H ₄ SiO ₄	706.57	-2.134	KCl	4.92	-4.180	FeCl+	.00	-8.990
H ₃ SiO ₄ -	1.46	-4.815	NaSO ₄ -	6.34	-4.273	FeCl2	.00	-12.668
H ₂ SiO ₄ --	.00	-9.575	KSO ₄ -	6.52	-4.316	FeCl++	.00	-19.421
NaH ₃ SiO ₄	.42	-5.448	CaSO ₄	30.42	-3.651	FeCl2+	.00	-20.581
H ₃ BO ₃	306.07	-2.305	MgSO ₄	246.22	-2.689	FeCl3	.00	-22.377
H ₂ BO ₃ -	.60	-5.003	CaCO ₃	.01	-7.269	FeCl4-	.00	-24.372
H ₂ CO ₃	8.40	-3.868	MgCO ₃	.00	-7.902	FeSO ₄	.00	-10.680
HCO ₃ -	.48	-5.102	CaHCO ₃ +	.74	-5.133	FeSO ₄ +	.00	-19.959
CO ₃ --	.00	-9.566	MgHCO ₃ +	.17	-5.694	Al+++	.00	-22.244
H ₂ S	7.59	-3.652	CaOH+	.19	-5.477	AlOH++	.00	-15.113
HS-	.76	-4.640	MgOH+	14.89	-3.443	Al(OH)2+	.00	-8.851
S--	.00	-12.966	NH ₄ OH	.00	.000	Al(OH)3	.09	-5.943
H ₂ SO ₄	.00	-12.114	NH ₄ +	.00	.000	Al(OH)4-	.00	-8.754
HSO ₄ -	.91	-5.028	Fe++	.00	-9.050	AlSO ₄ +	.00	-22.289
SO ₄ --	29.55	-3.512	Fe+++	.00	-23.441	Al(SO ₄)2-	.00	-23.627
HF	.00	.000	FeOH+	.00	-8.571	AlF++	.00	.000
F-	.00	.000	Fe(OH)2	.00	-8.990	AlF2+	.00	.000
Cl-	1473.40	-1.381	Fe(OH)3-	.00	-9.916	AlF3	.00	.000
Na+	663.06	-1.540	Fe(OH)4--	.00	-15.460	AlF4-	.00	.000
K+	149.77	-2.417	Fe(OH)++	.00	-15.407	AlF5--	.00	.000
Ca++	89.25	-2.652	Fe(OH)2+	.00	-8.737	AlF6---	.00	.000

Table A.9h. WATCH results for Sumikawa well SA-2 89/07/03. SA-2 is the well closest to Mt. Yake and shows magmatic influence. As with S-2, this well evolved from slightly alkaline (pH 8) to distinctly acid (pH 3.3) during a year of sampling. The sample chosen is early (pH 6.1) in this progression. Chloride in SA-2 discharge (and in the reservoir) is high and variable with almost no dissolved CO₂. The very low B/Cl and very high Cl/SO₄ ratios and the Ar-N₂-He gas concentration pattern also suggest strongly that this well fluid contains significant magmatic fluid. As for S-2, the water is supersaturated with anhydrite, undersaturated with calcite and approximately saturated with laumontite, wairakite, albite and muscovite.

Log solubility products of minerals in deep water (Al based on microcline)

	Theor.	Calc.		Theor.	Calc.		Theor.	Calc.
Adularia	-14.422	-15.108	Albite, low	-13.970	-14.220	Analcime	-11.525	-12.086
Anhydrite	-8.008	-7.439	Calcite	-12.632	-13.471	Chalcedony	-2.016	-2.134
Mg-Chlorite	-84.475	-70.668	Fluorite	-10.929	99.999	Goethite	1.978	-.045
Laumontite	-24.544	-23.999	Microcline	-15.108	-15.108	Magnetite	-17.446	-19.488
Ca-Montmor.	-72.615	-77.192	K-Montmor.	-34.014	-39.571	Mg-Montmor.	-74.113	-76.552
Na-Montmor.	-34.289	-38.682	Muscovite	-17.849	-17.573	Prehnite	-37.151	-34.866
Pyrrhotite	-24.050	-38.790	Pyrite	-45.186	-49.581	Quartz	-2.135	-2.134
Wairakite	-24.453	-23.999	Wollastonite	7.574	6.996	Zoisite	-37.722	-36.098
Epidote	-37.307	-34.911	Marcasite	-28.246	-49.581	Talc	8.870	20.772
Chrysotile	15.197	25.040	Sil. amorph.	-1.671	-2.134			

Table A.9i. WATCH results for Sumikawa well SB-1 89/08/08. The fluid chemistry of SB-1 is similar to that of SD-1 and lower Cl samples of S-4. It has high pH, low enthalpy and essentially no reservoir steam. The reservoir gas pressures are similar to those of SA-1 and S-4. The reservoir water is saturated with anhydrite, laumontite, wairakite and albite, and slightly supersaturated with calcite and muscovite.

Water sample (mg/kg)		Steam sample			
pH/deg.C	8.00/ 20.0	Gas (volume %)		Reference temperature	deg.C : 246.0
CO2	94.00	CO2	33.20		
H2S	.00	H2S	26.40	Sampling pressure	bar abs. : 1.0
NH3	.00	NH3	.00	Discharge enthalpy	kJ/kg : 1200.
B	107.00	H2	.36	Discharge	kg/s : .0
SiO2	627.00	O2	.19	Steam fraction at collection	: .3155
Na	248.00	CH4	.29		
K	44.00	N2	38.20	Measured temperature	deg.C : .0
Mg	.040				
Ca	6.40	Liters gas per kg			
F	4.300	condensate/deg.C	.53/20.0	Condensate (mg/kg)	
Cl	296.00			pH/deg.C	.00/ .0
SO4	126.00	Total steam (mg/kg)		CO2	.00
Al	.139	CO2	.00	H2S	.00
Fe	.050	H2S	.00	NH3	.00
TDS	1990.00	NH3	.00	Na	.00
Ionic strength = .01449					
Ionic balance : Cations (mol.eq.) = .01218349 Anions (mol.eq.) = .01389908 Diff(%) =13.16					
Deep water components (mg/kg)		Deep steam (mg/kg)		Gas pressures (bara)	
B	79.35	CO2	25.17	CO2	1852.76
SiO2	464.99	H2S	28.54	H2S	470.04
Na	183.92	NH3	.00	NH3	.00
K	32.63	H2	.00	H2	.65
Mg	.030	O2	.01	O2	5.39
Ca	4.75	CH4	.00	CH4	4.16
F	3.189	N2	1.01	N2	953.82
Cl	219.52			H2O	.372E+02
SO4	93.44			Total	.372E+02
Al	.1028				
Fe	.0371				
TDS	1475.80	Aquifer steam fraction = .0770			
Ionic strength = .01018					
1000/T (Kelvin) = 1.93					
Ionic balance : Cations (mol.eq.) = .00871992 Anions (mol.eq.) = .00999480 Diff(%) =13.62					
Oxidation potential (volts) : Eh H2S= -.675 Eh CH4= -.706 Eh H2= -.597 Eh NH3= 99.999					

Table A.9i. WATCH results for Sumikawa well SB-1 89/08/08. The fluid chemistry of SB-1 is similar to that of SD-1 and lower CI samples of S-4. It has high pH, low enthalpy and essentially no reservoir steam. The reservoir gas pressures are similar to those of SA-1 and S-4. The reservoir water is saturated with anhydrite, laumontite, wairakite and albite, and slightly supersaturated with calcite and muscovite (continued).

Chemical geothermometers (degrees C)

Quartz	244.8	(Fournier & Potter, GRC Bulletin, pp. 3-12, Nov. 1982)
Chalcedony	231.7	(Fournier, Geothermics, vol. 5, pp. 41-50, 1977)
Na/K	258.5	(Amorsson et al., Geochim. Cosmochim. Acta, vol. 47, pp. 567-577, 1983)

Activity coefficients in deep water

H+	.847	KSO4-	.832	Fe++	.486	FeCl+	.824
OH-	.822	F-	.822	Fe+++	.227	Al+++	.227
H3SiO4-	.824	Cl-	.819	FeOH+	.830	AlOH++	.479
H2SiO4--	.479	Na+	.824	Fe(OH)3-	.830	Al(OH)2+	.832
H2BO3-	.816	K+	.819	Fe(OH)4--	.475	Al(OH)4-	.827
HCO3-	.824	Ca++	.486	Fe(OH)++	.475	AlSO4+	.827
CO3--	.469	Mg++	.507	Fe(OH)2+	.832	Al(SO4)2-	.827
HS-	.822	CaHCO3+	.834	Fe(OH)4-	.832	AlF++	.479
S--	.475	MgHCO3+	.824	FeSO4+	.830	AlF2+	.832
HSO4-	.827	CaOH+	.834	FeCl++	.475	AlF4-	.827
SO4--	.463	MgOH+	.837	FeCl2+	.830	AlF5--	.469
NaSO4-	.832	NH4+	.816	FeCl4-	.824	AlF6---	.182

Chemical species in deep water - ppm and log mole

Deep water pH is 7.631

H+	.00	-7.559	Mg++	.01	-6.634	Fe(OH)3	.00	-7.911
OH-	7.70	-3.344	NaCl	2.80	-4.319	Fe(OH)4-	.08	-6.186
H4SiO4	707.93	-2.133	KCl	.24	-5.500	FeCl+	.00	-15.295
H3SiO4-	32.41	-3.468	NaSO4-	10.01	-4.075	FeCl2	.00	-19.561
H2SiO4--	.01	-7.009	KSO4-	7.89	-4.234	FeCl++	.00	-27.641
NaH3SiO4	3.82	-4.491	CaSO4	7.12	-4.282	FeCl2+	.00	-29.301
H3BO3	434.92	-2.153	MgSO4	.07	-6.257	FeCl3	.00	-31.747
H2BO3-	18.64	-3.514	CaCO3	.30	-5.523	FeCl4-	.00	-34.557
H2CO3	15.15	-3.612	MgCO3	.00	-9.095	FeSO4	.00	-15.418
HCO3-	19.03	-3.506	CaHCO3+	1.27	-4.901	FeSO4+	.00	-26.465
CO3--	.01	-6.782	MgHCO3+	.00	-8.410	Al+++	.00	-26.638
H2S	8.85	-3.586	CaOH+	.19	-5.482	AlOH++	.00	-17.833
HS-	19.11	-3.238	MgOH+	.02	-6.367	Al(OH)2+	.00	-9.872
S--	.00	-10.334	NH4OH	.00	.000	Al(OH)3	.29	-5.433
H2SO4	.00	-14.223	NH4+	.00	.000	Al(OH)4-	.01	-6.916
HSO4-	.16	-5.786	Fe++	.00	-14.826	AlSO4+	.00	-25.509
SO4--	74.53	-3.110	Fe+++	.00	-31.143	Al(SO4)2-	.00	-26.094
HF	.01	-6.134	FeOH+	.00	-12.686	AlF++	.00	-21.214
F-	3.17	-3.777	Fe(OH)2	.00	-11.564	AlF2+	.00	-17.530
Cl-	217.70	-2.212	Fe(OH)3-	.00	-11.102	AlF3	.00	-16.104
Na+	180.14	-2.106	Fe(OH)4--	.00	-15.438	AlF4-	.00	-16.774
K+	30.22	-3.112	Fe(OH)++	.00	-21.452	AlF5--	.00	-18.823
Ca++	1.90	-4.325	Fe(OH)2+	.00	-13.071	AlF6---	.00	-22.431

Table A.9i. WATCH results for Sumikawa well SB-1 89/08/08. The fluid chemistry of SB-1 is similar to that of SD-1 and lower Cl samples of S-4. It has high pH, low enthalpy and essentially no reservoir steam. The reservoir gas pressures are similar to those of SA-1 and S-4. The reservoir water is saturated with anhydrite, laumontite, wairakite and albite, and slightly supersaturated with calcite and muscovite (continued).

Log solubility products of minerals in deep water (Al based on microcline)

	Theor.	Calc.		Theor.	Calc.		Theor.	Calc.
Adularia	-14.416	-15.098	Albite, low	-13.966	-14.090	Analcime	-11.525	-11.957
Anhydrite	-8.033	-8.083	Calcite	-12.668	-11.750	Chalcedony	-2.011	-2.133
Mg-Chlorite	-84.579	-79.486	Fluorite	-10.936	-12.363	Goethite	2.053	-2.837
Laumontite	-24.550	-24.173	Microcline	-15.098	-15.098	Magnetite	-17.315	-27.672
Ca-Montmor.	-72.610	-87.424	K-Montmor.	-34.004	-44.591	Mg-Montmor.	-74.109	-89.715
Na-Montmor.	-34.279	-43.582	Muscovite	-17.847	-19.242	Prehnite	-37.194	-33.538
Pyrrhotite	-23.280	-58.378	Pyrite	-44.207	-73.063	Quartz	-2.129	-2.133
Wairakite	-24.477	-24.173	Wollastonite	7.551	8.491	Zoisite	-37.780	-35.610
Epidote	-37.351	-36.374	Marcasite	-27.312	-73.063	Talc	8.821	16.469
Chrysotile	15.137	20.734	Sil. amorph.	-1.667	-2.133			

Table A.9j. WATCH results for Sumikawa well SC-1 89/11/16. This water has both high Cl/(SO₄+HCO₃) and high B/Cl, suggesting magmatic influence (but less than S-2 and SA-2). This well was not injected with cold water in early 1989 and, perhaps as a result, shows close equilibrium with a wide range of minerals. Anhydrite, laumontite, wairakite, albite, calcite, and muscovite are saturated or nearly so, and analcime and epidote are not far off saturation.

Water sample (mg/kg)		Steam sample		
pH/deg.C	7.40/ 20.0	Gas (volume %)		Reference temperature deg.C : 268.0
CO2	39.00	CO2	28.60	
H2S	.00	H2S	21.50	Sampling pressure bar abs. : 1.0
NH3	.00	NH3	.00	Discharge enthalpy kJ/kg : 1250.
B	181.00	H2	1.07	Discharge kg/ s : .0
SiO2	825.00	O2	3.50	Steam fraction at collection : .3682
Na	320.00	CH4	.34	
K	51.60	N2	43.40	Measured temperature deg.C : .0
Mg	.030			
Ca	3.10	Liters gas per kg		
F	.000	condensate/deg.C	.96/20.0	Condensate (mg/kg)
Cl	456.00			pH/deg.C .00/ .0
SO4	90.30	Total steam (mg/kg)		CO2 .00
Al	.106	CO2	.00	H2S .00
Fe	.100	H2S	.00	NH3 .00
TDS	2420.00	NH3	.00	Na .00

Ionic strength = .01658

Ionic balance : Cations (mol.eq.) = .01536755 Anions (mol.eq.) = .01580329 Diff(%) = -2.80

Deep water components (mg/kg)				Deep steam (mg/kg)		Gas pressures (bara)	
B	119.92	CO2	40.74	CO2	3681.11	CO2	.804E-01
SiO2	546.59	H2S	50.87	H2S	1277.48	H2S	.360E-01
Na	212.01	NH3	.00	NH3	.00	NH3	.000E+00
K	34.19	H2	.02	H2	6.53	H2	.311E-02
Mg	.020	O2	.91	O2	336.43	O2	.101E-01
Ca	2.05	CH4	.03	CH4	16.75	CH4	.100E-02
F	.000	N2	7.44	N2	3700.58	N2	.127E+00
Cl	302.12					H2O	.534E+02
SO4	59.83					Total	.536E+02
Al	.0700						
Fe	.0663						
TDS	1603.34	Aquifer steam fraction =		.0463			

Ionic strength = .01051

1000/T (Kelvin) = 1.85

Ionic balance : Cations (mol.eq.) = .00987563 Anions (mol.eq.) = .01016728 Diff(%) = -2.91

Oxidation potential (volts) : Eh H2S= -.634 Eh CH4= -.684 Eh H2= -.614 Eh NH3= 99.999

Table A.9j. WATCH results for Sumikawa well SC-1 89/11/16. This water has both high Cl/(SO₄+HCO₃) and high B/Cl, suggesting magmatic influence (but less than S-2 and SA-2). This well was not injected with cold water in early 1989 and, perhaps as a result, shows close equilibrium with a wide range of minerals. Anhydrite, laumontite, wairakite, albite, calcite, and muscovite are saturated or nearly so, and analcime and epidote are not far off saturation (continued).

Chemical geothermometers (degrees C)

Quartz	267.4	(Fournier & Potter, GRC Bulletin, pp. 3-12, Nov. 1982)
Chalcedony	254.5	(Fournier, Geothermics, vol. 5, pp. 41-50, 1977)
Na/K	248.3	(Arnorsson et al., Geochim. Cosmochim. Acta, vol. 47, pp. 567-577, 1983)

Activity coefficients in deep water

H+	.832	KSO ₄ -	.815	Fe ⁺⁺	.448	FeCl ⁺	.807
OH-	.804	F-	.804	Fe ⁺⁺⁺	.193	Al ⁺⁺⁺	.193
H ₃ SiO ₄ -	.807	Cl-	.801	FeOH ⁺	.813	AlOH ⁺⁺	.441
H ₂ SiO ₄ --	.441	Na ⁺	.807	Fe(OH)3-	.813	Al(OH)2 ⁺	.815
H ₂ BO ₃ -	.798	K ⁺	.801	Fe(OH)4--	.436	Al(OH)4-	.810
HCO ₃ -	.807	Ca ⁺⁺	.448	Fe(OH) ⁺⁺	.436	AlSO ₄ ⁺	.810
CO ₃ --	.430	Mg ⁺⁺	.470	Fe(OH)2 ⁺	.815	Al(SO ₄)2-	.810
HS-	.804	CaHCO ₃ ⁺	.818	Fe(OH)4-	.815	AlF ⁺⁺	.441
S--	.436	MgHCO ₃ ⁺	.807	FeSO ₄ ⁺	.813	AlF2 ⁺	.815
HSO ₄ -	.810	CaOH ⁺	.818	FeCl ⁺⁺	.436	AlF4-	.810
SO ₄ --	.424	MgOH ⁺	.820	FeCl2 ⁺	.813	AlF5--	.430
NaSO ₄ -	.815	NH ₄ ⁺	.798	FeCl4-	.807	AlF6---	.150

Chemical species in deep water - ppm and log mole

Deep water pH is 6.971

H+	.00	-6.892	Mg ⁺⁺	.01	-6.634	Fe(OH)3	.01	-7.130
OH-	1.89	-3.954	NaCl	7.66	-3.883	Fe(OH)4-	.14	-5.954
H ₄ SiO ₄	867.39	-2.045	KCl	.53	-5.149	FeCl ⁺	.00	-14.402
H ₃ SiO ₄ -	6.16	-4.189	NaSO ₄ -	8.64	-4.139	FeCl2	.00	-17.652
H ₂ SiO ₄ --	.00	-8.543	KSO ₄ -	7.60	-4.250	FeCl ⁺⁺	.00	-25.565
NaH ₃ SiO ₄	.88	-5.128	CaSO ₄	3.06	-4.648	FeCl2 ⁺	.00	-27.088
H ₃ BO ₃	680.13	-1.959	MgSO ₄	.04	-6.432	FeCl3	.00	-29.340
H ₂ BO ₃ -	5.68	-4.030	CaCO ₃	.02	-6.750	FeCl4-	.00	-31.915
H ₂ CO ₃	49.36	-3.099	MgCO ₃	.00	-10.156	FeSO ₄	.00	-14.914
HCO ₃ -	7.69	-3.899	CaHCO ₃ ⁺	.36	-5.447	FeSO ₄ ⁺	.00	-24.757
CO ₃ --	.00	-8.053	MgHCO ₃ ⁺	.00	-8.708	Al ⁺⁺⁺	.00	-26.094
H ₂ S	39.80	-2.933	CaOH ⁺	.03	-6.249	AlOH ⁺⁺	.00	-17.379
HS-	10.75	-3.488	MgOH ⁺	.01	-6.671	Al(OH)2 ⁺	.00	-9.562
S--	.00	-11.101	NH ₄ OH	.00	.000	Al(OH)3	.20	-5.587
H ₂ SO ₄	.00	-12.686	NH ₄ ⁺	.00	.000	Al(OH)4-	.00	-8.258
HSO ₄ -	.91	-5.027	Fe ⁺⁺	.00	-14.177	AlSO ₄ ⁺	.00	-24.993
SO ₄ --	44.35	-3.336	Fe ⁺⁺⁺	.00	-29.693	Al(SO ₄)2-	.00	-25.695
HF	.00	.000	FeOH ⁺	.00	-12.496	AlF ⁺⁺	.00	.000
F-	.00	.000	Fe(OH)2	.00	-11.736	AlF2 ⁺	.00	.000
Cl-	297.22	-2.077	Fe(OH)3-	.00	-11.546	AlF3	.00	.000
Na ⁺	207.16	-2.045	Fe(OH)4--	.00	-16.562	AlF4-	.00	.000
K ⁺	31.71	-3.091	Fe(OH) ⁺⁺	.00	-20.191	AlF5--	.00	.000
Ca ⁺⁺	.98	-4.612	Fe(OH)2 ⁺	.00	-11.950	AlF6---	.00	.000

Table A.9j. WATCH results for Sumikawa well SC-1 89/11/16. This water has both high Cl/(SO₄+HCO₃) and high B/Cl, suggesting magmatic influence (but less than S-2 and SA-2). This well was not injected with cold water in early 1989 and, perhaps as a result, shows close equilibrium with a wide range of minerals. Anhydrite, laumontite, wairakite, albite, calcite, and muscovite are saturated or nearly so, and analcime and epidote are not far off saturation (continued).

Log solubility products of minerals in deep water (Al based on microcline)

	Theor.	Calc.		Theor.	Calc.		Theor.	Calc.
Adularia	-14.371	-14.999	Albite, low	-13.938	-13.950	Analcime	-11.566	-11.905
Anhydrite	-8.441	-8.669	Calcite	-13.242	-13.380	Chalcedony	-1.925	-2.045
Mg-Chlorite	-86.372	-84.683	Fluorite	-11.057	99.999	Goethite	3.286	-1.994
Laumontite	-24.717	-24.494	Microcline	-14.996	-14.996	Magnetite	-15.172	-26.612
Ca-Montmor.	-72.581	-80.845	K-Montmor	-33.864	-41.130	Mg-Montmor.	-74.087	-82.845
Na-Montmor.	-34.147	-40.081	Muscovite	-17.838	-18.257	Prehnite	-37.960	-35.507
Pyrrhotite	-10.789	-46.737	Pyrite	-28.408	-55.555	Quartz	-2.043	-2.045
Wairakite	-24.913	-24.494	Wollastonite	7.189	6.938	Zoisite	-38.801	-37.136
Epidote	-38.439	-37.502	Marcasite	-12.208	-55.555	Talc	8.054	12.767
Chrysotile	14.196	16.856	Sil. amorph.	-1.610	-2.045			

Table A.9k. WATCH results for Sumikawa well SD-1 89/08/09. This water is similar to that from S-3 and SB-1 in temperature (240 C) and in having some shallow groundwater influence, but is better equilibrated with relatively lower Mg and higher Cl. There is no aquifer steam and gas pressures are high. Unlike other wells, this water is nearly saturated (± 1 log unit) with Ca, Na and Mg montmorillonites and Mg chlorite. Like other wells, it is exactly saturated with anhydrite, albite and calcite and near saturation with laumontite, wairakite, epidote, and zoisite. Although this well was not injected in early 1989 with cold meteoric water, it was injected with a large amount of cooled water from well SC-1, so the wide range of saturated minerals is surprising unless the clays precipitated in the SC-1 cooling pond and did not fully dissolve after injection into SD-1.

Water sample (mg/kg)		Steam sample											
pH/deg.C	8.20/ 20.0	Gas (volume %)		Reference temperature	deg.C : 240.0								
CO2	39.00	CO2	42.20										
H2S	.00	H2S	50.50	Sampling pressure	bar abs. : 1.0								
NH3	.00	NH3	.00	Discharge enthalpy	kJ/kg : 1038.								
B	86.00	H2	.85	Discharge	kg/s : .0								
SiO2	582.00	O2	.10	Steam fraction at collection	: .2742								
Na	220.00	CH4	.19										
K	34.60	N2	6.01	Measured temperature	deg.C : .0								
Mg	.160												
Ca	6.95	Liters gas per kg											
F	3.800	condensate/deg.C	.93/20.0	Condensate (mg/kg)									
Cl	198.00			pH/deg.C	.00/ .0								
SO4	158.00	Total steam (mg/kg)		CO2	.00								
Al	.189	CO2	.00	H2S	.00								
Fe	.300	H2S	.00	NH3	.00								
TDS	2000.00	NH3	.00	Na	.00								
Ionic strength = .01253													
Ionic balance : Cations (mol.eq.) = .01075880 Anions (mol.eq.) = .01071822 Diff(%) = .38													
Deep water components (mg/kg)		Deep steam (mg/kg)		Gas pressures (bara)									
B	62.43	CO2	216.46	CO2	38822.17	CO2	.532E+00						
SiO2	422.49	H2S	180.39	H2S	9433.20	H2S	.167E+00						
Na	159.70	NH3	.00	NH3	.00	NH3	.000E+00						
K	25.12	H2	.15	H2	142.12	H2	.424E-01						
Mg	.116	O2	.29	O2	231.75	O2	.437E-02						
Ca	5.05	CH4	.25	CH4	340.49	CH4	.128E-01						
F	2.759	N2	14.21	N2	16046.79	N2	.346E+00						
Cl	143.73					H2O	.335E+02						
SO4	114.70					Total	.346E+02						
Al	.1371												
Fe	.2178												
TDS	1451.85	Aquifer steam fraction = .0002											
Ionic strength = .00853						1000/T (Kelvin) = 1.95							
Ionic balance : Cations (mol.eq.) = .00753019 Anions (mol.eq.) = .00750716 Diff(%) = .31													
Oxidation potential (volts) :						Eh H2S=	-.529	Eh CH4=	-.582	Eh H2=	-.587	Eh NH3=	99.99

Table A.9k. WATCH results for Sumikawa well SD-1 89/08/09. This water is similar to that from S-3 and SB-1 in temperature (240 C) and in having some shallow groundwater influence, but is better equilibrated with relatively lower Mg and higher Cl. There is no aquifer steam and gas pressures are high. Unlike other wells, this water is nearly saturated (± 1 log unit) with Ca, Na and Mg montmorillonites and Mg chlorite. Like other wells, it is exactly saturated with anhydrite, albite and calcite and near saturation with laumontite, wairakite, epidote, and zoisite. Although this well was not injected in early 1989 with cold meteoric water, it was injected with a large amount of cooled water from well SC-1, so the wide range of saturated minerals is surprising unless the clays precipitated in the SC-1 cooling pond and did not fully dissolve after injection into SD-1 (continued).

Chemical geothermometers (degrees C)

Quartz	239.9	(Fournier & Potter, GRC Bulletin, pp. 3-12, Nov. 1982)
Chalcedony	226.4	(Fournier, Geothermics, vol. 5, pp. 41-50, 1977)
Na/K	243.8	(Arnorsson et al., Geochim. Cosmochim. Acta, vol. 47, pp. 567-577, 1983)

Activity coefficients in deep water

H+	.859	KSO4-	.846	Fe++	.519	FeCl+	.840
OH-	.838	F-	.838	Fe+++	.257	Al+++	.257
H3SiO4-	.840	Cl-	.835	FeOH+	.844	AlOH++	.513
H2SiO4--	.513	Na+	.840	Fe(OH)3-	.844	Al(OH)2+	.846
H2BO3-	.833	K+	.835	Fe(OH)4--	.509	Al(OH)4-	.842
HCO3-	.840	Ca++	.519	Fe(OH)++	.509	AlSO4+	.842
CO3--	.504	Mg++	.538	Fe(OH)2+	.846	Al(SO4)2-	.842
HS-	.838	CaHCO3+	.848	Fe(OH)4-	.846	AlF++	.513
S--	.509	MgHCO3+	.840	FeSO4+	.844	AlF2+	.846
HSO4-	.842	CaOH+	.848	FeCl++	.509	AlF4-	.842
SO4--	.499	MgOH+	.850	FeCl2+	.844	AlF5--	.504
NaSO4-	.846	NH4+	.833	FeCl4-	.840	AlF6---	.214

Chemical species in deep water - ppm and log mole

Deep water pH is 6.449

H+	.00	-6.383	Mg++	.03	-5.948	Fe(OH)3	.10	-6.031
OH-	.48	-4.552	NaCl	1.46	-4.602	Fe(OH)4-	.37	-5.528
H4SiO4	673.44	-2.155	KCl	.11	-5.839	FeCl+	.00	-11.040
H3SiO4-	2.17	-4.642	NaSO4-	10.67	-4.048	FeCl2	.00	-15.730
H2SiO4--	.00	-9.342	KSO4-	7.05	-4.282	FeCl++	.00	-22.184
NaH3SiO4	.23	-5.719	CaSO4	8.60	-4.199	FeCl2+	.00	-24.007
H3BO3	356.04	-2.240	MgSO4	.42	-5.454	FeCl3	.00	-26.642
H2BO3-	1.02	-4.776	CaCO3	.03	-6.584	FeCl4-	.00	-29.662
H2CO3	277.38	-2.350	MgCO3	.00	-9.427	FeSO4	.00	-10.855
HCO3-	26.25	-3.366	CaHCO3+	1.64	-4.791	FeSO4+	.00	-20.699
CO3--	.00	-7.784	MgHCO3+	.00	-7.592	Al+++	.00	-22.638
H2S	154.67	-2.343	CaOH+	.01	-6.716	AlOH++	.00	-15.155
HS-	24.95	-3.122	MgOH+	.00	-6.946	Al(OH)2+	.00	-8.503
S--	.00	-11.456	NH4OH	.00	.000	Al(OH)3	.39	-5.296
H2SO4	.00	-11.866	NH4+	.00	.000	Al(OH)4-	.00	-7.831
HSO4-	2.54	-4.583	Fe++	.00	-10.376	AlSO4+	.00	-21.416
SO4--	92.16	-3.018	Fe+++	.00	-25.394	Al(SO4)2-	.00	-21.915
HF	.16	-5.096	FeOH+	.00	-9.463	AlF++	.00	-17.381
F-	2.61	-3.863	Fe(OH)2	.00	-9.603	AlF2+	.00	-13.848
Cl-	142.80	-2.395	Fe(OH)3-	.00	-10.439	AlF3	.00	-12.552
Na+	157.02	-2.166	Fe(OH)4--	.00	-15.973	AlF4-	.00	-13.342
K+	23.02	-3.230	Fe(OH)++	.00	-16.998	AlF5--	.00	-15.505
Ca++	1.85	-4.337	Fe(OH)2+	.00	-9.926	AlF6---	.00	-19.213

Table A.9k. WATCH results for Sumikawa well SD-1 89/08/09. This water is similar to that from S-3 and SB-1 in temperature (240 C) and in having some shallow groundwater influence, but is better equilibrated with relatively lower Mg and higher Cl. There is no aquifer steam and gas pressures are high. Unlike other wells, this water is nearly saturated (± 1 log unit) with Ca, Na and Mg montmorillonites and Mg chlorite. Like other wells, it is exactly saturated with anhydrite, albite and calcite and near saturation with laumontite, wairakite, epidote, and zoisite. Although this well was not injected in early 1989 with cold meteoric water, it was injected with a large amount of cooled water from well SC-1, so the wide range of saturated minerals is surprising unless the clays precipitated in the SC-1 cooling pond and did not fully dissolve after injection into SD-1 (continued).

Log solubility products of minerals in deep water (Al based on microcline)

	Theor.	Calc.		Theor.	Calc.		Theor.	Calc.
Adularia	-14.442	-15.141	Albite, low	-13.986	-14.074	Analcime	-11.525	-11.919
Anhydrite	-7.923	-7.942	Calcite	-12.514	-12.704	Chalcedony	-2.036	-2.155
Mg-Chlorite	-84.134	-85.323	Fluorite	-10.905	-12.501	Goethite	1.726	-.971
Laumontite	-24.525	-23.977	Microcline	-15.141	-15.141	Magnetite	-17.886	-21.861
Ca-Montmor.	-72.637	-71.634	K-Montmor.	-34.053	-36.814	Mg-Montmor.	-74.132	-73.230
Na-Montmor.	-34.325	-35.748	Muscovite	-17.857	-16.620	Prehnite	-37.010	-35.703
Pyrrhotite	-26.636	-34.794	Pyrite	-48.480	-36.976	Quartz	-2.155	-2.155
Wairakite	-24.375	-23.977	Wollastonite	7.653	6.122	Zoisite	-37.529	-36.442
Epidote	-37.181	-36.674	Marcasite	-31.386	-36.976	Talc	9.036	11.424
Chrysotile	15.402	15.733	Sil. amorph.	-1.683	-2.155			

Table A.91 WATCH results for Sumikawa well SM-2 78/09/25. The data may be less accurate and is certainly less complete (e.g. only CO₂ and H₂S) in this early analysis. Its relatively low temperature (200 C?) and high Mg suggests near-surface influence, but the high Cl/B and Cl/ other anions suggest the opposite. This water is saturated with anhydrite, muscovite and analcime, but apparently supersaturated with laumontite, wairakite, calcite and albite, possibly due to the low temperature or problems with the analysis..

Water sample (mg/kg)		Steam sample		
pH/deg.C	8.30/ 20.0	Gas (volume %)		Reference temperature deg.C : 215.5
CO2	102.00	CO2	79.10	
H ₂ S	.00	H2S	50.50	Sampling pressure bar abs. : 1.0
NH3	.00	NH3	.00	Discharge enthalpy kJ/kg : 1140.
B	70.00	H2	.00	Discharge kg/s : .0
SiO2	443.00	O2	.00	Steam fraction at collection : .3194
Na	356.00	CH4	.00	
K	11.30	N2	.00	Measured temperature deg.C : .0
Mg	6.000			
Ca	9.00	Liters gas per kg		
F	.000	condensate/deg.C	.62/20.0	Condensate (mg/kg)
Cl	265.00			pH/deg.C .00/ .0
SO4	242.00	Total steam (mg/kg)		CO2 .00
Al	.695	CO2	.00	H2S .00
Fe	.300	H2S	.00	NH3 .00
TDS	2090.00	NH3	.00	Na .00

Ionic strength = .01892

Ionic balance : Cations (mol.eq.) = .01655106 Anions (mol.eq.) = .01552782 Diff(%) = 6.38

Deep water components (mg/kg)				Deep steam (mg/kg)		Gas pressures (bara)	
B	53.88	CO2	30.21	CO2	2845.22	CO2	.248E-01
SiO2	340.95	H2S	42.70	H2S	898.05	H2S	.101E-01
Na	273.99	NH3	.00	NH3	.00	NH3	.000E+00
K	8.70	H2	.00	H2	.00	H2	.000E+00
Mg	4.618	O2	.00	O2	.00	O2	.000E+00
Ca	6.93	CH4	.00	CH4	.00	CH4	.000E+00
F	.000	N2	.00	N2	.00	N2	.000E+00
Cl	203.96					H2O	.213E+02
SO4	186.25					Total	.213E+02
Al	.5349						
Fe	.2309						
TDS	1608.56	Aquifer steam fraction =		.1157			

Ionic strength = .01343

1000/T (Kelvin) = 2.05

Ionic balance : Cations (mol.eq.) = .01214701 Anions (mol.eq.) = .01137942 Diff(%) = 6.53

Oxidation potential (volts) : Eh H2S= -.616 Eh CH4= 99.999 Eh H2= 99.999 Eh NH3= 99.999

Table A.91 WATCH results for Sumikawa well SM-2 78/09/25. The data may be less accurate and is certainly less complete (e.g. only CO₂ and H₂S) in this early analysis. Its relatively low temperature (200°C?) and high Mg suggests near-surface influence, but the high Cl/B and Cl/ other anions suggest the opposite. This water is saturated with anhydrite, muscovite and analcime, but apparently supersaturated with laumontite, wairakite, calcite and albite, possibly due to the low temperature or problems with the analysis (continued)..

Chemical geothermometers (degrees C)

Quartz	215.4	(Fournier & Potter, GRC Bulletin, pp. 3-12, Nov. 1982)
Chalcedony	198.7	(Fournier, Geothermics, vol. 5, pp. 41-50, 1977)
Na/K	96.0	(Arnorsson et al., Geochim. Cosmochim. Acta, vol. 47, pp. 567-577, 1983)

Activity coefficients in deep water

H+	.847	KSO4-	.830	Fe++	.484	FeCl+	.822
OH-	.819	F-	.819	Fe+++	.227	Al+++	.227
H3SiO4-	.822	Cl-	.816	FeOH+	.828	AlOH++	.476
H2SiO4--	.476	Na+	.822	Fe(OH)3-	.828	Al(OH)2+	.830
H2BO3-	.813	K+	.816	Fe(OH)4--	.472	Al(OH)4-	.825
HCO3-	.822	Ca++	.484	Fe(OH)++	.472	AlSO4+	.825
CO3--	.465	Mg++	.507	Fe(OH)2+	.830	Al(SO4)2-	.825
HS-	.819	CaHCO3+	.833	Fe(OH)4-	.830	AlF++	.476
S--	.472	MgHCO3+	.822	FeSO4+	.828	AlF2+	.830
HSO4-	.825	CaOH+	.833	FeCl++	.472	AlF4-	.825
SO4--	.459	MgOH+	.836	FeCl2+	.828	AlF5--	.465
NaSO4-	.830	NH4+	.813	FeCl4-	.822	AlF6---	.179

Chemical species in deep water - ppm and log mole

Deep water pH is 7.598

H+	.00	-7.526	Mg++	.99	-4.391	Fe(OH)3	.01	-6.918
OH-	5.52	-3.489	NaCl	2.24	-4.417	Fe(OH)4-	.50	-5.397
H4SiO4	509.32	-2.276	KCl	.03	-6.368	FeCl+	.00	-12.546
H3SiO4-	31.71	-3.477	NaSO4-	19.20	-3.792	FeCl2	.00	-18.218
H2SiO4--	.01	-6.840	KSO4-	2.27	-4.775	FeCl++	.00	-25.379
NaH3SiO4	4.92	-4.380	CaSO4	10.75	-4.103	FeCl2+	.00	-27.124
H3BO3	294.07	-2.323	MgSO4	15.29	-3.896	FeCl3	.00	-29.714
H2BO3-	13.85	-3.643	CaCO3	.38	-5.416	FeCl4-	.00	-32.698
H2CO3	11.66	-3.726	MgCO3	.01	-6.756	FeSO4	.00	-12.319
HCO3-	29.09	-3.322	CaHCO3+	1.65	-4.786	FeSO4+	.00	-23.929
CO3--	.03	-6.320	MgHCO3+	.06	-6.150	Al+++	.00	-23.982
H2S	8.34	-3.611	CaOH+	.12	-5.669	AlOH++	.00	-16.040
HS-	33.34	-2.996	MgOH+	.89	-4.669	Al(OH)2+	.00	-8.867
S--	.00	-10.302	NH4OH	.00	.000	Al(OH)3	1.36	-4.759
H2SO4	.00	-14.536	NH4+	.00	.000	Al(OH)4-	.23	-5.616
HSO4-	.11	-5.937	Fe++	.00	-11.825	AlSO4+	.00	-22.940
SO4--	149.26	-2.809	Fe+++	.00	-28.139	Al(SO4)2-	.00	-23.418
HF	.00	.000	FeOH+	.00	-10.076	AlF++	.00	.000
F-	.00	.000	Fe(OH)2	.00	-9.447	AlF2+	.00	.000
Cl-	202.58	-2.243	Fe(OH)3-	.00	-9.584	AlF3	.00	.000
Na+	268.45	-1.933	Fe(OH)4--	.00	-13.945	AlF4-	.00	.000
K+	8.02	-3.688	Fe(OH)++	.00	-19.166	AlF5--	.00	.000
Ca++	2.87	-4.145	Fe(OH)2+	.00	-11.577	AlF6---	.00	.000

Table A.91 WATCH results for Sumikawa well SM-2 78/09/25. The data may be less accurate and is certainly less complete (e.g. only CO₂ and H₂S) in this early analysis. Its relatively low temperature (200~C?) and high Mg suggests near-surface influence, but the high Cl/B and Cl/ other anions suggest the opposite. This water is saturated with anhydrite, muscovite and analcime, but apparently supersaturated with laumontite, wairakite, calcite and albite, possibly due to the low temperature or problems with the analysis (continued)..

Log solubility products of minerals in deep water (Al based on microcline)

	Theor.	Calc.		Theor.	Calc.		Theor.	Calc.
Adularia	-14.611	-15.390	Albite, low	-14.128	-13.631	Analcime	-11.573	-11.356
Anhydrite	-7.481	-7.608	Calcite	-11.901	-11.113	Chalcedony	-2.143	-2.276
Mg-Chlorite	-82.523	-68.439	Fluorite	-10.785	99.999	Goethite	.432	-1.902
Laumontite	-24.519	-23.137	Microcline	-15.390	-15.390	Magnetite	-20.162	-23.095
Ca-Montmor.	-72.928	-78.628	K-Montmor.	-34.355	-40.859	Mg-Montmor.	-74.400	-78.853
Na-Montmor.	-34.606	-39.101	Muscovite	-17.950	-17.811	Quartz	-2.274	-2.276
Wairakite	-24.040	-23.137	Wollastonite	8.092	8.459	Zoisite	-36.631	-33.684
Epidote	-37.010	-34.375	Marcasite	-47.834	-65.376	Talc	9.948	22.425
Chrysotile	16.527	26.977	Sil. amorph.	-1.755	-2.276			

Appendix B

Drilling and Completion Data for Sumikawa Area Boreholes

Drilling and Completion Data for Sumikawa Area Boreholes

50-HM-3 -- Borehole Summary

Surface Elevation: 974.0 mASL
 Coordinates: East= -4315.0
 North= -1490.0
 Vertical Borehole? T
 Vertical depth: 500.7 meters
 Total depth: 500.7 meters

History:

Start Time	End Time	Status
30sep75 00:00	19nov75 00:00	Drilling
25oct75 00:00		ShutIn
19nov75 00:00		ShutIn
27nov75 00:00		ShutIn
02dec75 13:30	02dec75 16:50	Injection
02dec75 16:50		ShutIn
31jan86 00:00		ShutIn

50-HM-3 -- Lost circulation

starting depth*	ending depth*	starting rate#	ending rate#	
25.0	25.0	250	250	total loss
45.0	45.0	250	250	total loss
93.0	93.0	250	250	total loss
108.1	108.1	250	250	total loss
109.6	109.6	56	56	
116.9	116.9	250	250	total loss
140.0	140.0	250	250	total loss
146.0	146.0	30	30	

* Vertical Depth (m)
 # 1/min

50-HM-3 -- Hole/Casing data

starting depth*	ending depth*	hole_size	casing_size	
0.0	11.5	7 5/8"	6"	cemented
0.0	120.0	146mm	4"	cemented
0.0	294.7	100mm	3"	cemented
290.9	500.7	79mm	73mm	uncemented

slotted regions:
 350.9 500.7

* Vertical Depth (m)

50-HM-3 -- Stratigraphy data

starting depth*	ending depth*	maj.code	maj.name	min.code	min.name
0.0	81.8	L	Andesitic lavas & pyro.	-	-
81.8	229.5	K	lake sediments	-	-
229.5	348.0	X	Dacitic lava	-	-
348.0	349.0	E	Black shales	-	-
349.0	410.0	F	Dacitic tuff & breccia	-	-
410.0	500.7	E	Black shales	-	-

* Vertical Depth (m)

Drilling and Completion Data for Sumikawa Area Boreholes

N60-KY-1 -- Borehole Summary

Surface Elevation: 991.0 mASL
 Coordinates: East= -4558.5
 North= -1610.5
 Vertical Borehole? T
 Vertical depth: 1604.0 meters
 Total depth: 1604.0 meters

History:

Start Time	End Time	Status
20oct85 00:00	13dec85 00:00	Drilling
14dec85 12:00		ShutIn
01may86 00:00	26jul86 00:00	Drilling
03aug86 00:00		ShutIn
03aug86 15:00	03aug86 16:00	Injection
03aug86 16:00		ShutIn
07aug86 13:20	07aug86 19:00	Injection
07aug86 19:00		ShutIn
10aug86 12:00		ShutIn

N60-KY-1 -- Lost circulation

starting depth*	ending depth*	starting rate#	ending rate#	
5.5	5.5	200	200	
12.9	12.9	300	300	
16.7	16.7	380	380	
38.8	38.8	202	202	
40.3	40.3	800	800	
346.5	346.5	76	76	
382.9	382.9	23	23	
530.0	530.0	35	35	
996.7	996.7	100	100	total loss
1160.0	1160.0	14	14	
1562.1	1562.1	7	7	

* Vertical Depth (m)
 # 1/min

N60-KY-1 -- Hole/Casing data

starting depth*	ending depth*	hole_size	casing_size	
0.0	42.5	14 3/4"	12"	cemented
0.0	290.7	10 5/8"	8 5/8"	cemented
0.0	501.0	7 5/8"	6"	cemented
0.0	1001.0	5 5/8"	4"	cemented
993.5	1604.0	101mm	3"	uncemented

slotted regions:

1140.8	1178.9
1271.6	1347.8
1380.6	1462.3
1467.8	1489.6
1511.3	1604.0

* Vertical Depth (m)

N60-KY-1 -- Stratigraphy data

starting	ending
----------	--------

Drilling and Completion Data for Sumikawa Area Boreholes

depth*	depth*	maj.code	maj.name	min.code	min.name
0.0	130.0	L	Andesitic lavas & pyro.	-	-
130.0	305.0	K	lake sediments	-	-
305.0	593.7	F	Dacitic tuff & breccia	-	-
593.7	1432.0	C/E	Black shales & Dacitic tu	-	-
1432.0	1604.0	B	Andesites	-	-

* Vertical Depth (m)

=====

Drilling and Completion Data for Sumikawa Area Boreholes

O-5T -- Borehole Summary

Surface Elevation: 835.0 mASL
 Coordinates: East= -3046.0
 North= -1589.0
 Vertical Borehole? T
 Vertical depth: 749.1 meters
 Total depth: 749.1 meters

History:

Start Time	End Time	Status
26jul68 00:00	23oct68 00:00	Drilling
31jul72 00:00		ShutIn
04aug77 00:00	12aug77 00:00	Drilling
13aug77 00:00		ShutIn
22sep78 16:22	22sep78 18:20	Injection
22sep78 18:20		ShutIn
05oct85 00:00		ShutIn
30sep87 00:00		ShutIn
26apr88 00:00		ShutIn

O-5T -- Lost circulation

starting depth*	ending depth*	starting rate#	ending rate#	
383.0	383.0	120	120	total loss
437.0	437.0	120	120	total loss
747.0	747.0	84	84	total loss

* Vertical Depth (m)

1/min

O-5T -- Hole/Casing data

starting depth*	ending depth*	hole_size	casing_size	
0.0	51.0	7 5/8"	6"	cemented
0.0	152.2	146mm	4"	cemented
0.0	251.4	92mm	86mm	cemented
233.7	446.7	92mm	73mm	uncemented
446.7	749.1	64mm	open hole	

slotted regions:

233.7 446.7

* Vertical Depth (m)

O-5T -- Stratigraphy data

starting depth*	ending depth*	maj.code	maj.name	min.code	min.name
0.0	51.0	L	Andesitic lavas & pyro. -	-	-
51.0	459.3	F	Dacitic tuff & breccia -	-	-
459.3	492.1	D	Andesitic tuff & black sh -	-	-
492.1	646.7	C/E	Black shales & Dacitic tu -	-	-
646.7	749.1	X	Dacitic lava -	-	-

* Vertical Depth (m)

Drilling and Completion Data for Sumikawa Area Boreholes

S-1 -- Borehole Summary

Surface Elevation: 1015.6 mASL
 Coordinates: East= -3700.3
 North= -2105.0
 Vertical Borehole? T
 Vertical depth: 448.4 meters
 Total depth: 448.4 meters

History:

Start Time	End Time	Status
06oct81 00:00	20nov81 00:00	Drilling
04nov81 20:00		ShutIn
17nov81 00:00		ShutIn
30apr82 00:00		ShutIn
05may82 00:00		Injection
20may82 17:05	20may82 18:19	Injection
26may82 03:26	26may82 04:14	Injection

S-1 -- Lost circulation

starting depth*	ending depth*	starting rate#	ending rate#	
436.0	436.0	250	250	total loss
437.5	437.5	250	250	total loss

* Vertical Depth (m)
 # l/min

S-1 -- Hole/Casing data

starting depth*	ending depth*	hole_size	casing_size	
0.0	31.0	9 5/8"	8"	cemented
0.0	304.8	7 5/8"	6"	cemented
304.8	448.4	5 5/8"	open hole	

* Vertical Depth (m)

S-1 -- Stratigraphy data

starting depth*	ending depth*	maj.code	maj.name	min.code	min.name
0.0	196.0	L	Andesitic lavas & pyro.	-	-
196.0	200.0	K	lake sediments	-	-
200.0	484.4	F	Dacitic tuff & breccia	-	-

* Vertical Depth (m)

Drilling and Completion Data for Sumikawa Area Boreholes

S-2 -- Borehole Summary

Surface Elevation: 1071.1 mASL
 Coordinates: East= -3702.7
 North= -2589.1
 Vertical Borehole? T
 Vertical depth: 1065.1 meters
 Total depth: 1065.1 meters

History:

Start Time	End Time	Status
20oct81 00:00	20may82 00:00	Drilling
23jun82 22:05	23jun82 23:02	Injection
24jun82 06:00		ShutIn
07jul82 00:00	08jul82 00:00	Production
16jul82 15:55	16jul82 16:55	Injection
04oct82 19:50	04oct82 21:38	Injection
06oct82 00:00	21oct82 00:00	Drilling
16oct82 17:23	16oct82 19:10	Injection
22oct82 00:00		ShutIn
23oct82 16:31	23oct82 18:05	Injection
24oct82 00:00		Injection
26oct82 00:00		ShutIn
10nov82 00:00		Production
12nov82 00:00		ShutIn
16may83 00:00		ShutIn
06aug84 00:00		Injection
02sep86 11:20	03nov86 16:30	Injection
30sep88 10:30	18oct88 00:00	Injection
03jul89 10:00	30nov89 12:00	Injection

S-2 -- Lost circulation

starting depth*	ending depth*	starting rate#	ending rate#	
771.4	771.4	120	120	total loss
797.2	798.5	60	60	
862.9	862.9	93	93	total loss
897.1	897.1	110	110	total loss
903.4	903.4	110	110	total loss
720.0	720.0	?	?	
914.8	914.8	120	120	total loss
935.0	935.0	?	?	

* Vertical Depth (m)
 # l/min
 ? missing data

S-2 -- Hole/Casing data

starting depth*	ending depth*	hole_size	casing_size	
0.0	30.5	9 5/8"	8"	cemented
0.0	305.6	7 5/8"	6"	cemented
0.0	703.3	5 5/8"	4"	cemented
703.3	1065.1	101mm	open hole	

* Vertical Depth (m)

S-2 -- Stratigraphy data

starting	ending
----------	--------

Drilling and Completion Data for Sumikawa Area Boreholes

depth*	depth*	maj.code	maj.name	min.code	min.name
0.0	280.0	L	Andesitic lavas & pyro.	-	-
280.0	430.0	K	lake sediments	-	-
430.0	570.0	F	Dacitic tuff & breccia	-	-
570.0	1065.1	C	Dacitic tuff	-	-

* Vertical Depth (m)

=====

Drilling and Completion Data for Sumikawa Area Boreholes

S-3 -- Borehole Summary

Surface Elevation: 1048.5 mASL
 Coordinates: East= -4248.6
 North= -2162.3
 Vertical Borehole? T
 Vertical depth: 805.1 meters
 Total depth: 805.1 meters

History:

Start Time	End Time	Status
22jul82 00:00	11jun83 00:00	Drilling
02sep82 12:51	02sep82 13:52	Injection
06oct82 16:13	06oct82 17:13	Injection
08dec82 00:00		ShutIn
16may83 13:45	16may83 16:35	Injection
12jun83 09:35	12jun83 14:30	Injection
16jun83 06:00		ShutIn
28jan84 00:00		ShutIn
15jun89 09:00	15jul89 15:00	Injection

S-3 -- Lost circulation

starting depth*	ending depth*	starting rate#	ending rate#	
112.0	112.0	20	20	
208.7	208.7	12	12	
419.0	419.0	55	55	
427.6	427.6	600	600	total loss
432.5	440.3	25	25	
441.3	450.0	125	125	
474.0	481.0	21	21	
508.8	508.8	325	325	
547.0	547.0	400	400	total loss
644.0	644.0	23	23	
647.5	647.5	90	90	total loss
755.0	755.0	?	?	

* Vertical Depth (m)
 # l/min
 ? missing data

S-3 -- Hole/Casing data

starting depth*	ending depth*	hole_size	casing_size	
0.0	38.1	12 1/4"	10"	cemented
0.0	254.8	9 5/8"	7 5/8"	cemented
1.9	601.3	5 5/8"	4"	cemented
4.9	804.5	101mm	3"	uncemented
804.5	805.1	101mm		open hole

slotted regions:
 602.8 804.5

* Vertical Depth (m)

S-3 -- Stratigraphy data

starting depth*	ending depth*	maj.code	maj.name	min.code	min.name

Drilling and Completion Data for Sumikawa Area Boreholes

0.0	290.0	L	Andesitic lavas & pyro.	-	-
290.0	410.0	K	lake sediments	-	-
410.0	610.0	F	Dacitic tuff & breccia	-	-
610.0	805.1	C/E	Black shales & Dacitic tu	-	-

* Vertical Depth (m)

=====

Drilling and Completion Data for Sumikawa Area Boreholes

S-4 -- Borehole Summary

Surface Elevation: 1106.7 mASL
 Coordinates: East= -4322.0
 North= -2763.0
 Vertical Borehole? T
 Vertical depth: 1552.0 meters
 Total depth: 1552.0 meters

History:

Start Time	End Time	Status
01jul83 00:00	01nov83 00:00	Drilling
11aug83 00:00		ShutIn
06nov83 19:50	06nov83 21:20	Injection
07nov83 09:11	07nov83 11:46	Injection
07nov83 11:46	07nov83 11:46	ShutIn
19nov83 00:00		ShutIn
30nov83 00:00		ShutIn
08nov84 00:00		ShutIn
24nov85 00:00		ShutIn
02sep86 11:20	03nov86 16:30	Production
03nov86 16:30		ShutIn
25oct88 09:05	24nov88 16:50	Production
24nov88 16:50		ShutIn
16may89 19:00	19may89 14:00	Injection
10jun89 08:51	23nov89 17:35	Production
23nov89 17:35		ShutIn

S-4 -- Lost circulation

starting depth*	ending depth*	starting rate#	ending rate#	
5.7	5.7	1000	1000	total loss
33.0	33.0	800	800	total loss
81.5	81.5	1845	1845	total loss
174.3	174.3	1394	1394	total loss
975.0	975.0	130	130	
1101.8	1108.3	140	140	
1172.4	1172.4	60	60	
1522.6	1522.6	800	800	total loss

* Vertical Depth (m)
 # l/min

S-4 -- Hole/Casing data

starting depth*	ending depth*	hole_size	casing_size	
0.0	37.0	26"	20"	cemented
0.0	291.6	17 1/2"	13 3/8"	cemented
1.1	695.3	12 1/4"	9 5/8"	cemented
7.9	1071.0	8 1/2"	7"	cemented
1071.0	1552.0	6 1/4"	open hole	

* Vertical Depth (m)

S-4 -- Stratigraphy data

starting depth*	ending depth*	maj.code	maj.name	min.code	min.name
0.0	420.0	L	Andesitic lavas & pyro.	-	-

Drilling and Completion Data for Sumikawa Area Boreholes

420.0	550.0	K	lake sediments	-	-
550.0	730.0	F	Dacitic tuff & breccia	-	-
730.0	840.0	E	Black shales	-	-
840.0	1160.0	C	Dacitic tuff	-	-
1160.0	1552.0	B	Andesites	-	-

* Vertical Depth (m)

=====

Drilling and Completion Data for Sumikawa Area Boreholes

SA-1 -- Borehole Summary

Surface Elevation: 1107.1 mASL
 Coordinates: East= -4369.2
 North= -2794.2
 Vertical Borehole? F
 Vertical depth: 1831.8 meters
 Total depth: 2002.0 meters

History:

Start Time	End Time	Status
29jul86 00:00	10oct86 00:00	Drilling
11oct86 20:56	12oct86 01:17	Injection
14oct86 00:00		ShutIn
16oct87 00:00		ShutIn
22oct88 09:45	25nov88 19:50	Production
15apr89 17:35	16may89 14:43	Injection
01jun89 09:10	29nov89 16:30	Production

SA-1 -- Lost circulation

starting depth*	ending depth*	starting rate#	ending rate#	
37.0	37.0	80	80	
122.0	122.0	200	200	
213.9	213.9	933	933	
1655.9	1655.9	130	130	
1726.4	1726.4	1660	1660	total loss
1735.8	1831.8	?	?	blind drilling

* Vertical Depth (m)
 # l/min
 ? missing data

SA-1 -- Hole/Casing data

starting depth*	ending depth*	hole_size	casing_size	
0.0	33.7	840mm	20"	cemented
0.0	367.3	17 1/2"	13 3/8"	cemented
0.0	1056.4	12 1/4"	9 5/8"	cemented
991.6	1830.9	8 1/2"	7"	uncemented
1830.9	1831.8	8 1/2"	open hole	

slotted regions:

991.6	1056.4
1089.3	1116.1
1255.6	1281.3
1323.8	1358.1
1435.9	1830.7

* Vertical Depth (m)

SA-1 -- Stratigraphy data

starting depth*	ending depth*	maj.code	maj.name	min.code	min.name
0.0	434.8	L	Andesitic lavas & pyro.	-	-
434.8	573.8	K	lake sediments	-	-
573.8	756.4	F	Dacitic tuff & breccia	-	-
756.4	1276.2	C/E	Black shales & Dacitic tu	-	-

Drilling and Completion Data for Sumikawa Area Boreholes

1276.2 1593.1 B Andesites - -
 1593.1 1831.3 Z Granodiorite and diorite - -

* Vertical Depth (m)

=====

SA-1 -- Deviation data (m)

Meas.depth	Vert.depth	E_dev.	N_dev.

100.0	100.0	0.00	0.00
360.0	359.9	-1.63	7.60
446.5	446.3	-2.13	10.69
476.5	476.3	-3.62	11.33
512.0	511.6	-7.12	11.32
550.0	549.2	-12.66	10.59
604.0	602.3	-22.18	9.30
666.0	662.8	-35.69	8.56
712.0	706.8	-49.00	9.10
767.0	758.3	-68.25	10.63
806.0	794.0	-83.92	12.07
842.0	826.7	-98.98	13.66
879.0	860.0	-114.98	15.34
933.0	908.4	-138.70	17.83
987.0	956.7	-162.80	20.36
1042.0	1005.8	-187.28	22.94
1125.0	1079.3	-225.89	25.18
1206.0	1150.1	-265.25	24.69
1300.0	1229.9	-314.82	23.82
1444.0	1351.0	-392.69	21.61
1644.0	1521.9	-496.39	16.72
1790.0	1650.2	-565.66	9.44
2002.0	1831.8	-672.44	-14.02

Drilling and Completion Data for Sumikawa Area Boreholes

SA-2 -- Borehole Summary

Surface Elevation: 1107.1 mASL
 Coordinates: East= -4355.8
 North= -2786.9
 Vertical Borehole? F
 Vertical depth: 1943.1 meters
 Total depth: 2004.6 meters

History:

Start Time	End Time	Status
19oct86 00:00	16nov86 00:00	Drilling
03aug87 00:00	25sep87 00:00	Drilling
22sep87 00:00		ShutIn
22sep87 16:45	22sep87 18:45	Injection
22sep87 18:45		ShutIn
22sep87 22:25	23sep87 01:00	Injection
23sep87 01:00		ShutIn
29sep87 00:00		ShutIn
24oct88 12:40	26nov88 11:50	Production
16apr89 17:53	17may89 13:36	Injection
07jun89 09:07	02dec89 14:05	Production

SA-2 -- Lost circulation

starting depth*	ending depth*	starting rate#	ending rate#	
107.0	107.0	250	250	
214.0	214.0	127	127	
270.0	270.0	74	74	
311.0	311.0	73	73	
676.9	676.9	2451	2451	total loss
1084.6	1943.1	?	?	Aerated Mud drilling
1903.5	1903.5	2077	2077	total loss

* Vertical Depth (m)

l/min

? missing data

SA-2 -- Hole/Casing data

starting depth*	ending depth*	hole_size	casing_size	
0.0	33.6	750mm	20"	cemented
0.0	334.0	17 1/2"	13 3/8"	cemented
0.0	1060.6	12 1/4"	9 5/8"	cemented
989.6	1941.5	8 1/2"	7"	uncemented
1941.5	1943.1	8 1/2"	open hole	

slotted regions:

1343.4 1941.5

* Vertical Depth (m)

SA-2 -- Stratigraphy data

starting depth*	ending depth*	maj.code	maj.name	min.code	min.name
0.0	434.7	L	Andesitic lavas & pyro.	-	-
434.7	571.1	K	lake sediments	-	-
571.1	767.4	F	Dacitic tuff & breccia	-	-

Drilling and Completion Data for Sumikawa Area Boreholes

767.4	897.2	C/E	Black shales & Dacitic tu	-	-
897.2	1069.4	C	Dacitic tuff	-	-
1069.4	1152.8	C/E	Black shales & Dacitic tu	-	-
1152.8	1941.5	C	Dacitic tuff	-	-

* Vertical Depth (m)

SA-2 -- Deviation data (m)

Meas.depth	Vert.depth	E_dev.	N_dev.
360.0	360.0	0.00	0.00
384.0	384.0	0.11	-0.45
403.0	403.0	0.50	-1.56
424.0	423.8	0.94	-3.73
442.0	441.7	1.08	-6.05
457.0	456.5	1.35	-8.45
466.0	465.3	1.56	-10.07
475.0	474.2	1.84	-11.84
524.0	521.9	3.50	-22.81
561.0	557.7	4.97	-31.96
607.0	601.7	7.37	-45.02
661.0	652.7	9.78	-62.80
715.0	703.0	11.14	-82.39
769.0	752.6	11.42	-103.56
827.0	806.0	11.16	-126.25
899.0	872.8	11.96	-153.03
990.0	958.1	13.14	-184.88
1040.0	1005.2	13.59	-201.57
1128.0	1088.3	14.35	-230.41
1168.0	1126.6	16.04	-241.81
1186.0	1144.1	17.01	-246.13
1269.0	1224.9	22.30	-264.02
1349.0	1303.1	28.97	-280.00
2004.6	1943.1	82.31	-411.48

Drilling and Completion Data for Sumikawa Area Boreholes

SA-4 -- Borehole Summary

Surface Elevation: 1107.1 mASL
 Coordinates: East= -4342.3
 North= -2779.6
 Vertical Borehole? F
 Vertical depth: 1738.6 meters
 Total depth: 2009.0 meters

History:

Start Time	End Time	Status
01oct87 00:00	15nov87 00:00	Drilling
13nov87 00:00		ShutIn
05may88 00:00	01jun88 00:00	Drilling
29may88 00:00		ShutIn
30may88 00:00		ShutIn
30may88 07:05	30may88 08:50	Injection
30may88 08:50		ShutIn
30may88 12:00		ShutIn
31may88 00:00		ShutIn
23oct88 09:20	27nov88 15:35	Production
28nov88 00:00		ShutIn
17apr89 19:20	18may89 13:10	Injection
29apr89 00:00	30apr89 14:32	ShutIn
04jun89 09:00	26nov89 10:30	Production

SA-4 -- Lost circulation

starting depth*	ending depth*	starting rate#	ending rate#	
123.0	123.0	35	35	
140.0	140.0	318	318	
754.4	754.4	2490	2490	total loss
782.1	782.1	308	308	
819.2	819.2	73	73	
841.9	841.9	137	137	
922.3	922.3	2108	2108	total loss
925.8	925.8	2108	2108	total loss
976.6	976.6	408	408	
1238.5	1738.6	?	?	Aerated Mud drilling

* Vertical Depth (m)
 # 1/min
 ? missing data

SA-4 -- Hole/Casing data

starting depth*	ending depth*	hole_size	casing_size	
0.0	33.6	750mm	20"	cemented
0.0	401.7	17 1/2"	13 3/8"	cemented
0.0	1129.7	12 1/4"	9 5/8"	cemented
1089.8	1731.3	8 1/2"	7"	uncemented
1731.3	1738.6	8 1/2"	open hole	

slotted regions:

1174.0	1426.4
1454.9	1497.5
1541.2	1645.6
1699.9	1723.5

* Vertical Depth (m)

Drilling and Completion Data for Sumikawa Area Boreholes

=====

SA-4 -- Stratigraphy data

starting depth*	ending depth*	maj.code	maj.name	min.code	min.name
0.0	432.7	L	Andesitic lavas & pyro.	-	-
432.7	577.2	K	lake sediments	-	-
577.2	780.3	F	Dacitic tuff & breccia	-	-
780.3	906.5	C/E	Black shales & Dacitic tu	-	-
906.5	1261.4	C	Dacitic tuff	-	-
1261.4	1587.9	B	Andesites	-	-
1587.9	1738.6	Z	Granodiorite and diorite	-	-

* Vertical Depth (m)

=====

SA-4 -- Deviation data (m)

Meas.depth	Vert.depth	E_dev.	N_dev.
100.0	100.0	-0.17	0.85
300.0	299.8	-4.40	6.77
515.0	511.5	-39.44	15.32
700.0	685.2	-101.68	25.92
926.0	889.9	-196.06	40.63
1113.0	1053.7	-282.31	65.39
1307.0	1217.2	-370.88	119.67
1516.0	1376.2	-495.86	170.30
1724.0	1524.1	-635.63	213.15
1900.0	1654.6	-746.16	254.63
2009.0	1738.6	-810.40	281.01

Drilling and Completion Data for Sumikawa Area Boreholes

SB-1 -- Borehole Summary

Surface Elevation: 1048.7 mASL
 Coordinates: East= -4289.9
 North= -2179.9
 Vertical Borehole? F
 Vertical depth: 2006.2 meters
 Total depth: 2086.1 meters

History:

Start Time	End Time	Status
11aug87 00:00	23oct87 00:00	Drilling
23oct87 00:00		ShutIn
25oct87 20:18	25oct87 22:40	Injection
25oct87 22:40		ShutIn
26oct87 11:41	26oct87 13:30	Injection
26oct87 13:30		ShutIn
08nov87 11:11	08nov87 17:50	Injection
08nov87 17:50		ShutIn
27may88 11:10	27may88 13:20	Injection
15aug88 04:30	15aug88 07:30	Injection
17nov88 10:20	22nov88 13:17	Injection
22nov88 13:17		ShutIn
25apr89 10:25	29may89 13:50	Injection
15jun89 09:07	01dec89 15:03	Production

SB-1 -- Lost circulation

starting depth*	ending depth*	starting rate#	ending rate#	
89.3	89.3	1990	1990	total loss
101.0	101.0	1990	1990	total loss
409.0	409.0	1590	1590	total loss
580.1	580.1	1990	1990	total loss
621.9	621.9	195	195	
646.3	646.3	1930	1930	total loss
1370.7	2006.2	?	?	Aerated Mud drilling

* Vertical Depth (m)

l/min

? missing data

SB-1 -- Hole/Casing data

starting depth*	ending depth*	hole_size	casing_size	
0.0	38.8	800mm	20"	cemented
0.0	274.9	17 1/2"	13 3/8"	cemented
0.0	1062.1	12 1/4"	9 5/8"	cemented
1062.1	2006.2	8 1/2"	open hole	

* Vertical Depth (m)

SB-1 -- Stratigraphy data

starting depth*	ending depth*	maj.code	maj.name	min.code	min.name
0.0	279.9	L	Andesitic lavas & pyro.	-	-
279.9	449.6	K	lake sediments	-	-
449.6	670.7	F	Dacitic tuff & breccia	-	-
670.7	1001.7	C/E	Black shales & Dacitic tu	-	-

Drilling and Completion Data for Sumikawa Area Boreholes

1001.7 1753.3 B Andesites - -
 1753.3 2006.2 Z Granodiorite and diorite - -

* Vertical Depth (m)

SB-1 -- Deviation data (m)

Meas.depth	Vert.depth	E_dev.	N_dev.
140.0	140.0	0.69	0.91
350.0	349.9	6.26	1.10
436.0	435.8	3.20	-1.21
485.0	484.2	-3.30	-4.60
523.0	521.4	-9.37	-9.26
561.0	558.2	-16.70	-15.24
608.0	603.1	-27.60	-23.76
675.0	666.1	-45.82	-37.67
760.0	744.8	-72.84	-54.88
818.0	798.5	-93.14	-63.18
874.0	850.0	-114.13	-69.60
931.0	902.2	-136.03	-75.98
988.0	954.0	-159.08	-82.16
1055.0	1015.5	-185.14	-87.33
1111.0	1067.7	-205.37	-89.57
1168.0	1120.7	-226.26	-90.12
1225.0	1174.2	-248.02	-90.60
1283.0	1227.3	-269.29	-90.87
1340.0	1280.6	-289.41	-92.53
1397.0	1334.3	-308.33	-95.36
1474.0	1407.7	-331.45	-98.51
1562.0	1492.3	-354.75	-104.40
1675.0	1602.0	-381.39	-110.44
1788.0	1712.1	-405.89	-116.73
1873.0	1795.4	-421.26	-123.48
1981.0	1902.1	-438.05	-123.89
2058.0	1978.4	-447.07	-120.70
2086.1	2006.2	-449.87	-118.74

Drilling and Completion Data for Sumikawa Area Boreholes

SB-2 -- Borehole Summary

Surface Elevation: 1048.7 mASL
 Coordinates: East= -4275.6
 North= -2173.0
 Vertical Borehole? F
 Vertical depth: 1308.0 meters
 Total depth: 1384.2 meters

History:

Start Time	End Time	Status
01nov87 00:00	10nov87 00:00	Drilling
28may88 00:00	23jun88 00:00	Drilling
21jun88 12:00		ShutIn
22jun88 10:43	22jun88 15:00	Injection
22jun88 15:00	22jun88 15:00	ShutIn
22oct88 12:18	24nov88 16:50	Injection
24nov88 16:50		ShutIn
29apr89 13:55	30may89 12:50	Injection
01jun89 12:45	29nov89 16:30	Injection

SB-2 -- Lost circulation

starting depth*	ending depth*	starting rate#	ending rate#	
95.0	95.0	1841	1841	total loss
120.0	120.0	487	487	
437.9	437.9	44	44	
472.7	472.7	199	199	
559.8	559.8	2240	2240	total loss
636.3	636.3	92	92	
828.9	1308.0	?	?	Aerated Mud drilling

* Vertical Depth (m)
 # l/min
 ? missing data

SB-2 -- Hole/Casing data

starting depth*	ending depth*	hole_size	casing_size	
0.0	38.8	750mm	20"	cemented
0.0	273.5	17 1/2"	13 3/8"	cemented
0.0	678.4	12 1/4"	9 5/8"	cemented
678.4	1308.0	8 1/2"	open hole	

* Vertical Depth (m)

SB-2 -- Stratigraphy data

starting depth*	ending depth*	maj.code	maj.name	min.code	min.name
0.0	283.4	L	Andesitic lavas & pyro.	-	-
283.4	446.6	K	lake sediments	-	-
446.6	653.9	F	Dacitic tuff & breccia	-	-
653.9	1109.9	E	Black shales	-	-
1109.9	1239.4	C/E	Black shales & Dacitic tu	-	-
1239.4	1306.9	C	Dacitic tuff	-	-

* Vertical Depth (m)

Drilling and Completion Data for Sumikawa Area Boreholes

SB-2 -- Deviation data (m)

Meas.depth	Vert.depth	E_dev.	N_dev.
0.0	0.0	0.00	0.00
220.0	219.9	-0.71	2.65
323.0	322.0	-5.31	14.86
440.0	436.9	-11.77	35.93
582.0	574.3	-16.69	71.26
709.0	691.9	-22.93	118.68
820.0	792.0	-35.01	164.92
936.0	896.4	-56.88	211.99
1048.0	997.1	-86.43	248.96
1125.0	1068.2	-107.99	269.18
1264.0	1197.0	-149.33	301.05
1384.2	1308.0	-189.04	324.42

Drilling and Completion Data for Sumikawa Area Boreholes

SB-3 -- Borehole Summary

Surface Elevation: 1048.7 mASL
 Coordinates: East= -4262.1
 North= -2166.5
 Vertical Borehole? F
 Vertical depth: 1365.9 meters
 Total depth: 1541.9 meters

History:

Start Time	End Time	Status
27jun88 00:00	05aug88 00:00	Drilling
16jul88 00:00		ShutIn
03aug88 00:00		ShutIn
05aug88 12:30	05aug88 15:30	Injection
05aug88 15:30		ShutIn
18nov88 13:18	22nov88 13:14	Injection
22nov88 13:14		ShutIn
25apr89 14:01	31may89 13:30	Injection
15jun89 09:07	01dec89 15:30	Injection

SB-3 -- Lost circulation

starting depth*	ending depth*	starting rate#	ending rate#	
101.0	101.0	192	192	
790.5	790.5	355	355	
804.9	1365.9	?	?	Aerated Mud drilling

* Vertical Depth (m)

1/min

? missing data

SB-3 -- Hole/Casing data

starting depth*	ending depth*	hole_size	casing_size	
0.0	16.9	26"	20"	cemented
0.0	278.5	17 1/2"	13 3/8"	cemented
0.0	681.6	12 1/2"	9 5/8"	cemented
681.6	1365.9	8 1/2"	open hole	

* Vertical Depth (m)

SB-3 -- Stratigraphy data

starting depth*	ending depth*	maj.code	maj.name	min.code	min.name
0.0	283.3	L	Andesitic lavas & pyro.	-	-
283.3	441.2	K	lake sediments	-	-
441.2	665.7	F	Dacitic tuff & breccia	-	-
665.7	1304.3	C/E	Black shales & Dacitic tu	-	-
1304.3	1366.0	B	Andesites	-	-

* Vertical Depth (m)

SB-3 -- Deviation data (m)

Meas.depth	Vert.depth	E_dev.	N_dev.
0.0	0.0	0.00	0.00

Drilling and Completion Data for Sumikawa Area Boreholes

130.0	130.0	0.17	-1.12
233.0	232.9	2.45	1.16
354.0	352.6	7.14	17.53
471.0	466.5	18.52	41.53
584.0	573.6	37.72	71.78
696.0	674.7	64.76	111.47
806.0	770.2	94.33	157.45
918.0	865.0	130.94	204.33
1020.0	950.0	175.14	239.12
1134.0	1047.7	228.66	262.65
1243.0	1138.6	287.31	275.97
1355.0	1226.7	354.41	292.56
1454.0	1299.8	419.33	307.72
1541.9	1365.9	473.40	328.40

Drilling and Completion Data for Sumikawa Area Boreholes

SC-1 -- Borehole Summary[†]

Surface Elevation: 1086.6 mASL
 Coordinates: East= -3885.5
 North= -2663.8
 Vertical Borehole? F
 Vertical depth: 2471.6 meters
 Total depth: 2486.0 meters

History:

Start Time	End Time	Status
27jul87 00:00	10nov87 00:00	Drilling
04oct87 00:00		ShutIn
05nov87 00:00		ShutIn
11nov87 00:00		ShutIn
15nov87 14:30	15nov87 17:05	Injection
16nov87 12:00		ShutIn
12may88 06:00		ShutIn
07jun88 12:45	07jun88 14:50	Injection
07jun88 14:50		ShutIn
30sep88 10:00	09oct88 10:00	Production
17oct88 10:00	15nov88 12:00	Production
15nov88 12:00		ShutIn
06oct89 09:08	28nov89 13:10	Production
28nov89 13:10		ShutIn
07apr90 16:00		ShutIn

SC-1 -- Lost circulation

starting depth*	ending depth*	starting rate#	ending rate#	
74.6	74.6	210	210	
1045.8	1045.8	100	100	
1080.7	1080.7	83	83	
1358.1	1358.1	190	190	
1380.0	1380.0	2100	2100	total loss
1387.9	1387.9	650	650	
1410.6	1410.6	583	583	
1430.6	1430.6	400	400	
1436.6	1436.6	1000	1000	
1448.6	1448.6	667	667	
1454.1	1454.1	1667	1667	
1499.5	1499.5	2000	2000	total loss
1703.3	1703.3	250	250	
1835.5	1835.5	600	600	
1861.3	1861.3	500	500	
1871.7	1871.7	750	750	
1977.5	2092.6	?	?	Aerated Mud drilling
2092.6	2471.6	?	?	blind drilling
2095.6	2095.6	1400	1400	total loss

* Vertical Depth (m)
 # l/min
 ? missing data

SC-1 -- Hole/Casing data

starting depth*	ending depth*	hole_size	casing_size	
0.0	40.7	1200mm	660mm	cemented
0.0	502.9	24"	18 5/8"	cemented
0.0	1018.4	17 1/2"	13 3/8"	cemented

Drilling and Completion Data for Sumikawa Area Boreholes

960.7	1799.3	12 1/4"	9 5/8"	cemented
1741.0	2466.8	8 1/2"	7"	uncemented
2466.8	2471.6	8 1/2"	open hole	

slotted regions:
1799.3 2466.8

* Vertical Depth (m)

SC-1 -- Stratigraphy data

starting depth*	ending depth*	maj.code	maj.name	min.code	min.name
0.0	339.9	L	Andesitic lavas & pyro. -	-	-
339.9	494.9	K	lake sediments -	-	-
494.9	654.9	F	Dacitic tuff & breccia -	-	-
654.9	2079.9	C/E	Black shales & Dacitic tu -	-	-
2079.9	2470.7	Z	Granodiorite and diorite -	-	-

* Vertical Depth (m)

SC-1 -- Deviation data (m)

Meas.depth	Vert.depth	E_dev.	N_dev.
50.0	50.0	-0.76	-0.83
150.0	150.0	-2.07	-2.39
250.0	249.9	-3.08	-3.85
350.0	349.9	-3.80	-5.19
450.0	449.9	-4.22	-6.42
550.0	549.9	-4.35	-7.54
650.0	649.9	-4.17	-8.55
750.0	749.8	-3.71	-9.44
850.0	849.8	-2.95	-10.22
950.0	949.8	-1.89	-10.89
1050.0	1049.8	-0.53	-11.44
1150.0	1149.7	0.55	-11.96
1250.0	1249.7	0.73	-12.52
1350.0	1349.7	0.76	-13.02
1450.0	1449.6	0.65	-13.46
1550.0	1549.4	0.54	-14.36
1650.0	1649.0	0.53	-16.01
1750.0	1748.6	0.52	-18.05
1850.0	1848.0	0.49	-20.48
1950.0	1947.0	3.53	-18.00
2050.0	2045.5	11.83	-6.83
2150.0	2143.7	22.91	8.73
2250.0	2241.5	36.76	28.68
2350.0	2339.1	48.44	49.18
2450.0	2436.6	57.15	69.60
2486.0	2471.6	60.11	77.37

†Original name: N61-SN-7D

Drilling and Completion Data for Sumikawa Area Boreholes

SD-1 -- Borehole Summary†

Surface Elevation: 1015.9 mASL
 Coordinates: East= -3752.8
 North= -2139.4
 Vertical Borehole? F
 Vertical depth: 1691.3 meters
 Total depth: 1704.3 meters

History:	Start Time	End Time	Status
	27aug86 00:00	10oct86 00:00	Drilling
	31aug86 00:00		ShutIn
	04sep86 18:40	04sep86 18:55	Injection
	12sep86 12:00		ShutIn
	12oct86 12:30	12oct86 16:20	Injection
	12oct86 16:20		ShutIn
	17oct86 15:30	17oct86 22:56	Injection
	17oct86 22:56		ShutIn
	03dec86 00:00		ShutIn
	05oct87 00:00		ShutIn
	17oct88 10:10	15nov88 12:00	Injection
	15nov88 12:00		ShutIn
	08aug89 09:15	01dec89 11:06	Production

SD-1 -- Lost circulation

starting depth*	ending depth*	starting rate#	ending rate#	
387.0	387.0	2800	2800	total loss
487.0	487.0	36	36	
799.7	799.7	400	400	
977.3	1691.3	?	?	Aerated Mud drilling

* Vertical Depth (m)
 # l/min
 ? missing data

SD-1 -- Hole/Casing data

starting depth*	ending depth*	hole_size	casing_size	
0.0	39.5	840mm	20"	cemented
0.0	183.9	17 1/2"	13 3/8"	cemented
0.0	706.9	12 1/4"	9 5/8"	cemented
641.0	1687.1	8 1/2"	7"	uncemented
1687.1	1691.3	8 1/2"	open hole	

slotted regions:
 781.6 922.7
 1043.5 1134.0
 1154.0 1244.7
 1274.9 1385.4
 1435.8 1496.0
 1515.6 1686.6

* Vertical Depth (m)

SD-1 -- Stratigraphy data

starting depth*	ending depth*	maj.code	maj.name	min.code	min.name

Drilling and Completion Data for Sumikawa Area Boreholes

0.0	190.0	L	Andesitic lavas & pyro.	-	-
190.0	200.0	K	lake sediments	-	-
200.0	475.0	F	Dacitic tuff & breccia	-	-
475.0	1242.9	C/E	Black shales & Dacitic tu	-	-
1242.9	1371.2	B/E	Black shales & andesitic	-	-
1371.2	1691.3	B	Andesites	-	-

* Vertical Depth (m)

SD-1 -- Deviation data (m)

Meas.depth	Vert.depth	E_dev.	N_dev.
0.0	0.0	0.00	0.00
700.0	700.0	0.00	0.00
1704.3	1691.3	101.24	101.81

†Original name: N61-KY-2

Drilling and Completion Data for Sumikawa Area Boreholes

52E-SM-1 -- Borehole Summary

Surface Elevation: 780.0 mASL
Coordinates: East= -3177.0
North= -1240.0
Vertical Borehole? T
Vertical depth: 1002.6 meters
Total depth: 1002.6 meters

History:

Start Time	End Time	Status
01jul78 00:00	24sep78 00:00	Drilling
23sep78 00:00		ShutIn
27sep78 00:00		ShutIn
30sep78 13:08	30sep78 14:17	Injection

52E-SM-1 -- Hole/Casing data

starting depth*	ending depth*	hole_size	casing_size	
0.0	44.5	10 5/8"	8"	cemented
0.0	147.5	7 5/8"	6"	cemented
0.0	399.5	5 5/8"	4"	cemented
0.0	618.5	101mm	3"	cemented
609.4	1002.6	79mm	73mm	uncemented

slotted regions:

799.6 1002.6

* Vertical Depth (m)

52E-SM-1 -- Stratigraphy data

starting depth*	ending depth*	maj.code	maj.name	min.code	min.name
0.0	423.0	F	Dacitic tuff & breccia	-	-
423.0	752.0	C	Dacitic tuff	-	-
752.0	993.1	E	Black shales	-	-
993.1	1002.6	B	Andesites	-	-

* Vertical Depth (m)

Drilling and Completion Data for Sumikawa Area Boreholes

52E-SM-2 -- Borehole Summary

Surface Elevation: 897.0 mASL
 Coordinates: East= -3105.0
 North= -1880.0
 Vertical Borehole? T
 Vertical depth: 1001.0 meters
 Total depth: 1001.0 meters

History:

Start Time	End Time	Status
01jul78 00:00	09sep78 00:00	Drilling
21aug78 00:00		ShutIn
26aug78 17:00	26aug78 19:52	Injection
26sep78 00:00	16oct78 00:00	Drilling
15oct78 00:00		ShutIn

52E-SM-2 -- Lost circulation

starting depth*	ending depth*	starting rate#	ending rate#	
111.8	111.8	500	500	total loss
187.8	187.8	8	8	
500.7	500.7	70	70	
548.5	548.5	70	70	
549.7	549.7	100	100	total loss
637.2	637.2	70	70	
979.1	979.1	500	500	total loss

* Vertical Depth (m)

l/min

52E-SM-2 -- Hole/Casing data

starting depth*	ending depth*	hole_size	casing_size	
0.0	20.7	12 1/4"	10"	cemented
0.0	66.0	9 7/8"	8"	cemented
0.0	147.4	7 5/8"	6"	cemented
0.0	399.8	5 5/8"	4"	cemented
0.0	803.2	101mm	3"	cemented
793.8	1001.0	79mm	73mm	uncemented

slotted regions:

510.4 586.2
 793.8 1001.0

* Vertical Depth (m)

52E-SM-2 -- Stratigraphy data

starting depth*	ending depth*	maj.code	maj.name	min.code	min.name
0.0	400.0	F	Dacitic tuff & breccia	-	-
400.0	462.5	D	Andesitic tuff & black sh	-	-
462.5	594.6	C	Dacitic tuff	-	-
594.6	770.5	C/E	Black shales & Dacitic tu	-	-
770.5	894.7	X	Dacitic lava	-	-
894.7	914.7	E	Black shales	-	-
914.7	1001.0	X	Dacitic lava	-	-

* Vertical Depth (m)

Drilling and Completion Data for Sumikawa Area Boreholes

N59-SN-5 -- Borehole Summary

Surface Elevation: 1040.0 mASL
 Coordinates: East= -5711.0
 North= -2462.0
 Vertical Borehole? T
 Vertical depth: 1700.5 meters
 Total depth: 1700.5 meters

History:

Start Time	End Time	Status
31oct84 00:00	13dec84 00:00	Drilling
13dec84 00:00		ShutIn
28apr85 00:00	20sep85 00:00	Drilling
01jun85 00:00		ShutIn
01aug85 00:00		ShutIn
20sep85 00:00		ShutIn
14oct85 00:00	07nov85 00:00	Drilling
07nov85 00:00		ShutIn
12nov85 16:17	12nov85 20:44	Injection
13nov85 12:00		ShutIn

N59-SN-5 -- Lost circulation

starting depth*	ending depth*	starting rate#	ending rate#	
6.0	6.0	520	520	
99.6	99.6	93	93	total loss
111.0	111.0	93	93	total loss
118.0	118.0	93	93	total loss
235.3	235.3	53	53	
263.7	263.7	92	92	total loss
272.0	272.0	500	500	total loss
273.7	273.7	93	93	total loss
277.9	277.9	1100	1100	total loss
281.1	281.1	700	700	total loss
287.3	287.3	93	93	total loss
334.5	334.5	90	90	total loss
337.9	337.9	90	90	total loss
340.6	340.6	56	56	
343.6	343.6	1000	1000	total loss
347.2	347.2	90	90	total loss
351.7	351.7	90	90	total loss
357.3	357.3	90	90	total loss
368.6	368.6	100	100	total loss
377.8	377.8	100	100	total loss
384.4	384.4	1000	1000	total loss
390.6	390.6	1000	1000	total loss
394.0	394.0	800	800	total loss

* Vertical Depth (m)
 # l/min

N59-SN-5 -- Hole/Casing data

starting depth*	ending depth*	hole_size	casing_size	
0.0	48.5	14 3/4"	12"	cemented
0.0	301.4	10 5/8"	8 5/8"	cemented
0.0	702.5	7 5/8"	6"	cemented
0.0	1002.0	5 5/8"	4"	cemented
998.6	1700.5	101mm	3"	uncemented

Drilling and Completion Data for Sumikawa Area Boreholes

slotted regions:

1302.4	1379.5
1417.6	1488.3
1510.1	1531.9
1580.8	1618.9
1651.5	1689.6

* Vertical Depth (m)

=====

N59-SN-5 -- Stratigraphy data

starting depth*	ending depth*	maj.code	maj.name	min.code	min.name
0.0	455.0	L	Andesitic lavas & pyro.	-	-
455.0	758.9	K	lake sediments	-	-
758.9	1051.7	B	Andesites	-	-
1051.7	1700.5	Z	Granodiorite and diorite	-	-

* Vertical Depth (m)

=====

Appendix C

Characteristic Mass Output Data for Sumikawa Boreholes

Slim Hole S-1

Test Interval: APRIL 25-30, 1982

Date	Wellhead Pressure (bars)	Total Flow Rate (T/HR)
04-25-82	8.07	34.70
	10.03	31.80
	11.70	25.90
	13.66	19.80
	15.62	15.20
	18.56	4.60
04-27-82	8.37	35.70
	10.23	32.00
	11.70	27.20
	13.37	22.00
	16.11	12.40
	18.27	5.70
04-30-82	8.66	34.40
	11.21	27.80
	13.17	21.40
	14.94	15.70
	17.49	7.00
	18.76	3.70

Note: The slim hole produces only steam. The feedzone (436 m TVD = 580 m ASL) temperature is at least 213°C. The feedzone pressure is at least 20 bars (i.e., saturation pressure at 213°C).

Characteristic Mass Output Data for Sumikawa Boreholes

Slim Hole S-2

Test Interval: July 8-12, 1982

Date	Wellhead Pressure (bars)	Total Flow Rate (T/HR)
07-08-82	0.90	4.08
	1.10	4.08
	1.59	4.03
	2.28	3.94
	3.06	3.99
	4.24	4.02
	6.30	3.47
	9.04	1.37
07-10-82	0.90	3.97
	2.28	3.97
	3.45	3.87
	5.32	3.73
	7.47	3.39
	9.34	2.95
	10.02	1.45
07-12-82	0.90	4.28
	0.89	4.06
	0.89	4.00
	2.46	3.95
	4.62	3.79
	7.66	3.17
	9.52	2.09
	9.72	2.09

Note: Discharge test of the partially drilled hole (Total depth = 904.6 m). Enthalpy of the produced fluid suggests a two-phase entry. Circulation loss data/spinner survey (07-16-82) imply fluid entries at ~800 m and at ~900 m.

Characteristic Mass Output for Sumikawa Boreholes

Slim Hole S-2

Test Interval: November 3-11, 1982

Date	Wellhead Pressure (bars)	Total Flow Rate (T/HR)
11-03-82	4.04	53.86
	5.27	50.89
	6.20	44.83
	7.28	29.24
	7.57	23.93
11-11-82	4.02	48.20
	4.81	50.19
	5.98	45.19
	6.86	42.16
	7.55	30.38

Note: Discharge test of the redrilled hole (Total depth = 1065.1 m). The borehole feeds from a liquid zone (pressure = 52.5 bars, temperature = $245 \pm 5^{\circ}\text{C}$) at a depth of 940 m.

Characteristic Mass Output Data for Sumikawa Boreholes

Slim Hole S-3

Test Interval: July and October, 1983

Date	Wellhead Pressure (bars)	Total Flow Rate (T/HR)
07-14-83	2.41	15.07
	2.41	15.80
	2.95	13.33
	3.54	12.10
	4.32	10.95
	4.28	10.02
	5.21	7.06
10-22-83	2.10	14.73
	2.93	15.73
	4.11	14.32
	5.21	13.62
	6.48	12.52

Note: The borehole produces from a liquid feedzone (temperature ~240°C) at a depth of 700 ± 50 meters (349 ± 50 m ASL).

Characteristic Mass Output for Sumikawa Boreholes

Well S-4

Test Interval: 1984, 1985, 1986, 1988

Date	Wellhead Pressure (bars)	Total Flow Rate (T/HR)
09-13-84	9.14	145.33
	13.16	143.03
	17.28	139.03
	21.20	130.50
	24.93	88.16
	26.89	49.32
10-20-84	9.24	162.79
	13.16	156.31
	16.10	151.16
	20.03	125.86
	23.95	59.18
11-06-84	9.33	164.66
	13.44	158.29
	17.56	150.44
	20.02	116.75
	22.76	40.97
11-16-85	10.01	175.79
	15.80	166.43
	19.92	148.03
	23.45	90.04
11-03-86	10.22	179.53
	16.40	174.31
	21.50	133.63
	24.44	107.57
11-24-88	6.15	172.62
	10.27	175.39
	14.68	174.60
	20.17	146.38
	21.94	84.10

Note: Completed hole (drilled depth: 1552 m) produces from several feedzones in the open interval (1071-1552 m) of the well. Wellhead enthalpies imply *in situ* boiling.

Characteristic Mass Output Data for Sumikawa Boreholes

Well SA-1

Test Interval: November 25, 1988 and August 6, 1989

Date	Wellhead Pressure (bars)	Total Flow Rate (T/HR)
11-25-88	4.87	33.59
	10.56	31.79
	21.45	26.68
	28.31	13.10
08-06-89	3.66	61.70
	4.21	61.81

Note: Completed hole (drilled depth: 2002 m MD or 1832 m TVD) produces from a feedzone at about 1800 m TVD. The maximum temperature at bottomhole exceeds 305°C. In 1989, cold water was injected into SA-1 in order to improve the productivity of this well; the 1989 flowrates are substantially higher than 1988 flowrates. The produced fluid is mostly (over 80% by mass at atmospheric conditions) steam.

Characteristic Mass Output for Sumikawa Boreholes

Well SA-2

Test Interval: November 26, 1988 and August 9, 1989

Date	Wellhead Pressure (bars)	Total Flow Rate (T/HR)
11-26-88	4.19	22.00
	5.02	27.50
	7.44	25.09
	10.86	22.10
08-09-89	3.65	25.99
	4.05	27.40

Note: Completed hole (drilled depth: 2005 m MD or 1943 m TVD) produces steam from a feedzone at about 1450 m TVD. The maximum temperature at bottomhole is 320°C. In 1989, cold water was injected into SA-2 in order to improve the productivity of this well; the 1989 flowrates are about the same as 1988 flowrates.

Characteristic Mass Output Data for Sumikawa Boreholes

Well SA-4

Test Interval: November 27, 1988 and August 3, 1989

Date	Wellhead Pressure (bars)	Total Flow Rate (T/HR)
11-27-88	3.50	24.08
	4.87	23.69
	10.15	23.00
	15.17	22.28
	19.78	21.38
08-03-89	3.64	29.09
	4.18	29.59

Note: Completed hole (drilled depth: 2009 m MD or 1739 m TVD) produces steam from a feedzone at about 1240 m TVD. The maximum temperature at bottomhole exceeds 300°C. In 1989, cold water was injected into SA-4 in order to improve the productivity of this well; the 1989 flowrates are somewhat higher than 1988 flowrates.

Characteristic Mass Output for Sumikawa Boreholes

Well SB-1

Test Interval: June 30 - December 1, 1989

Date	Wellhead Pressure (bars)	Total Flow Rate (T/HR)
07-15-89	2.63	105.50
07-31-89	2.89	108.00
08-15-89	2.94	105.80
08-24-89	3.16	102.60
08-25-89	5.07	94.60
09-15-89	2.99	102.80
09-30-89	2.91	101.40
10-15-89	2.86	96.40
10-30-89	2.72	91.40
11-15-89	2.52	86.20
11-29-89	2.72	89.60
11-30-89	4.78	78.10
12-01-89	7.37	48.10

Note: Completed hole (drilled depth: 2086 m MD or 2006 m TVD) produces mainly liquid water from a depth of about 1600 m TVD. The bottomhole temperature is about 300°C; by comparison, the feedzone temperature is estimated to be about 280°C.

Characteristic Mass Output Data for Sumikawa Boreholes

Well SC-1 (SN-7D)

Test Interval: Oct. & Nov. 1988; Oct. & Nov. 1989

Date	Wellhead Pressure (bars)	Total Flow Rate (T/HR)
10-01-88	19.49	182.90
10-09-88	18.80	134.30
10-18-88	14.78	281.90
10-18-88	13.60	409.80
10-31-88	12.23	446.70
11-04-88	19.09	171.70
11-06-88	19.29	198.20
11-06-88	17.23	349.60
11-08-88	18.21	309.40
11-11-88	15.76	382.90
11-13-88	18.80	290.20
11-15-88	16.84	116.70
11-15-88	13.90	62.60
10-06-89	12.72	490.70
10-09-89	12.43	477.20
10-12-89	12.62	491.80
10-16-89	12.33	472.20
10-20-89	17.33	109.60
10-26-89	19.88	252.40
10-31-89	12.43	481.10
11-05-89	12.62	484.60
11-10-89	13.01	489.50
11-15-89	13.01	487.20
11-20-89	13.11	487.60
11-23-89	13.31	496.80
11-25-89	15.37	461.10
11-26-89	17.52	422.20
11-27-89	20.07	352.30
11-28-89	17.13	80.70

Note: Completed hole (drilled depth: 2486 m MD or 2472 m TVD) produces mainly liquid water from several feedzones between 1950 m MD (temp = 307°C) and 2320 m MD (temp ~246°C). The well has a pronounced temperature inversion. SC-1 is the most prolific producer at Sumikawa.

Characteristic Mass Output for Sumikawa Boreholes

Well SD-1 (KY-2)

Test Interval: August 8 - December 1, 1989

Date	Wellhead Pressure (bars)	Total Flow Rate (T/HR)
08-10-89	2.42	96.90
08-20-89	2.32	87.50
08-24-89	2.47	84.90
08-25-89	4.17	79.80
08-26-89	5.36	50.70
08-31-89	2.37	98.30
09-10-89	2.23	81.40
09-20-89	2.42	81.50
09-30-89	2.32	78.00
10-10-89	2.37	79.60
10-20-89	2.42	81.10
10-31-89	2.40	78.50
11-10-89	2.40	80.70
11-20-89	2.28	76.60
11-27-89	2.81	87.00
11-28-89	3.94	69.70
11-29-89	5.12	53.80
11-30-89	2.62	82.00

Note: Completed hole (drilled depth: 1704 m MD or 1691 m TVD) produces from several feedzones in the depth interval from 800 m MD to 1570 m MD. At the start of the production test, in situ flashing is limited to the shallowest feedzone; eventually, flashing extends to the deepest feedzone. The decline in production rate is probably due to the spread of flashing conditions to deeper feedzones. The feedzone temperatures range from ~210°C (1450-1490 m MD) to ~250°C (1550-1570 m MD).

Characteristic Mass Output Data for Sumikawa Boreholes

Slim Hole 52-E-SM-2

Test Interval: September 23, 1978

Date	Wellhead Pressure (bars)	Total Flow Rate (T/HR)
09-23-78	1.11	5.18
	1.15	5.15
	1.18	5.11
	1.25	4.90
	1.36	5.00
	1.44	4.79
	1.59	4.72
	1.79	4.57
	2.06	4.36
	2.23	3.89
	2.37	2.77

Note: Partially-drilled hole (drilled depth: 803 m). Feedzone depth: 550 m (?). Wellhead enthalpies suggest *in situ* boiling.

Characteristic Mass Output for Sumikawa Boreholes

Slim Hole 52E-SM-2

Test Interval: October 1978 - October 1978

Date	Wellhead Pressure (bars)	Total Flow Rate (T/HR)
10-19-78	2.68	26.14
10-20-78	2.68	35.50
11-02-78	2.97	26.68
11-17-78	2.85	25.52
	3.83	24.44
	4.82	24.08
	5.80	23.62
	6.78	22.68
	9.23	20.34
	11.68	19.37
	13.15	17.32
06-26-79	2.86	18.97
08-24-79	2.86	20.56
10-27-79	3.07	20.09

Note: Completed hole (drilled depth: 1001 m). Feedzone depth: 980 m (?). Wellhead enthalpies suggest that the slim hole feeds from a liquid zone at a temperature of about 230-240°C. Flow data for 06-26-79 and later indicate some *in situ* boiling.

Appendix D

Flow Rate History for 1989 Injection Test

Table D.1. Flow rate history for cold water injection into Sumikawa wells in April and May, 1989.

Injection data for Sumikawa Wells (April 16–May 31, 1989)

All times are in hours from 00:00 hrs on March 01, 1989

All flow rates in in cubic meters per sec

Start (hrs)	Stop (hrs)	SA-1 (m ³ /s)	SA-2 (m ³ /s)	SA-4 (m ³ /s)	S-4 (m ³ /s)	SB-1 (m ³ /s)	SB-2 (m ³ /s)	SB-3 (m ³ /s)
1097.5833	1112.1667	0.0042	0.0000	0.0000	0.0000	0.0000	0.0000	0.0000
1112.1667	1113.5000	0.0031	0.0000	0.0000	0.0000	0.0000	0.0000	0.0000
1113.5000	1115.5000	0.0138	0.0000	0.0000	0.0000	0.0000	0.0000	0.0000
1115.5000	1117.5000	0.0314	0.0000	0.0000	0.0000	0.0000	0.0000	0.0000
1117.5000	1119.5000	0.0494	0.0000	0.0000	0.0000	0.0000	0.0000	0.0000
1121.8833	1136.6667	0.0000	0.0034	0.0000	0.0000	0.0000	0.0000	0.0000
1136.6667	1138.6667	0.0000	0.0189	0.0000	0.0000	0.0000	0.0000	0.0000
1138.6667	1140.8333	0.0000	0.0336	0.0000	0.0000	0.0000	0.0000	0.0000
1140.8333	1142.8333	0.0000	0.0481	0.0000	0.0000	0.0000	0.0000	0.0000
1147.3333	1160.5000	0.0000	0.0000	0.0050	0.0000	0.0000	0.0000	0.0000
1160.5000	1162.5000	0.0000	0.0000	0.0171	0.0000	0.0000	0.0000	0.0000
1162.5000	1164.5000	0.0000	0.0000	0.0306	0.0000	0.0000	0.0000	0.0000
1164.5000	1166.5000	0.0000	0.0000	0.0408	0.0000	0.0000	0.0000	0.0000
1185.0000	1189.7000	0.0783	0.0000	0.0000	0.0000	0.0000	0.0000	0.0000
1198.0000	1206.0000	0.0094	0.0000	0.0000	0.0000	0.0000	0.0000	0.0000
1208.2500	1214.3333	0.0874	0.0000	0.0000	0.0000	0.0000	0.0000	0.0000
1222.0000	1230.0000	0.0083	0.0000	0.0000	0.0000	0.0000	0.0000	0.0000
1232.3333	1243.7500	0.0649	0.0000	0.0000	0.0000	0.0000	0.0000	0.0000
1246.0000	1254.0000	0.0090	0.0000	0.0000	0.0000	0.0000	0.0000	0.0000
1256.1667	1262.1667	0.0000	0.0851	0.0000	0.0000	0.0000	0.0000	0.0000
1280.3333	1289.3333	0.0000	0.1017	0.0000	0.0000	0.0000	0.0000	0.0000
1294.0000	1302.0000	0.0000	0.0083	0.0000	0.0000	0.0000	0.0000	0.0000
1304.1667	1310.6667	0.0000	0.1097	0.0000	0.0000	0.0000	0.0000	0.0000
1318.0000	1326.0000	0.0000	0.0045	0.0000	0.0000	0.0000	0.0000	0.0000
1330.4167	1334.0000	0.0000	0.0000	0.0000	0.0000	0.0344	0.0000	0.0000
1334.0167	1336.3333	0.0000	0.0000	0.0000	0.0000	0.0000	0.0000	0.0300

Table D.1. Flow rate history for cold water injection into Sumikawa wells in April and May, 1989 (continued).

Start (hrs)	Stop (hrs)	SA-1 (m ³ /s)	SA-2 (m ³ /s)	SA-4 (m ³ /s)	S-4 (m ³ /s)	SB-1 (m ³ /s)	SB-2 (m ³ /s)	SB-3 (m ³ /s)
1342.0000	1350.0000	0.0000	0.0000	0.0188	0.0000	0.0000	0.0000	0.0000
1352.6667	1360.0833	0.0000	0.0000	0.0660	0.0000	0.0000	0.0000	0.0000
1366.0000	1374.0000	0.0000	0.0000	0.0118	0.0000	0.0000	0.0000	0.0000
1379.6167	1388.3333	0.0000	0.0000	0.0663	0.0000	0.0000	0.0000	0.0000
1390.0000	1398.0000	0.0115	0.0000	0.0000	0.0000	0.0000	0.0000	0.0000
1401.3333	1408.2500	0.0000	0.0000	0.0716	0.0000	0.0000	0.0000	0.0000
1414.0000	1422.0000	0.0000	0.0132	0.0000	0.0000	0.0000	0.0000	0.0000
1429.9167	1435.5000	0.0000	0.0000	0.0000	0.0000	0.0000	0.0498	0.0000
1449.1167	1450.3833	0.0838	0.0000	0.0000	0.0000	0.0000	0.0000	0.0000
1450.3833	1452.0333	0.0838	0.0000	0.0000	0.0000	0.0000	0.0000	0.0405
1452.0333	1454.5000	0.0000	0.0000	0.0000	0.0000	0.0000	0.0000	0.0405
1454.5333	1455.8833	0.0000	0.0000	0.0617	0.0000	0.0000	0.0000	0.0000
1472.5833	1488.0000	0.0000	0.0000	0.0000	0.0000	0.0521	0.0000	0.0000
1488.0000	1492.3333	0.0000	0.0000	0.0000	0.0000	0.0848	0.0000	0.0000
1497.7167	1502.0833	0.0000	0.0000	0.0765	0.0000	0.0000	0.0000	0.0000
1504.8333	1509.5000	0.1027	0.0000	0.0000	0.0000	0.0000	0.0000	0.0000
1520.5500	1527.0500	0.0000	0.0000	0.0824	0.0000	0.0000	0.0000	0.0000
1528.2500	1532.4667	0.1110	0.0000	0.0000	0.0000	0.0000	0.0000	0.0000
1544.3333	1551.0167	0.0000	0.0000	0.0850	0.0000	0.0000	0.0000	0.0000
1552.0000	1555.6667	0.1136	0.0000	0.0000	0.0000	0.0000	0.0000	0.0000
1568.8833	1575.0000	0.0000	0.0000	0.0893	0.0000	0.0000	0.0000	0.0000
1575.5000	1582.8333	0.0000	0.0883	0.0000	0.0000	0.0000	0.0000	0.0000
1592.3167	1598.5000	0.0000	0.0000	0.0892	0.0000	0.0000	0.0000	0.0000
1599.6667	1612.1333	0.0000	0.0000	0.0000	0.0000	0.0000	0.0000	0.0250
1616.3667	1622.0000	0.0000	0.0000	0.0893	0.0000	0.0000	0.0000	0.0000
1622.7500	1636.0000	0.0000	0.0000	0.0000	0.0000	0.0000	0.0000	0.0270
1640.2833	1646.0000	0.0000	0.0000	0.0913	0.0000	0.0000	0.0000	0.0000
1647.7167	1659.0833	0.0000	0.0000	0.0000	0.0000	0.0000	0.0636	0.0000
1664.2500	1671.0000	0.0000	0.0000	0.0921	0.0000	0.0000	0.0000	0.0000
1672.0833	1684.0000	0.0000	0.0000	0.0000	0.0000	0.0000	0.0835	0.0000
1688.1500	1700.0000	0.0000	0.0000	0.0938	0.0000	0.0000	0.0000	0.0000
1700.5167	1709.0000	0.0000	0.0000	0.0000	0.0000	0.0000	0.0000	0.0347
1713.2667	1719.8333	0.0000	0.0000	0.0000	0.0000	0.0807	0.0000	0.0000
1721.0000	1729.0000	0.0000	0.0887	0.0000	0.0000	0.0000	0.0000	0.0000
1729.0000	1734.0000	0.0000	0.0307	0.0000	0.0000	0.0000	0.0000	0.0000
1736.1667	1739.5000	0.0000	0.0956	0.0000	0.0000	0.0000	0.0000	0.0000

Table D.1. Flow rate history for cold water injection into Sumikawa wells in April and May, 1989 (continued).

Start (hrs)	Stop (hrs)	SA-1 (m ³ /s)	SA-2 (m ³ /s)	SA-4 (m ³ /s)	S-4 (m ³ /s)	SB-1 (m ³ /s)	SB-2 (m ³ /s)	SB-3 (m ³ /s)
1742.7833	1749.5000	0.1087	0.0000	0.0000	0.0000	0.0000	0.0000	0.0000
1760.1667	1781.0000	0.0000	0.0869	0.0000	0.0000	0.0000	0.0000	0.0000
1784.2500	1805.0000	0.0000	0.0802	0.0000	0.0000	0.0000	0.0000	0.0000
1808.9167	1813.0000	0.0000	0.0000	0.0000	0.0000	0.0000	0.0000	0.0416
1814.3333	1817.6667	0.1114	0.0000	0.0000	0.0000	0.0000	0.0000	0.0000
1817.6667	1831.5000	0.0157	0.0000	0.0000	0.0000	0.0000	0.0000	0.0000
1832.0000	1834.6667	0.0197	0.0000	0.0000	0.0000	0.0000	0.0000	0.0000
1834.6667	1836.6667	0.0407	0.0000	0.0000	0.0000	0.0000	0.0000	0.0000
1836.6667	1838.7167	0.0667	0.0000	0.0000	0.0000	0.0000	0.0000	0.0000
1843.0000	1850.0000	0.0000	0.0000	0.0000	0.1139	0.0000	0.0000	0.0000
1850.0000	1854.0000	0.0000	0.0094	0.0000	0.0000	0.0000	0.0000	0.0000
1854.8333	1857.5000	0.0000	0.0262	0.0000	0.0000	0.0000	0.0000	0.0000
1857.5000	1859.5000	0.0000	0.0436	0.0000	0.0000	0.0000	0.0000	0.0000
1859.5000	1861.6000	0.0000	0.0668	0.0000	0.0000	0.0000	0.0000	0.0000
1865.9333	1871.5000	0.0000	0.0000	0.0000	0.1230	0.0000	0.0000	0.0000
1876.0000	1878.1667	0.0000	0.0000	0.0098	0.0000	0.0000	0.0000	0.0000
1878.1667	1881.0000	0.0000	0.0000	0.0180	0.0000	0.0000	0.0000	0.0000
1881.0000	1883.0000	0.0000	0.0000	0.0294	0.0000	0.0000	0.0000	0.0000
1883.0000	1885.1667	0.0000	0.0000	0.0408	0.0000	0.0000	0.0000	0.0000
1889.1667	1894.5000	0.0000	0.0000	0.0000	0.1214	0.0000	0.0000	0.0000
1900.0000	1904.0000	0.0000	0.0000	0.0000	0.0191	0.0000	0.0000	0.0000
1904.0000	1906.0000	0.0000	0.0000	0.0000	0.0339	0.0000	0.0000	0.0000
1906.0000	1908.0000	0.0000	0.0000	0.0000	0.0689	0.0000	0.0000	0.0000
1908.0000	1910.0000	0.0000	0.0000	0.0000	0.0970	0.0000	0.0000	0.0000
1912.0000	1920.0000	0.0000	0.0000	0.0000	0.0000	0.0000	0.0000	0.0397
1920.0000	1944.0000	0.0000	0.0000	0.0000	0.0000	0.0000	0.0000	0.0438
1944.0000	1968.0000	0.0000	0.0000	0.0000	0.0000	0.0000	0.0000	0.0610
1968.0000	1992.0000	0.0000	0.0000	0.0000	0.0000	0.0000	0.0000	0.0649
1992.0000	2000.0000	0.0000	0.0000	0.0000	0.0000	0.0000	0.0000	0.0696
2003.0833	2024.0000	0.0000	0.0000	0.0000	0.0000	0.0000	0.0723	0.0000
2029.0000	2042.0000	0.0000	0.0000	0.0000	0.0000	0.0797	0.0000	0.0000
2048.6667	2072.0000	0.0000	0.0000	0.0000	0.0000	0.0000	0.0000	0.0735
2075.5000	2091.2500	0.0000	0.0000	0.0000	0.0000	0.0000	0.0591	0.0000
2097.2500	2116.1667	0.0000	0.0000	0.0000	0.0000	0.0705	0.0000	0.0000
2120.6667	2128.0000	0.0000	0.0000	0.0000	0.0000	0.0000	0.0863	0.0000

Table D.1. Flow rate history for cold water injection into Sumikawa wells in April and May, 1989 (continued).

Start (hrs)	Stop (hrs)	SA-1 (m ³ /s)	SA-2 (m ³ /s)	SA-4 (m ³ /s)	S-4 (m ³ /s)	SB-1 (m ³ /s)	SB-2 (m ³ /s)	SB-3 (m ³ /s)
2128.3333	2144.3333	0.0000	0.0000	0.0000	0.0000	0.0151	0.0000	0.0000
2144.3333	2146.8333	0.0000	0.0000	0.0000	0.0000	0.0343	0.0000	0.0000
2146.8333	2149.8333	0.0000	0.0000	0.0000	0.0000	0.0512	0.0000	0.0000
2154.6667	2167.3333	0.0000	0.0000	0.0000	0.0000	0.0000	0.0192	0.0000
2167.3333	2169.8333	0.0000	0.0000	0.0000	0.0000	0.0000	0.0351	0.0000
2169.8333	2172.8333	0.0000	0.0000	0.0000	0.0000	0.0000	0.0503	0.0000
2178.0000	2191.3333	0.0000	0.0000	0.0000	0.0000	0.0000	0.0000	0.0083
2191.3333	2194.5000	0.0000	0.0000	0.0000	0.0000	0.0000	0.0000	0.0283
2194.5000	2197.5000	0.0000	0.0000	0.0000	0.0000	0.0000	0.0000	0.0408